Retention Mechanism for Reversed Phase and Hydrophilic Interaction Liquid Chromatography: Development and Characterisation of Modified Silica Particles

Thesis

The Open University

Retention mechanism for reversed phase and hydrophilic interaction liquid chromatography:

Development and characterisation of modified silica particles

Sophie Bailes MChem(Hons)

Department of Life, Health, and Chemical Sciences

The Open University

Date of Submission: 6 November 2013

Date of Award: 31 March 2014

November 2013

ProQuest LLC.
789 East Eisenhower Parkway
P.O. Box 1346
Ann Arbor, MI 48106 – 1346

TABLE OF CONTENTS

AUTHORS DECLARATION

The work outlined in this thesis was carried out by the author between October 2010 and September 2013 under the supervision of Prof. Peter Taylor at the Department of Life, Health and Chemical Sciences, formerly the Department of Chemistry and Analytical Sciences, at The Open University, Milton Keynes.

This work contains no material which has been accepted for the award of any other degree or diploma in any university, and, to the best of my knowledge and belief, contains no material previously published or written by another person, except where due reference has been made.

Sophia Bailes

ACKNOWLEDGEMENTS

I would like to sincerely thank my supervisors Professor Peter Taylor, Professor Alan Bassindale, and particularly Professor Mel Euerby for their continued advice, guidance, patience, and understanding throughout my studies and beyond.

Additionally, I would like to thank the staff and students of the Department of Life, Health & Chemical Sciences, Open University, particularly Sergey Bylikin for his invaluable help and ongoing advice on synthetic chemistry routes, Allen Bowden for the many Solid State NMR analysis results, and Mabs Gilmor for her help and guidance during the hydrofluoric acid digestions. Thanks also to Gordon Imlach for his support and guidance in SEM imaging.

My thanks to Mel Euerby's team at Strathclyde University for providing a number of packed HPLC columns and prototype silica materials for comparison purposes. I would also like acknowledge and thank his team; Gesa Schad, Matthew James, Colin Pipe and Mark Fever for their assistance

On a more personal note I would like to dedicate this thesis to the memory of my mother, Elizabeth Bailes, from whom I got the drive and determination to finish it. I would also like to acknowledge the huge amount of support from Talia Flanagan, Sally van Pelt, Jodie Freeman, and all my family and friends who helped me along the way, thank you. Finally, thanks to Kirk; for switching everything in life to the easy setting.

ABSTRACT

Silanophilic interaction chromatography columns can give rise to complementary selectivity compared to the more commonly used hydrophobic interaction based HPLC columns. However, the former types of phase have historically caused issues of tailing and irreversible retention with polar or basic analytes. An investigation was therefore undertaken into the fundamental nature of their electrostatic, dipole-dipole and hydrogen bonding interactions. This was particularly focussed on interactions that are induced by the presence of residual silanols on the surface of HPLC phases, in order to fully understand the retention mechanism and the practical limitations of commercial stationary phases. Manufacturer's literature for these types of phase often contains specific applications and claims, however full independent testing of a range of acid, basic, phenolic, and polar compounds had not previously been demonstrated. Research in this area will aid in the development of new industrial applications by highlighting the stationary phase type with the most suitable mechanism to separate any combination of polar and non-polar compounds.

Initial investigations evaluated silanophilic interactions present in a set of Extended Polar Selectivity (EPS) phases utilising a set of known characterisation probes. Structural elucidation of these phases confirmed the intensity of these interactions is due to the accessibility of the silanols and the purity of the base silica. Shorter chains and sparsely bonded hydrocarbon ligands were shown to reduce hindrance and increase the degree of interaction. Endcapping was shown to decrease the accessibility of residual silanols and mask silanophilic interactions. High purity base silica was shown to reduce silanophilic interactions compared to similar phases bonded to a TYPE-A silica.

The control and restriction of silanophilic interactions is of great importance for the analysis of basic and polar molecules. Commercial TYPE-C™ phases are claimed to minimise silanophilic interactions through the "silanization" process. This converts the surface silanols to silica hydride prior to

derivatisation with a functionalised ligand. Characterisation of the TYPE-C™ Bidentate C18 phase showed higher silanophilic interactions than a typical TYPE-B octadecyl bonded phase with a trimethyl silane endcap. ^{29}Si NMR on the unpacked TYPE-C™ Bidentate C18 silica material confirmed the presence of silanols. These silanophilic interactions were shown to be coming from unreacted hydroxyl "wings" on polymeric silica hydride surface due to incomplete cross-linking of the triethoxy silane (TES) monomer during the "silanization" process.

Reduced efficiency observed in the characterisation of the TYPE-C™ Bidentate C18 phase was shown to be due to a high A Term in the van Deemter equation, due to a high level of Eddy dispersion in the silica bed. SEM imaging of the unpacked TYPE-C™ Bidentate C18 silica material showed a number of irregular particles present, these were identified as amorphous polyhydrosiloxane (PHS) formed through a cross-linking reaction of the TES monomer.

Investigation into the "silanization" reaction using TES indicated the process requires strict moisture control and monitored addition of the TES to reduce PHS formation Columns packed from the optimised "silanization" process showed lower silanophilic interactions in HILIC characterisation than the commercial TYPE-C™ phases. HILIC mode van Deemter analysis indicated the A Term contribution is comparable with unmodified bare silica; this suggests no added Eddy dispersion due to PHS particles in the packed silica bed.

HILIC analysis on the TYPE-C™ Diamond Bond and Silica-C phases coupled with ^{29}Si NMR spectroscopy confirmed the presence of accessible silanols on the surface of the silica. Principal component analysis found these phases to be similar to experimental and literature characterisation values for TYPE-B style bare silica. The efficiency and van Deemter contributions of these phases were comparable to unmodified TYPE-B silica indicating these phase are not prepared by "silanization" by TES but by a two step chlorination and reduction process.

GLOSSARY OF TERMS

List of Symbols

α	Separation factor
A_s	Asymmetry of peak
%B	Amount of organic modifier in the mobile phase
d_C	Internal column diameter
D_m	Solute diffusion coefficient
d_p	Particle size diameter
F	Flow rate
γ	Obstruction factor
φ	Polar volume fraction of the mobile phase
k	Retention factor
k_{corr}	Corrected retention factor
k_0	Retention factor in 100% solvent mobile phase
H/HETP	Column plate height
λ	Uniformity in packed silica bed
L	Column length
μ	Linear velocity of the mobile phase
m	Stoichiometric coefficient of the solvent in the mobile phase
η	Viscosity
N	Efficiency (Number of theoretical plates per column)
R_s	Resolution
r^2	Correlation coefficient
S	Neue selectivity value

t_D	Dwell time
T_{ext}	Extra column time
t_0	Column dead time
t_R	Retention time
t_G	Total time for the gradient
T	Temperature
T_M	Column dead time
V_D	Dwell volume
V_{ext}	Extra column volume
V_M	Column dead volume
$W_{0.5}$	peak width at half height
W_b	peak width at base
W_s	Column saturation capacity
W_x	Sample weight of an overloaded peak

List of Equations

Retention calculations:

$$t_o = \frac{V_m}{F} \qquad t_R = t_O(1+k) \qquad k = \frac{(t_R - t_O)}{t_O} \qquad t_{ext} = \frac{V_{ext}}{F} \qquad k_{corr} = \frac{(t_R - t_{ext}) - (t_O - t_{ext})}{t_O - t_{ext}}$$

Column efficiency calculations:

$$H = \frac{L}{N} \qquad N = 5.54\left(\frac{t_R}{W_{0.5}}\right)^2 \qquad N = 16\left(\frac{t_R}{W}\right)^2$$

$$H = \lambda d_p + 2\gamma\frac{D_m}{\mu} + c\frac{{d_p}^2}{D_m}\mu$$

$$V_m = \pi * \left(\frac{d_c}{2}\right)^2 * L_c * \frac{\varepsilon_t}{1000} \qquad V_m = 0.5\, L\, {d_c}^2$$

Resolution calculations

$$R_s = \left(\frac{1}{4}\right)\sqrt{N}\ \frac{(\alpha - 1)}{\alpha}\left(\frac{k}{1+k}\right)$$

$$R_s = \frac{1.176\,(t_{R2} - t_{R1})}{(W_{0.5_1} + W_{0.5_2})} \qquad R_s = \frac{2\,(t_{R2} - t_{R1})}{(W_1 + W_2)}$$

Selectivity factors

$$\alpha = \frac{k_1}{k_2} \qquad S = 100 \times \sqrt{(1 - r^2)}$$

Overloaded peak width calculations

$$W_b = \frac{16\, t_0^2\,(1+k_0)^2}{N_0} + \frac{6\, t_0^2\, k_0^2\, W_x}{W_S} \qquad W_s = \frac{N_0(6 t_0^2 k_0^2 W_x)}{(N_0 W_b - 16\, t_0^2\,(1+k_0)^2}$$

List of Abbreviations

AN(P)C	Aqueous Normal Phase Chromatography
ASEC	Aqueous Size Exclusion Chromatography
AEX	Anion Exchange
CE	Capillary Electrode
DEET	*N,N*-Diethyl-*meta*-toluamide
DRIFT	Diffuse reflectance infrared Fourier-transformed spectroscopy
DSC	Differential Scanning Calorimeter
ELSD	Evaporative Light Scattering Detection
EPS	Extended Polar Selectivity
GC	Gas Chromatography
HILIC	Hydrophilic Interaction Liquid Chromatography
HPLC	High Performance Liquid Chromatography
HSS	High Strength Silica
IEC	Ion Exchange Chromatography
IR	Infra Red
MeCN	Acetonitrile
MeOH	Methanol
MS	Mass Spectrometer
NMR	Nuclear Magnetic Resonance
NIR	Near Infra Red
NP-LC	Normal phase liquid chromatography
PEG	Polar Embedded Group
PCA	Principal Component Analysis
PQRI	Product Quality Research Institute

RI	Refractive Index
RP-LC	Reverse phase liquid chromatography
SB	Stable Bond (Zorbax)
SB	Selectivity for Bases (Waters)
SEC	Size Exclusion Chromatography
SEM	Scanning Electron Microscope
SFC	Supercritical Fluid Chromatography
TES	Triethoxysilane
TMS	Trimethoxysilane
TGA	Thermal Gravimetric Analysis
TLC	Thin Layer Chromatography
UHPLC	Ultra High Performance Liquid Chromatography
USP	United States Pharmacopeia
UV	Ultra Violet
ZIC	Zwitterionic Chromatography

Table of Figures

Table of Tables

1. INTRODUCTION

1.1 High Performance Liquid Chromatography

Liquid chromatography techniques range from home made traditional thin layer chromatography (TLC) plates to state of the art ultra-high performance liquid chromatography (UHPLC). The most commonly used of these is high performance liquid chromatography (HPLC) with packed silica based columns, which is employed in a number of industries including pharmaceutical, food and drinks manufacturing and academic research. HPLC is primarily utilised to separate a number of components in solution, often referred to as solutes, and can be coupled to a variety of detectors such as ultraviolet wavelength detectors (UV), refractive index (RI) and mass spectrometers (MS) to qualify and quantify these analytes.

HPLC is a reasonably complex piece of equipment which can mix and pump a number of solvents through the column at a constant flow until the column reaches a stable equilibrium; the sample of dissolved analytes or compounds, is then injected into this flow of the mobile phase without a drop in pressure. An HPLC column contains tightly packed silica particles in solvent, sometimes referred to as silica gel. This silica can be left untreated or can be modified by bonding silicon containing ligands to the surface, these are often termed silanes. As the mixture of compounds passes through the packed silica column some analytes will have a higher affinity to the surface of the column, the stationary phase, and some to the mobile phase. As the solutes in the starting mixture have different affinities as they pass down the column they are retained by the stationary phase forming bands and when they elute from the end of the column they will have separated into groups of like molecules. Different silanes will give different or complementary separation mechanisms under similar conditions. In reversed phase HPLC the mobile phase is aqueous and more polar than the stationary phase, which are commonly long chain hydrocarbons bonded to silica particles, therefore polar analytes will have a greater affinity for the mobile phase and will elute early whereas less polar

analytes or hydrophobic molecules will be retained on the stationary phase and elute later, Figure 1.1[1][2][3].

Figure 1.1 Schematic of separation mechanism

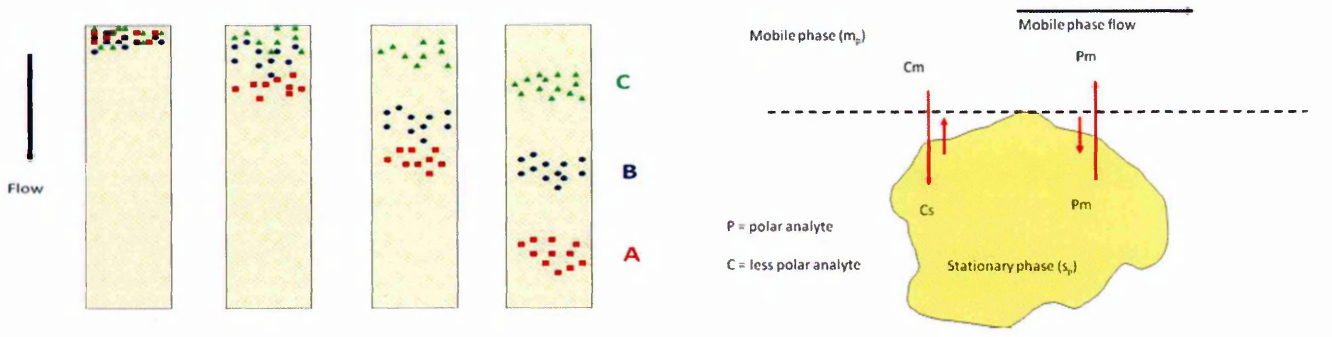

Although the exact separation mechanism of analyte retention is not fully understood it is known to involve intermolecular interactions between the mobile phase, stationary phase and solute. These interactions can be affected by polarity, pH, ionic strength and temperature of the mobile phase and the polarity and functionality of the stationary phase. There are three main theories to explain this; the first is based on the partition coefficient of the analyte between the stationary and mobile phase in which the solutes fully embed themselves into the bonded phase[4][5], however this may be over simplifying the process[6][7] as it doesn't allow for band broadening and peak tailing due to secondary interactions with residual silanols[8][9][10] and metals[11][12][13] on the surface of the stationary phase. The second theorises that the analyte is adsorbed directly onto the surface of the stationary phase[14][15] although this doesn't satisfactorily explain the retention differences of an analyte in different mobile phases. The third suggests preferential absorption of the mobile phase onto the stationary phase forming an absorbed solvent layer around the surface of the modified silica, followed by the partition of the analyte into this adsorbed layer[16][17].

Although the latter seems to be the most rounded proposal the study was carried out using large complex molecules and does not account for direct adsorption of small analytes onto the silica

surface. It is therefore likely that all three approaches are valid depending on the size and functionality of the solute and the mobile phase composition[18].

In reversed phase liquid chromatography (RP-LC) the hydrophobic solvent of the mobile phase will be attracted to the stationary phase forming a solvated layer around the surface of the silica. Hydrophobic analytes will then favour this solvated layer over the more polar water-rich bulk of the mobile phase[19-25]. This forces the analytes into the pores of the modified silica surface and into the vicinity of the bonded silane groups allowing both partition and adsorption to take place within the pores. Hydrophilic and polar molecules will not undergo the same interactions as they will favour the mobile phase, therefore a different mechanism must be used to separate polar analytes[26].

It is possible that the nature and strength of these intermolecular interactions dictates how the analyte is retained. For example chemical interactions such as hydrophobic, aromatic[31-33] and van der Waals forces[34][35] would most likely entail partitioning separations. The analytes undergo electrostatic interactions with the modified silica surface; these interactions are defined by the surface tension of the mobile phase. Therefore, using different organic solvents or a solvent gradient will result in retention differences being observed. The shape and size of the analytes is a key factor in how it binds to the stationary phase. For example a long chain linear molecule will be retained longer than its branched chain equivalent as the higher available surface area of hydrophobicity will be more likely to interact, and this interaction will occur more often[36-40], with the available silanes inside the pores of the silica surface[41-43]. There is the added complication of steric hindrance for branched chain molecules, as these interactions commonly happen inside the pores some analytes may not be retained simply because they cannot access the hydrophobic modified silica chains[44].

Physical interactions depend on the size of the molecule or functional group interacting with the stationary phase. Small or localised interactions such as ion-exchange chromatography (IEC) and dipole-dipole retention may be lead by adsorption directly onto the stationary phase[45]. The ionic

interaction between the oppositely charged molecule and the silane of the stationary phase leads to adsorption[46-48]. Ionic interactions can be very strong and often dominate the interaction between the analyte and stationary phase, the type, number and location of the ionic charges on the analyte will determine the strength of the interaction. The affect of these ionic interactions can be altered by changing the concentration of buffer salt. The smaller buffer ions will preferably bind to the ionic charges on the stationary phase which will alter the affinity of the solutes to the stationary phase. Weaker ionic interactions can be overcome with a lower buffer concentration; therefore in a buffer strength gradient the weaker ionic analytes will elute from the column first. Molecules that have a stronger ionic interaction require a higher salt concentration to affect the affinity between solute and stationary phase and these will elute later in the gradient[49].

Hydrogen bonding is an unusual chemical interaction as it is essentially a van der Waals force and should exhibit electrostatic characteristics[49][50]. However the polar nature of hydrogen bonding makes it appear to more aligned with adsorption interactions parallel to ionic interactions[51-53]. Stationary phases that exhibit hydrogen bonding will interact with the aqueous phase and other solvents in the mobile phase such as methanol so that for an analyte to be retained by hydrogen bonding the interactions have to be strong enough to overcome these forces. These types of interaction are prevalent in bare silica as the silanols groups are excellent hydrogen bonding groups (this will be covered in more detail in Section 1.5 and 1.6).

Size exclusion chromatography (SEC) is a type of partitioning separation of large molecules, sometimes simply by utilising the pores themselves, as bulky analytes will not fit into the pores and therefore are not be retained by the stationary phase[54][55]. Smaller molecules will be able to penetrate more pores and will be retained on the column for longer. Provided all the analytes are injected at the same time a SEC column will separate a mixture based on size, with the largest eluting first, and all analytes of the same shape and size eluting at the same time[56-58]. This applies

to large molecules such as proteins, peptides and oligonucleotides and is not suitable for molecules with a molecular weight below 1000 Daltons.

The strongest interaction will govern the retention characteristics however weaker, secondary interactions will contribute to the overall mechanism. The following Table 1.1 gives a summary of the types and strengths of interaction[59].

Table 1.1 Types of chromatographic interactions

Type of interaction	Characterization	Example	Energy[59] [kJmol^{-1}]
Hydrophobic interaction	Forces between molecules with low affinity for water in a high aqueous environment	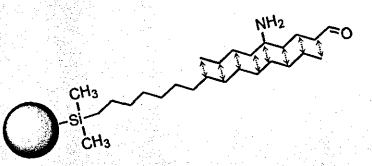	-4
π-π interactions	Non-covalent interactions between the π-electrons of aromatic systems (commonly through ring stacking)	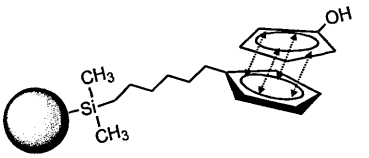	-4 to -12
Intermolecular interactions (van der Waals forces)	Attractive or repulsive electrostatic interactions between multipoles within the same or two different molecules	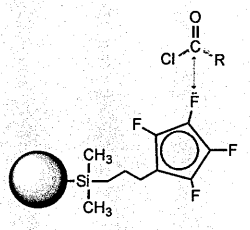	-2 to -4
Ionic interactions	Electrostatic interactions between a cation and an anion	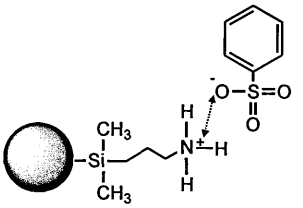	-20 to -100

Type of interaction		Characterization	Example	Energy[59] [kJmol^{-1}]
Physical interactions	Ion-dipole	The ionic force acting on the permanent dipole of a neutral molecule	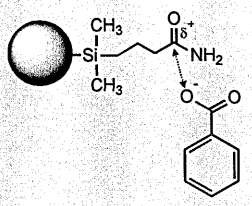	-4 to -17
	Dipole-dipole	Forces between determined dipole moments in electrically neutral compounds	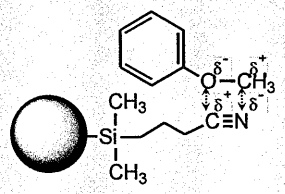	-4 to -17
Chemical interactions	Hydrogen bonding	Formed between a hydrogen donor and a hydrogen acceptor, these interactions can occur between atoms within the same molecule	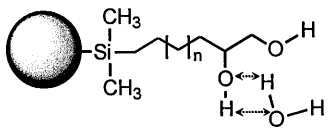	-4 to -17
	Electron donor-acceptor interaction	Formed between Lewis bases (electron donors) and Lewis acids (electron acceptor)	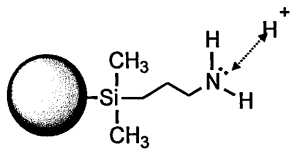	-4 to -17

The different types of interactions means the HPLC columns that exhibit each specific interaction type will separate the same mixture of analytes in a highly complementary way. For example, a long hydrocarbon chain such as a C18 column will give a different elution order to a mixture of aromatic and neutral compounds than a column bonded with phenyl rings.

The application of these retention mechanisms is to separate solutes of complex mixtures for qualification and quantification. In the majority of cases the desired resolution between these bands of analytes is the critical factor of any HPLC method, this can be mathematically determined by the resolution equation[60]:

(I) $$R_s = \left(\frac{1}{4}\right) N^{0.5} \left(\frac{\alpha - 1}{\alpha}\right) \left(\frac{k}{1+k}\right)$$

Where:

R_s =	resolution between two adjacent component peaks
N =	Efficiency of the column
α =	selectivity factor between two adjacent component peaks
k =	retention factor of the components of interest

This equation clearly indicates there are three main contributors to the relative retention of a mixture of analytes on a column and therefore the resolution between any two different analytes. These are seen to be efficiency (N) of the column, determined by the length (L), particle size (dp) and packing efficiency of the silica particles (λ)[61-63].

Secondly, the selectivity (α) term is determined by the functional groups of ligand used in the stationary phase and how this ligand is bonded to the phase[64]. The α term is also dependent on the organic composition[65][66], temperature[67], pH and buffer selection of the mobile phase[68]. Finally the retention factor (k) of the analyte is the ratio of the retention time of a given analyte under specific conditions (t_r) versus the dead time of the system (t_0). The retention time is not affected by column dimensions but can be significantly affected by the percentage of organic modifier and pH of the mobile phase[69][70] as shown in Figure 1.2 overleaf.

Figure 1.2 ***Plot of the effect of mobile phase concentration and pH on the retention factor of common analytes***

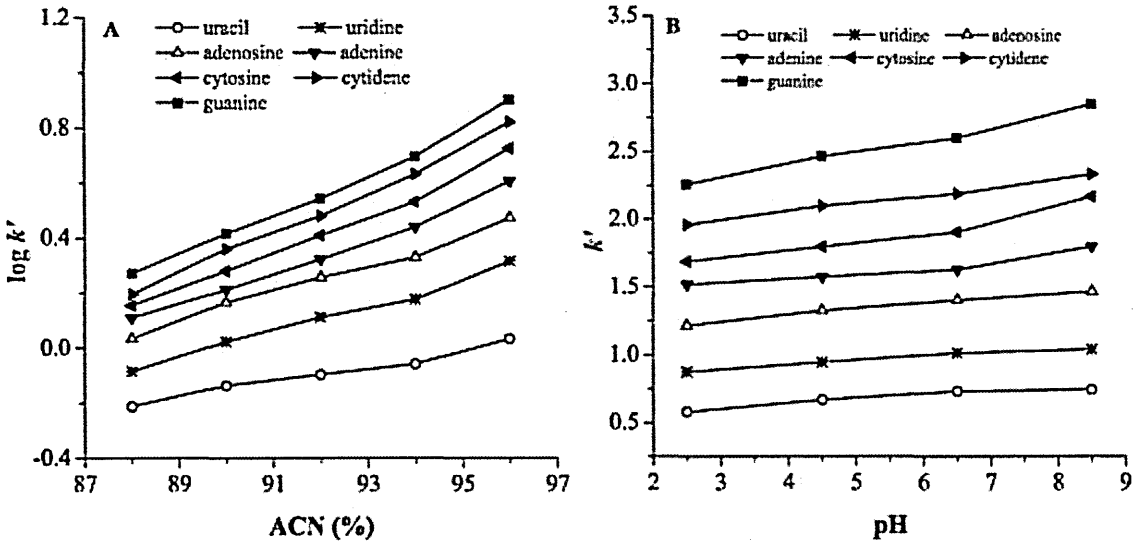

*Figure taken from ACT web seminar

So far these discussions have been based around reversed phase HPLC as it is the most versatile and commonly used. However it does have limitations, especially with the analysis of polar molecules as these would have greater affinity for the water rich polar mobile phase and will not be retained by the column. Therefore, further types of HPLC analysis for polar applications need to be researched.

1.2 Normal Phase Chromatography

In normal phase liquid chromatography (NP-LC) the stationary phase is predominantly polar, either through utilising the residual silanols on the base silica or by bonded diols, amines or cyano moieties to the silica surface. Whereas the mobile phase is usually a mixture of non-aqueous and non-polar solvents with a low eluotropic value (ε_o)[71][72]. Elutropic strength is based on the solubility parameters and the adsorbent properties of the solvent[73]. Previously solvents such as ether, tetrahydrafuran and chloroform were favoured due to their elutropic value. However due to health and safety issues with these solvents they are no longer routinely used. Iso-hexane is now the most commonly used base solvents combined with a more polar solvent such as methanol, iso-proponal or acetonitrile are used for the gradient. In normal phase, hydrophilic analytes will be repelled from the non-polar environment of the mobile phase and be forced towards the more polar stationary phase where it will be favourably adsorbed onto the silica surface or bonded silanes[74][72]. In gradient NP-LC the polarity of the mobile phase can then be increased to affect the retention of the analytes; as the polarity of the mobile phase increases the interaction with the stationary phase will become less favourable and the analyte affinity for the mobile phase increases based on the hydrophilic nature of the solute.

Solvents with a higher eluotropic value will favourably interact with the stationary phase as the polar functional group of the solvent will preferentially bind to the silanol or polar function of the stationary phase, resulting in a polar solvent layer around the stationary phase. As the retention in NP-LC is based on surface adsorption the retention factor of an analyte (k) can be modelled mathematically by the following equation[105]:

(II) $$\log k = \log k'_0 - m'.\log \varphi$$

Where:

φ = polar volume fraction of the mobile phase

m' = stoichiometric coefficient of polar mobile phase required to replace one molecule of analyte

k_0 = retention factor of the analyte in a 100% non-polar solvent mobile phase

This equation indicates that the retention factor is based on the polarity of the elutropicaly stronger solvent in the mobile phase versus the polarity of the stationary phase. As k_0 is a constant an analyte will be retained by adsorption onto the polar stationary phase and only be displaced when the polar fraction of the mobile phase is preferentially adsorbed and displaces the analyte. This retention time can be reduced by increasing the percentage of polar solvent in the mobile phase or by selecting a different stationary phase.

The adsorption coefficient can be affected by temperature changes as it will alter the interaction between the polar solvent fraction and the stationary phase. Buffers are not commonly used in NP-LC as they are commonly aqueous based.

As previously discussed, hydrophilic compounds are often not retained under reversed-phase conditions as they have a considerably higher affinity for the polar mobile phase. They are usually well retained under normal phase as the stationary phase is more polar than the organic rich mobile phase. However a major drawback to this method is that that very hydrophilic analytes are not usually soluble in the non-aqueous solvents used for normal-phase. Many of the solvents choices for NP-LC mobile phases are toxic reducing the likelihood of finding a suitable solvent for the desired analyte. Another disadvantage to NP-LC is that the system has a slow equilibration time making it non-reproducible and unsuitable for gradients or high throughput style analysis.

As many complex pharmaceuticals are hydrophilic and highly polar[75] there is a commercial requirement to develop methodology that quickly and efficiently separates these types of analytes by HPLC[76][77][80], capillary electrophoretic methods (CE)[79] or SFC[78]. HPLC equipment is usually cheaper, more versatile and simpler to use, creating a drive to develop HPLC methodology that would be suitable for analysis of water soluble polar compounds.

1.3 HILIC Retention Mechanism

Hydrophilic interaction liquid chromatography (HILIC) gives a truly orthogonal separation mechanism to those previously discussed[81-85]. Here the polar molecules, which are often not retained in RP-LC, now elute in order of increasing polarity. In RP-LC the aqueous component of the mobile phase is the stronger solvent and governs the affinity of the analytes. However in HILIC it is the organic phase which is the stronger solvent and the polar, hydrophilic analytes have greater affinity to the polar stationary phase. This type of chromatographic retention has been around for over 60 years, however it is only recently that the retention mechanism has been understood and recognised as a distinct mode of chromatography. HILIC, a term first published in 1990[86], utilises NP-LC type polar stationary phases giving rise to longer retentions of small polar, hydrophilic molecules along with mobile phase solvents with high eluotropic values similar to those used in RP-LC. Understandably HILIC has sometimes been referred to as a variant of normal phase and has previously been associated with Aqueous Normal Phase (ANP). However, the separation mechanism used in HILIC is now understood to be more complicated.

Current theories propose additional partitioning separation is the major contributing factor in the HILIC separation mechanism however it is likely the system also allows for adsorption of analytes, as in ANP chromatography. Due to the nature of the stationary phases used another large contribution to the retention mechanism will be from electrostatic interactions, this being especially important for charged analytes. Although a vast number of studies have been carried out since 1990 a unified theoretical explanation has not yet been agreed within the chromatographic community. As opposed to RP-LC the mobile phase in HILIC is organic solvent rich, commonly 60-95% acetonitrile is used, although it is said that true HILIC requires 70-98% acetonitrile[86]. There is still some argument about the amount of aqueous or weak solvent required for HILIC type retention mechanism; it is thought at least 2.5-3.0% is required. The small percentage of aqueous composition in the mobile phase forms an adsorbed solvated layer around the polar stationary phase, this has been proven

through Karl Fisher analysis[87] and molecular simulation dynamics[88]. Unlike RP-LC the organic contribution is the stronger solvent and the water is the weaker. Consequently the choice of stationary phase is important as it controls the degree of solvation that will take place[87].

The separation mechanism of pure HILIC[85] is said to be governed by the differential distribution of the sample analyte between this solvated layer and the solvent rich bulk of the mobile phase similar to liquid-liquid extraction mechanisms[86][87]. This is illustrated in Figure 1.2 below. Hydrophilic analytes will preferentially be retained by the partition and shift from the relatively hydrophobic bulk mobile phase into the immobilised polar aqueous-rich layer on the stationary phase[86][92].

Figure 1.2 ***Schematic of partitioning mechanism in HILIC***

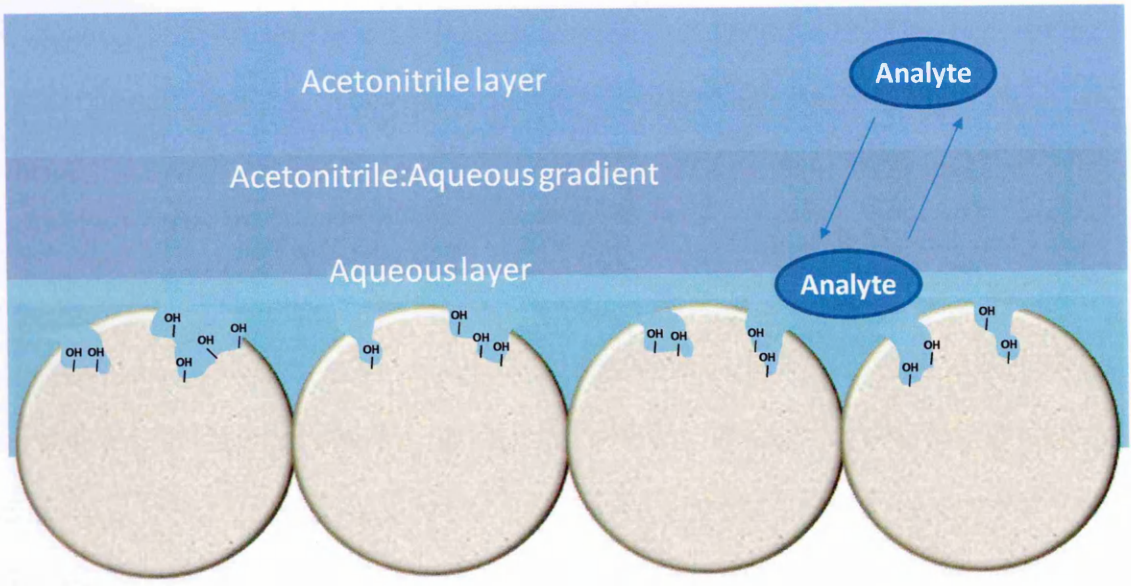

However the polar analytes are now in the same proximity as the hydrophilic silanols and polar silanes of the stationary phase and adsorption or electrostatic separation mechanism could potentially occur[93-95]. These secondary interactions are not typically counted as HILIC behaviour but it is impossible to separate the two retention mechanisms. Aqueous buffers can be used to preferentially adsorb onto to the polar functionality of the stationary phase and reduce the contributions to retention of polar analytes.

1.3.1 HILIC Mobile Phase

As the organic solvent is now the strong solvent in the mobile phase acetonitrile is favoured due to its elutropic strength, although methanol, ethanol and iso-proponal are also used. Water is the favoured choice for the weak solvent, as acetone can also be used but as it has a high UV absorbance it cannot be utilised with UV detection. As partitioning, adsorption effects and ion exchange interaction, contribute simultaneously to a complex retention mechanism in HILIC systems it can be referred to as a combination of NP-LC and RP-LC effects[96]. Research into binary HILIC using different compositions of aqueous-acetonitrile mobile phase has shown how the retention mechanism can flip between HILIC and RP-LC as the aqueous fraction of the solvent phase is increased[97]. HILIC can be run for gradient elution by increasing the percentage of aqueous concentration in the mobile phase, here the solvated layer around the stationary phase is affected which leads to changes in the partitioning effects. At high aqueous conditions the bulk of the mobile phase is no longer pure acetonitrile and the solvated aqueous layer dissipates into the bulk, therefore partitioning no longer occurs in the same way. In gradient mode the phase is no longer in equilibrium, however as long as the gradient is carried out in the same way the method should be repeatable. As the solvated layer takes a long time to reach equilibrium the post time for a HILIC gradient can be very long, often in excess of 20 column volumes. This means practically that running these gradients is very time consuming, however they do offer an extra degree of selectivity and reduced peak widths for very polar compounds which will be retained for a long time in isocratic HILIC due to the reduction in band broadening.

Analytes run between HILIC and RP-LC show a characteristic U-shaped plot of the log of the retention factor (k) versus the volume fraction of the aqueous buffer (φ[BUF]). Initially at low concentrations of water the main contribution to the HILIC retention model is the partitioning mechanism and the solvophobic analytes will favour the water rich adsorbed layer around the stationary phase over the mainly non-polar body of the solvent. Although adsorption will still occur

at high percent age organic composition these will be weaker, secondary interactions and have a lower contribution to the overall retention mechanism. As the percentage of water increases the polarity of mobile phase will increase altering the equilibrium co-efficient of the water layer around the stationary phase. The solutes will no longer be forced into close contact with the stationary phase and will have greater affinity for the mobile phase, therefore secondary retention factors such as ion exchange, dipole-dipole and H-bonding type interactions are now the main contributor to the retention mechanism as in RP-LC. This can be seen experimentally in Figure 1.3 below.

Figure 1.3 ***Retention of analytes in HILIC mode with different % organic modifier***[98]

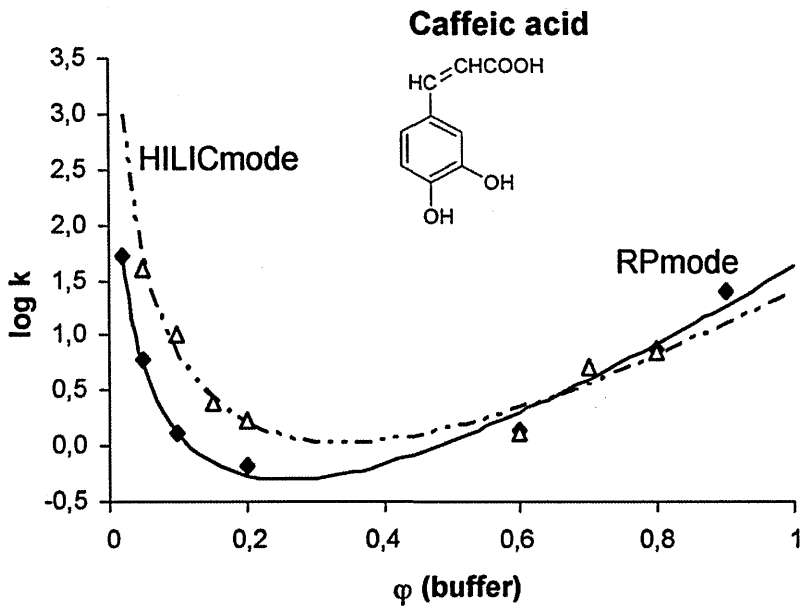

This effect can be shown mathematically using the following equation[98][105]:

(III) $$\log k = a_1 + m_1 \cdot \varphi(BUF) - m_2 \cdot \log \varphi(BUF)$$

Where:

a_1 = Empirical constant

m_1 = The increasing RP-LC mechanism, such as chemical and physical adsorption effect, based on the increasing aqueous fraction of the mobile phase.

m_2 = The decreasing HILIC contribution to the retention mechanism through partitioning of the polar fraction of the mobile phase.

As with NP-LC, organic solvents with a low eluotropic value are favoured for HILIC in order to form the solvent partioning layers. However solvents such as hexane, dimethyl ether or diethyl ether are not fully water miscible and therefore are not suitable. A polar protic solvent is required; although alcohols have been used for HILIC analysis, the most common solvent is acetonitrile as it has been found to give a longer retention time for the majority of polar analytes and therefore gives better separation of polar and non-polar mixtures.

Isocratic HILIC is often utilised as the polar stationary phases need a larger number of column volumes to equilibrate and establish the aqueous rich layer. Gradient HILIC is becoming more and more popular using a low concentration of water in the organic modifier at initial conditions increasing to higher water content over the analysis. However this technique has a number of drawbacks due to the slow kinetics and the added RP-LC type retention mechanism as the water concentration is increased as shown in Figure 1.3. This can be a reproducible technique but care needs to be taken to ensure that the aqueous layer is retained throughout the gradient and the column had adequate column volumes to equilibrate and reform the same density of the aqueous layer. As long as the aqueous layer is not completely depleted during analysis this should not require long equilibration times. This is comparable to phase collapse issues often seen with reversed phase columns. In reversed phase, phase collapse commonly occurs on long chain silanes that are run in completely aqueous mobile phases, here the stationary phase loses its organic solvation layer and when the pressure is released the long chain silanes "collapse" and fall in on each other. This results in reduced retention of molecules as the same area of hydrophobic alkyl chain is no longer available to interact with the solutes, until the organic solvent layer has reformed and the carbon chains are re-erected[106]. One of the major practical issues for HILIC mode is the choice of sample solvent. Here the aqueous component is not the strong solvent and the organic is the weak. Therefore a higher percentage of organic is required to give a higher detector response, however this may result in solubility issues for some compounds[89].

1.3.2 Buffer Salts in HILIC Analysis

The use of buffer salts is common in HPLC analysis to control pH and ionic strength of the mobile phase[1][20]. The pH of the mobile phase should be at least two pH units from the pK_a of the analyte to ensure the solute is fully in the ionised or unionised form otherwise peak splitting can occur. The ionic strength of the aqueous portion of the mobile phase can be used to suppress interactions from residual silanols on the stationary phase (this will be discussed further on page 24). Buffer salts need to be fully soluble in the mobile phase, although phosphate buffers are common in RP-LC these salts tend to precipitate in high concentration of solvents and are not suitable for HILIC. The main drawback of non-volatile buffers such as phosphate and sodium salts is their incompatibility with mass spectrometry.

Ammonium acetate and ammonium formate are favoured in HILIC as these salts can also contribute to the ionisation and polarity of the analyte; for example some highly polar analytes such as antibiotics need an ionic strength of >100mM to ensure the solute is in a single ionic form[105]. The buffer can also enhance the density of the solvated layer around the stationary phase by increasing the hydrogen bonding of the water molecules. This causes a shift in the partition equilibrium and the time an analyte is retained in the aqueous rich layer is increased. It is also thought that addition of the salt buffers decreases the electrostatic repulsion between the polar analytes and the polar stationary phase again increasing the retention[105]. The ammonium counter ion will preferentially adsorb onto the polar stationary phase significantly affecting the retention mechanism if the primary contribution is from ionic attraction and repulsion. Suppressing these ionic interactions will improve peak shape and reduce tailing from secondary interactions[80][108].

Ammonium based salt buffers have a near neutral pH in aqueous solution, in fact ammonium acetate has no buffering capacity at pH 6.8, however the high concentration of acetonitrile will increase this pH considerably. The high pH of the mobile phase may suppress the ionisation of weak

bases reducing retention from electrostatic interactions. This high pH can also affect the charge of the stationary phase. columns suitable for HILIC can be categorised as having either neutral or charged polar group; neutrals such as the amide and diol phases are not affected by the pH of the mobile phase and there is no change in the ionisation of the surface functionality. Charged ionic surfaces have ion exchange interactions, phases such as amino have an anion exchange mechanism at high pH whereas ionised bare silica phases will give rise to cation exchange at low pH. There are also Zwitterionic phases that display both anionic and cationic properties and can be greatly affected by the pH of the mobile phase. Charged stationary phases are more likely to become deprotonated at higher pH and the likelihood of electrostatic interactions contributing to the retention mechanism is increased[82].

1.3.3 HILIC Stationary Phases

As indicated previously, the type and character of a HILIC stationary phase will govern the hydrophilic partitioning mechanism and the RP-LC style adsorption and electrostatic interactions. The stationary phase requires a significant degree of polar functionality, hydrogen bonding capacity and ion exchange properties. These can be the same types of silica gel based columns used for RP-LC, such as diol, cyano and amine phases, however more recently specific HILIC columns such as zwitterions functionalities have been developed. Both polymeric and monofunctionally bonded phases can be used, as the conditions used in HILIC are often in neutral conditions the deterioration of silica through dissolving the silica bed is less of an issue. Some of the most commonly used stationary phases for HILIC mode are reviewed in Table 1.2 overleaf [94-98][112]

Table 1.2 *Types of HILIC stationary phase*

USP Classification	Stationary Phase Type	Schematic	Applications for columns	Problems with commercial columns
L3	Bare silica e.g. ACE™ 3 SIL	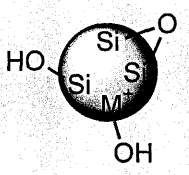	Highly common for HILIC applications. Used for oligonucleotides, peptides, and proteins.	The purity of the silica can cause issues with reproducibility due to variable distributions of silanols, siloxanes and in some cases small amounts of trace metals. Absorption effect and band broadening a possible for some peaks. Slow kinetics means long equilibration time
	Propyl-Amino e.g. Zorbax NH_2	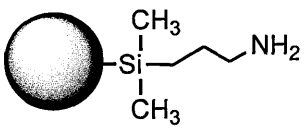	Polar compounds such as peptides. Commonly used in pseudo HILIC mode for carbohydrate and sugars analysis.	Highly charged stationary phase can lead to irreversible adsorption of some acids.
L10	Cyano e.g. Nucleosil CN	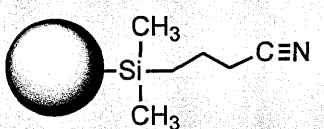	Hydrophobic proteins, these columns can also be used for NP-LC and HILIC gradient as faster equilibration time than bare silica.	Short alkyl chains have stability issues however polar and ion exchange interactions can be masked by the hydrophobic nature of long chain linkers.

USP Classification	Stationary Phase Type	Schematic	Applications for columns	Problems with commercial columns
L20	Diol e.g. Triart Diol-HILIC	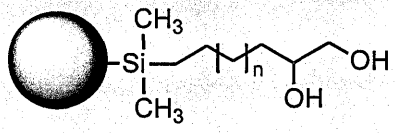	Proteins, steroids and sterols, phases can be used in conjunction with size exclusion separation depending on pore size. Hydrogen bonding abilities give complementary separations to other polar phases.	Polar and electrostatic forces are weak and can be over-shadowed by alkyl chain linkers; this can disrupt the portioning effect.
L8	Terminal- Amide e.g. Waters UPLC BEH Amide	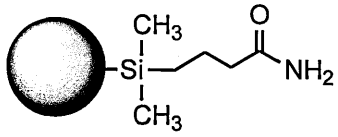	Polar compounds such as peptides.	
L3	Zwitterionic Sulfobetaine e.g. ZIC®-HILIC	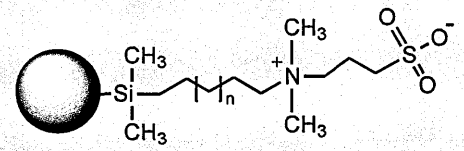	Used for carbohydrates, oligonucleotides, peptides, proteins and complex metabolites and polar pharmaceutical compounds.	Slow kinetics means long equilibration time and limited gradients due to water sensitivity Absorption effect and band broadening can be observed for some peaks.

USP Classification	Stationary Phase Type	Schematic	Applications for columns	Problems with commercial columns
	Mixed Mode e.g. SIELC Primesep N	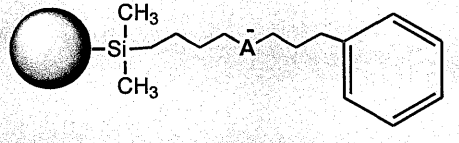	As with Zwitterions the dual retention mechanism allows for separation of complex mixtures containing acids, bases, and neutral solutes in a single run. Utilises same hydrophobic interactions as C18 but the addition of highly polar groups allow secondary interactions (such as ion exchange or pi-pi mechanisms).	Due to the complexity of making and bonding the silanes these phases can be very expensive.

Polar columns give complementary selectivity to alkyl phase columns during RP-LC method development; in most cases at least one polar phase is included in an initial column screen. However, these polar columns used under HILIC conditions have true orthogonality to a hydrophobic C_{18} phase in reversed phase as analytes will have an opposite retention mechanism. Consequently, there are a number of polar columns available on the market that can be used in both RP-LC and HILIC modes. Early HILIC separations were carried out using amino and amide functionalities for their polar character[104]. Subsequently amino columns such as Zorbax NH_2 phase, and the Phenomenex Luna phase, which is believed to have a polymeric structure, are now marketed for HILIC, NP-LC and RP-LC separations[113]. Common Amide phases that are used in HILIC include Waters XBridge and BEH phases, TSKgel Amide-80 and HALO-RP Amide[112][114].

HILIC phases have become more and more common in the past 15 years, many HILIC phases utilise the polar silanols available on the surface of unmodified bare silica. A number of manufacturers have launched bare silica as a HILIC phase, Waters BEH and XBridge HILIC phases[109-111], Phenomenex Luna silica and even fused core HILIC phases such as Halo and Kinetex (the types of silica and the respective pros and cons will be discussed in more detail in Chapter 1.5). As the silanols are relatively small the aqueous-rich layer formed around the surface is less dense. This leads to a smaller contribution from HILIC partioning and adsorption is more likely to control the retention mechanism. Silica gel has several advantages over bonded stationary phases such as a greater stability at intermediate and higher pH; some manufacturers suggest these phases are stable up to pH 9[92]. However at higher pH the surface silanols are fully ionised allowing for cation exchange to affect the retention mechanism which can allow for adsorption of charged bases[115][116]. At higher pH the silica framework of some columns has been seen to erode in aqueous analysis, this is discussed further in Section 1.9.2. Many column manufacturers state that their silica based columns are stable above pH 7 as silica is not as soluble in mobile phases with high acetonitrile content[92].

Cyano phases use the permanent induced dipole between the carbon and the electron rich nitrogen atom for their polar functionality[116][118]. They are one of the few HILIC style columns not to include hydrogen bonding in the retention mechanism. Cyano phases have been on the market for many years however many of these columns still have issues with robustness and stability in both RP-LC and HILIC[118][119] modes due to the pH and ionic strength of the mobile phase used. Often initial injections using these phases in HILIC mode show low retention for polar analytes, however if the analysis is continued the partitioning equilibrium is seen to shift towards the immobile aqueous-rich layer around the stationary phase increasing the columns HILIC capability. It is thought that this effect is due to the long equilibration time required to establish the adsorbed water layer around the polar stationary phase. However another possibility is that the cyano silane is being stripped from the column exposing the more polar silanols.

RP-LC investigations carried out on commercial cyano phases[118][119] have shown that the propyl linker is highly susceptible to cleavage at intermediate pH conditions as the nitrogen can form a covalent bond with the silicon and the resulting stable five-membered ring can be cleaved and washed off the column as shown in Figure 1.4 below.

Figure 1.4 ***Schematic of the possible ligand cleavage mechanism of cyano silane***

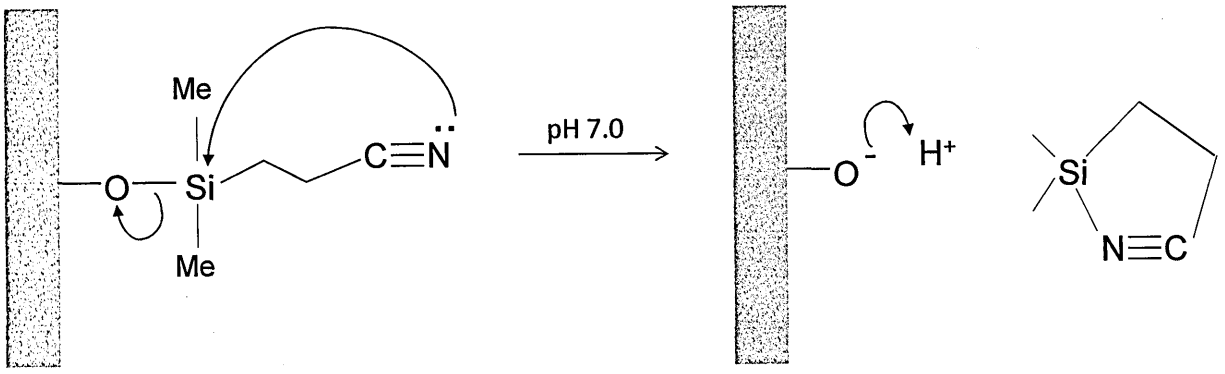

This type of ligand cleavage does not occur in NP-LC as hexane has no dissociated hydrogens and the analysis is usually carried out at low temperature and without any ionic buffers which may catalyse the stripping mechanism. HILIC analysis is often carried out using ammonium acetate buffer that has not been pH adjusted, as these aqueous solutions are approximately pH 7. However as the concentration of acetonitrile is increased so is the pH, in some cases HILIC analysis can be carried out in solution up to pH 9. This may catalyse silane stripping in a similar way. Theoretically by increasing the length of the ligand the likelihood of this cleavage mechanism occurring will be reduced as the spatial distance between the silicon and nitrogen atoms is too great for bond formation to occur[252]. However increasing the length of the linking alkyl chain will also increase the hydrophobicity of the phase, which will shift the partitioning equilibrium away from forming an aqueous-rich layer on the surface of the silica.

Diol phases can also be used in HILIC mode as the polar hydroxyl group of the diol gives rise to partitioning as well as hydrogen bonding, dipole-dipole and even ion exchange interactions when the surface silanols or hydroxyl wings on the silane are ionised[121]. These exhibit the same retention mechanism components as bare silica, however, as the hydroxyl groups are uniformly synthesised and bonded they have reproducible and uniformly distributed, albeit weaker, electrostatic forces[122][123]. As with the cyano phases the diols are bonded to alkyl chains, the length of which can add hydrophobic interactions to the retention mechanism which can overshadow the weaker dipole-dipole forces. Some column manufacturers have capitalised on this complementary separation mechanism. The Acclaim Mixed Mode HILIC column utilises a long alkyl chains to give hydrophobic interactions coupled with terminal diol functionality to give polar characteristics. These types of columns are often marketed as mixed mode phases due to this multi-component retention mechanism.

The polar nature of the Amino phase comes from the permanent dipole of the electron rich nitrogen and its adjacent carbocation. As nitrogen is not as electronegative as oxygen it would be expected that the HILIC character would not be as strong for an amino compared to a bare silica or a diol phase. However, the amino functionality has an approximate pK_a of 7 and will become ionised in the aqueous conditions at pH 3-7 giving these columns the added anion exchange character [124-126].

Amides are neutral phases however they are polar in nature due to the electron rich oxygen and nitrogen atoms bonded to the same carbocation. This results in resonance structures where the double bond can alternate between the more favourable oxygen and the charged nitrogen. Terminal amides are most effective in HILIC and normal phase separations as the polar charged group is available to form the aqueous layer and form electrostatic interactions with polar solutes. Amides are common in RP-LC as polar embedded groups as the bulky solvophobic amide group which reduces the likelihood of phase collapse and gives complementary separations[127-129].

Figure 1.5 Schematic of aqueous layer formed on different silica surfaces in HILIC

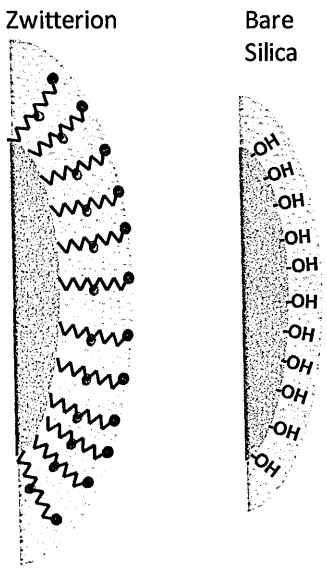

Zwitterionic phases were developed specifically for HILIC as both a charged and neutral stationary phase; they have a permanent formal charge giving an excess of both positive and negative charge across the silane. But overall they have zero charge and the silanes are classed as neutral compounds. The zwitterionic nature gives rise to both anion and cation exchange depending on the pH and the nature of the solute. The fixed charge acts as an internal counter ion to act as both electrostatic ionic interactions and a combined attraction-repulsion mechanism giving orthogonal separation from other charged phases[130][131].

Due to the size and complexity of the silane there is also an alkyl chain backbone which adds hydrophobicity to the retention process. Unlike the cyano and diol phases this hydrophobicity does not over-shadow the other interactions as the zwitterionic charges are spread across the silane. Another benefit of this is that the larger charged surface area produces a denser aqueous-rich layer around the silica surface, Figure 1.5[131][133]. Unlike some mixed-mode type phases where half the bonded ligands are hydrophobic chains which reduce the aqueous layer and half the bonded phase includes the electrostatic interaction functional group. The charged polar function of the zwitterions is embedded into the long chain hydrocarbons which reduces the hydrophobic repulsion of the alkyl groups. The increased partitioning effect coupled with both anionic and cation exchange makes the retention mechanism highly complex; this gives the Zwitterion an orthogonal separation approach[134][135].

Mixed mode columns can be highly diverse depending on the functionality of the silanes used. They usually incorporate a hydrophobic carbon chain with polar functionality to give cation (CX) or anion (AX) exchange interactions, or both such as in the Zwitterion phases. Many cyano, diol and phenyl

phases are mixed mode because of the propyl linker chains that bind the functional group to the silica base, as with the Acclaim HILIC Mixed Mode phase discussed above. However a lot of phases are not marketed as mixed mode because the hydrophobic interactions are secondary and suppressed by the main functionality of the column. Longer linker chains will contribute more to the retention mechanism creating a mixed-mode separation however as seen with the cyano phase this might over-power the desired polar-interactions and suppress a dual retention mechanism leaving a mainly hydrophobic mechanism that is not suitable for HILIC.

Manufacturing a mixed mode phase is complex; it can be achieved either by bonding on two different silanes or by synthesising a multifunctional silane and bonding this directly to the silica base as illustrated in Figure 1.6 below.

Figure 1.6 ***Schematic of possible types of mixed mode stationary phases***

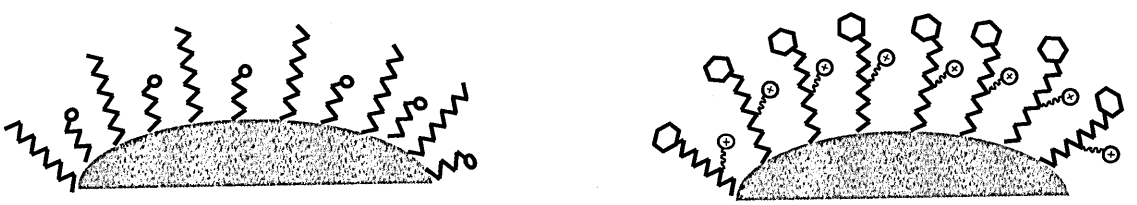

The first option is cheaper because the silanes are available readymade, however the difficulty arises in bonding the silanes in a uniform and reproducible way. One reason for this could be that the size and reactivity of the silanes may dictate the coverage on the silica base. If the long chain alkylsilanes are added first they are likely to bond readily to the surface, especially if a reactive leaving group, such as chloro, is used. Due to the difference in acidity of the surface silanols the silanes may not always bond evenly, however with effective pre-washing and silica preparation this can be overcome, this is covered in more detail in chapter 1.5. However the complex propylaminos, or aromatic silanes would need to be added in a second bonding, these groups are likely to be bulky so steric hindrance may decrease the bonding potential of the ligand. Also as the functional groups involved may be more reactive there is a possibility that a less reactive leaving group will be used to

reduce the possibility of cross linking and dimerising prior to bonding. Leaving groups such as amino or ethoxy have a lower reactivity therefore the second bonding may need to vary the ratios of ligand, solvent and catalyst or the reaction conditions may need to be adjusted to compensate for this. If the acidity of the silica, reactivity of the two different ligands, or impurities present in the ligand vary during these highly complex processes it may result in poor batch to batch reproducibility.

The second manufacturing process would bond all ligands in the same way which would overcome this issue. However, this process has its own drawbacks because the ligands are highly complex and costly to synthesise. The reactivity of the functional groups and leaving groups on the ligand may mean that they are prone to dimerising or crosslinking in solution prior to being bonded. As mentioned above this can be overcome by using a less reactive leaving group however this could reduce the ligand coverage on the silica surface and potentially leave exposed residual silanes or reduce the retention of neutral molecules. Some columns are believed to be produced in this way however because of the complexities they are usually very expensive. As the structure of the ligands used is proprietary information there are concerns over the repeatability and stability of these unknown bonded silanes.

HILIC mode analysis typically gives the reverse of what is expected from RP-LC which gives the chromatographer true orthogonal separations which is beneficial for method development. However the drawback to this is that HILIC does not readily retain highly hydrophobic solutes in the same way that RP-LC does not retain highly hydrophilic analytes. For solutions containing both hydrophobic and hydrophilic analytes a new technique would be required to separate these solutes in one analysis.

1.4 Aqueous Normal Phase Chromatography

In some of the literature Aqueous Normal Phase (ANP) and HILIC are used as analogous terms[136][137]. However there are some distinct physiochemical differences between the two modes[138][139]. As discussed in Section 1.3 the HILIC retention mechanism relies on partitioning between the aqueous layer around the silica base and the solvent rich bulk of the mobile phase. However, this is not effective for separating hydrophilic and hydrophobic molecules as the latter have a greater affinity with the mobile phase and is not well retained on the polar column. The term Aqueous Normal Phase (ANP) was coined in 2009 to describe the dual retention mechanism observed when separating a mixture of hydrophilic and hydrophobic solutes on a silica hydride stationary phase[140][141]. The reduction of the polar silanols and the addition of hydrophobic hydrocarbons disrupts the formation of the aqueous solvated layer on the surface of the column. Therefore the retention mechanism is likely to be governed through adsorption; however this is still not fully understood. Silica hydride is a fairly new and unique type of stationary phase (and will be investigated in further detail in chapter 1.7).

As the name suggests ANP is a mixture of the reversed phase retention mechanism expected for a predominately aqueous mobile phase coupled with the normal phase retention mechanism observed as the polarity of the mobile phase decreases with respect to the stationary phase. The types of HILIC mode columns discussed in chapter 1.3.3 would be unable to provide the former retention mechanism as addition of hydrocarbon chains to the surface of the stationary phase would disturb the equilibrium co-efficient of the water layer around the surface. Therefore other stationary phases must be investigated that contain polar functionality, for retention of hydrophilic compounds by electrostatic interaction in a solvent rich mobile phase, and long chain hydrocarbons for hydrophobic interaction in an aqueous rich mobile phase for non-polar species.

Some solute mixtures may be separated by isocratic analysis in ANP, by comparing the retention map of each solute it may be possible to find an ideal mobile phase composition to satisfactorily retain all analytes. However gradient analysis generally gives improved peak efficiencies and the gradient can be altered to reduce retention times and provide a more efficient analysis times. ANP is unique in being able to apply both standard and inverse solvent gradient; standard being from low to high organic solvent concentration and inverse being low to high water concentration gradient. This type of analysis has been shown to be highly beneficial for separating large complex molecules, such as proteins and peptides, which have multiple polar functionalities and a substantial hydrophobic backbone. This would have a number of applications within the fast-growing bio-pharmaceuticals industry in order to separate the active pharmaceutical ingredient from the smaller metabolites and impurities.

This type of analysis is not new in fact high organic-low aqueous based separations have been in use for as long as chromatographic instruments have existed[142]. It is only in the last 20 years that the distinction between HILIC and ANP retention mechanisms has been understood and there is still some debate as to how the analytes are retained and separated. The timeline in Figure 1.7 below shows some of the important points in history of the evolution of high organic chromatography.

Figure 1.7 Timeline of the evolution of HILIC and ANP mode chromatography

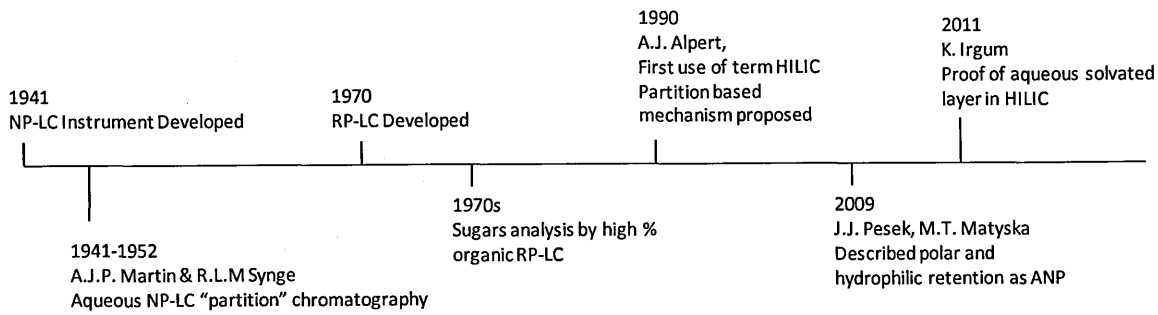

Advances in gradient HILIC and the development of specific HILIC mode columns would appear to have overshadowed ANP as the technique of choice for polar analytes. However, both of these techniques can contribute towards the understanding polar retention mechanisms. HPLC is a well established technique and in the current economic climate companies are unlikely to want to invest in new SFC and CE equipment for analysis of polar compounds. Therefore characterisation of polar interactions by HILIC and ANP as complementary techniques to RP-LC would be of benefit to the chromatographic community.

The research into different types of HPLC columns for RP-LC, NP-LC, and HILIC systems has brought to light the enormous variety of ligands and bonding techniques available. These different types of stationary phase allow for complementary and orthogonal separations of the same solution of analytes which is essential for method development. Although these different phases may utilise a number of functional groups for the ligands the vast majority of these columns use a modified silica particle base. Silica has many benefits for use as HPLC columns; however it was shown in Table 1.1 and Table 1.2 that the silica itself can give rise to electrostatic interactions that will retain polar and basic molecules on the surface of that stationary phase. In order to evaluate the chromatographic characteristics of an HPLC column firstly the type of silica must be investigated.

1.5 Silica Based Stationary Phases

As a result of its good mechanical properties and versatility, silica is the most commonly used support material for HPLC stationary phases[143][144]. Although alumina[145-147], titania[148][149] and zirconia[150] have also been used. The recent shift towards <2μm particle sizes for use in ultra high performance liquid chromatography (UHPLC) has capitalised on the ability to formulate a variety of particle sizes and porosities using silica. Another advantage of this material is the ease in which the surface can be modified and a variety of ligands can be chemically bonded to the silica base to produce HPLC columns with a range of interaction mechanisms[151][152]. Although considerable improvements have been made in the commercial processes for cleaning and bonding base silica over the last 40 years a lot of the research carried out is proprietary information and are not published in academic journals. The majority of commercial phases are chemically bonded using nucleophilic attack by one of the processes outlined in Figure 1.8 below.

Figure 1.8 ***Synthetic Route for Bonding Polymeric and Monomeric Ligands***

(i) Polymeric trifunctional bonding

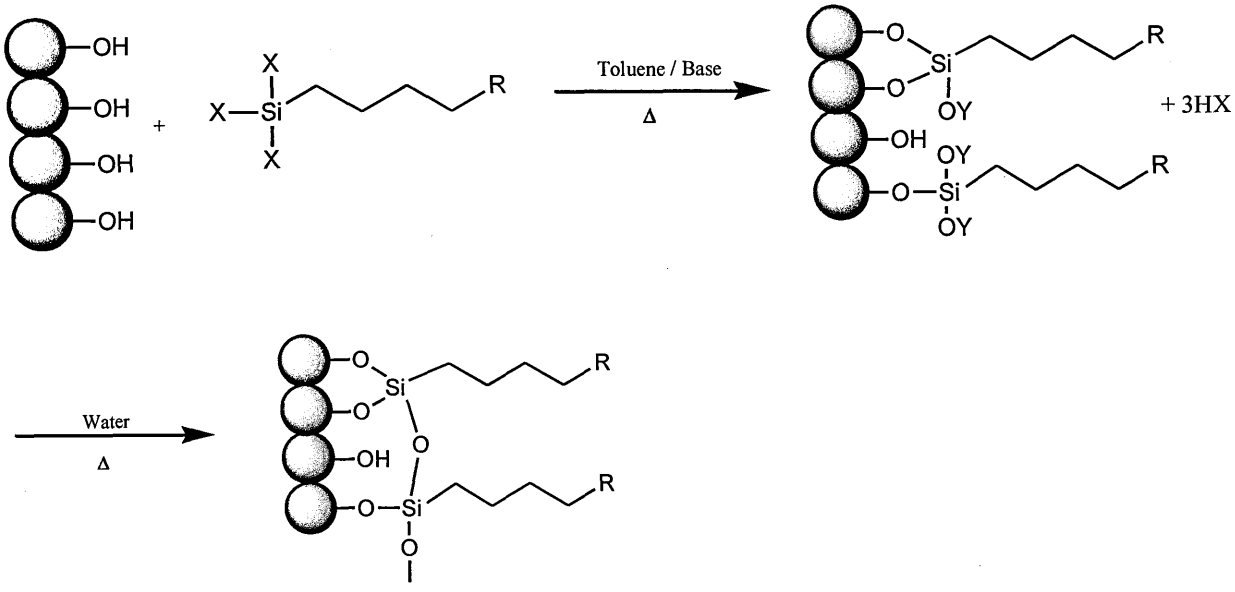

(ii) Monofunctional bonding

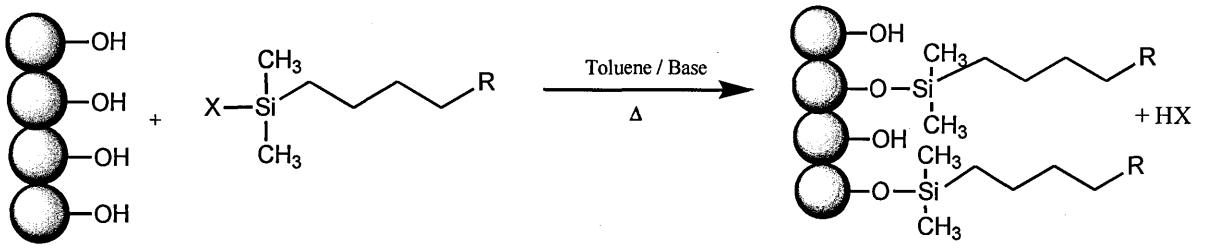

Where X can be Cl, EtO, NH_3

The first process is referred to as a polymeric stationary phase where the trifunctional organosilane is bonded to the surface silanols on the bare silica and then a controlled addition of water causes the silanes to crosslink forming a horizontal or vertical polymeric monolayer on the surface[154]. Historically this process is difficult to control due to the anhydrous conditions required resulting in low batch to batch repeatability as the density of the polymeric network can vary. Theoretically two types of crosslinking can occur during this reaction; the formation of a self assembly monolayer requires a highly controlled atmosphere using a humidifier to activate the base silica with a monolayer of moisture on the surface prior to bonding the organosilane[155] Vertical oligomeric linking (often termed laddering) occurs as the organosilanes add on top of each other forming strands of hydrocarbon chain that emanate out from the base silica[156]. In practice a combination of these two reactions are likely to occur which accounts for the lack of repeatability in these processes.

The latter bonding process is more commercially favourable as it involves a more straight forward single point bonding of a monofunctional organosilane onto the bare silica surface silanols. This is a considerably more reproducible process and can yield high surface coverage depending on the reactivity of the leaving group on the silane. For monofunctional bonding the two positions on the silane silica are commonly substituted with methyl groups as these are widely available, however research has shown that the substitution of bulky groups in this position can increase the stability of the stationary phases and reduces polar interactions with any residual silanol groups on the surface

of the silica. The Agilent Zorbax Stable Bond range utilise this technology and have developed a range of sterically protected ligands to increase stability of the phases and reduce secondary interactions with the base silica.

Secondary interactions with residual polar silanols have often caused issues for chromatographers, especially when separating mixtures containing basic compounds[157-160]. At low pH the active silanol groups are fully protonated but as the pH increases these groups lose a proton to become ionised, this can add a complex ionic exchange mechanism to the separation. Ionic binding is a strong retentive force for charged analytes and will cause basic analytes to have multiple retention points on the surface silica; this can result in poor mass transfer between the liquid and stationary phases and can cause band broadening of the solute on the column. In most cases this can be characterised by a non-Gaussian peak commonly termed peak tailing[160-162]. This can be an issue as integration is more subjective and quantification of the peak gives rise to greater error. In the worse cases multiply charged basic analytes can be irreversibly retained on the column. There are a variety of silanol types, as shown in Figure 1.9, which can be found on the surface of bare silica however these are not equivalent in behaviour, adsorption or chemical reactivity.

Figure 1.9 ***Types and Acidity of Residual Silanol Groups***

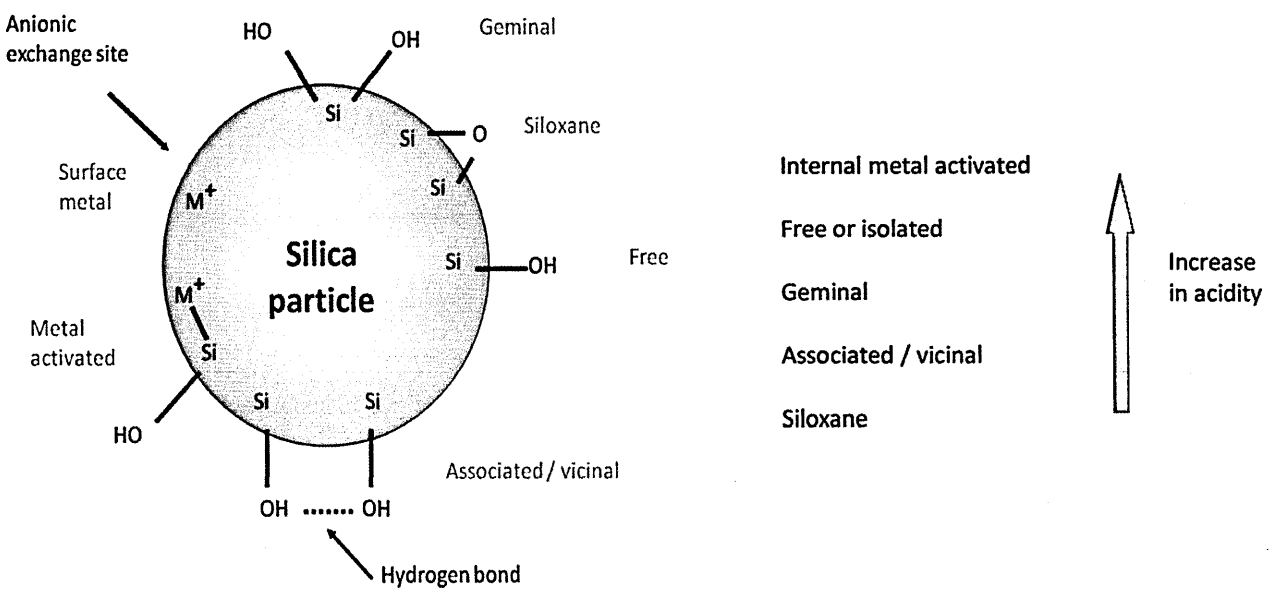

The early HPLC columns were prepared using silica precipitated from the solutions of silicates, due to this uncontrolled process the resulting silica contained a population of all the silanol types, this is often termed TYPE-A silica. This lead to a number of issues as the silica base was not homogeneous and metal active silanols were found to behave as more reactive sites when bonding the organosilane, resulting in variable coverage depending on the type of metal present. In addition to this the acidic nature of the metal activated silanols could cause basic moieties to be retained permanently on the column which could change the nature of the separation mechanism of the stationary phase causing issues for the chromatographer and give false results.

Therefore a cleaner type of silica was formed through aggregation of organo silica sols in air and pre-treatment was required to produce a homogeneous silica substrate with reduced metal content and activate the surface silanols prior to modification with an organosilane to give optimal coverage. This is commonly done in a two-step dehydroxylation and rehydroxylation process[163] where the silica is heated to a high temperature in an inert atmosphere, refluxed in aqueous hydrofluoric acid before being washed and dried. It is believed that another benefit of this process is to open the pores in the silica surface allowing more active sites to be available for bonding the organosilane[164].

In order to differentiate chromatography columns produced using pre-treated silica from those packed with the old-style 'dirty' silica this new generation of columns were referred to as TYPE-B phases. Although the TYPE-B silica overcame a number of the drawbacks of the previous (TYPE-A silica) commercial pre-treated silica has approximately 6-8 $\mu mol/m^2$ coverage of silanol groups, even after bonding with long chain hydrocarbons this figure is only reduced to 4-5 $\mu mol/m^2$ so that residual polar silanols can still be active on the surface of the silica.

Figure 1.10 Schematic of Endcapped C_{18} Bonded Silica

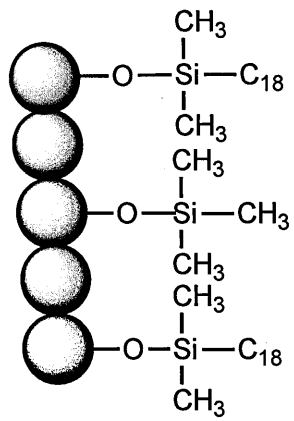

The most common method used by column manufacturers to reduce secondary interactions from residual silanol groups is known as Endcapping[165], Figure 1.10.

Here a second monofunctional silyl bonding is typically performed using a small hydrocarbon, most commonly trimethylsilane derivatives[166][167]. The smaller size and high reactivity of the endcap allow it to bond with the available unreacted silanols on the surface of the bonded silica. Although this is a proven and highly efficient technique it does not account for all residual silanol groups[168] in fact TMS endcapping has been shown to reduce residual silanols to 3-4 $\mu mol/m^2$.

As a chromatographer there are various methods to reduce unwanted secondary interactions from these residual polar silanols such as adding an amine modifier such as triethylamine (TEA), n-hexylamine and triethanolamine to the mobile phase such that at low pH the smaller charged ion will preferentially interact with the active silanol sites[169]. However, this can cause issues with coupling to mass-spec. This overview indicates how important it is for the chromatographer to be aware of residual silanols on the surface of the column. Silanols are highly active on bases that have multiply charges, i.e. nicotine, and some solutes may be irreversibly retained on the phase which could lead to those analytes not being detected.

1.6 Extended Polar Selectivity Columns

Silanol interactions can be advantageous to a chromatographer, they are often utilised for complex separations of steroid mixtures[170] and metabolites[171-173]. The Extended Polar Selectivity (EPS) range of stationary phases utilises these secondary interactions. These columns capitalise on the mixed hydrophobic and silanophilic retention to give complementary separations to a typical C18[174]. These range of columns combines the long alkyl chain with some form of hydroxyl group, either from the silica surface itself or manufactured in with the ligand. There are a number of ways which this could possibly be achieved, a few of these are shown in the section.

(i) Lightly bonded C18

As the name suggests this follows the same bonding principles as monofunctional bonding seen in the previous chapter using only a fraction of the organosilane commonly yielding <1 μmol/m^2 surface coverage of long chain hydrocarbons leaving a vast excess of accessible residual silanols, Figure 1.11.

Figure 1.11 Schematic of lightly bonded C_{18}

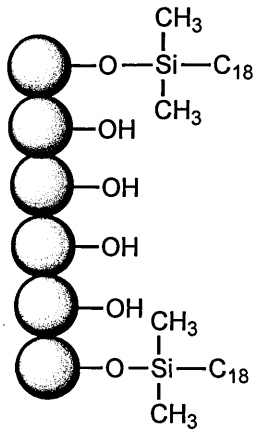

Although the process is relatively simple there are still issues with reproducibility to be overcome as it is important to ensure there is an even distribution ratio of hydrocarbons and silanols per μmol/m^2 surface area. This can be ensured by accurate weighing of the reagents and efficient and constant agitation during the bonding process. As the surface silanols are being incorporated into the retention mechanism it is also imperative that all the silanols have comparable acidity, it has already been seen that more acidic silanols on the silica surface can be deactivated through a two-step temperature and acid wash pre-treatment process.

(ii) Hydroxyl substituted silanes

These types of column can be thought of as "polar endcapped" as the hydroxyl substituted group both masks the residual silanols on the surface of the silica and gives the electrostatic interactions required for an EPS phase. However in this case the hydroxyl groups are incorporated into the ligand itself, rather than being added to the silica surface as a secondary bonding as in traditional endcapping, Figure 1.12.

Figure 1.12 Schematic of a hydroxyl substituted silanes

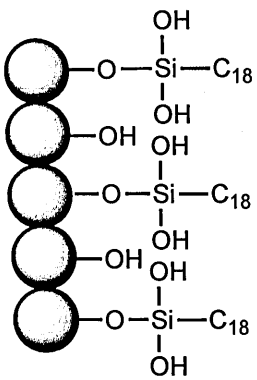

There are several advantages for the chromatographer of this type of stationary phase, first the carbon loading of the phase is more akin to that of a typical C18, and therefore the hydrophobic nature would be comparable giving longer retention for acidic, neutral and phenolic analytes than the lightly bonded phases when run in the ion suppressed mode. Secondly as the secondary interactions come from relatively less acidic silanols the reproducibility of these phases should be higher and tailing of basic moieties may be reduced. The disadvantages are that there is a lower distribution of silanols and the hydrogen bonding and ion exchange interactions may be masked by the hydrophobic interactions which would reduce the complementary separations.

(i) Polar endcapping

Unlike the hydroxyl substituted silanes shown above these types of phases are believed to undergo the traditional second bonding endcapping process using small polar organosilanes, for example where R is a cyano, diol or amino groups. The advantage is that the acidity of the polar interactions is controlled increasing batch to batch reproducibility. However a big disadvantage to this process is

that column manufacturers class their endcapping process as proprietary information and often the type or polarity of the endcap is not known. This can result in some solutes being irreversibly retained on the phase, Figure 1.13[223].

Figure 1.13 Schematic of a Polar Encapped Phase

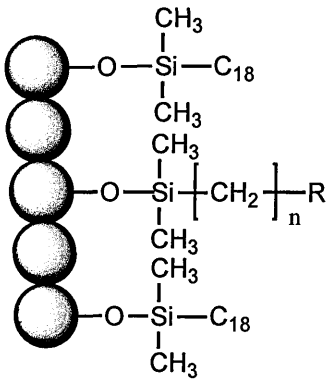

These types of phases are not that common, possibly due to the added complexity of the two step bonding processes and the stability of the polar endcaps is questionable as short chain silanes are highly susceptible to ligand cleavage at the base silica either through temperature or acid catalysed decomposition.

(ii) Terminal diols

The previous examples have shown stationary phases where the polar interactions occur at the silica surface; this can be a disadvantage for large bulky analytes due to steric hindrance of the long chain hydrocarbons, Figure 1.14.

Figure 1.14 Schematic of a Terminal Diol Phase

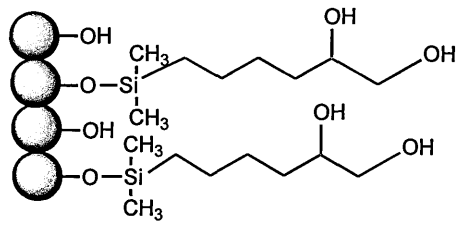

These columns have the advantage of having highly accessible polar groups of controlled acidity. However due to the reactivity of the diol functionality these phases cannot be endcapped in the traditional way without the endcapping reagent reacting with the terminal diols as well. Therefore it is likely there will still be some residual uncontrolled silanols on the surface of the silica which may cause unwanted tailing for small multiply charged bases.

The majority of these EPS phases have a USP classification of L1 as they contain octadecyl silanes, however the retention mechanisms, and hence chromatography selectivity, are wildly different to that of a typical endcapped C18 phase and to each other. There are a number of ways to characterise different types of columns[162-167], these will be discussed in more detail in Section 1.8. New phases should be independently subjected to these types of tests as column manufacturers will want to show their column in the best light and are likely to show only selected limited information in their marketing material literature.

The polar nature of these columns would make them a good starting point for characterisation of polar interactions. As these columns are commonly used in RP-LC this would be a good starting point for characterisation and evaluation of these types of phases. The types of ligand used for these columns are often proprietary information, therefore it may be useful to attempt to structurally evaluate these phases in order to categorise the type of polar interaction observed using chromatographic methods.

The electrostatic interactions described here are suitable for retaining polar solutes however they can also cause unwanted interactions and tailing on basic and polar analytes. Many chromatographers wish to suppress these secondary interactions; endcapping has been shown as one way of doing this. Another approach is by modifying the base silica itself to remove these residual silanols before the ligand is attached. Silica hydride phases have already been touched upon, these seem to be particularly interesting phases for this research as the literature seems to suggest that the residual silanols have been significantly reduced or even removed. Other types of modified silica such as SiON[181] have been produced, however, the silica hydride is favoured as it is now a more established technique and columns are commercially available for the evaluation process.

1.7 TYPE-C™ Silica

The previous sections have discussed bonding approaches for a fully hydroxylated silica base however in the last 20 years a new approach to the pre-treatment of silica particles has been explored in order to form a silica hydride surface[182-192] thereby theoretically eradicating any secondary interactions from residual silanols without the need of endcapping. The advantages of abolishing secondary H-bonding and ion exchange interactions with acidic silanols is clear, however a second advantage of this process is the direct formation of silica-carbon bonds on the particle surface rather than through a silicon-oxygen-silica linker. Silicon-carbon bonds are more covalent in nature and therefore much shorter and stronger[193] than the silicon-oxygen equivalent, this may give rise to greater stability of silica hydride based columns.

The increased polarity of the silicon-oxygen bond is due to the ability of (p-d)π back-bonding between the two atoms, this increases reactivity especially in the presence of halogenated compounds. Experimentally this is observed in the decreased Si-O bond length and an increase in the Si-O-Si bond angle[194]. Theoretically this can be explained by the silicon's unoccupied 3d orbitals acting as an acceptor for the oxygen lone pairs in the 2p orbitals. This donor-acceptor (p-d)π bond or π back donation is likely to be responsible for the stability of the Si-O-Si framework used in many HPLC columns[195]. This is illustrated in Figure 1.15 overleaf.

The shorter covalent bond energies in the Si-C can lead to a reduced activity but may still be liable to attack at neutral and high pH with some buffer ions (this will be covered in more details in Section 1.9). In theory a silica hydride modified silica base particle would yield a more stable stationary phase that was less susceptible to ligand cleavage at high temperatures and across a range of pH.

Figure 1.15 ***Molecular orbitals in (p-d)π back-donation for the Si-O bond***

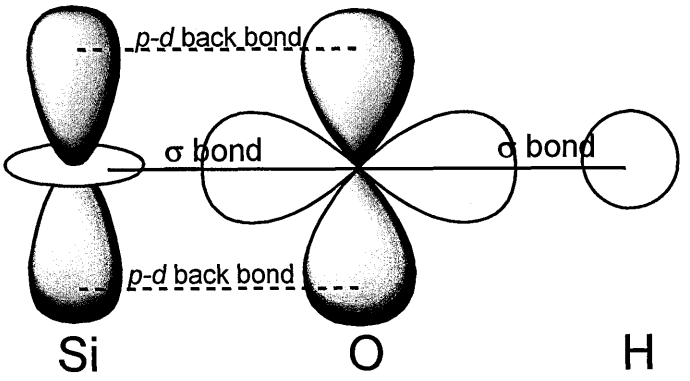

Initial investigations[182][183] into chemical derivatisation of an unmodified silica gel to form a silica hydride particle considered a two-step process of chlorination and reduction. The latter step can be carried out through a Grignard[192] reaction however this is less favoured due to the side reaction with the residual silanols, a more common reducing reagent would be lithium aluminium hydride[196] as shown in Figure 1.16 below.

Figure 1.16 ***Synthetic route for reduction of silica to silica hydride***

(I) $|\text{-O}\equiv\text{Si-OH} + SOCl_2 \xrightarrow[\text{reflux}]{\text{Toluene}} |\text{-O}\equiv\text{Si-Cl} + SO_2 + HCl$

(II) $|\text{-O}\equiv\text{Si-Cl} + LiAlH_4 \xrightarrow{\text{Ether}} |\text{-O}\equiv\text{Si-H} + LiCl + AlH_3$

The increased polarity of the Si-O bond may be an advantage in the bonding of chloro-silanes however it can be a disadvantage in these Grignard type reactions which need to be highly controlled. The intermediate Si-Cl species is extremely moisture sensitive and will rapidly hydrolyse back to the silanol, this could be a serious limitation for commercial manufacture as scaling up any anhydrous conditions could be highly labour intensive. The reduction step is also time consuming and requires constant monitoring due to the formation of extremely volatile by-products.

It has been shown that metal ions on the surface of the silica can have a drastic effect on the acidity and charge of the silica surface. Even though this technique should eliminate any metal activated silanols the addition of free Al^{3+} ions would leave a residual surface charge and facilitate unwanted secondary interactions. It is possible to carry out reductions through chemisorption of hydrogen from a pyrolytically activated support[198][199]. However this requires extremely high vacuum and pyrolysis temperatures (above 800°C) and would not be a simple reaction to scale up for manufacture.

Infra-red analysis carried out using this method has suggested a significant amount of residual silanols on the phase which may be due to the chloro-silane being converted back to a silanol due to high temperatures in the presence of water[183]. Research found that washing with excess hydrochloric acid following the reduction of the silica hydride particles should remove any residual aluminium hydride to <10ppm. However no analytical data is supplied to support these claims.

Derivatization of the hydride modified silica can then carried out using functionalised olefin species. Again the silica particles are being exposed to metals ions which may lead to unwanted positive charge on the silica surface; it is not clear whether a second hydrochloric acid wash is performed at this time to remove residual catalyst. Using the catalytic addition technique of hydrosilylation it is theoretically possible to bond any number of olefin species to the modified silica hydride resulting in a wide range of modified silica gels that do not require endcapping to mask secondary interactions from residual silanols. This leads to the production of a new class of HPLC stationary phase known as TYPE-C™[200]. The synthetic route is shown in Figure 1.17 below.

Figure 1.17 Synthetic route for ligand addition to the modified silica hydride

(III) $|\text{-O}\equiv\text{Si-H} + H_2C{=}CHR \xrightarrow{\text{Pt cat.}} |\text{-O}\equiv\text{Si-}CH_2CH_2R + \tfrac{1}{2}H_2$

Some of the disadvantages of this process have already been touched on, the time consuming and labour intensive three step manufacture appears to show little commercial benefit over the well established chlorosilane bonding and endcapping processes of full hydroxylated silica discussed in the introduction. However a much larger drawback to this methodology is that full conversion of silanol to silica hydride species is not observed. Spectroscopic techniques were utilised to determine the presence of Si-H bonds[201], in carrying out this analysis the presence of Si-OH was also observed on the surface of the silica. This was confirmed by solid state NMR when a comparison of the native and reduced silica particles were both found to contain both single (Q_3, $HOSi^*[OSi\equiv]_3$) and geminal silanols (Q_2, $(HO)_2Si^*[OSi\equiv]_2$) on the surface. GC analysis was used to quantify the surface coverage of Si-H from the generation of hydrogen gas in the presence of a strong base[202][203], as shown in Figure 1.18.

Figure 1.18 ***Oxidation of silica hydride***

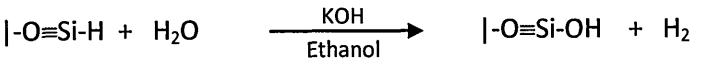

The process was found to be between 5-30% efficient depending on the type of native silica and pore size used; unsurprisingly it was found that the larger the pore size the more readily the silanols are converted to silica hydride, most likely due to the accessibility of the silanols during the chlorination step. As the platinum catalysed olefin addition will only bind to the silica hydride present the carbon load of any stationary phase produced in this will be low and may have a high ratio of residual silanols to hydrophobic silanes. This cannot be considered very efficient as it has already been seen that traditional bonding and endcapping approach will cover between 40-65% of the available silanols.

To overcome this disadvantage a second process was developed incorporating the benefits of a polymeric shell described earlier in this chapter, here triethoxysilane (TES) is used to form a monolayer of silica hydride[191][192] around a native silica particle. This is outlined in Figure 1.19 below.

Figure 1.19 Schematic for the formation of a TES monolayer

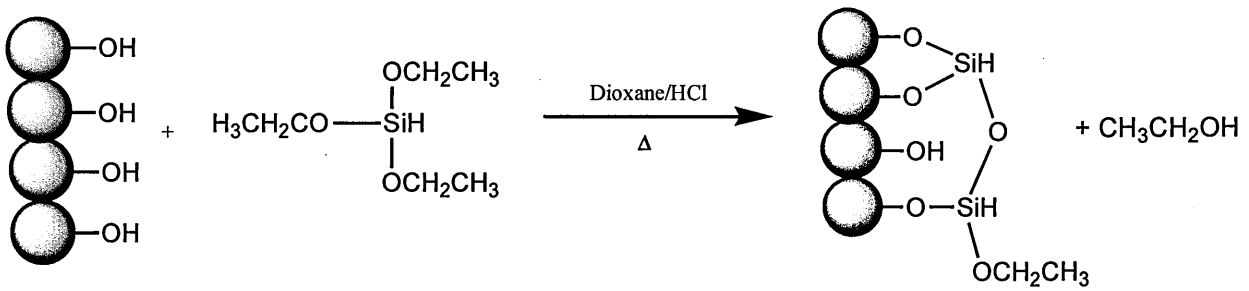

The use of the smaller TES monomer is favoured over an alkyl substituted monomer as this process should give a much higher surface coverage and a higher number of siloxane linkages than a traditional polymer phase. TES is highly reactive in the presence of water; as with the polymeric bonding described earlier this procedure should be carried out in the presence of argon using anhydrous dioxane to fully control the density of the monolayer on the surface of the silica. However research shows that aqueous hydrochloric acid is used which would result in an excess of water being present[185]. Although this would facilitate crosslinking of the TES polymer it would be uncontrolled and would most likely result in dense vertical oligomeric bonding which has been shown to have reproducibility issues for commercial phases. The main drawback of laddering for TES monomers is that any terminal ethoxy substituents would readily hydrolyse to silanols, which although less acidic than surface silanols would still facilitate ionic exchange and hydrogen bonding interactions. This was confirmed by solid state ^{29}Si CP-MAS NMR; although a significant increase of silica hydride coverage is shown on the TES polymer surface over the previous chlorination/reduction product, the presence of Q_2 and Q_3 silanols is still observed[185].

Optimisation of the TES concentration was carried out to reduce the unreacted silanol coverage on the silica surface, initial solid state ^{29}Si CP-MAS NMR data appears to indicate that increasing the molarity of TES decreases the peaks due to Q_2 and Q_3 silanols suggesting a greater surface coverage of the TES[203]. However in addition to reducing the Q_2 and Q_3 peaks the Q_4 siloxane ($Si^*[OSi\equiv]_4$) peaks were also eliminated. As the chemisorptions of TES would be unlikely to affect the nature of the silica surface these results would suggest a dense multilayered polymer is being formed. As TES is so reactive in the presence of water this is not surprising, it is also likely that the formation of an amorphous polyhydrosiloxane (PHS) will occur in solution without binding to the silica surface. Further analysis of a PHS product by DRIFT, DSC and TGA was shown to be indistinguishable from a TES monolayer bonded to a silica surface[185].

There are several benefits to forming a polymeric monolayer aside from masking the residual silanols on the particle surface[204]. It is possible that the formation of the monolayer provides a larger surface area for modification with functionalised olefins and could yield a higher carbon load. The commercial TYPE-C™ Bidentate C_{18} phase manufactured by Cogent is quoted as having a carbon load of 16% which is similar to traditionally monomeric bonded phases. Unlike the TYPE-C™ Bidentate C_{18} the majority of monomeric C18 columns will also be endcapped which has been shown to marginally increase carbon load. The hydrocarbon chains of the bidentate phase may be less densely packed than a traditionally bonded phase this could give rise to reduced shape selectivity. Another advantage of this type of polymeric coverage may be that the silica surface is protected from degradation at higher pH levels[205] which makes these phases considerably more versatile. The Commercial TYPE-C™ Bidentate C_{18} phase has a stated pH range of 2.0-9.2 and a maximum temperature of 80°C[273].

As with the previous silica hydride modified species these phases can be functionalised by platinum catalysed olefin, through addition reaction with the double or triple bond, as shown in Figure 1.20.

Figure 1.20 ***Schematic for possible modification of the silica hydride monolayer***

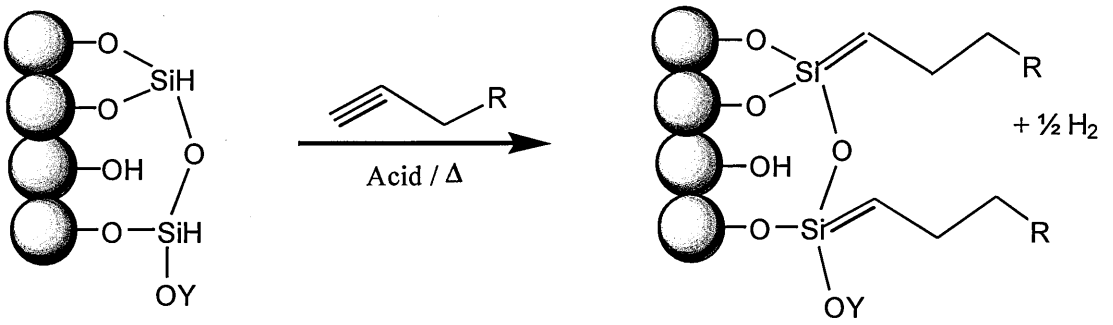

A large number of phases have successfully been synthesised using these reaction pathways and have been evaluated extensively by spectroscopic techniques with respect to silica hydride and silanol distribution[206-208]. Assessing the extent of the multilayered polymer formed during this process is spectroscopically challenging due to the broad peaks observed in DRIFT, solid state NMR and TGA/DSC and it has already been seen it is difficult to distinguish between the bonded TES monolayer and an unbound PHS species[185]. Theoretically silica hydride coverage can been determined by GC as shown previously with the chlorinated/reduced silica product. In some cases 100% coverage was obtained however the procedure was shown to have a ±20% error and these results depend on the initial surface coverage of silanols which is not easy to determine[183].

Due to the uncontrolled nature of this reaction complete horizontal coverage of a fully crosslinked TES monolayer bound to the surface of the silica is unlikely, therefore some residual silanols may be expected. It is unclear whether these can be readily identified by spectroscopic methods as current techniques seem to be unable to distinguish whether the silanols detected are on the surface of the silica or as terminal silanols on the polymeric shell. However the main question for a chromatographer is whether these silanols are accessible to polar, basic, and charged analytes and possess the potential to give rise to secondary interactions. The porous nature of the silica surface often means that silanols are often "buried" inside narrow pore channels[209] and therefore do not play a part in the retention mechanism. This can only be effectively assessed through

chromatographic characterisation using specific analytes to probe the different types of retention mechanism that is taking place on the column.

Commercial TYPE-C™ phases include a number of Bidentate phases[273]. As these columns are marketed as a polymeric monolayer they are highly likely to be produced by a similar route to the TES silanization discussed above. This would make it an excellent starting point to assess the presence of residual silanols on the surface of the phase and compare TYPE-C™ silica to the traditional bonded and endcapped TYPE-B phases. Due to the highly complex nature of the retention mechanisms of some phases it would be sensible to start with a simple C18 hydrocarbon chain. In theory this should rule out any π-π interactions that may contribute to the separation mechanism.

1.8 Characterisation of HPLC Columns

Given the vast range of stationary phases available on the market it can be difficult to find ways of chromatographically identifying similar or dissimilar columns. This task is made all the more complex due to restrictions imposed by column manufacturers, i.e. using phrases such as "typically", "classed as" and "proprietary information". Marketing and commercial information may be misleading or in some cases conflicting. HPLC columns are governed by a voluntary USP classification; however these generally only cover the primary separation mechanism and do not give the whole picture for the phase. For example, the majority of polar embedded group phases (PEG) as classed by the manufacturers as L1 denoting an Octadecyl silane functionality[210][211]. However in addition to the long chain hydrocarbon which gives the phase this classification the retention mechanism is also affected by the polar group, often an amide, carbamate, or sulphonamide functionality which gives significantly different retention for polar solutes[212][213]. Simply using this classification or the marketing information provided by the manufacture may lead to the wrong choice of column for the desired application. Consequently there has been increasing research into developing robust and transferable methodology to characterise and categorise stationary phase materials in an unbiased way[210-219].

1.8.1 Tanaka Methodology

The name Tanaka has been synonymous with column characterisation since 1989 due to the development of a robust and reproducible universal column characterisation method which can distinguish and numerically evaluate each of the chromatographic interactions for all types of stationary phase[220 - 223]. The method compares the relative retention times of a number of known analytes, shown in Figure 1.21, to characterise the selectivity and efficiency of HPLC columns. Following the original research the methodology has been extended to include additional probes to and amended to accommodate columns designed for UHPLC analysis[225].

Figure 1.21 Compounds used for Tanaka characterisation method

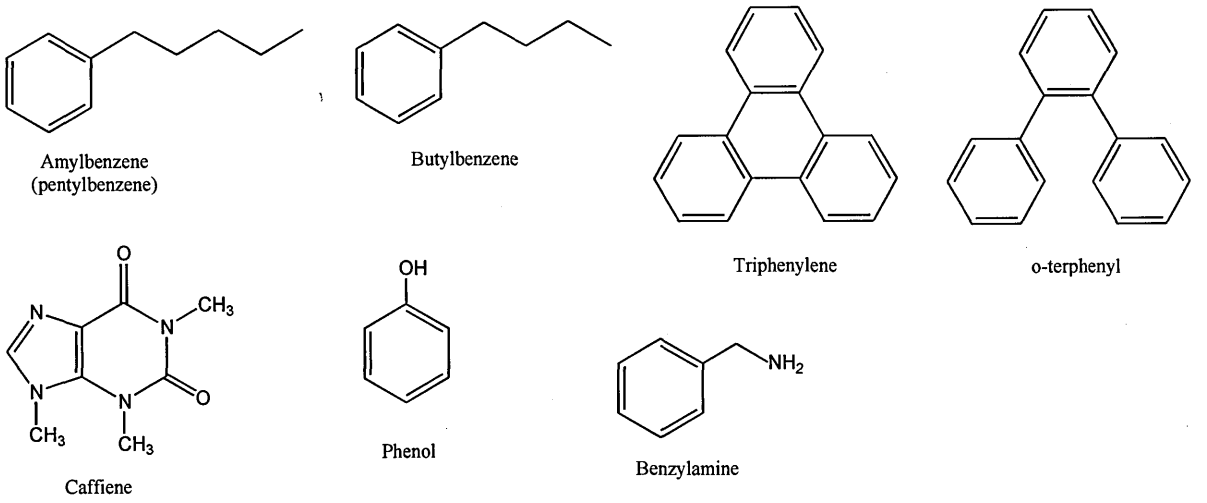

The ligand density or surface coverage can be evaluated by comparing the retention factor for amylbenzene (k_{AM}) across the different stationary phases. As amylbenzene has both hydrophobic and aromatic character it is the ideal solute to determine the surface coverage of ligands bonded to the stationary phase. The greater the coverage of hydrophobic ligands on the phase the more the long carbon chain of the amylbenzene interacts with these ligands and the solute has a higher retention time. The analysis is carried out using a mobile phase composition of 20:80 v/v water:methanol at 40°C. As no buffer or pH modifiers are used for this analysis and amylbenzene is a neutral analyte, the only interactions will be from the hydrophobic interactions.

The rest of the Tanaka values are calculated from the ratio of retention factors (k) of two different molecules analysed using the same mobile phase and temperature conditions. Hydrophobicity characteristics of the phase (α_{CH2}) can be evaluated by calculating the ratio of the relative retention times of amylbenzene and butylbenzene. As these two alkylbenzenes only differ by one methyl group the only difference in their interaction mechanism will be through hydrophobic retention, this is an excellent measure of surface coverage of alkyl ligands on the phase. The alkylbenzenes are injected as a low concentration homogenous mixture into a mobile phase composition of 20:80 v/v water:methanol at 40°C, to reduce any effects of band broadened or overloading. The molecules

and stationary phase will not be ionised ruling out any secondary electrostatic interactions. The greater the hydrophobic character of the bonded ligand the longer the amylbenzene will be retained with respect to the butylbenzene; the penta-carbon chain has more chances to interact and will therefore have a greater affinity to the stationary phase. The separation factor is calculated as the ratio of these two values, therefore the longer the amylbenzene is retained the higher the separation factor will be.

Shape selectivity can be determined by the separation factor for triphenylene and o-terphenyl ($\alpha_{T/O}$) this is usually the measure of the spacing or density of bonded ligands. This can also determine the steric nature of the ligands themselves, for example inclusion of bulky aromatic groups or branched chain functionalities. As triphenylene is a planar solute it is more likely to penetrate densely packed ligands and frequency of interaction with the silanes is increased which results in a longer retention time. O-terphenyl is a bulky solute due to the free rotation of the aromatic groups, therefore it is less likely to access a tightly packed stationary phase and the opportunities for interaction are reduced. Stationary phases that exhibit higher steric selectivity will retain the triphenylene longer than those that do not as the special arrangement of the bonded silanes allow the flatter analyte to interact with the base silica and the silanes. Phases that exhibit lower steric selectivity will not retain the o-terphenyl as long, therefore the alpha value between these two analytes gives an indication of the level of steric hindrance. As triphenylene is a more aromatic molecule this extra retention can also be attributed to π-π interactions therefore this test is not fully discriminatory and will depend on the type of ligand bonded. Theoretically the longer the triphenylene is retained the higher the separation factor, however steric selectivity cannot be measured numerically in the way that hydrophobicity can be, so that these values should be used to show the differences in stationary phases rather than saying a phase has high or low shape selectivity.

The hydrogen bonding capacity of a stationary phase is determined by the separation factor of caffeine and phenol ($\alpha_{C/P}$). Caffeine (LogP -0.55[285]) has a number of carbonyl and amine functional

groups which can form hydrogen bonding interactions whereas phenol (LogP 1.47[285]) is a neutral molecule with only a single hydroxyl group. In stationary phases with little or no capacity for hydrogen bonding the small polar caffeine molecule will elute early as it has a much greater affinity for the aqueous rich mobile phase. In stationary phases where residual silanols groups are available on the surface the caffeine will interact with these groups and be retained longer, often this peak will show tailing as the acidity of the silanols will vary which means the retention mechanism is not consistent across the column. The phenol retention time acts as a neutral marker and should be reasonably consistent across columns with a similar density of hydrophobic ligands. Therefore the larger the selectivity factor the more silanols are available for hydrogen bonding on the surface of the phase. If the selectivity factor is greater than one, i.e. if the caffeine elutes after the phenol there is a large capacity for hydrogen bonding on the stationary phase. For endcapped phases the selectivity factor can determine the degree of endcapping coverage as this analysis discriminates against residual silanols available for interaction on the silica surface.

Electrostatic interactions are measured at two different pH levels, these are the only characteristics that require mobile phase buffer as it ensures that any available ions on the stationary phase are in a fully ionised or unionised state. Ion exchange of the ligand or silanols activity can be measured by comparing the retention time of the charged analyte benzylamine against the retention of the neutral molecule phenol. At pH 7.6 the total silanol activity of ion exchange mechanism can be determined, whereas at pH 2.7 only the acidic silanols are active. The small benzylamine molecule will exist in the ionised form at low pH and therefore not be retained by residual silanols, only acidic silanols will be active at these conditions. At pH 7.6 the ionised benzylamine molecule will exhibit a charge which will undergo electrostatic interactions with the charged silanols or ions present on the stationary phase, therefore this molecule will be retained by these interactions. By comparing the retention time of benzylamine against the neutral phenol, which will not be affected by the charge, the level of silanol activity and electrostatic interactions can be estimated.

As more complex stationary phases have been developed over the past 20 years the Tanaka characterisation suite has been extended to include measures of aromatic character and dipole-dipole capacity of HPLC columns. This testing suite includes a number of methoxy- and nitro-substituted benzenes which are used to identify small differences in aromatic stationary phases. The selectivity factor of di- and trinitrobenzenes against the neutral toluene marker can determine the extent of π-π interactions on a phase as the retention times can distinguish the density of aromatic character on the phase. By comparing the retention times of the different dinitro solutes used it is possible to determine the level of dipole-dipole interaction capacity of a stationary phase.

1.8.2 PQRI Approach for Selecting Columns of Equivalent Selectivity

An alternative approach to the Tanaka testing is the Product Quality Research Institute (PQRI) approach developed for the United States Pharmacopeia Conversion (USP) to aid companies to find equivalent HPLC columns for analytical testing. The testing and correlating of data for a large amount of available HPLC columns has been in progress since 1998 and to date over 3000 retention time measurements have been performed on columns to determine suitable characterisation compounds to determine the five main column properties; hydrophobicity (H), steric selectivity (S*), hydrogen bonding acidity (A), hydrogen bonding basicity (B), and column cation exchange (C)[225-228].

The approach is similar to that of the Tanaka methodology described above in that characterisation compounds that exhibit specific interactions are selected and the retention factor of these compounds are compared against a neutral marker run under the same conditions. Data for the column comparison database is collated world-wide from a number of laboratories and has been tested for robustness and repeatability.

The database uses a linear regression approach to compare the five properties on the two columns, column 1 and 2, and determine a column comparison function (F_s) using the following equation:

$$F_s = \{[12.5(H_2 - H_1)]^2 + [100(S^*_2 - S^*_1)]^2 + [30(A_2 - A_1)]^2 + [143(B_2 - B_1)]^2 + [83(C_2 - C_1)]^2\}^{1/2} \quad \text{(IV)}$$

1.8.3 S Value Comparison

There are a number of specific column selectivity tests such as described above to compare one column to another to determine interaction types, bonded ligand density and packing efficiencies[233]. Although the chromatographic community tends to agree on measures for hydrophobicity there are still inconstancies with the approach, and consequently the results for determining other stationary phase interactions[234]. Much of the variation arises from the issue that only a single characterisation compound is used to determine the level of each type of interaction mechanism. It has been discussed at length throughout this chapter how secondary interaction mechanisms can affect the retention time of analytes depending on mobile phase composition, pH, ionic buffer concentration and temperature. Therefore it is unsurprising that the choice of a single characterisation compound is contested as being fully representative of the highly complex interactions between analyte and stationary phase.

The Neue approach to assessing selectivity differences of a column was initially carried out using a set of 33 characterisation compounds analysed in a variety of pH mobile phase conditions, especially different pH and organic modifiers, to cover the aspects of selectivity on a broader basis[235]. There are obviously practical implications with the time and effort required to run the myriad of columns available on the market using this approach, however as a comparison tool for a small number of stationary phases this gives a wealth of information.

The retention time of each analyte was compared on a graph and the correlation coefficient (r^2) determined for the entire data set. The findings concluded that the selectivity difference (S) of two columns could be determined numerically using the following equation:

(V) $$S = \sqrt{1 - r^2}$$

Figure 1.22 Neue's S Values for typical HPLC stationary phases[235]

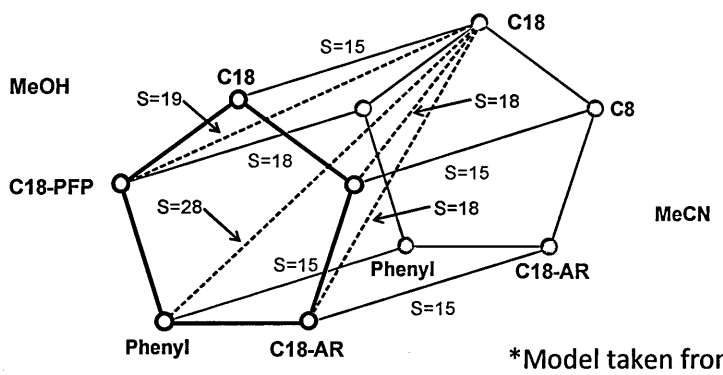

*Model taken from ACT web seminar

The S values for a number of complementary HPLC stationary phases can be seen in Figure 1.22 above. It is not surprising that the largest values are observed when comparing hydrophobic and aromatic ligands as the retention mechanisms are significantly different. The benefit of this approach is the number of similar compounds that can be evaluated, by grouping these into acidic, basic, neutral and phenolic analytes trends in separation mechanisms can be determined for each type of stationary phase.

1.8.4 Acids and Bases Separations

Column characterisation can also be determined using acidic and basic solutes against a neutral marker such as phenol or toluene[223]. As with Tanaka and other such approaches these characterisation compounds can be used to determine the extent of polarity, steric selectivity and anionic exchange on the phase. Small charged acids such as benzene sulphonic acid are only retained through electrostatic interactions therefore these are useful probes for comparing residual silanols, amino functionality, or charged bonded ligands. By evaluating the tailing factor of basic compounds the charge and silanol activity of a phase can also be determined. Small basic analytes with multiple charges such as nicotine are particularly susceptible to tailing through secondary interactions with residual silanols.

1.8.5 Characterisation of HILIC Phases

The increasing focus on HILIC interactions over the last 20 years has led to many more HILIC specific stationary phases being developed by manufacturers and existing column technologies, such as bare silica, to be improved by reducing particle size to improve separation efficiencies. However it can be difficult for the chromatographer to know which type of phase will give the desired interaction for their particular set of compounds. Earlier approaches for column characterisation for HILIC separations tended to be more application and instrument specific [236-238]. Later a consolidated methodology was developed as a general evaluation of chromatographic interactions on HILIC phases[239-241]. The analytes can be classified by their LogD values, as determined by equation VI. Where analytes with high LogD values will have greater affinity to the bulk mobile phase and have a lower retention and the low LogD values are more suitable for HILIC analysis, however this can be complicated by ion exchange interactions.

(VI) $$\log D = \frac{([neutral + ionised\ solute]_{acetonitrile})}{([neutral + ionised\ solute]_{water})}$$

Unlike RP-LC characterisation methods the main requirement for HILIC probes is to determine the degree of hydrophilicity on the column. A selection of nucleosides, saccharides and xanthenes were chosen to identify the selectivity, position and configuration of hydrophilic groups on the surface of the silica. All of these compounds have a low LogD value making them ideal candidates for HILIC partitioning. As HILIC columns can have neutral or acidic/basic functionalities the probes need to be able to characterise both anion- and cation exchange properties on the stationary phases. As with all stationary phases the characterisation compounds need to evaluate the steric selectivity of the phase so steric isomers of the analytes are included in the mixture. These compounds, shown in Figure 1.23, were chosen as they have minimal secondary electrostatic interactions from ion exchange mechanisms to maximise the correlation between retention and LogD values[241] and uses toluene as a t_0 marker.

Figure 1.23 Compounds used for HILIC characterisation method

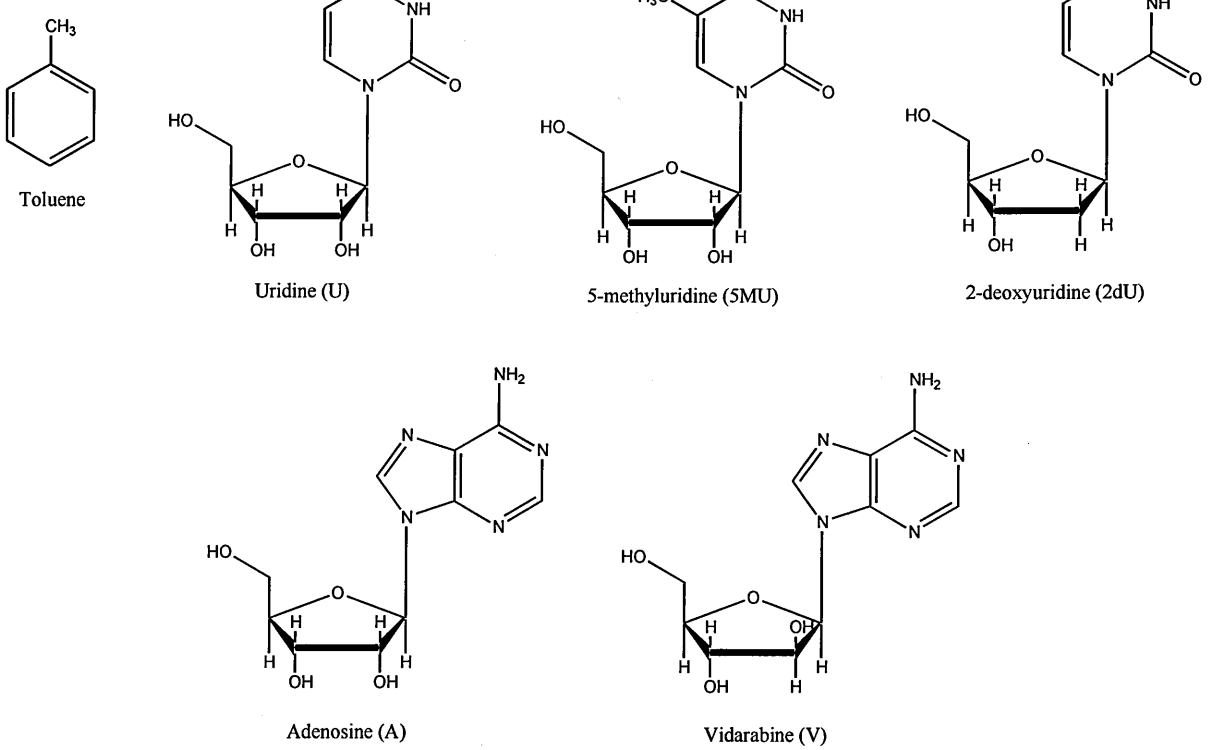

Figure 1.23 Compounds used for HILIC characterisation method (cont.)

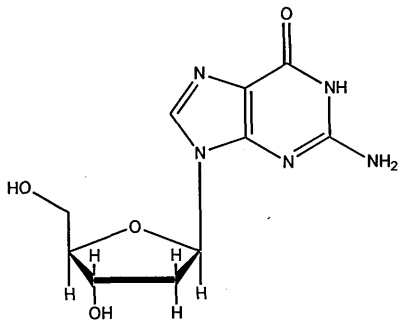

2'-deoxyganosine (2-dG)

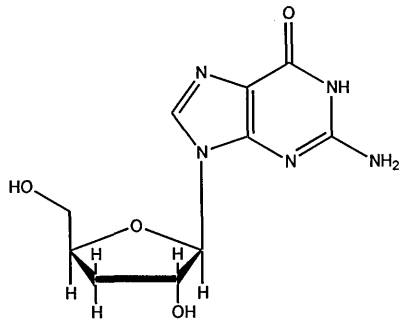

3'-deoxyganosine (3-dG)

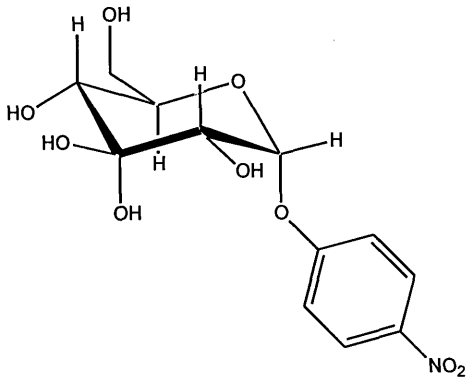

4-nitrophenyl-α-D-glucopyranoside (NPαGLu)

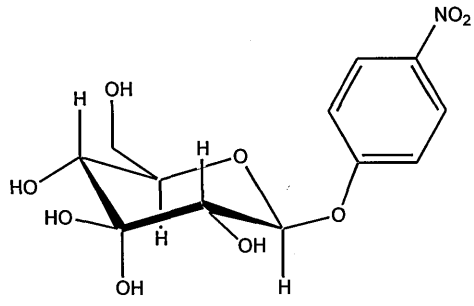

4-nitrophenyl-β-D-glucopyranoside (NPβGLu)

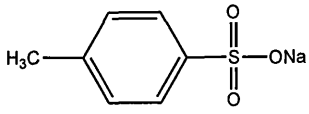

Sodium p-toluenesulfonate (SPTS)

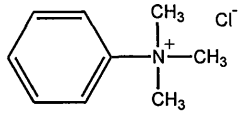

N,N,N-trimethyl-phenylammonium chloride (TMPAC)

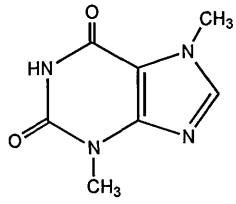

Theobromine

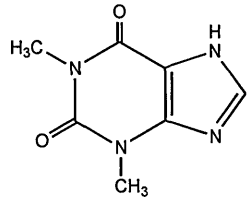

Theophylline

The hydrophobicity of the phases (α_{CH2}) can be determined by the ratio of separation factors of uridine and 5-methyluridine as the difference in these two structures is a single methyl group. The 5-methyluridine has the extra methyl functionality therefore will be retained longer on the phase relative to the uridine. The additional retention time will be dependent on the hydrophobicity of the stationary phase. Again the ratio of retention times can provide a numerical comparison for the degree of hydrophobic interactions between stationary phases.

The degree of selectivity factors due to active hydroxyl groups (α_{OH}) can be determined by assessing the retention ratio of uridine and 2-deoxyuridine. The former has an extra hydroxyl group substituted on the five-membered ring structure which can interact with hydroxyl groups on the column, either present from silanols or from diol functionalised ligands. The longer retention time of uridine compared to that of 2-deoxyuridine represents the degree of hydroxyl group interactions.

The shape selectivity factor can be determined for both configurational ($\alpha_{V/A}$) and regio ($\alpha_{2dG/3dG}$) isomers. As both these pairs of isomers have the same nucleobase any secondary electrostatic interactions from ion exchange should be cancelled out, it is not about the length of time the analytes are retained for but the difference in retention time of the two isomers. As with RP-LC it is difficult to assign a numerical value to steric selectivity therefore these characterisation probes are designed to bring out differences in columns.

The density of the bonded ligand is another selectivity factor ($\alpha_{NP\alpha Glu/NP\beta Glu}$) that requires evaluation of a pair of isomers. The principle of this pairing is similar to the triphenylene and o-terphenyl analysis in the Tanaka methodology. Here the 4-nitrophenyl-α-D-glucopyranoside probe is more linear in nature as the nitrophenyl functionality is substituted on the axial position. This would allow the molecule to penetrate densely packed ligands whereas the 4-nitrophenyl-β-D-glucopyranoside has the nitrophenyl substituted on the equatorial position making the molecule bulky and less likely to assess these ligands.

The pH of the stationary phase is an important factor in HILIC separations, this can be probed by using the relative retention times of theophylline and theobromine (α_{pH}). The characterisation method is carried out using 5:95 20 mM ammonium acetate at pH 5.8:acetonitrile, under these conditions theobromine, a stronger base, should exist in its protonated form as it has a pK_a of 10[242]. Theophylline is a tertiary amine and has a pK_a of 8.6 making it less likely to be protonated under these mobile phase conditions. For basic phases the protonated theobromine will be repelled by the

positively charged stationary phase surface and will elute earlier than the neutral theophylline resulting in a selectivity factor less than one. For acidic phases the theobromine will be more strongly retained than the theophylline giving a selectivity factor greater than one.

The final characterisation probes for HILIC analysis are the only ones to take into account electrostatic interactions. Sodium-*p*-toluenesulfonate is used to determine the degree of anion exchange interactions on the phase (α_{AX}) and *N,N,N*-trimethyl-phenylammonium chloride to determine the level of cation exchange interactions (α_{CX}). The retention time of both of these solutes is measured against uridine which should not undergo any degree of electrostatic interaction with the stationary phase. Therefore the longer the electrostatic moieties are retained with respect to the uridine retention time the greater the stationary phase's capacity for electrostatic interactions.

1.8.6 Principal Component Analysis

The characterisation methods described in this chapter can generate a vast amount of data which may require interpretation and comparison. Depending on the size of the data sets in question this can sometimes be an arduous task to do by eye. Often it is best to employ a chemometric approach to the data analysis in order to sort and visualise differences between the characterisation data from a vast number of stationary phases with different functionalities.

Principal component analysis (PCA) is an exploratory data analysis tool employed by researchers to visualise the different aspects and variations contained in a data set[243]. It is a predictive method that helps find differences and correlations in sample sets and pick out any major trends in the data. Each separate component of the data set is used to create a 2D model and the samples can then be weighted using any number of factor variables set by the user and are then mapped onto the PCA.

For the case of the Tanaka data all the components will have equal weighting therefore the PCA will be used as a canonical correlation analysis (CCA) tool, as developed by Harold Hotelling in the 1930s, to assess correlations of a data set[244].

PCA is based on the mathematical Eigen decomposition covariance matrix of the variables in a data set, for example a given data set $\mathbf{A}^T$ with *x* rows of samples and *y* columns of variables, the covariance matrix of **A** is defined as shown in equation (VII). The data matrix A is then broken down into individual components based on score (t_i) and loading vectors (p_i) of the residual matrix (E) as shown in equation (VIII).

(VII) $$cov(A) = \frac{A^T A}{m-1}$$

(VIII) $$A_{xy} = t_1 p_1{}^T + t_2 p_2{}^T + t_3 p_3{}^T \ldots . + t_n p_n{}^T + E_{xy}$$

The score and loading vectors are defined using the information on how each component relates to one another. The model is based on plotting these components as straight lines in variable space where first principal component (t_1, p_1) is the direction which best describes the overall variation in the data matrix A. The direction of the second principal component is selected by the data that best describes the variation not covered by the first principal component and so on. Overall a complex data set can be adequately modelled in 2D space using just a few orthogonal principal components rather than all of the original variables[245]. For comparison of Tanaka or similar values all the data set can be used and each alpha value is set as a principal component. By plotting the characterisation results for each stationary phase against each other, relations between phases are easily detected[222][226].

1.9 Stability of HPLC Columns

HPLC columns need to be robust and give reproducible results therefore the stability of the silica base and the bonded silanols is imperative to the design of the phase. Although the majority of RP-LC methodology is carried out at low pH the analysis of compounds with a low pK_a or compounds that degrade in acidic media is becoming more common. It has already been discussed (in Chapter 1.3) that HILIC analysis is often carried out in a low to neutral pH mobile phase, however the high concentration of acetonitrile may result in a higher pH than the buffer. Chromatographers are facing increasingly difficult separations from polar compounds, complex sugars, metabolites, and biopharmaceuticals which require a stationary phase to be versatile to a range of pH and temperatures.

1.9.1 Stability in Acidic Conditions

Considerable research has been carried out into the integrity of the covalent bond between the bonded ligand and the silica base in a range of pH, organic modifiers and buffer salts[246-251]. Studies at low pH show conclusively how the covalent bond is hydrolysed[252] in the mobile phase and ligand cleavage occurs resulting in irreversible changes in the integrity of the column which alters the retention mechanism. Although the exact mechanism is not fully understood it has been shown that the rate of hydrolysis is increased at high temperatures[253][254].

Acid hydrolysis is the most common reason for column ligand degradation which leads to irreversible changes to the stationary phase. Phases that have functional groups susceptible to hydrolysis, for example polar embedded phases such as amides and carbamates are more likely to undergo this process. The relative stability of column can be determined by an extrapolated stability test using a high percentage aqueous mobile phase containing 1%v/v trifluoroacetic acid as a

catalyst[252]. Acid hydrolysis is more favourable in aqueous conditions due to the greater disassociation of the water molecules, using an elevated temperature also increases the rate of hydrolysis. As these are not real-life chromatographic conditions only a small number of column volumes are required to assess the relative/comparative stability of each column. The same analyte is injected a number of times, in this case *o*-cresol is used as it is not charged in this highly acidic media, and the relative retention time (k) is recorded. The reduction of k is an indication of the percentage of ligand that is being cleaved during the analysis. Some typical phases are shown in Figure 1.24 below.

Figure 1.24 ***Relative acid stability for a range of HPLC stationary phase ligand[252][255]***

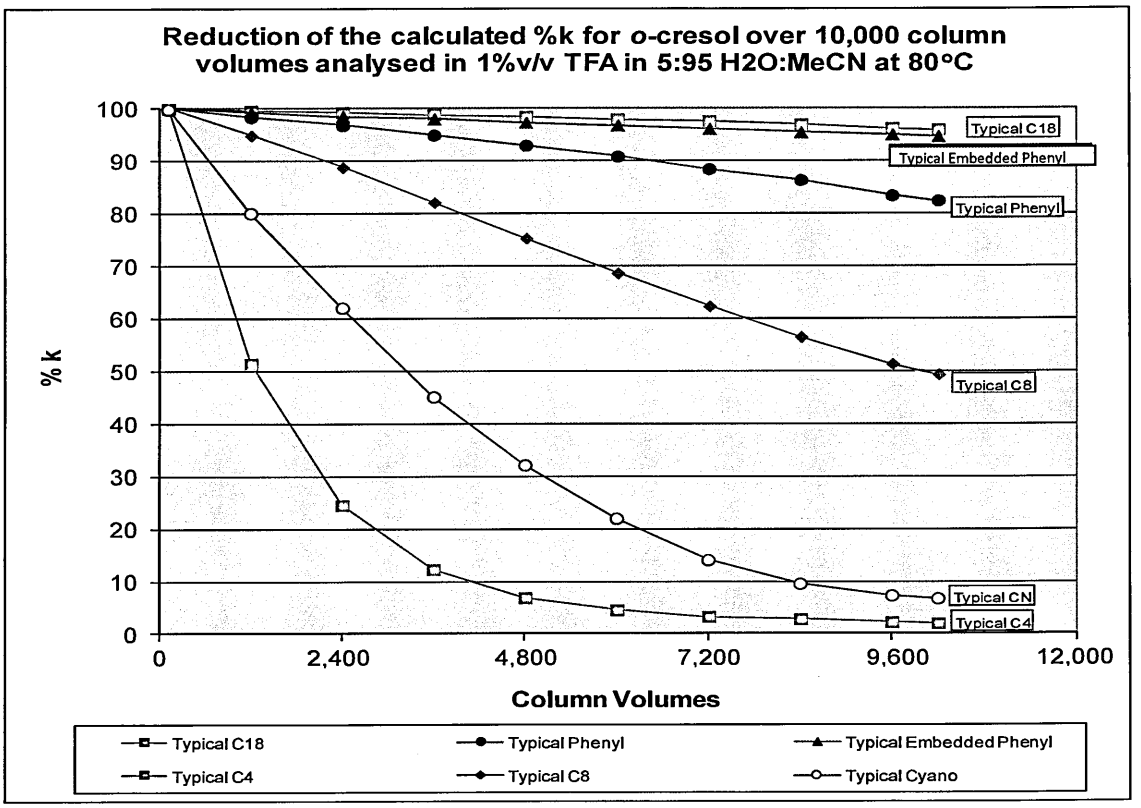

This data can only be used as an indication of the relative stability as only a single column is degraded and small variances may occur due to differences in the batch to batch bonding reproducibility, packing and experimental changes. It can clearly be seen that the long chain hydrocarbons, such as C_{18} are significantly more stable than shorter one such as C_8 and C_4. As these

ligands are likely to be bonded in the same way with a similar coverage it is likely that the steric hindrance of the longer chain silanes prevent the H^+ ions from penetrating the surface and catalysing the hydrolysis.

Another factor that can affect the rate of hydrolysis and subsequent ligand cleavage is the type of silica used. It has been seen in chapter 1.5 that older columns where prepared using Type-A silica which are said to be less stable than the modern column technologies of Type-B silica. This can be shown experimentally in the same way using the Waters Spherisorb ODS phases which, due to the age of these phase types are believed to be bonded onto Type-A silica, shown in Figure 1.25.

Figure 1.25 ***Relative acid stability for a range of HPLC stationary phases silicas***[252][255]

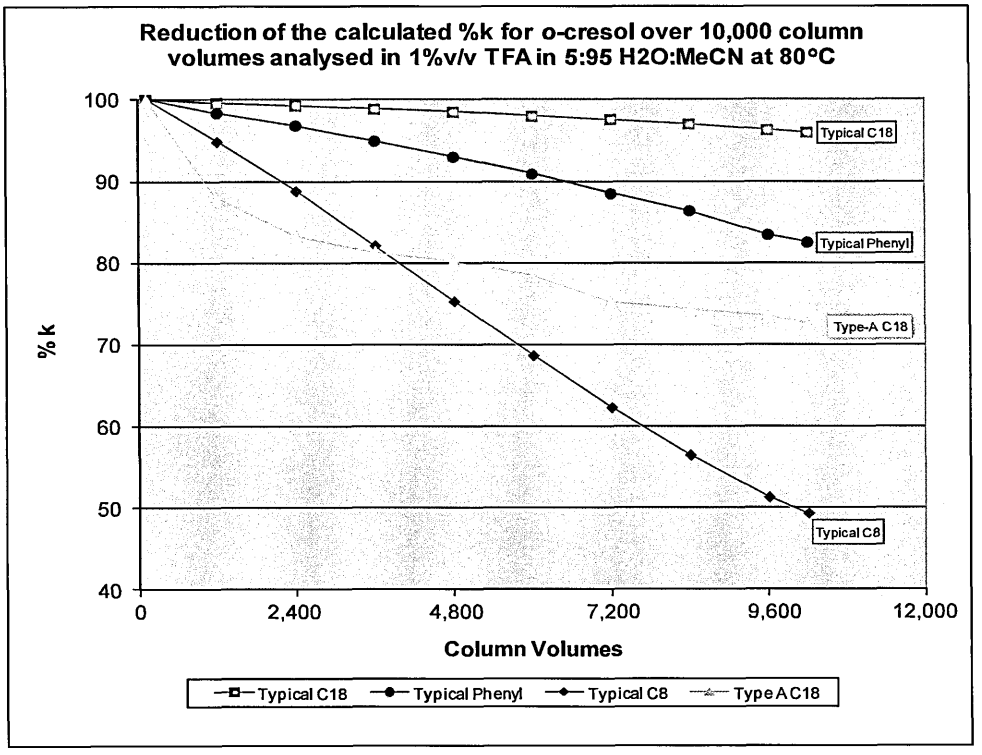

Although the ligand is believed to be a C18 it can be seen that the Spherisorb ODS phases are highly susceptible to acid hydrolysis which indicates that the lower quality Type-A silica is more readily hydrolysed in acidic conditions. This could be due to the presence of metals which weakens the Si-O-R linker bond of the silane to the silica surface.

1.9.2 Stability at High pH

High pH has always been a difficult area from chromatographers to work in as experimentation showed premature column failure in this media[256]. Previously it was believed that a similar mechanism to that observed at low pH was occurring, but research has shown that in media of pH 9-10 the hydrolysis of siloxane bonds from their silica support occurs very slowly[251] concluding that it is the silica base that is being affected. It has been shown that the type and purity of the silica base along with the type of silane and density of the bonding dictates the rate at which the silica particles are dissolved in high pH mobile phase[257][258]. The percentage of organic solvent in the mobile phase is also a large factor here as a higher organic component will reduce the solubility of the silica and therefore decrease the rate of dissolution[257]. This would indicate that a higher carbon load on the column will improve stability at high pH as the inorganic anions and cations cannot readily penetrate the silica surface in order to catalyse the degradation of the silica particles. This suggests that polymeric bonded stationary phases would have a greater stability at medium and high pH as the dense polymeric shell should shield the silica surface from attack.

Another large factor in the stability of monomeric silica columns at neutral and high pH is the concentration of anion and cations present in the mobile phase. It has been shown that a high concentration of anionic salts such as aqueous carbonate and phosphate buffers resulted in a significantly higher degradation affect than organic buffers such as glycine and borates[257] The counter-ion is also shown to have an effect, is was shown experimentally that, in increasing order of aggressiveness, ammonium<potassium<sodium cations will reduce the lifetime of a column[257].

1.9.3 Temperature Effects on Stability

The majority of columns are stable to around 70-80°C however continuous analysis at this temperature will decrease column lifetime as the elevated temperature will catalyse the hydrolysis of the covalent silane-silica bond or the degradation of the base silica particles.

1.9.4 Structural Effects of Stability of HPLC phases

Different silanes will have different stability coefficients depending on the functionality and spatial arrangement and their susceptibility to hydrolysis[259][260]. As with the cyano silane (discussed in Chapter 1.3.3) this ligand cleave can be the result of snippage at the base of the silica enabled by cyclisation of the ligand, which can then elute from the column as a neutral species, as shown in Figure 1.26 below. The shorter the length of the linker chain the more likely this mechanism is to occur as the formation of four, five and six membered rings are more favourable. The likelihood of this type of ligand cleavage is also increased by the presence of polar functional groups as a highly electronegative atom such as nitrogen will increase the chances of cyclisation. For example amides and amine highly favour this type of ligand cleavage as the Si-N bond is shorter, and therefore stronger than the Si-C bond,.

Figure 1.26 Cyclisation cleavage mechanism

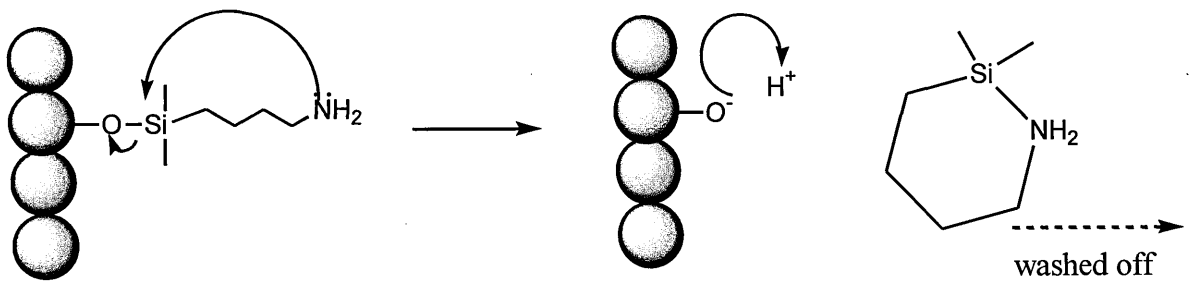

This type of base ligand cleavage is less favourable with long chain hydrocarbons as the Si-C bonds are fairly covalent in nature and acid or base hydrolysis requires increased energy to overcome this. Without an energetically more favourable structure to rearrange to the alkyl chain would simply have to cleave leaving a primary carbocation which is less common although it does occur more readily in high pH solutions. It has already been shown the shorter the alkyl chain the more susceptible it is to acid hydrolysis, even though the coverage of smaller ligands should theoretically be higher it has been seen that trimethylsilane columns will readily hydrolyse to form methane as a leaving group as there is less steric hindrance from H_3O^+ attack.

Endcapped stationary phases are seen to have improved stability, this may be because the dense packing of a small endcapping reagent (typically TMS) at the silica surface protects the phase through steric hindrance. Another theory is that as the TMS endcap ligands are more readily hydrolysed these will be cleaved first preserving the silane which allows the characterisation analyte to continue to be retained even though ligand hydrolysis is taking place.

The Zorbax Stable-Bond range of stationary phases utilises this steric hindrance affect to improve stability of a stationary phase by actually incorporating it into the bonded ligands. Here large, bulky, inert functional groups are substituted onto the linking silica molecule of the ligand. As these groups are inert hydrocarbons they should have little effect on the retention mechanism of the column but these bulky groups will protect the silica base from acid hydrolysis and silica dissolution in high pH conditions.

This can be thought of as an endcapping process as these large substituents also suppress unwanted secondary interactions from residual silanols on the surface of the silica. However, unlike traditional endcapping only a single bonding process is required; this is advantageous if the ligand is susceptible to hydrolysis or degradation in acid or base conditions. The structures of commonly used Stable-Bond "wings" are shown in Figure 1.27 shown overleaf.

Figure 1.27 Schematic of Common Structures for Zorbax Stable Bond Technology[265]

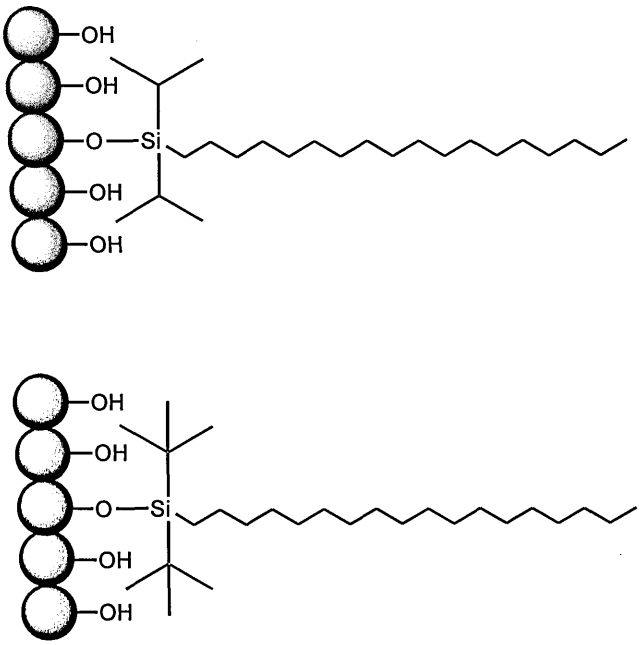

The literature research has shown the importance of stability in an HPLC column. The literature shows a number of real-life and extrapolated tests to determine stability of stationary phases which needs to be incorporated into the characterisation methodology in this research.

2. AIMS

The aim of this research is to gain a greater understanding of the fundamental nature of the retention mechanism of a number of commercial stationary phases with known and unknown polar functionality. These findings will be reviewed against the claims made by the column manufacturers. The investigation will focus on determining where the polar interaction is taking place and the relative degree of this retention mechanism under different conditions. This knowledge will give insight into the selectivity and limitations of these columns to aid the correct choice of stationary phase for commercial applications.

1) Initially a determination of the retention mechanism for the Extended Polar Selectivity range of stationary phase materials will be carried out. Each phase will be evaluated by using different groups of characterisation compounds in a variety of mobile phase ionic buffers and pH to determine the different retention mechanisms present on each phase. These results will be represented pictorially using principal component analysis to compare the main interactions of these phases against more traditional RP-LC phases. In order to determine the limitations of the columns for real-life industrial applications; an assessment of overall stability and robustness of these columns will be performed. Finally a structural elucidation of these stationary phases will be carried out to determine how different spatial arrangements and functional groups of the bonded ligands will produce different degrees of polar retention mechanism.

2) The greater understanding of the hydrophilic and polar interactions will be used in the comparison of the retention mechanism for the TYPE-C^{TM} Bidentate C18 stationary phase in RP-LC. An evaluation of the retention mechanism using the same characterisation compounds with particular reference to secondary interactions from residual silanols. Chromatographic assessment of the nature and structure of the silica hydride monolayer by

evaluation of physical attributes of the stationary phase. This will be compared to spectroscopic analysis of the Bidentate C18 TYPE-C™ bonded silica to determine the functionality of the base silica and the structure of the bonded ligand. An investigation into the efficiency of the TYPE-C™ Bidentate C18 phase will be performed using van Deemter analysis and Microsoft Solver to determine the contributions to dispersion. This will be coupled with SEM imaging to evaluate the efficiency packed bed of the Bidentate C18 TYPE-C™ bonded silica.

3) HILIC mode will be used to determine the retention mechanism for TYPE-C™ Diamond Hydride and Silica-C in HILIC mode by evaluation of polar characterisation compounds. This data will be used to compare the retention mechanism against traditional silica based HILIC phases in a PCA comparison. The degree of electrostatic interactions of the TYPE-C™ Diamond Hydride and Silica-C phases will be chromatographically characterised and the silanol activity confirmed by spectroscopic analysis. Due to the nature of HILIC analysis the stability of the TYPE-C™ Diamond Hydride stationary phase will be determined through *in-vitro* testing. The efficiency of the TYPE-C™ Diamond Hydride and Silica-C phases will be investigated using a modified HILIC mode van Deemter analysis.

4) A small scale controlled "silanization" process of bare silica using triethoxy silane monomer will be carried out through design of experiment to attempt to maximise the coverage of silica hydride. The results will be evaluated through ^{29}Si NMR spectroscopy and SEM imaging. The optimised conditions will be used to scale up the bonding process and the prepared silica hydride particles packed into columns. These phases will be evaluated chromatographically using the learnings from the previous analysis.

3. INSTRUMENTS, MATERIALS AND METHODOLOGY

3.1 Instruments

The HPLC system consisted of an Agilent® Technologies 1260 Infinity equipped with 1260 binary pump (with the mixer and dampener removed), 1260 ALS auto sampler, 1260 TCC oven and 1260 DAD detector along with OpenLAB CDC software. The dwell volume, temperature validation, and repeatability of the instrument were determined prior to any experimental work being performed.

The stability testing was carried out on an Agilent® Technologies 1100 Series HPLC system consisting of an 1100 binary pump, 1100 auto sampler and 1100 DAD detector along with Chemstation software. The system was stripped down to mimic the dwell volume of a 1260 series by removing the column oven fins and replacing all the tubing with 0.12mm internal diameter tubing. The dwell volume, temperature validation, and repeatability of the instrument were determined prior to any experimental work being performed.

The NMR system consisted of a Jeol® DX400 module equipped with a Doty Scientific® 609 probe with 4mm zirconia rotors for solid state samples. Tetramethylsilane (TMS) was used as chemical shift reference for the ^{29}Si and ^{13}C nuclei.

The GC-MS system consisted of a Agilent® Technologies 6890 gas chromatograph fitted with a ThermoSc TG-5MS 15m x 0.25mm x 0.25µm column with an Agilent® Technologies 5973 mass-selective detector. An auto tune was performed on the instrument prior to use.

The scanning electro-microscope system consists of a Zeiss® Supra 55VP Analytical FEG-SEM equipped with Everhart-Thornley® Secondary Electron Detector, Variable Pressure Secondary Electron Detector mode (VPSE) and HKL Electron Backscattered Diffraction system (EBSD). The samples were coated with carbon prior to analysis to enhance image.

3.2 HPLC Method Parameters

The following instrument parameters were used for each specifically named method:

Tanaka Hydrophobic, Silanophilic and Steric Selectivity analysis

Mobile Phase A:	Water	80% / 30%
Mobile Phase B:	Methanol	20% / 70%
Flow Rate:	0.21 mL/min	Isocratic
Oven Temperature:	40 °C	
Injection Volume:	0.2 µL	
Wavelength:	UV 254 and 210 nm; referenced at 360 and 100 nm	
	DAD collection over the range of 190 – 360 nm	

Tanaka Ion Exchange analysis

Mobile Phase A:	20 mM KH_2PO_4 pH 2.7 in 70:30 Water:Methanol*	
Mobile Phase B:	20 mM KH_2PO_4 pH 7.6 in 70:30 Water:Methanol**	
Flow Rate:	0.21 mL/min	Isocratic
Oven Temperature:	40 °C	
Injection Volume:	0.2 µL	
Wavelength:	UV 254 and 210 nm; referenced at 360 and 100 nm	
	DAD collection over the range of 190 – 360 nm	

* 200 mM Stock buffer prepared by dissolving 27.22 g KH_2PO_4 in ~800 mL H_2O, 85 % H_3PO_4 added to adjust to pH 2.7 prior to making up to 1000 mL with H_2O.

** 200 mM Stock buffer prepared by dissolving 27.22 g KH_2PO_4 in ~800 mL H_2O, KOH added to adjust to pH 7.6 prior to making up to 1000 mL with H_2O.

Tanaka AROMATICS / DINITRO

Mobile Phase A:	Water	50% / 60%
Mobile Phase B:	Methanol	50% / 40%
Flow Rate:	0.21 mL/min	Isocratic
Oven Temperature:	40 °C	
Injection Volume:	0.2 µL	
Wavelength:	UV 254 and 210 nm; referenced at 360 and 100 nm	
	DAD collection over the range of 190 – 360 nm	

ACIDS I/II

Mobile Phase A:	5 mM KH_2PO_4 pH 2.5 in MeOH/H_2O (35 : 65 v/v)*	
Flow Rate:	0.21 mL/min	Isocratic
Oven Temperature:	40 °C	
Injection Volume:	1 µL	
Wavelength:	UV 254 and 210 nm; referenced at 360 and 100 nm	
	DAD collection over the range of 190 – 360 nm	

ACIDS III

Mobile Phase B:	5 mM KH_2PO_4 pH 2.5 in MeOH/H_2O (65 : 35 v/v)*	
Flow Rate:	0.21 mL/min	Isocratic
Oven Temperature:	40 °C	
Injection Volume:	1 µL	
Wavelength:	UV 254 and 210 nm; referenced at 360 and 100 nm	
	DAD collection over the range of 190 – 360 nm	

* 200 mM Stock buffer prepared by dissolving 27.22 g KH_2PO_4 in ~800 mL H_2O, 85 % H_3PO_4 added to adjust to pH 2.5 prior to making up to 1000 mL with H_2O.

BASES_Gradient

Mobile Phase A:	20 mM KH_2PO_4 pH 2.7 in water*	
Mobile Phase B:	20 mM KH_2PO_4 pH 2.7 in MeOH/H_2O (65:35v/v)*	
Gradient	Time	%B
	0	5
	7	100
	10	100
Post time:	5 minutes	
Flow Rate:	0.21 mL/min	
Oven Temperature:	60 °C	
Injection Volume:	1 µL	
Wavelength:	UV 254 and 214 nm; referenced at 360 and 100 nm	
	DAD collection over the range of 190 – 360 nm	

BASES_Hydrohobic / Hydrophilic

Mobile Phase A:	20 mM KH_2PO_4 pH 2.7 in water*	30% / 95%
Mobile Phase B:	20 mM KH_2PO_4 pH 2.7 in MeOH/H_2O (65:35v/v)*	70% / 5%
Flow Rate:	0.21 mL/min	Isocratic
Oven Temperature:	60 °C	
Injection Volume:	1 µL	
Wavelength:	UV 254 and 214 nm; referenced at 360 and 100 nm	
	DAD collection over the range of 190 – 360 nm	

* 200 mM Stock buffer prepared by dissolving 27.22 g KH_2PO_4 in ~800 mL H_2O, 85 % H_3PO_4 added to adjust to pH 2.7 prior to making up to 1000 mL with H_2O.

H-Bonding_Snyder Protocol (dimethylacetamide versus ethylbenzene)

Mobile Phase A:	Water	50%
Mobile Phase B:	Acetonitrile	50%
Flow Rate:	0.42 mL/min	Isocratic
Oven Temperature:	35 °C	
Injection Volume:	2 µL	
Wavelength:	UV 215 nm; referenced at 360 and 100 nm	
	DAD collection over the range of 190 – 360 nm	

H-Bonding_Engelhardt Protocol (pyridine versus phenol)

Mobile Phase A:	Water	40%
Mobile Phase B:	Methanol	60%
Flow Rate:	0.21 mL/min	Isocratic
Oven Temperature:	35 °C	
Injection Volume:	2 µL	
Wavelength:	UV 254 nm; referenced at 360 and 100 nm	
	DAD collection over the range of 190 – 360 nm	

H-Bonding_Alltech Protocol (N,N-diethyl-meta-toluamide versus toluene)

Mobile Phase A:	Water	42%
Mobile Phase B:	Acetonitrile	58%
Flow Rate:	0.21 mL/min	Isocratic
Oven Temperature:	35 °C	
Injection Volume:	2 µL	
Wavelength:	UV 254 nm; referenced at 360 and 100 nm	
	DAD collection over the range of 190 – 360 nm	

100 Compounds Gradient

Mobile Phase A:	0.03 %v/v TFA in water	
Mobile Phase B:	0.03 %v/v TFA in Methanol / Acetonitrile	
Gradient	Time	%B
	0	3
	5.5	100
	6	100
Post time	2 minutes	
Flow Rate:	0.21 mL/min	
Oven Temperature:	35 °C	
Injection Volume:	2 µL	
Wavelength:	UV 214, 254 nm; referenced at 360 and 100 nm	
	DAD collection over the range of 190 – 360 nm	

Loadability

Mobile Phase A:	20 mM KH_2PO_4 pH 2.7 in water*	
Mobile Phase B:	20 mM KH_2PO_4 pH 2.7 in 30:70 water:Acetonitrile/Methanol*	

The composition was adjusted for each column until the analytes had a retention time of ~4 minutes

Flow Rate:	0.21 mL/min	Isocratic
Oven Temperature:	60 °C	
Injection Volume:	2 µL	
Wavelength:	UV 256 nm; referenced at 360 and 100 nm	
	DAD collection over the range of 190 – 360 nm	

* 200 mM Stock buffer prepared by dissolving 27.22 g KH_2PO_4 in ~800 mL H_2O, 85 % H_3PO_4 added to adjust to pH 2.7 prior to making up to 1000 mL with H_2O.

Stability

Mobile Phase A:	25 mM KH_2PO_4 pH 2.5 / pH 7.0 in water	40%
Mobile Phase B:	Methanol	60%
Flow Rate:	0.05 mL/min	Isocratic
Oven Temperature:	60 °C	
Injection Volume:	2 µL	
Wavelength:	UV 256 nm; referenced at 360 and 100 nm	
	DAD collection over the range of 190 – 360 nm	

Forced Stability

Mobile Phase A:	1.0 %v/v TFA in 95:5 H_2O:MeCN	Isocratic
Flow Rate:	1.0 mL/min	
Oven Temperature:	80 °C	
Injection Volume:	2 µL	
Wavelength:	UV 210 nm; referenced at 360 and 100 nm	
	DAD collection over the range of 190 – 360 nm	

Neutrals Testing

Mobile Phase A:	Water	
Mobile Phase B:	Methanol	Isocratic

The mobile phase composition is varied until all neutral molecules elute in 10 minute analysis

Flow Rate:	0.21 mL/min
Oven Temperature:	22 °C
Injection Volume:	2 µL
Wavelength:	UV 210 nm; referenced at 360 and 100 nm
	DAD collection over the range of 190 – 360 nm

van Deemter

Mobile Phase A:	0.1 %v/v TFA in Water	
Mobile Phase B:	0.1 %v/v TFA in Acetonitrile	

The composition was adjusted for each column to keep the k comparable at both temperatures

Flow Rate:	0.05 mL/min	0.90 mL/min
	0.10 mL/min	1.10 mL/min
	0.20 mL/min	1.30 mL/min
	0.30 mL/min	1.50 mL/min
	0.50 mL/min	1.70 mL/min
	0.70 mL/min	2.00 mL/min
Oven Temperature:	40 °C and 60 °C	
Injection Volume:	2 µL	
Wavelength:	UV 256 nm; referenced at 360 and 100 nm	
	DAD collection over the range of 190 – 360 nm	

Cox Plot

Mobile Phase A:	200 - 5mM Ammonium Acetate pH 3.0/7.0*	65%
Mobile Phase B:	Methanol	35%

The composition was adjusted for each column to keep the k comparable at both mobile phase pH

Flow Rate:	0.21 mL/min	Isocratic
Oven Temperature:	30 °C	
Injection Volume:	4 µL	
Wavelength:	UV 210 and 254 nm; referenced at 360 and 100 nm	
	DAD collection over the range of 190 – 360 nm	

* 200 mM Stock buffer prepared by dissolving 15.42g $C_2H_4O_2.NH_3$ in ~800 mL H_2O, CH_3COOH added to adjust to pH 3.0 prior to making up to 1000 mL with H_2O

HILIC Characterisation / Loadability

Mobile Phase A:	20 mM Ammonium Acetate pH 4.7*	10%
Mobile Phase B:	Acetonitrile	90%
Flow Rate:	0.105 mL/min	Isocratic
Oven Temperature:	25 °C	
Injection Volume:	4 µL	
Wavelength:	UV 210 and 254 nm; referenced at 360 and 100 nm	
	DAD collection over the range of 190 – 360 nm	

HILIC Cox Plot

Mobile Phase A:	5 -200mM Ammonium Acetate pH 3.0/7.0*	10%
Mobile Phase B:	Acetonitrile	90%
Flow Rate:	0.105 mL/min	Isocratic
Oven Temperature:	25 °C	
Injection Volume:	4 µL	
Wavelength:	UV 210 and 254 nm; referenced at 360 and 100 nm	
	DAD collection over the range of 190 – 360 nm	

* 200 mM Stock buffer prepared by dissolving 15.42g $C_2H_4O_2.NH_3$ in ~800 mL H_2O, CH_3COOH added to adjust to pH 3.0 prior to making up to 1000 mL with H_2O. For pH 7.0 solution 35% NH_3 was added to adjust to pH 7.0 prior to making up to 1000 mL.

On Column Endcapping

The detector and sampler modules were disconnected from the system and the lines thoroughly cleaned with acetonitrile to remove any water from the system.

Solvent		Flow rate:
Mobile Phase A:	20% N,O-Bis(trimethylsilyl) acetamide in toluene (anhydrous)	0.05 mL/min
Mobile Phase B:	Toluene (anhydrous)	1.0 mL/min
Mobile Phase A2 & B2	Acetonitrile	1.0 mL/min
Oven Temperature:	80 °C	

The system and column were primed for 2 hours with acetonitrile, then 2 hours with toluene to prior to the endcapping procedure. The N,O-Bis(trimethylsilyl) acetamide solution was run for 5 hours following which the column flushed for 2 hours with toluene and 2 hours of acetonitrile. Prior to use the column was conditioned with 50:50 water:acetonitrile for one hour.

4.3 Spectroscopic Method Parameters

The following instrument parameters were used for each technique:

Solid State NMR

Instrument:	Jeol DX400
Probe:	Doty Scientific 609
Temperature:	
Mode:	MAS-GHD (magic angle spinning gate proton decoupling)
	CP-MAS (cross-polarisation magic angle spinning)
Field Strength:	400 MHz
Acquisition time:	0.2 s
^{1}H Domain:	
Scans:	32
Gain:	5
Relaxation delay:	2.5 s
^{29}Si Domain:	
Scans:	1024
Gain:	15
Relaxation delay:	60 s
^{13}C Domain:	
Scans:	512
Gain:	10
Relaxation delay:	15 s

Liquid NMR Analysis

Instrument:	Jeol DX400
Mode:	BCM
Temperature:	23.5 °C
Frequency:	6000 Hz
Acquisition time:	0.5s
Solvent:	$CDCl_3$
^1H Domain:	
Scans:	128
Gain:	18
Spin:	17 Hz
Relaxation delay:	15 s
^{13}C Domain:	
Scans:	15000
Gain:	25
Spin:	15 Hz
Relaxation delay:	15 s

GC-MS

Instrument:	Agilent 6890 GC-MS
Column:	ThermoSc TG-5MS 15 m x 0.25 mm x 0.25 um

GC Parameters

Carrier Gas: He

Flow: 1 mL/min (1.09 psi with average velocity 51 cm/sec)

Split: 25:1

Total flow: 27.7 mL/min

Gradient:

Initial Temp (°C)	Ramp Rate (°C/min)	Final Temp (°C)	Total Time (min)
50	-	-	2
50	20	250	14

Injector Port: 270 °C

Injection Volume: 1 µL

Post Wash A: 3

Post Wash B: 3

MS Parameters

Inlet Temperature: 280 °C

Gain: 1.0

EM Voltage: 1500 V

Source Temperature: 230 °C

Quad Temperature: 150 °C

Scan Range: 50 – 550 m/z

Number of Scans: $4s^{-1}$

Scan Time: 14 minutes

Solvent Delay: 5 minutes

Scanning Electron Microscope

Fully motorised 5-axis stage, and a range of detectors:-

Everhart-Thornley Secondary Electron detector

Zeiss Gemini In-Lens Secondary Electron detector

Backscattered Electron Detector (Centaurus)

VPSE Variable Pressure Secondary Electron Detector

EDAX Genesis 4000 Energy Dispersive X-Ray system for elemental analysis

HKL Electron Backscattered Diffraction system (EBSD)

Stage Parameters

5-axis, motorised

X-Y ranges (depends on sample size)	+/- 65 mm maximum, from stage centre.
Z (Height) range	0 – 50 mm
R (Rotation)	Full 360 deg.
T (Tilt)	-4 deg. to +70 deg.
EHT (Accelerating Voltage)	20 kV
Working Distance	15 mm +/- 0.1 mm
Tilt Compensation (at 70 deg.)	ON
Dynamic Focus	ON
Secondary Imaging on conductive sample	5 kV
Backscattered Imaging on conductive sample	10 kV
X-Ray Analysis (EDS)	15 kV (WD = 10.5 +/- 0.1 mm)
Electron Backscatter detection (EBSD)	20 kV (WD = 15 +/- 0.1 mm)

3.4 Synthetic Methods

The silica particles recovered from unpacked HPLC columns were prepared using the following synthetic techniques.

Silane Cleavage by Hydrofluoric Acid Sample Preparation

The aqueous HF solution for the silane cleavage was prepared prior to use; 25 mL 48% $v/v_{(aq)}$ hydrofluoric acid was added to 25 mL methanol and 50 mL distilled water in a plastic reaction vessel. Approximately 100 mg of unpacked, dried silica was weighed into 30 mL polypropylene screw cap scintillation vials and a plastic coated magnetic stirrer added. 10 mL of the aqueous HF solution was added to each reaction vessel and stirred at room temperature for 5 hours. 5 mL hexane was added to each solution; the vials were gently shaken and stirred at room temperature for a further 1 hour. The hexane layer was removed with a syringe and transferred to glass scintillation vials for GC analysis.

***In-vitro* Sample Preparation**

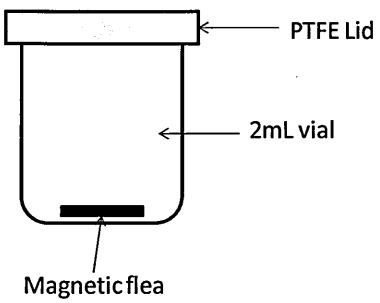

Approximately 100mg of bonded silica was weighed into a 10mL glass vial and approximately 2mL of 100mM ammonium acetate and acetonitrile solution added. In order to emulate the HPLC methodology a 5:95 v/v buffered H_2O:MeCN solution was used, however in order to compensate for wetting and ensure the silica is fully submersed two further solution of 25:75 and 50:50 buffered H_2O:MeCN was also used. These solutions were added as per the table below. The vial was then sealed with a PTFE lid prior to being heated at 80°C over a period of at least 36 hours with continuous stirring. The vials were removed from the heating block and allowed to cool to room temperature.

Table 3.1 ***Silica and solvents used for in-vitro sample preparation***

Silica		Aqueous Phase		
Type	Weight (mg)	2M Ammonium Acetate (mL)	Water (mL)	Acetonitrile (mL)
TYPE-C™ Diamond Hydride	102	0.1	-	1.9
	101	0.1	0.4	1.5
	99	0.1	0.9	1.0
Experimental C1 Bonded Phase	100	0.1	-	1.9
	98	0.1	0.4	1.5
	101	0.1	0.9	1.0

The contents of the vial were shaken and filtered using a 20mm diameter Buchner funnel using a <2µm nylon filter paper. The silica particles were then washed with 0.5mL water and then 0.5 mL MeCN. The silica was then transferred to a watch glass and dried in a 40°C oven for 20 minutes prior to being transferred to a sample vial.

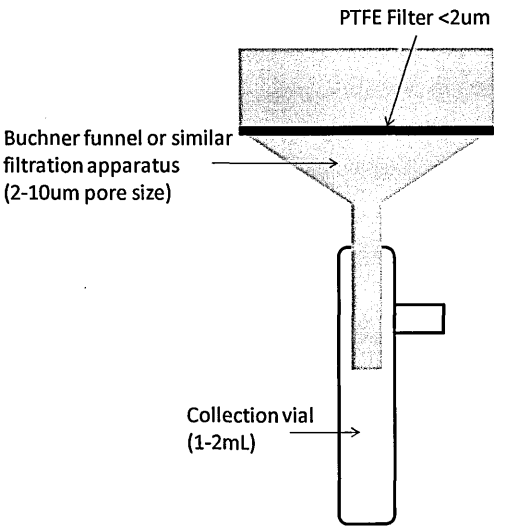

A liquid-liquid extraction was performed by addition of 2mL of anhydrous deuterated chloroform to each of the filtrates and shaken vigorously, before being left to settle. The chloroform supernatant was removed with a pipette and transferred to an oven dried vial. Magnesium sulphate was added to the vial and the extract shaken again before being left to settle for approximately 1 hour. The extract was shaken and filtered through glass wool directly into an oven dried glass NMR tube for analysis.

Silanization Preparation

The unbonded silica is washed in 4 M HCl in 1,4 dioxane prior to being dried in a vacuum oven. The silica was heated incrementally from 40 °C to 120 °C with a 1 hour equilibration period over 20 °C increments. The silica was then heated at 120 °C over a 48 hour period for complete removal of water. In a typical procedure, a 1.00 g sample of pre-washed and dried silica was placed in a 3-neck, 100 mL round bottom flask equipped with a condenser topped with a argon flow and equalizing tube, an addition funnel with equalizing tube was also attached. The flask was fitted with a thermometer and placed on a heating mantle with a magnetic stirrer.

Table 3.2 Silica and solvents used for TES "silanization" sample preparation

Silica (g)	TES Silane (M)	Water		Catalyst		
		Percentage (%v/w)	Volume (mL)	Type	Molarity (M)	Volume (mL)
1.00	0.5	-	-	HCl (in dioxane)	4M	0.80
1.00	0.5	1.00	0.01	HCl (in dioxane)	4M	0.80
1.00	0.5	5.00	0.05	HCl (in dioxane)	4M	0.80
1.00	0.5	10.0	0.10	HCl (in dioxane)	4M	0.80
1.00	0.5	5.00	0.05	HCl (in dioxane)	4M	1.60
1.00	0.5	5.00	0.05	TFA (anhydrous)	4.33M	0.75
1.00	0.5	5.00	0.05	Imidazole (in dioxane)	4M	0.80
1.00	1.0	5.00	0.05	HCl (in dioxane)	4M	0.80
1.00	2.5	5.00	0.05	HCl (in dioxane)	4M	0.80
-	2.5	5.00	0.05	HCl (in dioxane)	4M	0.80

A 50mL aliquot of anhydrous 1,4 dioxane was then added, followed by the amount of water and catalyst shown in the Table 3.2. The mixture was heated to about 70-80°C, and then a 10mL amount of TES/1,4 dioxane solution was added dropwise, over a period of 15-20min prior to gentle reflux for approximately one hour.

The product was centrifuged and washed consecutively with 10mL portions of 20:80 water:THF, THF, and diethyl ether (twice with each solvent). The final product was dried at room temperature and then in a vacuum oven at 110°C for 6 h or more.

3.5 Stationary Phase Materials

The columns purchased for use in the TYPE-C RP-LC investigations are shown in the table below.

Table 3.3 Columns purchased for TYPE-C RP-LC evaluation

Supplier	Column Type	Lot Number	Serial Number	Column Dimensions
Microsolve	Cogent Bidentate C18 ™	0412-100-13	M12-CP04-013	50 x 2.1mm
Microsolve	Cogent Bidentate C18 ™	0412-100-13	M12-CP04-010	50 x 2.1mm
ACT	ACE 3 C18	V11-6820	A103330	50 x 2.1mm
ACT	ACE 3 C18	V11-6820	A103331	50 x 2.1mm

The columns purchased for HILIC investigations are shown in the table below.

Table 3.4 Columns purchased for TYPE-C HILIC evaluation

Supplier	Column Type	Lot Number	Serial Number	Column Dimensions
Microsolve	Cogent Diamond Hydride	1211-350-04	M11-ST12-231	50 x 2.1mm
Microsolve	Cogent Type-C Silica™	0511-147-03	M11-ST05-237	50 x 2.1mm
ACT	SIL 3	V11-6413	A105958	50 x 2.1mm
ACT	SIL 3	V11-6413	A105959	50 x 2.1mm

The following columns were purchased directly from the manufacturer, the silica was then unpacked, slurried in an appropriate solvent and repacked into 50 x 2.1mm column dimensions for direct comparison to the TYPE-C^{TM} phases:

Table 3.5 Columns purchased to be re-packed for the EPS RP-LC evaluation

Supplier	Column Type	Lot Number	Serial Number	Column Dimensions
Thermo	HyPURITY Aquastar	6430	22503-052130	150 x 2.1mm
Agilent	Zorbax SB AQ	B10313	863953-914	150 x 4.6mm
Waters	Acquity HSS C18 SB		18600749	150 x 4.6mm
Grace	Alltima HP C18 EPS	36/132	87715	150 x 4.6mm
Grace	Platinum C18 EPS	29/176	32183	150 x 4.6mm

A number of experimental bonded and unbonded silica phases were donated by Mel Euerby at Strathclyde University to be used as standards for direct comparison to the recovered silica during the spectroscopic testing.

3.6 Mobile Phase Materials

The following mobile phase solvents and buffers were purchased from Fisher-Scientific to be used for chromatographic experiments; Acetonitrile (Far UV grade) Methanol (HPLC grade), trifluoroacetic acid (Analytical grade), Formic acid (Analytical grade), 85% Phosphoric acid (Analytical grade), Potassium dihydrogen phosphate buffer salt (Anhydrous, Analytical grade) and Ammonium acetate buffer salt (Analytical grade), 35% Ammonia (HPLC grade). Water was purified on a Milli-Q apparatus (Millipore, Bedford).

3.7 Characterisation Chemicals

The specifically named characterisation solutes were purchased from Sigma-Aldrich, Fluka, Acros and Merck and were prepared at a concentration between 1 and 100μg/mL in water, MeCN, MeOH, 50:50 water:MeCN or 50:50 water:MeOH depending on their solubility.

4. RESULTS AND DISCUSSIONS: EPS PHASE EVALUATION

The five EPS phases chosen to undergo characterisation are shown in Table 4.1 below.

Table 4.1 Manufacturer's data of EPS phases for characterisation

Phase	Pore size (Å)	Surface coverage (m^2/g)	Endcapping	Carbon Load (%)	pH range	Max temp (°C)
HyPURITY Aquastar 3um [262]	190	200 *(200)*	Polar	10 *(13)*	2-8[a]	80[c]
Platinum EPS C18 3um [263]	100	200 *(200)*	None	5 *(6)*	2-7.5	80[c]
XSelect HSS SB C18 3.5um[264]	100	230 *(230)*	None	8.5 *(15)*	2-8	45
Zorbax-SB AQ 3.5um [265]	80	180 *(200)*	None	Proprietary *(10)*	1-8	60
Alltima HP C18 EPS 3um[266]	190	200 *(340)*	None	4 *(16)*	1-10[b]	80[c]

Values shown in parenthesise indicate the data for the equivalent C18 phase from same column manufacture
[a] pH range for HyPURITY silica type rather than individual phase
[b] Value stated on suppliers website rather than manufacturers literature on phase
[c] Temperature quoted as general range for manufacturers phases rather than specific phase

Although the structure of the bonded ligands is proprietary information and are not fully disclosed the manufacturers provide some data on these phases. This information indicates that the Platinum EPS C18, Alltima HP C18 EPS and XSelect HSS SB C18 are all lightly bonded phases[263][264][266] although the Waters phase is believed to be trifunctionally bonded where as the other two phases are monomeric bondings. The age of the Platinum EPS C18 phases suggests that it may be bonded onto old style TYPE-A silica[259], where as the Alltima HP C18 EPS and XSelect HSS SB C18 are much newer column technologies and are most likely produced using TYPE-B silica[264][266].

The Zorbax-SB AQ phase is part of the stable-bond (SB) range as discussed in Section 1.9[265]. The bulky stable-bond technology is designed to increase stability, however it there is a possibility that these bulky groups could sterically suppress any available silanols on the surface of the silica. The phase is classed as an EPS phase indicating added polar interaction mechanism either from residual silanols or from hydroxyl groups , therefore it is possible that the bulky stable-bond groups have been modified to include some hydroxyl functionality. The HyPURITY Aquastar phase is more of an unknown; the characterisation work described in the following chapter was designed to attempt to identify the structure of the bonded ligands on these phases[262].

4.1 RP-LC Chromatographic Evaluation of EPS Phases

4.1.1 Tanaka Characterisation Testing of EPS Phases

The EPS phases that underwent analytical evaluation are classed as L1 type columns, except for the Zorbax SB-AQ, as they include octadecyl silane functionality in the bonded ligands[262-266][232]. As discussed in Section 1.6 these phases contain both hydrophobic and polar characteristics however due to proprietary information the exact structure and functionality of these phases is not known. The Tanaka characterisation compounds have been chosen to probe the different retention interactions of a column as discussed in Section 1.8, it was possible to determine more about the chemical structure from these results. The α values for the full Tanaka characterisation are shown in Table 4.2 and graphically in Figure 4.1.

Comparison of the $k_{(am)}$ value indicates the density of bonded ligands on each phase; it can be seen that the XSelect HSS has the highest value and the Platinum and Alltima phases the lowest. This correlates with the carbon load data from the manufacturer's information which can be seen in Table 4.1, where the higher the carbon load of the phase the higher the value of $k_{(am)}$. The $\alpha_{(A/B)}$ value

is comparable across all five columns which indicates the hydrophobic interactions is similar for all phases even though the ligand density may vary.

Some differences are observed in the $\alpha_{T/O}$ values; the XSelect, Alltima and Platinum phases are thought to be lightly bonded C18 ligands[263][264][266], these phases are shown to be grouped together with a similar steric selectivity. This would indicate that the octadecyl silanes are spread out across the silica surface allowing for shape selectivity to be part of the retention mechanism for these types of phases. The XSelect HSS phase has been seen to have a higher carbon load[264] which may explain the small difference in the alpha values. However triphenyl and o-terphenyl are small molecules and may not be discriminatory for these types of phases[224]. The differences observed here could equally be from the electron rich conjugated systems interacting with polar silanols or with aromatic groups present on the phase rather than being an indication of the shape selectivity of the phases. Further characterisation work using methoxy and nitro benzenes is required to determine the aromatic selectivity of these phases (this is shown on page 97).

Table 4.2 Tanaka characterisation values – comparison of EPS phases

					pH 2.7		pH 7.6	
	$k_{(am)}$	$\alpha_{(A/B)}$	$\alpha_{(T/O)}$	$\alpha_{(C/P)}$	$\alpha_{(P/BnOH)}$	$\alpha_{(B/P)}$	$\alpha_{(P/BnOH)}$	$\alpha_{(B/P)}$
HyPURITY Aquastar 3um	1.097	1.401	2.779	0.894	0.885	0.141	0.890	3.043
Platinum EPS C18 3um	0.545	1.352	2.234	2.217	0.818	0.351	1.026	8.101
XSelect HSS SB C18 3.5um	1.951	1.377	1.938	1.735	0.836	0.129	0.852	5.341
Zorbax-SB AQ 3.5um	0.866	1.303	1.181	2.590	0.886	0.135	0.870	1.107
Alltima HP C18 EPS 3um	0.357	1.294	2.375	1.610	0.867	0.217	0.879	5.617

A(am) = amylbenzene, B = butylbenzene, T = triphenylene, O = *o*-terphenyl, C = caffeine, P = phenol, $BnNH_2$ = benzylamine, BnOH = benzyl alcohol

The $\alpha_{C/P}$ values are designed to show polar interactions from residual silanols[224], as these phases are developed to include this retention mechanism it is no surprise that all phases show a degree of silanol interaction. An endcapped C18 phase would have a selectivity factor of <0.5[222] as the silanols activity is minimised as discussed in Section 1.5. The three columns that are believed to be lightly bonded C18 phases are seen to have higher $\alpha_{C/P}$ values due to the high level of exposed silanols[263][264][266].

Figure 4.1 Tanaka characterisation values – comparison of EPS phases

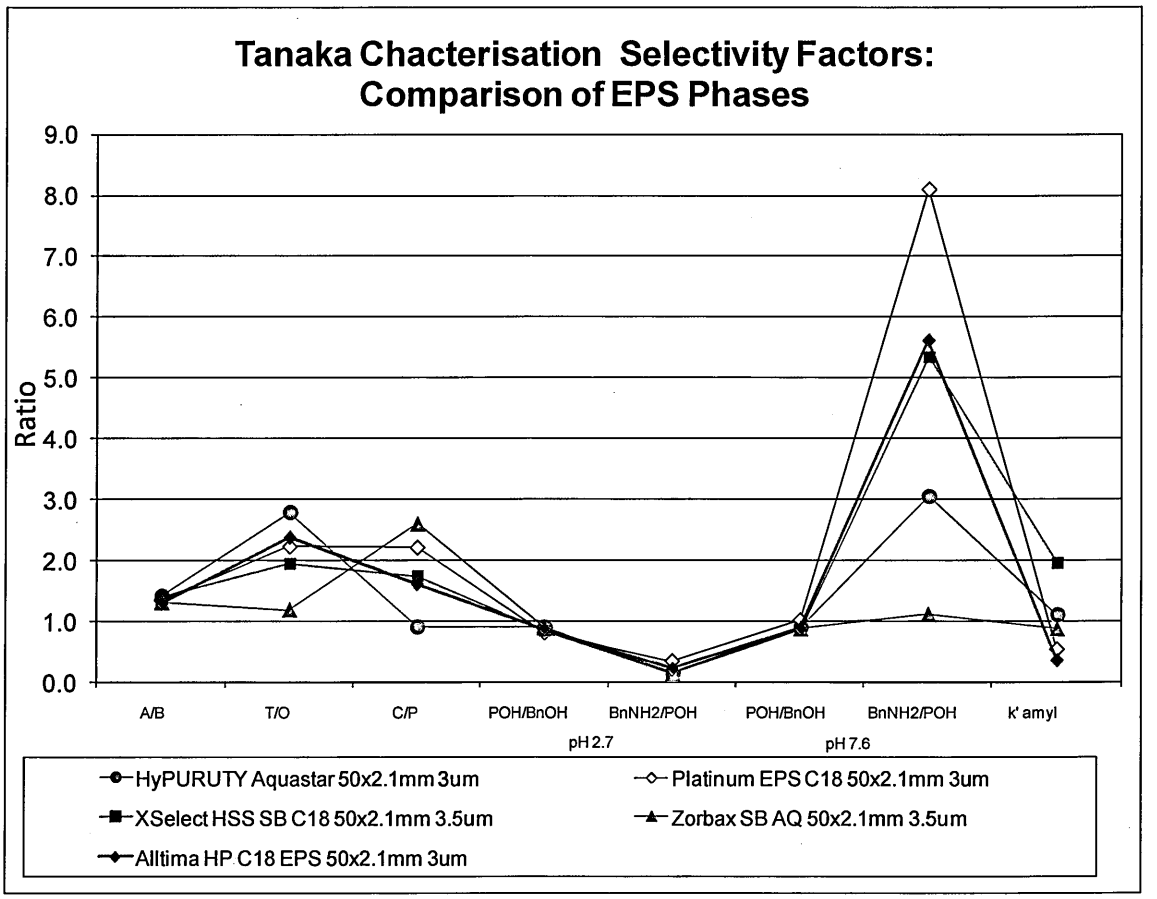

A(am) = amylbenzene, B = butylbenzene, T = triphenylene, O = *o*-terphenyl, C = caffeine, P = phenol, $BnNH_2$ = benzylamine, BnOH = benzyl alcohol

The Platinum EPS and Alltima HP phases are manufactured by the same company and it is likely they are produced by very similar synthetic routes[263][266]. The Platinum is believed to be TYPE-A silica[263] with a high percentage of acidic silanols which is indicated by the higher $\alpha_{C/P}$ value. The Alltima HP and XSelect HSS phases show a lower $\alpha_{C/P}$ value which corroborates the manufacturers claims that these phase are bonded to TYPE-B silica[263][264][266]. The Zorbax-SB AQ has the highest selectivity

factor of all the phases; this indicates a significant number of polar functionalities are available on the phase. This result is comparable to the $\alpha_{C/P}$ values determined for other Stable Bond phases, the Zorbax-SB C3 has an $\alpha_{C/P}$ value of 2.71[222], possibly indicating a secondary mechanism occurring due to the Stable Bond technology. As discussed in the Introduction, the Stable Bond range has bulky substituted groups on the bonded silane, the high $\alpha_{C/P}$ value suggests these substituents could be modified with a large number of hydroxyl groups which give raise to the polar selectivity of the Zorbax-SB AQ phase. Another possibility is that the bulky Stable Bond ligands contain aromatic functionality that are retaining the caffeine through π-π interactions, without knowing the structure of the phase these alpha values cannot be definitely allocated to specific interactions. Further analysis into the possible contribution from aromatic retention mechanism, see Figure 4.2, and the full structural elucidation of the Zorbax-SB AQ phase, see Section 4.3, would be required to fully understand this $\alpha_{C/P}$ value. The HyPURITY Aquastar has low $\alpha_{C/P}$ value indicating a lower level of silanols interaction. However it is still not clear whether this polar functionality comes from a small number of residual silanols in the surface of the silica or from less acidic polar hydroxyl-style groups on the bonded ligand, again structural elucidation will be carried out to determine this.

Phenolic selectivity is determined by the $\alpha_{POH/BnOH}$ value; for all these phases the values are comparable indicating a similar level of phenolic activity on all of the phases. The variation in $\alpha_{T/O}$ values discussed on the previous page did bring up the possibility of aromatic groups being present on the phases. Although the similar $\alpha_{POH/BnOH}$ values observed here do not rule out this as a possibility it would suggest that the level of phenolic interaction is similar for all the phases which would suggest that all phases have equal aromatic substituents or, as is more likely, none .

Finally the $\alpha_{BnNH2/POH}$ values indicate the level of electrostatic interactions from ion exchange. For the EPS phases, this component of the retention mechanism will most likely come from the residual silanols on the surface of the silica, as in the three lightly bonded phases, or from the hydroxyl

groups on the bonded ligand, which may be the case with the HyPURITY Aquastar phase. At intermediate pH all of ion exchange sites are active and the total degree of electrostatic interactions is observed. At low pH only the very acidic ionic sites are active and only the level of acidic interactions is detected.

For the three lightly bonded phases it can be seen that there are a significant number of ion exchange sites active on all three phases. The trend shows reducing activity in both total electrostatic activity and acidic ion exchange activity across Platinum>Alltima>HSS phases. As the electrostatic retention component is coming from the residual silanols on the phase it would indicate that the purity of the silica is increasing across Platinum>Alltima>HSS phases. The $\alpha_{BnNH2/POH}$ values at low pH show a smaller spread, however it is important to note that a fully endcapped C18 phase would have a $\alpha_{BnNH2/POH}$ value of <0.1[222][224]. Therefore the determined $\alpha_{BnNH2/POH}$ value for the Platinum phase indicates a difference in the base silica. This confirms the idea that the Platinum phase is bonded to TYPE-A silica as the intensity of both total and acidic silanols activity is seen to be significantly higher than the two similar phases. The Alltima and HSS phases show comparable values for the total silanols activity however the HSS phase shows a lower value for acidic silanol activity. This may be due to the HSS phase using trifunctionally bonded ligands which will preferentially bind to the acidic sites on the silica surface during the bonding process, or it may be because the HSS has purer base silica than the Alltima phase.

The Zorbax-SB AQ phase has the lowest $\alpha_{BnNH2/POH}$ value of all the phases tested at pH 7. This is an odd result as it had been seen previously that the $\alpha_{C/P}$ value for this phase was slightly higher than the other phases. The previous results were thought to indicate a large number of hydroxyl groups present on the bulky substituents on the octadecyl silane functionality however the latter results indicate they are not active ion exchange sites. It is possible that these interactions are coming from residual silanols on the base silica and the bulky substituents on the ligands incorporate other functional groups that interact with the caffeine; for example phenyl groups would be large enough

to sterically hinder solutes from interacting with the base silica. These groups would also bring secondary π-π interactions to the phase which would retain caffeine for longer. However the phase has comparable phenolic retention to the other columns which suggests all phases have comparable aromatic character which would not explain the increased $\alpha_{C/P}$ value for the Zorbax-SB AQ phase. Further characterisation work is required to determine the aromatic nature of these phases.

The HyPURITY Aquastar phase is seen to have a lower level of total silanols or ion exchange activity than the lightly bonded C18 phases and very little degree of acidic ion exchange activity. This would lead to the conclusion that the electrostatic component of the retention mechanisms of this phases comes from a small number of sites. If the interaction is from residual silanols the base silica must have a high purity with a low proportion of acidic silanols.

The extended Tanaka characterisation was carried out with these phases; however no significant differences were seen. As these methoxy- and nitro-benzene interactions are designed to pick out variations in aromatic phases the EPS phases showed a high level of co-elution with these probe analytes as these phases cannot discriminate between the differences in the molecules[222][224]. The low alpha values seen suggest little to no aromatic character on the phases. The Zorbax-SB AQ previously showed a high result for the caffeine which suggested there may be some phenyl substituents in the bulky Stable Bond ligands, however the aromatic molecules show poor retention on this phase and the results are comparable to the other EPS phases. It is possible that the fixed orientation of a bulky substituent phenyl may not give rise to phenolic interactions as the conjugated rings are not free to rotate and stack giving rise to the π-π interactions. Further investigation into the structural elucidation will be carried out, see Section 4.3, to fully assess this. The Dinitrobenzene results are shown overleaf in Figure 4.2, as an example, the full set of the results is given in the appendix.

Figure 4.2 ***Tanaka characterisation values – comparison of EPS phases***

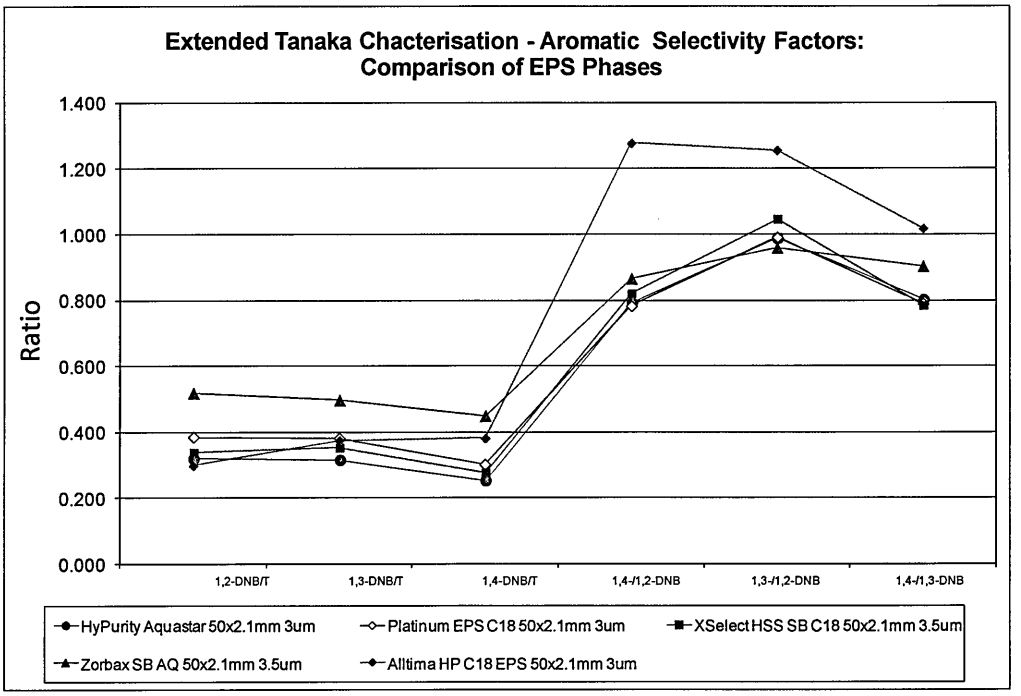

A(am) = amylbenzene, B = butylbenzene, T = triphenylene, O = *o*-terphenyl, C = caffeine, P = phenol, $BnNH_2$ = benzylamine, BnOH = benzyl alcohol

4.1.2 Principal Component Analysis of EPS Phases against Common Stationary Phase Types

Principal Component Analysis (PCA) is a chemometric tool employed to evaluate data, as discussed in Section 1.8.6. Using the alpha values from the Tanaka data described in the previous chapter, the selectivity of the EPS phases were compared against a variety of stationary phases to fully assess the retention mechanism. In order to evaluate the EPS phases the parameters of the PCA must be defined; here the alpha values from the Tanaka data shown in Section 4.1.1 and the extended Tanaka data shown in the appendix were used to determine the types of interactions involved in the retention mechanism. Data for a range of typical C18 phases and some common stationary phase types were taken from publications to compare to the EPS phases[222]. Initially the PCA model was created by mapping the different components on a loading plot, Figure 4.3. The plot captures >95% of the population and the intensity of each interaction is demonstrated by the length of the vector.

Figure 4.3 Loading plot for PCA using Tanaka Characterisation data comparison of EPS phases

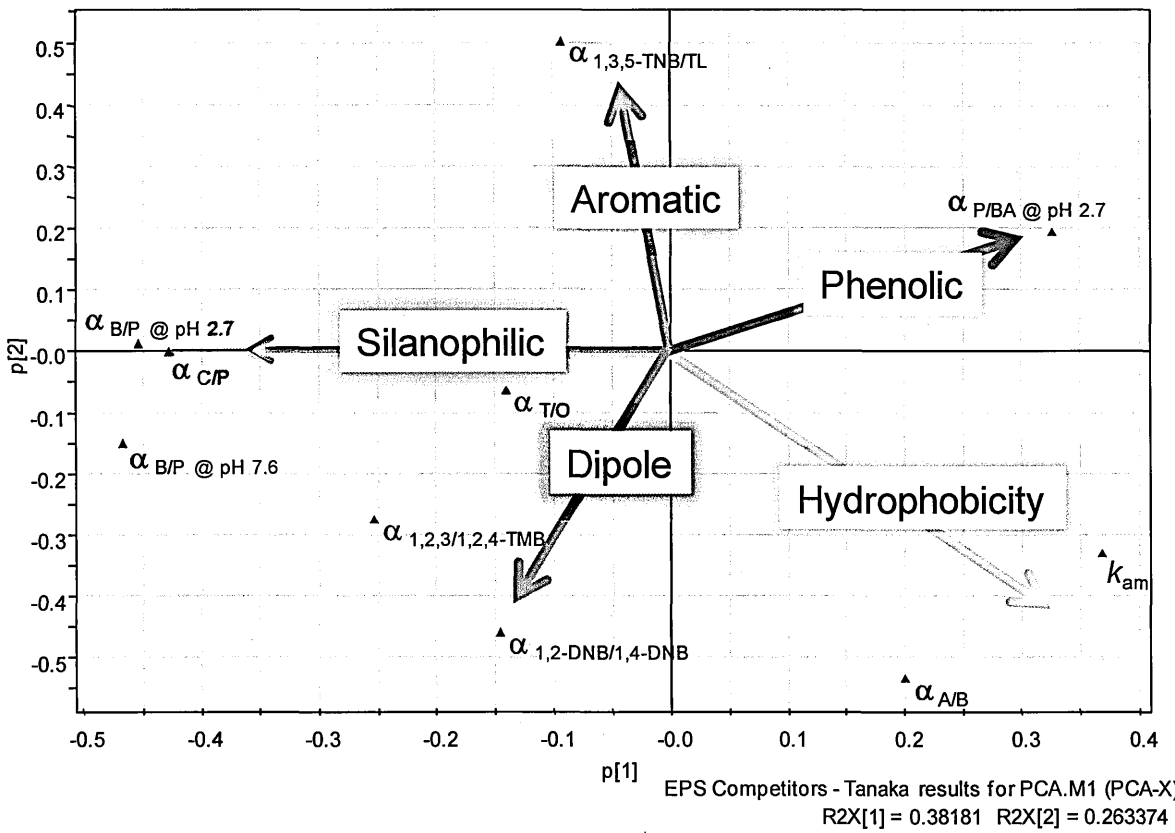

A(am) = amylbenzene, B = butylbenzene, T = triphenylene, O = *o*-terphenyl, C = caffeine, P = phenol, $BnNH_2$ = benzylamine, BnOH = benzyl alcohol

Based on these data points the directional vector for each type of interaction is overlaid onto the loading plot, these vectors will then be transferred into the model itself. Figure 4.4 below shows loading plot and PCA for the stationary phases assessed. In this instance the EPS phases are highlighted in blue, the C18 in red and the other typical stationary phases in black.

Figure 4.4 PCA using Tanaka Characterisation data comparison of EPS phases

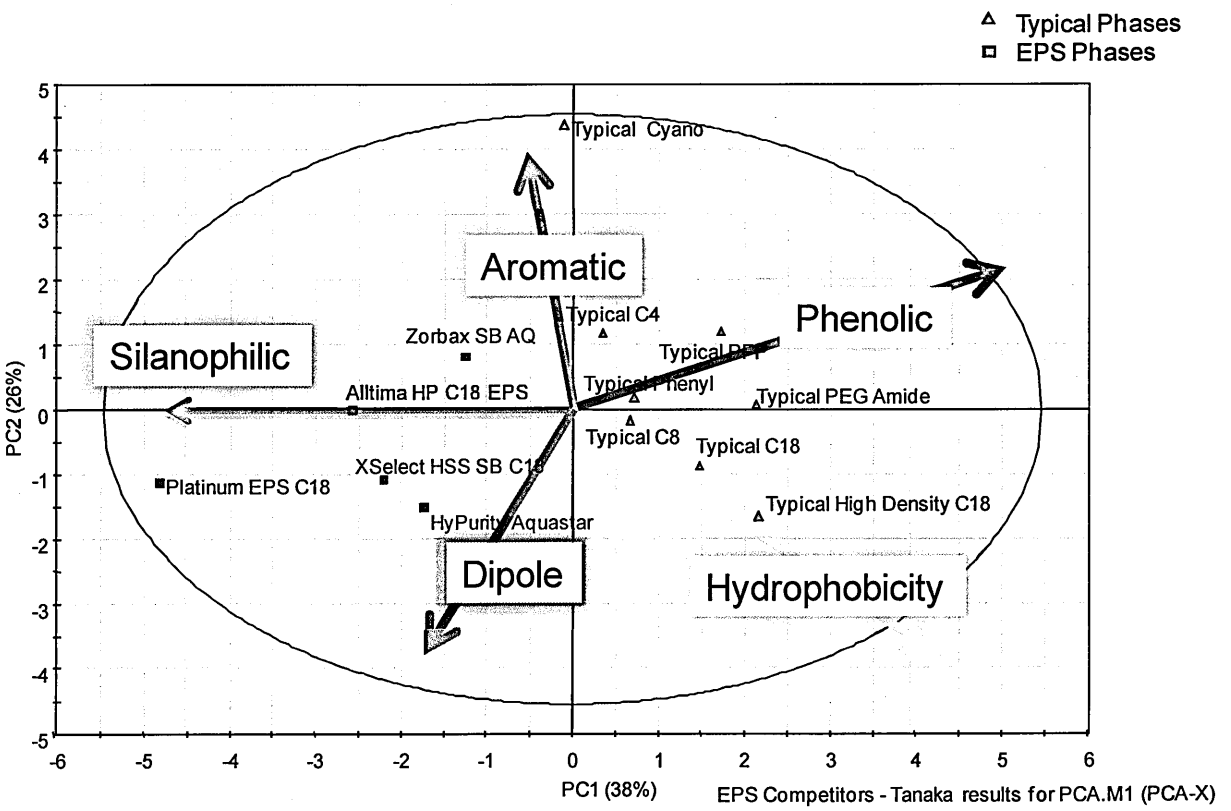

Every PCA model is different as the mathematical algorithm will automatically assess the data and assign each of the principal components in the order of bearing it has in the variance of the overall data set. With this data set a large number of octadecyl silane phases have been used therefore it is no surprise that hydrophobicity is the primary component in this model. The loading plot shows the k_{am} and $\alpha_{A/B}$ points to be located in the bottom right hand section of the model, indicating that the hydrophobicity vector will go from low hydrophobicity in the top left, diagonally down to higher hydrophobicity values in the bottom right. This can be seen from the linear progression in the

Typical C4, C8, C18 and high density C18 phases along the hydrophobicity vector as the carbon chain length increases.

As this data set contains the EPS phases the second principal component is seen to be the silanophilic interactions which increase across the x axis from right to left. This can be seen in the loading plot as the $\alpha_{B/P}$ and $\alpha_{C/P}$ values are observed in the middle left of the model. Unsurprisingly all of the EPS phases are grouped in this area with the Platinum EPS being the furthest to the left as it has exhibited the highest silanols interactions.

The visual assessment of these results brings out some interesting comparisons that were not immediately apparent from the graphs of the Tanaka data. From the manufacturer's information it was believed that the XSelect HSS and Alltima HP phases were similar phases; both being lightly bonded octadecyl silanes on high purity silica with the former being a trifunctional bonding and the latter being a monfunctional. However looking at the grouping on the PCA model it would seem that the XSelect HSS exhibits a very similar retention mechanism to the HyPURITY Aquastar and the Alltima HP is more similar in selectivity to the Zorbax-SB-AQ.

As these results would suggest the HyPURITY Aquastar is comparable to the trifunctionally bonded XSelect HSS phase further work to determine the structure of these two phases was required, see Section 4.3. From the Tanaka results it was seen that the HyPURITY Aquastar had a lower degree of silanophilic and electrostatic interactions. From this it was suspected that the polar interaction could be attributed from substituents on the bonded silane rather than the base silica. Coupled with the manufacturer's data that this is a polar endcapped phase it was assumed that the phase would have electron rich groups substituted to the linker silane, possibly on alkyl chains. From this data it is speculated that these electron rich groups could be hydroxyl groups, substituted directly to the linker silica atom on the silane, as in the hydroxyl substituted silane seen in Figure 1.12 in Section 1.6 of the introduction. If this is the case it is possible that during the bonding process these

electronegative hydroxyl groups bonded to the silica surface or crosslinked with neighbouring silanes through a dehydration reaction. The result would be a cross between a tri-functionally bonded and a polymerically bonded C18 with some hydroxyl groups unreacted across the surface. This is shown in the bonding schematic in Figure 4.5 below.

Figure 4.5 ***Schematic of possible structure for HyPURITY Aquastar stationary phase***

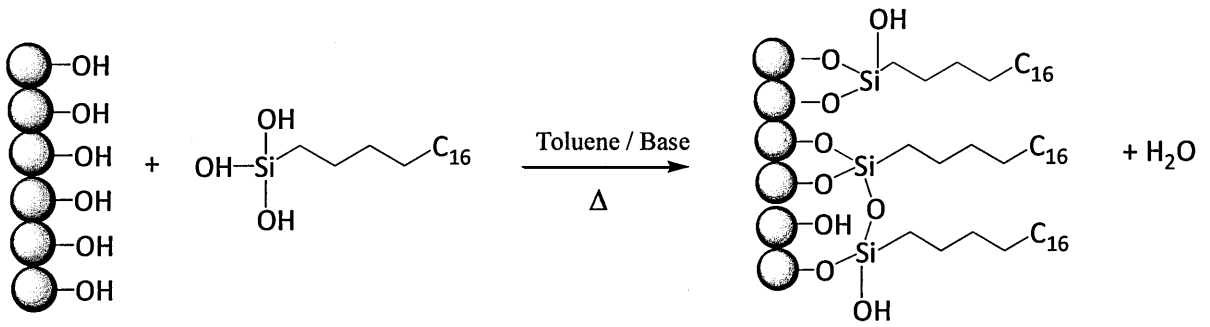

Due to its highly reactive nature $C_{18}H_{37}Si(OH)_3$ cannot be readily purchased, therefore it is more likely that a $C_{18}H_{37}Si(EtOH)_3$ ligand is used[270] and the ethoxyl groups hydrolysed to hydroxyl groups in the presence of water. The degree of crosslinking would depend on the amount of ligand used and how spatially close the silanes are to each other on the phase. This would result in some degree of electrostatic and silanophilic interactions but with little to no contribution from acidic silanols which is what was seen in the Tanaka characterisation probe results.

In the previous section some interesting results were seen for the $\alpha_{C/P}$ values for the Zorbax-SB AQ indicating the possible presence of aromatic groups. The Zorbax-SB AQ appears to lie in the aromatic region relative to the other EPS phases, however there is no positive aromatic character observed. This suggests that both the HyPURITY Aquastar and Zorbax-SB-AQ phases are not straightforward octadecyl silane bondings and further investigation is required to structurally evaluate these phases. To fully understand the structure and bonding of the silanes it would be necessary to cleave the ligand using an oxidative cleavage method followed by GC-MS analysis and full structural elucidation[271][272]. This can be seen in Section 4.3.

4.1.2 Basic Solutes and Further Characterisation of EPS Phases

The EPS phases have been shown to have significant levels of silanols or hydroxyl group interactions as part of the retention mechanism. As was discussed in the introduction this has historically been an issue for adequate separation of basic compounds as the charged analytes tend to be unevenly retained on the phases resulting in tailing and poor peak shape. Therefore a mixture of hydrophilic and lipophilic bases (Figure 4.6) were analysed on the EPS phases in both gradient and isocratic mode to determine the degree of tailing, phenol was included as a neutral molecule for comparison.

Figure 4.6 Basic molecules used for evaluation of EPS phases

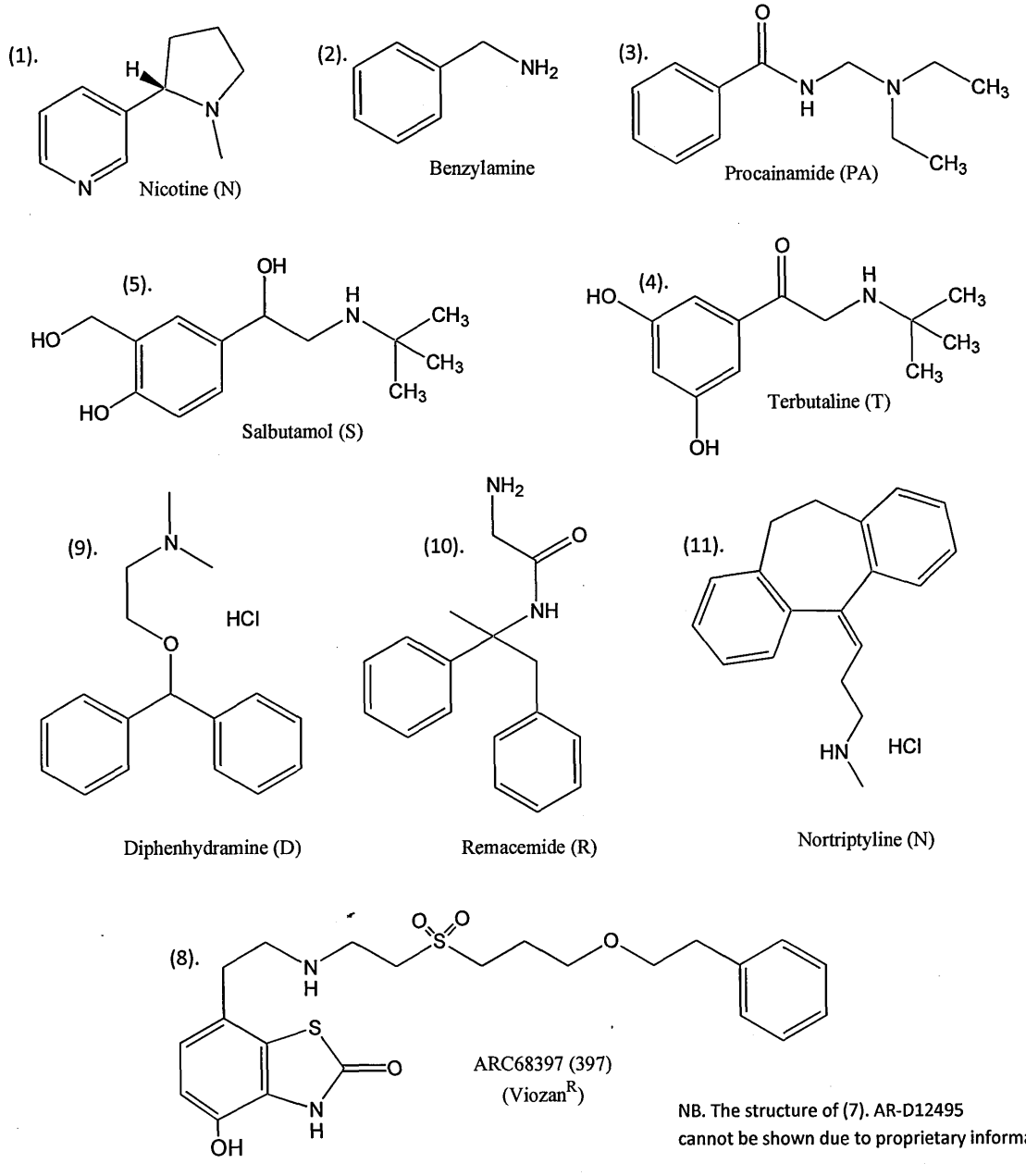

NB. The structure of (7). AR-D12495 cannot be shown due to proprietary information

Figure 4.7 ***Chromatograms of gradient analysis of all basic compounds and phenol on the EPS phases***

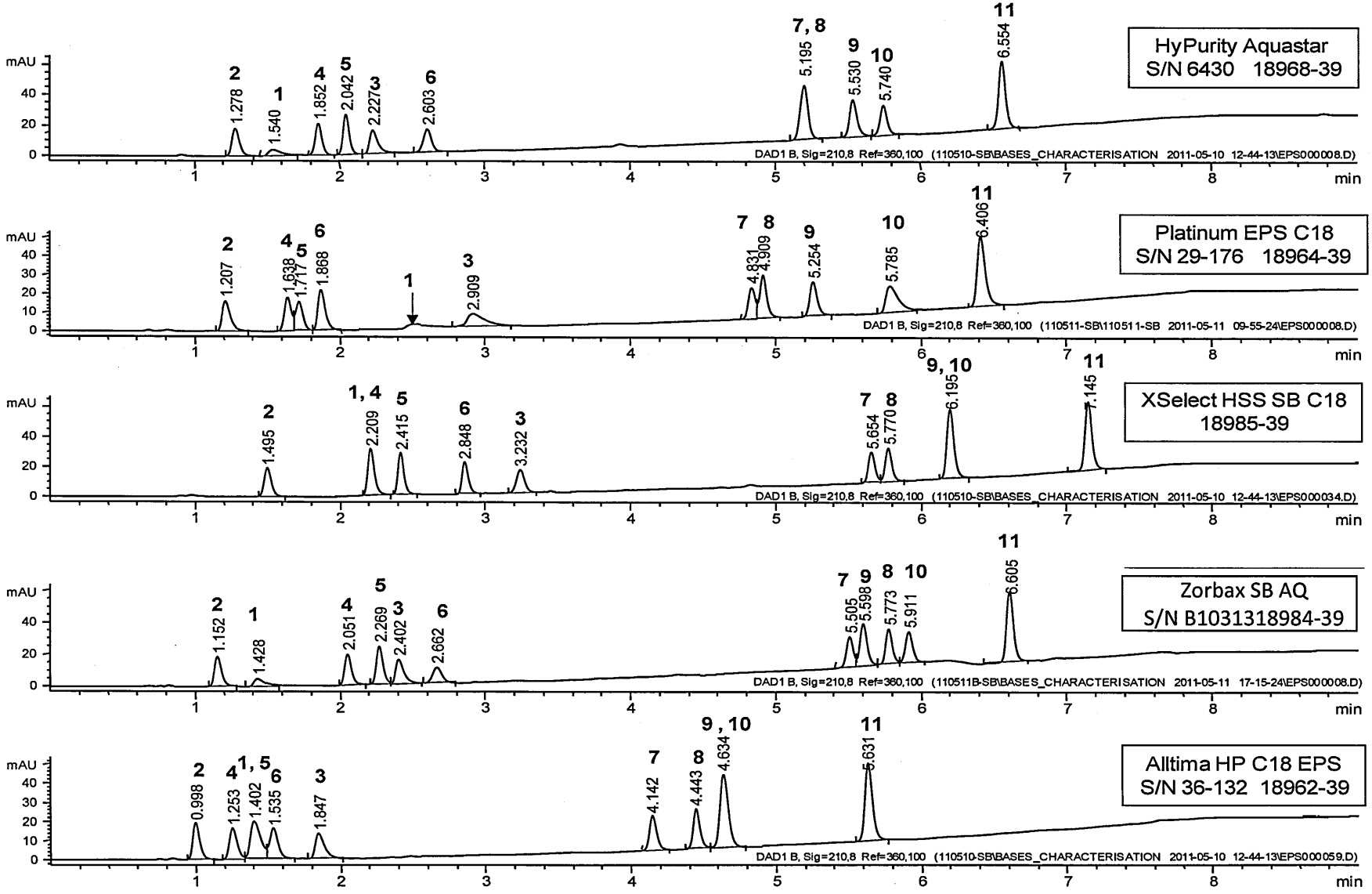

1: Nicotine, 2: Benzylamine, 3: Procainamide, 4: Terbutaline, 5: Salbutamol, 6: Phenol, 7: AR-D12495, 8: AR-C68397, 9 :Diphenhydtamine, 10: Remacemide, 11: Nortriptyline

Figure 4.8 ***Chromatograms of isocratic analysis of hydrophilic basic compounds and phenol on the EPS phases***

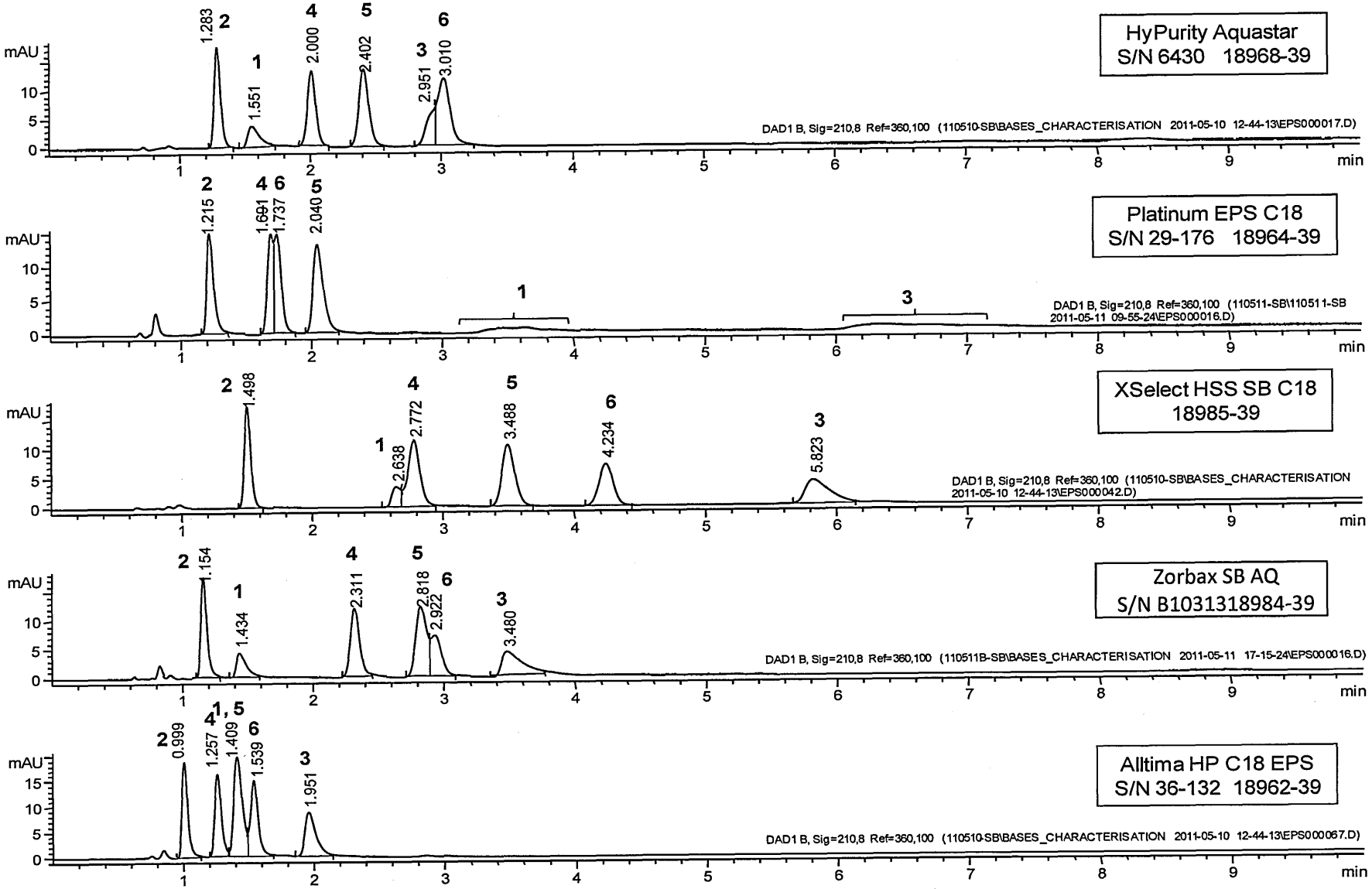

1: Nicotine, 2: Benzylamine, 3: Procainamide, 4: Terbutaline, 5: Salbutamol, 6: Phenol

Figure 4.9 ***Chromatograms of isocratic analysis of lipophilic basic compounds and phenol on the EPS phases***

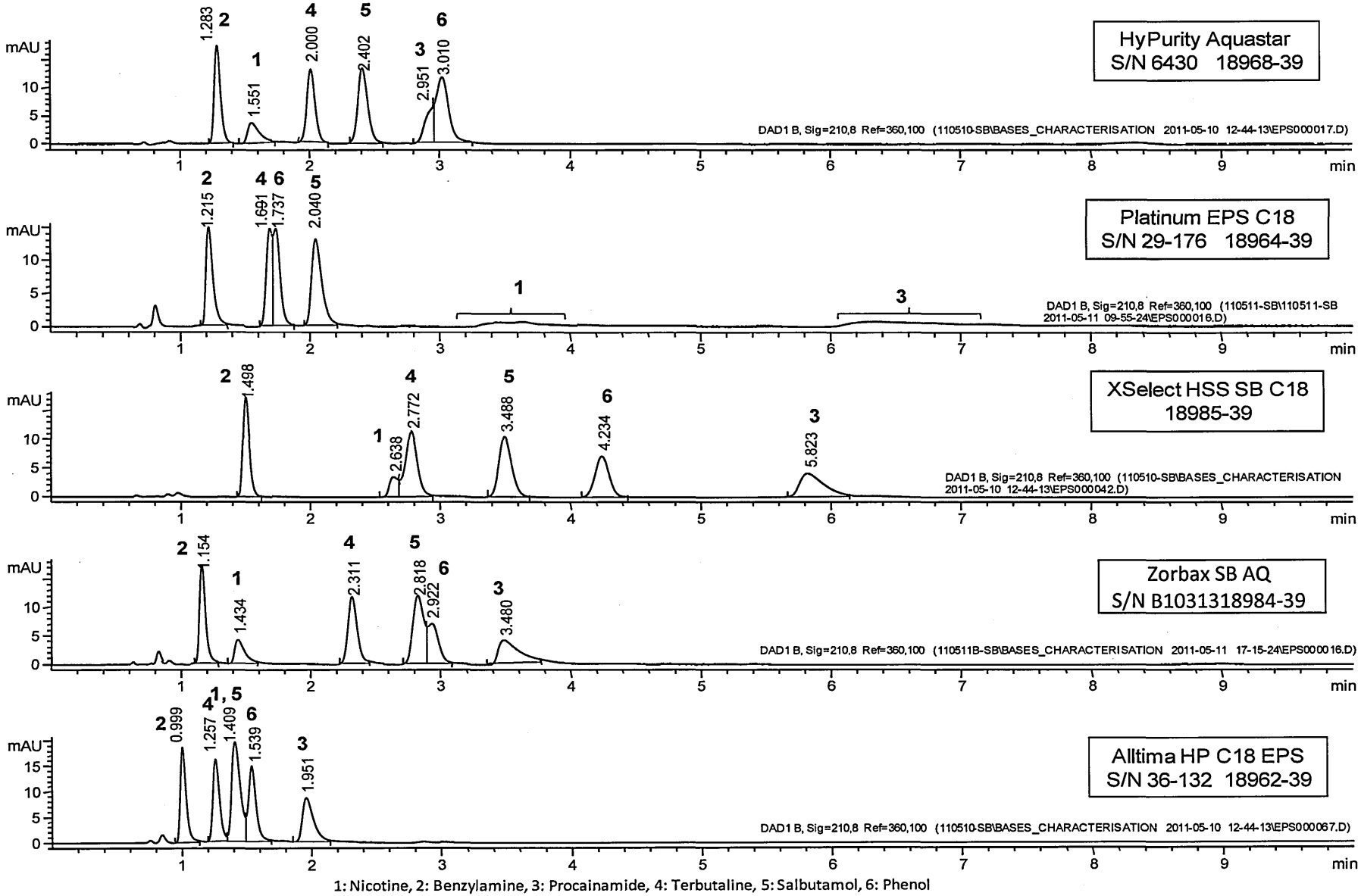

1: Nicotine, 2: Benzylamine, 3: Procainamide, 4: Terbutaline, 5: Salbutamol, 6: Phenol

The chromatograms for the gradient analysis are shown in Figure 4.7 above, the isocratic analyses are shown in Figures 4.8 and 4.9 for the hydrophilic and lipophilic bases respectively. The retention time data were tabulated and α values calculated to numerically compare the retention mechanism of the EPS phases, these are shown in Tables 4.3 and 4.4 overleaf.

Nicotine and procainamide are the most discriminatory bases as these molecules have multiple charged sites; nicotine is a diprotic base with pK_a of 3.12 and 8.02 where as procainamide is a stronger base with a pK_a of 9.32. Evaluation of the retention time and peak shape for these two solutes gives a good indication of availability of residual silanols on the phase. The longer the retention and more pronounced tailing of these peaks the greater the degree of polar functionality through silanols or hydroxyl groups. Due to co-elution with other bases the peak shape of nicotine cannot be evaluated for the XSelect HSS and Alltima HP phases. The lipophilic bases have a more Gaussian peak shape as the higher concentration of organic solvent in the mobile phase reduces the interactions between the silanols groups and the analytes.

The Platinum is the most prominent outlier; it has a much lower $\alpha_{P/B}$ value for the gradient analysis but a considerably higher $\alpha_{PA/B}$ value for the hydrophilic isocratic run. Here it is likely that the ionised amino substituents on the benzylamine and the procainamide are retained by the more acidic silanol groups caused by metal ions on the surface silica whereas the phenol, which has no positive character, is not affected by this. The procainamide has multiple amine groups that will be ionised to quaternary nitrogen atoms at this low pH and therefore is retained significantly longer than benzylamine. This can also be seen in the chromatogram as the procainamide peak is broad and tailing, even on the gradient analysis, through its interactions with the variable acidic silanols.

The hydrophilic bases also showed a difference with the Platinum phase on the $\alpha_{P/Ni}$ value, the difference in α value is not as pronounced however the chromatograms show how different this base silica is. Here the peaks for nicotine and procainamide are so broad and tailed it is difficult to

distinguish them from the base-line. The plot of the lipophilic bases shows the Platinum again to have different values from the other phases although the trend of α values is comparable across all phases. The chromatograms generally show all peaks to be reasonably Gaussian even on this isocratic run this is not surprising due to the higher percentage of organic solvent used.

Table 4.3 Selectivity factors for all basic compounds by gradient analysis on EPS phases

	$\alpha_{P/B}$	$\alpha_{S/T}$	$\alpha_{397/P}$	$\alpha_{397/495}$	$\alpha_{397/D}$	$\alpha_{No/P}$
HyPURITY Aquastar 3um	3.353	1.167	2.381	1.002	0.932	3.099
Platinum EPS C18 3um	1.971	1.241	4.079	1.019	0.829	5.523
XSelect HSS SB C18 3.5um	3.065	1.132	1.984	1.023	0.923	2.518
Zorbax-SB AQ 3.5um	4.789	1.168	2.628	1.056	1.036	3.063
Alltima HP C18 EPS 3um	3.123	1.293	4.681	1.089	0.951	5.501

N = nicotine, B = benzylamine, PA = procainamide, S = salbutamol, T = terbutaline, D = diphenhydramine, R = remacemide, N = nortriptyline, 397 = ARC68397

Both the Platinum and the Alltima show a higher value of $\alpha_{397/P}$ which may be because the lower coverage of these two phases relative to the other EPS phases and this could have resulted in a lower retention of phenol. This would also account for the lower $\alpha_{397/P}$ value of the XSelect HSS phase as it was seen in the Tanaka characterisation that this phase has a higher ligand density which would increase the retention time for phenol.

This trend is also seen in the variation in $\alpha_{No/P}$ as the nortriptyline also has a long hydrocarbon chain which is retained through hydrophobic interactions, the phases with a greater ligand density such as the XSelect HSS phase have higher retention time for nortriptyline. However these phases also have

a higher retention time for phenol so the resulting $\alpha_{No/P}$ value is actually smaller than the phases with a lower ligand density. In isocratic analysis these values are significantly different as here the phenol has greater affinity for the higher percentage of organic solvent in the mobile phase and it is therefore not well retained.

Table 4.4 Selectivity factors for basic compounds by isocratic analysis on EPS phases

	Hydrophilic Bases				Lipophilic Bases			
	$\alpha_{P/S}$	$\alpha_{S/T}$	$\alpha_{P/Ni}$	$\alpha_{PA/B}$	$\alpha_{397/P}$	$\alpha_{495/P}$	$\alpha_{D/P}$	$\alpha_{No/P}$
HyPURITY Aquastar 3um	1.347	1.327	2.749	3.958	1.817	1.464	2.437	5.698
Platinum EPS C18 3um	0.776	1.351	0.357	10.723	3.979	2.127	2.831	9.317
XSelect HSS SB C18 3.5um	1.263	1.340	1.806	6.150	1.630	1.800	2.825	6.163
Zorbax-SB AQ 3.5um	1.048	1.302	2.853	5.447	1.801	1.907	1.980	4.494
Alltima HP C18 EPS 3um	1.198	1.302	1.198	4.870	1.783	1.783	2.934	5.660

N = nicotine, B = benzylamine, PA = procainamide, S = salbutamol, T = terbutaline, D = diphenhydramine, R = remacemide, N = nortriptyline, 397 = ARC68397

A similar evaluation for acidic compounds was carried out with the results showing very few differences in the majority of the α values. These results are shown in the Appendix. This analysis was also run at low pH and therefore both the analytes and hydroxyl groups of the stationary phases are unionised and the only interactions would be from the stronger hydrophobicity of the octadecyl silane and the weaker hydrogen bonding of the hydroxyl groups themselves. The main variation in the acid characterisation was observed in the $\alpha_{PP/P}$ value, by assessing the k values it can be seen that the retention factor of the 4-hydroxybenzoic acid propyl ester is the cause of this variation. As the trend of higher retention time is comparable with the increased hydrophobicity of the phases this is likely to be due to the ester group on this analyte.

4.1.3 100 Compounds Evaluation: S Value Calculation for EPS Phases

A large selection of basic, acidic, neutral and phenolic compounds were chosen to evaluate the retention mechanisms of each of the EPS phases. The retention mechanisms were compared against a typical monofunctionally bonded and endcapped C18 phase; in this case a ACE 3 C18 column was used for comparison. The analytes were split into the separated functional type so each group can be assessed. The retention time of each analyte was determined by gradient analysis using both methanol and acetonitrile as an organic solvent and using formic acid and phosphate buffer as a pH modifier. To ensure the validity of these results a sample of toluene was injected every 20 samples and the retention time, peak area, symmetry, and width were compared and shown to have an RSD <3%. These are tabulated in the appendix.

Only the results of the acetonitrile gradient using 0.1% v/v formic acid as a pH modifier is shown here as all sets of analysis showed the same trends, the remaining results are shown in the appendix. The retention times for methanol are slightly longer due to the lower solvating power of this organic modifier. Mass transfer is also improved for many analytes, giving better peak shape. The retention times were compared graphically and the linearity and correlation coefficient (R^2) of all compounds was also determined.

Comparison of the HyPURITY Aquastar phase against the ACE C18, in Figure 4.10 overleaf, shows the correlation coefficient to be >0.9 which indicates the phases have similar retention mechanisms. From previous characterisation results and manufacturer's information it is thought that the Aquastar phase is a mixture of mono-functionally and tri-functionally bonded octadecyl silane with no endcapping on the surface. The ACE 3 C18 is thought to be a mono-functionally bonded octadecyl silane with small hydrocarbon endcap (i.e. a non-polar endcap). The tri-functionally bonded Aquastar has been shown to have a small amount of non-acidic silanophilic interactions, likely from unreacted arms of the ligand which are hydrolysed to hydroxyl groups or from the residual silanols on the

surface of the silica. The two phases are similar in structure with the main difference to the retention mechanism being the more readily accessible silanols on the Aquastar. The difference between mono- and tri-functional bonding may have an effect on the retention mechanism but it is not possible to determine that from this data as the base silica and ligands for these two phases are not comparable. The acids, neutrals and phenols are seen to elute earlier on the EPS phase which is as expected due to the lower hydrophobicity of the phase. The lower carbon load and $k_{(am)}$ value seen in the Tanaka testing indicates there is a lower percentage of the octadecyl silane ligands bonded to the Aquastar phase. Bases are seen to elute at a comparable or slightly longer retention times most likely due to the extra interaction with the hydroxyl groups on the EPS being comparable to their affinity on the more hydrophobic C18.

Figure 4 .10 Comparison of HyPURITY Aquastar and ACE C18 using Formic Acid and Acetonitrile

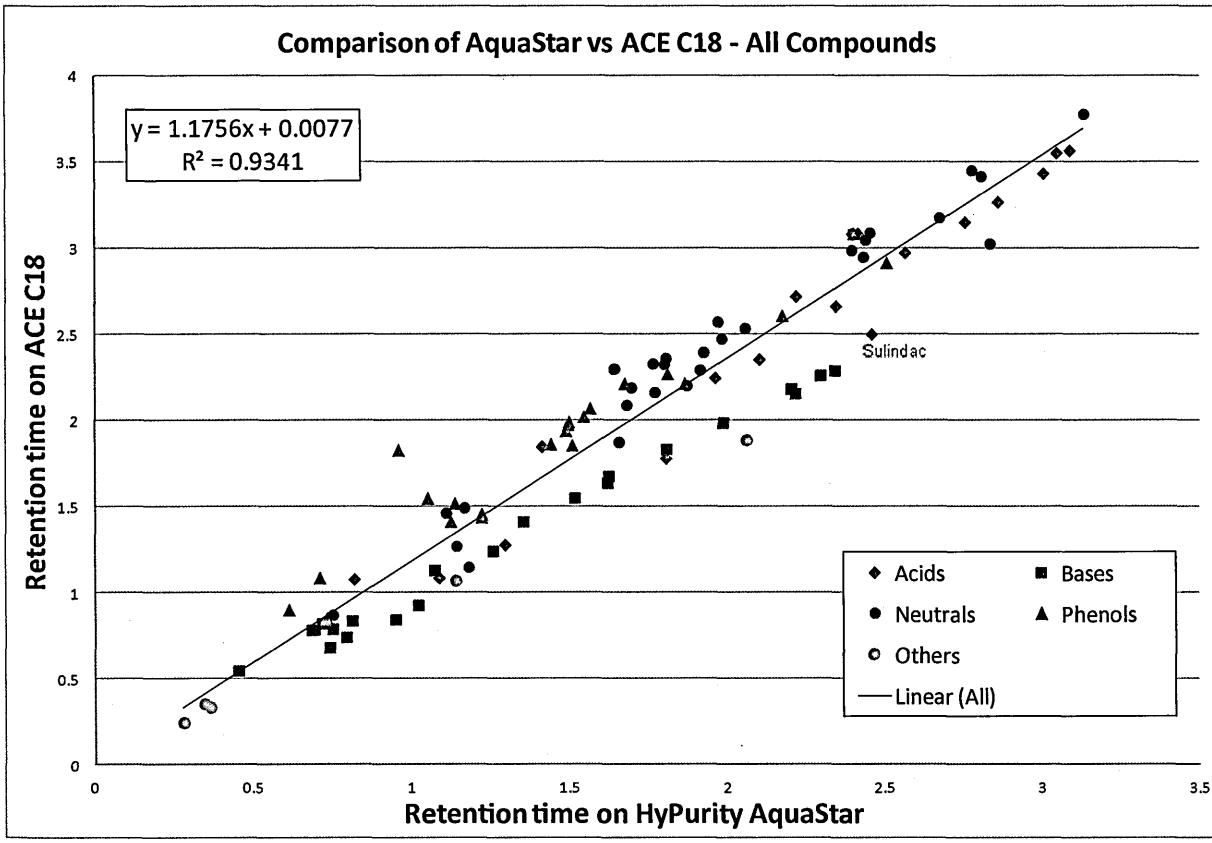

The Platinum EPS phase (Figure 4.11) shows significantly different retention times; here the correlation to the ACE C18 is extremely low with a coefficient <0.4. Again the neutrals, acids and phenols have a shorter retention time on the Platinum than the ACE C18, as the phase is only lightly bonded this is most likely due to the lower hydrophobicity, as seen from the Tanaka characterisation testing. In this case the bases are seen to elute later on the Platinum phase, indicating that there are strong interactions between basic analytes and the stationary phase which are greater than the hydrophobic interaction the same analytes would have with the ACE C18. Trimethylbenzylamine is also shown to have a long retention time on the Platinum EPS phase. This molecule contains a quaternary amine salt; the positively charged nitrogen will be retained by ionised acidic silanols on the Platinum EPS phase similar to the retention mechanisms seen for the basic molecules.

Figure 4.11 Comparison of Platinum EPS C18 and ACE C18 using Formic Acid and Acetonitrile

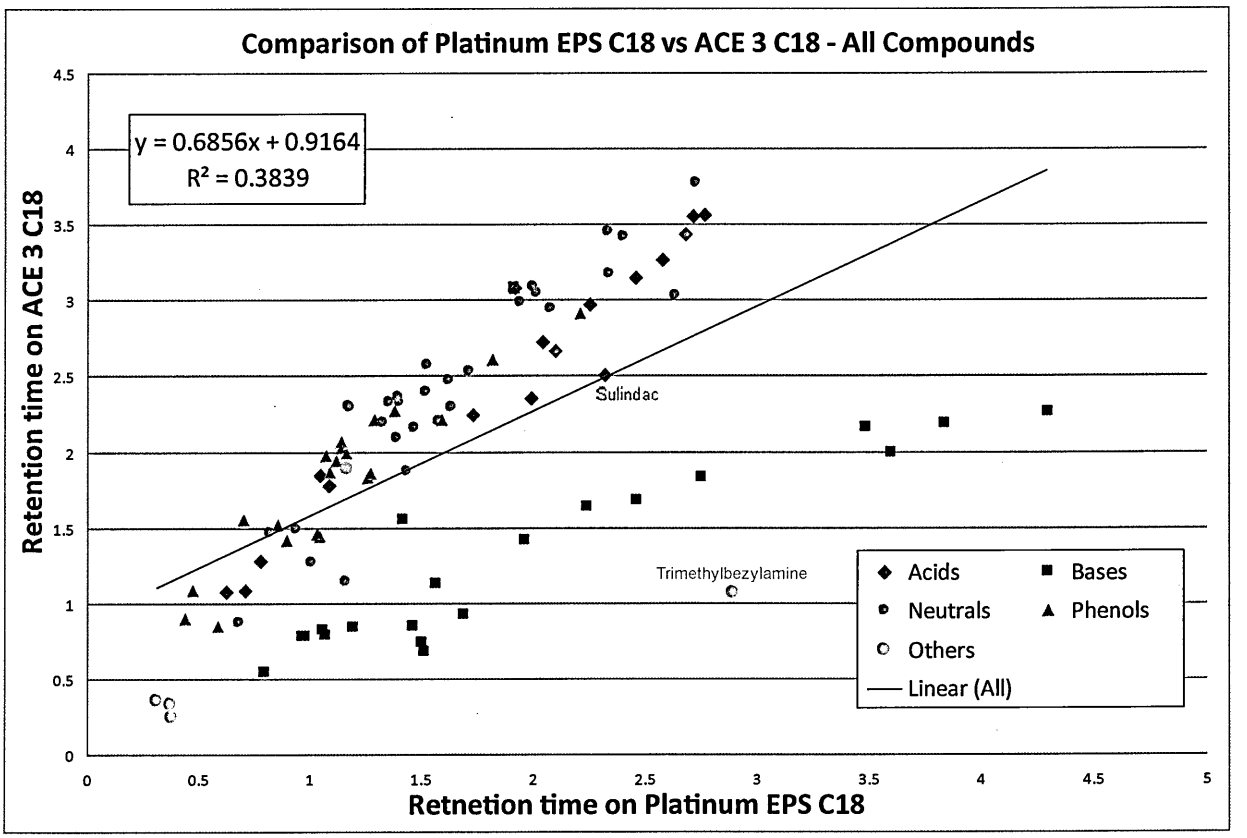

These interactions are most likely occurring on the silica itself and the bases are being retained by strong anionic interactions with the residual silanols. Again this mirrors the findings from the Tanaka characterisation and evaluation of basic molecules shown earlier in this chapter. It is believed from these characterisation probes that the Platinum silica is the TYPE-A silica which contains a higher level of metal ions. This was confirmed by the longer retention and poor peak shape of the hydrophilic bases on Platinum phase compared to the other EPS phases analysed.

Evaluation of the peak width of each solute analysed in the 100 compound mixes gave an interesting insight to the Gaussian nature of these retention mechanisms. By reviewing the sum of all peak widths it is possible to get a general feel for the peak shape, Table 4.5 shows a summary of the sum of peak widths, it can be seen that although all EPS phases have a slightly higher peak width result than the ACE C18, between 10% and 30% increase is observed for most phases. However the sum of the peak widths analysed on the Platinum EPS phase is seen to be double those analysed on the ACE C18. This shows that although the Platinum EPS gives highly complementary separations to the ACE C18 the pay-off from this is a large reduction in peak symmetry which may not be acceptable for analytical methodology.

Figure 4.12 overleaf shows the comparison plot for the XSelect HSS phases, a correlation co-efficient of >0.95 indicates this phase does not demonstrate a significantly different retention mechanism to ACE C18. This confirms the findings of the Tanaka characterisation work which showed this phase to have the highest $k_{(am)}$ value which indicates a higher level of ligand density than the other EPS phases.

Figure 4.12 Comparison of XSelect HSS SB C18 and ACE C18 using Formic Acid and Acetonitrile

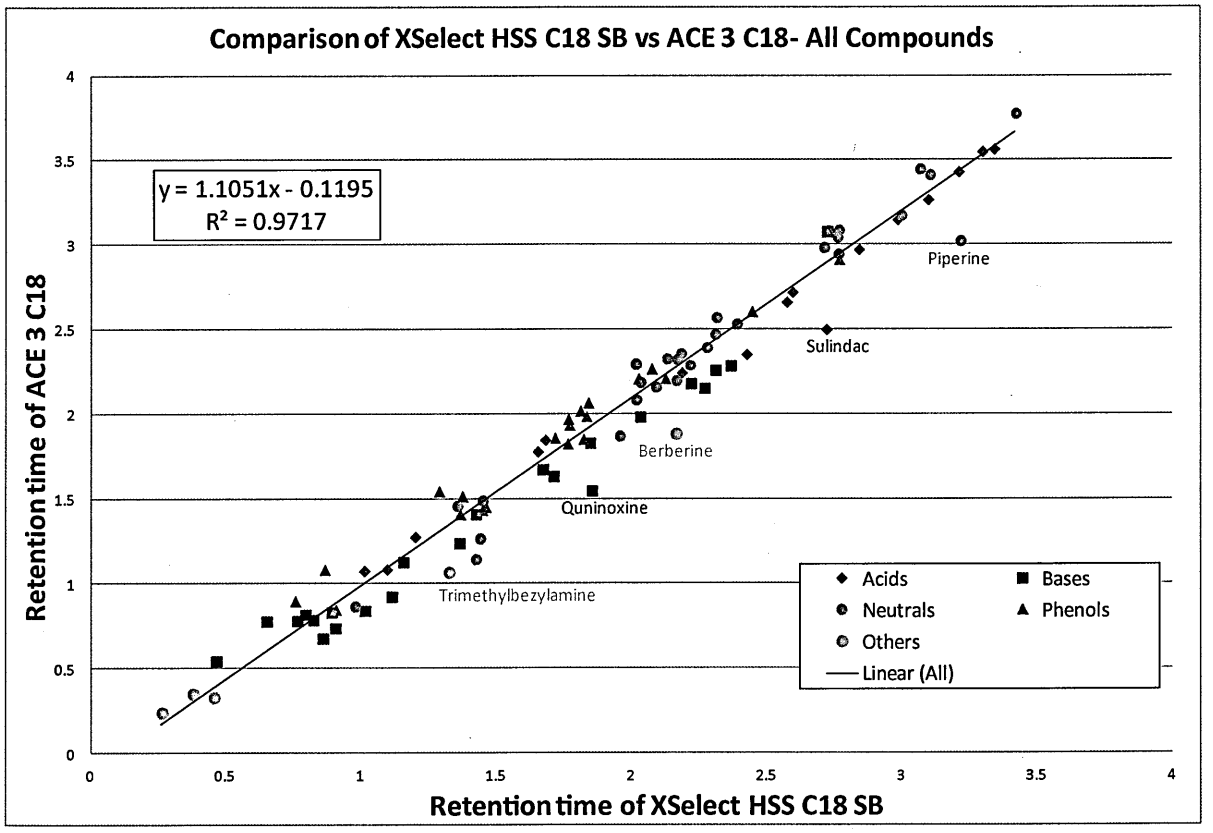

The Tanaka characterisation results indicated a degree of silanophilic interaction was contributing to the overall retention mechanism which is likely to be a result of residual silanol groups on the phase. The majority of these interactions were shown to be non-acidic silanols resulting from the highly pure TYPE-B silica used for this phase. This would explain the high level of correlation with the ACE 3 C18 phase observed here.

The few outliers, indicated in Figure 4.12 above, that are seen to be retained longer on the XSelect HSS phase all contain functional groups such as amine and sulphonic groups that would become charged at low pH. These dipole-dipole charged nitrogen or sulphur atoms would then show a greater level of interaction with the available silanols. The sum of the peak widths is shown to be lower on the XSelect HSS phase than the other EPS phases, showing a lower tailing factor for these analytes. Again this confirms the purity of the silica used for this phase.

Figure 4.13 Comparison of Zorbax-SB AQ C18 and ACE C18 using Formic Acid and Acetonitrile

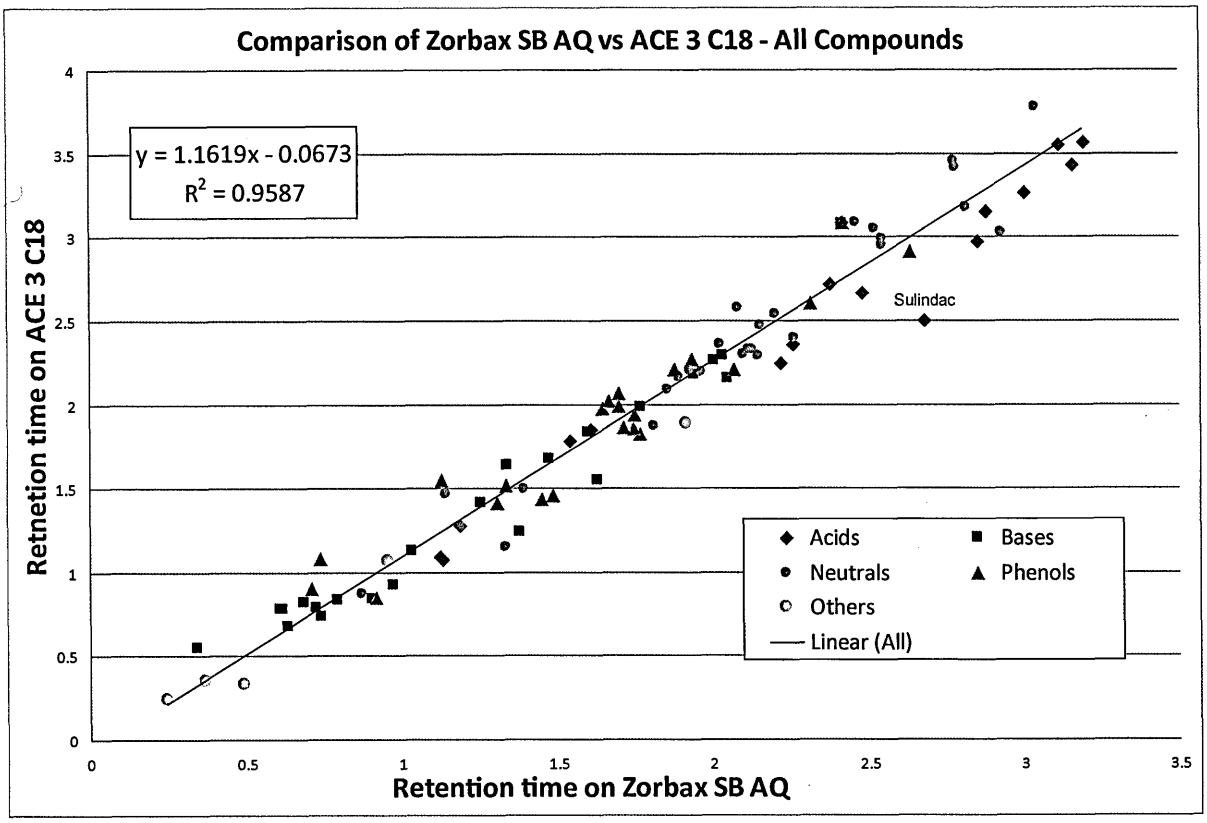

The Zorbax-SB AQ results (Figure 4.13) showed that this phase also has a comparable retention mechanism to the ACE C18 phase and again the correlation coefficient is >0.95. Some of the neutral and phenol molecules are shown to have a lower retention on the Zorbax-SB AQ phase which may be due to the lower carbon load but not to the degree of the Platinum or Aquastar phases shown earlier.

From the Tanaka characterisation work shown in Section 4.1.1 it was seen the retention time of caffeine was longer than expected on the Zorbax-SB AQ phase. The possible reasons for this were theorised as silanophilic interactions from the non-acidic silanols either in the bulky Stable Bond groups or on the silica surface or through π-π interactions with phenyl groups within the Stable Bond. Comparison of the retention time for all phenyl compounds analysed are shown below in Figure 4.14. If it is assumed that the ACE 3 C18 phase has no aromatic functionality, based on the manufacturer's data[265] then the retention mechanism for this phase is purely through hydrophobic

and a small amount of silanophilic interactions. As retention times for the phenyl analytes is comparable on both the Zorbax-SB AQ and the ACE 3 C18 phases this indicates there are no π-π interactions contributing to the retention mechanism. Further structural elucidation of the ligands would be needed to confirm this however from the chromatographic results it would appear that the bulky stable bonds are branched hydrocarbon chains and do not contain any aromatic functionality.

Figure 4.14 ***Comparison of neutral and phenolic compounds on Zorbax-SB AQ C18 and ACE C18 using Formic Acid and Acetonitrile***

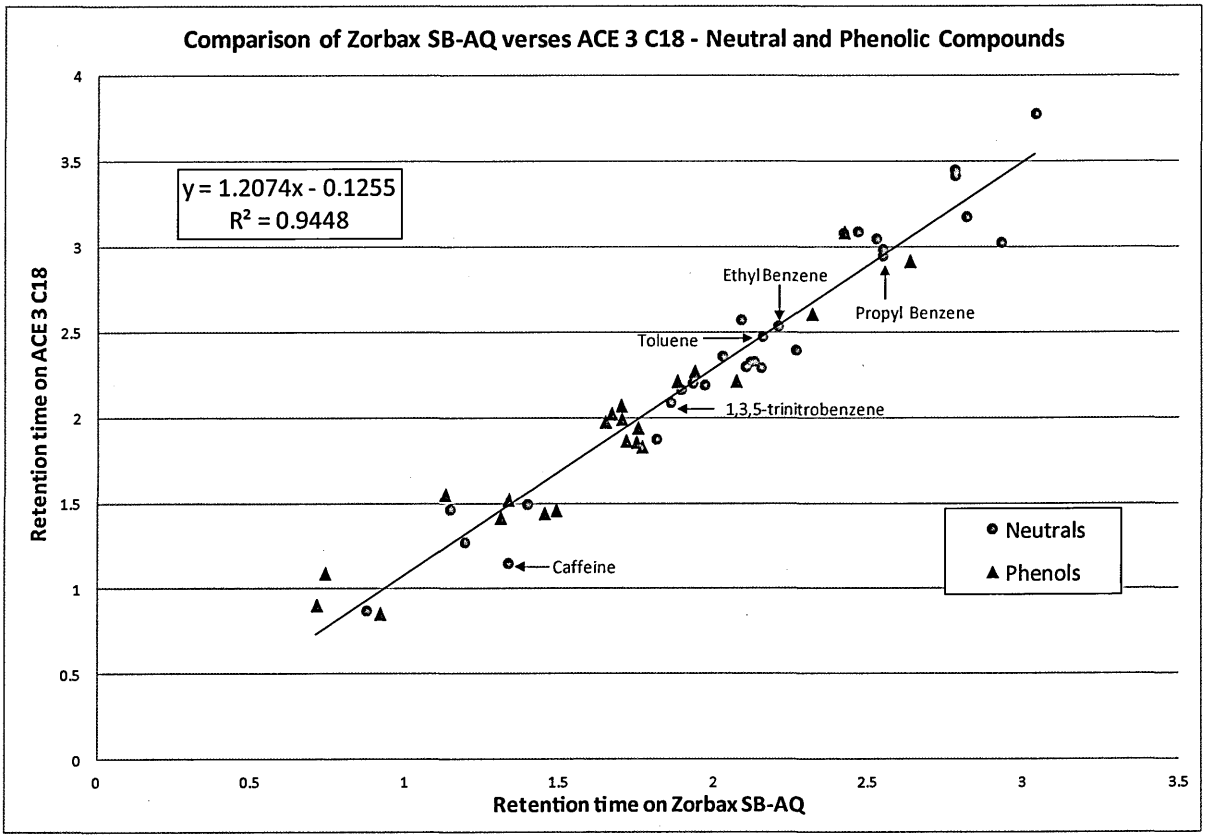

The Alltima HP EPS phase comparison is shown in Figure 4.15, this phase also shows a marked difference in retention mechanism from the ACE C18 with a correlation coefficient of 0.8. The trends are comparable to the previous phases with acids, neutrals and phenols having a slightly lower retention time on the EPS but the basic compounds are retained for longer. The manufacturer's data

and the Tanaka characterisation has shown the Alltima phase to be similar in bonded ligand structure and density to the Platinum EPS however the difference in silica purity is most pronounced when comparing the peak widths for this analysis. The sum peak width for all compounds is shown in Table 4.5 overleaf; the increased value observed for the Platinum phase is an indication of the degree of tailing seen on the basic compounds and other charged analytes during this analysis.

Figure 4.15 Comparison of Alltima HP EPS and ACE C18 using Formic Acid and Acetonitrile

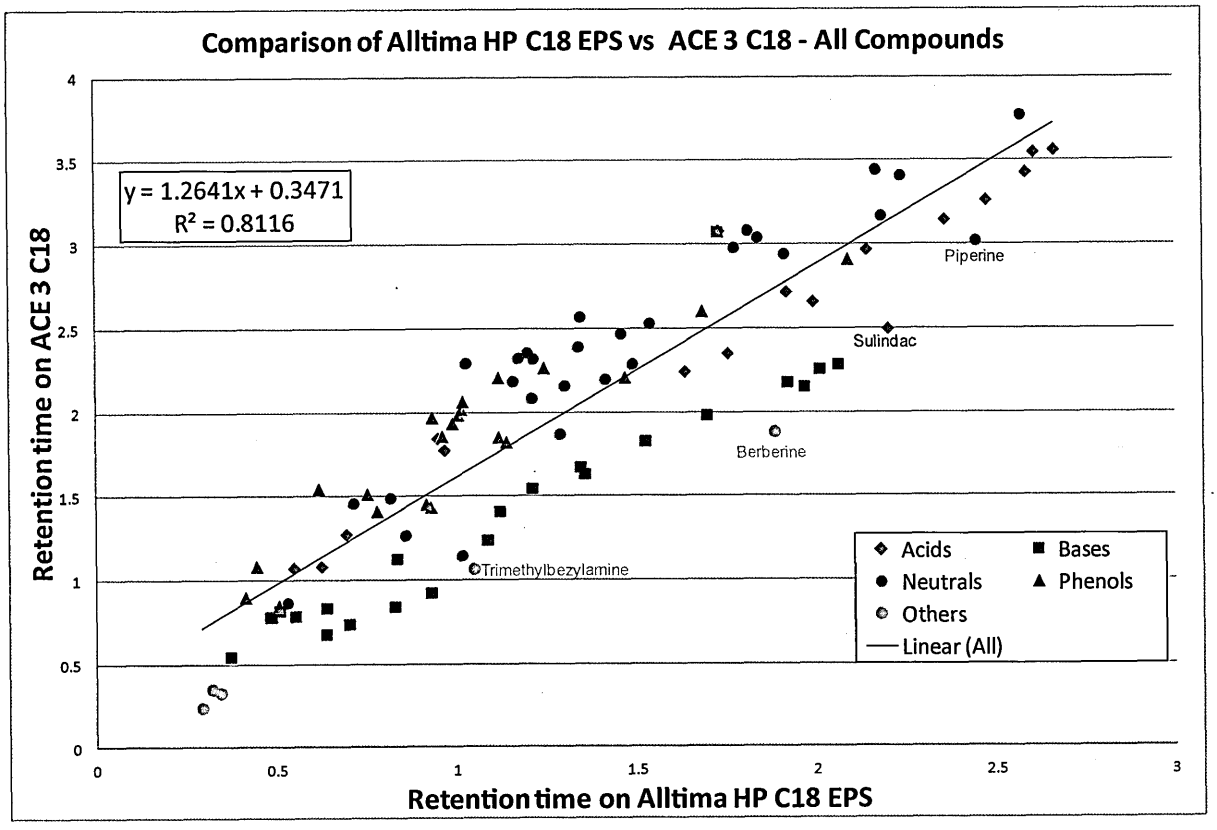

One interesting outlier for all the EPS phases is seen to be sulindac; as an acidic compound analysed at low pH it would be expected that the retention mechanism would be based solely on the hydrophobic interactions of the octadecyl silane and would not be affected by the silanol interactions. However it has been shown that sulindac has a longer retention than expected on the EPS columns. One possible reason for this may be that the sulphoxide exists as two resonance structures of the polarised double bond and the dative bond between the oxygen and the sulphur as shown in Figure 4.16 overleaf. The oxygen of the sulphinyl group will carry a partial charge which

may become protonated, the resulting partial positive charge on the sulphur would be retained longer of the EPS phases through electrostatic interactions.

Figure 4.16 Resonance structures of sulphinyl group of sulindac

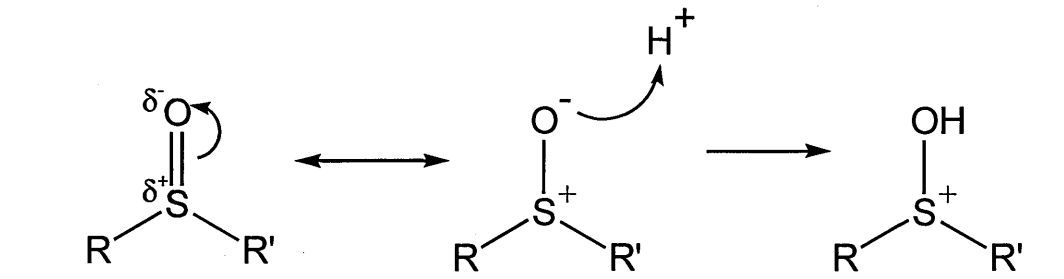

Polarised double bond form Dative bond form Protonated form

This would be the most probable explanation as no contribution from aromatic interactions has been seen for the retention mechanism on any of the EPS phases which would cause an increase in retention time for this analyte. It would be likely that the electronegative fluorine and hydroxy groups present on sulindac would actually be repelled by the residual silanols on the stationary phase at low pH, this would cause a decrease in retention time.

The S Values were calculated from the correlation coefficient as discussed in Section 1.8.3 for each of the columns against the ACE 3 C18 phase. These can be seen in Table 4.5 overleaf. The calculated S Value for a typical phenyl phase against a C18 would be around 16 to 20 depending on the length of the carbon linker chain[235].

It can be seen that the added polar functionality of the residual silanols, or possibly hydroxyl groups in the case of the Zorbax-SB AQ and HyPURITY Aquastar phases, allows the EPS phases a highly complementary selectivity against an endcapped octadecyl silane phase.

Table 4.5 ***Comparison of S values, correlation coefficient and peak width for all EPS columns***

Phase	Correlation Coefficient (r^2)	S Value	Σ All Peak Width of 100 Compounds (seconds)
ACE 3 C18	1.0000	-	2.8183
HyPURITY Aquastar	0.9341	26	3.7405
Platinum EPS	0.3839	78	5.6731
HSS C18-SB	0.9717	17	3.1471
Zorbax AQ-SB	0.9587	20	3.3633
Alltima HP EPS	0.8116	43	3.6404

The differences in these phases can be shown to be greatly affected by selecting a small group of compounds that are seen to have the greatest differences in selectivity across the columns and comparing the retention times on each phase. The Zorbax-SB AQ and XSelect HSS phases have been omitted from this analysis as they did not show significantly different retention times against the ACE C18 phase.

The chromatograms of this test mixture on each of the four columns are shown in Figure 4.17 overleaf. The main areas of co-elution on the ACE 3 C18 are highlighted and the corresponding peaks are indicated on the three EPS phases. This mixture was designed to give the greatest selectivity on the Alltima HP phase therefore it is no surprise that all fourteen compounds are separated in a little over 2 minutes run time. The change in elution order is more pronounced on the Alltima HP and Platinum EPS phases than on the Aquastar column. In the case of the phenols, methyl paraben and vanillin, the peak shape is actually sharper on the Platinum phase. However for basic analytes such as amiloride, the peak shape is significantly more tailed.

Figure 4.17 *Multiple compound test mix on ACE C18 and EPS phases using Formic Acid and Acetonitrile*

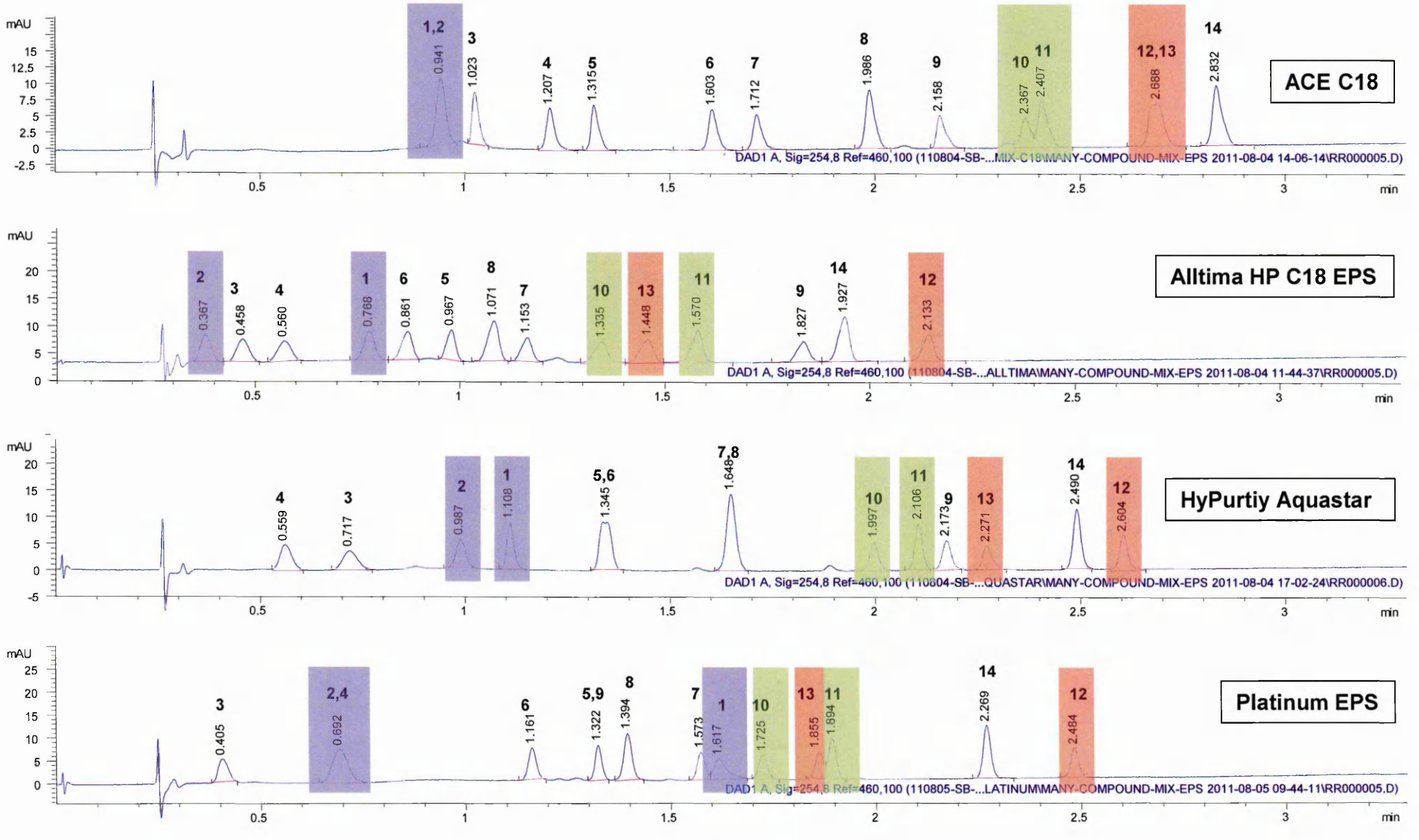

1. Amiloride 2. Metronidazole 3. 1,3-dihyrdoxybenzene 4. 4-hydroxybenzoic acid 5. Caffeine 6. Vanillin 7. Qunioxaline 8. Methyl paraben 9. Berberine 10. 1,2,3,4-tetrahydro-1-naphthaol 11. Furosemide 12. Sulindac 13. Methylbenzoate 14. Tolmetin

The overall peak shape appears to be Gaussian on the Alltima phases although some tailing is observed especially for the basic or charged analytes. However the peak widths are seen to be larger than expected given the low concentration of these analytes, which should minimise any band broadening or overloading effects. The columns used in this analysis were re-packed from silica material recovered from unused large bore columns into the small dimension HPLC columns. It may be possible that the bonded silica may have been modified during this process. It is also possible that the column packing may not have been uniform across all the EPS phases which may account for variations in efficiency. Due to the volume of material available it was not possible to repeat this analysis on a second column; ideally this analysis would have been performed on a brand new Alltima EPS phase to assess whether the increase in peak width was due to the packing process.

A second test mix was also analysed, the chromatogram is shown in Figure 4.18. This time the retention times on the HyPURITY Aquastar phase were utilised to show optimum separation for this column. Again the areas of co-elution on the ACE C18 are highlighted, here it is noted that although quinoxaline and salicyamide are separated on the ACE C18 they are not fully resolved on the Aquastar. This is likely to be a result of the higher degree of hydrophobicity on the ACE C18 phase and the increased retention of the quinoxaline on the Aquastar phase due to the electrostatic interaction between the charged nitrogen atoms of the analyte and the silanols or hydroxyl groups of the stationary phase.

As with the previous test mix the Alltima shows a greater difference in elution order however the peak shape is significantly improved on the Aquastar phase. It is interesting to compare the Alltima and Platinum phases on this mix, although it is believed that these two phases have comparable silane structures and coverage the difference in selectivity is notable. Basic analytes such as amiloride and nortriptyline are much more strongly retained on the lower purity silica due to the presence of the more acidic silanols.

The two test mixes shown here were developed to pick out the differences in the additional polar selectivity component to the retention mechanism of the EPS phases compared to a straight forward hydrophobic interaction on an endcapped C18 phase. This analysis shows is how the test mix selection can be utilised by column manufacturers to display their own phases in the best light when comparing them to competitor phases. It has already been discussed how the overall retention mechanism is the sum of all interactions from the bonded ligand functional groups, base silica and the degree of these contributions will vary in strength depending on the structure of the analyte, organic modifier and buffer salts present, temperature, pH and ionic strength of the mobile phase. Therefore by altering just one of these parameters will produce variations in the retention time and peak shape.

As column manufacturers will have different procedures for cleaning the silica and bonding the silane ligands there are bound to be some variations in stationary phases even those with the same basic structure. These variations in the retention mechanisms can be enhanced or minimised by choosing the right analysis conditions and compounds for the test mix.

This indicates the importance of fully understanding the retention mechanism of a particular phase; a manufacture's brochure or scientific paper can make a specific phase look like it can separate a wide selection of analytes .

Figure 4.18 ***Multiple compound test mix on ACE C18 and EPS phases using Formic Acid and Acetonitrile***

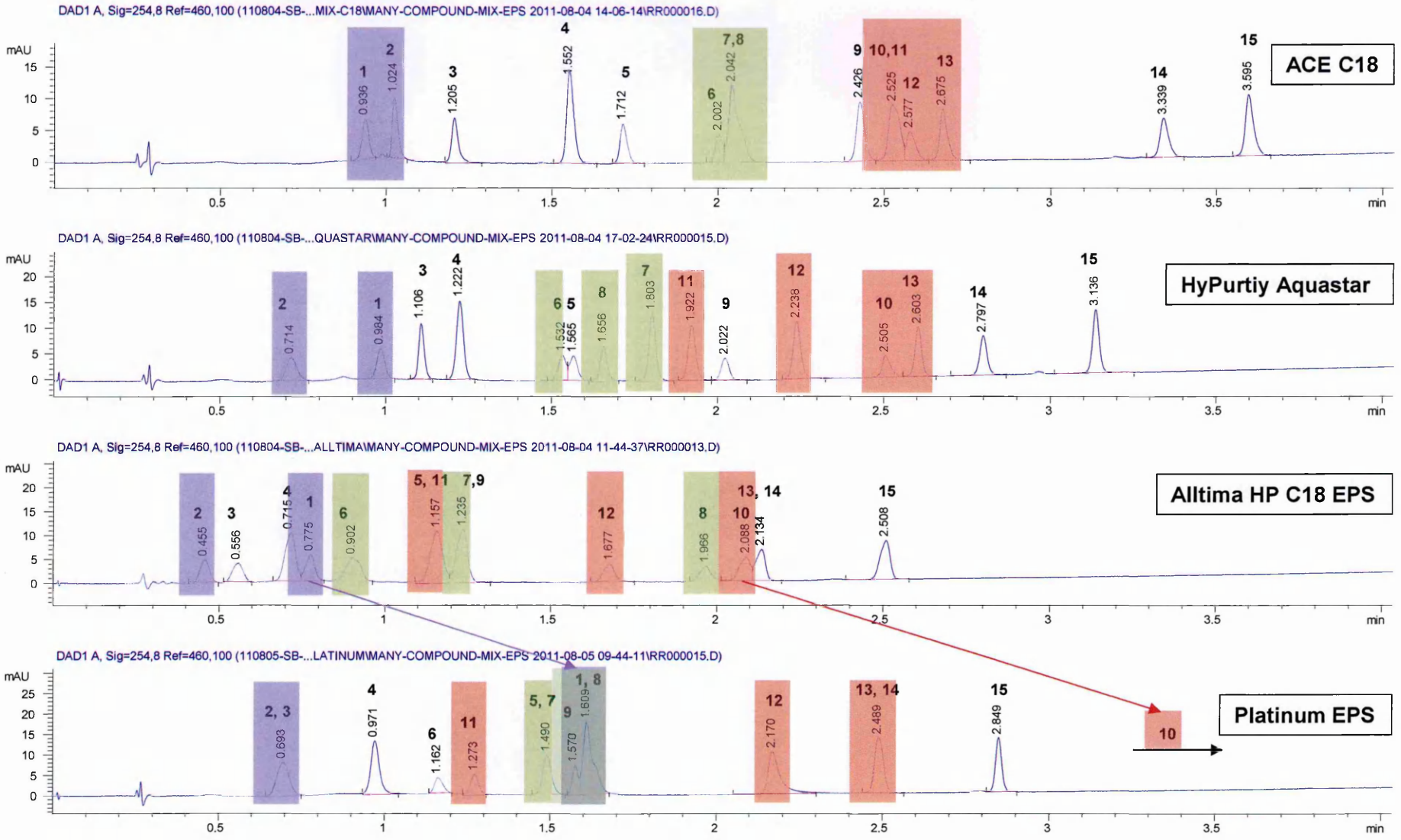

1. Amiloride 2. Metronidazole 3. 4-hydroxybenzoic acid 4. Salicyamide 5. Qunioxaline 6. Sailcylic acid 7. Phenacetin 8. Unknown impurity 9. 1,2-dinirtobenzene 10. Nortriptyline 11. 4-chlorophenol 12. Piroxicam 13. Sulindac 14. Benzophenone 15. Celecoxib

4.2 Stability Assessment of EPS Phases

HPLC analysis should be carried out at least two pH units away from the pK_a of the analytes being separated to ensure the compounds are in a fully ionised or unionised state. Consequently an HPLC stationary phase may be exposed to mobile phase in a range of pH and buffer concentrations. As discussed in Section 1.9 the stationary phase must be stable across these different pHs as modifications to the surface or bonded ligand may result in changes to the retention mechanism and therefore variations in retention times.

As the EPS phases being evaluated here are thought to consist of an octadecyl silane with polar functionality coming from either the base silanols or from hydroxyl groups attached to the bonded ligand. The stability of the phase would centre around cleavage of these ligands and therefore a loss of hydrophobicity or modification of the silanols or hydroxyl groups resulting in a variation in electrostatic interactions. This can be evaluated chromatographically by injecting the same compound multiple times over a long analysis and comparing the retention time and peak shape.

Initially the columns were subjected to a forced stability assessment which was carried out using extreme pH and temperature conditions, these results were then extrapolated to get an overall picture of the stability of the phases. A longer term analysis was then carried out to assess the stability of the columns in real-time using temperature, pH and buffer ion concentrations that would be typical in HPLC applications.

Characterisation compounds were chosen to assess the hydrophobic and polar interactions of the stationary phases during this analysis to determine any changes in ligand functionality, density or structure of the silica base.

4.2.1 Forced Stability Analysis of EPS Phases

The characterisation compound *o*-cresol was chosen to assess hydrophobic interactions during this analysis. Highly acidic conditions and elevated temperature have been known to cause ligand cleavage which would result in a reduction of retention time of the *o*-cresol solute. As an extra test a mixture of neutral compounds (dimethyl phthalate, toluene, biphenyl, and phenanthrene) was analysed before and after the forced stability testing and the chromatograms compared to determine any changes to the phase. This is a standard set of neutrals used as a quality control (QC) test mix by a number of column manufacturers.

The change in relative retention factor of the *o*-cresol was calculated as a percentage and this result plotted against the number of column volumes for each of the EPS phases, shown in Figure 4.19 below. Only the retention factor percentage observed on every tenth injection, equivalent to 1200 column volumes is displayed on the graph.

Figure 4.19 Evaluation of the change in retention time for o-cresol injected on EPS phases

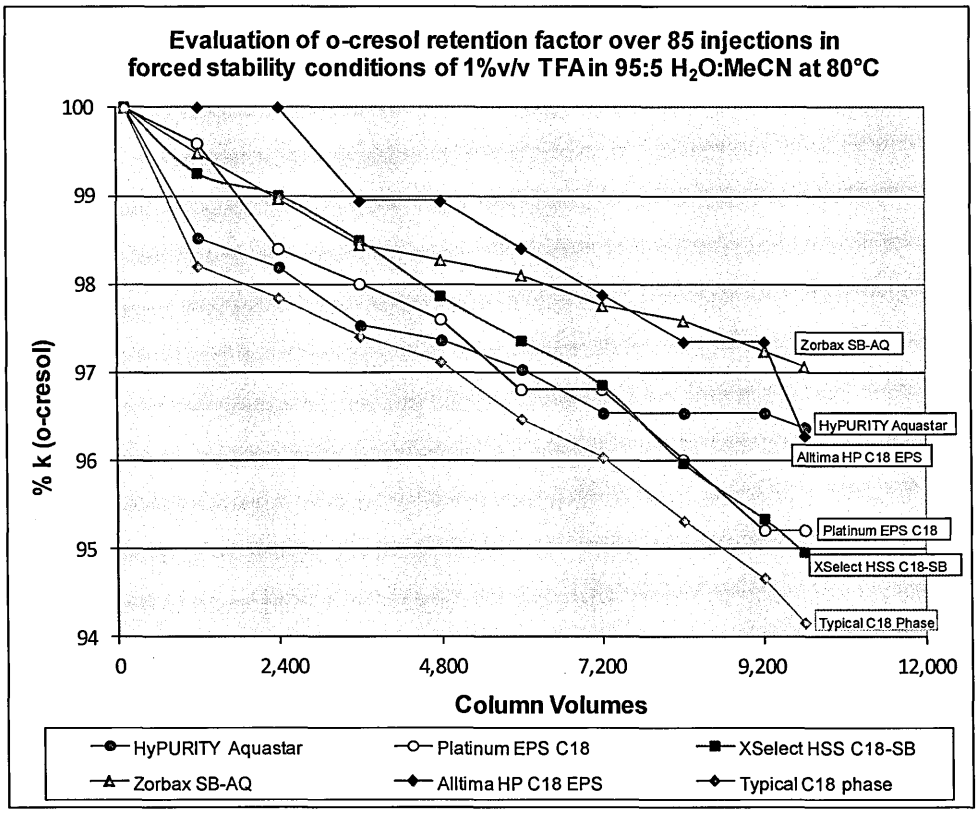

All columns show a very small decrease in the retention time of *o*-cresol and very little change between the neutral peaks before and after, the most pronounced change is observed in the XSelect HSS phase where the *o*-cresol is seen to decrease from 0.967 to 0.927 minutes, this is approximately a 5% decrease overall. The neutrals solution for the XSelect HSS column shows the most variation (Figure 4.20). The peak shift observed here is not pronounced and would be said to be a negligible variation, the neutral chromatograms for the other phases are not shown as no change is observed before or after testing.

Figure 4.20 ***Comparison of neutrals test mix before and after the forced stability analysis on the XSelect HSS phase***

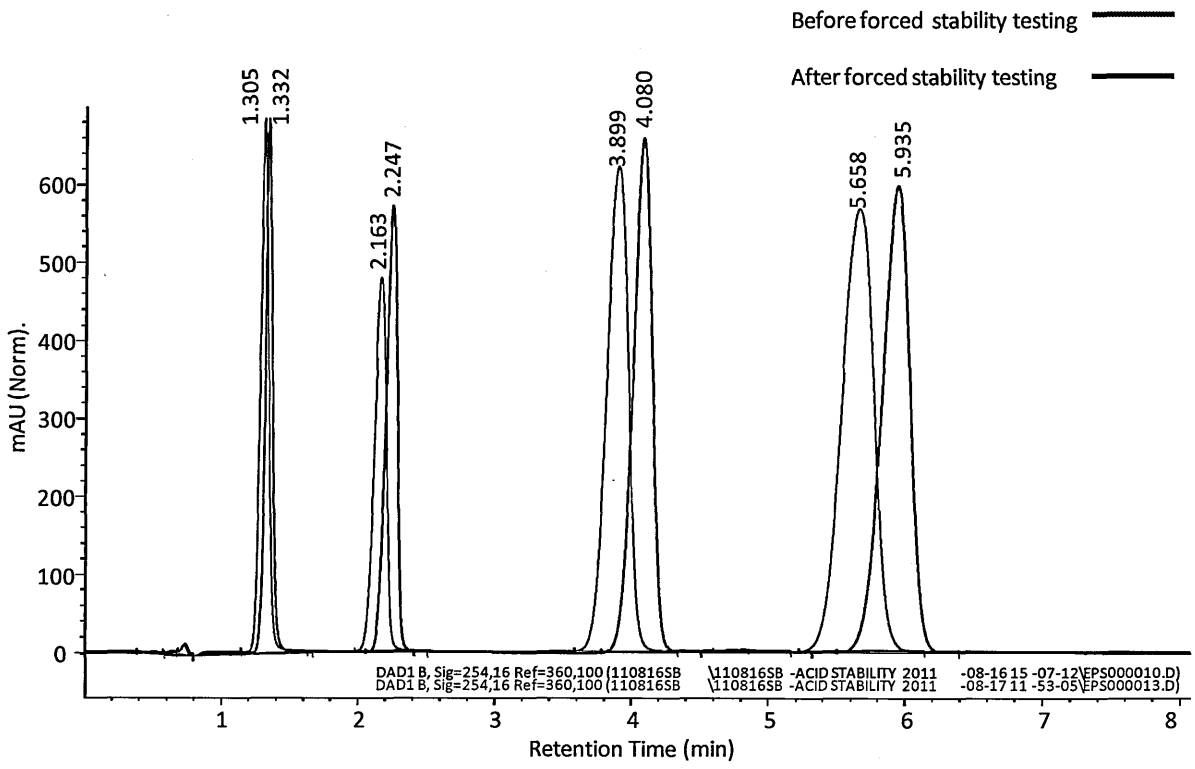

Elution order: [1] dimethyl phthalate, [2] toluene, [3] biphenyl, [4] phenanthrene

Figure 4.19 shows the stability of the EPS phases in comparison to typical C18 phases that are considered to have good stability for analysis at low pH. The plot shows that these EPS phases are seen to be more stable than a typical C18 phase. This is an unusual result as the theory dictates that

phases with a high surface coverage are less susceptible to acid hydrolysis due to steric hindrance of the bonded ligands. In other words if the H_3O^+ groups are blocked from reaching the Si-O linking bond to the densely packed silanes bonded to the phase. Manufacturer's data[269] commonly show their high carbon load columns to possess higher stability than the equivalent C18 in acidic conditions. If it is assumed that the phases are prepared using similar purity of silica, bonding conditions, and silane and the only difference is the density of the bonded ligand then the additional stability observed is unlikely to come from this steric hindrance effect.

Manufacturer's literature has shown that the Platinum EPS, XSelect HSS and Alltima HP phases are all lightly bonded C18 phases and therefore the predicted stability would be low as the Si-O linker bonds would be easily accessible by the H_3O^+ ions. However the experimental data shown in Figure 4.19 along with manufacturer's specification[267][268] indicates that very little ligand cleavage through hydrolysis occurs. There are a couple of possible explanations for this, firstly it could be that the base silica is becoming positively charged and actively repelling the H_3O^+ ions away from the surface and reducing the likelihood of hydrolysis occurring at the Si-O linker bond. Even at this low pH it is highly unlikely that the silanols will become ionised, therefore the only possible change could be from the exposed metal ions in the silica. If this was the case it would be expected that the Platinum EPS would have greater stability as the Tanaka and Bases testing had shown that the surface silanols have a greater level of acidity compared to the other EPS columns which is most likely due to the metals present in the TYPE-A silica. This hypothesis is unlikely as a strong degree of positive charge of this nature would have been identified during the characterisation analysis.

As discussed in Section 1.5 historically HPLC columns were bonded onto unpurified, TYPE A, silica which has previously been shown to be less stable than the equivalent TYPE-B phases (Section 1.9.1). Some of these columns are still in production today as they are employed for chemical analysis of pharmaceutical products and the specific column is registered on the pharmacopeia. Therefore a

similar stability assessment was carried out using a C18 phase that is known to be bonded onto the old style TYPE-A silica. A C18 was chosen as these are liable to ligand cleavage at the base of the silica rather than exhibiting any side reactions through hydrolysis of the silane itself. These results were then compared to the EPS phases as shown in Figure 4.21 overleaf.

Figure 4.21 ***Evaluation of the change in retention time for o-cresol injected EPS phases and Waters Spherisorb 3 ODS-2***

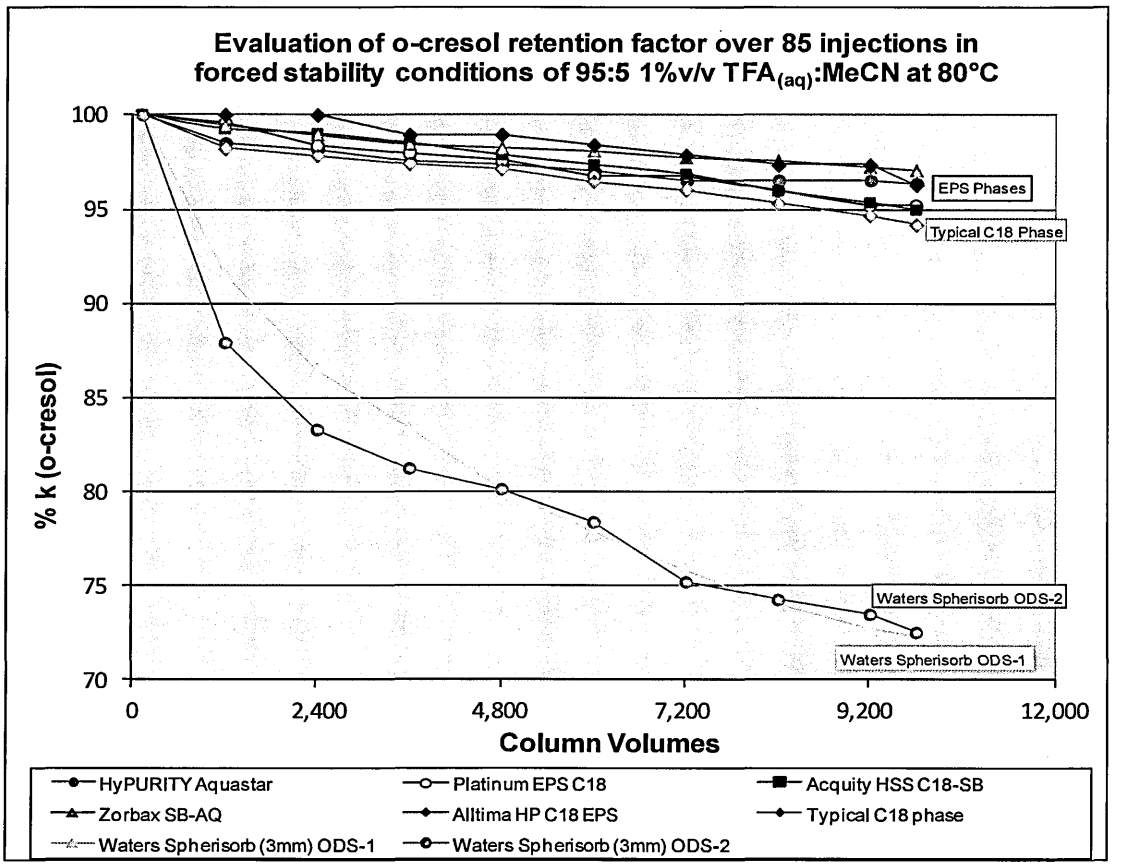

The Waters Spherisorb ODS-2 phase shows a significant reduction in the retention time of *o*-cresol which is indicative of the octadecyl silane being cleaved in the presence of acid. Although the ligand density is significantly higher on the Waters Spherisorb ODS-2 phase the reduction in retention time is calculated as a percentage to show the relative change in ligand density over time rather than the amount being cleaved. This result appears to indicate that the TYPE-A silica does not make a column more stable in acidic conditions. However only one phase of TYPE-A material has been tested and the bonding route is not known for this phase therefore this result is not conclusive.

The second possible explanation for the apparent high stability of the EPS phases is that the sparse covering of the octadecyl silane means the H_3O^+ ions are less likely to encounter a bonded ligand which makes this type of silane cleavage less favourable. Again this is unlikely due to the high concentration of TFA used the H_3O^+ ions are in excess. It has previously been thought that surface of bare silica stationary phases does not interact with analytes as much as the silica surface for bonded columns as the solute molecules use the ligands as a sort of ladder to travel down and reach the base silica. As some of the EPS phases are more lightly bonded the H_3O^+ ions in solution might not be penetrating the base of the silica and therefore reducing the likelihood of acid hydrolysis. Although this may give an explanation for the three lightly bonded phases it would not explain the comparable levels of stability observed for the HyPURITY Aquastar and the Zorbax-SB-AQ. Therefore there may be something intrinsic in the polar nature of these columns which somehow protects from acid hydrolysis or repels H_3O^+ ions from the phase and therefore reduces the likelihood of ligand cleavage by acid hydrolysis.

As all the EPS columns tested show a high degree of stability the variations shown may just be through experimental error. As only a small amount of EPS stationary phase was available and as this test renders the column unusable afterwards the analysis could not be duplicated. However to evaluate the repeatability of this analysis testing of a ACE 3 C18 phase was carried out in triplicate and the %RSD variation in overall stability was found to be <1.0%. The full results of this are shown in the Appendix. This suggested that these results are precise and the EPS phases display a high level of stability in acidic conditions. These columns have been re-packed from recovered material therefore it is possible that this has changed the stability of the bonded phases, although the manufacturer's literature for these phases also state a high degree of stability in acidic conditions[267][268].

4.2.2 *Real-time Stability Analysis of EPS Phases*

The forced stability analysis is an excellent tool in assessing the relative stability of a phase against its peers. However it does not always give enough information about how a column will age under everyday use. The analysis is commonly carried out over 20,000 column volumes which accounts for approximately 3 months analysis time at 8 hours a day, 5 days a week. For this a longer term analysis is required with a number of acidic, basic and neutral probes to bring out any small changes to the retention mechanism of a phase over an extended period of use. Different types of analyte are chosen as the changes in retention time indicate changes to the surface of the phase. For example amitriptyline is a tertiary amine with a pK_a of 9.4 and will be ionised in most pH conditions used for analysis. Therefore the charged nitrogen will be retained by any residual silanols that are present on the phase and as ligands are cleaved and more silanols are exposed the retention time of amitriptyline will increase and the peak may become more tailed. As a result real-time stability assessment is not just about the change in retention time but includes any changes in peak shape, tailing or efficiency of the column during the analysis.

For the EPS phases the real-time stability was carried out using a range of mobiles phases with different pH and buffer salts. As the phases showed little change in low pH the initial analysis was carried out using 10 mM potassium phosphate buffer at pH 2.5. With all columns there are no downwards trends observed for the retention factor and efficiency across the 20,000 column volumes analysed. The full results are shown in the Appendix. Some variation in the efficiency of butyl benzene is observed however that is likely to be due to the change in peak height as the sample evaporates over time.

Although no downwards trend is observed in the plots of retention factor and efficiency for the Alltima HP EPS column and the overlaid pressure traces shows no increase in pressure over the 20,000 column volumes. However the overlaid pressure traces shows some variation which may

cause small differences in the retention time of all the analytes. This does not indicate a reduced stability of the column as the trend is not a decrease in retention time but a random variation across all injections. The first four chromatograms (representing the initial 2500 column volumes) on the column show more variation in retention time and after that they become more stable, as the analysis is isocratic and the flow rate remains constant this is likely to be the point where the column reaches equilibrium. However this observation is only based on a single column and one that was repacked from recovered silica material rather than the commercial column. Overall no trends were observed and the column can be considered stable using 10 mM potassium phosphate buffer at pH 2.5

The columns were tested at neutral pH using 20 mM ammonium acetate at pH 6.8 and 10mM potassium phosphate at pH 7.6. The full results for these are also shown in the appendix. For all phases the retention time of the amitriptyline is seen to increase a small amount across the 20,000 column volumes run. This is indicative of a small amount of cleavage of the C18 ligand which would expose silanols on the surface of the silica. These silanols will have a negative charge at pH 6.8 and will interact with the positively charged amitriptyline increasing the retention time.

The other neutral and acidic analytes are not seen to decrease in retention time so the amount C18 phase lost must have a negligible effect on the hydrophobic contribution to the retention mechanism. It has been well covered in this thesis that the strength of electrostatic retention through ionic exchange interactions can be significantly higher than hydrophobic. Even a small percentage of silane cleavage will have an effect on the retention of basic analytes but not on the neutrals. Column manufacturers often use neutral test mixes as a validation test mix to check packing efficiency and identify any changes to the phase during testing. This testing shows that a small amount of silane cleavage would not be picked up by comparison of retention time of neutral compounds. This is shown numerically in Table 4.6 where the initial and final retention times of the basic amitriptyline and the neutral toluene are compared over the 20,000 column volumes. It can be

seen that even in cases of a significant increase of retention time in the amitriptyline peak there is <2.0% change in the neutral compounds which would be classed as analytical error and therefore be counted as negligible.

Table 4.6 Change in retention times of neutral and basic analytes

Phase	Amitriptyline			Toluene		
	Initial R_t (min)	Final R_t (min)	Δ (%)	Initial R_t (min)	Final R_t (min)	Δ (%)
HyPURITY Aquastar	0.534	0.570	+6.7	0.224	0.222	-0.9
Platinum EPS	0.651	0.756	+16.1	0.423	0.431	+1.9
XSelect HSS C18-SB	0.910	0.928	+2.0	0.919	0.921	+0.2
Zorbax AQ-SB	0.376	0.403	+7.2	0.553	0.550	-0.5
Alltima HP EPS	0.169	0.182	+7.7	0.365	0.369	+1.1

The Platinum EPS phase shows the greatest increase in retention time over the 20,000 columns volumes, this is shown in the graph in Figure 4.22. The calculated increase in retention time is ~16%, although this would indicate a significant loss of ligand this is not mirrored by a loss in retention time of the other analytes during the run. It is likely that some ligand is being cleaved resulting in silanols being exposed. However as ionic interactions have a greater degree of strength the increase in retention time of the amitriptyline is exaggerated and in practice it is likely that only a small amount of ligand is lost. The pressure traces were assessed to see if the stripping of the phase was apparent through an increase in pressure but no significant difference was observed.

Figure 4.22 Evaluation of the change in retention time for amitriptyline on Platinum EPS phase

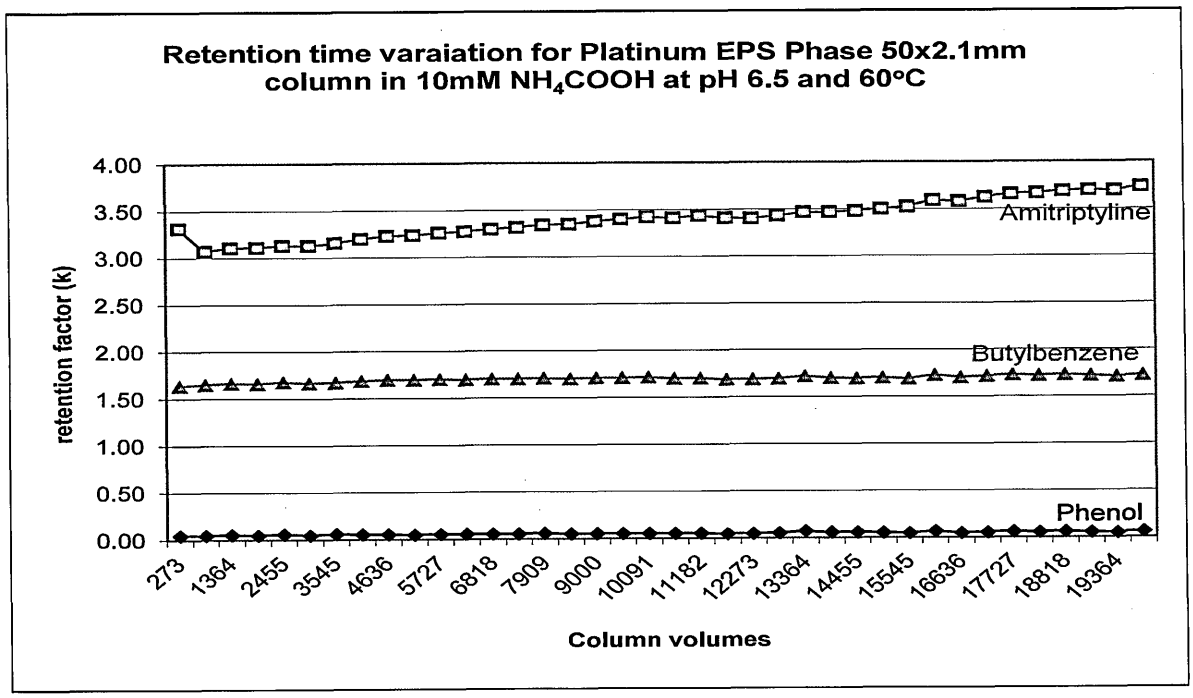

Very little increase in the retention time for amitriptyline is observed for the Alltima HP phase, although as the amitriptyline co-elutes with the larger phenol peak a small movement in retention may be masked. As the phenol peak is approximately 0.14 minutes wide and that tends to be the increase in retention time seen in the other columns this may be misleading.

The most interesting result from some of the phases is that the neutrals analysed before and after are actually seen to increase in retention time after the stability analysis, this is shown for the HyPURITY Aquastar phase (Figure 4.23). This is very unusual as it would suggest that the phase has gained hydrophobicity which is in direct contrast to the indication that some C18 ligand has been lost. There are a number of possible explanations for this in that the phase has not fully reached equilibrium however by overlaying the 5 injections of the neutrals show that the retention times before and after are stable within the sets of repeat injections, just not comparable to each other. It may be possible that the pumps of the instrument are not delivering the correct flow which would account for small differences in the retention times however if this was the case it would be more likely that the retentions times would vary randomly and here the two sets of repeat injections show

the same retention times. Another possibility would be some sort of ion pairing with the buffer and the exposed silanols or hydroxyl groups on the phase however it is unclear as to how this would add hydrophobicity to the phase and if this was the case then it would reduce the hydrogen bonding capacity of the silanols and therefore the amitriptyline retention would not be seen to increase.

Figure 4.23 ***Evaluation of a mixture of neutral analytes before and after the stability testing on the HyPURITY Aquastar phase***

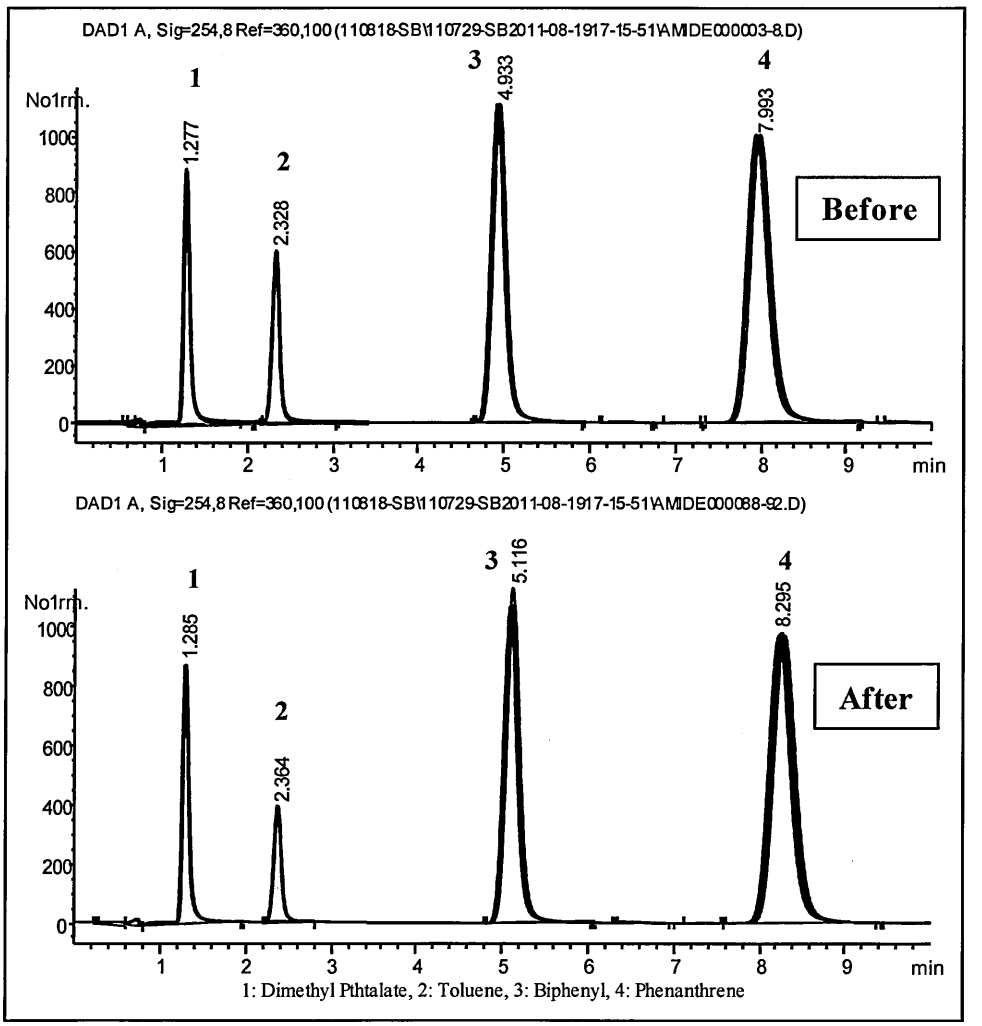

Evaluation of the toluene retention time shows a 1.5% increase, which again is classed as negligible. One possible reason for the increase of the retention time would be changes in the organic percentage of the mobile phase. The analysis takes around 48 hours and as the mobile phase for the

neutrals test mix is pre-mixed the small changes in composition may have a small change in retention time.

Overall the EPS columns appear to be stable at neutral pH using ammonium acetate buffer, therefore the same analysis was tried using 20 mM potassium phosphate buffer at pH 7.6. These results showed an entirely different story; again the full results are shown in the appendix. The analysis was originally set to run for 38 injections of each sample however for the majority of phases after a small number of injections of each sample the back pressure was seen to rise significantly and the instrument automatically cut out. This is likely due to the silica base of the column being eroded and these particulates of silica and hydrocarbon silane then blocked the frit at the base of the column. This can be seen in the overlay of the pressure traces, on each injection the pressure increases step-wise as the frit becomes blocked. The only phase that managed to run through the entire analysis was the Platinum EPS phase however the retention times and efficiencies observed for all phases showed a significant decrease.

The longer the initial retention time of the analyte the more pronounced the decrease, the peak width also increases considerably across the run as the stationary phase deteriorates and changes the mass transfer rates of the analyte. Comparing the graphs in Figure 4.24 and Figure 4.25, the retention factor does appear to decrease gradually indicating the columns is being eroded slowly; however the efficiency plot shows the column has a drastic change in integrity after only 5000 column volumes. The loss of phase caused by this erosion of silica can clearly be seen in the overlaid chromatograms for all columns, here the shift in retention time is observed from the first few injections and the change in peak shape, width and tailing can clearly be seen in the butyl benzene and the toluene peaks. The retention factor and efficiency show an immediate downwards trend for all analytes although this is not as apparent with phenol, butyl benzoic acid and 2-hydroxybenzoic acid because they elute so close to the solvent front.

Figure 4.24 ***Evaluation of retention time of a mixture of basic and neutral analytes over 20,000 column volumes at neutral pH on the Platinum EPS phase***

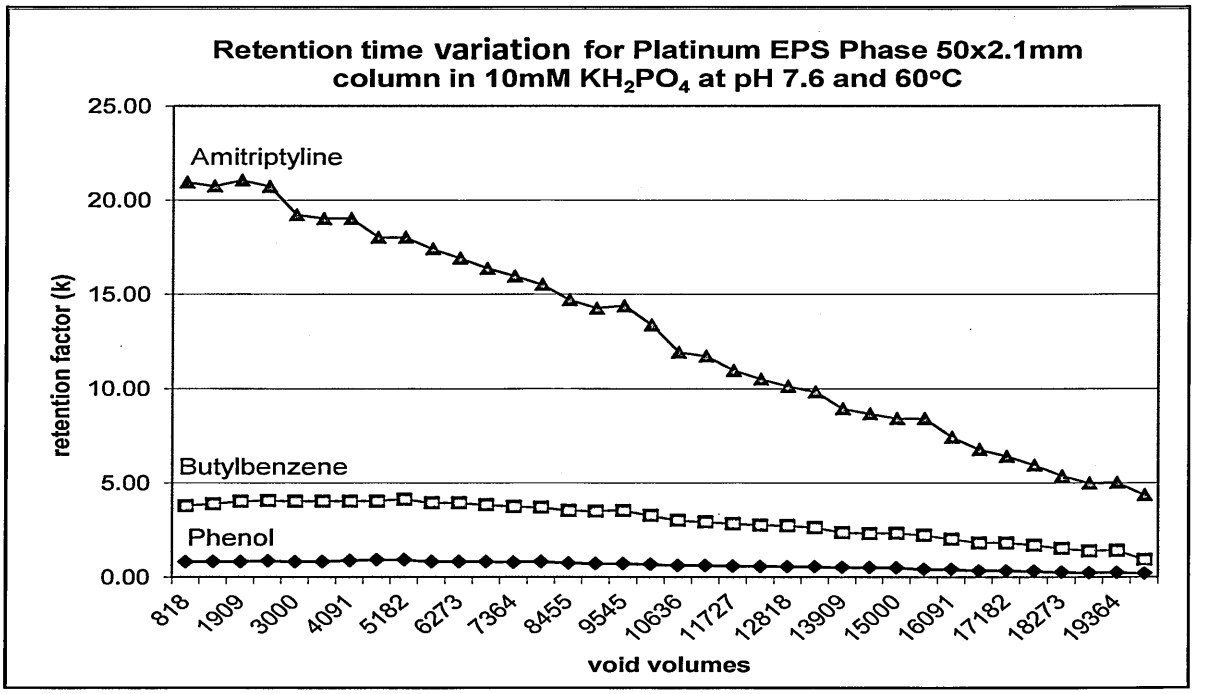

Figure 4.25 ***Evaluation of efficiency values of a mixture of basic and neutral analytes over 20,000 column volumes at neutral pH on the Platinum EPS phase***

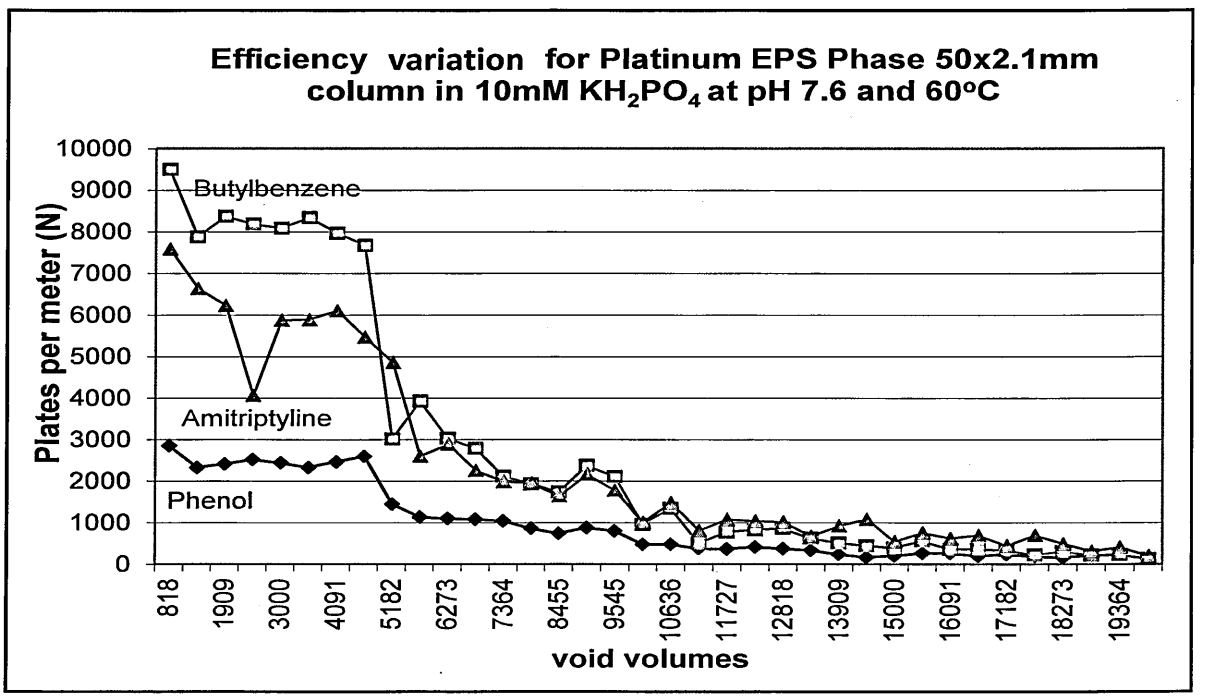

The Zorbax-SB-AQ was the only phase to show a gradual decrease in efficiency in tune with the reduction of the retention time. The phase only managed to run for 16,000 column volumes before the eroded silica forced the instrument to cut out due the exceeding the pressure limit, however it is likely that the branched ligand of the stable-bond technology protected the silica from erosion and the loss of phase was more gradual and uniform than observed in the other phases.

It is well documented that potassium phosphate will erode the silica particles[257][258][261] at neutral pH and as some of these phases only have a sparsely bonded ligand density there is no protection from sterically bulky ligands. Many column manufacturers claim that the columns they produce are stable in neutral pH and although this may be the case it is important to specify the range of ionic buffers as well as a pH range and temperature.

4.3 *Oxidative Cleavage and Structural Elucidation of EPS Phases*

The EPS phases were subjected to aqueous hydrofluoric acid digestion along with experimental monomerically bonded C4, C8 and C18 phases endcapped with trimethyl silanes. Under digestion the silane ligand will be cleaved from the base silica, any oxygen atoms on the phase will be replaced by fluorine atoms forming a stable fluorinated silane. Some of the silica structure may be dissolved depending on the digestion period. The digests were extracted with hexane, any hydrocarbon present will be transferred to the solvent layer, which was then analysed by GC-MS. Solid state ^{13}C CP-MAS NMR was carried out on the bonded silica materials to confirm the structures.

The experimental silica materials were structurally evaluated as standards, these phase are known to be bonded using a high purity silanes with methyl substituents, monomerically bonded with a trimethylsilane endcap. The ultra pure silica base is likely to be digested; however as only trace metals are present this should not interfere with the silane recovery. No silane peak was observed in the C4 extract, it is likely that the fluorosilane is too volatile and not stable in hexane. This would also explain why no peaks are observed for the TMS endcap, these small, volatile fluorosilanes would require headspace GC-MS analysis for structural elucidation. However as the EPS phases are not endcapped the recovery of TMS does not need to be confirmed for these columns.

Table 4.7 ***Assignment of mass fragments for standard silica phases***

Phase	Molecular Mass (m/z)	Structure
All silanes	77.0	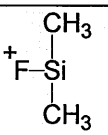
	105.1	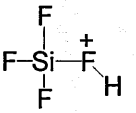

Table 4.7 ***Assignment of mass fragments for standard silica phases (cont.)***

Phase	Molecular Mass (m/z)	Structure
C8	190.2 $[M]^+$	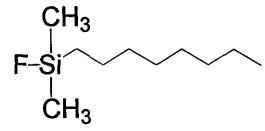
	175.1 $[M-(CH_3)]^+$	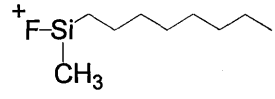
C18	330.3 (not seen) $[M]^+$	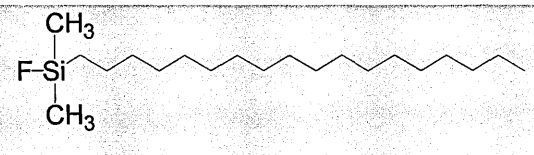
	315.3 $[M-(CH_3)]^+$	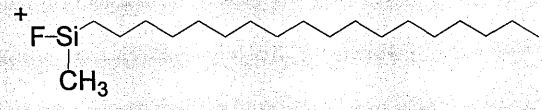
	$[M-SiF(CH_3)_2]$ 252.3	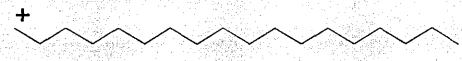

Both phases show similar fluorosilane fragments; the fragment at *m/z* 77.0 which is simply the di-methyl substituted silica cleaved of the hydrocarbon. The fragment at *m/z* 105.1 is a little more complex, the highly electronegative fluorine atoms will replace all substituents on the silica making a tetrahedral fluoro-silane, this becomes ionised by addition of a hydrogen ion to the lone pair of the silica making a charged species that can be detected by mass spec.

For the standard phases the parent ion is observed for the C8 phase, another prominent fragment is that observed at *m/z* 175.1 as the parent ion can lose a methyl from the silica substituents or from the end of the hydrocarbon chain. For the C18 phase the parent ion is not observed, this is common for long chain silanes, however the fragment at *m/z* 252.3 confirms the hydrocarbon present is $C_{18}H_{32}$.

Table 4.8 ***Assignment of mass fragments for EPS bonded silica phases***

Phase	Molecular Mass (m/z)	Structure
HyPURITY Aquastar	338.3 $[M]^+$	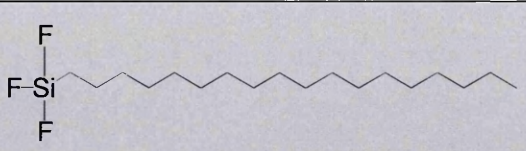
	127.0	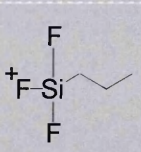
	85.1 $[M-(C_{18}H_{37}]^+$	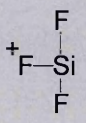
Platinum EPS	330.3 (not seen) $[M]^+$	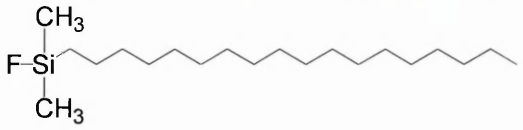
	315.3 $[M-(CH_3]^+$	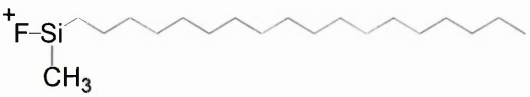
	$[M-SiF(CH_3)_2]^+$ 252.3	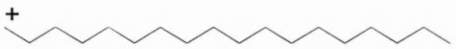
XSelect HSS C18	338.3 $[M]^+$	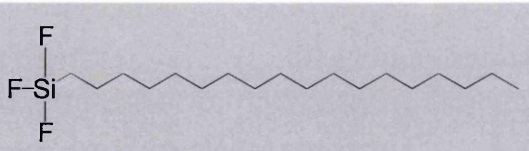
	127.0	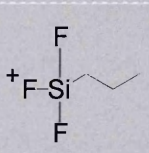
	85.1 $[M-(C_{18}H_{37}]^+$	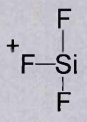

Table 4.8 ***Assignment of mass fragments for EPS bonded silica phases (cont.)***

Phase	Molecular Mass (m/z)	Structure
Zorbax-SB AQ	176.1 $[M]^+$	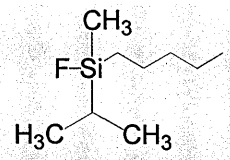
	133.1 $[M-(C_3H_7)]^+$	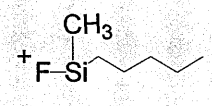
	105.1 $[M-(C_5H_{11})]^+$	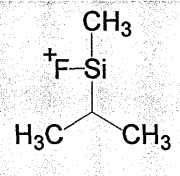
Alltima HP C18	330.3 (not seen) $[M]^+$	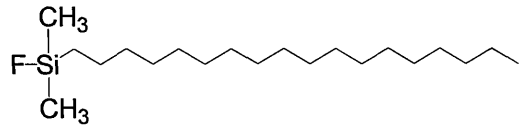
	315.3 $[M-(CH_3)]^+$	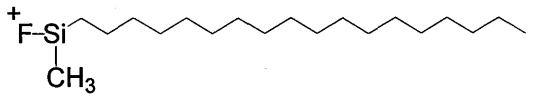
	$[M\text{-}SiF(CH_3)_2]^+$ 252.3	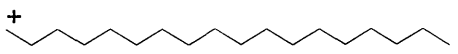

The EPS phases show some striking similarities in their mass fragmentation patterns; the Platinum EPS and Alltima HP EPS are identical and comparable to the standard C18 phase. This is not surprising as the two phases are produced by the same manufacturer and literature states them to be lightly bonded dimethyl octadecyl silanes. The solid state ^{13}C CP-MAS NMR carried out on these two silica materials indicate a number of carbon environments in the hydrocarbon region however it is not possible to assign these as the chemical shift are seen to overlap. No other environments are observed which confirm these two phases as bonded dimethyl octadecyl silanes with no endcap.

The HyPURITY Aquastar and XSelect HSS SB C18 phases also show the same fragmentation pattern in the GC-MS indicating the bonded silane has the same structure for each phase, albeit the purity may be different. Although only a low abundance of the parent ion is observed, the GC-MS shows a typical fragmentation pattern for long chain hydrocarbons. The initial fragment observed at *m/z* 309.2 indicates the loss of $^{\cdot}CH_2CH_3$ from the parent ion. Further fragments observed every *m/z* 28.0 are observed indicating the loss of $^{\cdot}CH_2CH_2$ until the C18 chain is depleted. The silane base observed at *m/z* 85.0 indicates a trifluorosilane which corresponds to a trihydroxyl octadecyl bonded to the surface of the silica. As discussed in Section 4.1.2, this type of ligand can give rise to mono-, di- and tri-functional bonding with the substituent hydroxyls undergoing cross-linking or remaining protonated and contributing electrostatic cationic exchange to the retention mechanism. The similarities between the HyPURITY Aquastar and XSelect HSS SB C18 bonded silane explains the similar chromatographic results, the manufacturer's data suggest a different carbon load which may explain the different retention times for neutral and acidic solutes. The purity of the silica is likely to be different for each phase which would explain the different retention times and tailing factors of basic solutes. This is seen in a greater extent in the Platinum EPS and Alltima HP C18 phases, however it is likely that both the HyPURITY Aquastar and XSelect HSS SB C18 phases are bonded onto TYPE-B silica as the tailing on the basic analytes is shown to be minimal.

The Zorbax AQ SB appears to be a unique phase; the retention time of the silane in the GC is considerably lower than other EPS phases. For the standard C18, Platinum EPS and Alltima HP C18 phases, which are known to be dimethyl octadecyl silanes, the peaks are observed to be around 10.9 minutes. Whereas the HyPURITY Aquastar and XSelect HSS SB C18 phases are seen to elute at approximately 9.7 minutes and the standard dimethyl C8 phase is observed at 5.0 minutes. The Zorbax AQ SB peak, by contrast is seen to elute at 3.8 minutes indicating the length of the hydrocarbon is shorter than the C8 chain. In order to get a better idea of the peak and fragments the sample was reanalysed using a lower starting temperature and a shallower temperature gradient.

The resulting chromatogram shows two partially coeluting peaks; the resulting mass fragments for these peaks are identical indicating the fluorosilane exists as two isomers. Although the standard C18 phase does not show the parent ion but the $[M-(CH_3]^+$ fragment, the standard C8 phase is smaller and the parent ion appears to be stable in the gaseous phase. The shorter retention time on the GC and lower mass observed for the Zorbax AQ SB phase indicates the hydrocarbon chain is much shorter. Therefore it is assumed that the cleaved fluoro-hydrocarbon is stable in the gas phase and the mass peak observed at m/z 176.1 is the parent ion.

The mass spectrum shows a fragment at *m/z* 133.1 which indicates the parent ion losing an isopropyl group. From the manufacturer's data it is thought that the Zorbax-SB range incorporates large bulky groups into the substituents on the linking silica, from these mass spec results it is likely that these are isopropyl groups. As no fragment is observed at *m/z* 90.1 and the parent ion is *m/z* 176.1 rather than *m/z* 204.1 it indicates that only one isopropyl substituent is bonded to the silane. This would correspond to the level of electrostatic exchange observed in the chromatographic characterisation, as only half of the residual silanols are masked by the bulky isopropyl groups.

If it is assumed the phase has a single isopropyl substituent and a methyl substituent on the linking silica the resulting mass of the parent ion corresponds to a C_5H_{11} hydrocarbon chain. The manufacturers state that the carbon load is proprietary information however the retention factor of amyl benzene shown in Section 4.1.1 indicates that the coverage is greater than the Platinum EPS and Alltima HP C18 Phases, with a carbon load of approximately 5%, but lower than the HyPURITY Aquastar and XSelect HSS SB C18 phases, with a carbon load of 8.5% and 10% respectively. The shorter C5 silane of the Zorbax AQ SB would cause less steric hindrance which would explain the difference in the $\alpha_{T/O}$ values observed in Section 4.1.1. These shorter hydrocarbon chains would allow easier access to the ionic exchange sights of the base silica allowing for the higher $\alpha_{C/P}$ value.

Previously it was believed that there were hydroxyl groups or aromatic groups bonded to the bulky propyl groups as the strength of the cationic interactions observed in the Tanaka characterisation was lower than the other EPS phases. The MS shows a fragment at m/z 77.0 which is often observed for benzene rings with a carbocation, however the mass of the parent ion spectrum results shown here indicates this is not the case. A fluorinated silica with a benzene and methyl substituent would show a fragment of m/z 139.0 which is not observed. A possible explanation is that the fluoro-silica fragment rearranges in the gaseous phase and forms the more stable di-methyl substituent. As this seems an unusual rearrangement a di-isopropyl substituted cyano silane was analysed by GC-MS, the fragment at m/z 77.0, although less abundant, was observed, confirming the gaseous rearrangement. No environments were observed at δ 100-150ppm in the solid state ^{13}C CP-MAS NMR spectrum which would indicate the presence of aromatic carbons. Therefore it must be concluded that no hydroxyl or aromatic substituents are present and the electrostatic interactions for the Zorbax-SB AQ are coming from residual silanols on the base silica. The low ion exchange interaction results shown in Section 4.1.1 suggests a high purity TYPE-B is likely to be used for the base silica in the Zorbax-SB AQ phase. However the short C_5 alkyl chain reduces steric hindrance and allows analytes to interact with the base silica resulting in the high $\alpha_{C/P}$ value.

The mass spectrum results obtained here give a good indication of the structures of the silanes used for the EPS phases. These proposed structures are shown overleaf in Figure 4.26. Although the solid state ^{13}C CP-MAS NMR spectrum were not clear enough to pick out individual environments they were used to confirm the types of carbon environments present in these structures. All of the solid state ^{13}C CP-MAS NMR spectrum showed an environment around δ 71ppm which does not correspond to any of the structures shown. It is likely this is due to residual polyethylene glycol (PEG) which is a common lab contaminant. All of the solid state ^{13}C CP-MAS NMR spectrum are shown in the appendix.

Figure 4.26 ***Proposed structures of all EPS phases***

HyPURITY Aquastar and XSelect HSS SB C18

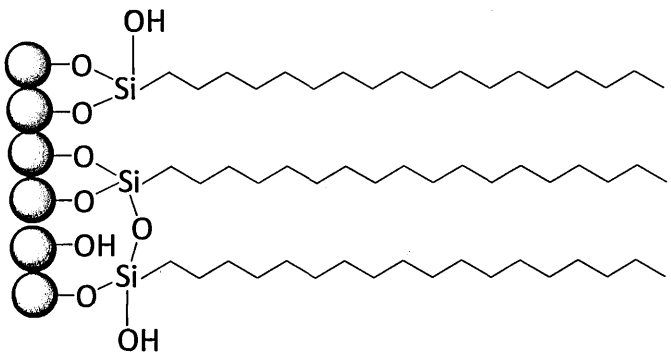

Platinum EPS C18 and Alltima HP C18

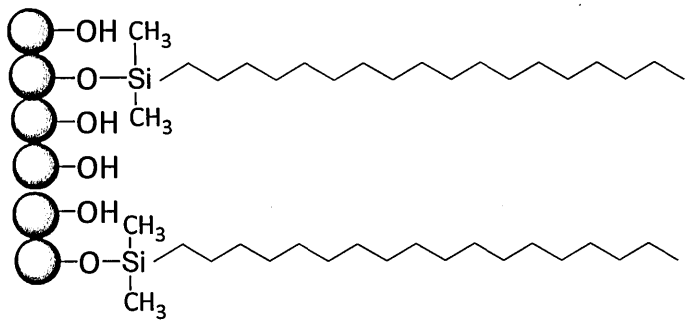

Zorbax-SB AQ

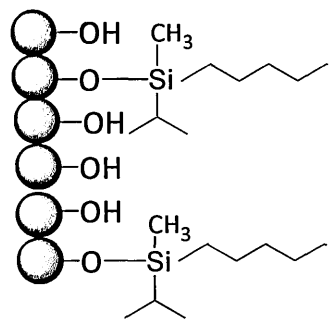

4.4 Conclusion of Chromatographic Analysis

The EPS phases have all been shown to have a retention mechanism made up of hydrophobic interactions from the octadecyl silane and ionic interactions from the residual silanols or hydroxyl groups. The degree of the ionic interaction component has been shown to be greater in the lightly bonded C18 phases, the Platinum EPS and Alltima HP C18, where the interaction comes from the residual silanols. However an increase in the contribution of ionic interaction, as shown in the Tanaka evaluation, results in an increase in tailing of basic molecules. This is shown by the evaluation of the Platinum EPS phase which has a high degree of ionic interaction due to the more acidic base silica however this phase would be unsuitable for analysing bases as it yields poor peak shape, however the phase has been shown to be suitable for acidic and neutral compounds. The Alltima HP C18 phase has been shown to have the same bonded silane and comparable carbon load; however the purity of the base silica appears to be higher resulting in more Gaussian peak shape for basic analytes.

The XSelect HSS C18 and HyPURITY Aquastar phases are seen to have a more Gaussian peak shape for basic and charged compounds however the payoff to this is that the selectivity difference for these phases versus the ACE C18 is not as marked. From the GC-MS and solid state ^{13}C CP-MAS NMR it was confirmed the ionic component for these columns come from a combination of residual silanols and hydroxyl substituents bonded to the silica linker. The carbon load of the XSelect HSS C18 is lower than the HyPURITY Aquastar allowing for a greater contribution of silanophilic and ionic interactions. The use of a high purity TYPE-B silica in the X-Select HSS C18 means that the contribution of acidic silanols is minimised. For the HyPURITY Aquastar the degree of acidity of ionic interactions is likely to be more controlled and consistent as the hydroxyl substituent groups also crosslink to mask any secondary interactions from the residual uncontrolled silanols on the surface. However this reduces the "polar" nature of the phase.

The Zorbax-SB AQ was also shown to have Gaussian peak shape and a lower degree of electrostatic cationic exchange through controlling the number of accessible silanols available on the surface of the silica. This is done through a bulky isopropyl substituent on the linking silica atom which hinders the accessibility of the residual silanols on the silica surface. The structural elucidation indicates that there are no polar substituents on the phase as originally thought. Therefore the cation exchange retention mechanism is likely to be coming from silanols on the base silica. Unlike the other EPS phases which incorporate an octadecyl silane the hydrophobic contribution to the retention mechanism comes from a pentyl hydrocarbon silane, although the exact carbon load is not know it is believed to be around 6-8% based on the chromatographic comparisons with the other EPS phases.

Overall the Extended Polar Selectivity phases are shown to have a complementary selectivity to a typical endcapped C18 phase making them a useful addition to the method development tool kit. However due to the increased peak width and tailing these phases may not be suitable for the analysis of polar and basic compounds. This evaluation highlights potential issues of using stationary phases that have residual silanols present on the surface of the silica with polar and basic compounds. As the degree of ionic interaction is much higher than other interaction components that make up the retention mechanism even a small amount of these residual silanols can cause peak tailing with some analytes if used in an unbuffered system. It has been discussed in Section 1.5 how additives can be used to minimise these effects. The degree of electrostatic interactions from hydroxyl groups within the bonded silane are much easier to control however the level of crosslinking and laddering would need to be controlled during the bonding process.

5. RESULTS AND DISCUSSIONS: REVERSED PHASE EVALUATION OF TYPE-C™ BIDENTATE PHASE AND COMPARISON AGAINST TYPICAL TYPE-B C18 PHASE

The TYPE-C™ phases have been shown to be based on a modified silica hydride particle that has been "silanized" by the formation of a triethoxy silane polymer shell and functionalised by addition of olefin or alkyne ligands[181] (Section 1.7). The process for manufacturing the commercial TYPE-C™ materials, available from Cogent, is proprietary information so it is unknown whether this process is used. For this analysis it was assumed that the "silanization" process and ligand bonding is similar to those described in Section 1.7.

In theory these phases should exhibit a more stable linkage than traditional TYPE-A or TYPE-B bonded silica and no secondary interactions from the residual silanols on the surface. The following section will describe the chromatographic and spectroscopic analysis carried out to determine whether these claims can be substantiated. A typical endcapped TYPE-B C18 phase will be analysed alongside the TYPE-C™ Bidentate C18 to validate the analysis, an ACE 3 C18 column was chosen as characterisation data for this phase has been published in literature[223][269]. The properties of the two phases to be evaluated are compared in Table 5.1 below.

Table 5.1 ***Manufacturer's data of TYPE-B and TYPE-C™ phases for characterisation***

Phase	Pore size (Å)	Surface coverage (m^2/g)	Endcapping	Carbon Load (%)	pH range	Max temp (°C)
Cogent TYPE-C™ Bidentate C18 4µm[273]	100	350	N/A	16.0	2.0-9.2	80
ACE 3 C18 3µm[269]	100	300	YES	15.5	1.5-10.0[a]	60

[a] Manufacturers catalogue states for optimum column lifetime a pH range of 2-8 is recommended, column lifetime may decrease depending on the type of inorganic buffers, organic modifiers and temperature.

5.1 *Chromatographic Selectivity Evaluation of TYPE-C™ Bidentate Phase Compared against Typical TYPE-B C18 Phase*

Although there are some publications available of the chromatographic properties of the TYPE-C™ silica stationary phases there does not appear to be a great deal of current independent analysis on characterising these phases using Tanaka probes and similar methodology. The initial step in this investigation was to carry out this type of chromatographic evaluation in order to better understand the retention mechanism.

In order to simplify the process the TYPE-C™ Bidentate C18 was selected for evaluation as the octadecyl bonded ligand should only exhibit hydrophobic interactions. An ACE 3 C18 phase was chosen as a comparison phase as this stationary phase is fully endcapped which minimises the residual silanols on the surface of the silica. The ACE materials use highly pure, TYPE-B silica therefore any residual silanols that may still be accessible on the surface of the silica will be low acidity, thereby minimising the degree of silanophilic interactions.

5.1.1 *Tanaka Characterisation of TYPE-C™ Bidentate Phase*

The Tanaka characterisation compounds have been chosen to probe the different retention mechanisms of a column as discussed in Section 1.8.1; in this case as both columns are marketed as C18 it is no surprise that the alpha values determined are very similar for the hydrophobicity characterisation markers. This can be seen Table 5.2 and graphically in figure 5.1 overleaf, here the retention factor (k) for amylbenzene and the separation factor ($\alpha_{A/B}$) for amylbenzene and butylbenzene are comparable. When looking at the surface area and carbon load of these two phases, shown in the Table 5.1, it stands to reason that these values should be similar as there will be an analogous number of available hydrocarbon chains to interact with these molecules.

Table 5.2 ***Tanaka characterisation values – comparison of ACE 3 C18 and TYPE-C^{TM} Bidentate C18 phases***

					pH 2.7		pH 7.6	
	$k_{(am)}$	$\alpha_{(A/B)}$	$\alpha_{(T/O)}$	$\alpha_{(C/P)}$	$\alpha_{(P/BnOH)}$	$\alpha_{(B/P)}$	$\alpha_{(P/BnOH)}$	$\alpha_{(B/P)}$
ACE 3 C18	5.45	1.47	1.50	0.37	1.01	0.09	1.04	0.34
Type C^{TM} Bidentate C18	5.54	1.44	1.90	0.94	1.10	0.12	1.12	4.56

A(am) = amylbenzene, B = butylbenzene, T = triphenylene, O = *o*-terphenyl, C = caffeine, P = phenol, $BnNH_2$ = benzylamine, BnOH = benzyl alcohol

The separation factor for triphenylene and o-terphenyl gives an indication of the steric selectivity of the phase; triphenylene is a planar solute whereas o-terphenyl is bulky due to the free rotation of the aromatic groups. Stationary phases that exhibit steric selectivity will retain the triphenylene longer than the o-terphenyl as the spatial arrangement of the bonded silanes allow the flatter analyte to insert itself between the silanes allowing for a greater degree of interaction. As triphenylene is a more aromatic molecule this extra retention can sometimes be attributed to π-π interactions. However in this case the silanes are stated to be octadecyl ligands and no aromatic functionality is expected from either of these columns.

If we compare the retention times of triphenylene on the two phases, the TYPE-C^{TM} Bidentate C18 column shows a longer retention than the ACE 3 C18 where as the o-terphenyl is comparable on both phases. The monomeric bonding process of the ACE 3 C18 silica means the hydrocarbon chains are likely to be vertically aligned and packed in a dense uniform manner, we have already seen the hydrophobicity of the two phases is comparable, which indicates there are a similar number of octadecyl ligands on both phases. The difference in the $\alpha_{(T/O)}$ value suggests that the way the ligand bonds to the polymeric monolayer of the TYPE-C^{TM} Bidentate C18 yields a different spatial arrangement of the hydrocarbon chains. The uneven surface of the silica-hydride layer may result in the C18 ligands sticking out in different directions and having a larger space in between the

hydrocarbon chain which allows the planar analyte more chances to fit in between the ligand and gives added shape selectivity.

As the manufacturers claim the TYPE-C^{TM} Bidentate C18 phase has no residual silanols on the surface of the stationary phase there should be no capacity for H-bonding from hydroxyl groups and the caffeine should have a low retention time. Looking at the ACE 3 C18 the retention time for caffeine is lower than that of a neutral phenol marker indicating the endcapping on the phase suppresses any secondary interaction of the silanols. However the TYPE-C^{TM} Bidentate C18 phase shows a longer retention time, eluting closer to the neutral phenol showing there are some secondary H-bonding interactions, this is confirmed by the larger $\alpha_{(B/P)}$ as discussed on the following pages.

Figure 5.1 ***Graph of Tanaka comparison of ACE 3 C18 and TYPE-C^{TM} Bidentate C18 phases***

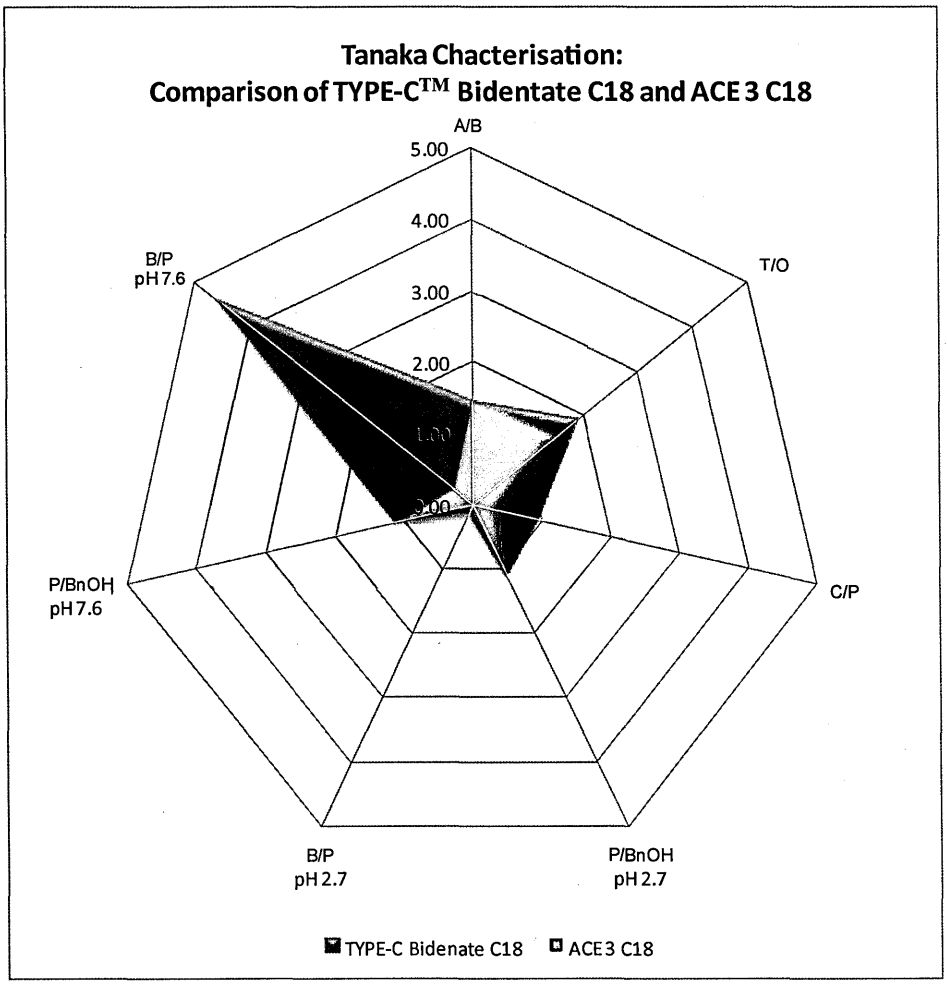

A(am) = amylbenzene, B = butylbenzene, T = triphenylene, O = *o*-terphenyl, C = caffeine, P = phenol, $BnNH_2$ = benzylamine, BnOH = benzyl alcohol

When these alpha values are compared to the same interactions on the EPS phases from Section 4.1.1 it can be seen how a higher level of H-bonding from the stationary phase yields a longer retention time of caffeine and thus a higher alpha value. This comparison is shown in Table 5.3. The results from the previous chapter suggest that the Platinum EPS and Alltima HP phases are lightly bonded dimethyl substituted octadecyl silane based phases. These phases use the high percentage of residual silanols on the surface of the TYPE-B silica, or TYPE-A silica in the case of the Platinum EPS, for the polar interactions which would account for the high alpha values shown. The TYPE-C™ Bidentate C18 phase does not exhibit this level of silanophilic interaction but is more comparable with the HyPURITY Aquastar and XSelect HSS phases. The results in the previous chapter have shown that these phases use the hydroxyl-group endcapping for the polar interaction contributions. This suggests that the H-bonding occurring on the TYPE-C™ Bidentate C18 phase is not from residual silanols on the surface of the silica but from hydrolysed triethoxy silanes within the silica hydride Bidentate layer.

Ionic exchange is an exceedingly strong retention mechanism in chromatographic terms, as the silanol groups on the stationary phase will be ionised or unionised at different pH levels, in this case it is believed that the only ion exchange interactions on the stationary phase will come from ionisation of the residual silanols. Here the retention times of the neutral phenol marker against charged benzylamine were compared at low pH, where only acidic silanols will be ionised, and at neutral pH which will show total silanophilic activity. It has been seen in Section 1.5 that free and geminal silanols have a high acidity.

The ACE 3 C18 results can be used as an example of a phase that has a low level of ion exchange interactions; the retention times of phenol and benzyl alcohol are reasonably similar at both pH 2.7 and pH 7.6. Although there has been a small increase in the retention of benzylamine at neutral pH it is not a significant shift. Due to the high purity of the silica and the endcapping process used for this phase there are a low number of available acidic silanols. When looking at the same comparison for

the TYPE-C™ silica column a significant shift in retention time was seen, so that at neutral pH the benzylamine co-elutes with the phenol, indicating the column is exhibiting a large ion exchange character. The silanophilic activity observed by the value of $\alpha_{(B/P)}$ at low pH is comparable to the ACE C18 phase; however at neutral pH this is significantly higher indicating a higher level of "less-acidic" silanol activity on the TYPE-C™ Bidentate C18 phase.

Table 5.3 ***Tanaka characterisation values – Comparison of TYPE-C™ Bidentate C18 and EPS phases***

					pH 2.7		pH 7.6	
	$k_{(am)}$ [221]	$\alpha_{(A/B)}$	$\alpha_{(T/O)}$	$\alpha_{(C/P)}$	$\alpha_{(P/BnOH)}$	$\alpha_{(B/P)}$	$\alpha_{(P/BnOH)}$	$\alpha_{(B/P)}$
Type C™ Bidentate	5.45	1.44	1.90	0.94	1.10	0.12	1.12	4.56
HyPURITY Aquastar	1.39	1.40	2.78	0.89	0.89	0.14	0.89	3.04
Platinum EPS C18	0.70	1.35	2.23	2.22	0.82	0.35	1.03	8.10
XSelect HSS SB C18	2.52	1.38	1.94	1.74	0.84	0.13	0.85	5.34
Zorbax-SB AQ	1.13	1.30	1.18	2.59	0.89	0.14	0.87	1.11
Alltima HP C18 EPS	0.45	1.29	2.38	1.61	0.87	0.22	0.88	5.62

A(am) = amylbenzene, B = butylbenzene, T = triphenylene, O = *o*-terphenyl, C = caffeine, P = phenol, $BnNH_2$ = benzylamine, BnOH = benzyl alcohol

Comparison of the alpha values between the TYPE-C™ Bidentate C18 and the EPS phases, as seen in Section 4.1.1, confirms these deductions on the level of electrostatic interactions. For phases which are known to have a high level of available silanols on the surface of the silica, the Platinum EPS and Alltima HP phases[263][266], the $\alpha_{(B/P)}$ is significantly higher at neutral pH. At low pH only the Platinum EPS and Alltima HP phases are seen to have a higher $\alpha_{(B/P)}$ value, the former has a higher value as it is bonded using a TYPE-A silica which will contain a greater number of metal ions which give rise to more acidic silanols.

Although the main polar contribution of the HyPURITY Aquastar and XSelect HSS phases has been shown to come from hydroxyl groups substituted on the silane, these phases have a lower carbon

load than the ACE 3 C18 and according to the manufacturers are not endcapped[262][264] therefore some of the base silica is likely to be accessible. Due to the low number of acidic silanols observed in the Tanaka data in the previous chapter the phases are believed to be bonded onto a highly pure TYPE-B silica base. The purity of the base silica used to manufacture the TYPE-C™ Bidentate phase is not known. The $\alpha_{(B/P)}$ values are comparable with those of the XSelect HSS and HyPURITY Aquastar phases which suggests that a high purity silica has been used if the electrostatic interactions observed arises from silanols on the surface. However the bidentate monolayer formation would block any surface silanols and the observed cationic exchange would most likely be from hydrolysed TES within the cross-linked shell. A possible schematic for the TYPE-C™ Bidentate C18 phase defining these two different types of silanol groups is shown in figure 5.2 below.

Figure 5.2 ***Diagram of acidic and non-acidic silanols/hydroxyl groups on a possible structure of the TYPE-C™ Bidentate phase***

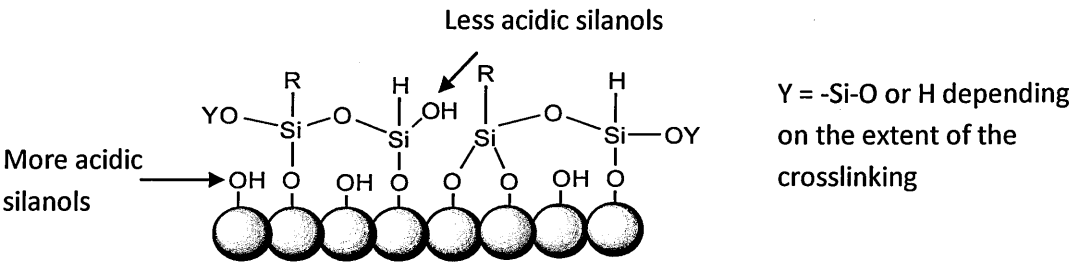

Overall the Tanaka characterisation results determined here are relatively comparable to the values reported in the PQRI database found in the USP Database[231][232][274] as shown in Table 5.4. Again the PQRI results indicate the hydrophobicity of the two columns is comparable and the TYPE-C™ Bidentate C18 phase shows enhanced steric selectivity, hydrogen bonding and ion exchange separations. Previous studies have shown a good correlation between the PQRI database and experimental Tanaka results for hydrogen bonding where no π-π interactions are observed[45]. This is shown in further detail in Section 5.1.4.

Table 5.4 ***PQRI Characterisation Values – Comparison of ACE 5 C18 and TYPE-C^{TM} Bidentate C18 phases***

	Hydrophobicity	Steric Selectivity	Hydrogen Bonding		Cation Exchange		Silica Type
			Acidic	Basic	pH 2.8	pH 7.0	
ACE 5 C18	1.00	0.027	-0.096	-0.007	0.143	0.096	B
Cogent Bidentate C18	0.95	0.059	-0.130	0.004	0.785	2.266	A

The TYPE-C^{TM} Bidentate C18 phase is quoted to be a TYPE-A silica base; however this is not documented in the manufacturer's data. The purity of the silica used is an interesting question, the Tanaka results shown on page 149 show a lower $\alpha_{B/P}$ value at lower pH when compared to the Platinum EPS phase which is known to be a TYPE-A phase. However if the phase has a full bidentate mono-layer of silica hydride as described in the introduction this should block any of the residual silanols on the surface. If this is the case the manufacturers may have used a low purity TYPE-A style silica, this would be difficult to test and as the Tanaka results have shown that there are little or no acidic silanols contributing to the retention mechanism it would be an academic activity.

5.1.2 *Further Column Characterisation of TYPE-C™ Bidentate Phase*

The evidence of residual silanol or hydroxyl group activity can also be observed in the chromatograms of the basic solute analysis shown in Figure 5.3 below.

Figure 5.3 ***Chromatographic gradient comparisons of 10 basic solutes and phenol on TYPE-C™ Bidentate C18 and ACE 3 C18 phases***

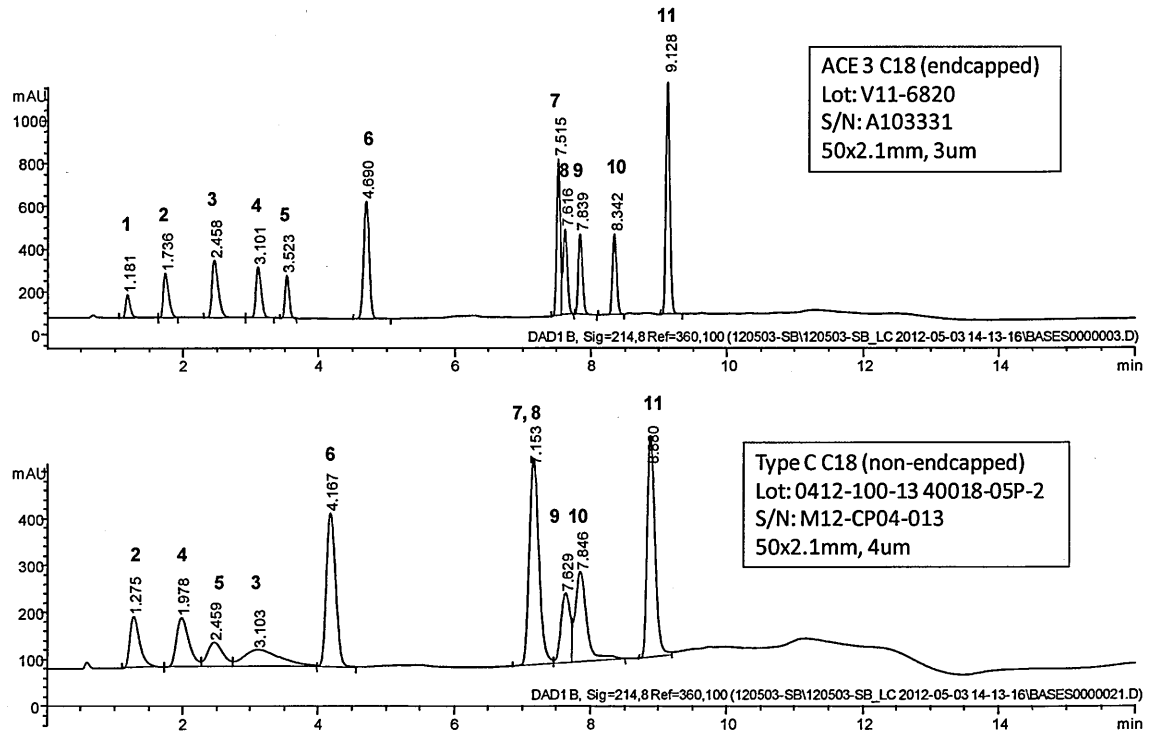

1. Nicotine, 2. Benzylamine, 3. Procainamide, 4. Terbutaline, 5. Salbutamol, 6. Phenol, 7. ARD-12495, 8. ARC-68397, 9. Diphenhydramine, 10. Racemide, 11. Nortripyline

Here the effect of the secondary electrostatic interaction was seen, this occurs on the TYPE-C™ Bidentate C18 stationary phase in a real-life situation. At low pH multiple charged bases such as procainamide and nicotine are significantly more retained on the TYPE-C™ Bidentate C18 phase than the ACE 3 C18. Nicotine (compound 1) is so well retained it is not observed to elute as a peak and is either co-eluting with another analyte or is lost in the rising baseline between 10 and 12 minutes. In general the peak shapes on the TYPE-C™ Bidentate C18 phase are significantly broader which will reduce resolution between peaks. Even the phenol marker, which will not be affected by silanophilic interactions, shows a broader peak on the TYPE-C™ Bidentate C18 phase. The peak is

still Gaussian in shape however the peak width is significantly broader on the TYPE-C™ Bidentate C18 than the ACE 3 C18 (0.1493min compared to 0.0882min measured at half height at 214nm). This indicates the TYPE-C™ Bidentate C18 phase is giving rise to poor mass transfer or a sub optimum packed column which is allowing for greater dispersion of the analytes as they travel down the column.

The two phases were also compared for the retention times of hydrophilic and lipophilic bases using the isocratic analysis. The results are shown below in Figures 5.4 and 5.5.

Figure 5.4 ***Chromatographic isocratic comparisons of hydrophilic bases and phenol on TYPE-C™ Bidentate C18 and ACE 3 C18 phases***

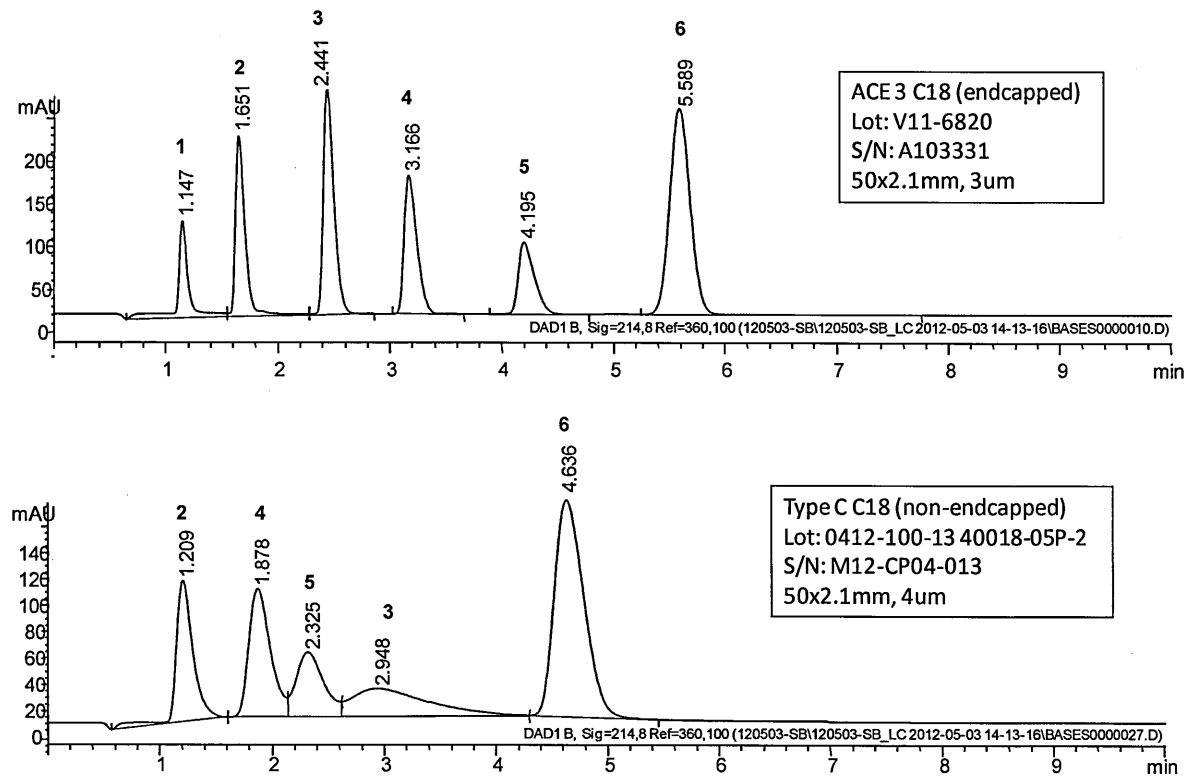

1. Nicotine, 2. Benzylamine, 3. Procainamide, 4. Terbutaline, 5. Salbutamol, 6. Phenol

The longer retention time and poor peak shape for procainamide is more exaggerated in the isocratic analysis. Comparison of peak shapes for all analytes shows the peaks on the TYPE-C™ Bidentate C18 to be significantly broader and exhibit a greater degree of tailing than those on the

ACE 3 C18. Although this is expected for many of the hydrophilic bases due to the silanophilic interaction between the charged analyte and the silanols on the phase, the difference in lipophilic bases and the neutral phenol marker indicates that the poor peak shape is not just through these secondary interactions.

Figure 5.5 ***Chromatographic isocratic comparisons of lipophilic bases and phenol on TYPE-C^{TM} Bidentate C18 and ACE 3 C18 phases***

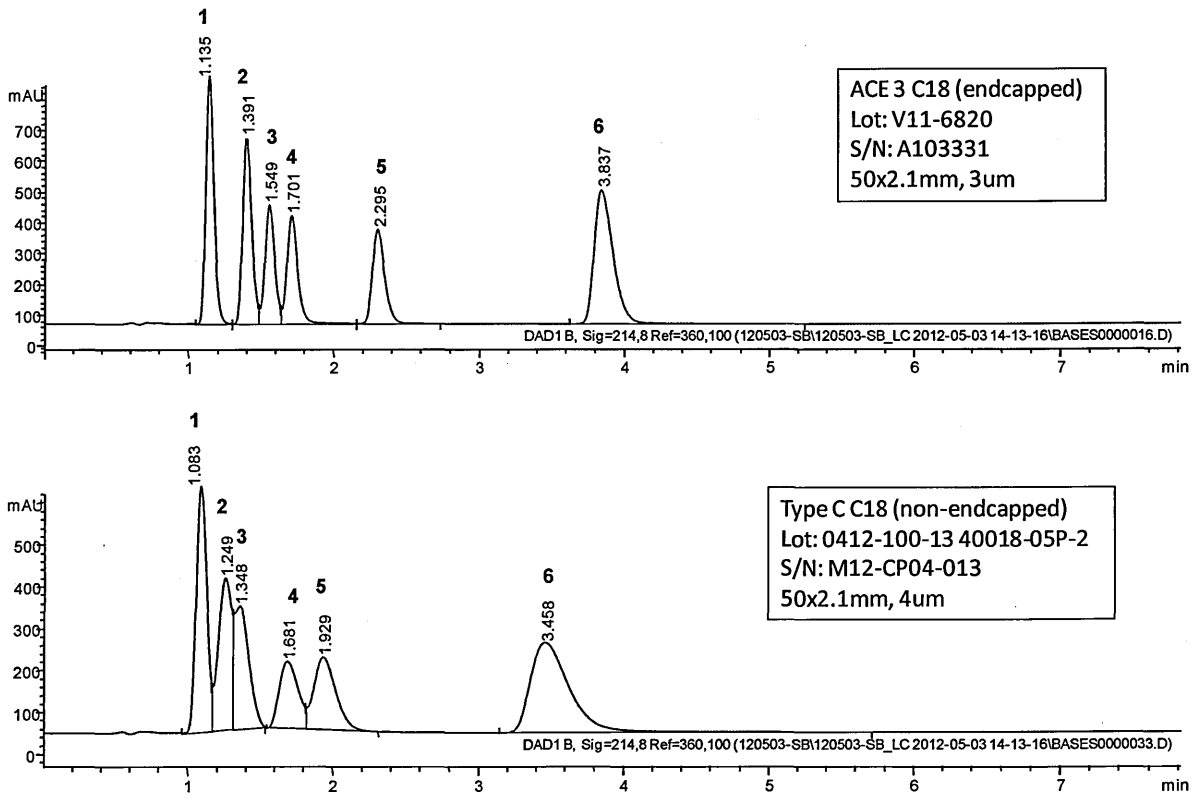

1. Phenol , 2. ARD-12495, 3. ARC-68397, 4. Diphenhydramine, 5 Racemide, 6. Nortripyline.

To ensure the column had not deteriorated through use the amyl benzene and butyl benzene samples from the Tanaka characterisation were re-run and the retention times and peak shapes compared. No difference in retention factor and peak shape was observed in either column before and after the basic solutes analysis. Although it was noted that the peak widths at half height for these neutral analytes was larger than on the TYPE-C^{TM} Bidentate C18 phase than the same injection volume on the ACE 3 C18. These results indicate that there are larger differences between the two phases than the retention mechanism requires further investigation.

The chromatograms show a marked difference in the two phases; however numerical comparison of the alpha values for the gradient analysis, shown in Table 5.5 below, does indicate any great difference in the phases. The main disparity observed is in the $\alpha_{P/B}$ value which arises from the increased retention time of procainamide on the TYPE-C™ Bidentate C18 phase due to the secondary electrostatic interaction with the silanols. Simply looking at these figures does not convey the variation seen in the two phases.

Table 5.5 ***Basic Solutes Characterisation Values – Comparison of ACE 3 C18 and TYPE-C™ Bidentate C18 silica***

	$\alpha_{P/B}$	$\alpha_{S/T}$	$\alpha_{397/P}$	$\alpha_{397/495}$	$\alpha_{397/D}$	$\alpha_{No/P}$
ACE 3 C18	3.76	1.17	1.73	1.01	0.97	2.10
TYPE-C™ Bidentate C18	5.22	1.35	1.83	1.00	0.93	2.32

N = nicotine, B = benzylamine, PA = procainamide, S = salbutamol, T = terbutaline, D = diphenhydramine, R = remacemide, N = nortriptyline, 397 = ARC68397

Further characterisation work with using acidic and neutral solutes was also carried out; these results are shown in the appendix. The analysis showed comparable retention times on both the ACE 3 C18 and TYPE-C™ Bidentate C18 phases although in the majority of cases the peak widths were noticeable broader and more tailed on the TYPE-C™ Bidentate C18 phase. This difference in peak width may be due to the difference in particle size across the two columns but as it is a continuing trend observed for the TYPE-C™ Bidentate C18 phase it merited further investigations.

5.1.3 On-Column Endcapping of TYPE-C™ Bidentate Phase

The long retention times and poor peak shape observed on the TYPE-C™ Bidentate C18 phase for basic analytes indicates a larger number or residual silanols accessible on the surface of the phase. To investigate this further one of the TYPE-C™ Bidentate C18 columns was subjected to on-column endcapping using N,O-Bis(trimethylsilyl) acetamide. Any accessible silanols or hydroxyl groups on the phase should be capped with the N,O-Bis(trimethylsilyl) acetamide as in the schematic shown in Figure 5.6 below. Unlike the chloro substituted silanes the by-product from this reaction is neutral which would be washed off the column without further reaction.

Figure 5.6 Schematic of possible endcapping reaction pathway on TYPE-C™ Bidentate C18 phase using N,O-Bis(trimethylsilyl) acetamide

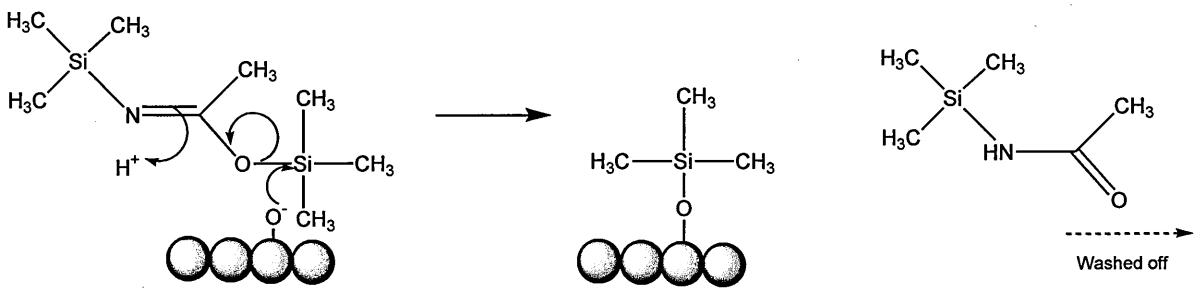

The column used had previously been subjected to characterisation and stability work therefore the structure of the silica hydride monolayer may have changed since the initial bases evaluation. The gradient and isocratic bases methods were run prior to the endcapping procedure and the same samples and mobile phases run immediately following the procedure to assess the change in accessible silanols, the results from the gradient run are shown in Figure 5.7 overleaf.

Figure 5.7 ***Chromatographic gradient comparisons of hydrophilic bases and phenol on TYPE-C^{TM} Bidentate C18 before and after on-column endcapping***

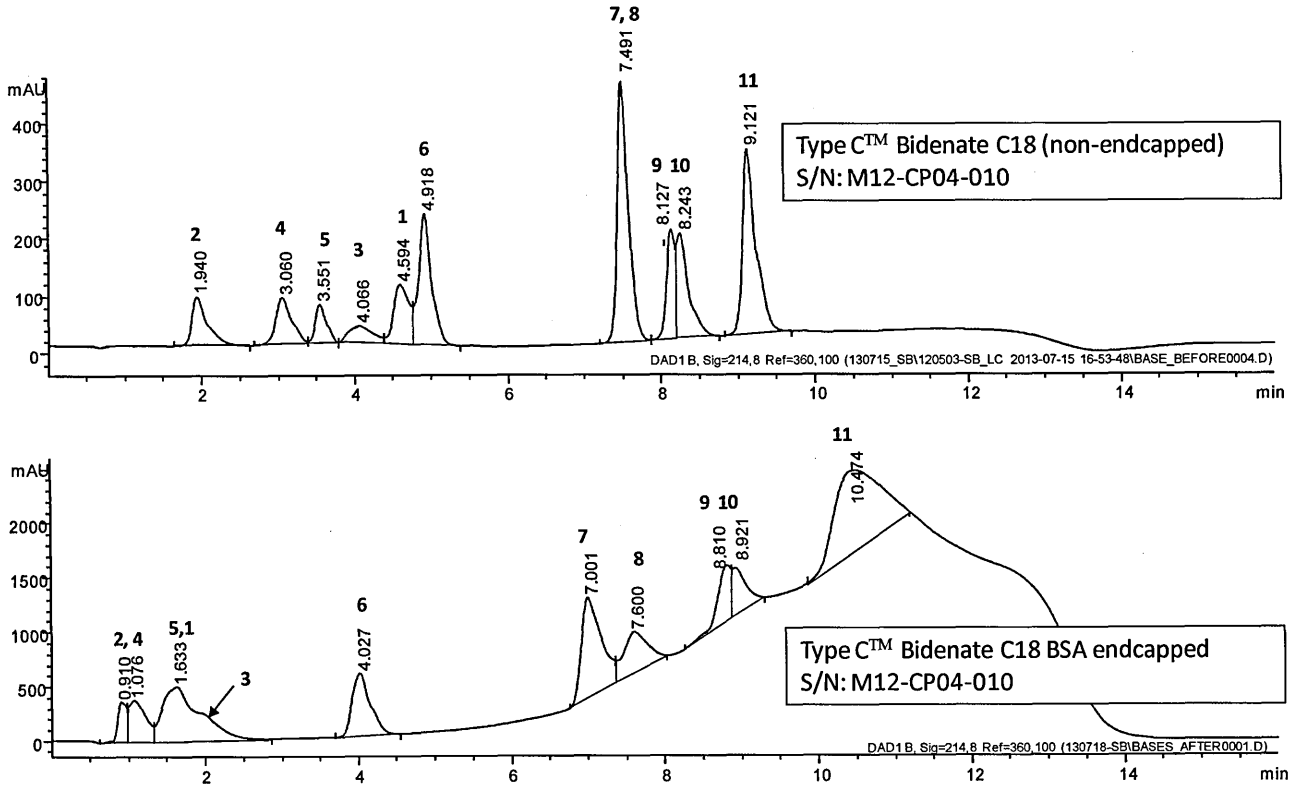

1. Nicotine, 2. Benzylamine, 3. Procainamide, 4. Terbutaline, 5. Salbutamol, 6. Phenol, 7. ARD-12495, 8. ARC-68397, 9. Diphenhydramine, 10. Racemide, 11. Nortripyline

Prior to endcapping the peak shape of the bases are wider and more tailed than previously seen on page 155. However, as this column has been exposed to harsh conditions and elevated temperatures during other characterisation work the structure of the silica hydride monolayer may have been altered resulting in further silanols being exposed or octadecyl ligands being cleaved. On this phase the nicotine peak is now distinguishable from the procainamide and phenol peaks whereas on the previous TYPE-C^{TM} Bidentate C18 column it was not possible to assign this analyte. Again this may be due to the silica hydride and octadecyl ligand structure being altered during testing or it may be due to differences in the packing.

Following the endcapping procedure the baseline was noted to rise excessively with the blank gradient analysis, therefore the injection volume for the bases experiment was increased to compensate for this. Several injections were run and it was noticed that the peak shape and

retention time appeared to deteriorate over the runs, indicating the phase is leaching silane, most likely the BSA endcap which may be being cleaved due to the elevated temperature of this analysis. The chromatogram shows a marked difference in retention time of the bases; the majority of the analytes appear to have a reduced retention time however ARC-68397, diphenhydramine, and remacemide are seen to have comparable retention. The nortriptyline may have an increased retention time however due to the sharply rising baseline and peak due to cleaved BSA silane at the end of the gradient it is difficult to accurately assign this peak.

The neutral phenol marker also appears to have reduced retention time, this is indicative of loss of the octadecyl phase and it may indicate that the structure of the silica hydride and C18 ligands was altered during the bonding process. The procedure was carried out at 80°C which is at the top end of the temperature range suggested by the manufacturers. However it is probably that the elevated temperature caused some ligand cleavage during the bonding process. The decreased retention times may be due to a reduction in electrostatic interaction due to minimising the silanol activity on the phase or it may simply be due to the ligand cleavage of the octadecyl phase reducing the hydrophobic interactions with the basic analytes. Due to co-elution of the peaks it is not possible to determine and compare peak tailing of the basic analytes before and after the endcapping process.

The on-column endcapping shown does indicate that the residual silanols are readily accessible as some of the BSA endcap appears to have bonded. However the rising baseline suggests that the bonding is not very stable and it liable to cleave off at elevated temperatures. Overall the analysis is not conclusive and ideally it would be useful to repeat this using less harsh conditions and a small, more reactive endcapping agent such as trimethyl silane however as there were only two TYPE-C™ Bidentate C18 columns available it was not possible to carry out further experiments.

5.1.4 *Hydrogen-Bonding Assessment of TYPE-C™ Bidentate Phase*

So far evidence has been shown that the TYPE-C™ Bidentate C18 phase does exhibit hydrogen-bonding and electrostatic interactions from ion exchange which are contrary to the claims of the manufacture. However these tests are performed using methanol as the organic modifier rather than acetonitrile, although the manufacturers do not discourage the use of methanol with their phases it may be possible that the silica hydride surface of the phase is being converted to silanols during analysis. To ensure this was not the case a brand new column was used to determine the retention time of caffeine and phenol over 1500 column volumes. The column was used straight from the box without being allowed to equilibrate in order to determine any changes in peak shape. The main shift in retention times is observed in the first few injections as shown in Figure 5.8 below, following this a further 2.1% reduction in retention time of the co-eluting peak was seen from 2.485 to 2.43 minutes as shown in Figure 5.8 below.

Figure 5.8 ***Initial 5 injections of phenol and caffeine on TYPE-C™ Bidentate C18***

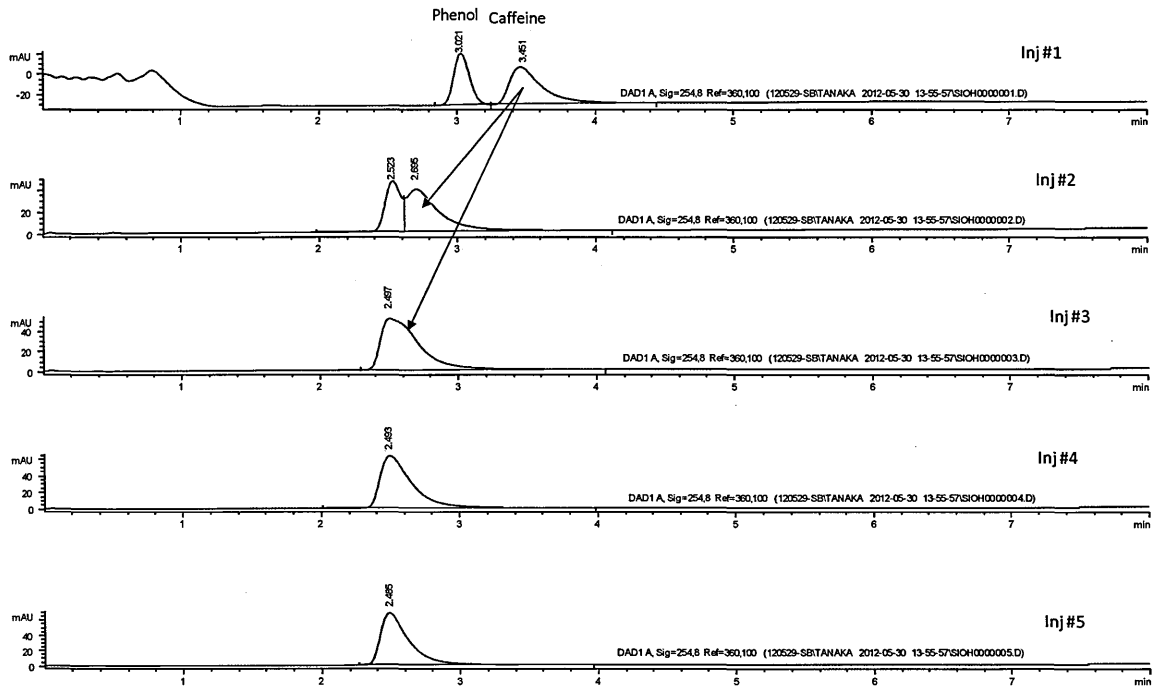

As the TYPE-C™ Bidentate phases are packed and stored in 50:50 Water:Acetonitrile solvent mix the initial shift of retention time is likely to be due to the different mass transfer properties of acetonitrile versus methanol. The manufacturers state that only 7 – 10 column volumes are required to condition a new column for use[273], as a single 8 minute injection would equate to 15 column volumes the column should be fully equilibrated and conditioned following this first injection. However a significant amount of retention shift is observed for caffeine between the 2nd and 5th injection. Overall the retention time of caffeine is decreasing equating to a loss in residual silanol activity; this indicates that methanol is not causing the silica hydride to be converted to silanol on the silica surface.

This reduction in retention time denotes a loss of H-bonding interactions on the phase, this may occur as some of the polymeric monolayer is lost through silane snippage either at the base silica or across the polymeric covering itself. Although a 2.1% shift in retention time appears to be relatively small decrease it should be noted that this occurs over a low number of column volumes at neutral pH and 40°C which are typical operating conditions. As the manufacture claims these columns are very stable due to the shorter covalent Si-C bond formed with the silica-hydride monolayer even this small reduction in retention time is unexpected. Further stability work to fully assess the phase is shown later in Section 5.3. These results may suggest the phase loss is due to cleavage of the octadecyl ligand from the polymeric monolayer. This could be explained by cleavage of the ladder phenomenon alluded to in Section 1.5 as these irregular strands of organocarbon chains are susceptible to severing from the crosslinked triethoxysilane shell. However this effect is more likely to be due to slow equilibration of the phase due to the change in organic modifier. This is common for around 40% of HPLC phases[275] although it does contradict the manufacturer's claims for fast equilibration in 7-10 column volumes.

The previous results discussed in this chapter indicate that hydrogen bonding is occurring on the TYPE-C™ Bidentate phase; there are a number of documented characterisation methods and probes for H-bonding[277][279] all containing a tertiary nitrogen atom as a hydrogen bond acceptor. These are shown in more detail in Section 3.2. These solutes are compared against a neutral analyte in an unbuffered aqueous/organic mobile phase and the resultant retention and selectivity factors are calculated. The figures for the TYPE-C™ Bidentate phase were compared against the ACE 3 C18 and the EPS phase results from Chapter 4 are shown in Table 5.6 below.

Table 5.6 ***Hydrogen Bonding Selectivity Factor Values - Comparison of ACE 3 C18, EPS phases and TYPE-C™ Bidentate C18 silica***

	$\alpha_{DMA/EB}$	$\alpha_{D/T}$	$\alpha_{C/P}$	$\alpha_{Py/Ph}$
ACE 3 C18	0.02	0.41	0.37	0.54
TYPE-C™ Bidentate C18	0.05	0.52	0.94	2.67
HyPURITY Aquastar	0.07	0.60	0.89	1.47
Zorbax SB AQ	0.07	0.62	2.59	1.56
XSelect HSS SB C18	0.09	0.72	1.74	1.68
Platinum EPS C18	0.15	0.80	2.22	2.96
Alltima HP C18 EPS	0.18	0.78	2.34	2.34

DMA = Dimethylacetamide, EB = Ethylbenzene, D = N,N-Diethyl-meta-toluamide, T = toluene, C = caffiene, P(Ph) = phenol, Py = pyridine

Visually comparing the values in Table 5.6 we can see that the ACE 3 C18 has relatively low α values, this is to be expected as it has already been seen that there is a low percentage of available silanols on the surface of this phase. Although there does not appear to be any correlation between the different α values for each pair of analytes. However the ACE 3 C18 values are the lowest across all four analyses. As with previous results the TYPE-C™ Bidentate phase is more comparable with the EPS phases than a typical C18. For the first two α values the TYPE-C™ Bidentate C18 phase is more comparable to the HyPURITY Aquastar and Zorbax SB AQ EPS phases. Here a trend was observed, as the carbon load on the phase decreases the α value increases. It is known that the Platinum EPS C18

is bonded to TYPE-A silica[259] therefore the more acidic silanols would be expected, however as this analysis is carried out at neutral pH it is the overall silanol distribution that is being assessed.

For the $\alpha_{C/P}$ value a similar trend is noticed, as discussed in Section 4.1.1 the Zorbax SB AQ phase shows a higher value than expected based on the level of electrostatic interactions observed in the Tanaka analysis. The value is high due to the longer retention of caffeine over phenol. This may be due to the extra interactions from the bulky isopropyl silane substituents that make up the Stable-Bond of these Zorbax phases. Again the column manufacturers do not publish the exact structure of these silanes as it is proprietary information but from Section 4.3 it was thought that this phase is a pentyl hydrocarbon chain with a single isopropyl substituent. In this type of analysis caffeine would be susceptible to secondary interactions from aromatic (π-π) interactions. However, as shown in Section 4.1.2 and 4.3 there is no aromatic functionality present on this phase and the hydrogen bonding capacity is coming highly accessible silanols on the surface of the silica.

As discussed in Section 5.1.1, literature has shown that the Snyder $\alpha_{DMA/EB}$ results can be directly correlated to the Tanaka $\alpha_{C/P}$ values for phases that have no contribution for π-π interactions[45]. The experimental data shown here was correlated in the same way and shown in Figure 5.9-5.11 overleaf.

Figure 5.9 *Correlation of Snyder and Tanaka Style Hydrogen Bonding Results*

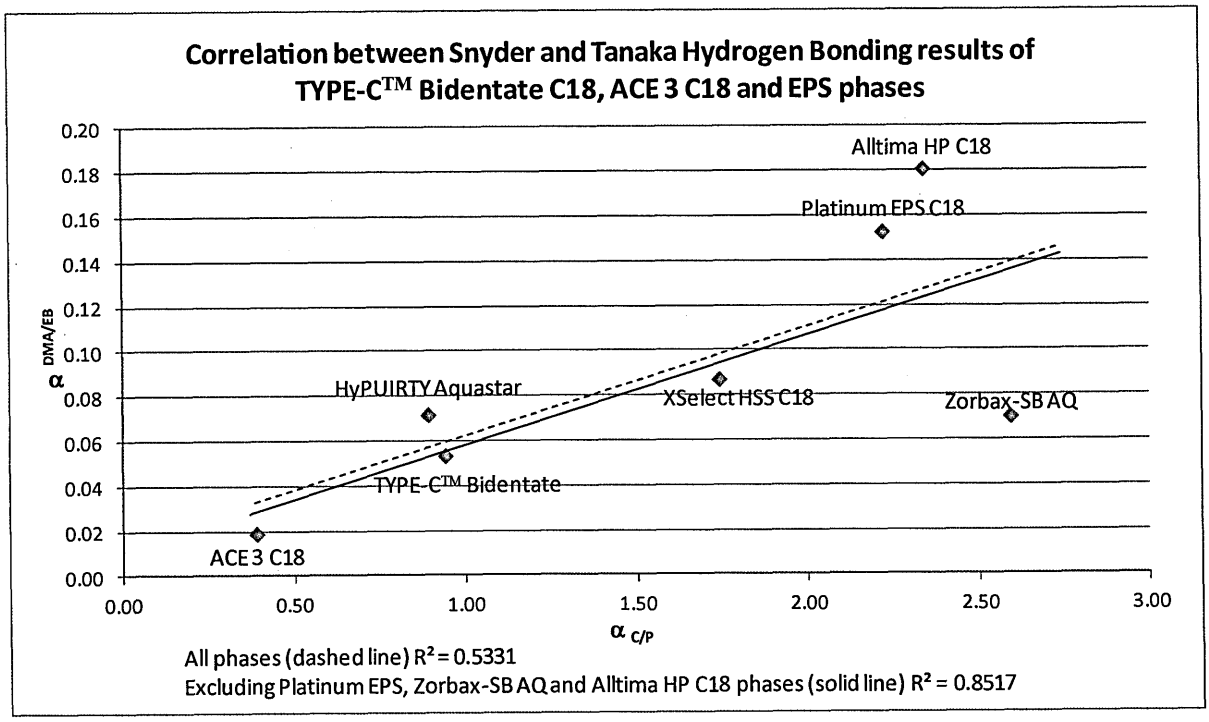

Figure 5.10 *Correlation of Alltech and Tanaka Style Hydrogen Bonding Results*

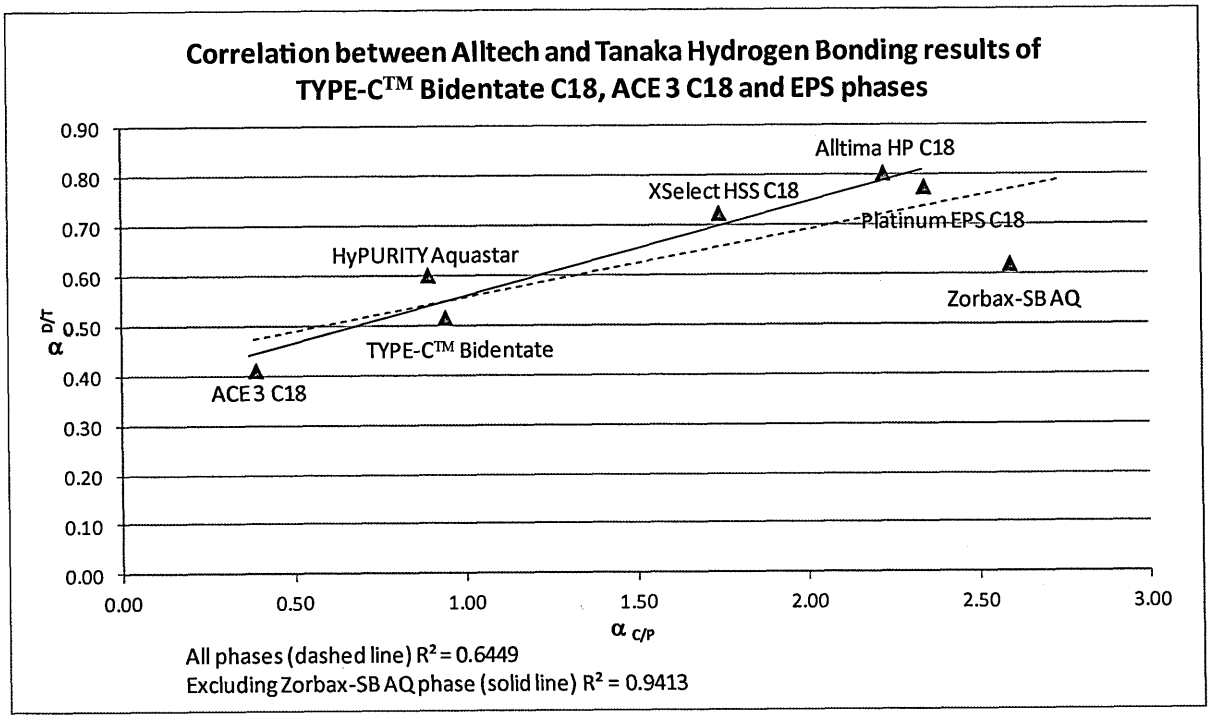

The TYPE-C™ Bidentate , ACE 3 C18 and some of the EPS phases show a correlation of the Snyder and Alltech testing against the Tanaka results as shown in the plots above. The two lightly bonded phases and the Zorbax-SB AQ phase are shown to be outliers in the Snyder and Tanaka correlation; these phases are known to have highly accessible silanols which may give rise to electrostatic interactions with the caffeine and a longer retention time. Removing these results from the data set shows a higher correlation although the number of phases shown is much lower than the literature results[45] which might account for the difference.

For the Alltech versus Tanaka comparison the full data set shows a higher correlation and it is only the Zorbax-SB AQ phase that is seen to be an outlier. In Section 5.1.1 the Zorbax-SB AQ and Zorbax-SB C3 phases have been shown to have a longer retention of caffeine compared to similar columns. This is likely to be due short aliphatic chains leading to very accessible silanols on the surface allowing for greater electrostatic interactions.

Figure 5.11 ***Correlation of Engelhardt and Tanaka Style Hydrogen Bonding Results***

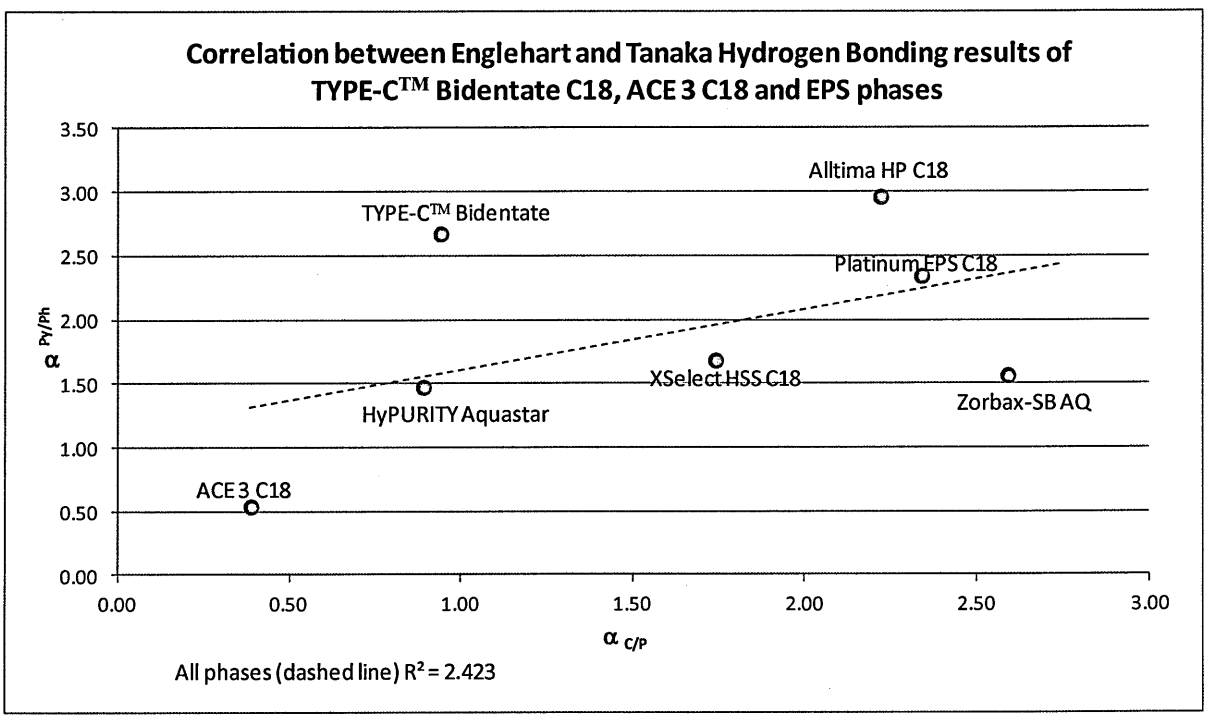

The comparison of the Engelhardt and Tanaka results shows no correlation between the two data sets. This may be due to the pK_a of pyridine being close to that of the unbuffered mobile phase making it an unsuitable probe for hydrogen bonding in these conditions. In all cases it can be seen that the TYPE-C™ Bidentate phase has higher α values than the ACE 3 C18; this mirrors previous findings that suggests the residual silanols are more accessible on the TYPE-C™ Bidentate C18 silica. This is especially apparent in the analysis of pyridine (pK_a 5.20, LogP 0.77, LogD 0.65 quoted at pH 7[284][285]) and phenol (pK_a 9.95, LogP 1.47, LogD 1.63 quoted at pH 7[284][285]), however it should be noted that the pK_a of pyridine is very close to that of the unbuffered methanol:water mobile phase[284] resulting in a percentage of the analyte in solution being ionised. This makes the method non-reproducible[274][276] and consequently further studies were done using buffering additives to understand the retention mechanism and determine a more robust method[278], a similar experiment was carried out for the TYPE-C™ Bidentate phase, the results are shown overleaf.

In the unbuffered state the pyridine peak elutes at 1.5 minutes and is observed to exhibit significant peak tailing; this is likely because the ionised and unionised solutes will show different affinities for the stationary phase as the positive charge on the ionised form will be retained longer by any negative acidic silanols available on the surface of the phase.

At lower pH it has already been seen the retention mechanism is governed by the distribution of acid silanols on the phase. As the pyridine is now fully ionised we would expect to see peak tailing again due to secondary interactions with the silanols, however in this case the tailing factor is noticeably lower than previously observed. The retention time of pyridine has decreased as the buffer ions will compete with the available active surface silanols and reduce the interaction with the pyridine itself. The three chromatograms for the different pHs are stacked for visual comparison and shown in Figure 5.12 below.

Figure 5.12 ***Comparison of Engelhardt Hydrogen-Bonding analysis at different pH levels on TYPE-C^{TM} Bidentate C18 phase***

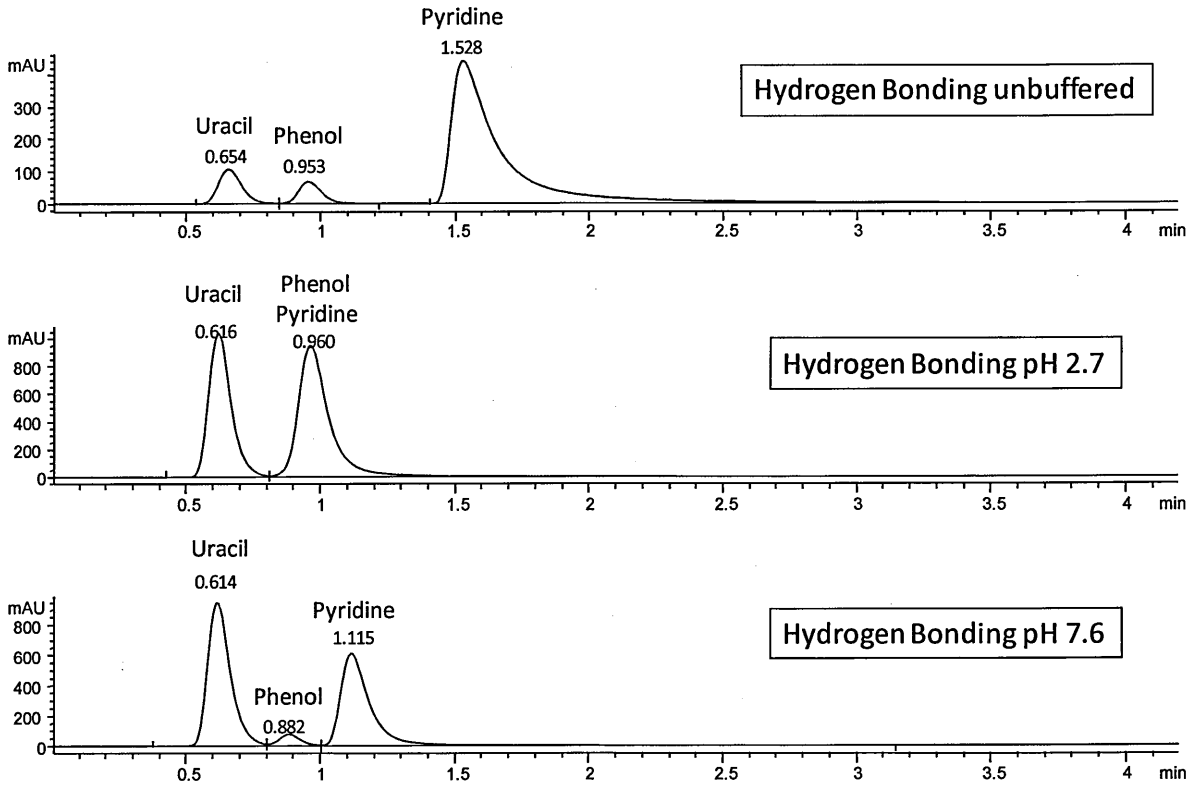

At higher pH the pyridine will be fully un-ionised as the pH is now two units above the pK_a of pyridine therefore the H-bonding effect will be reduced and the retention time decreases, however, the separation observed between phenol and pyridine indicates that H-bonding is still playing a role in the retention mechanism. As with the ion exchange characterisation the hydrogen bonding at pH 7.6 is due to all residual silanols, here the pyridine is retained for longer than observed at pH 2.7, which only indicates hydrogen bonding for the more acidic silanols sites. The retention of the phenol appears to decrease slightly at pH 7.6. Again this is another indication that whatever is responsible for the hydrogen bonding on the TYPE-C^{TM} Bidentate C18 phase are unlikely to be from acidic surface silanols species.

5.1.5 *Mobile Phase Ionic Strength and pH Effects on TYPE-C™ Bidentate Phase*

It has been seen from the Tanaka characterisation that the TYPE-C™ Bidentate C18 phase exhibits a degree of electrostatic interaction which is likely to be due to un-reacted hydroxyl groups within the bidentate monolayer, and possibly from a small number of residual silanols groups accessible on the surface of the silica. The majority of these silanol groups appear to be weakly acidic, as the $\alpha_{(B/P)}$ value is seen to be significantly higher at neutral pH, however some of these silanols groups appear to be ionised at low pH.

Considerable research has been carried out on characterising the different types of silanol found on the surface of the silica stationary phase and the subsequent interactions with charged analytes[279]-[283]. The main contribution to the retention mechanism is from electrostatic ion exchange, at low pH the cation exchange mechanism can be shown to be in equilibrium with the potassium base:

(I) $$SiO^-H^+ + K^+H^+PO_4^{-2} \leftrightarrows SiO^-K^+ \; H_2^+PO_4^{-2}$$

The equilibrium constant for the ion exchange interaction (k_{IE}) can be calculated by the following equation[283]:

(II) $$k_{IE} = \frac{[SiO^-K^+][H_2^+PO_4^{-2}]}{[SiO^-H^+][K^+H^+PO_4^{-2}]}$$

Therefore the ionisation constant is controlled through the concentration of the ionic buffer. The distribution coefficient (D_{IE}) for a single analyte can be derived for this relationship and the retention factor (k), assuming that the analyte is in the fully ionised form.

(III) $$D_{IE} = \frac{[SiO^-K^+]}{[SiO^-H^+][K^+H^+PO_4^{-2}]} = k_{IE}.\frac{[SiO^-H^+]}{[H^+]} \cdot \frac{1}{1 + k/[H^+]}$$

As the distribution coefficient is dependent on both the ion exchange equilibrium constant and number of accessible silanols on the surface of the silica it is also related to the inverse of the concentration of counter ions in the mobile phase. Therefore by plotting the retention factor against the inverse of the ionic concentration of the mobile phase should determine the relationship between the accessible silanols and their contribution to the retention mechanism. As the ionic strength is increased the counter ion will compete with the free silanols groups and suppress these electrostatic interactions with the charged analytes thereby reducing the retention factor.

Again this was run at pH 3.0 where only the acidic silanols will be ionised, and pH 7.0 where all the silanols will be active. Ammonium acetate was used as an ionic buffer as potassium phosphate at neutral pH can degrade the silica surface. Three organic bases were chosen for the analysis; nortriptyline (pK_a 9.7), quinine (pK_a 8.4) and pyridine (pK_a 5.2)[285]. The plots for these three basic analytes run at pH 3.0 is shown in Figure 5.13 below and pH 7.0 in Figure 5.14 overleaf.

Figure 5.13 ***Effect of ionic concentration on retention factor of basic analytes for ACE 3 C18 and TYPE-C™ Bidentate C18 phase at pH 3.0***

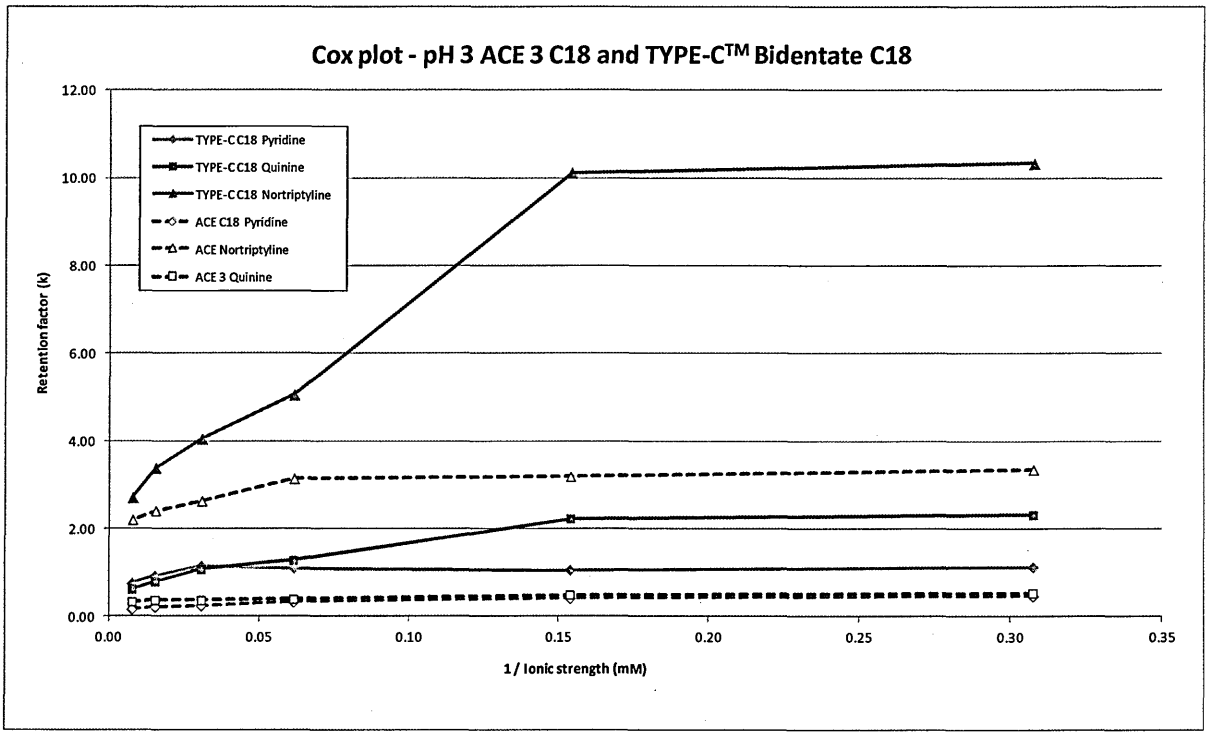

The nortriptyline, as the strongest base, shows the greatest retention time on both columns. As the molarity of the ionic buffer increases the retention factor decreases as the silanophilic interactions are being suppressed by the ammonium counter ion. At pH 3 the retention factor is seen to plateau at low concentrations of counter ion, the more acidic silanophilic interactions are dominating the retention mechanism and the low levels of counter ion are not able to suppress these charged groups. As the counter ion concentration increases over 20 mM the retention factor decreases sharply as the silanophilic interactions are being suppressed by the counter ion. As the strength of these electrostatic interactions is much higher than the less acidic silanols or hydrophobic interactions even a tiny percentage of unsuppressed silanols can have a significant contribution to the retention factor which accounts for the higher plot. The plot cannot be extrapolated to zero for any of the analytes as even at infinite concentration of counter ion there will still be a hydrophobic contribution to the retention factor from the C18 ligands.

Figure 5.14 ***Effect of ionic concentration on retention factor of basic analytes for ACE 3 C18 phase at pH 7.0***

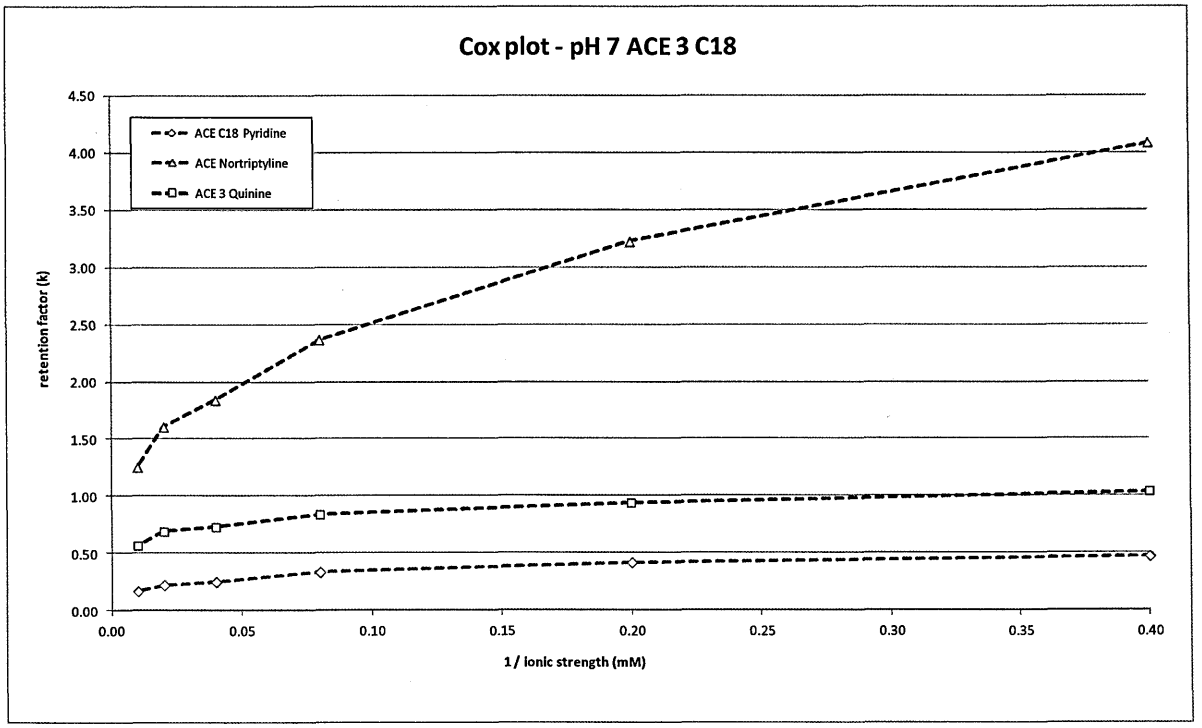

Ammonium acetate has a pH of around 6.8 therefore an excess of acetic acid was required to adjust the pH to 3 however only a small amount of ammonia was required to adjust the mobile phase to pH 7. As acetic acid is an ion pair reagent this analysis is not directly comparable to the pH 3 results shown previously, however the two columns were run on the same mobile phase and therefore can be directly compared. The plot for the retention factor of nortriptyline at pH 7 shows a more linear progression and proportionally decreases as the concentration of the counter ion increases. At high ionic concentrations the counter ions will be suppressing the silanophilic interactions therefore the retention factor is lower than that at pH 3 as the majority of silanols will be suppressed. As the strength of these silanophilic interactions is lower the small amount of unsuppressed silanols will have less of a contribution. However, as the counter ion concentration decreases the silanophilic contribution to the retention mechanism increases significantly. The plot does not plateau out as previously observed indicating a greater number of the lower acidic silanols.

The plots for quinine follow the same trend; however as this is a weaker base the retention factors are lower. Even at pH 7 the retention factor appears to plateau out as the concentration of the counter ions tends to zero. Pyridine shows no change between pH 3 and pH 7 as it is a less basic analyte, therefore it is in the conjugated acid form at pH 3 and unionised at pH 7[285]. Consequently the only contribution to the retention mechanism will be from the hydrophobic interactions and as the silanophilic interactions will not retain neutral or acidic molecules and increasing the concentration of the counter ion has minimal affect the retention mechanism.

The same analytes were run on the TYPE-C™ Bidentate C18 phase, the results for the pH 7 analysis are shown in Figure 5.15 overleaf. Here the retention factors at pH 3 are a little higher than those observed for the ACE 3 C18 phase however the retention factors for nortriptyline and quinine at pH 7 are over 20 fold higher. The pyridine shows no change as before due to the molecule being in its unionised or neutral form and only being affected by the hydrophobic retention mechanism.

The vast difference in the pH 7 results confirms the significantly increased number of lower acidity silanols accessible on the TYPE-C™ Bidentate C18 stationary phase surface. A much smaller percentage of acidic silanols are also present however these are only marginally higher than those observed in the ACE 3 C18 phase and may go some way to contributing to the increased peak tailing on basic compounds as seen in the previous sections. However it can be seen from these results that there is a significant contribution from non-acidic silanophilic interactions to the retention mechanism.

Figure 5.15 ***Effect of ionic concentration on retention factor of basic analytes for TYPE-C™ Bidentate C18 phase***

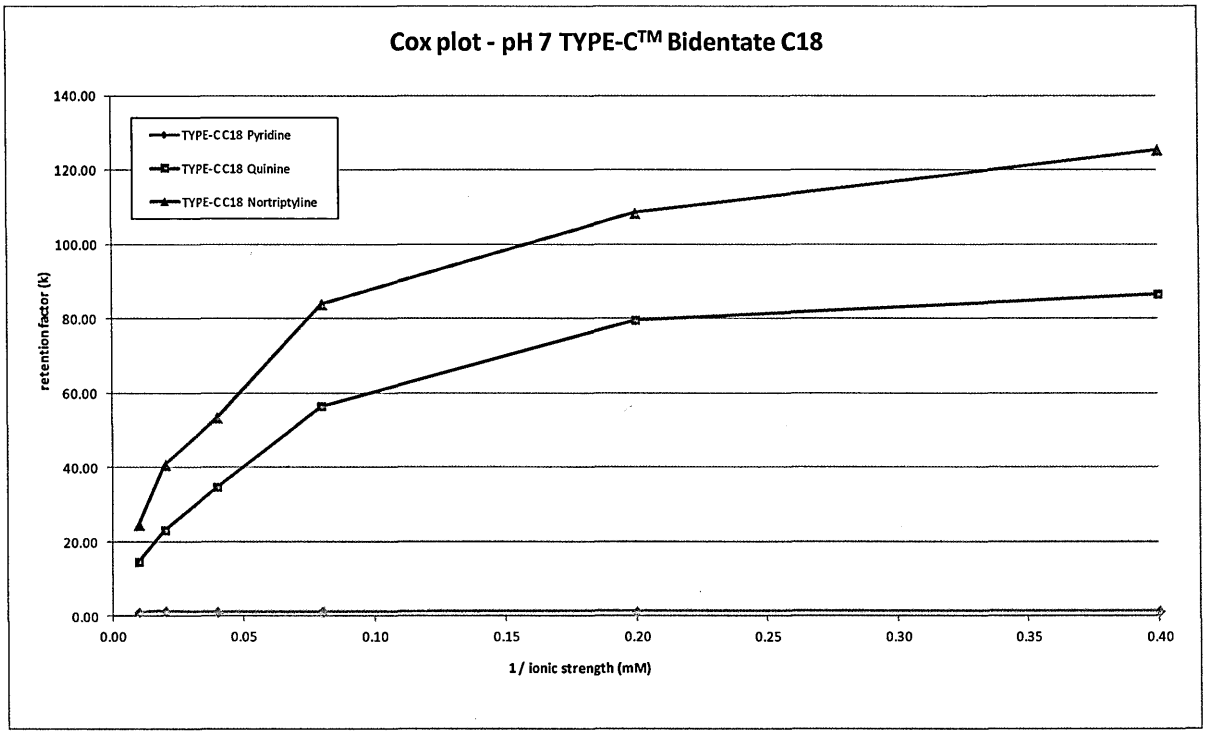

This mirrors the findings from the previous characterisation work, these results confirm the presence of accessible silanol groups on the surface of the TYPE-C™ Bidentate C18 stationary phase and that the majority of these are non-acidic silanols. These interactions could be coming from hydroxyl groups within the bidentate monolayer or they could be coming from the silica itself. The purity of the base silica used for the Cogent TYPE-C™ phases is not known as this is proprietary information.

It has been discussed in the introduction how modern high purity silicas, such as TYPE-B style silica, yield a lower percentage of acidic silanols.

At high concentrations of buffer the secondary interactions from the silanols groups should be minimal as the charged silanols will preferentially interact with the smaller buffer ions. Interestingly when the peak widths for the two columns are compared it is noted that those observed on the TYPE-C™ Bidentate C18 are significantly higher than those on the ACE 3 C18. As already discussed the pyridine solute will be unionised at pH 7 and at high concentrations of buffer and secondary interactions from hydrogen bonding or dipole-dipole interactions from the silanols will be minimised. Under these conditions it can be seen that the peak width for the pyridine peak is around one and a half times wider for the TYPE-C™ Bidentate C18 phase, 0.093min compared with 0.067min on the ACE 3 C18. Although the peak areas are comparable (506 versus 466) the height for the pyridine peak is reduced on the TYPE-C™ Bidentate C18 phase, 77mAU and the ACE 3 C18, 116mAU. This difference in peak width has been seen previously, these results indicate it is not solely through secondary interactions with silanophilic groups and requires further investigation.

5.1.6 *Analyte Overloading on TYPE-C™ Bidentate C18*

The findings so far have indicated the peak shape on the TYPE-C™ Bidentate C18 are less Gaussian and more tailed than the same concentration of analytes on the ACE 3 C18 phase. It has been shown that this is especially prominent for basic compounds at low and neutral pH which indicates the presence of secondary silanophilic interactions occurring during the retention mechanism. In these previous characterisation models it has been assumed that the low concentration of solutes analysed have little to no overloading capacity on these stationary phases and the sample bands travel down the column independently of each other. However it is known that some stationary phases can exhibit overloading even at very low concentrations of analytes and overloading occurs more readily at ionisable silanols sites on the surface of the silica [286]. As efficiency (N) is a function of width at base (W_b) of a peak it may be possible that the poorer peak shape observed on the TYPE-C™ Bidentate C18 is caused by overload tailing[287].

Increased bandwidth of basic analytes on the column is common for both TYPE-A and TYPE-B silicas that have residual accessible silanols[288] although more pronounced on the former due to the more acidic silanols. These occur as the analytes travel in a band down the column and as each charged solute molecule interacts with an accessible silanols it will form a temporary ionic bond, this essentially blocks the site for other molecules in the group due to the mutual repulsion effect. The next molecule in the group will be repelled by the positively charged base now retained on the stationary phase and has to travel onto the next available site for ionic interaction thereby increasing the width of the band of molecule. For acidic silanols sites the strength of the ionic interaction is higher and the charged analyte will be retained for longer increasing this affect. Overloading effects can be mitigated by increasing the ionic strength of the buffer as the smaller charged ions will preferentially pair with the silanols and thus render them inactive. As we have already seen ionic binding is a very strong retention mechanism and even a small distribution of highly acidic silanol sites can lead to rapid overloading at low pH[286].

Figure 5.16 and 5.17 below describe the overloading properties for both the TYPE-C™ Bidentate C18 and ACE 3 C18 columns using methanol as an organic modifier. The percentage of organic was altered for each compound and column to try and keep the retention factor (k) as comparable as possible. Here the change in peak shape for a neutral and basic analyte was assessed as the sample concentration is increased until the efficiency of the peak reaches half its initial value (N-50%). The ACE 3 C18 phase exhibits classic column overloading characteristic commonly known as "shark-fin" peaks for the basic analyte (I) as the peak shape became more akin to a right angle triangle which resemble the dorsal fin of a shark. Whereas the neutral moiety (II) retains a more Gaussian appearance with an increases in sample concentration. Previous characterisation of this phase using basic analytes indicated a low distribution of active silanols; these results may indicate a small number of highly acidic silanols are still accessible even on the surface of this highly inert silica.

Figure 5.16 ***Overloading of (I) Nortriptyline and (II) Phenol injections on ACE 3 C18 at pH 2.7***

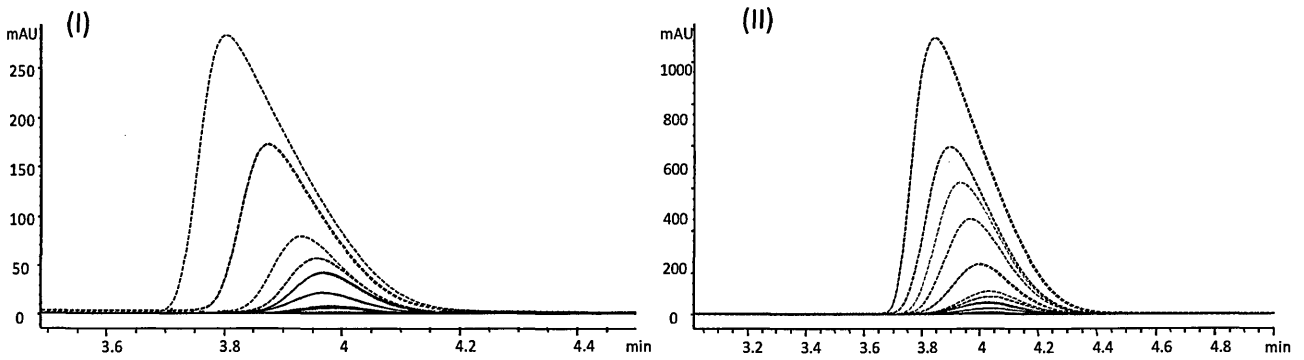

Figure 5.17 ***Overloading of (I) Nortriptyline and (II) Phenol injections on TYPE-C™ Bidentate C18 at pH 2.7***

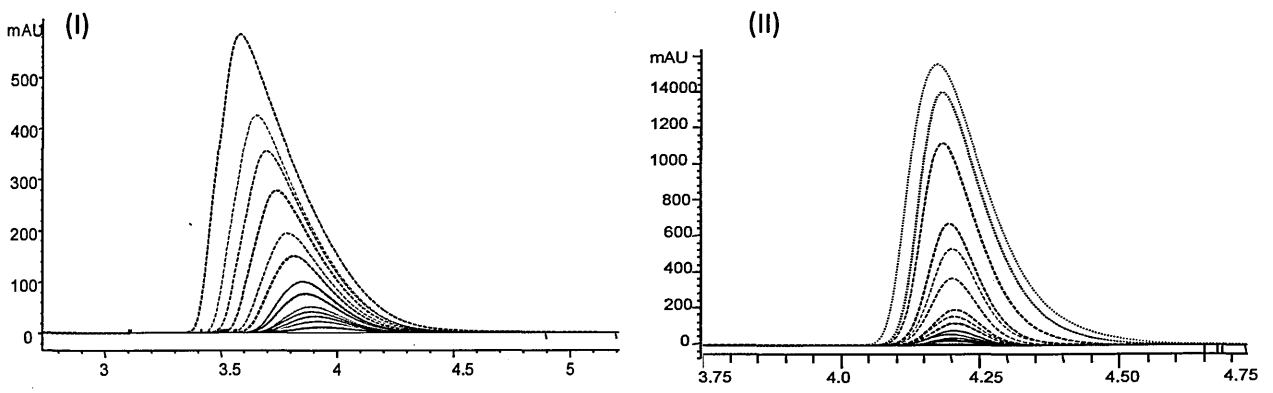

Initial observation of the chromatograms suggests that the ACE 3 C18 exhibits greater overloading capacity than the TYPE-C™ Bidentate C18 however the overall peak widths for the phenol are significantly higher on the latter phase. This mirrors the findings with the characterisation investigations although this would suggest that the increase in peak width is not caused by column saturation. The column saturation capacity (W_s) can be calculated numerically[286] by manipulation of the equation for the width at base (W_b) for heavily overloaded peaks:

(IV) $$W_s = \frac{N_0(6t_0^2k_0^2W_x)}{(N_0W_b - 16\,t_0^2\,(1+k_0)^2}$$

Where:
W_s = Saturation capacity
N_0 = Initial efficiency of the column
t_0 = Column dead time
k_0 = Initial retention factor
W_x = Sample weight at column saturation
W_b = Peak width at base

The saturation capacity of a phase is directly proportional to the sample weight (W_x) that can be injected onto the column. The saturation capacities for both the TYPE-C™ Bidentate C18 and the ACE 3 C18 were calculated for overloading using both methanol and acetonitrile as the organic modifier. These results are shown in Table 5.7 below.

Table 5.7 ***Column Saturation Values at N_0-50%– Comparison of ACE 3 C18 and TYPE-C™ Bidentate C18 silica***

	Nortriptyline				Phenol			
	MeOH		MeCN		MeOH		MeCN	
	N_0	W_s (mg)	N_0	W_s (mg)	N_0	W_s (mg)	N_0	W_s (mg)
ACE 3 C18	5844	0.24	5472	0.13	4682	5.41	4372	4.45
TYPE-C™ Bidentate C18	918	1.20	1045	0.62	1946	8.49	1791	8.43

As previously discussed the W_s value is reduced for ionised samples hence it is not surprising that the values calculated for the basic moieties are considerably lower than the neutral marker for the

sample concentrations. However what was not expected is that the W_s values for the TYPE-C™ Bidentate C18 is 5 fold higher than that of ACE 3 C18 for the ionised nortriptyline and one and a half times higher for the neutral phenol. This analysis was run at both 214nm and 254nm however only the results from 254nm are reported below. As the phenol moiety shows much greater absorption at the lower wavelength resulting in a greater peak area and peak width, as efficiency is inversely proportional to peak width this reduces the sample concentration for N-50% resulting in a lower W_s value at 214nm.

It can be seen in the calculated W_s values that the saturation concentration for the phases using methanol as an organic modifier is significantly higher than the same analysis using acetonitrile. This may be due to the size and polarity of the organic molecules, as methanol is a smaller and more highly polar molecule it does not obstruct the analytes proximity from the silica surface and the octadecyl ligand. Essentially, the methanol allows more analytes to access the stationary phase and is likely to encourage larger number of solute molecules to interact with a single ligand through hydrogen bonding of the hydroxyl groups. Acetonitrile is a more commonly used organic modifier in HPLC analysis as it is thought to give sharper peaks which often results in better resolution between peaks. However these results indicate that methanol is a superior organic modifier for column saturation effects for these phases.

The calculated column saturation values indicates that overloading is not responsible for the larger peak widths observed on the TYPE-C™ Bidentate C18 phase, however it does show an interesting difference in the efficiencies calculated for the two phases. As 50x2.1cm columns are being used for this isocratic analysis efficiency are not expected to be that large but considering the N_0 value for the ACE 3 C18 is nearly 7 fold that of the TYPE-C™ Bidentate C18 phase this indicates significant differences in the columns. Efficiency of a peak is calculated from the retention time and width of the peaks. In this analysis the organic percentage for each column was adjusted in order to keep the

retention times as similar as possible for both analytes across the two columns. Therefore this large variation in efficiency is due to the differing peak widths.

Previous characterisation work has shown that the peak width for the TYPE-C™ Bidentate C18 phase are significantly higher on all solutes than the same concentration injected on the ACE 3 C18 phase. As efficiency is inversely proportional to the peak widths these increased widths are having a detrimental effect on the efficiency of this phase. Efficiency is a function of the height equivalent to a theoretical plate (HETP) which is dependent on a number of parameters shown by the van Deemter equation[289].

(V) $$HEPT = \lambda d_p + 2\gamma \frac{D_m}{\mu} + c \frac{d_p^{\,2}}{D_m} \mu$$

Where:

$HEPT$ =	height equivalent to a theoretical plate
λ =	particle shape (with regard to the packing)
d_p =	particle diameter
γ =	regularity of interparticle spaces
D_m =	diffusion coefficient of the mobile phase
μ =	linear velocity

There are a number of parameters that can affect efficiencies therefore further investigation is required to determine why the efficiencies of the TYPE-C™ Bidentate C18 phase are lower than expected for this type of stationary phase, these are shown in Section 5.2.3.

5.1.7 Multiple Compounds Evaluation of TYPE-C™ Bidentate: S Value Calculation

The Tanaka analysis shown in Section 5.1.1 uses a small number of characterisation compounds as probes to understand the retention mechanism of a stationary phase. To get a fuller picture of how different functional groups will be retained on a particular phase a larger number of compounds are required, here a mixture of acidic, basic, neutral and phenolic compounds were run by a short gradient analysis using both 0.03% (v/v) $TFA_{(aq)}$ and 20 mM potassium phosphate buffer at pH 2.5 in methanol and acetonitrile organic solvents. The retention times for each solute were compared for each phase and represented graphically in Figure 5.18 below.

A 10 mg/mL solution of toluene was injected periodically to check the system; the relative standard deviation for these phases is typically <3%. The full calculations for mean and standard deviation on retention time, peak area, width, and symmetry for these injections can be seen in the appendix.

Figure 5.18 ***Comparison of retention times on TYPE-C™ Bidentate C18 verse ACE 3 C18***

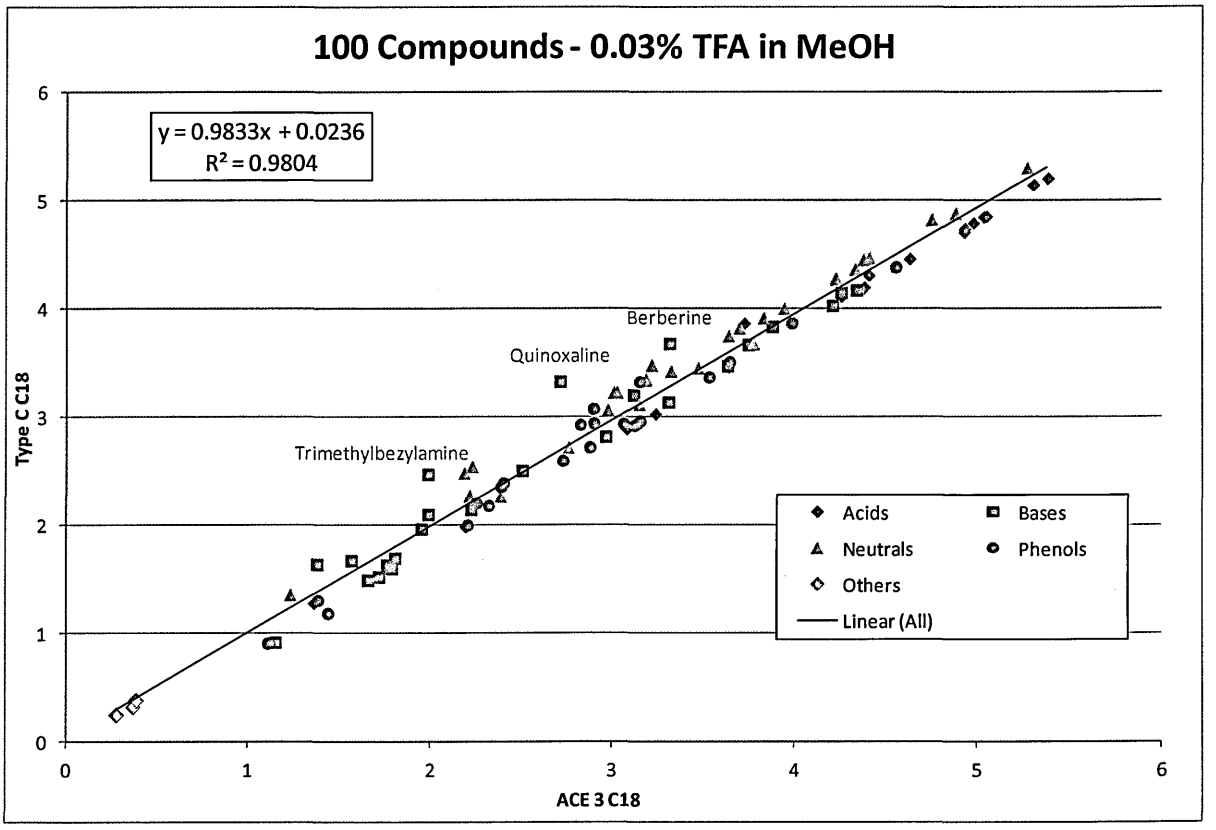

TFA is often used as a reagent in ion pair chromatography, in aqueous solution the hydroxyl group dissociates and forms a conjugated base which is stabilised by the dipole moment of the trifluoromethyl group. It can form complexes with acidic and neutral analytes[246][256] in solution forming neutral or negatively charged species respectively which can alter the retention order of a mixture of analytes. The negatively charged conjugated base can also be adsorbed onto the surface of the column surface resulting in a negative charge which repels negatively charged ionic solutes but retains positively charged ones for longer. A low concentration of TFA has been used for this analysis however in order to ensure the results are not being skewed by ion pair interactions the retention times for all analytes were compared in both the TFA and potassium phosphate analysis. This comparison can be seen below in Figure 5.19; the retention times are comparable which suggests any effect from ion pairing is minimal on these phases.

Figure 5.19 ***Comparison of retention times on TYPE-C^{TM} Bidentate C18 using TFA pH modifier and 25mM KH_2PO_4 (pH 2.7) buffer salt to assess the degree of ion pairing***

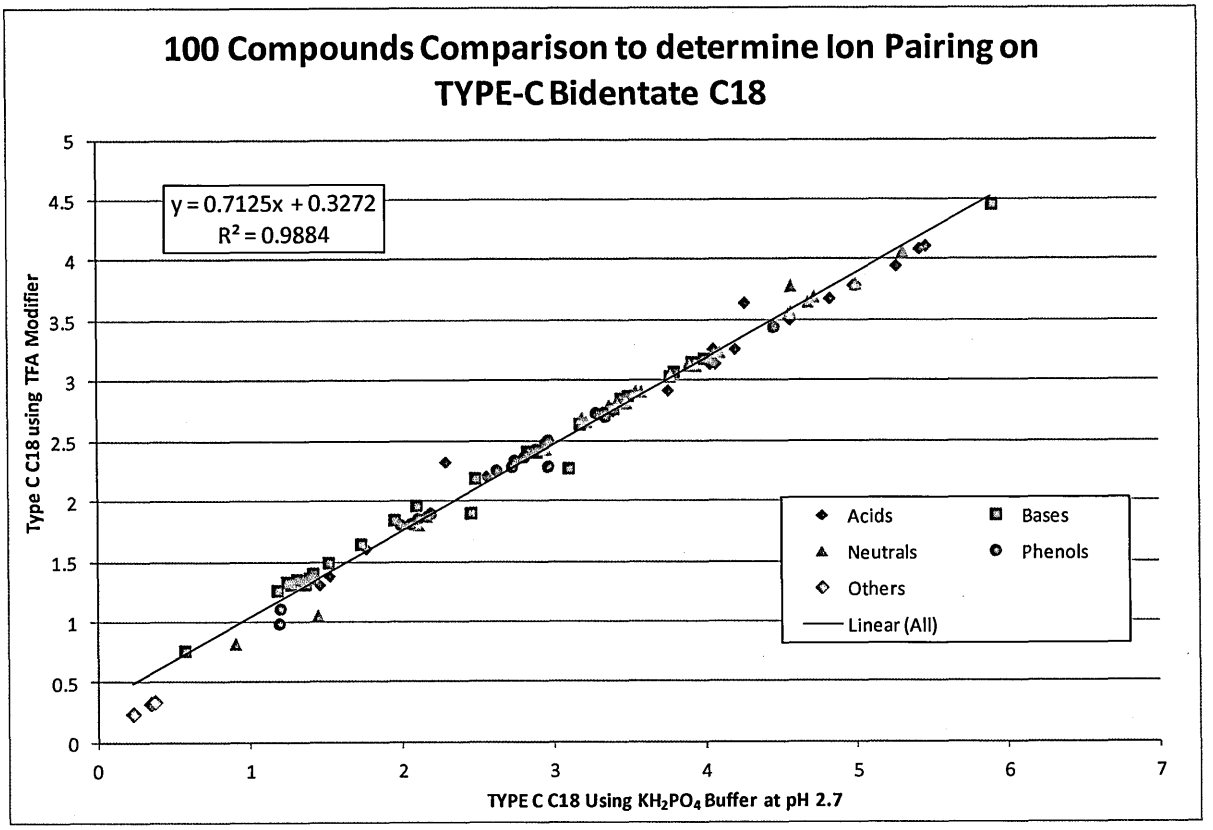

It can be seen that the majority of analytes have a very similar retention on both the ACE 3 C18 and the TYPE-C^{TM} Bidentate C18 phase. The ion suppressed acids, neutrals and phenols show a linear distribution on the plot, the majority of retention times have <5% RSD between the two phases and this indicates there is relatively little difference in the hydrophobic, π-π interactions, steric selectivity and dipole-dipole retention mechanism as has been seen previously with the Tanaka characterisation in previous sections.

Looking at the neutrals it can be seen in Figure 5.20 below, the toluene, ethyl benzene and propyl benzene are perfectly linear and follow a trend of increasing hydrocarbon chains increases retention time equally on both the columns confirming the identical hydrophobic retention mechanism on both phases.

Figure 5.20 ***Neutral Analytes on TYPE-C^{TM} Bidentate C18 verse ACE 3 C18***

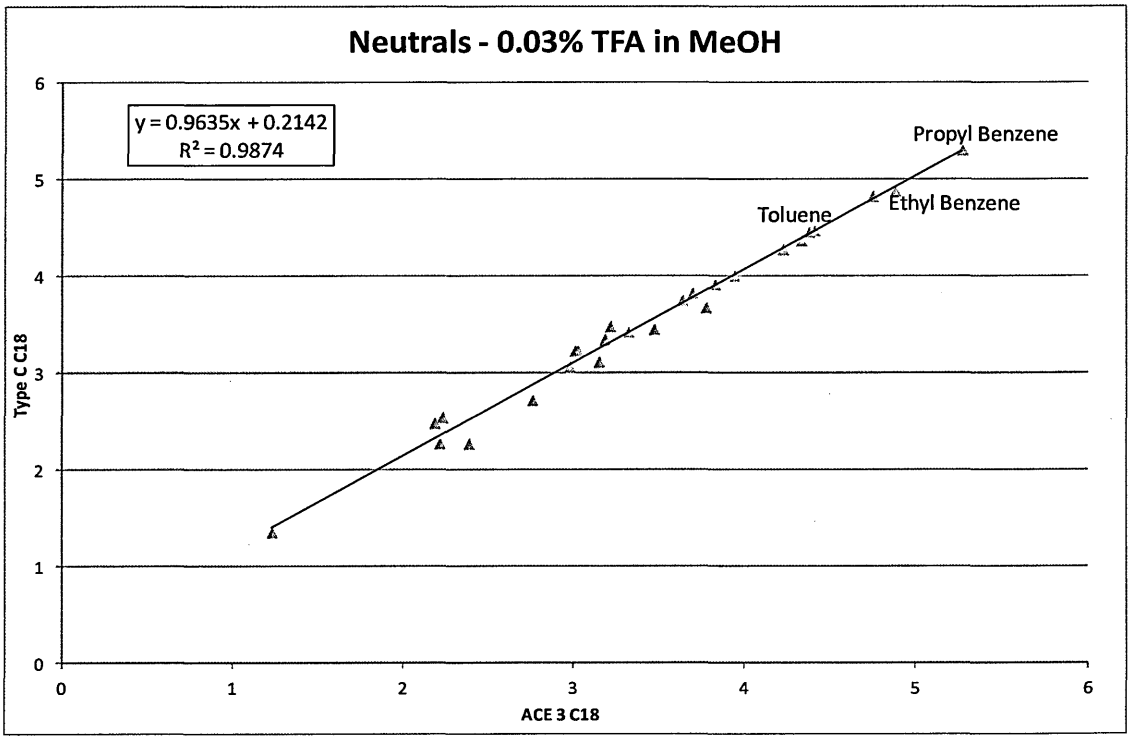

The phenol solutes and ion suppressed acids show a highly linear retention comparison on both phases, the only outlier is piroxicam, which has a number or secondary and tertiary nitrogen atoms and a hydroxyl group which may contribute to H-bonding and therefore be retained by the residual hydroxyl or silanol groups on the TYPE-C™ Bidentate C18 phase. The graphic comparisons of the phenols and acid analytes can be seen in the Appendix. The main differences observed in the retention factors comparison for the two phases can be seen in the analysis of basic solutes; the reduced correlation coefficient indicates some variation in retention times especially in the quaternary nitrogen containing compounds which show greater affinity for the TYPE-C™ Bidentate C18 column. It has already been discussed how the silanol or hydroxyl groups on stationary phases which give rise to secondary ionic binding and hydrogen bonding of basic analytes can also cause peak tailing so it is not a surprise that when we compare the peak symmetry of the basic moieties on both the TYPE-B and TYPE-C™ phases the correlation coefficient is dramatically lower.

Figure 5.21 ***Peak asymmetry calculations and examples[290]***

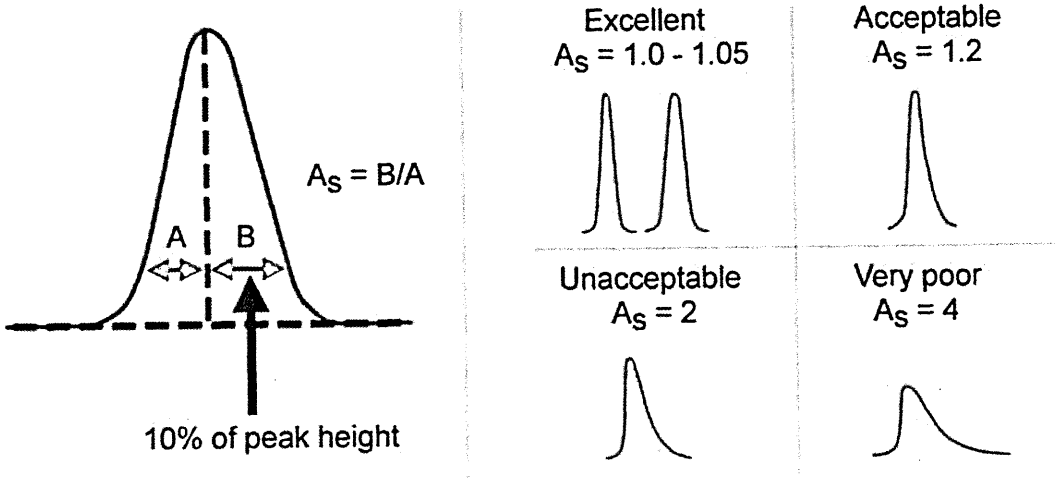

For a perfectly Gaussian peak a symmetry value of 1.0 would be expected, however in practice a symmetry measurement between 0.8 and 1.2 is considered acceptable as calculated by the equation shown in Figure 5.21. Peak tailing is more common than fronting especially with basic moieties we would expect the A_s values to be <1 for both these columns. However for the ACE 3 C18 we can see

that the majority of peaks have an A_s value between 0.6 and 1.0 but the same concentration of analytes run on the TYPE-C™ Bidentate C18 column shows A_s values of 0.3 to 0.8. The retention times and peak asymmetry figures for both the TYPE-C™ Bidentate and ACE 3 C18 phases were compared graphically and the correlation coefficients calculated, these are shown in Figure 5.22 below.

Figure 5.22 ***Comparison of retention times and peak symmetry of basic compounds of TYPE-C™ Bidentate C18 and ACE 3 C18 phases***

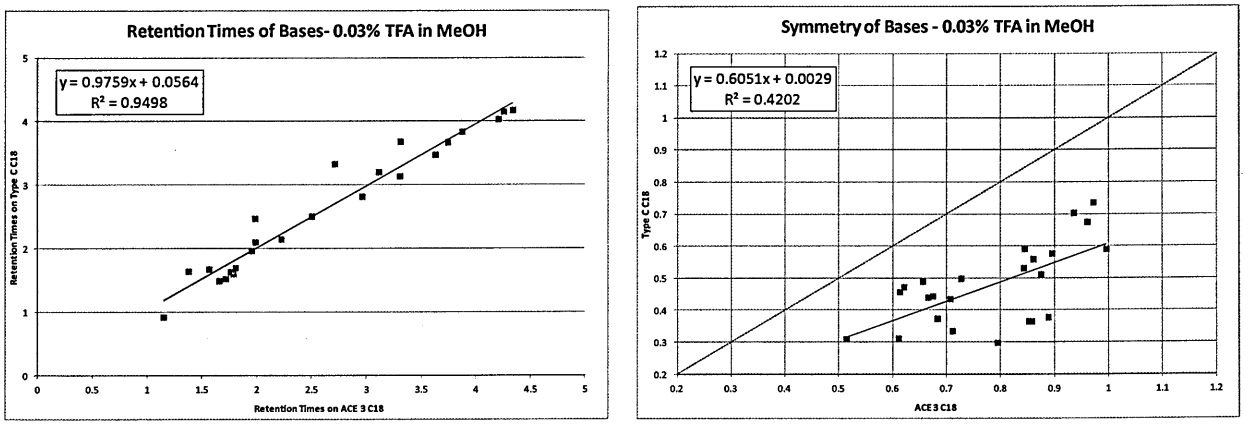

A number of previous studies have been carried out with a large set of analytes to assess the different aspects of selectivity on a broader basis. A large range of functional groups were analysed in various mobile phase conditions, especially pH and organic modifiers, to focus on specific selectivity differences between stationary phase and column packing types.

These selectivity differences (S) can be quantified numerically using the Neue equation[291], the selectivity differences of some typical stationary phases were discussed in Section 1.8.3. It can be seen that the same column analysed in different organic modifiers can give an S value of 15 due to different interactions of the analytes between the mobile and stationary phases. Whereas the different stationary phase functionalities in these two different organic modifiers can give an S value

as high as 28 as there are added variations with the interaction mechanism as well as the solvents selectivity differences, hydrophobic and π-π selectivity are shown to have the largest differences .

By comparing the S value of the TYPE-C^{TM} Bidentate C18 column and the EPS phases from Chapter 4 against a typical C18 phase we can see the S values vary significantly, this is shown in Table 5.8. The sum of all peak widths determined at half height is also included for each column in Table 5.8. By comparing the retention plots of these phases we can see the retention mechanism for the TYPE-C^{TM} Bidentate C18 phase is more comparable to the HyPURITY Aquastar and the XSelect HSS than the lightly bonded and Zorbax-SB AQ phases. For these trifunctionally bonded octadecyl phases the majority of the analytes have comparable retention times to the ACE 3 C18, however the bases show a longer retention time due to the added H-bonding and ion exchange interactions from the accessible hydroxyl substituents. This can be seen in greater detail in Section 4.1.4 and is shown below in the S values. The Zorbax SB-AQ, Alltima HP, and Platinum EPS phases show significantly different retention plots and selectivity values due to the added steric selectivity on the phases and highly accessible silanols on the surface of the phase.

Table 5.8 Neue Characterisation Values of TYPE-C^{TM} Bidentate C18, ACE C18 and EPS phases

	S value (vs. ACE C18)	Retention r^2 (vs ACE C18)	$\sum$ All Compounds Peak Width$_{0.5}$ (seconds)
ACE 3 C18	0	1.0000	5.0233
TYPE-C^{TM} Bidentate C18	14	0.9804	8.1504
HyPURITY Aquastar	23	0.9457	8.2480
XSelect HSS C18-SB	31	0.9040	6.8864
Zorbax SB-AQ	41	0.8331	6.8983
Alltima HP-C18	42	0.8242	8.0419
Platinum EPS C18	78	0.3915	10.3004

The Platinum EPS phase has a high selectivity value as the TYPE-A silica is significantly more acidic and therefore has a much longer retention of basic compounds, however the lower carbon load means it has a shorter retention time for the acidic, neutral and phenolic moieties. As with the TYPE-C™ Bidentate C18 column the payoff for this added selectivity is large peak widths. The secondary silanophilic interactions results in band broadening and increased transfer rate between mobile and stationary phase resulting in high tailing factors.

Although the HyPURITY Aquastar and Alltima HP phases have a higher peak width this is not solely due to tailing of bases, by comparing the peak width of toluene we can see that the relative peak widths are significantly higher on these phases (0.0326 and 0.0406 seconds respectively) than on the ACE 3 C18 (0.276 seconds) even though the symmetry is >0.8 for this peak. These columns were repacked from recovered material rather than purchased directly from the manufacture. As efficiency is a function of peak width the variation may be caused by a decrease in efficiency due to this process rather than any differences in retention mechanism of these phases.

The same type of analysis was carried out using acetonitrile as the organic modifier, these results showed no significant differences although the peak width was smaller due to the faster mass transfer of this solvent. Likewise the analysis using 20mM KH_2PO_4 as a buffer salt in both methanol and acetonitrile showed no significant differences in peak width. These results can be seen in the appendix. Overall the S values calculated have confirmed the findings from the previous characterisation analysis shown in this chapter. The retention mechanism from the TYPE-C™ Bidentate C18 phase has been found to comprise of both hydrophobic and silanophilic interactions. The same increased peak width has been observed for neutral, acidic, basic and phenolic compounds which indicate that this is not due to secondary interactions but is a function of the stationary phase itself. This is linked with the lower efficiencies observed in the previous chapter and further investigation will be carried out to determine the cause (Section 5.2.3).

5.1.8 Conclusion of Chromatographic Selectivity Evaluation

The findings in this chapter have shown the selectivity for the TYPE-C™ Bidentate C18 column to be between the ACE 3 C18 phase, which has minimal electrostatic interactions due to its endcapping, and the EPS phases from Section 4.1, which use the residual silanols and substituted hydroxyl groups to add polar and electrostatic interactions to the overall retention mechanism. These results indicate that the TYPE-C™ Bidentate phase contains a number of Si-OH bonds which cause secondary electrostatic reactions with charged species. The majority of these electrostatic interactions have been shown to occur at the lower acidity hydroxyl groups which are likely to be produced through cross-linking or incomplete formation of the triethoxy silane monolayer shell as described in Section 1.7. An alternative source of these silanophilic interactions could be from residual silanols on the surface of the silica which are accessible due to incomplete coverage of the silica hydride monolayer. Determining the type and location of these silanophilic groups requires further spectroscopic investigation of the bonded silica itself, carried out in Section 5.2.1.

Another trend indicated by the chromatographic analysis is the lower efficiency values of the TYPE-C™ Bidentate C18 phase when compared to a typical endcapped TYPE-B C18. The results from the analyte overloading showed no significant decrease in efficiency due to band broadening on the TYPE-C™ Bidentate C18 over that observed for the TYPE-B C18. Comparison of efficiencies even at low concentrations shows a significant disparity between the two phases. From the current data it is difficult to determine why the efficiency of the TYPE-C™ Bidentate C18 phase is so low and whether this is typical of these columns. Further chromatographic analysis have been carried out through van Deemter curves to assess the calculated HETP values and which parameters are contributing to the low efficiency values, see Section 5.2.3.

5.2 *Chromatographic and Spectroscopic Evaluation of Physical Properties of TYPE-C™ Bidentate*

The chromatographic selectivity analysis indicated a number of unresolved questions around the structural properties and packing of the TYPE-C™ Bidentate C18 phase. The silica particles used in this chapter were unpacked from a commercial column before being washed in diethyl ether and dried at 80°C overnight before use. The recovery process for these particles may have altered the chemistry and density of the surface bonding of the silica so the results gained from them can only be used for indication purposes and may not fully reflect the nature of the commercial TYPE-C™ Bidentate C18 silica.

A number of experimental monofunctionaly bonded TYPE-B silica phases were used for comparison; these are shown in Table 5.9 below.

Table 5.9 ***Properties of silica particles for characterisation***

Phase	Particle Size (µm)	Bonded Ligand	Pore size (Å)	Surface coverage (m^2/g)	Endcapping	Carbon Load (%)
Cogent TYPE-C™ Bidentate C18	4	C_{18}	100	350	N/A	16.0
Bare Silica	3	-	100	300	-	-
C4	3	C_4	100	300	TMS	5.5
C8	3	C_8	100	300	TMS	9.0
C18	3	C_{18}	100	300	TMS	15.5
C18 (uncapped)	3	C_{18}	100	300	-	Unknown

5.2.1 *^{29}Si MAS NMR Spectroscopic Analysis of TYPE-C™ Bidentate*

The silica particles were studied by solid-state ^{29}Si MAS NMR spectroscopy to determine the number and types of silica environments present in the phases. The samples were referenced against an external tetramethylsilane standard. The spectra for the TYPE-C™ Bidentate C18 silica is shown in Figure 5.23 below; overlaid with the spectra for the TYPE-B unbonded and C18 endcapped silica for comparison.

Figure 5.23 ***Comparison of TYPE-C™ Bidentate C18 and TYPE-B bare silica and endcapped C18 by Solid State ^{29}Si NMR***

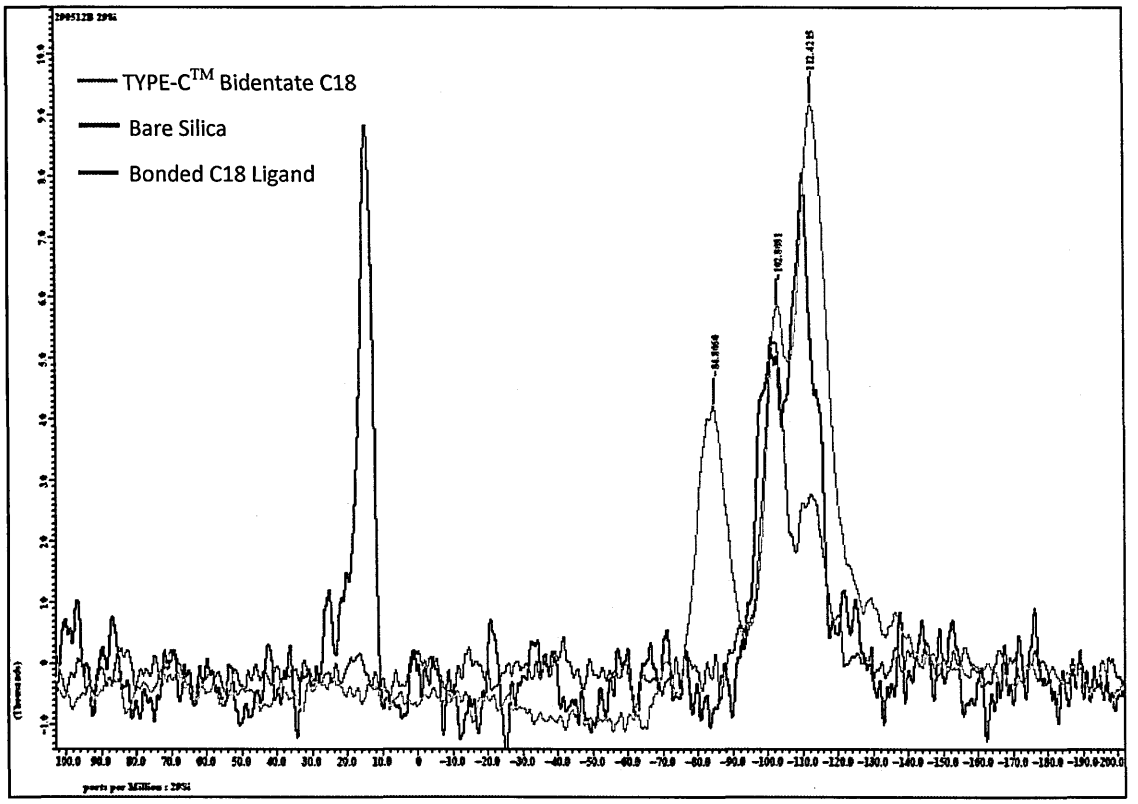

The chemical shifts of three naturally occurring silica environments common in a tetrahedral silica oxide structure are well documented[292-295] as well as the modified silica hydride environments[185]. These are shown in Table 5.10 overleaf. The chemical shift pattern of the two silica hydride groups is comparable with previous investigations that showed the addition of a hydroxyl group to a silica hydride structure will increase the delta shift about 10ppm[296].

The TYPE-B silica materials show a strong response for both the Q_3 and Q_4 environments present in the base silica, no resonance for the Q_2 shift is observed however the peaks are quite broad so they may be masked by the abundance of Q_3 and Q_4 silica environments present. The TYPE-B C18 also shows a resonance shift around -14 ppm which is due to the silicon of the octadecyl bonded ligand. This silicon is less de-shielded, moving the delta shift downfield, as the O-Si-C bonds are more covalent in nature and there is only one electronegative oxygen to pull electrons away from the silicon nucleus. The TYPE-B bare silica and TYPE-C™ Bidentate C18 silica do not have a resonance shift in this area.

Table 5.10 ***Chemical shift data for silica oxide and silica hydride environments***

Nomenclature	Molecular architecture	Structure	δ^- (ppm)
SiH_1	$HSi^*(OH)(OSi\equiv)_2$	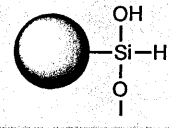	-70 to -73
SiH_2	$HSi^*(OSi\equiv)_3$	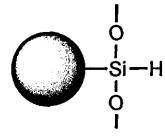	-83 to -85
Q_2	$(OH)_2Si^*(OSi\equiv)_2$	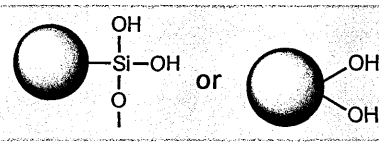	-90 to -92
Q_3	$HOSi^*(OSi\equiv)_3$	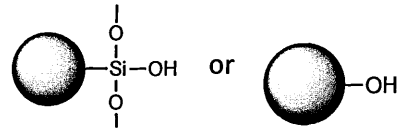	-100 to -102
Q_4	$Si^*(OSi\equiv)_4$		-110 to -112

The TYPE-C™ Bidentate C18 silica shows clear resonance shifts indicating the presence of silica hydride, however it also shows a large Q_3 delta shift. Solid-state ^{29}Si MAS NMR spectroscopy does not differentiate between surface silanols and "buried" silanols[209] within the crystalline structure of

the silica, considering the level of silanophilic interactions shown in the previous chapter it is likely that a large percentage of these are readily accessible.

No other silicon environments are observed confirming that the bonding ligands used are more likely to be double or triple bond olefins and not chlorosilanes or similar silica based ligands, as in the traditional bonding routes discussed in Section 1.4.

5.2.2 *Further Spectroscopic Analysis of TYPE-C™ Bidentate C18 Phase*

Further studies by solid-state ^{13}C and ^{1}H MAS NMR were carried out on the unpacked TYPE-C™ Bidentate C18 silica and the experimental TYPE-B silica materials. The observed carbon environments are shown in Table 5.11 below, the corresponding environments are shown in Figure 5.15 overleaf.

Table 5.11 *^{13}C MAS NMR δ shift pattern for ACT silicas and TYPE-C™ Bidentate C18 silica*

Phase	δ Shift					
	0 ppm	12 ppm	18 ppm	22 ppm	27-28 ppm	30 ppm
Cogent TYPE-C™ Bidentate C18		X		X		X
Bare Silica						
C4	X	X	X		X	
C8	X	X		X	X	
C18	X	X		X		X
C18 (uncapped)	X	X		X		X

Comparisons of the monfunctionally bonded TYPE-B C4, C8 and C18 endcapped and C18 unendcapped materials could not readily differentiate between endcapped and non-endcapped phases. The chemical shift for the carbon environments of the TMS endcap, observed around 0ppm, is not distinguishable from the substituent methyl carbons adjacent to the silica of the octadecyl silane. This environment was not observed in the TYPE-C™ Bidentate C18 silica which indicates that the phase is not endcapped with trimethyl silane. Other endcapping agents could have been used however no other carbon environments are observed that are not attributed to the octadecyl silane.

The manufacturer's data suggests the phase is not endcapped as the silica hydride monolayer suppresses 97% of residual silanols on the surface of the phase. The ^{13}C MAS NMR data shown here appears to confirm no endcap is present. The TYPE-C™ Bidentate C18 phase only appears to show three carbon environments which can readily be attributed to the octadecyl bonded ligand as shown in Figure 5.24 below.

Figure 5.24 ***^{13}C MAS NMR environments for the bonded silicas***

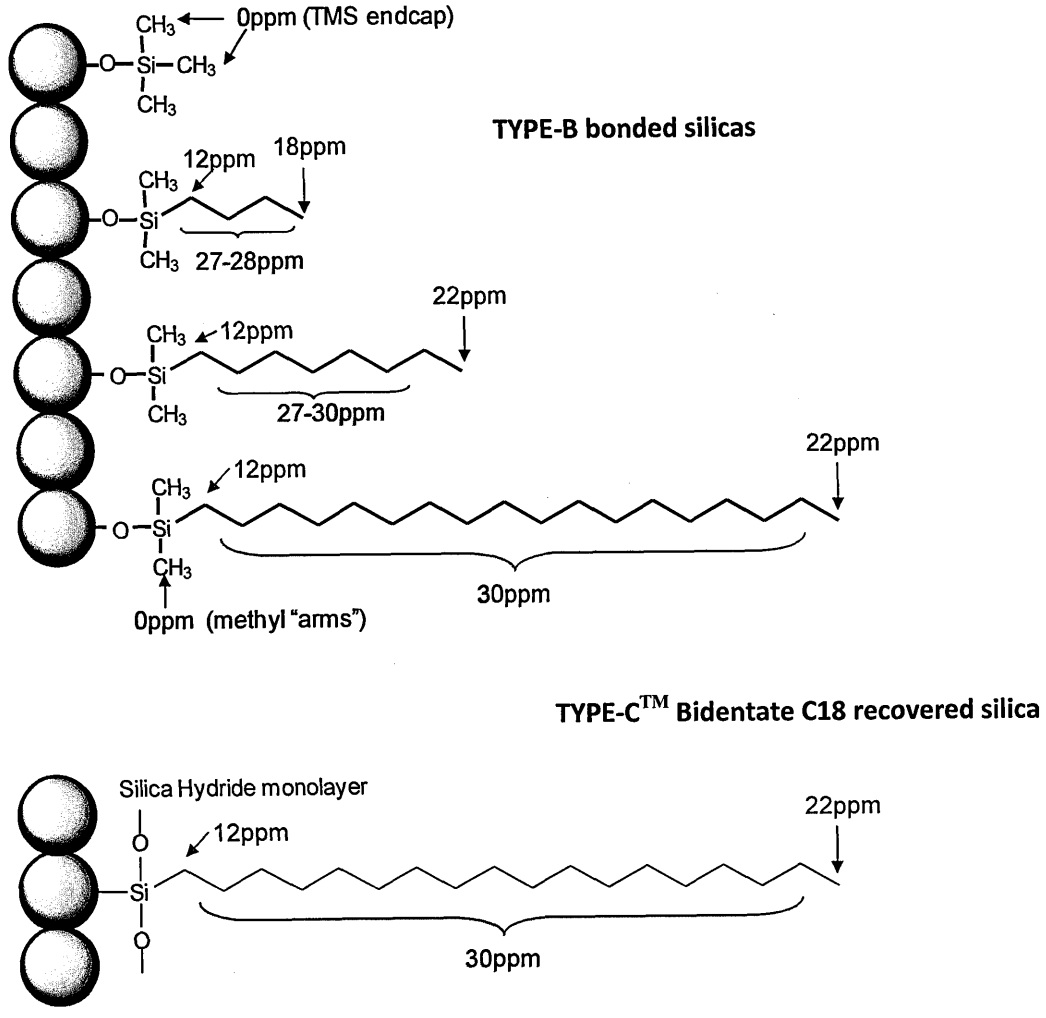

Further investigation work of the TYPE-B C18 endcapped and unendcapped material was carried out by Thermogravimetric analysis (TGA) and Differential scanning calorimetry (DCS) however these techniques also showed no significant differences in the results. The changes in relative weight and heat flow are shown in Figure 5.25 overleaf. The reduction in weight seen by TGA appears to occur

around 225°C, both phases show a single, rapid decay. The non-endcapped phase was expected to show a single decay as only the octadecyl ligands are being cleaved, however the endcapped phase was expected to show a stepped decay as the less stable TMS endcap would be cleaved first then the more stable octadecyl ligand. However this instrument may not be discriminatory enough to detect the two stages. The peak in heat flow on the DCS occurs around 225°C as the octadecyl silanes are being cleaved and atomised. Again the two phases show no significant changes and the endcapped phase does not show a step-wide increase in heat flow as the TMS endcap is cleaved first. The TYPE-C™ Bidentate C18 silica was analysed and showed a single weight decay and heat flow spike however, this data does not confirm or deny the presence of endcapping on the phase.

Figure 5.25 ***TGA and DSC Results of ACE3 C18 silica with and without TMS endcapping***

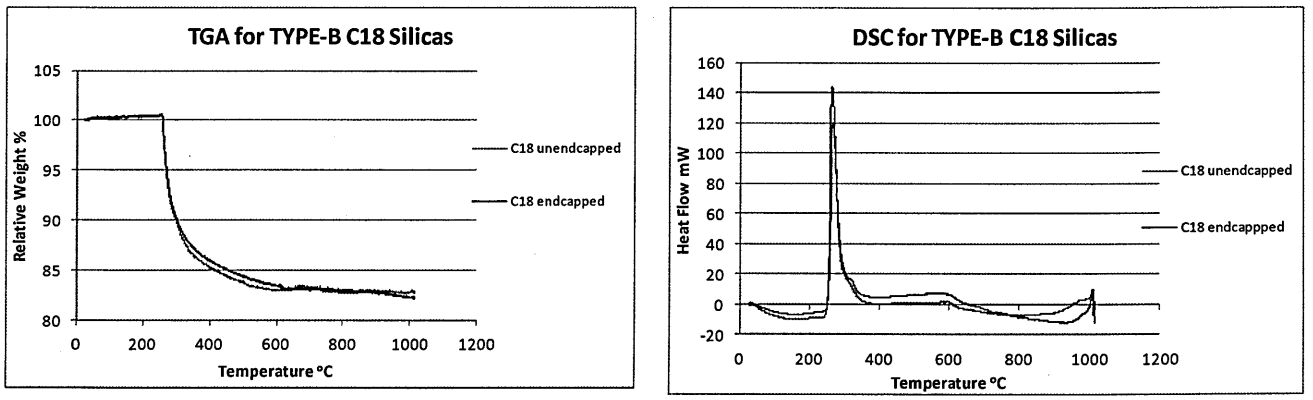

No delta shift is observed between 50 to 90 ppm which would be expected for ethoxyl carbon environments[293] on the TYPE-C™ Bidentate C18 silica which indicates that all of the branched arms have either been cross-linked or hydrolysed to Si-OH as shown in Figure 5.26 below.

Figure 5.26 ***Schematic of hydrolysis of ethoxyl "arms" during bonding procedure***

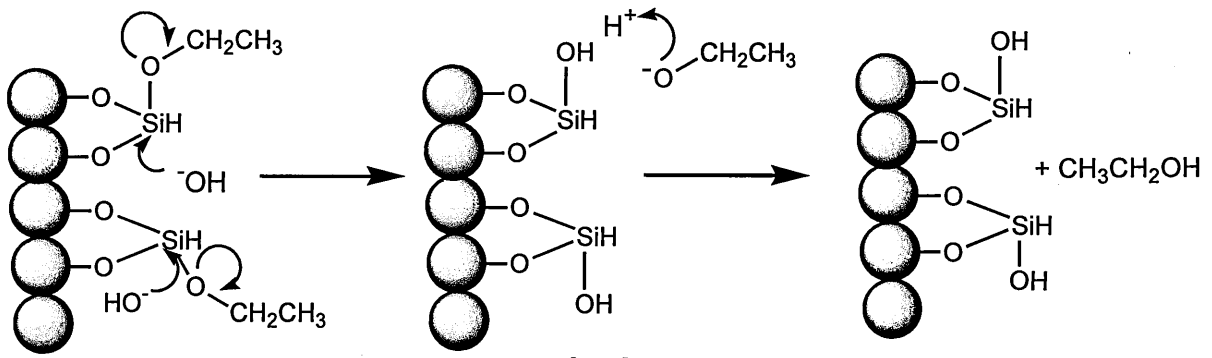

5.2.3 *Efficiency Characterisation of TYPE-C™ Bidentate*

The efficiency of a column is measured in terms of plate height, each plate represents a theoretical slice of the column where the analyte is in equilibrium between the solid and liquid phase. The greater the number of these plates the higher the likelihood to the analyte undergoing retention through adsorption, partition or electrostatic exchange, therefore the more efficient the column is. A number of models[297-300] have been developed to assess and measure the height equivalent to a theoretical plate (HETP). The main issue with modelling these effects is that the column is not a homogenous system and band broadening effects can occur differently at the middle and edge of the column resulting in a parabolic profile rather than a single band[301][302] therefore these models need to assess each area of the column and combine the patchwork cross section of the column and average them[299][302]. The main contributions to band broadening on the column are the mass transfer of the analyte absorbance process, the natural diffusion of the analyte within the system and the length of the pathway through the column. However, recently the advances in small particle sizes and shorter column lengths have brought other "smaller" band broadening effects into play; system dispersion effects, radial dispersion temperature differences across the column[304], and "wall effects"[303].

With advances in instrumentation and the development of ultra high performance chromatography (UHPLC) more interest has been placed on decreasing the dispersion volume of a system.

(VI) $$N_{app} = \frac{\mu_{system} + \mu_{column}}{\sigma_{system} + \sigma_{column}}$$

Where:
μ = linear velocity
σ = dispersion

For longer columns the $\sigma_{column} >> \sigma_{system}$ therefore any band broadening caused by the system dispersion volume is negligible. However for short columns the effects of large system dispersion volume can be a major contribution to band broadening and $\sigma_{column} < \sigma_{system}$, which can reduce the efficiency of a column by more than half[305]. Another issue brought about through small particle and

high flow rate analysis is the diffusion coefficient at high velocity. Previously, in large particle columns, it was thought that diffusion was a constant and the apparent effect decreased as the velocity increases. However more recently it has been thought to be variable and highly dependent on the velocity of the analyte[308][310], friction between the surface of the silica stationary phase and the mobile phase compressibility [306][307].

The van Deemter equation[289] was introduced over 50 years ago and was designed to model the band broadening and efficiency observed in gas chromatography columns. These columns are very long capillary columns therefore some of the "smaller" band broadening effect discussed above where not considered. Later it was shown how this equation could be linked to >3µm particle sized packed bed HPLC columns. The equation represents the three main factors for band broadening; multiple paths through the packed column (A), molecular diffusion (B), and mass transfer effects (C_s for the stationary phase and C_m for the mobile phase). These contributions to peak efficiency (N) can be shown using the equation below:

$$H = \lambda d_p + 2\gamma \frac{D_m}{\mu} + c \frac{d_p^{\,2}}{D_m} \mu \qquad \text{(V)}$$

The first parameter, commonly known as the Eddy (radial) diffusion term is determined through the uniformity of the particle bed of a packed column. Here the particle diameter and the way the particles are packed is assessed as a function of how an analyte travels down the column. Previously this was thought to be a constant value; however more recent work has shown this is not the case. The "wall effects" discussed earlier means that the pathway for analytes in this boundary region is restricted and this leads to these molecules travelling slower than the molecules in the centre of the column. This "long range eddy dispersion" results in a radial dispersion pattern that is irrespective of particle uniformity or packing efficiency[303-309]. In order to accurately model the Eddy diffusion term the cross section idea needs to be replaced with Infinite Parallel Zones[304] and systems such as Parallel Segmented Flow (PSF) or Curtain Flow (CF)[303] can now be used to create virtual "wall less"

columns to minimise this effect in small particle size columns. This is an academic approach to get a greater understanding of the model; however the approach could never be applied practically as "wall effects" will always need to be included in the system.

In the case of the TYPE-C™ Bidentate C18 phase the extent of the polymeric layer may cause the particles to be non-uniform if the density of the polymeric layer is not controlled. If this bonding is similar to the TES crosslinking method discussed in Section 1.7 it is also possible that the stationary phase may contain a percentage of unbound amorphous polyhydrosiloxane (PHS) material which would affect the packing[185] (this is shown in the next section). The particle size stated by the manufacture is 4 μm which should be large enough to be modelled using the van Deemter equation and the column length is only 5 cm which should minimise the effects of long range Eddy dispersion.

The molecular (longitudinal) diffusion term is dependent of the diffusion coefficient of the analyte in the mobile phase and is inversely proportional to the flow rate. As previously discussed the solute diffusion coefficient (D_m) can be affected by the velocity difference between the analyte in the mobile phase and the analyte in the stationary phase. As the particle size of the TYPE-C™ Bidentate C18 and the ACE 3 C18 are different the pressure of the system may need to be taken into account when modelling these parameters. However the instrument has a maximum pressure of 600 bar and the columns 400 bar and 275 bar respectively the velocity differences for this analysis should be negligible and the B term should be satisfactorily modelled for these phases.

The final parameter, resistance to mass transfer, may have an effect as it is dependent on the pore distribution of the phase; again an uncontrolled polymer layer on the surface of the silica would have a detrimental effect on band broadening as the analytes may be trapped in the uneven surface created by the polymer which would result in poor mass transfer. It is widely thought that the A and C term are linked, however there is some disagreement about whether they have a harmonic[300] or decay[307] based coupling. This leads to a discrepancy in model and experimental data and it may not

be possible to accurately determine the C terms. However in practical terms the difference in the model used is marginal as the analysis carried out here is based on direct comparison of the two phases the type of coupling model used will not have an impact on the results.

Many of the models discussed above are highly mathematical and consider one or more of the "smaller" band broadening effects. Although the van Deemter equation may not be the best model for calculating absolute values for these parameters it is an excellent model for comparison. In this analysis the percentage organic will be altered to achieve a comparable k value. The same system and flow rates will be used for both phases to keep the dispersion of the system (σ_{system}) value comparable and any differences should be due to the column.

The effect of these three parameters can be represented graphically by the effect of the height equivalent to a theoretical plate (HEPT) of the stationary phase against linear velocity of the mobile phase as shown in Figure 5.26 below. Although we know this model to be inaccurate for the A and the C terms the overall effect on the HETP will be the same.

Figure 5.26 ***Theoretical graph of contribution of van Deemter terms to calculate HETP***

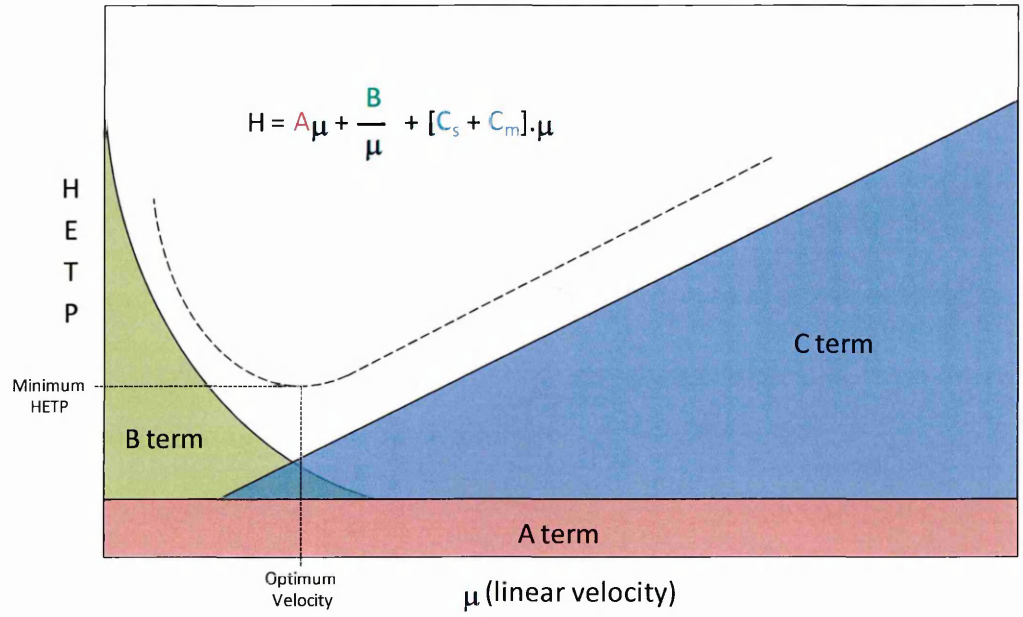

The main practical application of the van Deemter equation is to assess the optimum mobile phase velocity for the phase. This is the point where the minimum HETP is achieved as this will equate to the maximum number of plates achievable by the column, and therefore the maximum efficiency. Due to the shape of the curve it can be seen that as the flow rate is increased beyond this point it results in a sharp increase in HETP, therefore a significant decrease in efficiency, whereas an increase in flow rate will yield only a slight decrease in efficiency.

The analysis for the ACE 3 C18 and TYPE-C^{TM} Bidentate C18 phases was carried out at 40°C and 80°C; at higher temperatures the viscosity of the mobile phase is reduced which reduces resistance to mass transfer coefficient (C). In practice this should diminish the effect of the C term and the calculated HEPT should plateau off as linear velocity increases. Ketoprofen was used as a retention time marker as it will be unionised at low pH which reduces the effect of the ionised silanols accessible on the surface of the phases. The mobile phase composition was adjusted on each column until the ketoprofen had a retention factor of approximately 10. The van Deemter plots for both phases at 40°C are shown in Figure 5.27 below.

Figure 5.27 van Deemter plots for ACE 3 C18 and TYPE-C^{TM} Bidentate C18 phases at 40°C

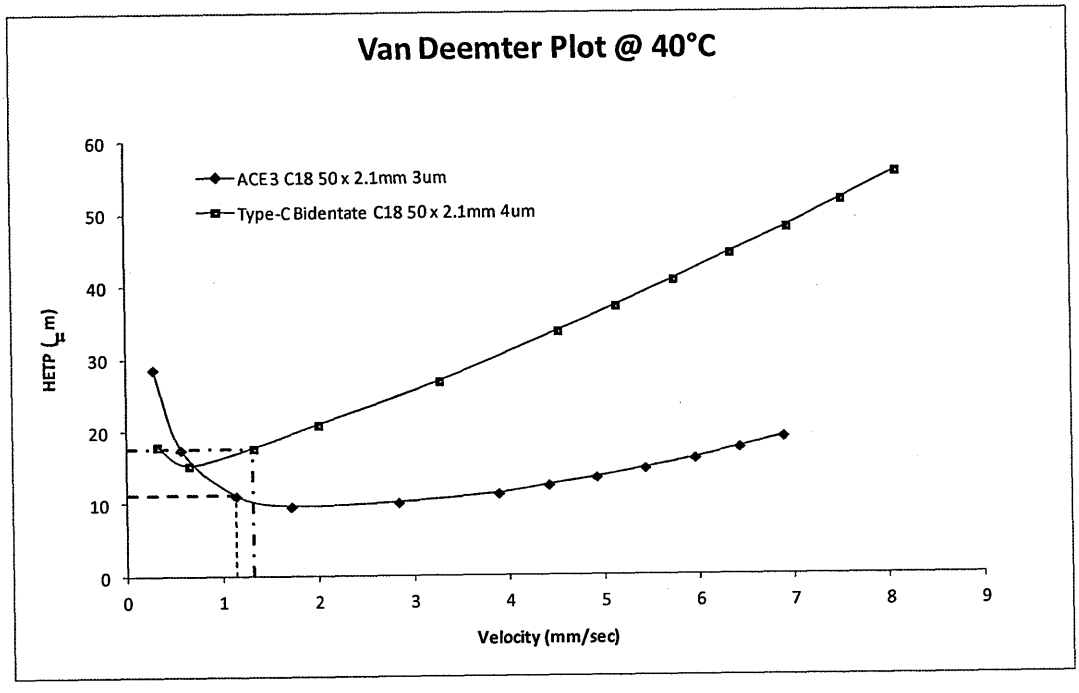

Most of the analysis work has been done at 0.21 $mLmin^{-1}$ (1.33 mm/sec) due to scale-down to 50x2.1 mm columns; the velocity of the analytes in mm/sec was calculated for each column running at a flow rate of 0.21 $mLmin^{-1}$ and is shown on the graph. The TYPE-C™ Bidentate C18 phase shows an optimum flow rate around 0.1 $mLmin^{-1}$ (0.51 mm/sec) and steep inclines either side indicating a large decrease in efficiency away from the optimum. There is a significant difference in HETP vales at this flow rate which explains significant difference in peak widths and efficiencies observed.

The steep gradient of this part of the TYPE-C™ Bidentate C18 plot indicates the repeatability of these phases may be an issue as small changes in instrument flow or column packing may result in significant variation in the HETP. Even at the optimum velocity the calculated HETP for the TYPE-C™ Bidentate C18 phase is seen to be higher than that of the ACE 3 C18 phase. The difference in particle size for the two phases may account for some of this difference, a reduced plate height van Deemter curve is in Figure 5.28 shown overleaf.

The equation shown in Figure 5.26 can be solved for each of the phases using the experimental data; the calculated best fit figures for the parameters A, B, and C are shown in Table 5.12 overleaf. In some models the following equation is used:

(VI) $$HETP = A\mu + \frac{B}{\mu} + [C_s + C_m]\mu$$

However it was found that using the $A\mu^{1/3}$ parameter gave a better fit for this data and because the equation is being used for direct comparison between the two phases. The differences in the parameters for the two temperatures are calculated using Microsoft Solver and is shown in Table 5.12 overleaf. The variations in calculated values between the two temperatures were calculated as a percentage and are shown in parentheses' underneath the 80°C results.

Table 5.12 ***Calculated van Deemter Terms Values - Comparison of ACE 3 C18 and TYPE-C™ Bidentate C18 phases***

	40°C			80°C		
	A	B	C	A	B	C
ACE 3 C18 (3µm)	1.14	7.72	2.14	0.32 *(-71.9%)*	15.5 *(+101%)*	1.86 *(-13.0%)*
TYPE-C™ Bidentate C18 (4µm)	6.26	3.92	5.12	1.86 *(-70.2%)*	8.43 *(+115%)*	4.92 *(-3.9%)*

The analysis of the data shows that for the ACE 3 C18 phase the major contribution to dispersion effects is from the B term. This is due to the dispersion coefficient of the solutes itself and the natural band broadening of the band of molecules in solution; it has been shown that analytes will disperse in solution regardless of the porosity, packing distribution and mobiles phase used. Therefore the B term is more reliant on the analyte used rather than the column. The calculated values for the A and C terms are seen to be much lower for this phase. At higher temperatures the viscosity of the mobile decreases therefore it is easier for the analytes to move through the system. This can be seen by a vast increase in the B term as the natural dispersion of the band of analytes is increased due to the reduced hindrance from friction and interactions with the mobile phase molecules. This can also be seen in the reduced A term as the change in compressibility of the mobile phases reduces the effect of friction and radial temperature gradients as the band of analytes travel down the column. Only a small change in the C term is observed which is likely to be due to the easier mass transition of the analyte travelling from the stationary phase to the, now less viscous, mobile phase.

However, the results for the TYPE-C™ Bidentate C18 phase show a greater contribution from both the A and C terms and a lesser dependency on the natural diffusion of the analyte shown in the B term. The same analyte is used and although the mobile phase composition is changed slightly to

keep the k value consistent these small changes should have a negligible effect. As the k values are comparable the analyte will spend approximately the same amount of time "on-column" therefore the natural dispersion should also be comparable for each case. This indicates there is a much greater contribution from the nature of the column packing and material than seen for the ACE 3 C18. As discussed previously the A and C term are linked and are based on how well the column is packed as poor packing or irregular particle sizes lead to higher Eddy diffusion terms and poor mass transfer between the mobile and stationary phases. The same trends are seen as the temperature is increased; a drastic increase of B, a decrease in A and a smaller decrease in C. This pattern indicates that the surface of the silica hydride monolayer TYPE-C^{TM} Bidentate C18 phase does not undergo any changes at higher temperature. The TYPE-C^{TM} Bidentate C18 phase is said to be a 4µm phase as opposed to the 3µm ACE 3 C18, therefore a reduced plate height plot is shown in Figure 5.28 below, to compensate for these different particle sizes.

Figure 5.28 ***Reduced plate height plot for ACE 3 C18 and TYPE-C^{TM} Bidentate C18 phases at 40°C***

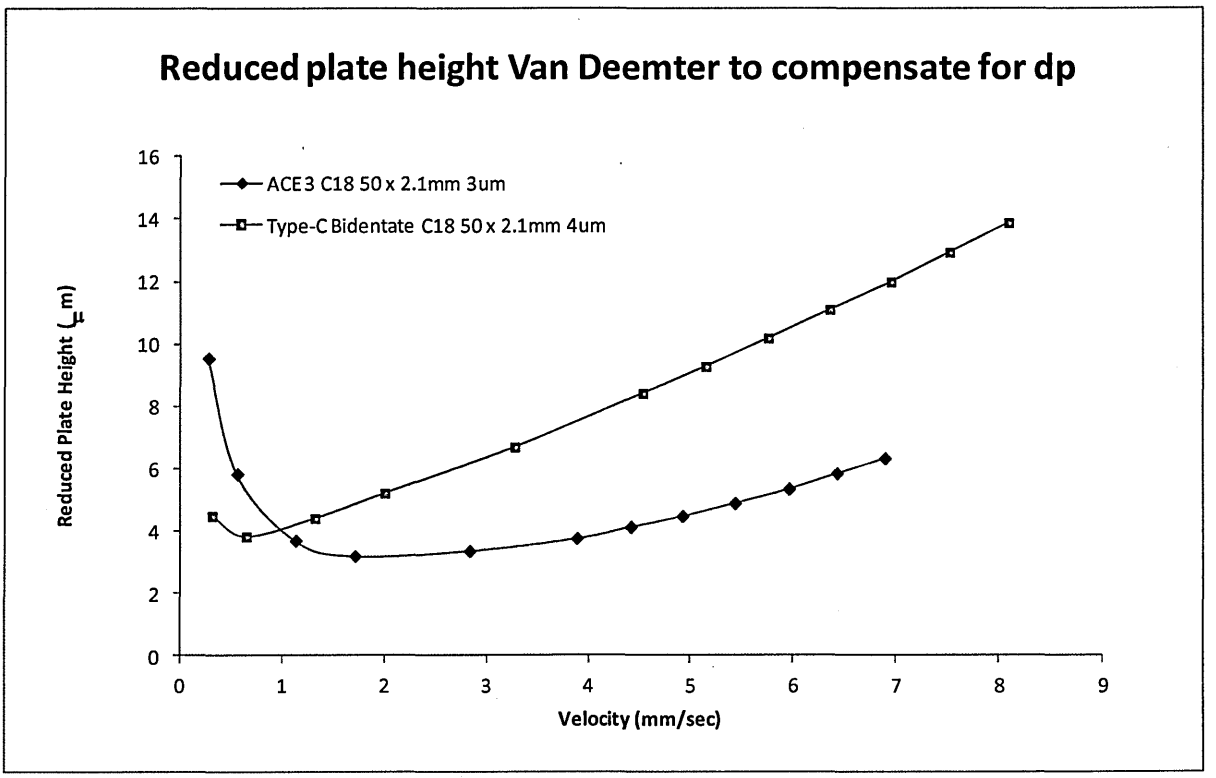

The plot still shows the same trend even though the reduced plate height at optimum velocity is now more comparable across the two columns. The plot shows the reduced plate height for the ACE 3 C18 and TYPE-C™ Bidentate C18 phase at 0.2mL/min is 3.7mu and 4.4um respectively. This indicates that the difference in efficiency of the two phases is due to the A and C terms rather than the difference in particle size.

The efficiency of the TYPE-C™ Bidentate C18 phase was originally investigated due to the higher peak width observed in the characterisation probe analysis. Literature has shown that for UHPLC phases the peak width can be affected by the pressure exerted on the analyte in the system[314][315] therefore it is possible that difference in system pressure may affect the peak width. The peak widths of the ketoprofen peak were compared and found to be comparable at similar pressures. The ACE 3 C18 has a higher system pressure overall due to the 3 µm particle size as opposed to the 4 µm of the TYPE-C™ Bidentate C18 phase. It is known that very high system pressure can have an effect on analyte dispersion as the natural band broadening, shown in the B term of the van Deemter, is reduced under the elevated pressure. At a flow rate of 2.0 mL/min the TYPE-C™ Bidentate C18 phase has the greatest amount of pressure exerted on the phase at 211 bar. This is the equivalent of the ACE 3 C18 at 0.9 mL/min which has a pressure of 203 bar exerted on the phase. The peak widths for ketoprofen are comparable in these runs; the TYPE-C™ Bidentate C18 phase yielding 0.0606 minutes and the ACE 3 C18 showing 0.0748 minutes.

This comparison of peak width with pressure cannot be considered to be accurate as the flow rate is varied and therefore the dispersion of the analyte will be different across the two phases. In order to accurately perform a pressure comparison the flow rates would need to be kept constant and a pressure regulator applied to exert the same pressure on system for both phases. This comparison only shows that the different pressure of the system caused by the difference in particle size does not have a large effect on the peak width of the analyte. The maximum pressure observed for either column is less than 300 bar and literature[316] has shown that for small molecules the effect on peak

width is negligible at a system pressure <500 bar. Therefore it can be assumed that the effect of pressure is going to be comparable for both phases and the difference observed in the van Deemter plots is likely to be due to packing efficiencies rather than a difference in particle sizes.

Overall this analysis appears to show the reduced efficiency of the TYPE-C^{TM} Bidentate C18 phase can be attributed to the A and C term of the van Deemter. This may indicate an issue with the packing and the particle size uniformity of the phase and further investigations need to be carried out to determine the actual size and uniformity of the particles used in this column. In Section 1.7 it was discussed how an excess of TES monomer used in the formation of the silica hydride monolayer could lead to PHS particulates being formed. This could explain the poor peak packing efficiencies seen here. Other explanations could be that the formation of the silica hydride monolayer actually binds two or more silica particles together making large lumps within the silica base which give rise to non-uniform packing. It is possible that the column used for this testing was just badly packed and it could be a one-off result. Ideally it would be good to perform this testing again on a brand new TYPE-C^{TM} Bidentate C18 phase column to confirm these results, however as the number of columns available for this research was limited this phase will have to be investigated by Scanning Electron Microscope to assess the issue with packing uniformity.

5.2.4 *Particle Uniformity Assessment by Scanning Electron Microscope*

The van Deemter analysis from the previous chapter indicated the reduced efficiency observed in the TYPE-C™ Bidentate C18 phase is likely to be due to non-uniformity of the packed stationary phase giving rise to a higher degree of radial diffusion within the phase. This may be due to a variation in particle size, a small amount of the unpacked stationary phase was analysed by scanning electron microscopy (SEM) along with a sample of 5 µm bare, unbonded, TYPE-B silica for reference. The TYPE-B silic (Figure 5.26(a) below) shows a small variation in particle size from approximately 4 to 8 µm diameter and a low level of surface defects on the silica particles. Experimental and commercial columns have been produced using a mixed silica bed packing technique in order to achieve bimodal distribution of particle size and pore size[310-314]. From this literature it has been shown that a wide particle size distribution did not yield systematic differences in Eddy dispersion and it is the particle porosity that is thought to be a much greater contribution to hydrodynamic dispersion. The variation of particle size seen in Figure 5.29(a) would have a negligible effect on the van Deemter curve.

Figure 5.29 ***SEM image of (a) Typical 5µm TYPE-B unbonded silica and (b) recovered TYPE-C™ Bidentate C18 silica***

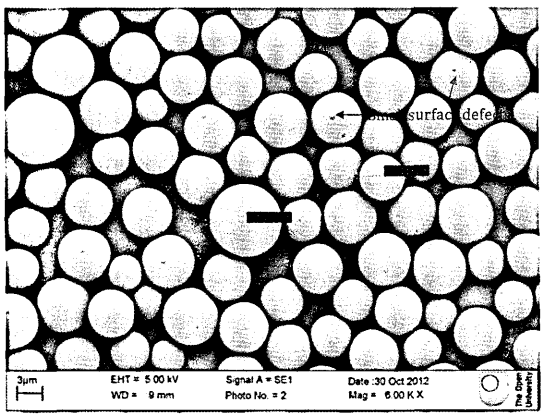

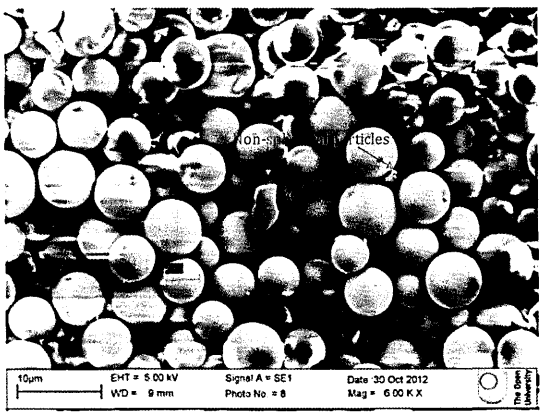

However the unpacked TYPE-C™ Bidentate C18 silica, seen in figure 5.30(b), shows not only a similar variation in particle size but also a number of non-spherical particles within the phase which may be

due to unbound PHS material as discussed in Section 1.7. The presence of non-uniform and non-spherical particles would explain the shape of the van Deemter curve seen in the previous section[181].

The irregular particle shapes will affect analytes pathway down the column. Uniform size and shaped particles will result in a tightly packed bed; this means the time it takes for each of the analyte molecules to travel through the stationary phase will be identical regardless of the pathway taken. As the analytes will travel in a tight band the only affect on the retention of these analytes will be from interactions with the stationary phase itself, resulting in a sharp Gaussian peak shape. However for non-uniform particle shapes or significant variations in particle sizes the packed bed may contain voids where eddies can form. Eddies are vortexes that can cause turbulent mixing of the mobile phase and the solutes. In this type of packed stationary phase the analytes can take pathways of significantly different lengths and can be retained in Eddies which leads to band broadening and increased peak widths. Here the retention time of an analyte is made of both the chemical and physical interactions with stationary phase forces and these varying longitudinal pathways.

Figure 5.30 ***Schematic of analyte pathway in uniform and irregular packed silica bed***

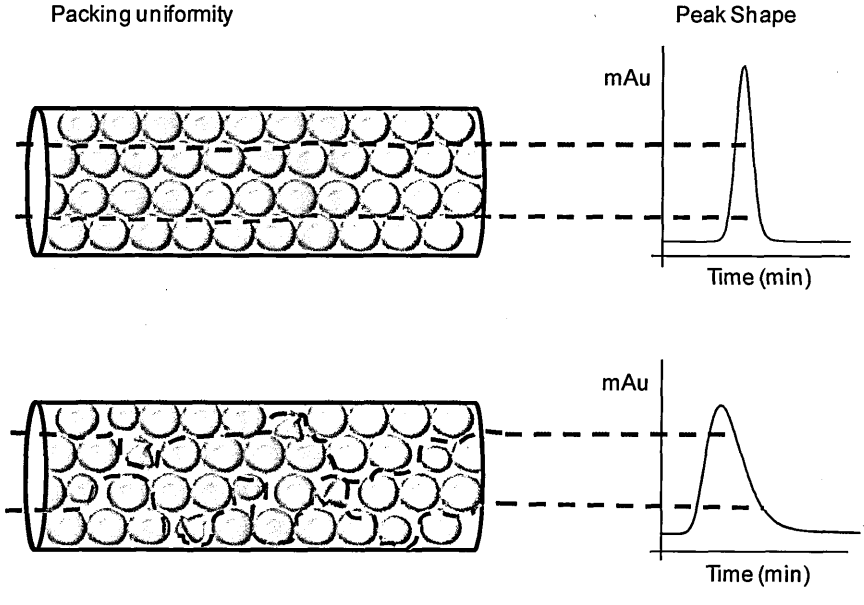

The exact bonding process for the TYPE-C™ Bidentate C18 is proprietary information and therefore it cannot be confirmed that the Si-H monolayer is formed from crosslinking TES monomers as discussed in Section 1.7. On the assumption that the phase is produced by this or a similar process the non-spherical particles could be explained through the formation of large amorphous polyhydrosiloxane complexes. These PHS particles are likely to form through crosslinking and laddering of the TES monomer which break free from the silica particle during the washing process. This may result in an area on the surface of the base silica that is not covered by the silica hydride monolayer leaving residual silanols exposed. The variations in particle size and the addition of non-spherical particles would explain the increased peak widths and lower efficiencies and high contribution from the A term observed in the chromatographic testing in the previous section.

Although the phase is classed as a 4 μm particle size this SEM image shows the majority of particles to be larger. This may not significantly affect the packing uniformity of the silica bed, it has been seen from the typical 5 μm silica that a level of variation is common in silica batches with negligible effect on the resulting efficiency[311-314]. This is only a small sample of the phase which has been recovered from a commercial column and may not be representative.

5.3 *Stability Assessment of TYPE-C™ BidentateC18 Phase*

The silanization of a porous silica particle to create the silica hydride monolayer and the subsequent modification with long chain hydrocarbon olefins should theoretically make the stationary phase less susceptible to acid hydrolysis. The formation of the direct Si-C linker should be much shorter and therefore harder to break than the traditional bonding formation of the Si-O bond, as discussed in Section 1.7. The theoretical knowledge substantiates the claims made by the manufacturers that the TYPE-C™ Bidentate C18 has enhanced stability against a typical TYPE-B C18 phase[269]. This section aims to investigate these claims by subjecting the TYPE-C™ Bidentate C18 phase to forced stability and real-life stability testing.

5.3.1 *Forced Stability Assessment of TYPE-C™ BidentateC18 Phase*

The forced stability plot is shown in Figure 5.31 overleaf. The stability, based on the relative reduction in retention factor of a neutral molecule compared to the literature results of the retention factor of the same molecule on a typical monofunctionaly bonded TYPE-B C18 phase[255]. The TYPE-C™ Bidentate C18 phase shows a small decrease in retention factor indicating a small amount of the octadecyl ligand is being cleaved. The relative reduction in retention factor on the TYPE-C™ Bidentate C18 phase is seen to be lower than the literature values of the TYPE-B C18, 2% reduction compared to a 6% reduction. However the two sets of analysis were not run on the same system therefore this difference may be due to small variations in mobile phase composition or oven temperatures. The comparison can be used for a general comparison to say the TYPE-C™ Bidentate C18 phase has similar stability to the TYPE-B C18 when exposed to acid hydrolysis at elevated temperatures.

Figure 5.31 ***Stability Evaluation of TYPE-C^{TM} Bidentate C18 silica under elevated temperature and low pH conditions***

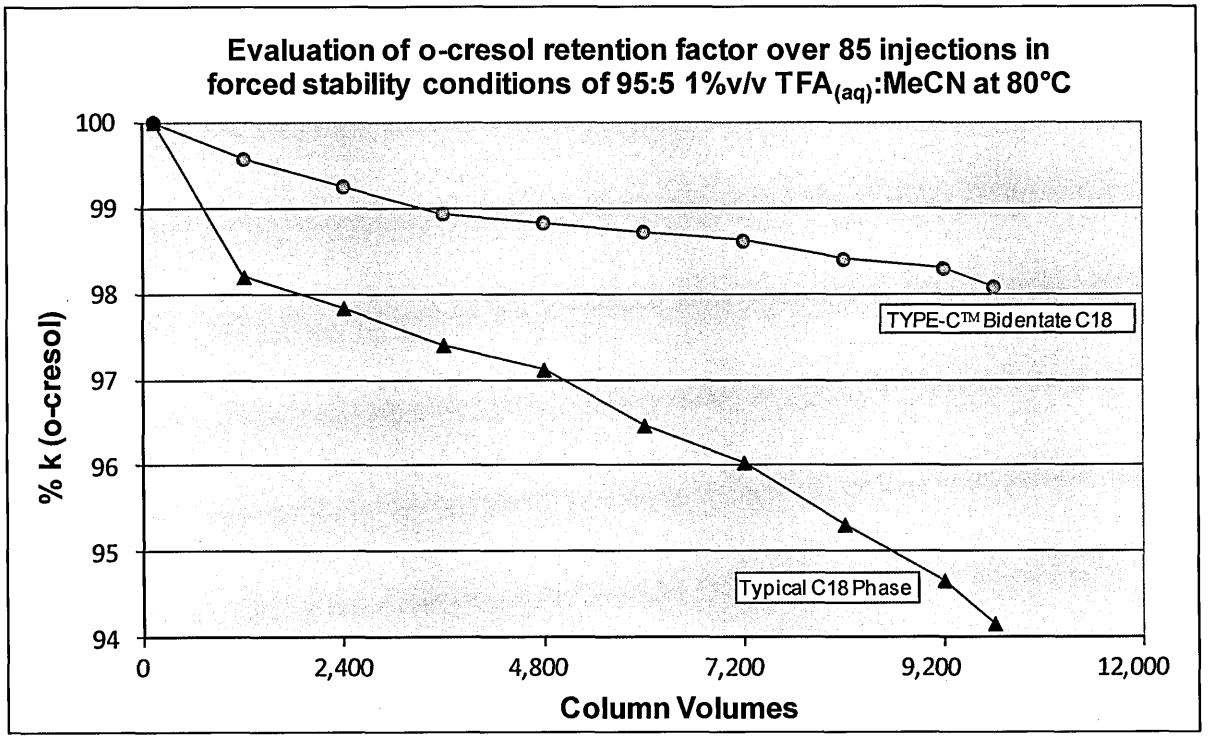

O-cresol was chosen as a stability probe as it is highly sensitive to hydrophobic interactions under these conditions. Only a small amount of phase loss was seen in extreme acidic and high temperature conditions. Under other conditions this type of acid hydrolysis may not be apparent. This can be seen in the neutral characterisation probes analysed before and after the forced stability conditions (Figure 5.32 overleaf). The retention time of the set of neutral compounds shows no change before and after the extrapolated stability testing even though a small amount of phase cleavage was observed.

These results agree with the manufacturer's claims that the formation of the direct Si-C bond gives a high level of stability in acid conditions and elevated temperature. In Section 5.1.4 a small amount of variation of retention was observed in neutral conditions using methanol mobile phase at 40°C on a brand new column. This may indicate a low level of silane cleavage; this could be due to over cross-linking of the polymeric silica hydride coverage and this "laddering" is snipped off during the initial

analysis or it could be due to basic hydrolysis brought on by dissociated methanol in neutral conditions. However it is more likely to be due to longer column equilibration than expected following the switch from acetonitrile to methanol organic component of the mobile phase.

Figure 5.32 ***Evaluation neutral probes of TYPE-C^{TM} Bidentate C18 silica under elevated temperature and low pH conditions***

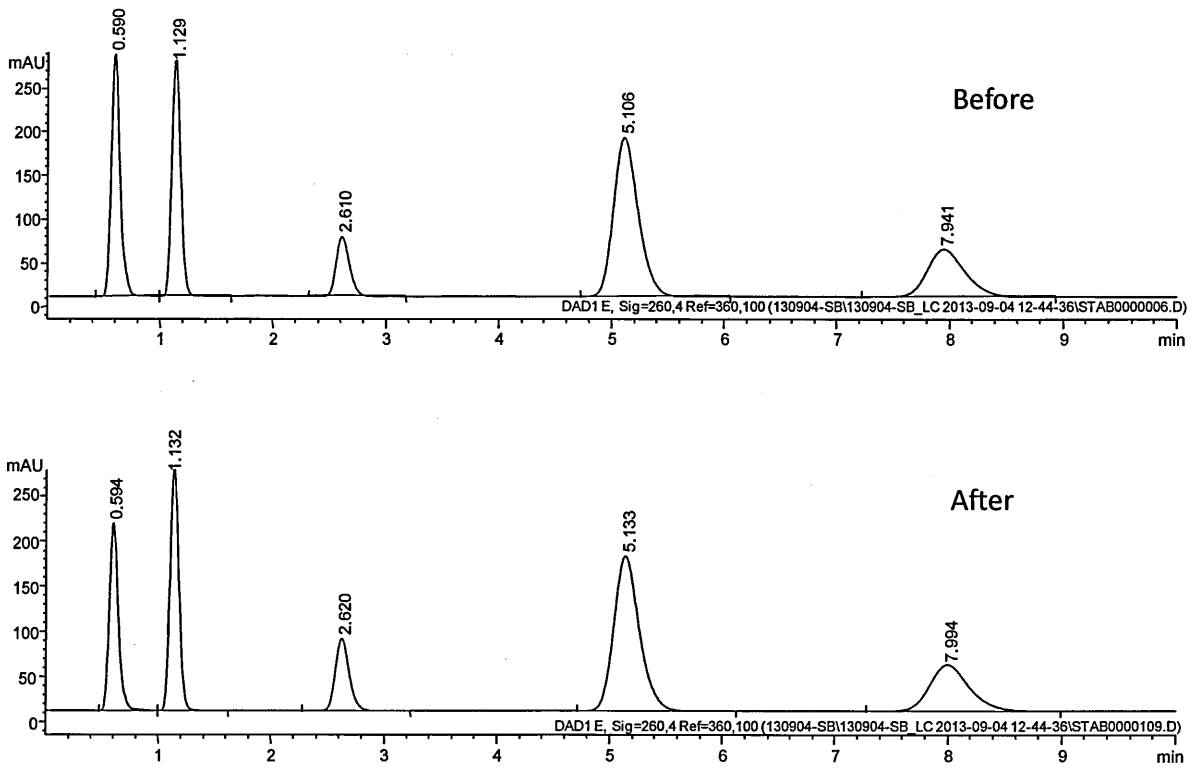

Elution order: [1] uracil, [2] dimethyl phthalate, [3] toluene, [4] biphenyl, [5] phenanthrene

Further analysis is required to assess the stability of the phase under different pH conditions using "real-life" conditions; these are shown in the next section.

5.3.2 *Real-Time Stability Assessment of TYPE-C™ BidentateC18 Phase*

As with the EPS phases the forced stability data only gives an indication of relative stability and it is the real-time stability in typical mobile phase and temperature conditions that most interests the chromatographer. The manufacturer states that the phase is stable over the pH range 2.0 to 9.2 and temperatures up to 80°C. However during the characterisation work in Section 5.1.4 the stability of the TYPE-C™ Bidentate C18 phase had been put into question. The forced stability results in the previous chapter showed comparable stability to TYPE-B C18 phases under extreme conditions.

The initial testing on the TYPE-C™ Bidentate C18 phase was carried out at low pH as the column should be less susceptible to acid hydrolysis. A selection of acidic, basic and neutral solutes were analysed over 20,000 column volumes. The results of the retention factor of each of the analytes are shown in Figure 5.33 below.

Figure 5.33 Real-time Stability Evaluation of TYPE-C™ Bidentate C18 silica at pH 2.5

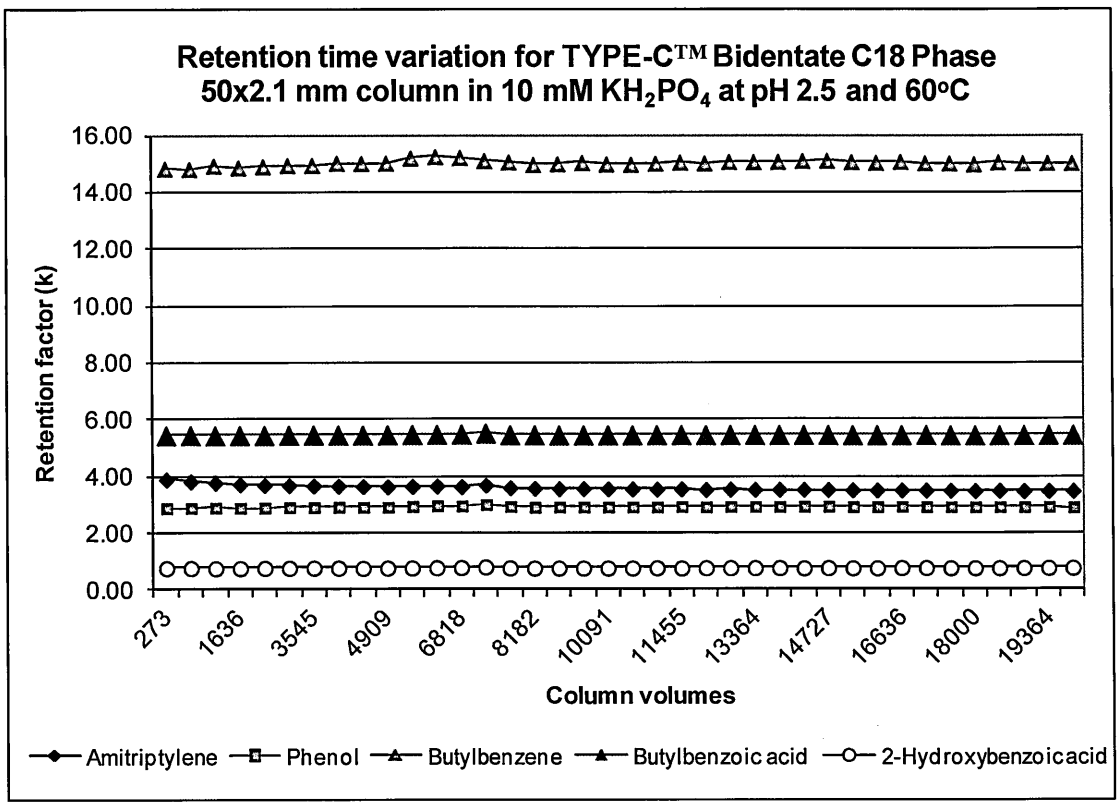

No significant change in retention factor is observed for any of the analytes during this analysis, the efficiency calculation for each of the peaks over the analysis was also found to be consistent throughout the analysis; this is shown in Figure 5.34 below. As a further assessment a mixture of neutrals was analysed before and after the stability testing, no change in retention time was observed for the neutral peaks.

Figure 5.34 ***Efficiency Evaluation of TYPE-C^{TM} Bidentate C18 silica During Real-time stability Testing at pH 2.5***

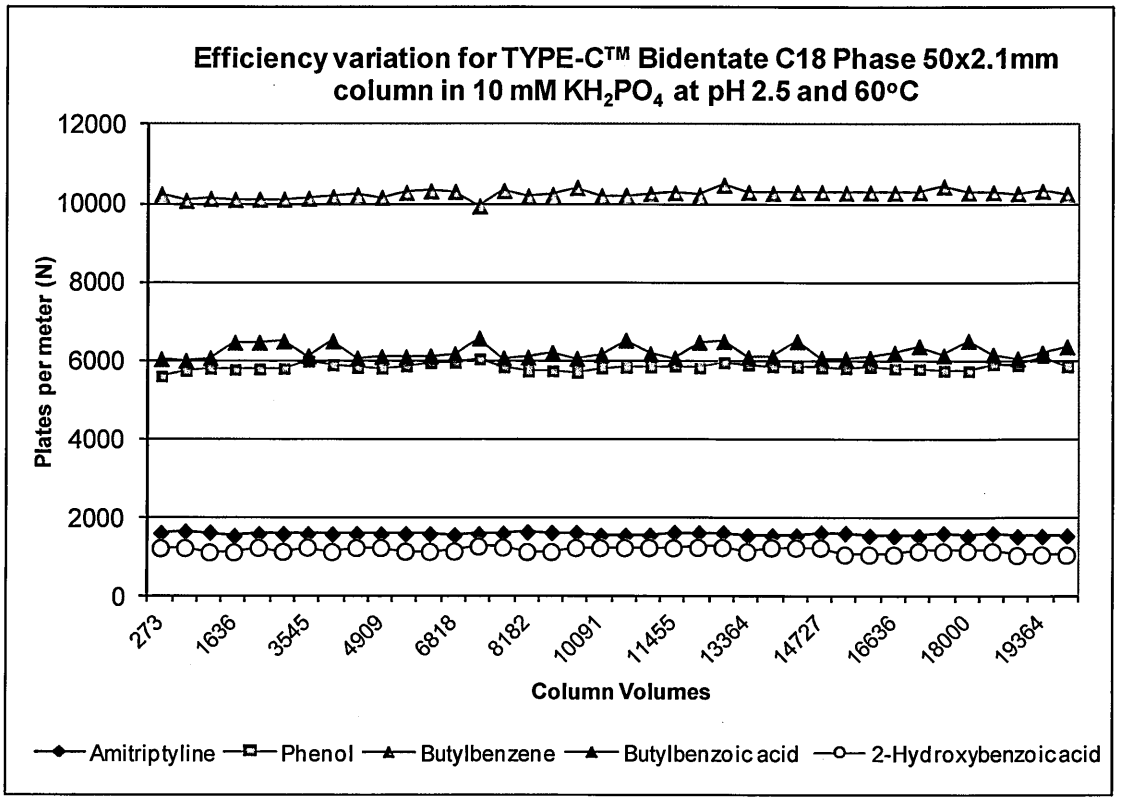

The stability evaluation at pH 7.0 is run in ammonium acetate as it has been shown in Section 4.2.2 that potassium phosphate at pH 7.0 and 60°C can result in the degradation of the silica base of an HPLC column. The same set of acid, basic and neutral analytes were used. At pH 7.0 the basic solute amitriptyline is observed to have a higher retention time than at pH 2.5 due to the activated silanol groups available on the phase. During the analysis the retention factor of the amitriptyline increases indicating that more silanols are being activated as a small amount of octadecyl ligand is being

cleaved from the surface of the phase. In contrast to this the retention factor of the neutral butyl benzene is seen to decrease over the analysis as the cleaved silanes reduced the hydrophobic interactions. The butyl benzoic acid retention factor is also seen to reduce a small amount however as the retention time is lower the effect is less pronounced, no significant change is observed in the retention factor of the phenol and 2-hydroxbenzoic acid. The amitriptyline retention factor is seen to increase around 11% over the 20,000 column volumes however the butyl benzene is only seen to decrease 5% as the electrostatic interactions are much stronger than the hydrophobic interactions from the C18 ligands. These results are shown in Figure 5.35 below.

Figure 5.35 ***Real-time Stability Evaluation of TYPE-C™ Bidentate C18 silica at pH 7.0***

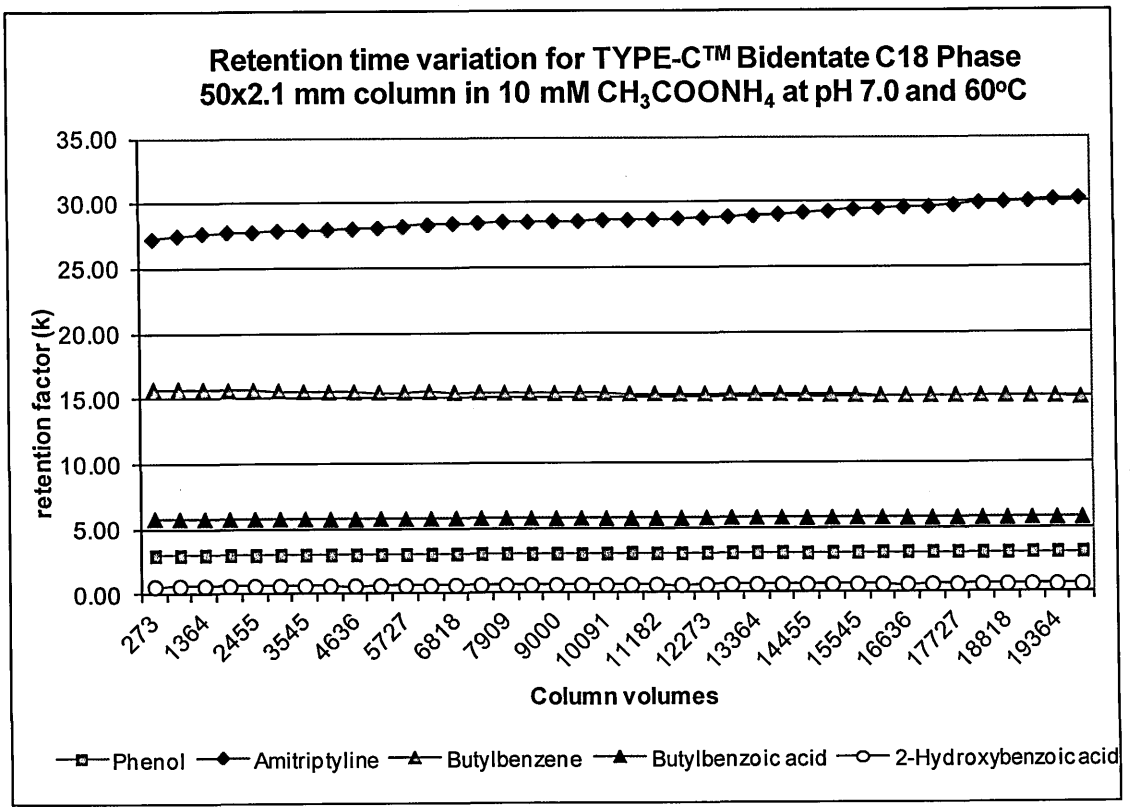

The efficiency values were also calculated for the peaks over the 20,000 column volumes but no significant change was observed, as shown in Figure 5.36 overleaf. A small rise in efficiency is observed for the amitriptyline peak around 10,000 column volumes however it is likely to be due to the increase in peak area as a new sample is used for the analysis.

Figure 5.36 *Efficiency Evaluation of TYPE-C™ Bidentate C18 silica During Real-time stability Testing at pH 7.0*

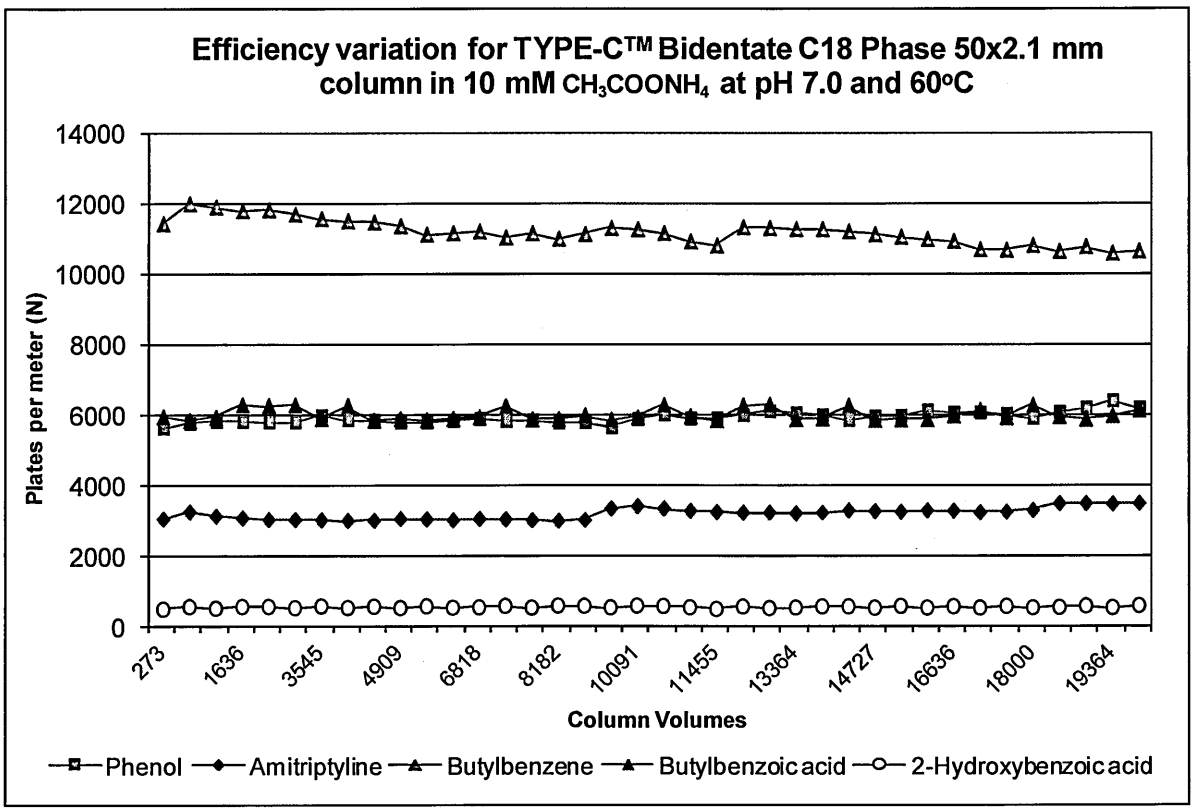

The change in retention time indicates some of the octadecyl silane is being cleaved which suggests the phase is not completely stable under these conditions. This goes against the manufacturer's information but this is a very sensitive test assessing small changes in retention factor and it may be that the change in retention time shown here would not be picked up during day to day analysis.

As with the previous stability evaluations a neutral solute test mix was analysed before and after the stability assessment to probe the changes in the phase. The stability testing has indicated a small amount of phase is being snipped. This is confirmed by comparing the retention times of the peaks in the neutral test mix. These retention times are seen to decrease between 2% and 8%, as shown in Figure 5.37 overleaf.

Figure 5.37 Neutrals Test Mix Assessment of TYPE-C^{TM} Bidentate C18 silica Before and After Real-time stability Testing at pH 7.0

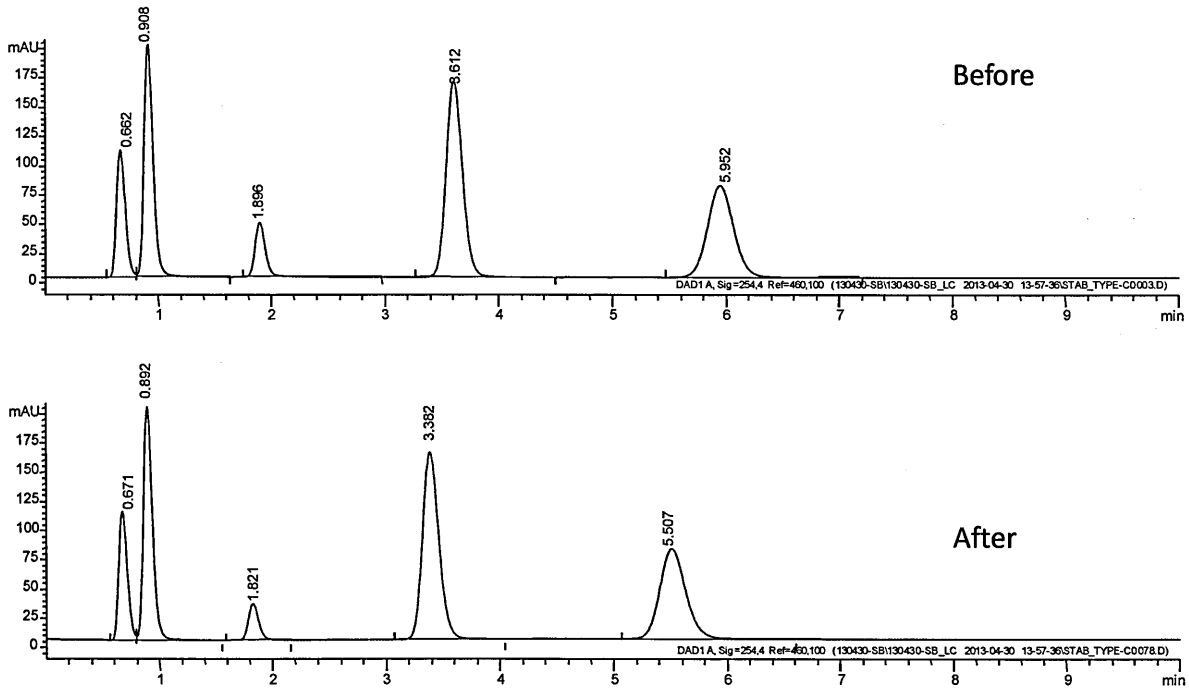

Elution order: [1] Uracil, [2] Dimethylphthalate, [3] Biphenyl, [4] Phenanthrene, [5] Toluene

Overall the TYPE-C^{TM} Bidentate C18 phase has been shown to be highly stable in acidic conditions however some ligand cleavage is observed at neutral pH. This is common for bonded silica HPLC phases and is more likely to be due to the silica base being dissolved rather than hydrolysis of the octadecyl ligand[257][258]. This suggests that the silica hydride polymer formed through cross-linking the triethoxy silane coverage does not protect the silica surface from attack.

5.4 *Conclusion of Physical Properties of TYPE-C™ BidentateC18 Phase*

The solid-state ^{29}Si MAS NMR spectra shown in this chapter has confirmed the presence of silanols on the TYPE-C™ Bidentate C18 stationary phase. It is not possible to tell from the spectra where these silica environments are located on the silica and bonded silane. However, in conjunction with the chromatographic data showing the level of silanophilic interaction it can be concluded that a high percentage of these silanols are accessible on the surface of the stationary phase.

Comparison of these results with the same characterisation probes run on the EPS phases, shown in Chapter 4, suggest that the silanophilic interactions are coming from residual hydroxyl groups within the structure of the silica hydride monolayer rather from surface silanols. This makes sense when considering the nature of the triethoxy silane monomers used to form the silica hydride monolayer. The ^{13}C MAS NMR spectra indicates that there are no ethoxyl groups present on the silica surface suggesting complete crosslinking of the monomer, which is statistically highly unlikely, or all of the remaining ethoxyl groups have been hydrolysed to hydroxyl groups through the presence of water.

The phase has been shown to have high stability against acid hydrolysis at elevated temperatures; this is due to the direct formation of the Si-C bond by derivatisation of the silica hydride using olefins. However the polymeric triethoxy silane coverage does not appear to protect the silica surface from degradation at neutral pH in methanol conditions. Therefore the stability range of 2.0-9.2 as stated by the manufacturers has not been confirmed in this analysis.

Endcapping the hydroxyl "arms" on the column showed a reduced retention time of some of the basic analyte. Due to co-elution of the peaks it was difficult to tell whether the endcapping improved the peak tailing and as the neutral phenol also shows a reduction in retention time this could also be due to cleavage of the octyldecane ligand. The results indicate that hydroxyl groups present on the surface of the phase are easily accessible however further work would be required to confirm this.

van Deemter and SEM results give a good insight into issues with bonding and packing of the TYPE-C™ Bidentate C18 stationary phase; the low efficiency values observed throughout the characterisation work can be explained by the high A and C values determined through van Deemter modelling. On further investigation by SEM these values were found to be due to irregular particles, likely to be amorphous polyhydrosiloxane particles formed during the addition of the silica hydride monolayer. The high eddy dispersion value caused by the non-uniform packing bed account for the low efficiency values and high peak widths observed in the characterisation testing.

Both the presence of the hydroxyl "arms" and the presence of irregular PHS particles suggest that the formation of the silica hydride monolayer is sub-optimal. As the manufacturing process is proprietary information the exact method is unknown. It has already been seen how the concentration of TES used in the "silanization" process needs to be controlled to reduce the formation of PHS particles[185]. Therefore further investigation is required by varying the parameters of the "silanization" process as discussed in literature[185-195]. The formation of the mono-layer and PHS particles was assessed by experimental design to determine the critical parameters for the bonding procedure. This investigation work is discussed in Chapter 7.

6. RESULTS AND DISCUSSIONS: HILIC EVALUATION OF TYPE-C™ SILICA AND DIAMOND HYDRIDE PHASES AND COMPARISON AGAINST TYPICAL TYPE-B SILICA

Hydrophilic interaction liquid chromatography is the ideal separation mechanism for polar hydrophilic compounds; as discussed in the introduction its retention mechanism is a mixture of partitioning, adsorption and ion exchange interactions. In theory the TYPE-C™ silica should not be suitable for HILIC or ANP interactions as the hydrophobic silica hydride would not form a aqueous solvent layer around the stationary phase and the quoted low level of silanols available on the surface would minimise any cationic interactions. However the previous chapter showed that electrostatic interactions from silanophilic groups are a major contributor to the retention mechanism for the TYPE-C™ Bidentate C18. The TYPE-C™ manufacturers themselves claim the phases give complementary selectivity when used in HILIC or ANP. Many HILIC column characterisation methods are available and in this chapter the TYPE-C™ Silica-C and TYPE-C™ Diamond Hydride phases was evaluated using some of these characterisation probes. As with the C18 characterisation typical TYPE-B phase will be used as a reference and validation, in this can the ACE 3 SIL was used. The manufacturer's specifications for all columns are shown in Table 6.1 below.

Table 6.1 Manufacturer's data of TYPE-B and TYPE-C™ phases for characterisation

Phase	Pore size (Å)	Surface coverage (m^2/g)	Endcapping	Carbon Load (%)	pH range	Max temp (°C)
TYPE-C™ Silica-C 4µm[273]	100	350	N/A	-	1.0-7.0	60
TYPE-C™ Diamond Hydride 4µm[273]	100	350	N/A	<2.0	2.5-7.0	60
ACE 3 SIL 3µm[269]	100	300	-	-	1.5-10.0[a]	60

[a] Manufacturers catalogue states for optimum column lifetime a pH range of 2-8 is recommended, column lifetime may decrease depending on the type of inorganic buffers, organic modifiers and temperature.

6.1 *Chromatographic Selectivity Evaluation of TYPE-C™ Silica-C and Diamond Hydride Compared against a Typical TYPE-C silica*

Manufacturing specification for the TYPE-C™ Silica-C and TYPE-C™ Diamond Hydride phases states that the hydrophilic nature of the silica hydride surface means these phases do not form the aqueous solvated layer required for HILIC partitioning. However it does state that the TYPE-C™ Diamond Hydride phase performs similarly to HILIC phases for the elution of polar compounds. The retention mechanism is thought to be purely through adsorption and ion exchange interactions and therefore is more akin to the aqueous normal phase as discussed in Section 1.4. However, as the distinction between HILIC and APN is blurred it was decided to use the HILIC characterisation probes to evaluate the separation mechanism occurring here.

6.1.1 *Ikegami/Tanaka Evaluation of TYPE-C™ Silica-C and Diamond Hydride*

In order to evaluate the different contributions to the retention mechanism the Ikegami/Tanaka characterisation probes discussed in Section 1.8.5. These compounds were chosen to minimise the contribution from electrostatic ion exchange interactions which are much stronger and tend to dominate the retention mechanism. The results for the three columns are shown in Table 6.2 below.

Table 6.2 Tanaka characterisation values – comparison of TYPE-B and TYPE-C™ silica

	k_U	$\alpha_{(pH)}$	$\alpha_{(CH_2)}$	$\alpha_{(OH)}$	$\alpha_{(V/A)}$	$\alpha_{(2dG/3dG)}$	$\alpha_{(\alpha/\beta)}$	$\alpha_{(AX)}$	$\alpha_{(CX)}$
TYPE-C™ Silica-C	0.85	1.23	0.98	1.13	1.00	1.11	1.27	-0.03	32.17
TYPE-C™ Diamond Hydride	0.40	1.17	1.01	0.90	1.01	1.00	1.03	-0.26	58.33
ACE 3 SIL	0.58	1.05	1.09	1.07	1.13	1.11	1.25	-0.17	22.80

U = uridine, pH = 5-methyluridine, CH_2 = 2-deoxyuridine, A = adenosine, V = vidarabine, 2dG = 2-deoxyganosine, 3dG 3-deoxyganosine, α = 4-nitrophenyl-α-D-glucopyranoside, β = 4-nitrophenyl-β-D-glucopyranoside, AX = sodium p-toluenesulfonate, CX = N,N,N-trimethyl-phenylammonium,

A significant observation, which is not readily apparent from the α values shown above, is the relatively short retention of the selected nucleosides solutes. These solutes were chosen for their low logD value[317]. However in the majority of cases the calculated k value for these analytes is <1.00. The exception to this is for those analytes which have a high capacity for cationic interactions or hydrogen bonding, here the retention values increase, this can be seen in the $\alpha_{(CX)}$ values. These low k values indicate that "true" HILIC partitioning has a minimal contribution to the retention mechanism for these phases. These types of values are typical for bare silica phases[241] where the main contribution if from electrostatic interactions.

Uridine is a hydrophilic molecule with a logD value of -3.01 at neutral pH[317] therefore the calculated k_U for the three phases gives an indication of HILIC partitioning contributions to the retention mechanism. As expected the k_U for the TYPE-C™ Diamond Hydride phase is low as the hydrophobic methyl silanes bonded to the phase disrupt the aqueous solvated layer and therefore reduce the partitioning effect. It is surprising that the TYPE-C™ Silica-C phase has a higher k_U value than the TYPE B silica as it would be expected that the silica hydride coverage would also reduce the likelihood of the aqueous layer forming on the silica surface. However it has been seen from the TYPE-C™ Bidentate C18 phase that a significant number of silanols are still active on the TYPE-C™ silica. Also it must be noted that the k_U values are <1.00 and for phases such as the ZIC-HILIC and Amide-80 phases these values are 2.20 and 4.58 respectively[241].

For all three phases the theobromine is retained for longer than the theophylline, giving a selectivity factor greater than one. As this analysis is run at pH 5.8 this suggests the phases are acidic and the negatively charged surface is predominately the cause for the difference in retention times. There are orientation effects with these two analytes, however as the phases are unbonded or very lightly bonded with small silanes these effects would be negligible. The TYPE-C™ Silica-C phase has the highest α(pH) value however it is comparable to other TYPE-B bare silica phases[241], the TYPE-C™

Diamond Hydride phase has a slightly lower value suggesting the trimethyl silanes are reducing the electrostatic interactions on this phase.

The $\alpha_{(CH2)}$ value indicates the level of hydrophobicity on the phase, therefore it would be expected that the TYPE-C™ Diamond Hydride would have a high value compared to the other two phases due to stated carbon load[273]. However both the TYPE-C™ phases show little selectivity, this may be due to that lack of partitioning effect from these phases and the more hydrophobic 5-methyluridine does not get close enough to the stationary phase to undergo adsorption. The TYPE-C™ Silica-C is the only phase to retain 5-methyluridine for longer than uridine, however the difference and the k values for both analytes are so low this may be natural variation in retention times.

The $\alpha_{(OH)}$ value gives the level of selectivity from the hydroxyl groups, again from manufacturer's information the TYPE-C™ phases would be expected to show little selectivity. However, again it is the TYPE-C™ Silica-C that shows a marked difference in retention times between the two analytes. Although a higher $\alpha_{(OH)}$ value was expected for the TYPE-B silica the results are comparable to other bare silica columns[241].

The values for shape selectivity, $\alpha_{(V/A)}$ and $\alpha_{(2dG/3dG)}$ and silane density $\alpha_{(\alpha/\beta)}$ are not very descriptive for these types of columns and it is likely that the differences observed here are due to secondary electrostatic interactions. The TYPE-C™ Diamond Hydride is the only phases tested that has any bonded silane which might give rise to these retention mechanism contributions, however this phases showed co-elution for all three pairs of analytes.

The $\alpha_{(AX)}$ and $\alpha_{(CX)}$ are notably the most significant results here; for all three phases the sodium-p-toluenesulfonate eluted before the void volume marker toluene indicating electrostatic repulsion. The very high $\alpha_{(CX)}$ values observed indicate the extent of cation exchange interaction occurring due to silanophilic retention. The high $\alpha_{(CX)}$ value for the TYPE-C™ Diamond Hydride phase may be a little

misleading; it suggests there is a greater extent of silanophilic interactions on this phase than on the TYPE-C™ Silica-C and TYPE B bare silica. However *N,N,N*-trimethyl-phenylammonium chloride is significantly more hydrophobic than uridine due to the methyl groups, therefore the high retention is due to both electrostatic interactions with the silanols and hydrophobic adsorption with the hydrocarbon silane on the phase[273]. The TYPE-C™ Silica-C is seen to have a higher $\alpha_{(CX)}$ value than the TYPE-B silica, this may be because the TYPE-B silica is a higher purity silica. Evaluation of the current data does not give any indication as to the nature of the surface silanols therefore further investigation into buffer concentration to aid ion exchange suppression and pH variation to determine the contribution from more acidic silanols would be required.

Overall the three phases appear to show very little selectivity for HILIC separations and the main contribution to the retention mechanism is seen to be coming from cationic exchange with the silanol groups on the surface. As the contribution is so large, it is likely to mask any secondary interactions from partitioning and hydrophobic adsorption when analysing polar analytes, however this retention mechanism appears to give rise to poor peak shape. The $\alpha_{(CX)}$ value has been removed from the graphical representation of the result, shown in Figure 6.1 below.

Figure 6.1 Tanaka characterisation values – comparison of TYPE-B and TYPE-C™ silica

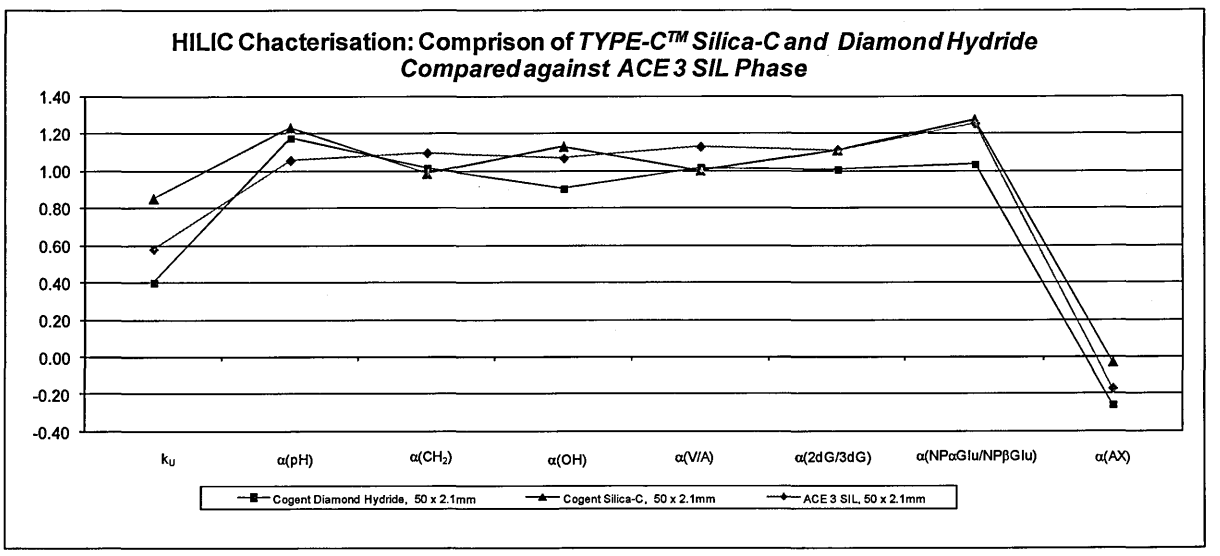

U = uridine, pH = 5-methyluridine, CH_2 = 2-deoxyuridine, A = adenosine, V = vidarabine, 2dG = 2-deoxyganosine, 3dG 3-deoxyganosine, α = 4-nitrophenyl-α-D-glucopyranoside, β = 4-nitrophenyl-β-D-glucopyranoside, AX = sodium p-toluenesulfonate, CX = N,N,N-trimethyl-phenylammonium,

One of the manufacturer's claims for the TYPE-C™ Diamond Hydride phase is that it requires much less equilibration than typical HILIC phases. The results seen above indicate that this is because the phase is not forming an aqueous solvated layer on the surface of the phase which is required for "true" HILIC partitioning separations. However the uridine is still being retained on the phase, even though the k_U is low compared to commonly used HILIC phases. From the results above it is unclear whether the uridine is being retained through a partitioning mechanism or through a combination of adsorption and electrostatic interactions.

This retention mechanism can be further investigated through the movement in retention time of uridine over 70 column volumes. Prior to use the columns were washed and stored in a 50:50 water:acetonitrile solution, the columns were not allowed any equilibration period and the uridine solution was injected in 5 minute intervals, equivalent to 4.8 column volumes. The retention times for each phases were recorded and are shown in Figure 6.2 below.

Figure 6.2 ***Movement in retention time of uridine over 70 column volumes to assess column equilibration period***

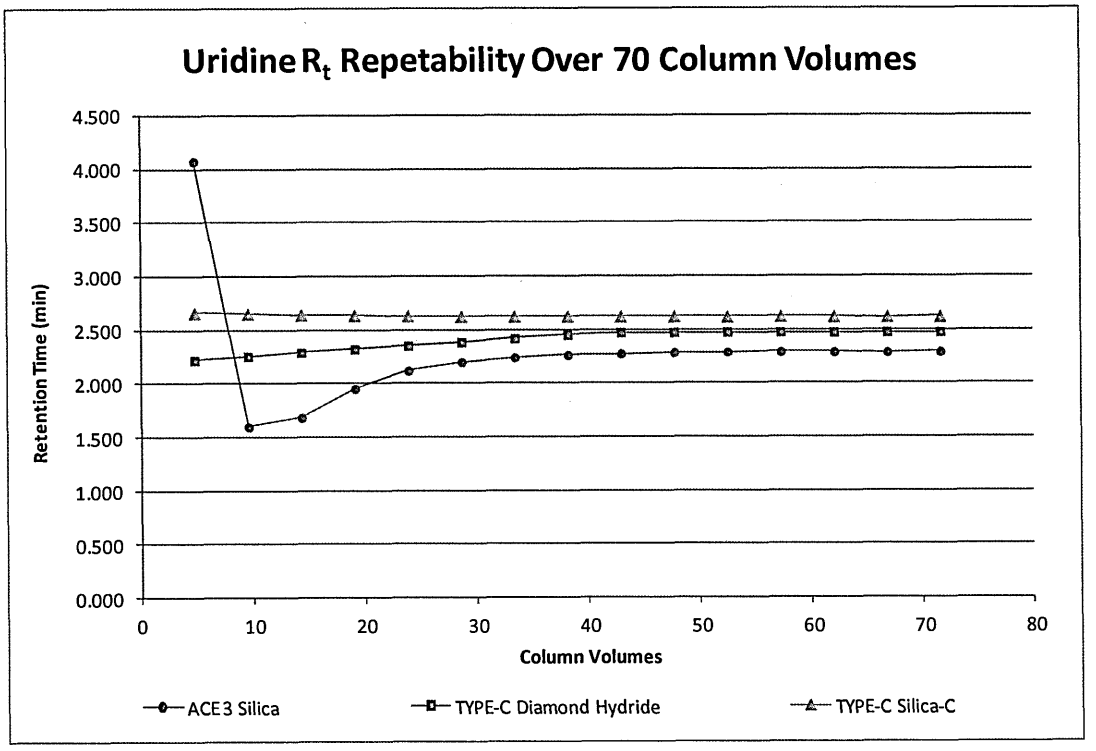

The retention time is used rather than the retention factor as this is comparison work and it is the variation in the raw data rather than the value itself that is being assessed. As the determination of the solvent front can be subjective, especially in HILIC as the sample solvent has similar composition to the mobile phase, calculating the retention factor may allow for a small error in the results.

The TYPE-B Silica exhibits a typical equilibration pattern; the initial injection has a significantly higher volume of water surrounding the silica and the aqueous layer has not had time to form therefore the retention time is significantly longer. As the aqueous layer begins to establish itself the retention mechanism is now governed by partitioning, it can be seen that the column takes around 45-50 column volumes for the aqueous layer to be fully formed and give a repeatable retention time. This equates to around 50 minutes equilibration time and as the phase had been conditioned for at least 60 minutes prior to the Ikegami/Tanaka characterisation work shown above.

The TYPE-C™ phases shows much less variation in the initial injection, this may be because all three columns are in the same thermostatic oven has therefore been allowed to time to reach correct temperature prior the first injection, whereas the TYPE-B silica may not have done. The TYPE-C™ Diamond Hydride phase shows less variation in retention time however it does not fully equilibriate until 40-45 column volumes have been run down it. This is significantly different to the 7-10 column volumes stated in the manufacturer's specifications. The 7-10 column bed volumes stated by the manufacture may be the case for analytes that are retained through adsorption and electrostatic ion exchange, however uridine was chosen specifically for this investigation as it is retained through the partitioning contribution to the retention mechanism. This indicates that the aqueous layer is being formed around the TYPE-C™ Diamond Hydride phase surface and partitioning is a factor in the retention mechanism.

The TYPE-C™ Silica-C results were the most surprising as the Ikegami/Tanaka characterisation work implies the phase is very similar to the TYPE-B bare silica, and it was expected that the conditioning

results would mirror those of the ACE 3 SIL. However the TYPE-C™ Silica-C phase is seen to reach equilibrium in less than 30 column volumes. This may be due to the reduced silanophilic nature of the phase means that the aqueous layer formed is less dense and consequently forms faster.

All phases, once they have reached equilibrium were seen to have a variation of ≤0.1% RSD. Once the phases were fully conditioned the ACE 3 SIL and TYPE-C™ Silica-C have comparable retention times to the Ikegami/Tanaka characterisation work shown above. However the uridine retention time observed on the TYPE-C™ Diamond Hydride phase has increased from 2.01 seen previously to 2.47 minutes in this analysis. This indicates there may have been a change in the bonding coverage or silanol distribution of the phase. As the other two columns show the same retention time it is unlikely to be analytical variation due to mobile phase composition, pH or oven temperature, which are the most common causes of retention time changes. This requires further investigation into the stability of the TYPE-C™ Diamond Hydride phase.

6.1.2 *PCA Characterisation of TYPE-C™ Diamond Hydride and Silica-C*

In the last 20 years there have been a large number of HILIC mode stationary phases developed, and consequently a large number of PCA characterisation of these columns[319-321]. The two major parameters for the formation of the aqueous layer required for HILIC partition are the pH of the phase and the contribution of silanophilic interactions from the hydroxyl groups on the phase. The Ikegami/Tanaka characterisation shown in the previous section uses these two parameters as the basis for a simplified PCA plot which can clearly categorise the different types of stationary phase[322]. The relative α values of the retention factors of theobromine and theophylline, and uridine and 2-deoxyuridine respectively taken from publications[241] are shown in Figure 6.2 below. Although it has been seen the TYPE-C™ Silica-C and TYPE-C™ Diamond Hydride phases have a predominately ionic exchange contribution to the retention mechanism rather than true HILIC partitioning, the experimental results are compared against this literature data.

Figure 6.3 Simplified PCA of Ikegami/Tanaka Characterisation data for HILIC phases

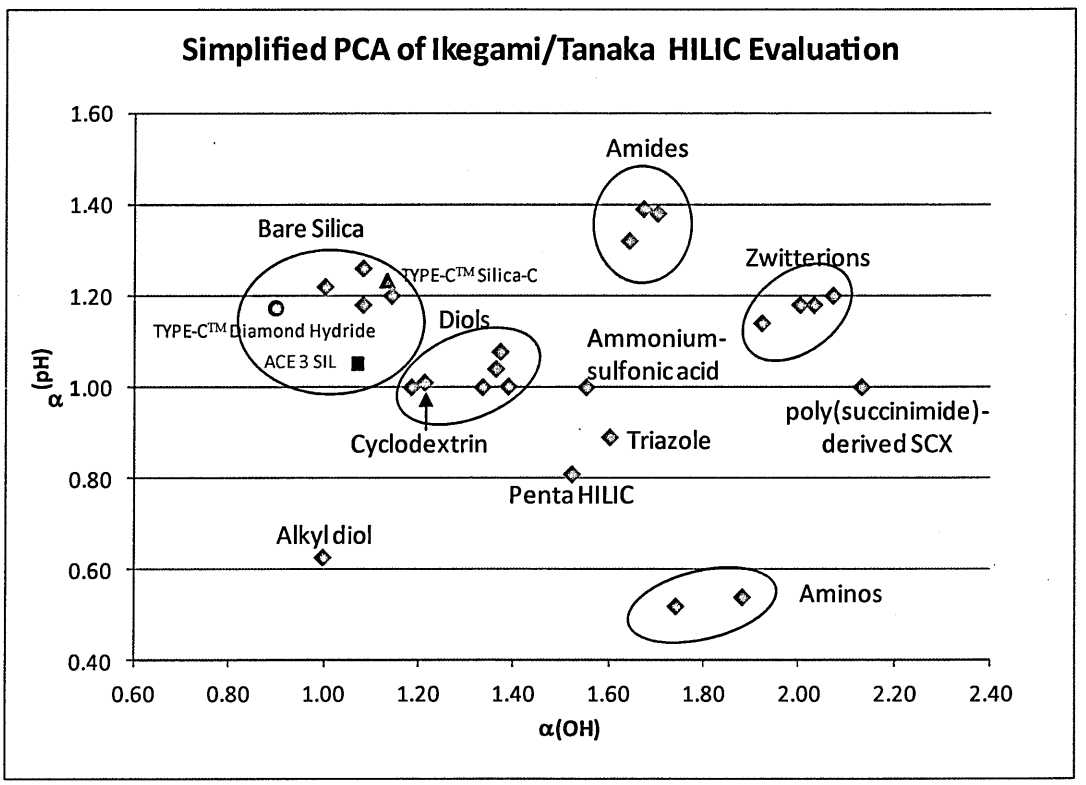

To ensure the integrity of this data the ZIC-HILIC phase was analysed along with the TYPE-C™ phases during the Ikegami/Tanaka characterisation. These results were compared to the results taken from publications and the RSD values shown to be around 1.0%, the full results can be seen in the appendix. The simplified PCA shows that the columns tested can be grouped together and similar phases can be characterised and defined through the two parameters. Although there is not enough data to substantiate the designated areas of the plot there are a number of bare silica phases within this data set that appear to have similar properties.

The ACE 3 SIL and the two TYPE-C™ phases also show the same properties as the bare silica phases. The ACE 3 SIL has a lower $\alpha_{(pH)}$ value due to its high purity silica base, the $\alpha_{(OH)}$ values are comparable with the other silica phases. The TYPE-C™ Diamond Hydride phase has a comparable $\alpha_{(pH)}$ with the other bare silica columns but a lower $\alpha_{(OH)}$ value as the coverage of silica hydride and the unknown hydrocarbon silane reduces the percentage of available silanols. This lower result may be caused by hydrophobic silane restricting the formation of the aqueous layer on the surface which reduced the contribution of partitioning in the retention mechanism and may actively repel the hydrophilic probe solutes. The TYPE-C™ Silica-C phase appears to be comparable with the other bare silica phases for both $\alpha_{(OH)}$ and $\alpha_{(pH)}$ values, this suggests the coverage of silanols on the surface of the phase is similar to unbonded TYPE-B silica.

Overall the simplified PCA is a useful way of quickly characterising a HILIC phase however as it does not include electrostatic attraction and repulsion of the exposed silanols on the surface of bare silica it may not give the full picture. Further investigation is required to probe the ion exchange interactions observed on the two TYPE-C™ phases. Therefore these results will be compared using a full PCA incorporating all Ikegami/Tanaka characterisation data. The loading plot for the PCA captured >95% of the population, Figure 6.4 overleaf. Some interesting variations in the vectors is observed as the two sets of regio-isomeric probes for stereo-selectivity do not lie in the same quadrant. The $\alpha_{(2dG/3dG)}$ regio-isomers probes are observed in the top left hand and have similar

retention characteristics to the $\alpha_{(\alpha/\beta)}$ probes which indicates the ligand density of the phase which is linked to stereoselectivity. However the other pair of region-isomers, the $\alpha_{(V/A)}$ probes are observed in the right hand quadrant, in a similar area to the $\alpha_{(OH)}$ characteristic which identifies hydroxyl group on the surface of the phase. Hydroxyl groups on a HILIC stationary phase will cause the formation of the aqueous layer which gives rise to the partition retention mechanism. The adenosine and vidarabine probes have a number of accessible hydroxyl groups which will be retained through the partition retention mechanism, as these probes are aligned with the uridine and 2-deoxyuridine probes it indicates that the partition contribution has a greater contribution and over powers the stereoselective contribution to the retention mechanism.

Figure 6.4 PCA Loading Plot for HILIC phases using Ikegami/Tanaka Characterisation data

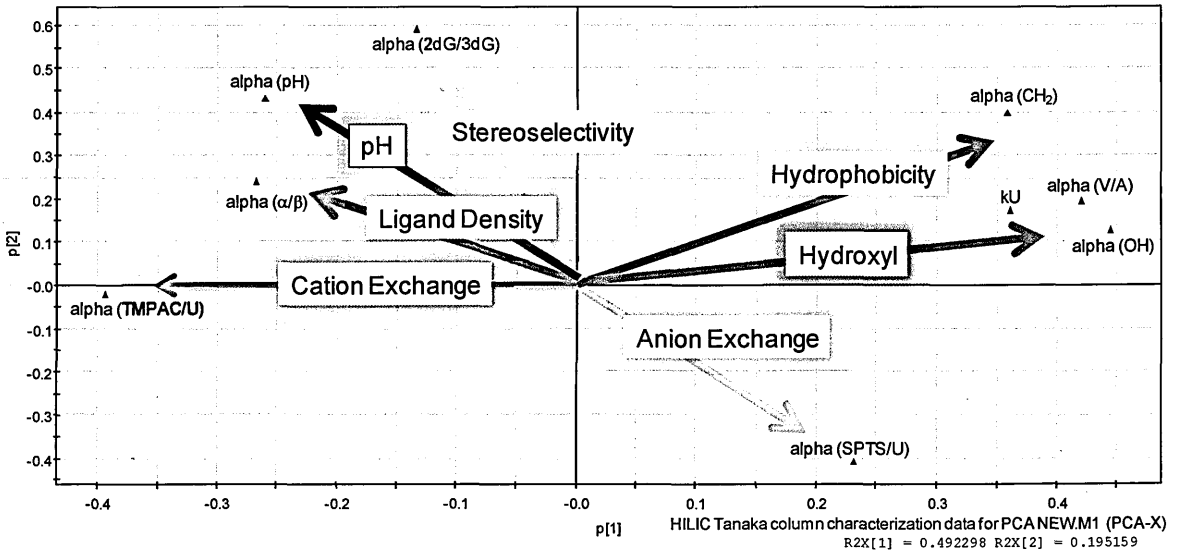

U = uridine, pH = 5-methyluridine, CH_2 = 2-deoxyuridine, A = adenosine, V = vidarabine, 2dG = 2-deoxyganosine, 3dG 3-deoxyganosine, α = 4-nitrophenyl-α-D-glucopyranoside, β = 4-nitrophenyl-β-D-glucopyranoside, AX = sodium p-toluenesulfonate, CX = N,N,N-trimethyl-phenylammonium,

The retention factor of uridine is also observed to be in the same area as the $\alpha_{(OH)}$ characteristic; this may suggest that uridine is governed by the partition retention mechanism. The $\alpha_{(TMPAC/U)}$ characterisation term indicates the electrostatic nature of the phase due to cation exchange retention mechanism. On the loading plot the $\alpha_{(TMPAC/U)}$ is observed to be in the opposite quadrant to the $\alpha_{(OH)}$ which suggests that in these conditions the hydroxyl groups do not dissociate to ions which would give rise to electrostatic interactions. The ammonium acetate is buffered at pH 5.8 however

due to the high concentration of acetonitrile in the mobile phase composition the working pH is likely to be higher. The full Ikegami/Tanaka characterisation PCA including the columns from publications[241] are shown in Figure 6.5 below.

Figure 6.5 PCA for HILIC phases using Ikegami/Tanaka Characterisation data

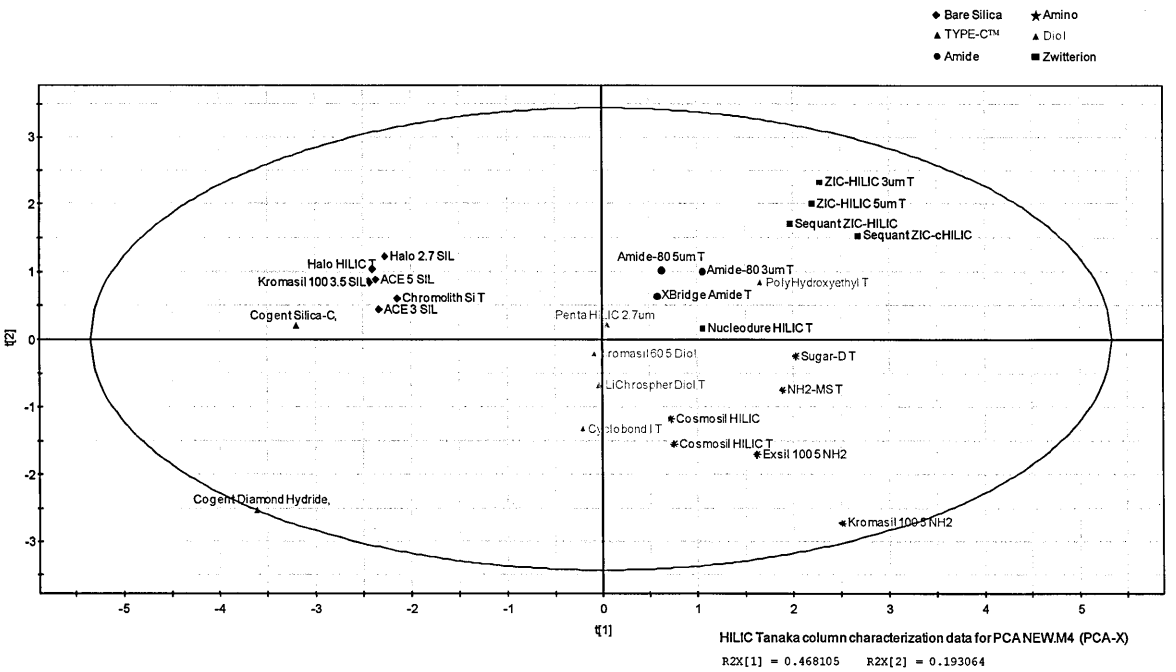

As with the simplified PCA shown in Figure 6.3 this full PCA shows fairly distinct groupings of the different column types. The TYPE-C™ Silica-C phase is still seen to be observed with the TYPE-B bare silica phases. However the TYPE-C™ Diamond Hydride phase is seen to differ, although it has the same level of cation exchange as the silicas it also lies on the $\alpha_{(CH2)}$ vector, due to the lightly bonded hydrocarbon coverage. This is a comparable result to those observed in the simplified PCA however the differences are amplified here.

Both PCAs have confirmed the presence of residual silanols accessible on the TYPE-C™ Silica-C and Diamond Hydride phases. This data also indicates that the electrostatic cation exchange component of the retention mechanism observed in the TYPE-C™ phases is due to silanol activity rather than hydroxyl, amide or zwitterion. The extent and acidity of these silanol groups will be investigated further in the next section.

6.1.3 The effect of Ionic Strength on Diamond Hydride and TYPE-C™ Silica Phases Under HILIC Conditions

The level of cationic exchange observed for both the TYPE-C™ Silica-C and TYPE-C™ Diamond Hydride phases indicates that the coverage there is a number of hydroxyl or silanol groups on these phases. As with the TYPE-C™ Bidentate C18 phase the nature of the silanophilic activity can be investigated by evaluating the retention factor of certain analytes in mobile phase of different ionic concentrations and pH. As the columns need to remain in HILIC mode the mobile phase composition needs to remain at 95% acetonitrile therefore the previous methods, seen in Section 5.1.5 cannot be used. However the same principle of increasing the ionic concentration of ammonium acetate at both pH 3.0 and 7.0 can be utilised.

In order to investigate partitioning interactions and the contribution from adsorption and electrostatic retention on each phase three analytes were chosen from the Ikegami/Tanaka characterisation probes. Uridine, theobromine and theophylline were chosen as they had a similar retention factor. As cationic exchange has such a significant affect in the retention factor the retention time of *N,N,N*-trimethyl-phenylammonium chloride was seen to be very long and was therefore not included in the selection.

The manufacturers suggest that the TYPE-C™ Diamond Hydride phase is best used in ANP and the light coverage of the hydrocarbon based silane groups bonded to the surface of the silica reduced the formation of the aqueous solvent layer. This should minimise the contribution from partitioning from the retention mechanism and only allow adsorption and electrostatic interactions. Therefore it would be expected that all three analytes would behave as the reversed phase model and the retention factor would decrease as the ionic strength increases and the silanol groups are suppressed by the counter ion. The results can be seen in Figure 6.6 overleaf.

Figure 6.6 HILIC mode Cox Plots at pH 3.0 and pH 7.0 on TYPE-C™ Diamond Hydride phase

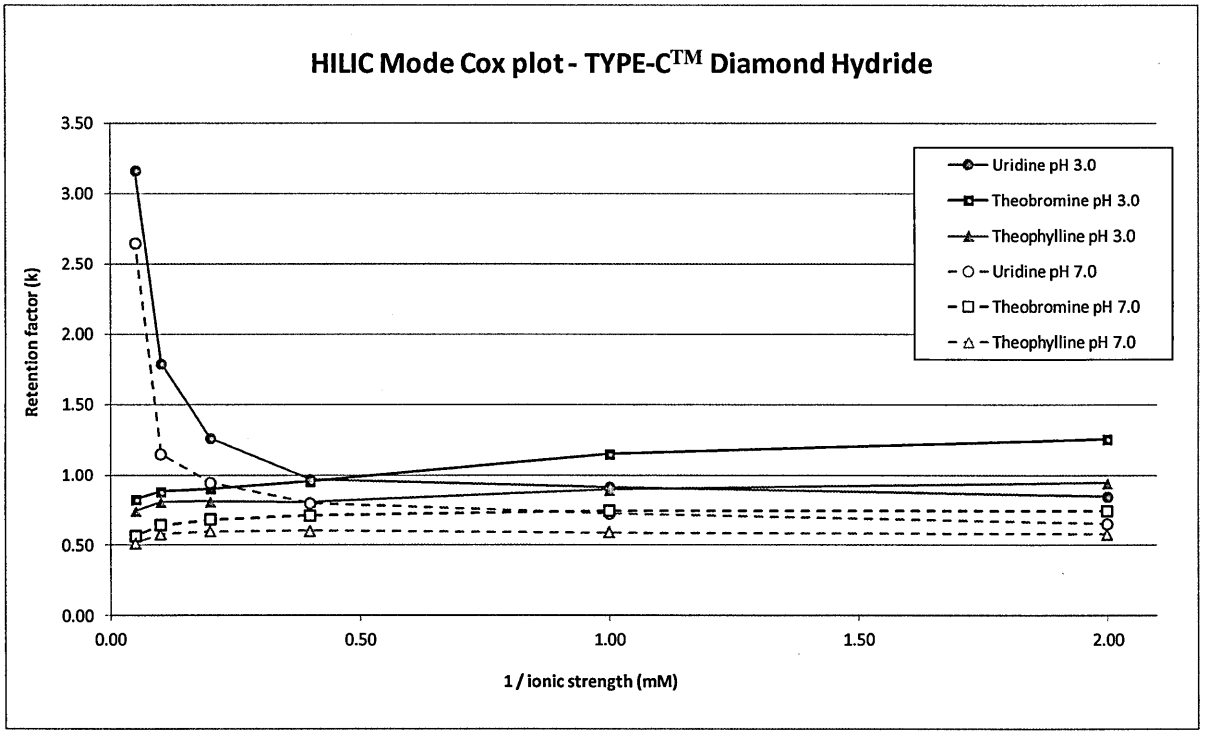

The theobromine and theophylline results behave as expected, at high ionic strength the silanols are suppressed and the retention factor is reduced. This is more pronounced for pH 3.0 than it is for pH 7.0; due to the large concentration of acetonitrile the actual pH of the mobile phase may be significantly higher than the ammonium acetate buffer used.

The results for uridine are not as expected from an adsorption/electrostatic interaction retention mechanism. As the ionic strength of the mobile phase decreases so does the retention factor of uridine. This result indicates that a partitioning mechanism is contributing to the retention of the analyte and as the ionic strength is increased the density of the aqueous layer around the silica surface is also increases allowing the analyte to be retained in this aqueous layer for longer. The width of the uridine peak also increases as the retention time increases; this may be due to natural dispersion of the analyte as it spends more time in the column. The increased peak width may suggest that the movement between the aqueous layer and the acetonitrile rich bulk of the mobile

phase is impeded by the buffer ions. This is possibly because the higher concentration of buffer makes the aqueous layer denser and mass transfer between the two layers is increased.

This pattern is similar for the TYPE-C™ Silica-C phase as seen in Figure 6.7 below and Figure 6.8 overleaf. At pH 3.0 the retention factor for the theobromine and theophylline is reduced as the concentration of buffer increases and the counter ion suppresses the residual silanols on the surface of the phase. However the uridine retention factor increases significantly as the concentration of ionic buffer increases and alters the partition interaction mechanism of the aqueous layer around the column surface.

Figure 6.7 HILIC mode Cox Plots at pH 3.0 and pH 7.0 on TYPE-C™ Silica-C phase

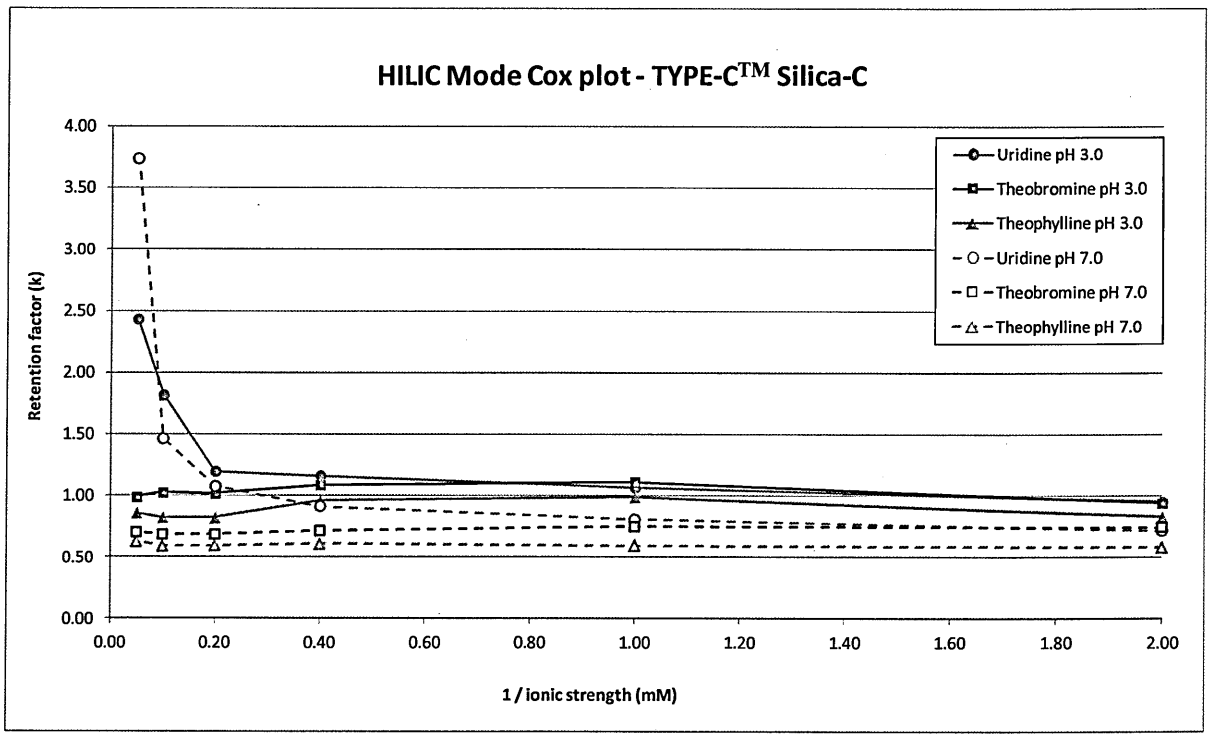

At pH 7.0 the effect on uridine is more pronounced however there is no significant different observed across the retention factors of theobromine and theophylline as the ionic strength increases. This result mirrors those of the TYPE-C™ Diamond Hydride phase and may be due to the elevated pH of the mobile phase due to the high concentration of acetonitrile.

The ACE 3 SIL also shows this trend to a lesser extent; at pH 7.0 the uridine retention factor shows the same trend as the TYPE-C™ phases. However at pH 3.0 the uridine retention factor still decreases as the ionic strength decreases however not in the same degree of exponential decay. At pH 3.0 the retention factors of theobromine and theophylline decrease as the ionic buffer increases but show no significant change at pH 7.0.

Figure 6.8 HILIC mode Cox Plots at pH 3.0 and pH 7.0 on TYPE-C™ Silica-C phase

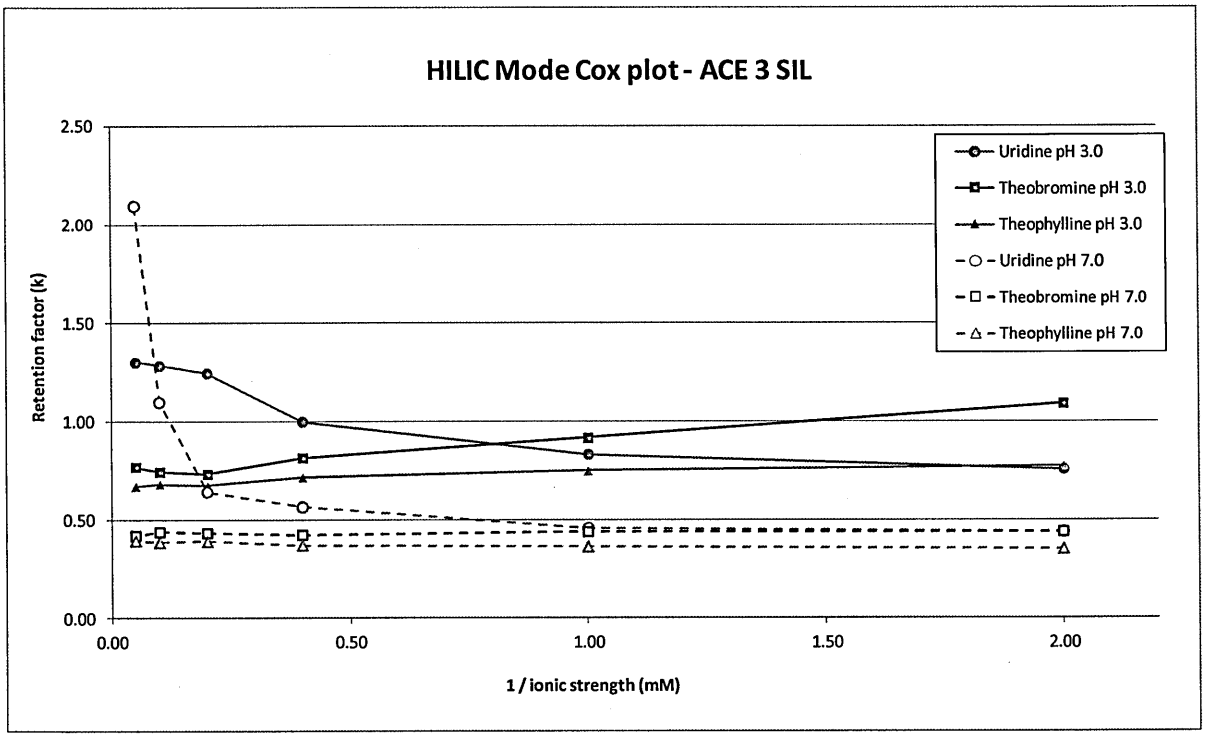

These results confirm the presence of silanols on the surface of the TYPE-C™ phases which contributes to the formation of an aqueous layer allowing for HILIC partition separation mechanism to take place. Although this is contrary to the manufacturer's information it does agree with the findings for the TYPE-C™ Bidentate C18 findings shown in the previous chapter. Although the TYPE-C™ phases do not exhibit the same characteristics of a TYPE-B silica the results do indicate the same trends for contribution to the retention mechanism.

6.1.4 *Overloading Assessment of Diamond Hydride and TYPE-C™ Silica: Ws Value Calculation in HILIC Mode*

In reversed phase chromatography analyte overloading is often characterised by the peak tailing, especially for basic analytes, due to secondary interactions with residual silanols on the surface. In HILIC mode it has been seen that a large contribution to the retention mechanism is due to the electrostatic interactions with these silanol groups. However due to the abundance of available silanols on the surface of the silica the analytes are less likely to overload at one specific site and exhibit peak tailing in the same way. In HILIC mode the analytes are retained through a combination of partition, adsorption and electrostatic mechanisms, again uridine and adenosine are chosen as they have the highest retention factor of all of the Ikigami/Tanaka characterisation probes.

The retention factors for the probes are too low to give an accurate evaluation of the overloading capacity of these phases; however characterisation work shown in Section 6.1.1 showed short retention time for all analytes tested under these conditions. The column saturation capacity (W_s) was calculated using the equation discussed in Section 5.1.6 and the results along with the determined initial retention factor and efficiency of the analyte are shown in Table 6.3.

Table 6.3 ***Column Saturation Values at N_0-50%– Comparison of TYPE-C™ Diamond Hydride and Silica-C phases against ACE 3 SIL phase***

	Uridine			Adenosine		
	k	N_0	W_s (mg)	k	N_0	W_s (mg)
ACE 3 SIL	0.58	2202	0.82	1.15	3204	3.84
TYPE-C™ Diamond Hydride	0.45	1655	0.48	1.39	1999	5.76
TYPE-C™ Silica-C	0.76	2086	1.33	1.87	2803	10.0

Unlike the TYPE-C™ Bidentate C18 phase the TYPE-C™ Silica-C phase show comparable efficiency to the ACE 3 SIL, the TYPE-C™ Diamond Hydride phase has a lower efficiency however it also has a lower retention factor which may account for the lower efficiency values. As shown in Section 6.1.1 the light bonding of alkyl chain on the TYPE-C™ Diamond Hydride phase reduces the formation of the aqueous layer around the surface of the silica. This results in the lower retention factor for uridine which has been shown to be retained through the partitioning mechanism. Adenosine is retained through a mixture or partition and electrostatic interactions and is retained for longer on the two TYPE-C™ phases which also show an increase in the efficiency values.

Although these values are not as high as the ACE 3 SIL phase the TYPE-C™ phases are stated by the manufacturers to be 4 µm particle size phases[273]. The ACE phase is a 3 µm phase[269] which allows for a lower HETP value and subsequently a higher efficiency. It has been shown in Section 5.2.3 and 5.2.4 that the reduced efficiency of the TYPE-C™ Bidentate C18 phase may be attributed to sub-optimum packing and irregular particles within the packing bed most likely due to formation of PHS particles during the bonding of the bidentate monolayer of silica hydride. These results show the TYPE-C™ Diamond Hydride and Silica-C phases do not have the same reduced efficiency which may indicate the silica hydride coverage is not formed through crosslinked triethoxy silane bonding. This will be investigated further using spectroscopic analysis in Section 6.2 and by a HILIC mode van Deemter analysis shown in Section 6.4.

Figure 6.9 Overloading of (I) Uridine and (II) Adenosine injections on ACE 3 SIL

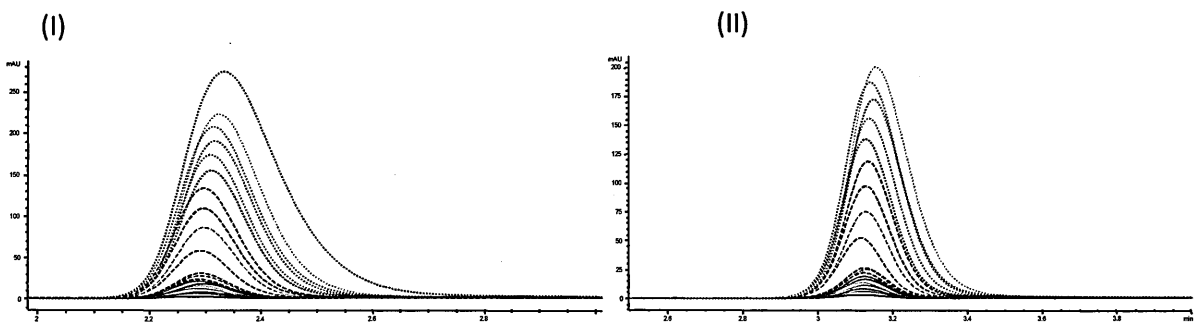

Unlike the reversed phase analysis the overloaded chromatographs show a Gaussian peak shape with little change to the retention factor as the sample concentration increases. The reversed phase analysis of nortriptyline shown in Section 5.1.6. gave the classic "shark-fin" tailing associated with basic analytes. Neither of the chromatograms for HILIC mode analytes shown here exhibit shark-fin tailing which indicates that ionic exchange interaction is not the main contribution to the retention mechanism. The previous section has shown that the retention mechanism for uridine has a high contribution from partitioning interactions. It can be seen in the overlaid chromatograms shown in Figures 6.9 to 6.11 that the peak width for uridine is higher and the peak shape less Gaussian than for the adenosine peak in the same concentrations. The chromatograms for the ACE 3 SIL show a reduced peak width for the adenosine when compared to the peak widths observed on the TYPE-C^{TM} Diamond Hydride and Silica-C phases. However the calculated column saturation capacity for adenosine shown in Table 6.3 is nearly half that of the TYPE-C^{TM} Diamond Hydride nearly three times lower than the TYPE-C^{TM} Silica-C phase.

Figure 6.10 Overloading of (I) Uridine and (II) Adenosine injections on TYPE-C^{TM} Diamond Hydride

(I) (II)

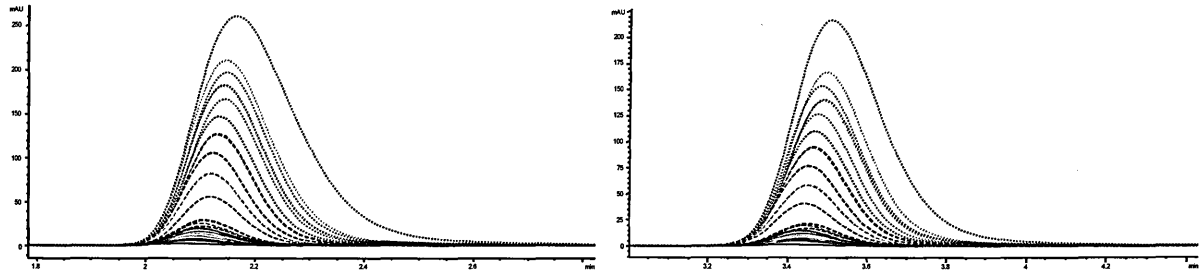

Figure 6.11 Overloading of (I) Uridine and (II) Adenosine injections on TYPE-C^{TM} Silica-C

(I) (II)

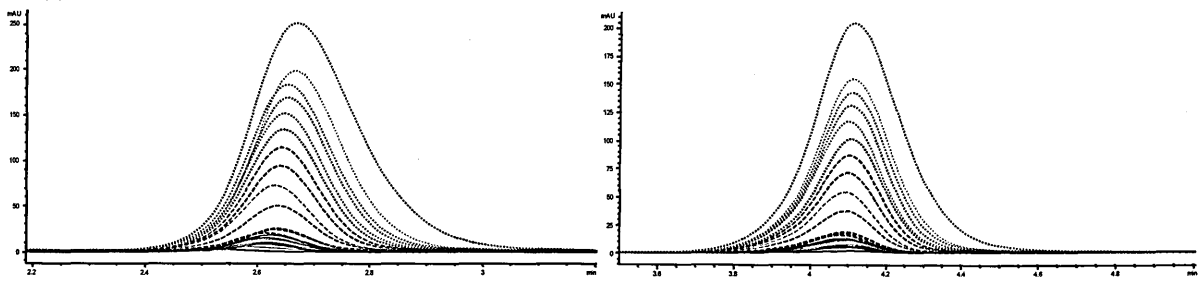

The two TYPE-C™ phases show comparable peak shape and widths for both the uridine and adenosine phases, the TYPE-C™ Diamond Hydride phase exhibits a small degree of fronting on both analytes. The calculated column saturation value for adenosine on the TYPE-C™ Silica-C is double that of the TYPE-C™ Diamond Hydride phase. This is likely because the phase has a greater number of accessible silanols that are easy for the solutes to access. The TYPE-C™ Silica-C will also give rise to a higher density of aqueous solvated layer around the silica as the hydrophobic nature of the TYPE-C™ Diamond Hydride will disturb this layer. It was shown in Section 6.1.3 that adenosine is most likely retained through a combination of ion exchange and partioning the conditions are ideal for the analytes to be retained in bands with low dispersion. The dispersion coefficient of these phases will be investigated in greater detail in Section 6.4 during the van Deemter analysis.

Overall both the TYPE-C™ phases show a high columns saturation point and Gaussian peak shape even at high sample concentration. The column efficiencies shown are comparable with the ACE 3 SIL phase however this will be investigated further in Section 6.4 during the van Deemter analysis.

6.1.5 Conclusion of Diamond Hydride and TYPE-C™ Silica-C Retention Mechanism in HILIC Mode

The Ikegami/Tanaka results indicate the retention mechanism for the TYPE-C™ Diamond Hydride and Silica-C phases is mainly from electrostatic interactions with a small contribution of adsorption and partitioning retention. The results clearly show a high number or residual silanols accessible on both TYPE-C™ phases which contradicts the manufacturer's claims of a full silica hydride coverage. Both phases have been shown to form an aqueous layer around the surface of the silica under HILIC conditions. Consequently the TYPE-C™ phases should be allowed to equilibrate for at least 30 column volumes in the case of the Silica-C and 45 column volumes for the Diamond Hydride in order to obtain repeatable results in HILIC or ANP mode. This is contrary to the advice given by the manufacturers with regard to the TYPE-C™ Diamond Hydride phase.

The principal component analysis shows both TYPE-C™ phases to be comparable with TYPE-B bare silica phases however the TYPE-C™ Diamond Hydride shows additional hydrophobicity due the lightly bonded alkyl phase. The nature of this hydrocarbon coverage will be investigated further in Section 6.2. The TYPE-C™ Diamond Hydride phase also showed a change in retention time of uridine across two sets of analysis using the same HILIC conditions. This also calls into question the stability of the phase, as with the TYPE-C™ Bidentate C18 phase the column will be unpacked and the structure and stability of the bonded silica material will investigated in Section 6.2 and 6.3 respectively.

Both TYPE-C™ phases show ionic interactions comparable with the ACE 3 SIL phase due to the presence of silanols on the surface of the silica. The results of Section 6.1.3 indicate that the electrostatic interactions are comparable at pH 3.0 and pH 7.0 suggesting a similar population of silanols groups on the surface of the phase. As the mobile phase used has high acetonitrile content

the working pH of the mobile phase will be higher than the buffer which may affect the results however it indicates that the TYPE-C™ phases use a high purity of silica.

The efficiencies of the TYPE-C™ phases are comparable with the ACE 3 SIL which indicates the issues with packing efficiencies and irregular particle shapes observed for the TYPE-C™ Bidentate C18 phase are not present in the Silica-C and Diamond Hydride phases, this will be investigated in greater detail in Section 6.4. The column saturation factor of the TYPE-C™ phases has been shown to be high, mostly likely due to the high number of accessible silanols on both phases.

Overall it would appear from these preliminary results that the TYPE-C™ Diamond Hydride and Silica-C phases have different physical properties than the TYPE-C™ Bidentate C18 phase from the previous chapter. It is thought that the TYPE-C™ Bidentate C18 was produced by a crosslinking reaction of triethoxysilane on the surface of the phase to form a polymeric layer of silica hydride which masks the surface silanols. Due to the level of ionic exchange and column saturation shown for the TYPE-C™ Diamond Hydride and Silica-C phases it is likely that these phases have been produced by a different process. Section 1.7 in the introduction showed a two-step route of chlorination and reduction of a base TYPE-B silanol onto the silica hydride. One of the drawbacks to this process is low silica hydride coverage of the material, however as the characterisation probes have shown the TYPE-C™ Diamond Hydride and Silica-C phases have a greater cation exchange capability than the unmodified ACE 3 SIL phase in HILIC mode. This indicates a large number of unconverted silanols on the surface, therefore it is possible that the two-step chlorination and reduction process has been utilised for the manufacture of the TYPE-C™ Diamond Hydride and Silica-C phases.

6.2 *Solid State NMR Analysis of TYPE-C™ Diamond Hydride and Silica-C Phases*

The manufacture state that the TYPE-C™ Diamond Hydride phase has a carbon load of <2.0%, the extra hydrophobic interactions have been confirmed in Section 6.1.1 and 6.1.2. The TYPE-C™ Diamond Hydride and TYPE-C™ Silica-C phases were unpacked and analysed using solid state ^{29}Si NMR spectroscopy, the full spectra were compared to the bare TYPE-B silica from Section 5.2.1 and are shown in Figure 6.12 below.

Figure 6.12 ***Solid State ^{29}Si NMR Spectra of TYPE-C™ Diamond Hydride Silica Material against the ACT TYPE-B unbonded silica***

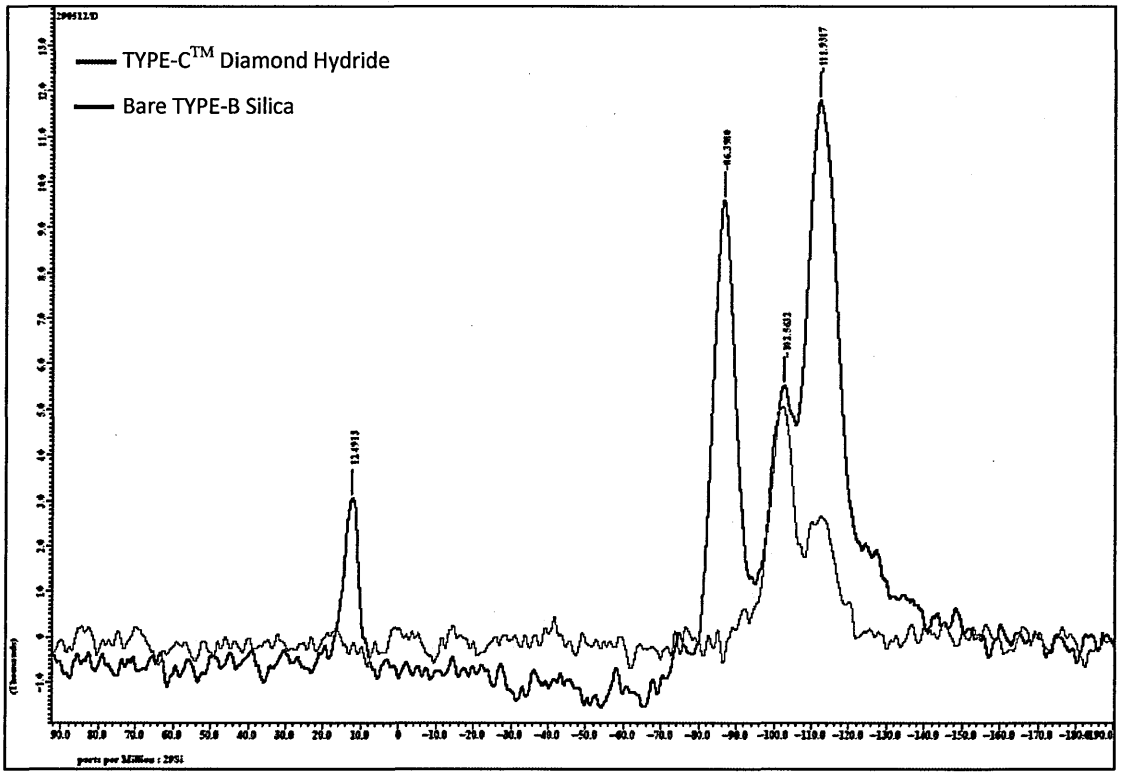

As with the TYPE-C™ Bidentate C18 both the TYPE-C™ phases display both Q_3 and Q_4 silica environments indicating a level of residual silanols. The Ikigami/Tanaka results shown in Section 6.1.1 have already shown these are a large number of accessible silanols on the surface of the silica phases. The TYPE-C™ phases also show a delta shift at approximately -86 ppm which confirms the presence of a silica hydride environment. Only the TYPE-C™ Diamond Hydride phase shows a delta

shift of approximately 12 ppm which would correspond to a silane bonded to the surface of the silica material. The solid state ^{29}Si NMR spectra for the TYPE-C™ Bidentate C18 silica material shown in Section 5.2.1 does not show a silica environment at this delta shift as the octadecyl bonding is carried out using alkene or alkyne hydrocarbons forming a direct Si-C bond. This suggests a different method of bonding for the TYPE-C™ Diamond Hydride silica material, the presence of a silane type environment indicates a typical monofunctional silane bonding as shown in Section 1.5.

The TYPE-C™ Diamond Hydride silica material was analysed by solid state ^{13}C NMR spectroscopy, only a single carbon environment was observed at 0.3 ppm which is a typical delta shift for trimethyl silane (TMS). This is shown below in Figure 6.13.

Figure 6.13 Solid State ^{13}C NMR Spectra of TYPE-C™ Diamond Hydride Silica Material

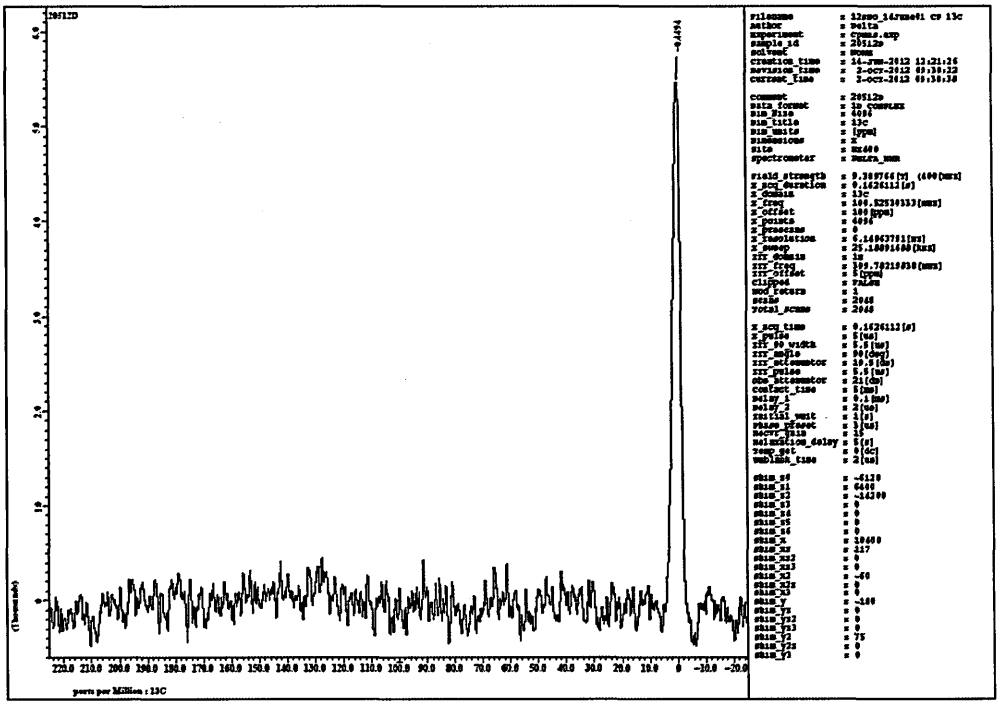

The NMR spectroscopy results suggest that the hydrophobic interactions observed for the TYPE-C™ Diamond Hydride phase may come from a light coverage of monofunctionally bonded trimethylsilane. No evidence of the bidentate silica hydride monolayer is observed from this data.

6.3 *In-vitro stability of TYPE-C™ Diamond Hydride and C1 Bonded Silica*

The results from the characterisation probes seen in Section 6.1 raised some questions about the stability of the TYPE-C™ Diamond Hydride phase as the uridine probe showed an unexplained change in retention time across different sets of analysis. The NMR results from the previous section indicate that the phase is likely to be a monofunctionally bonded trimethyl silane. Literature has shown that many short alkyl chain phases are susceptible to hydrolysis[118][119][259][260] resulting in ligand cleavage. Although the HILIC analysis shown here has been carried out using buffered ammonium acetate the high composition of acetonitrile in the mobile phase may elevate the pH above pH 7. There is a possibility that the TMS is being cleaved through high pH hydrolysis due to the excess of ^{-}OH ions in the mobile phased. This would expose further residual silanols, consequently enhancing the density of the aqueous salvation layer around the silica increasing the retention of analytes through partition interactions. In addition the greater number of available silanols on the phase would cause the analytes to be retained for longer through electrostatic cationic interactions.

To investigate this further some of the recovered silica material from the unpacked TYPE-C™ Diamond Hydride phase was subjected to in-vitro stability testing. An experimental TYPE-B silica with a monofunctionally bonded C1 silane was used as a comparison for this analysis work. The silica material was an ultra-pure TYPE-B silica material with a monofunctionally bonded trimethyl silane as shown in Table 6.4 below.

Table 6.4 Manufacturer's data of silica materials for comparison

Phase	Particle Size (µm)	Bonded Ligand	Pore size (Å)	Surface coverage (m^2/g)	Endcapping	Carbon Load (%)
Cogent TYPE-C™ Diamond Hydride	4	TMS	100	350	N/A	<2.0
Experimental C1	3	TMS	100	300	-	3.0

Both silica materials were subjected to high temperature stability testing using a high concentration of unbuffered ammonium acetate in a number of mobile compositions with different concentrations of acetonitrile. A variety of mobile phase compositions were carried out due to the wettability of the silica material to ensure the surface of the silica was fully submerged. The mobile phase was then evaporated down and the residue extracted into deuterated chloroform before being analysed by ^{13}C NMR spectroscopy.

Due to the excess of acetonitrile in the sample it was not possible to identify any carbon environments around 0 ppm in order to confirm the presence of trimethyl silanes cleaved from the surface of the silica materials. However this does not verify the stability of phase in HILIC conditions. The volatile nature of the TMS means it is possible that the silanes underwent hydrolysis cleavage during the stability analysis but did not form a stable molecule that could be extracted into the chloroform. The low coverage of the TYPE-C^{TM} Diamond Hydride and experimental C1 material may have resulted in a very low concentration of trimethyl silane being cleaved from the silica material. This low concentration may not have been detected in the ^{13}C NMR spectra due to the high concentration of acetonitrile masking the delta shift. Table 1.1 in the introduction showed the relative strength of an electrostatic interaction through ion exchange can be five time higher than hydrophobic and partition exchange mechanism. Consequently only a small amount of the TMS phase would need to be cleaved to give a large increase in electrostatic retention through silanophilic interactions. In order to investigate these deductions further stability analysis could be carried out in a sealed container and analysed using headspace GC-MS to determine the presence of TMS[272] without the interference from residual acetonitrile.

6.4 *HILIC mode van Deemter Characterisation of TYPE-C™ Diamond Hydride and Silica-C Phases*

The reversed phase van Deemter analysis of the TYPE-C™ Bidentate C18 phase shown in Section 5.2.3 gave an insight into the possible sub-optimum packing and irregular particles present in the phase. Although the column efficiencies of the TYPE-C™ Diamond Hydride and Silica-C phases are shown to be comparable with the ACE 3 SIL phase this analysis will determine the dispersion contributions that will affect the dispersion of analytes on the phase based on the van Deemter equation:

$$H = \lambda d_p + 2\gamma \frac{D_m}{\mu} + c \frac{d_p^{\,2}}{D_m} \mu \qquad \text{(I)}$$

The Eddy (A), Longitudinal (B) and Mass Transfer (C) terms can be determined using Microsoft Solver as before. As the TYPE-C™ Diamond Hydride and Silica-C phases have low hydrophobic interactions it is not possible to carry out the van Deemter in the same way. Ketoprofen was analysed as a characterisation probe in HILIC mode on the phases but was found to have a retention factor of around 3 which is not high enough to accurate determine the B Term in the van Deemter equation. Salbutamol was chosen as a characterisation probe as the accessible hydroxyl and amine groups give a longer retention time on the silica phases. The HILIC parameters were kept the same as the previous analysis and only the flow rate changed to calculate the height equivalent to a theoretical peak (HETP) of the column against the velocity of the analyte.

As with the TYPE-C™ Bidentate C18 analysis the particle size of the phases will affect the calculation of HETP. The ACE 3 SIL is stated to be a 3 µm particle size where as the two TYPE-C™ phases are 4 µm. Therefore a reduced plate height plot was determined using the experimental data and is shown in Figure 6.14 overleaf.

Figure 6.14 ***Reduced Plate Height HILIC Mode van Deemter Pot for TYPE-C^{TM} Diamond Hydride and Silica-C versus ACE 3 SIL phases***

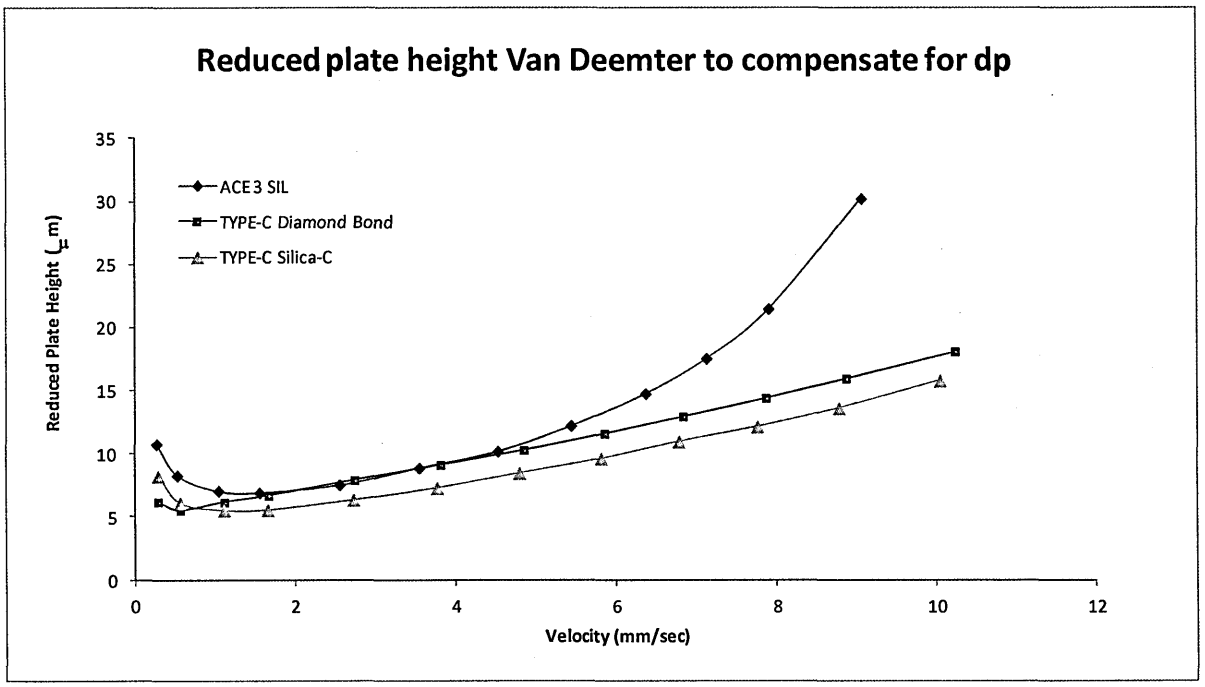

The HILIC characterisation shown previous was run at 0.105 mL/min which is around the optimum flow rate for the two TYPE-C^{TM} phases, although it is slightly lower than the optimum velocity for the ACE 3 SIL the phases show a reasonable comparable HETP at this flow rate. The ACE 3 SIL shows a more gradual decrease in HETP at low velocity than the TYPE-C^{TM} phases indicating a greater contribution from the B term due to the natural dispersion of the salbutamol solute. This phase also shows a sharper rise at high velocity than the TYPE-C^{TM} phases which suggests the mass transfer coefficient, the C term, has a greater effect at high flow rates. This may be due to the higher contribution from partition interactions in the retention mechanism of the ACE 3 C18 phase. As the velocity is increased the analyte has less time to partition between the acetonitrile bulk of the mobile phase and the aqueous solvated layer around the surface of the silica. This suggests that the ACE 3 SIL phase has a greater contribution from partitioning and a lower degree of electrostatic interactions in the retention mechanism as shown in the Ikigami/Tanaka characterisation seen in Section 6.1.1.

The two TYPE-C™ phases show very similar plots, the Diamond Hydride is seen to have a slightly higher efficiency at the lowest velocity but the Silica-C shows a higher efficiency above the optimum velocity. As this analysis is only done on a single column of each type this small difference may be due to small variations in packing.

Microsoft Solver was used to calculate numerical values for the A, B and C terms, shown in Table 6.5 below, for the three phases using the following equation:

$$H = A\mu^{1/3} + \frac{B}{\mu} + [C_s + C_m].\mu$$

Table 6.5 ***Calculated HILIC Mode van Deemter Terms Values – Comparison of TYPE-C™ Diamond Hydride and Silica-C versus ACE 3 SIL phases***

	A	B	C
ACE 3 SIL (3µm)	1.73	3.28	2.13
TYPE-C™ Diamond Hydride (4µm)	3.35	1.10	0.99
TYPE-C™ Silica-C (4µm)	1.94	1.93	1.06

As indicated visually by the plot the ACE 3 SIL phase shows the largest contribution from the B Term which is due to the natural dispersion of the salbutamol. The TYPE-C™ Diamond Hydride on the other hand shows the largest contribution to be from the A Term which is due to packing inefficiencies. The degree of the A Term is approximately three times the B and C Terms calculated however all the terms are low for the three phases. The TYPE-C™ Silica-C shows the A and B Term to be comparable and higher than the C Term.

6.5 Conclusion of Physical Properties of TYPE-C™ Diamond Hydride and Silica-C Phases

The characterisation probes indicated the presence of residual silanols on both the TYPE-C™ Diamond Hydride and Silica-C phases; this was confirmed by Solid State ^{29}Si NMR on the unpacked silica material from these columns. In HILIC mode the two TYPE-C™ phases showed similar retention mechanisms to the TYPE-B bare silica phases as the degree of electrostatic interactions from the accessible silanols overpowers any contributions from partitioning and adsorption.

The calculated column efficiencies and HETP for the TYPE-C™ phases are equivalent to the ACE 3 SIL. The van Deemter calculation shows the TYPE-C™ Diamond Hydride and Silica-C phases relatively low A and C terms compared to the TYPE-C™ Bidentate C18 results shown in Section 5.2.3. This indicates the TYPE-C™ Diamond Hydride and Silica-C phases do not have the same packing inefficiencies due to irregular particles as the TYPE-C™ Bidentate C18 phase. It is likely that the TYPE-C™ Silica-C phase is prepared by the two-step chlorination and reduction reaction as shown on page 39 rather than the formation of the silica hydride monolayer formed through the cross-linking triethoxy silane as shown on page 42.

The characterisation and van Deemter results indicate that the TYPE-C™ Diamond Hydride and TYPE-C™ Silica-C phases are produced through a similar process. The presence of a bonded silane on the TYPE-C™ Diamond Hydride phase, shown by Solid State ^{29}Si NMR, suggests the likelihood of a mono-functional bonding using a TMS ligand substituted with a good leaving group such as chloro-, amino- or ethoxyl-trimethyl silane. The trimethyl silane may react preferentially with the residual silanols on the surface of the phase over the reduced silica hydrides. However as only a light coverage is used there are still a number of accessible silanols on the surface of the phase.

Further investigation into the production of a bare silica hydride phase would be an interesting academic piece of research; however the practical application for these silica materials would be limited. The literature shows poor coverage through the two-step chlorination and reduction reaction, between 5-30% depending on the type of silica use[192][203]. Although it is possible that this process could be improved it has been shown to be highly moisture sensitive and can be a complex reaction. It has been shown that HILIC and ANP mode retention occurs between a mixture of partitioning, adsorption and electrostatic interactions, the formation of a full coverage silica-hydride phase would not be suitable for this type of HPLC analysis. Silica-hydride would not encourage the formation of the aqueous solvated layer required to give rise to partitioning and would not readily ionise to undergo electrostatic interactions. It is possible that the phase may exhibit some adsorption retention mechanism however this would rely on hydrogen exchange interactions which have been shown to be weak. As the phase would not exhibit any hydrophobic, π-π, or dipole-dipole interactions the phase would not be suitable for reversed phase HPLC either.

The main reason to investigate the formation of a silica hydride particle would to be use it as a base silica material for bonding different functional silanes for HPLC retention without secondary interactions with residual silanols. It has been shown that cross-linking the triethoxy silane monomer to form the silica hydride polymeric layer yields a higher coverage and masks the majority of residual silanols. Therefore the following investigation will be based on this route rather than the more complex and labour intensive two-step chlorination and reduction process.

7. *Synthesis of Silica Hydride Monolayer Particles*

From the results in Chapter 5 it was seen that the retention mechanism of the TYPE-C™ Bidentate phase exhibits a large contribution from electrostatic interactions. This has been shown to be due to the hydroxyl ends of the cross-linked triethoxysilane (TES) monomers bonded to the surface of the silica and from the presence of unbound amorphous polyhydrosiloxane (PHS) particles packed in with the silica bed. Research had shown that increasing the concentration of TES during the initial "silanization" step increases the likelihood of the amorphous PHS particles forming[185]. The formation of these particles indicates that the processes are difficult to control especially once the method is scaled up to a commercial level; this Chapter will focus on modelling and understanding the critical parameters of the "silanization" process and the boundaries for the reaction model.

7.1 *Small Scale Process Control Modelling*

The "silanization" and bonding process for the commercial TYPE-C™ Bidentate phase is proprietary information however there is available research into a polymeric "silanization" reaction using triethoxysilane which will be used for comparison purposes. The reaction uses hydrochloric acid as a catalyst as opposed to common chlorosilane bonding reactions which use a basic catalyst. The reaction scheme, shown in Figure 7.1 below, yields a neutral by-product which might account for the choice in catalyst[191][192].

Figure 7.1 ***Schematic for the formation of a TES monolayer***

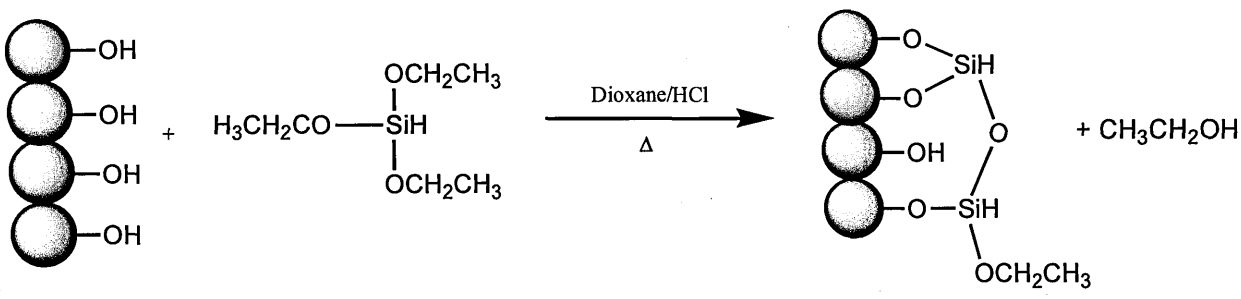

Therefore the type and molarity of the catalyst will be investigated to monitor how this affects the reaction outcome. The research has shown that dioxane is the optimum solvent due to its eluotropic value and polarity[189-191] therefore this will be kept constant throughout the process control modelling. Triethoxy silane is highly reactive so the moisture content is controlled using anhydrous dioxane and carrying out the reaction under argon. However the literature shows that an unknown volume of water is added to the reaction through the use of an aqueous hydrochloric acid catalyst. This uncontrolled addition of water may leave the reaction open to error; therefore the percentage of water will also be investigated. Lastly the amount of triethoxy silane will be investigated as it has already been seen this may result in laddering and the formation of unbound particles[185]. The reaction protocol was carried out as outlined in Table 7.1 below:

Table 7.1 Results from TES "silanization" sample preparation

Silica (g)	TES Silane (M)	Water	Catalyst		Product	
		Volume (mL)	Type	Molarity (M)	Recovered (g)	Yield (%)
0.958	0.5	-	HCl	4M	0.991	56.3
1.057	0.5	0.01	HCl	4M	1.101	59.3
1.044	0.5	0.05	HCl	4M	1.085	58.8
1.014	0.5	0.10	HCl	4M	1.116	61.5
0.969	0.5	0.05	HCl	8M	1.002	56.6
1.014	0.5	0.05	TFA	4.33M	1.047	57.7
1.050	0.5	0.05	Imidazole	4M	1.136	61.4
0.971	1.0	0.05	HCl	4M	1.003	56.6
1.053	2.5	0.05	HCl	4M	1.062	57.3
-	5.0	0.05	HCl	4M	-	-

After washing, the silica materials were left to dry over night at 60°C to remove any residual solvent prior to analysis. It was noted that the 4 M imidazole catalyst product had different physical properties and appeared to have more flow in the drying vessel than the other silica materials. This may be due to the triethoxy silane bonding to the surface of the silica in a different way so that the resultant particles repelled each other. It also may be due to solvent molecules binding to the silica-hydride surface and not evaporating off during the drying period.

As the amount of triethoxy silane was increased the product became more difficult to wash as the silica particles stuck together and had to be gently agitated in the washings to get them to separate. This is likely due to the cross-linking and laddering effect of the excess of triethoxy silane monomer binding to more than one silica particle. Conversely the triethoxy silane reaction without the presence of silica gave a very low yield that was difficult to recover. Initially a lower concentration of triethoxy silane was used but the resultant particles were so fine they were not recovered in the filtering process. Therefore a 10 fold increase in the concentration of triethoxy silane was required and filtered through 0.45 μm filter paper. As the resultant product was so difficult to recover from the filter paper an accurate yield could not be recorded prior to analysis.

7.1.1 NMR and SEM Analysis of Small Scale Process Modelling

The bonded silica were analysed by Solid State ^{29}Si NMR spectroscopy for the presence of silica hydride, either in the fully crosslinked form, SiH_2, which has a delta shift of -80 to -85 ppm or the practically crosslinked with a hydroxyl substituent, SiH_1, which is observed at -70 to -73 ppm[185][296]. The silanol environment, Q_3, shows a delta shift of -100 to -102 ppm[292-295]. The spectra of the bare silica and the structure of the silica environments can be seen in Section 5.2.1. SEM imagery was also carried out on the silica materials to determine the presence of any PHS particles present in the products. The SEM of the bare silica can be seen in Section 5.2.4. The results for each process are shown in Figure 7.2 to 7.11 below:

Figure 7.2 (a) ^{29}Si NMR Spectra and (b) SEM Image: No Water : 4 M HCl : 0.5 M TES

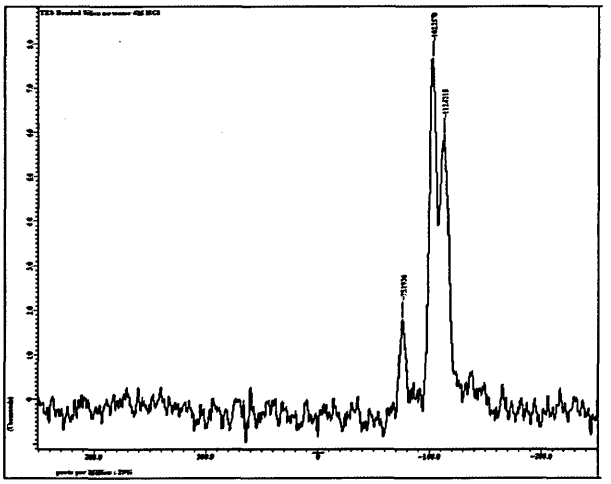

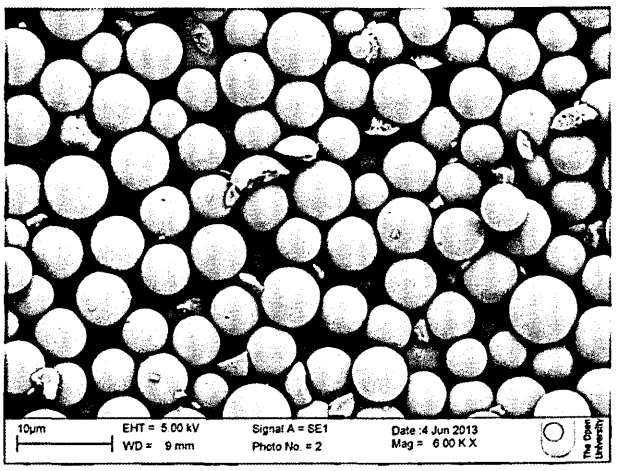

***Figure 7.3 (a) ^{29}Si NMR Spectra and (b) SEM Image:* 1% Water : 4 M HCl : 0.5 M TES**

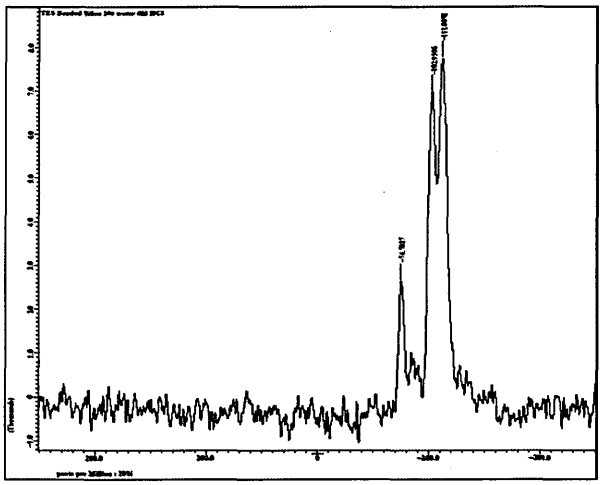

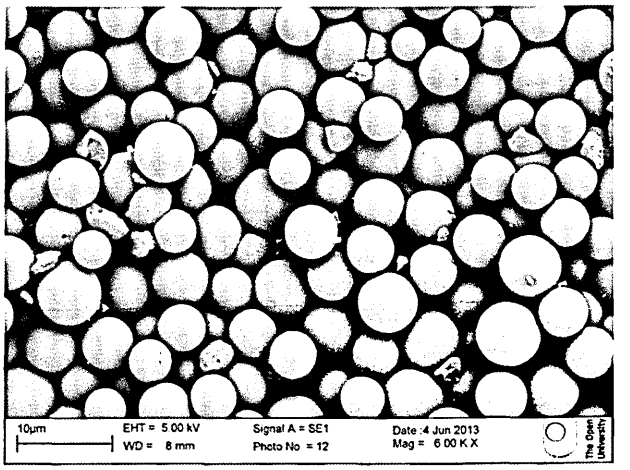

Figure 7.4 *(a) ^{29}Si NMR Spectra and (b) SEM Image:* **5% Water : 4 M HCl : 0.5 M TES**

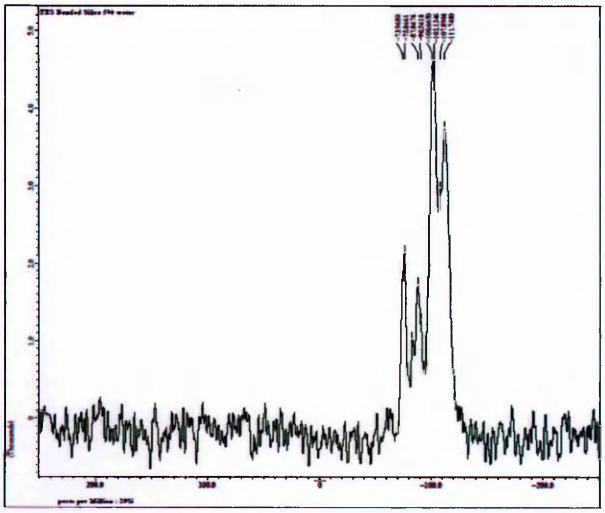

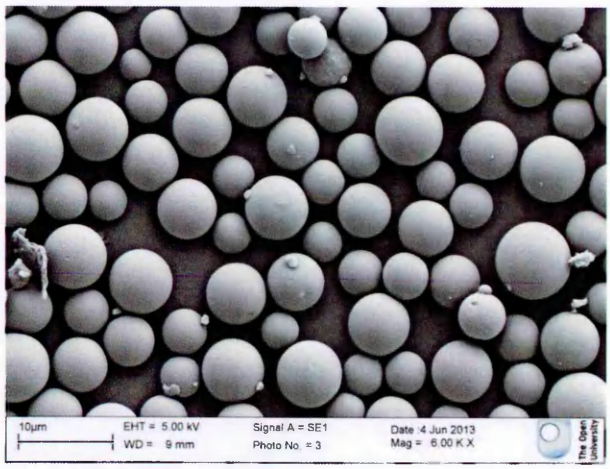

Figure 7.5 *(a) ^{29}Si NMR Spectra and (b) SEM Image: 10% Water : 4M HCl : 0.5M TES*

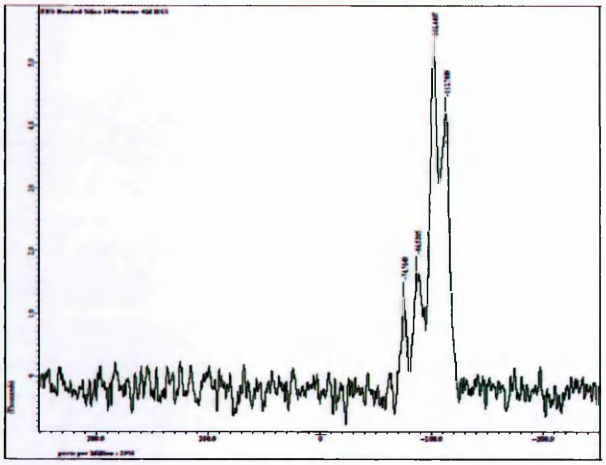

Figure 7.6 *(a) ^{29}Si NMR Spectra and (b) SEM Image:* **5% Water: 4M Imidazole : 0.5M TES**

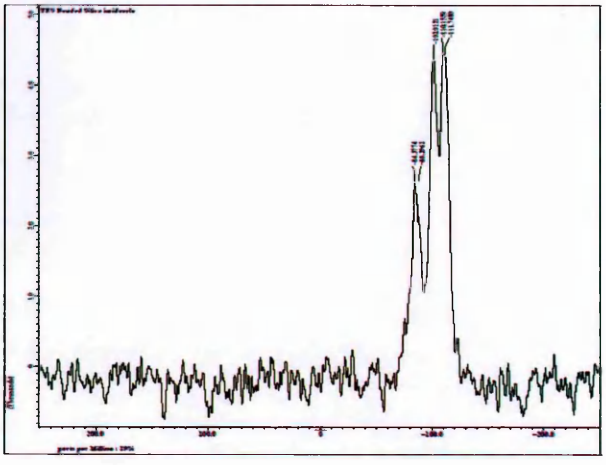

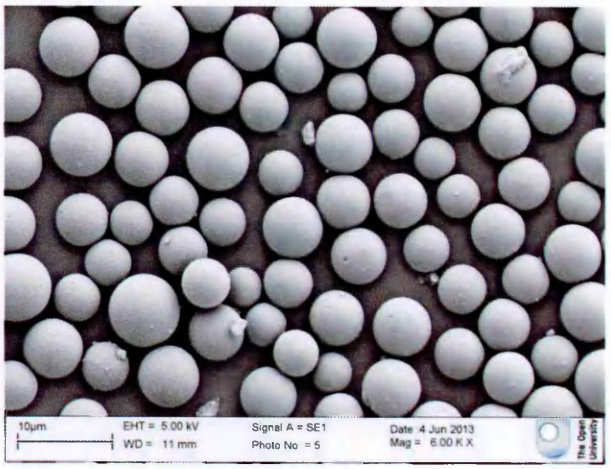

Figure 7.7 (a) ^{29}Si NMR Spectra and (b) SEM Image: 5% Water: 4M TFA : 0.5M TES

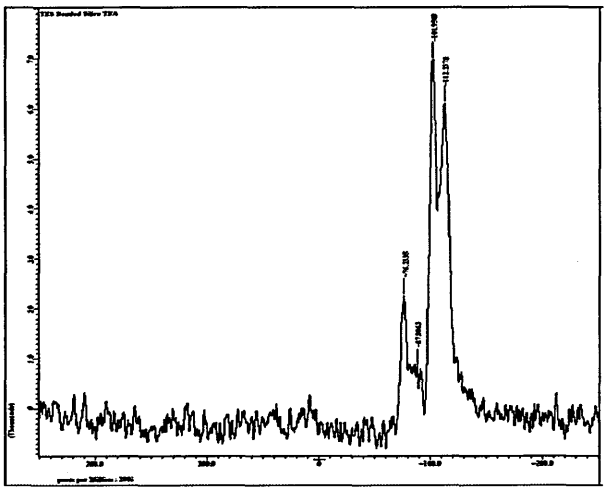

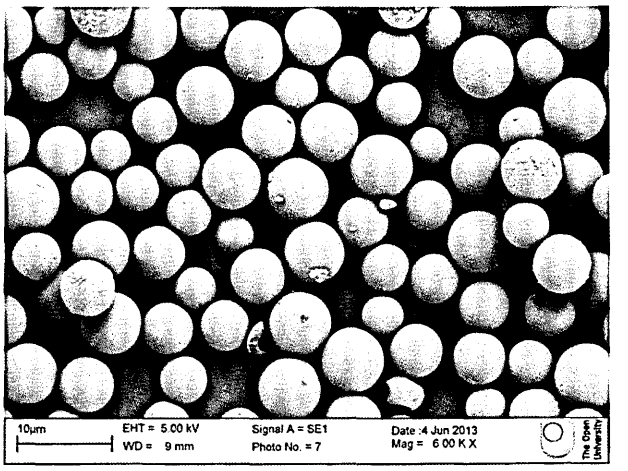

Figure 7.8 (a) ^{29}Si NMR Spectra and (b) SEM Image: 5% Water : 8 M HCl : 0.5 M TES

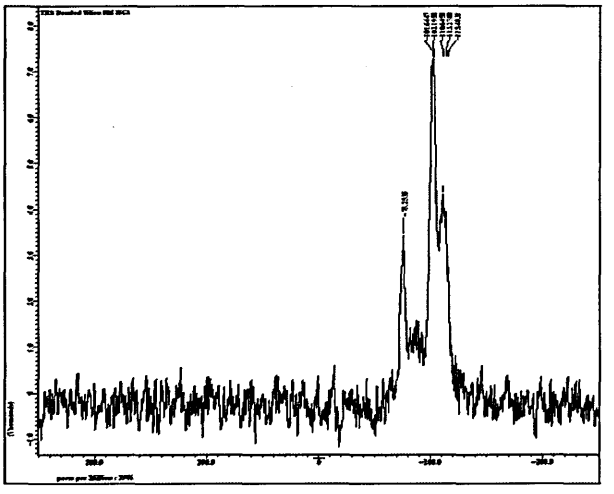

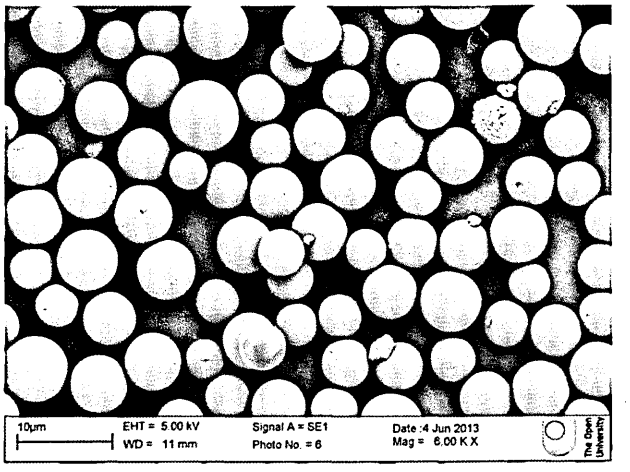

Figure 7.9 (a) ^{29}Si NMR Spectra and (b) SEM Image: 5% Water : 4 M HCl : 1.0 M TES

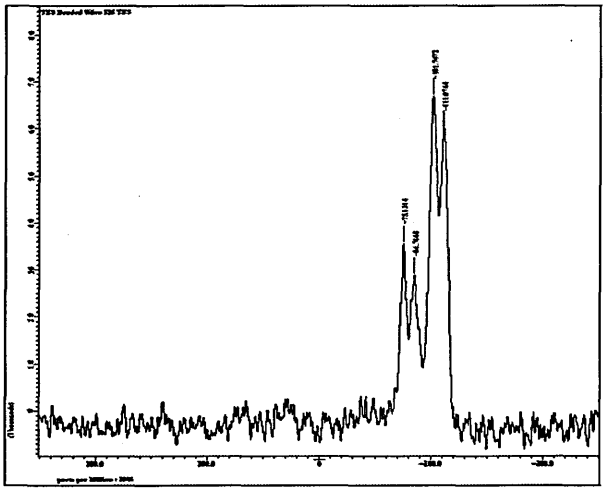

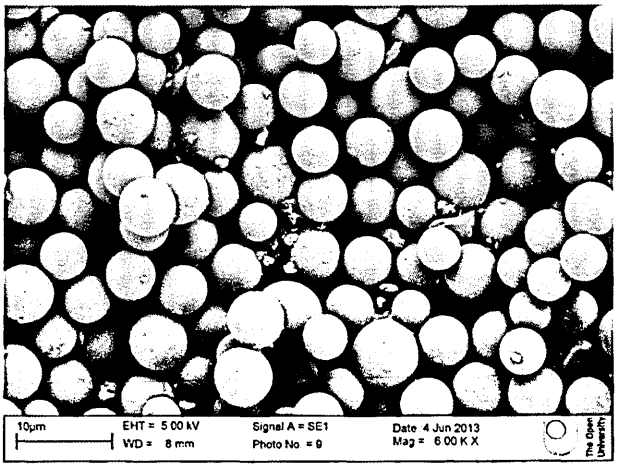

Figure 7.10 *(a) ^{29}Si NMR Spectra and (b) SEM Image:* **5% Water: 4M HCl : 2.5M TES**

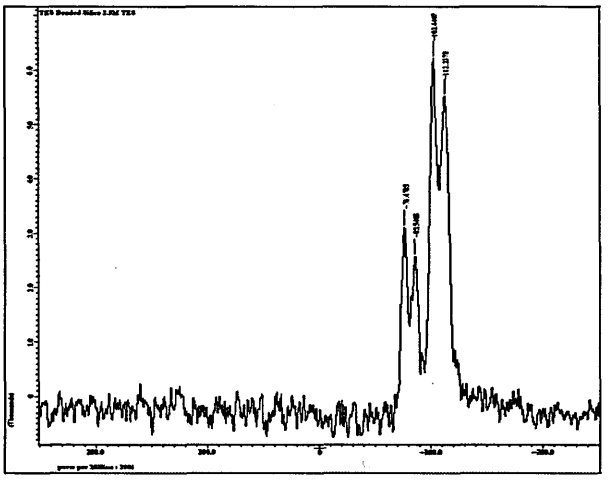

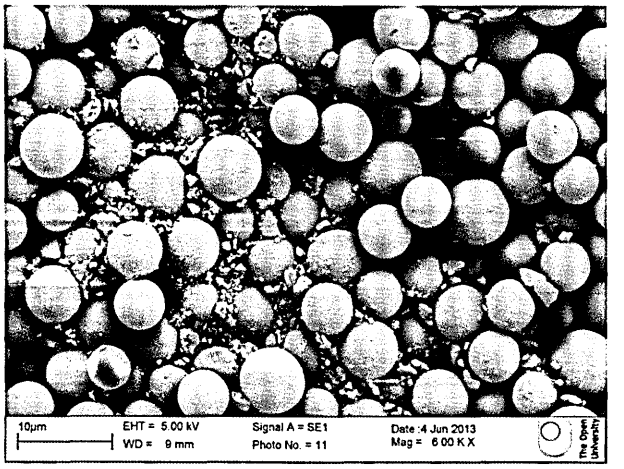

Figure 7.11 *(a) ^{29}Si NMR Spectra and (b) SEM Image:*5% Water : 4M HCl : 5M TES (No Silica)

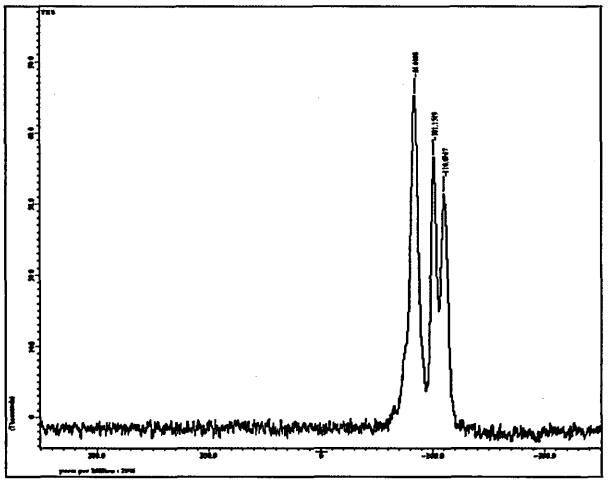

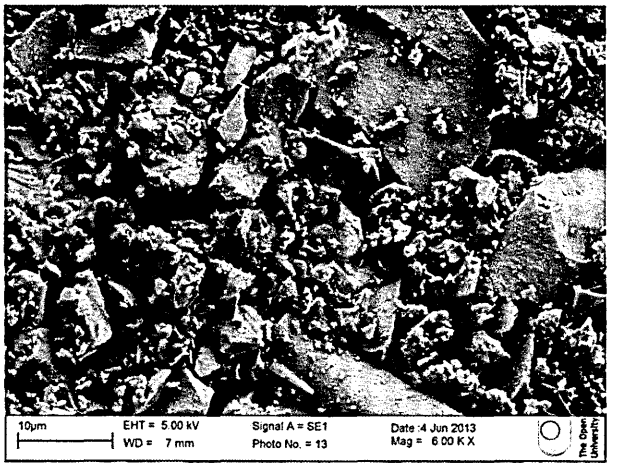

Assessment of the results shows some interesting trends; increasing the concentration of water actually appears to decrease the number of PHS particles. It was originally thought that in completely anhydrous conditions the TES monomers would not crosslink or bind to each other as no water is present to initiate the hydrolysis reaction and the anhydrous HCl cannot dissociate. However it would appear that this is not the case, it is most likely that the anhydrous dioxane becomes protonated allowing the HCl to dissociate and protonate the ethoxyl groups on the TES monomer in the solvent. This would allow the TES to cross-link in solution prior to binding to the silica particle. In the 1%, 5%, and 10% water reactions the water is added to the reaction vessel prior

to the TES monomer and will likely to be attracted to the porous surface of the silica. As the TES solution is added the ethoxyl groups will be protonated at the surface of the silica making it more likely that they will bind to the particle and then crosslink to form the polymeric coverage. This can also be seen in the relative abundance of the SiH_1 and SiH_2 environments, shown in Figure 7.2 to 7.5, as the water content increases the SiH_1 shift reduces and the SiH_2 increases as the coverage on the particles becomes more polymeric in nature.

The comparison for type and concentration of catalyst shows the 4 M HCl reaction to have the highest concentration of PHS particles, however this SEM is taken from a very small volume of the particles and overall all four products would seem to be comparable. The imidazole catalyst appears to show an abundance of SiH_2 environments and only a very small shoulder of the SiH_1 environments. This may be because the charged amine counter-ion becomes associated with the deprotonated silanol on the surface of the silica through hydrogen bonding. Therefore all of the TES monomers are laid down onto the silica surface in the same orientation. This allows a more controlled addition of the TES monomers allowing the formation of a single monolayer and reducing crosslinking. Research has shown the use of polyamines yields a more controlled precipitation of silica particles during the formation of diatoms[323] therefore it is likely that the reaction works the other way round, as shown in Figure 7.12 below.

Figure 7.12 ***Schematic of amine controlled polymerisation of silica base***

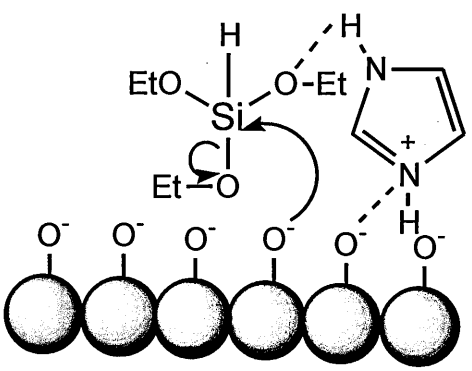

The TFA catalyst reaction also shows a low concentration of PHS particles in the SEM however the NMR spectra shows only a low abundance of SiH_1 and SiH_2 environments relative to the Q_3 environment, suggesting the reaction has a low coverage. It was found in the low concentration of TES reaction without silica present that the resultant PHS particles were hard to recover so it may be that these small particles were removed during the washing process.

As expected the increase of TES concentration showed a marked increase in the number and size of the PHS particles. The excess of TES will crosslink in solution and form these irregular particles, once seeded the TES monomers will continue to bind to the protonated ethoxyl substituents within the particles. The NMR shows the intensity of SiH_1 and SiH_2 environments increases but this is likely due to the presence of PHS particles. The NMR of the unbound PHS itself shows some Q_3 and Q_4 environments as well as the SiH_2, this is due to the tetrahedral silica complexes formed by the crosslinked TES monomers. As these particles form in solution they can freely orientate into the highly stable tetrahedral silica oxide structure.

These results show that analysis by silica environments on the NMR may not give the full picture of the nature of the silica surface as the PHS material gives rise to Q_3 and Q_4 environments. Therefore these phases need to be assessed chromatographically to understand the level of accessible silanols available on the phase. It is not possible to test all phases therefore the optimal process was determined using these results and scaled up to a 5 gram scale.

7.1.2 Conclusion of Small Scale Process Modelling

Overall it has been shown that a small amount of water is required to protonate the ethoxyl substituents at the surface of the silica, therefore a controlled addition of 5% was seen to be the optimum. The concentration of TES monomer also needs to be strictly controlled to minimise the formation of PHS particles but still ensure full coverage of the silica particle, 0.5 M was chosen as the optimum level. For the catalyst, both the 8 M hydrochloric acid and 4 M imidazole products showed low levels of PHS particles and a reasonable coverage of silica hydride. Interestingly the imidazole products appears to show a majority of SiH_2 environments and the hydrochloric acid shows mostly SiH_1 environments. These two processes where chosen for scale up to a 5 gram reaction in order to pack a 50 x 2.1 mm column for characterisation and van Deemter testing.

As the small scale processes showed the presence of irregular particles the scaled up silica materials were washed over a 3 μm filter paper to remove any PHS that may have formed during the reaction. As the silica particles were calibrated to 5 μm in diameter they could easily be recovered however this process resulted in a low yield and would not be suitable for large scale manufacturing. Both the batches were dried at 80°C overnight prior to being slurried in the appropriate solvent and packed into stainless steel 50 x 2.1 mm columns. Both columns were packed in the same way using the same batch of solvent making them suitable for comparison.

7.2 *Evaluation of Silica Hydride Particles*

The scale up process was completed in the same way and the silica materials packed into stainless steel HPLC column housing. The silica materials will be compared against the commercial TYPE-C™ Silica-C phase, as they do not have comparable hydrophobicity to the TYPE-C™ Bidentate phase. It is likely that the TYPE-C™ Silica-C phase is prepared using the two-step chlorination and reduction process discussed in Section 1.7 and therefore may have different packing and efficiency properties. This will be determined by van Deemter analysis shown in Section 7.2.4.

No information for pH and temperature range is known on the Silica Hydride materials however a summary of the physical properties of the base silica compared to the commercial TYPE-C™ Silica-C phase are shown in Table 7.2 below.

Table 7.2 ***Specification for the Silica Hydride and TYPE-C ™ Silica-C phases for characterisation***

Phase	Particle size (µm)	Pore size (Å)	Surface coverage (m^2/g)	Pore volume (mL/g)	Column Dimension (mm)
Silica Hydride #1 8 M Hydrochloric acid[a]	5	100	400	1.0	50 x 2.1
Silica Hydride #2 4 M Imidazole	5	100	400	1.0	50 x 2.1
Cogent TYPE- C ™ Silica-C	4	100	350	0.92	50 x 2.1

[a] Information based on the unbonded silica prior to "silanization" process

7.2.1 *Spectroscopic Evaluation of Silica Hydride Particles*

The loose silica hydride materials were analysed by Solid State ^{29}Si NMR spectroscopy for the presence of silica hydride coverage as before. The spectra confirms the presence of both Q_3 and Q_4 environments in the silica hydride materials, with chemical shift of -100 to -102 ppm and -110 to -112ppm respectively. The Silica Hydride #1 Hydrochloric Acid material shows the presence of both SiH_1 and SiH_2 environments as seen previously in the small scale process, with chemical shift of -70 to -73 and -85 to -88 respectively. These results are shown in Figure 7.13 below.

Figure 7.13 **Solid State ^{29}Si NMR spectroscopy (a) 8 M Hydrochloric, (b) 4 M Imidazole**

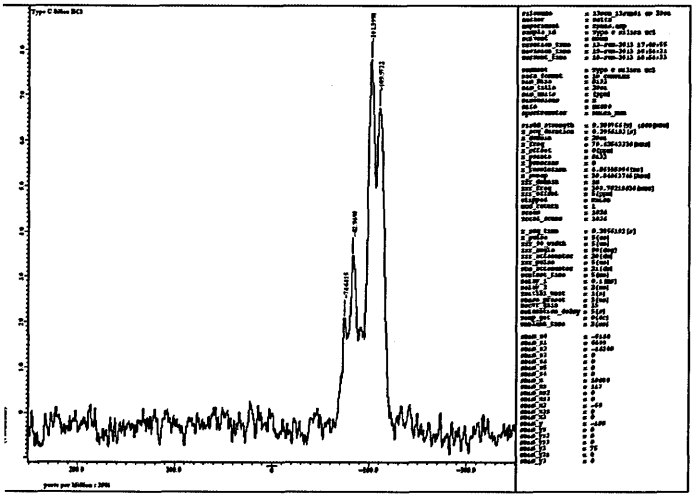

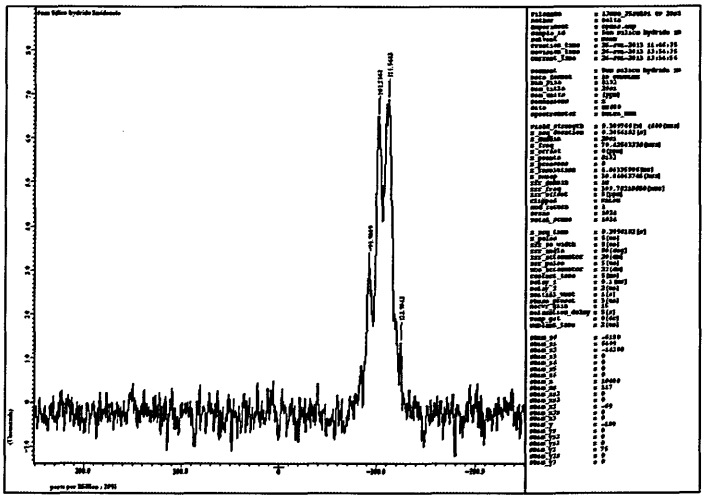

However the Silica Hydride #2 Imidazole material shows a chemical shift at -92 ppm which is slightly different from the small scale results which showed a peak around -88 ppm. It is possible that the chemical shift observed at -92ppm is due to a Q_2 environment, which has not previously been observed with this silica. However, that would mean there are no silica hydride environments on the surface of the phase. The column characterisation carried out in Section 7.2.2 indicates a similar coverage of silica hydride in both prepared silicas therefore it is more likely that the chemical shift for the SiH_2 environment has moved upfield.

7.2.2 *Ikigami/Tanaka HILIC Characterisation of Silica Hydride Particles*

The two phases were analysed using the Ikigami/Tanaka HILIC characterisation probes, the TYPE-C™ Silica-C column was also analysed at the same time as a control column and the results found comparable to those shown previously in Section 6.1.2. The numerical results are shown in Table 7.3 below.

Table 7.3 ***Tanaka characterisation values – comparison of TYPE-C™ Silica-C and Prepared Silica Hydride Columns***

	k_U	$\alpha_{(pH)}$	$\alpha_{(CH_2)}$	$\alpha_{(OH)}$	$\alpha_{(V/A)}$	$\alpha_{(2dG/3dG)}$	$\alpha_{(\alpha/\beta)}$	$\alpha_{(AX)}$	$\alpha_{(CX)}$
TYPE-C™ Silica-C	0.85	1.23	0.98	1.13	1.00	1.11	1.27	-0.03	32.17
Silica Hydride #1 8 M HCL	0.69	1.15	1.13	1.12	0.97	1.10	0.98	0.12	14.69
Silica Hydride #2 4 M Imidazole	0.62	1.00	1.12	1.14	0.99	1.10	0.92	0.11	13.56

U = uridine, pH = 5-methyluridine, CH_2 = 2-deoxyuridine, A = adenosine, V = vidarabine, 2dG = 2-deoxyganosine, 3dG 3-deoxyganosine, α = 4-nitrophenyl-α-D-glucopyranoside, β = 4-nitrophenyl-β-D-glucopyranoside, AX = sodium p-toluenesulfonate, CX = N,N,N-trimethyl-phenylammonium,

Overall the results for the two Silica Hydride phases are shown to be fairly comparable to the TYPE-C™ Silica-C phase with the exception of the cation exchange value. The lower $\alpha_{(CX)}$ observed for the two Silica Hydride materials indicates there are fewer residual silanols accessible on the surface of the phase, this suggests there is a greater coverage of silica hydride. The lower concentration of silanols will reduce the formation of the aqueous layer around the surface of the silica decreasing the contribution from partitioning retention; this can be seen in the lower retention factor for uridine. The Solid State ^{29}Si NMR spectra for the Silica Hydride #1 (prepared using 4 M hydrochloric acid) showed the presence on SiH_1 environments, where the silica hydride has a hydroxyl group attached to it. Chromatographically this does not appear to show any different characteristics to the Silica Hydride #2 (prepared using imidazole) which does not show any SiH_1 environments and the silanophilic interaction comes from the Q_3 environment, likely to be residual silanols or hydroxyl substituents on the silica hydride monolayer.

There are no identifiable trends in the Silica Hydride material characterisation other than the cation exchange, the analytes show very little retention and the pairs of probes co-elute. These phases are shown to have a large contribution from cation exchange and only a small amount of partition and adsorption interactions making them unsuitable for HILIC retention. Some small variation is seen in the α values however these are outweighed by the $\alpha_{(Cx)}$ values, Figure 7.14 below shows the plot of the α values excluding $\alpha_{(Cx)}$.

Figure 7.14 ***Plot of Tanaka characterisation values excluding cationic exchange– comparison of TYPE-C™ Silica-C and Prepared Silica Hydride Columns***

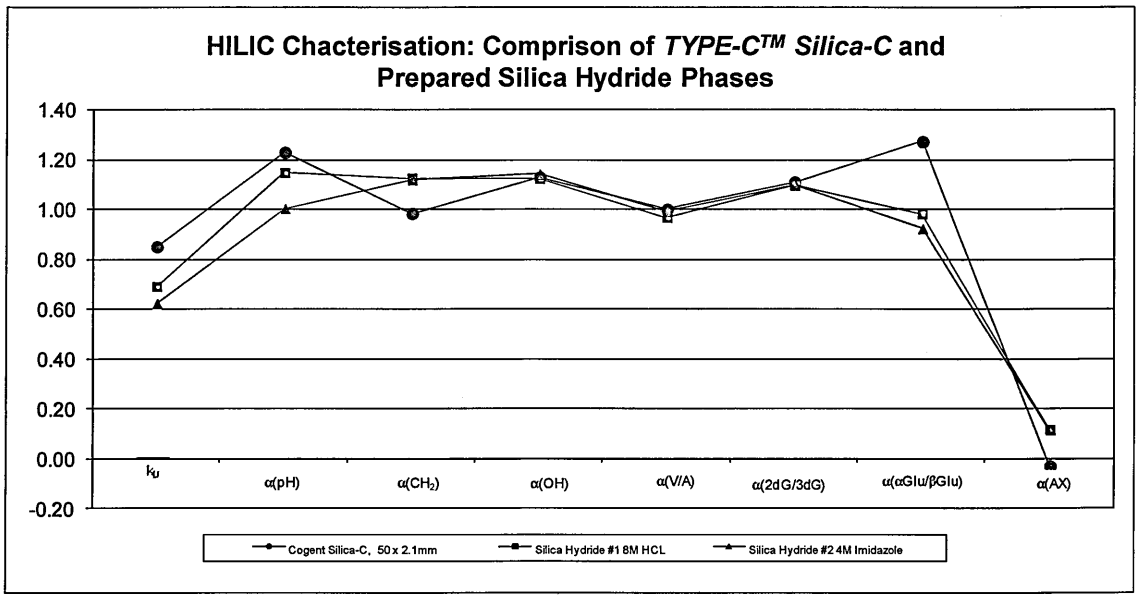

U = uridine, pH = 5-methyluridine, CH_2 = 2-deoxyuridine, A = adenosine, V = vidarabine, 2dG = 2-deoxyganosine, 3dG 3-deoxyganosine, α = 4-nitrophenyl-α-D-glucopyranoside, β = 4-nitrophenyl-β-D-glucopyranoside, AX = sodium p-toluenesulfonate, CX = N,N,N-trimethyl-phenylammonium,

7.2.3 *PCA of Silica Hydride Particles*

The Ikigami/Tanaka results shown in the previous section indicated that the Silica Hydride materials have a lower coverage of accessible silanols than the TYPE-C™ Silica-C phase although they showed very little retention for HILIC probes. Section 6.1.2 showed how HILIC columns can be grouped together based on the $\alpha_{(pH)}$ and $\alpha_{(OH)}$ values, the plot is shown below in Figure 7.15.

Figure 7.15 ***Simplified PCA of Silica Hydride phases against literature HILIC results using Ikegami/Tanaka Characterisation data***

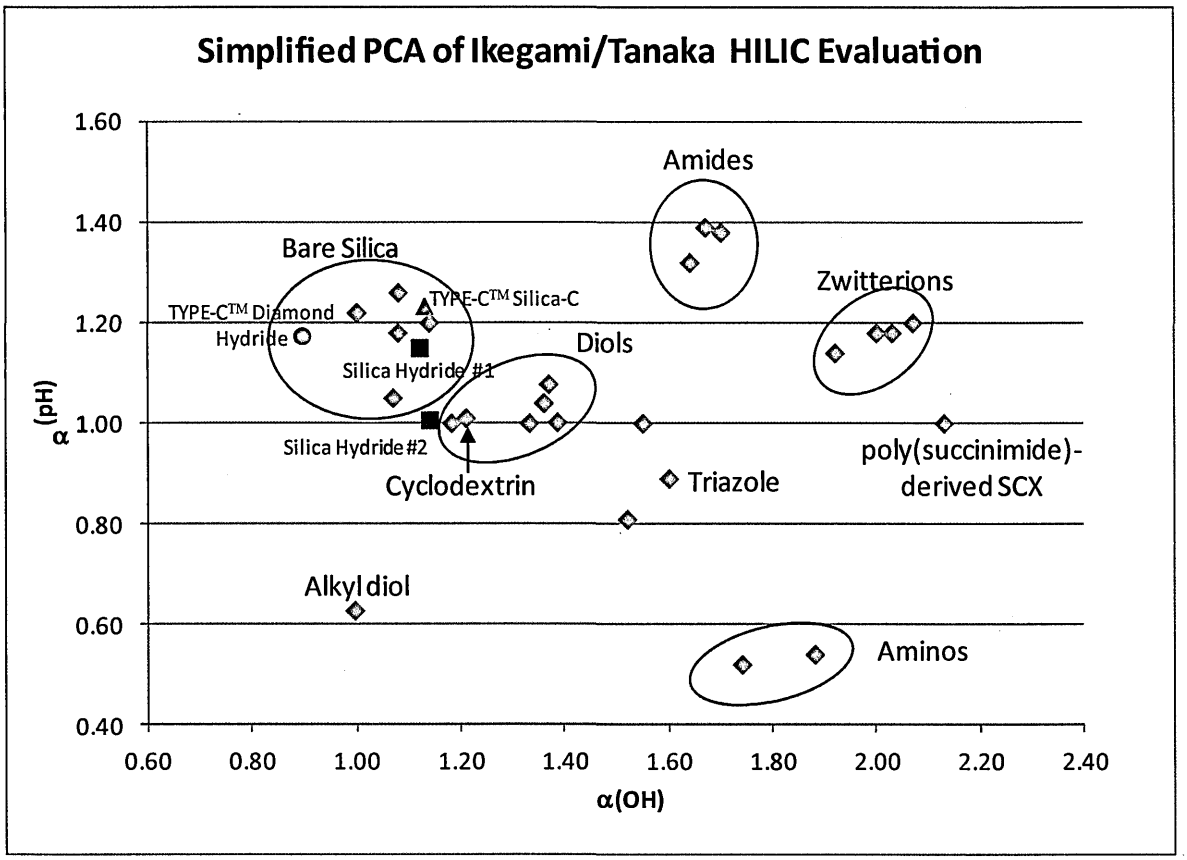

This indicates the Silica Hydride phases are comparable to bare silica and diol phases, most likely due to the silanophilic interactions from the residual hydroxyl arms on the silica hydride polymer. As the simplified PCA does not take into account the cation exchange interactions the results were added to the full principal component analysis for HILIC phases in order to get an full indication of the

properties of the phase compared to HILIC columns on the market. The loading plot for the PCA is shown in Figure 7.16 below.

Figure 7.16 PCA Loading Plot for HILIC phases using Ikegami/Tanaka Characterisation data

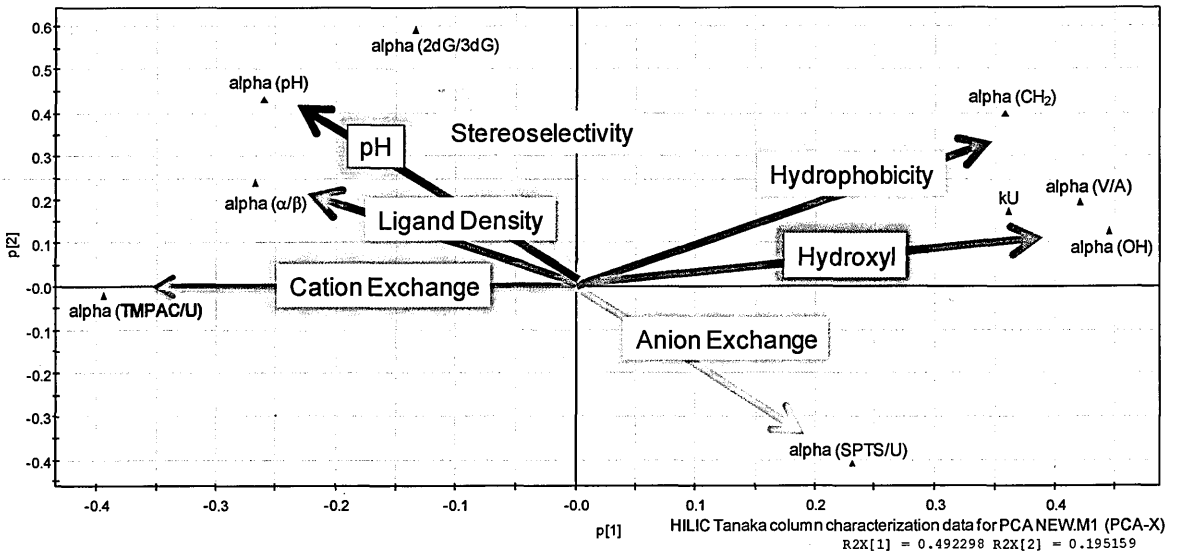

U = uridine, pH = 5-methyluridine, CH_2 = 2-deoxyuridine, A = adenosine, V = vidarabine, 2dG = 2-deoxyganosine, 3dG 3-deoxyganosine, α = 4-nitrophenyl-α-D-glucopyranoside, β = 4-nitrophenyl-β-D-D-glucopyranoside, AX = sodium p-toluenesulfonate, CX = N,N,N-trimethyl-phenylammonium,

The loading plot shows the same configuration as previously, the columns are modelled in Figure 7.17 below.

Figure 7.17 PCA on HILIC phases including Silica Hydride columns

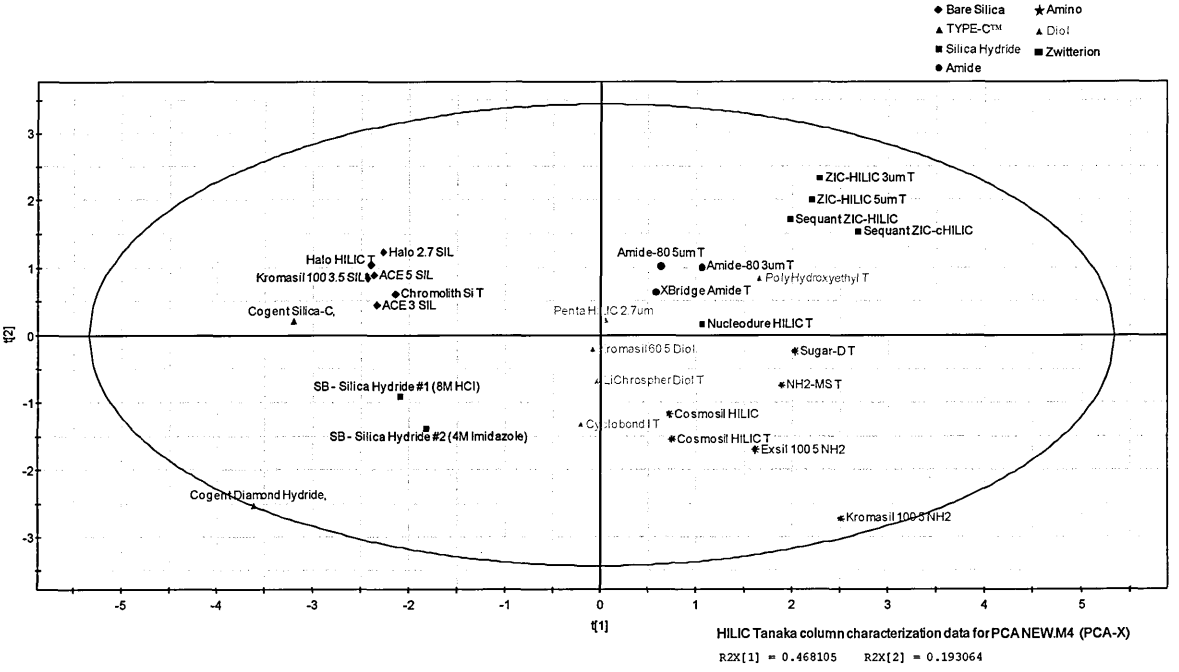

It has been seen previously that the TYPE-B bare silica phases are grouped in the upper left quadrant and the TYPE-C™ Silica-C phase is observed at the bottom of the group. The two Silica-Hydride materials can be seen in the bottom left quadrant along with the TYPE-C™ Diamond Hydride phase. This is due to the added hydrophobicity of these phases makes it lie along the diagonal axis due to the $\alpha_{(CH2)}$ values. The degree of cation exchange of the Silica Hydride materials is seen to be lower than observed on the TYPE-B bare silica columns and considerably lower than observed on the TYPE-C™ phases. The two columns are seen to be grouped together indicating comparable characteristics, they do not readily fit into one of the categories of columns; however they are most comparable to the bare silica and diol phases.

The results indicate that the silica hydride coverage of the prepared phases is greater than the commercial TYPE-C™ phases. As the synthesis route for the "silanization" of the TYPE-C™ Silica-C phase is unknown it is not possible to draw any conclusions about the optimised process, however these results do show that the silanophilic interactions have been reduced through the controlled TES "silanization" process.

7.2.4 *van Deemter Analysis of Silica Hydride Particles*

The investigation into the TYPE-C™ Bidentate C18 phase shown in Chapter 5 found the phase to have a reduced efficiency compared to the ACE 3 C18 phase. This was shown to be due to irregular PHS particles within the silica packing material, these particles give rise to eddies within the packing base which increase the A term of the van Deemter equation and results in a higher HETP value. Section 6.4 showed the TYPE-C™ Diamond Hydride and Silica-C phases did not have the same reduced efficiency values compared to the ACE 3 SIL indicating the phase does have the same issues with the packing bed. This is possibly due to a different "silanization" process as discussed in the previous chapter.

The optimised TES "silanization" processed developed in this section should minimise the presence of PHS particles in the packing bed and show a lower contribution from the A Term for the van Deemter calculation. The silica hydride materials were prepared using a 5 µm silica particle, as the TYPE-C™ Silica-C phase is stated to be a 4 µm particle the results were compiled using the reduced plate height van Deemter as shown below in Figure 7.18.

Figure 7.18 van Deemter plot for Prepared Silica Hydride against TYPE-C™ Silica-C Phases

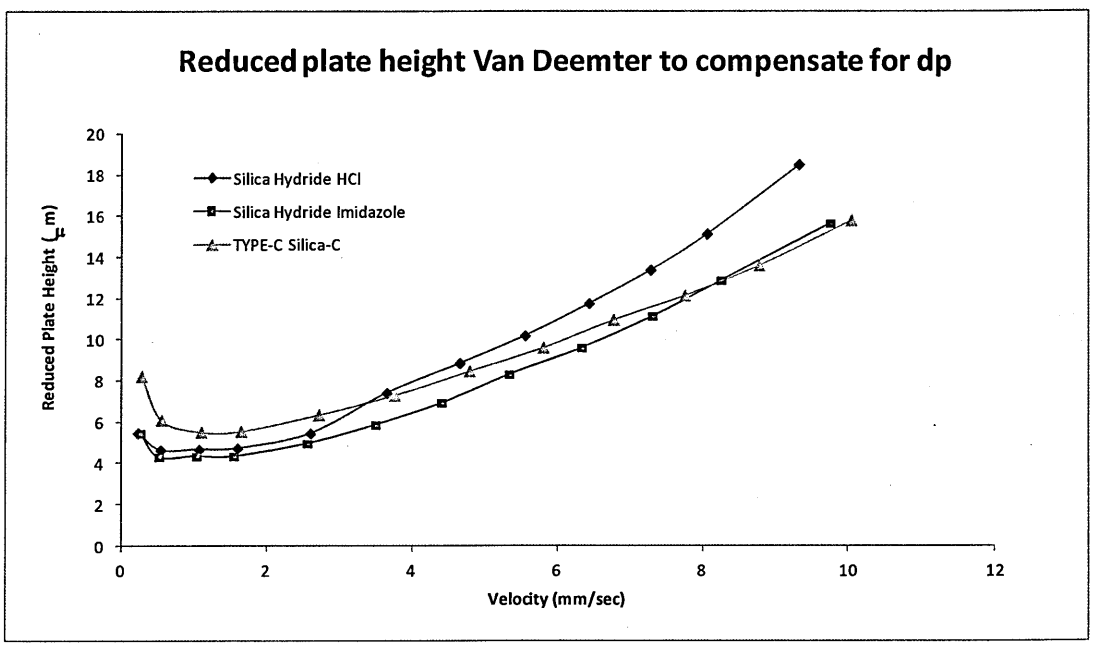

The analysis was carried out with salbutamol rather than ketoprofen as the former gave a retention factor of approximately 10 under HILIC conditions. The plots for the two prepared Silica Hydride phases are comparable with each other and the TYPE-C™ Silica-C phase. The plots are seen to rise exponentially as the flow rate increases which suggests a larger contribution from the C Term, due to poor mass transfer between the stationary and mobile phase. However this analysis is run at 25°C and reversed phase van Deemter plots are usually run at higher temperatures to improve mass transfer. As this is HILIC analysis the increase at high flow rate may also be due to the reduced contribution from partitioning interactions. As the flow rate increases the analytes are less likely to effectively partition between the aqueous solvated layer around the silica base and the acetonitrile rich bulk of the mobile phase.

The van Deemter terms were calculated using Microsoft Solver as before and are shown in Table 7.4 below along with the efficiency values calculated from the average plate count for the 0.5 mL/min runs.

Table 7.4 ***Calculated HILIC Mode van Deemter Terms Values – Comparison of Prepared Silica Hydride phases versus Silica-C phase***

	Efficiency at 0.5 mL/min	A	B	C
Silica Hydride #1 8 M Hydrochloric Acid (5 µm)	2027	2.11	2.03	-0.25
Silica Hydride #2 4 M Imidazole (5 µm)	2036	1.94	1.93	1.07
TYPE-C™ Silica-C (4 µm)	1974	1.94	1.93	1.06

As expected the A and B Terms are comparable across all three columns. The low A Term indicates a small contribution from Eddy dispersion in the packing bed, indicating minimal interference from irregular PHS particles. The B Term is due to natural dispersion of the analyte within the system, the

similarity of these values indicates the columns have comparable path length as the analyte spends the same amount of time on each column.

The only variable result is from the C Term, the Silica Hydride #1 particles (prepared using 4 M hydrochloric acid) is seen to have a different contribution from the C Term than the other two phases. This is not surprising as the plot in Figure 7.18 shows a steeper increase of HETP as the velocity increases. However the result given by Microsoft Solver shows a negative contribution for the C Term, this does not seem likely as the C Term indicates dispersion of analytes due to the mass transfer between the stationary phase and mobile phase. This is unlikely as the phase has been shown to exhibit cation exchange retention which requires the analyte to interact directly with the surface of the bonded silanes. This would lead to some mass transfer between the analyte in the mobile phase and the interaction with the stationary phase.

This result suggests that the Microsoft Solver program cannot accurately model van Deemter contributions in HILIC mode. This may be due to the lack of data points at low velocity measurements, which results in a poor model for the B Term as this is at its maximum when velocity is at a minimum. The minimum flow rate analysed is at 0.05 mL/min, this is the lowest flow rate the system can accurately deliver therefore any points below this would not be a discriminative measurement.

Although the model may not be useable to give accurate numerical values the plots shown in Figure 7.18 and the efficiency values calculated by the instrument appear to be comparable across the three phases. This shows that the Prepared Silica Hydride Particles have a particle size distribution comparable to the TYPE-C™ Silica-C phase.

7.3 Conclusion of Synthesis of Silica Hydride Particles

The Ikegami/Tanaka HILIC characterisation data for the optimised Silica Hydride phases shows a reduced contribution from cationic exchange interactions when compared to the ACE 3 SIL and TYPE-C™ Diamond Hydride and Silica-C phases. This suggests a greater coverage of silica hydride and minimised secondary interactions from residual silanols or hydroxyl substituents on the silica hydride monolayer. As this was the aim of the optimisation process these phases are a success however the characterisation probes have shown these Silica Hydride phases are not suitable for HILIC separations.

The packed columns were shown to have comparable van Deemter plots and efficiencies to the commercial TYPE-C™ Silica-C phase and the contributions from the A Term have been minimised. This indicates that the presence of irregular PHS particles within the packed silica bed have been reduced through the controlled addition of water during the "silanization" process and by filtration through a larger pore filter paper.

The optimised "silanization" process yielded a successful product for small scale academic research, however due to the complexity and low yield of the final product this process is not suitable for large scale commercial manufacturing.

Ideally these modified silica materials would have been derivatised further using an octadecyl functionalised olefin to yield a C18 phase with minimal residual silanols without the need of an endcap and analysed in reversed phase against the TYPE-C™ Bidentate C18 phases. Unfortunately due to resource and time restraints this has not been possible. However the optimisation of the "silanization" process has shown how the issues found in the commercial TYPE-C™ Bidentate C18 phase can be solved.

8. CONCLUSIONS

Silanophilic interactions have historically caused issues with peak tailing and irreversible retention of polar and basic analytes. However, ionic, dipole-dipole, and hydrogen bonding interactions can be a powerful tool for separating polar molecules. In order to utilise these interactions a better understanding of the mechanism is required to overcome the issues. The work presented here gives a greater understanding of the separation mechanism and the practical limitations of a number of commercial stationary phases. The manufacturer's information for these columns often contains specific applications, however full independent testing of a range of acid, basic, phenolic, and polar compounds has not been demonstrated previously. This research will aid in the development of new industrial applications by highlighting the stationary phase with the most suitable mechanism to separate any combination of polar and non-polar compounds.

The initial research in this investigation was carried out to indentify and characterise the intensity and location of the silanophilic interactions in phases which are known to have accessible silanols on the surface. This confirmed a high level of cationic exchange and hydrogen-bonding interactions present in the Extended Polar Selectivity (EPS) phases. Structural elucidation determined the exact structures and thusly the location of the electrostatic interactions was identified. Hydrofluoric acid digestion and the subsequent analysis by GC-MS was proven to be suitable for the structural elucidation of silanes of equal or greater molecular weight as a dimethyl(octyl)silane.

The main interactions were shown to come from exposed silanols on the surface of the silica base. The accessibility of the silanols and the purity of the base silica dictated intensity of these interactions. Shorter chain and sparsely bonded hydrocarbon silanes on the silica surface were shown to reduce hindrance and result in more accessible silanophilic groups, therefore

increased interactions. Monofunctionally bonded silanes were shown to have a higher level of silanophilic interaction than trifunctionally bonded phases, again due to the easier accessibility of the surface silanols. High purity base silica was shown to reduce the level of silanophilic interactions; whereas the presence of metal ions in the lower purity silica used in the Platinum EPS phase increased the degree of retention of basic analytes.

Interestingly the Extended Polar Selectivity phases were shown to have a higher stability when exposed to acid hydrolysis conditions than typical octadecyl bonded phases with a trimethyl silane endcap. The reason for this is unclear; it is thought to be due to the charge on the surface on the silica arising from the exposed silanols. Further investigation into the cause of this added stability would be beneficial as understanding the mechanism further could be used to increase the stability of commercial HPLC phases. The phases show limited stability at neutral pH due to the degradation of the base silica particles. However dissolution of silica particles in neutral pH is well documented in literature and commonly occurs in all types of HPLC phases.

The retention mechanism for the EPS phases have been shown to have contributions from hydrophobic, silanophilic, dipole-dipole interactions, and hydrogen bonding which give them complementary selectivity to a monofunctionally bonded end-capped C18 phase. The end-capping process masks the residual silanols on the surface of the phase and reduces contribution from silanophilic interactions. Overall these findings gave insight into how silanophilic interactions can be identified and categorised as arising from the silica surface or from polar substituents on the bonded silane. These results were then used as a bench mark to evaluate the retention mechanism of the more complex silica hydride phases.

TYPE-C^{TM} silica phases were developed to convert the silanols on the surface of the silica to silica hydride prior to derivatisation with a functionalised ligand. In theory these phases should not exhibit any silanophilic interactions; however this investigation has shown the retention

mechanism to have contribution from cation exchange, dipole-dipole and hydrogen bonding interactions. ^{29}Si NMR spectroscopy on the unpacked silica materials confirmed the presence of silanols on the surface of the TYPE-C™ phases. The investigation showed that the silanophilic interactions are likely to be coming from unreacted hydroxyl "wings" on polymeric silica hydride surface due to incomplete cross-linking of the TES monomer. The preliminary investigation into "on-column" endcapping of these residual hydroxyl ends was not successful, further investigation into endcapping processes on the unpacked silica would be necessary to optimise this process.

The TYPE-C™ Bidentate C18 phase, which is thought to be unendcapped, showed comparable stability to monomerically bonded encapped TYPE-B C18 phase when exposed to acid hydrolysis at high temperatures. At neutral pH the TYPE-C™ Bidentate C18 phase showed silica dissolution indicating the silica hydride polymeric coverage does not protect the silica from degradation. Unlike the EPS phases the TYPE-C™ Bidentate C18 phase shows similar selectivity to a monofunctionally bonded endcapped C18 phase bonded to a highly pure TYPE-B silica base. This indicates the contribution from the silanophilic interactions has minimal effect on the overall selectivity of the phase.

However the investigation has shown that the "silanization" process of converting the silica base to a silica hydride monolayer has a considerable effect on the peak shape and efficiency of the TYPE-C™ Bidenate C18 phase. van Deemter analysis shows a higher contribution from the A Term resulting from high Eddy diffusion in the column pathway when compared to a monofunctionally bonded TYPE-B C18 phase. Scanning electron microscope imagery of the unpacked TYPE-C™ silica material showed a number of irregular particles present, these were identified as amorphous polyhydro-siloxane (PHS) formed through a cross-linking reaction of the triethoxy silane (TES) monomer.

Investigation into the "silanization" reaction using TES indicated the process needs strict moisture control and monitored addition of the TES to reduce PHS formation The product requires slurrying and filtration through a wide pore filter to remove any PHS particulates prior to packing. This process is time consuming and leads to poor yields, making it unsuitable for commercial processes, however it was acceptable for small scale academic purposes. Process modelling also showed the choice of catalyst may affect the level of coverage of the TES monolayer; imidazole leads to a more ordered lattice formation due to hydrogen bonding between the surface silanols and the amine ion. HPLC columns packed using the controlled "silanization" process showed a lower contribution from silanolphilic interaction in HILIC mode than the commercial TYPE-C™ Silica-C phases. The HILIC van Deemter analysis for this phase also showed a lower contribution from the A Term, comparable with commercial TYPE-C™ and TYPE-B silica phases.

The manufacturers of the TYPE-C™ commercial phases state the Diamond Hydride and Silica-C phases can be used for aqueous normal phase analysis without the need of a high number column volume equilibration as required for HILIC analysis. However this investigation has shown that both the TYPE-C™ Diamond Hydride and Silica-C phases have accessible silanols on the surface of the silica. These silanols allow the formation of the aqueous solvated layer required for the partitioning interactions required for HILIC mode separations. Analysis into the effect of ionic strength in the TYPE-C™ phases has shown partitioning separations may be occurring with certain analytes. The Tanaka/Ikegama HILIC characterisation has shown these two phases to have comparable selectivity's to unbonded TYPE-B silica phases. ^{29}Si NMR on the unpacked silica materials confirmed the presence of silanols on the surface of the silica. The van Deemter analysis run on the TYPE-C™ Diamond Hydride and Silica-C phases showed comparable efficiencies and A-Term contributions to the TYPE-B bare silica phase. Indicating there is no added dispersion from eddies caused by irregular PHS particles in the silica bed. This suggests

the TYPE-C™ Diamond Hydride and Silica-C phases are not prepared by the same "silanization" process as the TYPE-C™ Bidentate C18 phase and are more likely prepared by a two-step chlorination and reduction process.

Overall the commercial TYPE-C™ phases exhibited a contribution from silanophilic interactions in the observed retention mechanisms. Although the conversion of residual silanols to silica hydride is a good idea in theory the practical considerations for the "silanization" of bare silica by TES is difficult to control and yields a number of hydroxyl group accessible on the surface of the polymeric layer. These hydroxyls give rise to electrostatic, dipole-dipole, and hydrogen bonding interactions that are similar to those of residual silanols. The formation of PHS particulates can be controlled during the "silanization" process however this is time consuming and results in low yields. The controlled process has only been proved in small scale reaction conditions and may not be suitable for scale up due to the need for moisture control during the TES addition.

8.1 Further work

During this investigation a number of areas where identified for further research, due to time and resource constraints it was not possible to investigate these fully.

1. The increased stability of the EPS phases; it was hypothesised that the silica surface may become charged which repelled the H^+ ions in the mobile phase reducing the likelihood of acid hydrolysis at the surface of the silane, although it is unclear how this would happen. Another theory is that the sparsely bonded EPS phases are less likely to be cleaved from the surface as there are fewer bonds to attack. Neither of these reasons are satisfactory and further investigation would be required to determine the cause of the increased stability.

   The columns tested during this investigation were packed from recovered silica materials rather than sourced directly from the column manufacture. It is possible that the recovery and packing process has altered the physical properties of the silica material. Ideally this analysis would be repeated using brand new columns directly from the manufacture. A longer analysis time and the use of different acidic additives would also be beneficial to determine any trends or differences between the different types of EPS phase. Additionally further bondings of an octadecyl silane would be carried out using different carbon loads to evaluate how the coverage affects the stability of the phase.

2. Optimising the endcapping process on the TYPE-C™ Bidentate C18; initial investigations into "on-column" endcapping using N,O-Bis(trimethylsilyl) acetamide yielded poor results due to a rising baseline in the subsequent analysis. This indicates the endcap was being cleaved during the analysis. Further investigation into endcapping the silica material prior to packing the silica material would be required to optimise the endcapping process.

There are a number of endcapping reagents such as chloro-, ethoxyl or amino-trimethyl silane, and hexamethyldisilazane, once bonded these phases could be packed and evaluated for basic analytes.

3. Stability of the TYPE-C™ Diamond Hydride silica material in neutral pH; the *in-vitro* stability testing showed very little cleavage of the trimethyl silane. However the characterisation of the TYPE-C™ Diamond Hydride phase showed retention time changes for some of the probes during analysis. This indicates a change to the surface of the silica and the bonded phase. Due to the small amount of the TYPE-C™ Diamond Hydride silica material available it was not possible to assess the stability of the material in different mobile phase compositions therefore further work into the stability of different pH, ionic strength and solvent composition could be carried out to evaluate the phase.

4. Derivatisation of the produced silica hydride materials with olefins. The process controlled silica hydride produced in this investigation showed a reduced level of silanophilic interactions. The packed phases could only be analysed for HILIC characterisation, ideally the produced silica material would be derivatised using an alkene or alkyne octadecyl species and the resulting phase characterised for reversed phase analysis and compared against the TYPE-C™ Bidentate C18. The evaluation of the endcapping processes discussed above could then be utilised to endcap this phase and reduce the silanophilic interaction further.

REFERENCES

[1] L. R. Snyder, J. J. Kirkland and J. L. Glajch, Practical HPLC Method Development 2nd Edition, *Wiley-Blackwell*; **1997**.

[2] L. R. Snyder, J. J. Kirkland and J. W. Dolan, Introduction to Modern Liquid Chromatography, *Wiley-Blackwell*, **2010**.

[3] L. R. Snyder and J. W. Dolan, High-performance Gradient Elution: The Practical Application of the Linear-solvent-strength Model, *Wiley-Blackwell*, **2007**.

[4] K. A. Dill, J Phys Chem., **1987**, 91, *p.1980–1988*.

[5] P. T. Ying, J. G. Dorsey, K. A. Dill, Anal Chem., **1989**, 61, *p.2540–2546*.

[6] F. Gritti, G. J. Guiochon, Chromatogr A., **2005**, 1099, *p.1-42*.

[7] F. Gritti, G. J. Guiochon, Chromatogr A., **2006**, *1115*, *p.142-163*.

[8] U. D. Neue, K. V. Tran, A. Méndez, P. W. Carr, J. Chromatogr A., **2005**, 106 (1-2), *p. 35-45*

[9] P.C. Sadek, P.W. Carr. J. Chromatogr. Sci., **1983**, 21, *p. 314*

[10] J. Kohler, D.B. Chase, R.D. Farlee, A.J. Vega, J.J. Kirkland, J. Chromatogr., **1986,** 352, *p. 275*

[11] D. L. Dugger, J. H. Stanton, B. N. Irby, B. L. McConnell, W. W. Cummings, R. W. Maatman, J. Phys. Chem., **1964**, 68(4), *p. 757–760*

[12] J. J. Gilroy, J.W. Dolan, P.W. Carr, L. R. Snyder" J.Chromatogr *A.*, **2004**, 1026 (1-2), *p.77-89*

[13] B. D. Karcher, I. S. Krull, J Chrom Sci., **1987**, 25(10), *p. 472-478.*

[14] H. L. Wang, U. Duda, C. J. Radke. J Colloid Interface Sci., **1978**, 66, *p.153–165*.

[15] F. Riedo, E. S. Kováts, J Chromatogr A, **1982,** 239, *p.1–26*.

[16] J. H. Knox, A. J. Pryde., J Chromatogr A. **1975**, 112, *p.171–188.*

[17] A. Dabrowski., Adv Colloid Interface Sci., **2001** 8;93 (1-3), *p.135-224.*

[18] B. Law, S. J. Houghton, P. Ballard, J. Pharm and Biomed Anal., **1998,** 17, (3), *p. 443-453*

[19] U. D. Neue, J. E. O'Gara, A. Mendez, J Chromatogr A., **2006**, 1127, *p.161-174*

[20] L. R. Snyder, J. J. Kirkland, An Introduction to Modern Liquid Chromatography, 2nd Edition, *Wiley-Interscience, New York*, **1979**, Chapter 6

[21] M. R. Euerby, P. Petersson, J Chromatogr A., **2003**, 994, *p.13–36*

[22] L. R. Snyder, J. W. Dolan, P. W. Carr, J Chromatogr A., **2004**, 1060, *p.77-116*

[23] J. J Kirkland, J. L. Glajch. J Chromatogr A., **1983**, *255, p.27-39*

[24] U. D. Neue, HPLC Columns, Theory, Technology, *Wiley-VCH, New York*, **1997**, *p.369*

[25] L. R. Snyder, J. J. Kirkland, J. L. Glajch, Basics of Separation, Practical HPLC Method Development, *Wiley-Interscience, New York*, **1997**

[26] W. Bicker. J. Y. Wu, H. Yeman, K. Albert, W. Lindner, J Chromatogr A., **2011**, 1218 *p. 882–895*

[27] T. Ikegami, K. Tomomatsu, H. Takubo, K. Horie, N. Tanaka, J. Chromatogr. A., **2008**, 118, p. 4474

[28] M. Lämmerhofer, J. Sep. Sci., **2010**, 33, *p. 679.*

[29] M. A. Strege, S. Stevenson, S. M. Lawrence, Anal. Chem., **2000**, 72, *p. 4629-4633.*

[30] M. A. Strege, Am. Pharm. Rev., **1999**, 2 (3), *p. 53-58.*

[31] M. Douša, K. Lemr, J Sep Sci., **2011**, 34, (12), *p. 1402-1406*

[32] L. Nondek, J. Chromatogr, **1986**, 373, *p. 61.*

[33] J. D. Goss, J. Chromatogr. A, **1998**, 828, *p. 267.*

[34] K. Jinno, K. Kawasaki, Chromatographia, **1983,** 17, *p. 578.*

[35] X. Liu, H. Tanaka, A. Yamauchi, B. Testa, H. Chuman, Helvetica Chimica Acta, **2004**, 87, (11), *p. 2866–2876*

[36] A. Pagliara, E. Khamis, A. Trinh, P. A. Carrupt, R. S. Tsai, B. Testa, J Liquid Chrom., **1995**, 18, (9)

[37] B. Buszewski, R. M. Gadzała-Kopciuch, M. Markuszewski, R. Kaliszan, Anal. Chem., **1997,** 69, *p, 3277-3284*

[38] B. Buszewski, J. Schmid, K. Albert, E. Bayer. J. Chromatogr. **1991**, 552, *p. 415.*

[39] J. Zhao, P. W. Carr, Anal. Chem., **1998.**, ACS Publications

[40] K. B. Sentell, J. G. Dorsey, Anal Chem., **1989.**, ACS Publications

[41] O. V. Krokhin, Anal. Chem. **2006,** 78, *p .7785-7795*

[42] P. Aimar, M. Meireles, V. Sanchez, J Membrane Sci, 1990, 54, *p. 321–338*

[43] R. Kaliszan, M.A. van Straten, M. Markuszewski, J Chromatogr A, **1999**, 855, (2), *p. 455–486*

[44] A. Stauba, D. Guillarmea, J. Schapplera, J. L. Veutheya, S. Rudaz, J Pharma and Biomedical Anal, **2011**, 55, *p. 810–822*

[45] C. Markopoulou, T. Tweedlie, D. Watson, G. Skellern, H. Reda, P. Petersson, H. Bradstock, M. Euerby, Chromatographia, **2009**, 70, *p. 705–715*

[46] J. H. Knox, A. Pryde, J. Chrom, **1975**, 112, *p.171-188*

[47] G. Lei, X. Xiong, Y. Wei, X. Zheng, J. Zheng. *J Chromatog A*, **2008**, 1187 *p. 197-204*

[48] W. Kopaciewicz, M.A. Rounds, J. Fausnaugh, F.E. Regnier, J. Chromatogr. A **1983,** 266 *p. 3.*

[49] Y. B. Yang, F. E. Regnier, J. Chromatogr. A, **1991**, 544, *p. 233.*

[50] A. Berthod, W. Li, D. W. Armstrong, Anal Chem, **1992**, 64, *p. 873-879*

[51] T.D. Booth, I. W. Wainer, J. Chromatog A, **1996**, 737(2), *p. 157-196*

[52] J. S. Kiel, S. L. Morgan, R.K. Abramson - J Chromatog A, **1985**, 320(2), *p. 313-323.*

[53] K. Yoshizako, K. Hosoya, Y. Iwakoshi, K. Kimata, N. Tanaka, Anal. Chem., **1998**, 70, *p. 386*

[54] A. Striegel, W. W. Yau, J. J. Kirkland, D. D. Bly, Modern Size-Exclusion Liquid Chromatography: Practice of Gel Permeation and Gel Filtration Chromatography, **2009**, *Wiley-Blackwell*; 2nd Edition.

[55] W. Kopaciewicz, F.E. Regnier, Analytical biochemistry, **1982**, 126(1), *p. 8-16.*

[56] B. E. Boyes, D. G. Walker, P. L. McGeer - Analytical biochemistry, **1988**, 170, *p. 127*

[57] P. Marialice, C. Silvestre , M. Hamon , M. *Yvon* J. Agric. Food Chem., **1994**, 42 (12), *p. 2778–2782*

[58] J. P. Larmann, J. J. Destefano, A. P. Goldberg, R. W. Stout, L. R. Snyder, M. A. Stadalius, J. Chromatogr., **1983**, 255, *p. 163*

[59] J. Zhao, P. W. Carr, Anal Chem, **1998**, 70 (9), *p 1934–1942*

[60] U. D. Neue, J. E. O'Gara, A. Mendez, J Chromatogr A, **2006**, 1127, *p.161-174*

[61] R. E. Majors, Anal Chem, **1973**, 43, *p. 755*

[62] F. Gritti, G. Guiochon, J Chromatogr A, **2001**, 1218, *p. 1592–1602*

[63] U. D. Neue, N. Brady, S. Serpa, P. Iraneta, B. Alden, T. Walter, K. Wyndham, 32nd International Symposium on High Performance Liquid Phase Separations and Related Techniques, **2008**

[64] U. D. Neue, HPLC Columns: Theory, Technology, and Practice, *Wiley-Blackwell* **1997**

[65] M. R. Euerby, F. Scannapieco, H. J. Rieger, I. Molnar, J Chromatogr A, **2006**, 1121, *p. 219–227*

[66] J. L. Rafferty, L. Zhang, J. Ilja Siepmann, M. R. Schure, Anal. Chem. **2007,** 79, *p. 6551-6558*

[67] D. V. McCalley, J Chromatogr A, **2000**, 902, *p. 311–321*

[68] N. H. Davies, M. R. Euerby, D. V. McCalley, J Chromatogr A, **2008**, 1178, *p. 71-78*

[69] M. C. Gennaro, D. Giacosa, C. Abrigo, J Liquid Chrom, **1994**, 17(20),

[70] M. T. W. Hearn, D.J. Lyttle, J. Chromatogr. **1981**, 218, *p. 483-495*

[71] V. J. Barwick. Trends in Analytical Chemistry, **1997**, 16(6), *p. 293–309*

[72] H. B .Patel, T. M. Jefferies, J. Chromatog A, **1987**, 389, *p. 21–32*

[73] H. Colin, G. Guiochon, P. Jandera, Chromatographia, 1982, 15(2), p.133-139

[74] P. Sandera, Liquid chromatography—normal phase. In: Encyclopedia of analytical science, 2nd Edn. **2005** *Elsevier*, Oxford, *p. 142–152.*

[75] H.T. Rasmussen, W. Li, D. Redlich, M.I. Jimidar S. Ahuja, M. Dong (Eds.), Handbook of HPLC in Pharmaceutical Analysis, **2005** *Elsevier*

[76] N. W. Smith, M. B. Evans - Chromatographia, **1995**, 41, *p. 197*

[77] X. Wang, W. Li, H. T. Rasmussen, J Chromatogr A, **2005**, 1083 (1–2), *p. 58–62*

[78] Y. Zhao, G. Woo, S. Thomas, D. Semin, P. Sandra, J. Chromatogr. A, **2003,** 1003, *p. 157*

[79] K. D. Altria, A. B. Chen, L. Clohs, LC–GC Eur., **2001**, 14, *p. 736*

[80] A. J. Alpert J. Chromatogr., **1990**, 499, *p. 177*

[81] N. P. Dinh, T. Jonsson, K. Irgum, J Chromatogr A, **2011**, 1218, *p. 5880– 5891*

[82] P. Hemström, K. Irgum., J Sep Sci., **2006**, 29, *p. 1784–1821*

[83] M. A. Strege, Anal. Chem., **1998**, 70, *p. 2439-2445*

[84] M. Godejohann , J Chromatogr A., **2007**, 1156, *p. 87–93*

[85] P. Hemstr, K. Irgum J. Sep. Sci. **2006**, 29, *p. 1784 – 1821*

[86] A. J. Alpert, J Chromatogr A. **1990**, 499, *p. 177–196*

[87] F. Mihci, K. Irgum, Water Adsorption Isotherms among HILIC Phases, **2011,** Final Thesis, *Department of Chemistry, Umeå University, Sweden.*

[88] S. Melnikov, A. Höltzel, A. Seidel-Morgenstern, U. Tallarek, Angewandte Chemie International Edition, **2012**, 51(25), *p. 6251-6254*

[89] D. V. McCalley, J Chromatogr A, **2010**, 1217(20), *p. 3408-3417*

[90] J. Ruta, S. Rudaz, D. V. McCalley, J. Veuthey, D. Guillarme., J Chromatogr A, **2010**, 1217(52), *p. 8230-8240*

[91] P. Hemström, K. Irgum. J Sep Sci. **2006**, 29, *p. 1784–1821*

[92] B. Buszewski, S. Noga, Anal Bioanal Chem. **2012**, 402(1), *p. 231–247.*

[93] F. Gritti, Y.V. Kazakevich, G. Guiochon. J Chromatogr A. **2007**, 1169, *p. 111–124.*

[94] S. Bocian, P. Vajda, A. Felinger, B. Buszewski. J Chromatogr A. **2008**, 1204, *p. 35–41.*

[95] D.V. McCalley, U.D. Neue UD. J Chromatogr A. **2008**, 1192, *p. 225–229.*

[96] P. Sandera, J Sep Sci. **2006**, 29, *p. 1763–1783*

[97] P. Sandera et al. J. Chromatogr. A., **2010**, 1217, *p. 22–33*

[98] J. Urban, V. Skeříková, P. Jandera, R. Kubíčková, M. Pospíšilová, J. Sep. Sci., **2009**, 32, *p. 2530.*

[99] A.R. Oyler, B.L. Armstrong, J.Y. Cha, M.X. Zhou, Q. Yang, R.I. Robinson, R. Dunphy, D.J. Burinsky. J Chromatogr A., **1996**, 724, *p. 378–383*

[100] S. D. Garbis, A. Melse-Boonstra, C. E. West, R. B. Breemen. Anal Chem. **2001**, 73, *p. 5358–5364*

[101] B. A. Olsen. J Chromatogr A. **2001**, 913, *p. 113–122.*

[102] R. Li, J. Huang. J Chromatogr A. **2004,** 1041, *p. 163–169.*

[103] Y. Guo, S.J. Gaiki., J. Chromatogr A. **2005**, 1074, *p. 71–80*

[104] J. C. Linden, C. L. Lawhead. J Chromatogr A. **1975**, 105, *p. 125–133.*

[105] L. R. Snyder, J. W. Dolan. Adv Chromatogr. **1998**, 38, *p. 115–185.*

[106] M. Przybyciel, R. E. Majors. LC-GC North America, **2002**, 20(6), *p. 516-520*

[107] T. Zhou, C. A. Lucy. J Chromatogr A. **2010**, 1217, *p. 82–88*

[108] N. T. Hong Bui, J.J. Verhage, K. Irgum. J Sep Sci. **2010**, 33, *p. 2965–2976*

[109] J. Pesek, M.T. Matyska., LC-GC North America, **2007**

[110] W. Naidong, J. Chromatogr B, **2003**, 796, *p. 209.*

[111] D. S. Bell, Jones, A. Daniel, J. Chromatogr A., **2005**, 1073, *p. 99.*

[112] H. Tanaka, X. Zhou, M. Ohira., J Chromatogr A, **2003**, 987, *p. 119–125*

[113] T. Yoshida., Anal Chem, **1997**, 69, *p. 3038–3043*

[114] M. C. Xu, D.S. Peterson, T. Rohr, F. Svec, J.M.J. Fréchet, Anal Chem, **2003**, 75, *p. 1011–1021*

[115] D. McCalley, J Chromatogr A., **2007**, 1171 (1-2), *p. 46-55*

[116] A. P. McKeown, M. R. Euerby, H. Lomax, C. M. Johnson, H. J. Ritchie, M. Woodruff, J. Sep. Sci., **2001**, 24, *p. 835*

[117] Z. Hao, B. Xiao, N. Weng, J. Sep Sci., **2008**, 31(9), *p. 1449-1464*

[118] C. McClintic, D.M. Remick, J.A. Peterson, D.S. Risley, J. Liq. Chromatogr. Rel. Technol., **2003**, 26(18), *p. 3093*

[119] C. Markopoulou, T. Tweedlie, D. Watson, G. Skellern, H. Reda, P. Petersson, H. Bradstock, M. R. Euerby., Chromatographia, **2009**, 70 (5-6), *p 705-715*

[120] E. M. Borges, M. R. Euerby., J. Pharma and Biomed Anal., **2013**, 77,

[121] H. Tanaka, X. Zhou, O. Masayoshi, Journal of Chromatography A., **2003**, 987 (1-2), *p. 119–125*

[122] C. Brons, C. Olieman, J. Chromatogr., **1983**, 259, *p. 79*

[123] M. Lafosse, B. Herbreteau, M. Dreux, L. Morin Allory., J. Chromatogr., **1989**, 472, *p. 209*

[124] A. R. Oyler, B. L. Armstrong, J. Y. Cha, M. X. Zhou, Q. Yang, R. I. Robinson, R. Dunphy, D. J. Burinsky., J Chromatogr A, **1996**, 724, *p. 378–383*

[125] Y. Guo, S. Gaiki, J Chromatogr A, **2005**, 1074 (1–2), *p. 71–80*

[126] B. A. Olsen, J Chromatogr A, **2001**, 913 (1–2), *p. 113–122*

[127] M. R. Euerby, P. Petersson, J Chromatogr A, 2005, 1088, p. 1-15

[128] R. E. Majors, M. Przybyciel. LC-GC North Am. **2002**, 20, *p. 584-593*

[129] T. Greene, P. Wuts, *Protective Groups in Organic Synthesis*, 2nd Ed., Wiley, New York, **1991**

[130] E. S. Grumbach, D. M. Diehl, D. R. McCabe, J. R. Mazzeo, U.D. Neue., LC-GC North Am., Suppl., **2003**, *p. 53*

[131] C. Dell'Aversan, G. K. Eaglesham, M. A. Quilliam., J. Chromatogr. A, **2004**, 1028, *p. 155*

[132] W. Bicker, J. Wu, M. Lämmerhofer, W. Lindner J. Sep. Sci., **2008**, 31, *p. 2971*

[133] A. Kumar, J.C. Heaton, D.V. McCalley – J. Chromatogra A, 2013, 1276, p. 33-46

[134] S. Vikingsson, R. Kronstrand, M. Josefsson, J Chromatogra. A., **2008**, 1187 (1-2), *p. 46-52*

[135] Y. Guo, S. Gaiki., J. Chromatogr. A, **2005**, 1074, *p. 71*

[136] M. K. L Bicking, R. A. Henry., LC-GC North America, **2010**

[137] W. Way., The Reporter (Europe), **2007**, 24, *p. 8-10*

[138] P. Hemstroem, K. Irgum, J. Sep. Sci., **2006**, 29, *p. 1784*

[139] Y. Guo, S. Gaiki, J. Chromatogr., A., **2011**, 1218, *p. 5920*

[140] J. J. Pesek, M. T. Matyska, J. Sep. Sci., **2009**, 32, *p. 3999*

[141] J. J. Pesek, M. T. Matyska, R. I. Boysen, Y. Yang, M. T.W. Hearn., Trends in Analytical Chemistry,, **2013**, 42, *p.61-73*

[142] R. I. Boysen, M. T. W. Hearn., *Amino Acids, Peptides and Proteins in Organic Chemistry*, Wiley-VCH Verlag GmbH & Co. KGaA, Weinheim, Germany, **2012,** *p. 167*

[143] R. Iler, The Chemistry of Silica. Wiley, New York **1979**

[144] K. K. Unger, Porous Silica. Elsevier, Amsterdam **1979**

[145] W. Buchberger, K. Wlnsauer, J Chromatogr. **1989**, 482(2), *p. 401-6.*

[146] J. J. Pesek, V.H. Tang - Chromatographia, **1994**, 39, *p. 649*

[147] J. Nawrocki, C. Dunlap, A. McCormick, J. Chromatogra A, **2004**, 1028(1), *p. 1-30*

[148] T. Zhou, C.A. Lucy, J. Chromatogr. A, **2010**, 1217, *p. 82.*

[149] T. Zhou, C.A. Lucy, J. Chromatogr. A, **2008**, 1187, *p. 87*

[150] J. Randon, S. Huguet, C. Demesmay, A. Berthod, J. Chromatogr. A., **2010**, 1217, *p. 1496.*

[151] K. K. Unger (Ed.), Packing and Stationary Phases in Chromatographic Techniques, M. Dekker, New York **1989**

[152] S. H. Hansen, P. Helboe, M. Thomsen. J. Chromatogr., 544 **1991,** *p.53*

[153] J. J. Hetem, Hüthig Buch Verlag, Heidelberg Chemically Modified Silica Surfaces in Chromatography. A Fundamental Study. **1993**

[154] J. J. Kirkland, J. L. Glajch, R. D. Farlee, J Anal Chem **1989,** 61, *p.2-11*

[155] M. J Wirth, H. O Fatunmbi, J Anal Chem **1993,** 65, *p.822-826*

[156] L. C. Sander, S. A. Wise, J Anal Chem **1984,** 56, *p.505-510*

[157] J. Nawrocki, Chromatographia, 31 (3/4) **1991**, *p.193*

[158] M. A. Stadalius, J. S. Berus, L. R. Snyder LC-GC, 6 (6) **1988**, *p.494*

[159] G. B. Cox, J. Chromatogr. A, 656 **1993**, *p.353*

[160] J. Nawrocki. J. Chromatogr., 779 **1997**, *p.29*

[161] S. M. C. Buckenmaier, D. V. McCalley, M. R. Euerby, Anal. Chem. **2002**, 74, p. 4672.

[162] U. D. Neue, D. J. Phillips, T. H. Walter, M. Capparella, B. Alden, R. P. Fisk, LC/GC, **1994**, 12 (6), *p. 468.*

[163] P. J. van den Driest, H. J. Ritchie, Chromatographia **1987**, 24, *p.324-328*

[164] D. B. Marshall, K. A. Stutler, & Lochmüller, C. J Chrom Sci, **1984,** 22(6) *p.217-220*

[165] C. Lochmüller, D.B. Marshall, Analytica Chimica Acta, 142 **1982,** *p.63-72*

[166] D. B. Marshall, C. Cole, A. D. Norman, J Chrom Sci, 25(6) **1987**, *p.262-266*

[167] K. D. Mc Murtrey, J Liq Chrom, 11(16) **1988** *p.3375-3384*

[168] J. E. Sandoval, J Chromatogr. A, 852(2) **1999** *p.375-381*

[169] , J. Pernak, J Chromatogra A, **2004**, 1030(1-2), *p. 263-271*

[170] Analytical Proceeding 30 **1993** *p.46 - 51*

[171] R. t'Kindt, G. Alaerts, Y. Vander Heyden, D. Deforce, J van Bocxlaer, J. Sep. Science 30 **2007** *p. 2002–2011*

[172] A. Nahum, C. Horváth . J Pharma Biomed Anal, **1987**, 5(7), *p. 723-727*

[173] R. J. Ruane, I. D. Wilson, J Chromatogra A, **1988**, 441, *p. 355–360*

[174] U. D. Neue, K. van Tran, A. M´endez, P. W. Carr, J Chromatogra A, 1063 **2005**, *p.35-45*

[175] K. Kimata, K. Iwaguchi, S. Onishi, K. Jinno, R. Eksteen, K. Hosoya, M. Araki, N. J Tanaka, Chromatogr. Sci. 27, **1989**, *p.721–728*

[176] M. R. Euerby, P.Petersson, J Chromatogra A, 994(1), **2003**. *p.13-36*

[177] P. Petersson , M.R. Euerby , J Sep Sci. 28(16), **2005**, *p.2120-9*

[178] J. Köhler, D.B. Chase, R.D. Farlee, A.J. Vega, J.J. Kirkland. J Chromatogr A., 352, **1986**, *p.275*

[179] E. Cruz, M. R. Euerby, C. M. Johnson, C. A. Hacket, Chromatographia, 44, **1997**, *p.151-161*

[180] M. R. Euerby, P.Petersson, LC GC Europe, 13,**2000**, *p.665–677*

[181] W. Huihui, X. Xingya, D. Yuguang, L. Xinmiao., Anal. Methods., **2012**. 4, *p. 3524*

[182] J. E. Sandoval, J. J. Pesek, Anal. Chem., 61, **1989** *p.2067-2075*

[183] J. E. Sandoval, J. J. Pesek, Anal. Chem., 63, **1991,** *p.2634-2641*

[184] J. J. Pesek, J. Sandoval, D. Chu, E. Jonsson, "Chemically Modified Oxide Surfaces", H.A. Mottola, J.R. Steinmetz, eds., Elsevier, **1992**, *p.57-72*

[185] C. H. Chu, E. Jonsson, M. Auvinen, J. J. Pesek, J. E. Sandoval, Anal. Chem., 65, **1993**, *p.808-816*

[186] J. J. Pesek, I. Leigh, eds., Royal Society of Chemistry, Cambridge, **1994**, *p.1-23*

[187] J. J. Pesek, M. T. Matyska, J. E. Sandoval, E. Williamsen, J. Liq. Chromatogr., 19, **1996**, *p.2843-2865*

[188] J. J. Pesek, M. T. Matyska, M. Oliva, M. Evanchic, J. Chromatogr. A, 818, **1998**, *p.145-154*

[189] J. J. Pesek, M. T. Matyska, P.F. Fu, Chromatographia, 53, **2001,** *p.635-640*

[190] J. J. Pesek, M. T. Matyska in "A Century of Separation Science", H. Issaq, ed., *Marcel Dekker*, New York, **2001**, *p. 349-364*

[191] J. J. Pesek, M. T. Matyska, J. Sep. Sci., 28, **2005**, *p.1845-1854*

[192] J. J. Pesek, M. T. Matyska, S. Larrabee, J. Sep. Sci., 30, **2007**, *p.637-647*

[193] R. David, Jr. Lide. Tetrahedron, 17(3-4), **1962**, *p.125–134*

[194] H. Oberhammer, J. E. Boggs, J. Am. Chem. Soc., 102, **1980**, *p. 7241-7244*

[195] M. G. Voronkov, V.P. Mileshkevich, Y.A. Yuzhelevskii, "The Siloxane Bond"; Consultants Bureau: New York, **1978**.

[196] J. J. Pesek, S. A. Swedberg., Chromatogr, 361, **1986**, *p.83-92*

[197] D. H. Saunders, P. M. Barford, L. T. Olszewski, H. L. Rothbart., Anal Chem. 46, **1974**, *p.834-8838*

[198] C. Morterra, M. J. D. Low., Phys Chem 73, **1969**, *p.321-326*

[199] C. Morterra, M. J. D. Low., Phys Chem 73, **1969**, *p.321-326*

[200] J. E. Sandoval, J. J. Pesek, US Pat. 5017540, **1991**

[201] A. L. Smith, J. A McHard., Anal Chem 31(7), **1959**, *p. 1174-1179*

[202] A. L. Smith., *Analysis of Silicones*, J Wiley & Sons, New York, **1974**

[203] J. J. Pesek, M. T. Matyska, Chromatography Today, 3, **2010**, p.24-26.

[204] J. J. Pesek, M. T. Matyska, J. Sep. Sci., 32, **2009**, p.3999-4011.

[205] H. Claessens, M. van Straten, J. Kirkland, Journal of Chromatography A, 728 (1),**1996**, *p-259-270*

[206] M. T. Matyska, J. J. Pesek, A. M. Siouffi, Chem. Anal., 40, **1995**, *p.517-530*

[207] J. J. Pesek, M. T. Matyska, R. J. Yu, J. Chromatogr. A, 907, **2002**, *p.195-203*

[208] J. J. Pesek, M. T. Matyska, S. Prabhakaran, J. Sep. Sci., 28, **2005**, *p.2437-2443*

[209] M. T. Matyska, J. J. Pesek, G. Shetty, J. Liq. Chromatogr. & Rel. Technol., 33, **2009**, *p.1-26*

[210] B. Bidlingmeyer, C. C.Chan, P.Fastino, R. Henry, P. Koerner, A.T. Maule, M. R.C. Marques, U. Neue, L.Ng, H. Pappa, L. Sander, C. Santasania, L. Snyder, T.Wozniak., Pharmacopeial Forum, **2005**, 31(2), *p.637-64*

[211] USP 27–NF 22. Rockville, MD: United States Pharmacopeial Convention, Inc., **2004**, *p. 2281.*

[212] M. R. C. Marques., Pharm Forum., **2000**, 26(1), *p. 273–288.*

[213] M. R. C. Marques., Pharm Forum., **2001**, 27(4), *p. 2882–2911.*

[214] H. Engelhardt, M. Jungheim, Chromatographia, **1990**, 29, *p. 59.*

[215] H. Engelhardt, H. Low, W. J. Gotzinger, Chromatogr. **1991**, 544, *p. 371–379.*

[216] D. V. McCalley, J. Chromatogr. A **1994**, 664, *p. 139–147.*

[217] H. Engelhardt, M. Arangio, T. Lobert, LCGC **1997**, 15, *p. 856–866.*

[218] D. V. McCalley, J. Chromatogr. A **1999,** 844, *p. 23–38.*

[219] M. R Euerby, P. Petersson., LC-GC Europe., **2000**, 13, *p. 665–677.*

[220] L. R. Snyder, J. W. Dolan, LC GC North America **2002**, 20, *p. 1016–1026.*

[221] M. R. Euerby, P. Petersson, A. P. McKeown., J. Sep. Sci. **2003**, 26, *p. 295–306.*

[222] M. R. Euerby, P. Petersson, J. Chromatogr. A **2003**, 994, *p. 13–36.*

[223] M. R. Euerby, P. Petersson, J. Chromatogr. A **2005**, 1088, *p. 1–15.*

[224] K. Kimata, K. Iwaguchi, S. Onishi, K. Jinno, R. Eksteen, K. Hosoya, M. Araki, N. J. Tanaka., Chromatogr. Sci. **1989**, 27, *p. 721–728*

[225] M. R. Euerby, P. Petersson, M. James., J. Chromatogr A, **2012,** 1228, *p. 165-174*

[226] M. R. Euerby, P. Petersson J. Sep. Sci. **2005**, 28, *p. 2120–2129*

[227] L. C. Sander, S. A. Wise, J. Separation Science, **2003**, 26, *p. 283*

[228] U. D. Neue, E. Serowik, P. Iraneta, B. A. Alden, T. H. Walter J. Chromatogr A, **1999**, 849, *p. 87*

[229] L. R. Snyder, J. W. Dolan and P. W. Carr, J. Chromatogr. A, **2004**, 1060, *p. 77-116.*

[230] L. R. Snyder, J. W. Dolan and P. W. Car, Anal. Chem., **2007**, 79, *p. 3255-3261.*

[231] L. R. Snyder , A. Maule, A. Heebsch, R. Cuellar, S. Paulson, J. Carrano, L. Wrisley,, C. C. Chan, N. Pearson, J. W. Dolan and J. Gilroy, J. Chromatogr. A, **2004,** 1057, *p. 49-57.*

[232] J. W. Dolan, A. Maule, L. Wrisley,, C. C. Chan, M. Angod, C. Lunte, R. Krisko, J. Winston, B. Homeierand, D. M. McCalley and L. R. Snyder, J. Chromatogr. A, **2004**, 1057, *p. 59-74*.

[233] L. R. Snyder, J. W. Dolan, P. W. Carr, J. Chromatogr. A., **2004**, 1060, *p. 77*

[234] U. D. Neue, K. Tran, P. C. Iraneta, B. A. Alden, J. Sep. Sci. **2003**, 26, *p. 174.*

[235] U. D. Neue, J. E. O'Gara, A. Mendez., J. Chromatogr. A., **2006**, 1127, *p. 161-174*

[236] R. I. Chirita, C. West, A. L. Finaru, C. Elfakir., J. Chromatogr. A, **2010**, 1217, *p. 3091*

[237] C. West, E. Lesellier., J. Chromatogr. A, **2006**, 1110, *p. 200*

[238] G. Marrubini, B. E. C. Mendoza, G. Massolini., J. Sep. Sci., **2010**, 33, *p. 803*

[239] M. Lämmerhofer, M. Richter, J. Wu, R. Nogueira, W. Bicker, W. Lindner ., J. Sep. Sci., 31, **2008**, p. 2572

[240] B. Chauve, D. Guillarme, P. Cléon, J. L. Veuthey., J. Sep. Sci., **2010**, 33, p. 752

[241] Y. Kawachi, T. Ikegami, H. Takubo, Y. Ikegami, M. Miyamoto, N. Tanaka., J. Chromatogr. A., **2011**, 1218 (35), *p. 5903–5919*

[242] A. Turner Jr., A. Osol., J. Am. Pharm. Assoc., **1949**, 38, *p. 158.*

[243] K. Pearson., *Philosophical Magazine,* **1901**, 2(11), *p. 559–572*.

[244] R. A. Johnson, D. W. Wichern., *Applied Multivariate Statistical Analysis,* **2007**.

[245] B. M. Wise, N. B. Gallagher., *J. Proc. Cont.,* **1996**, 6(6), *p. 329–348*

[246] L. Snyder, J.J. Kirkland, An Introduction to Modern Liquid Chromatography, 2nd Edition, *Wiley-Interscience, New York*, **1979**, Chapter 6.

[247] J. J. Kirkland, LC-GC, **1996**, 14, *p. 486.*

[248] J. J. Kirkland, J. Chromatogr. Sci., **1996**, 34, *p. 309.*

[249] J. Kohler, J. J. Kirkland, J. Chromatogr.,**1987**, 385, *p. 125.*

[250] J. J. Kirkland, C.H. Dilks, Jr., J. J. DeStefano, J. Chromatogr., **1993**, 635, *p. 19.*

[251] J. J. Kirkland, J. W. Henderson, J. Chromatogr. Sci., **1994,** 32, *p. 473.*

[252] B. C. Trammell, C. A. Boissel, C. Carignan, D. J. O'Shea, C. J. Hudalla, U. D. Neue, P. C. Iraneta, J Chromatogra A, **2004**, 1060, *p. 153–163*

[253] S. D. Fazio, S. A. Tomellini, H. Shih-Hsien, J. B. Crowther, T. V. Raglione, T. R. Floyd, R. A. Hartwick., Anal Chem, **1985**, 57(8), p. 1559-1564

[254] A. Yang, T. Li., Anal. Chem. **1998**, 70, p. 2827-2830

[255] M. R. Euerby, Strathclyde University, Personal correspondence, **2013**

[256] U. D. Neue, *HPLC Columns, Theory, Technology, and Practice*, Wiley-VCH, New York, **1997**, *p. 369.*

[257] H. A. Claessens, M. A. van Straten, J. J. Kirkland, J Chromatogr A, **1996**, 728, *p. 259-270*

[258] J. J. Kirkland , J. W. Henderson, J. J. DeStefano , M. A. van Straten , H. A. Claessens, J Chromatogra A, **1997**, 762, *p.97-112*

[259] J. E. O'Gara, B. A. Alden, C. A. Gendreau, P. C. Iraneta, T. H. Walter, J Chromatogr A, **2000**, 893, *p. 245–251* (cyano)

[260] C. R. Silva, C. H. Collins, I. C. S. Fontes Jardim, C. Airoldi, J Chromatogr A, **2004**, 1030, *p. 157–166.*

[261] J. Kohler, D. B. Chase, R.D Farlee, A.J Vega, J. Kirkland, J Chromatogr., 352, **1986**, *p.275-305*

[262] Thermo Scientific Manufacturer's specification (Online); http://www.thermoscientific.com.

[263] Alltech® Platinum Columns Manufacturer's brochure (Online); http://www.crawfordscientific.com.

[264] Waters Manufacturer's data (Online); http://waters.com.

[265] Agilent Zorbax Datasheet (Online); http://chem.agilent.com.

[266] Alltech® Alltima Columns Manufacturer's brochure (Online); http://www.crawfordscientific.com

[267] Platinum Stability Specification, Alltech White Paper (Online); http://www.mandel.ca/products/Chromatography/Liquid_Chromatography/HPLC_Columns/Alltech_Platinum/Grace%20Platinum%20Stability.pdf

[268] FisherScientific, Alltech Manufacturer's Specification (Online); http://www.fishersci.com/ecomm/servlet/fsproductdetail_10652_698439

[269] ACT Manufacturer's Specification (Online); www.**ace-hplc**.com/.../a12_u1100-**ace catalogue**-39227_web_small.pdf

[270] Silanes Catalogue, Gelest Inc (Online); http://www.gelest.com/gelest/forms/GeneralPages/prod_list.aspx?pltype=1&classtype=silanes&alpha=65

[271] A. Yang, T. Li., Anal. Chem. **1998**, 70, *p. 2827-2830*

[272] S. D. Fazio, S. A. Tomellini, H. Shih-Hsien, J. B. Crowther,' T.s V. Raglione, T. R. Floyd, R A. Hartwick., Anal. Chem. **1985**, 57, *p. 1559-1564*

[273] MicroSolve Technology; Cogent Specification (Online); http://www.microsolvtech.com/cogent_udc.asp

[274] PQRI Column Database, US Pharmacopeia Conventions (Online): http://www.usp.org/usp-nf/compendial-tools/pqri-approach-column-equiv-

[275] J. J. Gilroy, J. W. Dolan, L. R. Snyder, J Chromatogr A, **2003**, 1000 (1–2), *p. 757-778*

[276] H. Engelhardt, H. Müller. . J. Chromatogr., 218, **1981**, *p. 395*

[277] L. R. Snyder., J Chromatogr A., **1983**, 255, *p. 3-26.*

[278] H. Engelhardt, H. Löw, W. Götzinger. J. Chromatogr., 544, **1991**, *p. 371*

[279] G. B. Cox., J Chromatog A., **1993**, 656(1), *p.353-367*

[280] J. Köhler, D. B. Chase, R. D. Farlee, A. J. Vega, J. J. Kirkland, J Chromatogra., **1986**, 352, *p. 275*

[281] R. K. Iler, The Chemistry of Silica, *Wiley*, New York, **1979**.

[282] J. Glajch, J. J. Kirkland, J. Kohler., J. Chromatogra., **1987**, 384, *p. 81*

[283] G. B. Cox, R. W. Stout, J Chromatog A., **1987**, 384, *p.315-336*

[284] D. V. McCalley., J Chromatogr A, **2000**, 902, *p. 311–321*

[285] David R. Lide (Eds.) CRC Handbook of Chemistry and Physics, Internet Version, **2007**, 87th ed., Taylor and Francis, Boca Raton, FL.

[286] N. H. Davies, M. R. Euerby, D. V. McCalley., J Chromatogr A, 1119, **2006**, *p. 11-19*

[287] L. R. Snyder, J. J. Kirkland, J. L. Glajch., Practical HPLC Method Development, **1997**, Wiley: New York

[288] S. M. C. Buckenmaier, D. V. McCalley, M. R. Euerby., Anal Chem, 74, **2002**, *p. 4672-4681*

[289] J. J. van Deemter, F. J. Zuiderweg, A. Klinkenberg.,. *Chem. Eng. Sci.*, 5, **1956**, *p. 271*

[290] LC-GC Chrom Academy, *Crawford Scientific*

[291] U. D. Neue, H. J. Kuss, Chromatogr A, 1217(24), **2010**, *p. 3794-3803*

[292] G. Engelhardt, H. Koller, NMR: basic principles and progress, **1994**, 31, *p. 1-29*

[293] P. Diehl, E. Fluck, H. Günther, R. Kosfeld, J. Seelig., NMR: basic principles and progress (eds), **1994**, *p. 34*

[294] F. Uhlig, H. Chr. Marsmann., ^{29}Si NMR Some Practical Aspects, Gelest Inc (Online); http://www.pascal-man.com/periodic-table/29Si.pdf

[295] R. Casasnovas, J. Frau, J. Ortega-Castro, A. Salvà, J. Donoso, F. Muñoz, J Molecular Structure, **2009**, THEOCHEM 912, *p. 5–12*

[296] Z. Liu., *Synthesis and reactions of novel silsesquioxane cages*, PhD Thesis, The Open University, **2004**.

[297] G. J. Kennedy and J. H. Knox, J. Chromatogr. Sci.,**1972**,10, *p.606*

[298] J. Huber, Chromatogr. A., **1976**, 126, *p. 401-420*

[299] F. Gritti, G. Guiochon, Anal Chem, **2006**, 78(15), *p. 5329-5347*

[300] J. C. Giddings, *J. Chromatogr.*, **1961**, 5, *p.46.*

[301] G. Desmet, Anal Chem., **2008**, 80, *p. 8076-8088*

[302] K. Broeckhaven, J. Chromatogr. A., **2009**, 1216, *p.1325-1337*

[303] R. Shalliker, 2013, Active Flow Technology Presenting the 'Infinite Diameter Column' in Curtain Flow Mode of Operation, *HPLC2013 presentation,* **2013**

[304] U. D. Neue, J. Chromatogr. A., **1990**, 535, *p.189-190*

[305] F. Gritti, G. Guiochon, , J. Chromatogr. A., **2010**, 1217, *p. 3000-3012*

[306] G. Desmet, S. Deridder, J. Chromatogr. A., **2011**, 1218, *p. 32-45*

[307] S. Deridder, G. Desmet, J. Chromatogr. A., **2012**, 1227, *p. 194- 202*

[308] G. Desmet, Anal Chem, **2008**, 90, *p. 8076-8088*

[309] F. Gritti, J. Chromatogr. A, **2011**, 1218, *p. 3476*

[310] A. Daneyko, A. Itzel, S. Khirevich, U. Tallarek, Anal Chem, **2011**, 83(10), *p. 3903–3910*

[311] J. J. Kirkland, J. Yau., US. Patent No. 4160728

[312] J. J. Kirkland, T.J. Langlois, J.J. DeStefano., Am. Lab., **2007**, 39, *p. 18–21*

[313] A. Daneyko, S. Khirevich, A. Höltzel, A. Seidel-Morgenstern, U. Tallarek, J. Chromatogr A, **2011**, 1218(45), *p. 8231-8248.*

[314] J. E. MacNair, K.C. Lewis, J.W. Jorgenson., Anal Chem, **1997**, 69(6), *p. 983-989.*

[315] B. A. Bidlingmeyer, L.B. Rogers, Sep. Sci., **1972**, 7, *p. 131*

[316] M. M. Fallas, N. Tanaka, S. Buckenmaier, D.V. McCalley., J Chromatogr A, **2013**, 1297, *p. 37-45*

[317] T. Ikegami, J. Ichimaru, W. Kajiwara, N. Nagasawa, K. Hosoya, N. Tanaka., J. Anal. Sci., **2007**, 23, *p. 109*

[318] G. Marrubini, B. E. C. Mendoza, G. Massolini, J. Sep. Sci., **2010**, 33, *p. 803*

[319] N. P. Dinh, T. Jonsson, K. Irgum., J. Chromatogr A, **2011**, 1218(35), *p. 5880-5891.*

[320] M. Lämmerhofer, M. Richter, J. Wu, R. Nogueira, W. Bicker, W. Lindner., J Separation Sci., **2008**, 31(14), *p. 2572-2588*

[321] Y. Guo, S. Gaiki., J Chromatogr A, **2011**, 1218(35), *p. 5920-5938.*

[322] T. Ikegami, N. Tanaka, HPLC 2013 Lecture, **2013**

[323] M. Chiacchia., *Biometric approach to silabe based namomaterials,* PhD Thesis, The Open University, **2012**.

APPENDIX

Appendix 1 Retention factor (k) and alpha (α) values for Nitro- and Methoxy-Benzene Characterisation for EPS phases

	k values			
	NB	DNB	TNB	Toluene
HyPurity Aquastar 50x2.1mm 3um	0.892	0.912	0.533	2.317
Platinum EPS C18 50x2.1mm 3um	0.607	0.603	0.366	1.333
Aquity HSS SB C18 50x2.1mm 3.5um	1.703	1.575	1.381	4.040
Zorbax SB AQ 50x2.1mm 3.5um	1.300	1.276	0.956	2.260
Alltima HP C18 EPS 50x2.1mm 3um	0.376	0.378	0.244	0.846

	MB	1,2-DMB	1,3-DMB	1,4-DMB	1,2,3-TMB	1,2,4-TMB	1,3,5-TMB	Toluene
HyPurity Aquastar 50x2.1mm 3um	1.258	1.210	0.777	1.108	1.484	0.919	1.487	2.352
Platinum EPS C18 50x2.1mm 3um	0.762	0.595	0.521	0.684	0.871	0.650	0.962	1.337
Aquity HSS SB C18 50x2.1mm 3.5um	2.096	0.731	1.279	2.079	2.826	2.025	2.826	4.036
Zorbax SB AQ 50x2.1mm 3.5um	1.337	1.208	1.814	1.609	1.022	1.313	2.396	2.279
Alltima HP C18 EPS 50x2.1mm 3um	0.503	0.478	0.469	0.451	0.338	0.403	0.499	0.854

	α values							
	TNB/NB	DNB/Tol	TNB/Tol	1,2,3-TMB/T	1,2,3-TMB/MB	1,2,3/1,2,4-TMB	1,4-DMB/MB	1,2-DMB/MB
HyPurity Aquastar 50x2.1mm 3um	0.598	0.394	0.230	0.631	1.180	1.615	0.881	0.962
Platinum EPS C18 50x2.1mm 3um	0.602	0.453	0.274	0.651	1.142	1.339	0.897	0.780
Aquity HSS SB C18 50x2.1mm 3.5um	0.811	0.390	0.342	0.700	1.349	1.396	0.992	0.349
Zorbax SB AQ 50x2.1mm 3.5um	0.735	0.565	0.423	0.448	0.765	0.778	1.203	0.904
Alltima HP C18 EPS 50x2.1mm 3um	0.648	0.447	0.288	0.396	0.673	0.839	0.897	0.951

Appendix 2 Comparison of alpha values for Nitro- and Methoxy-Benzene Characterisation for EPS phases

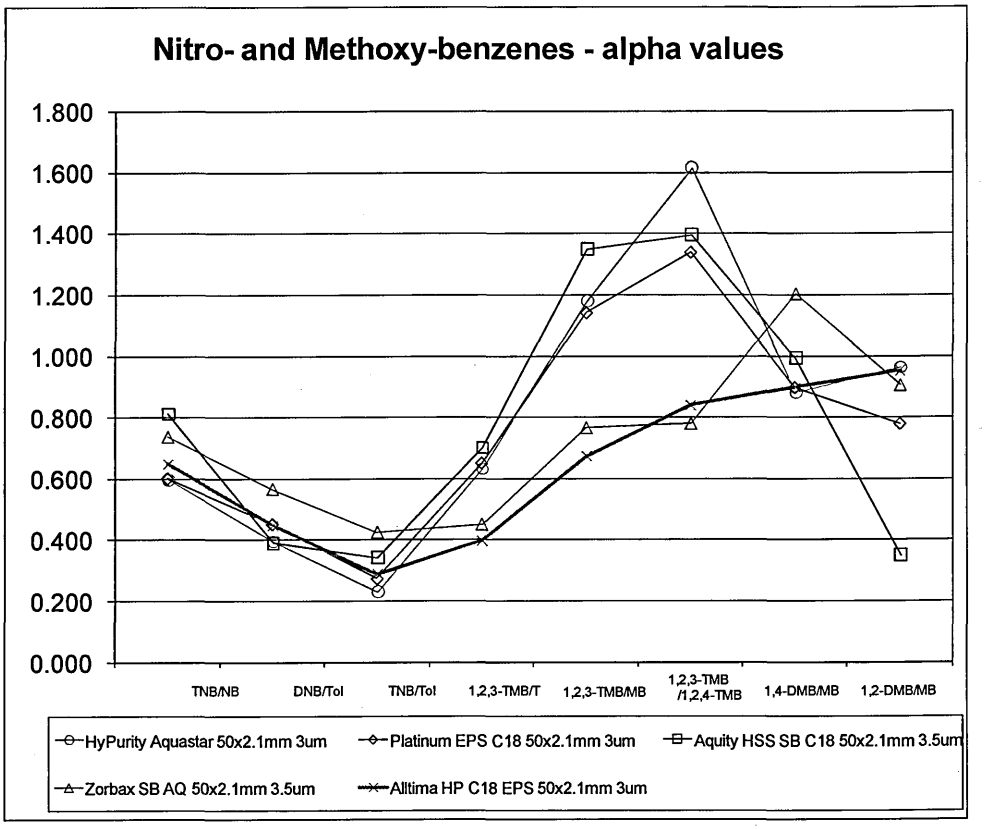

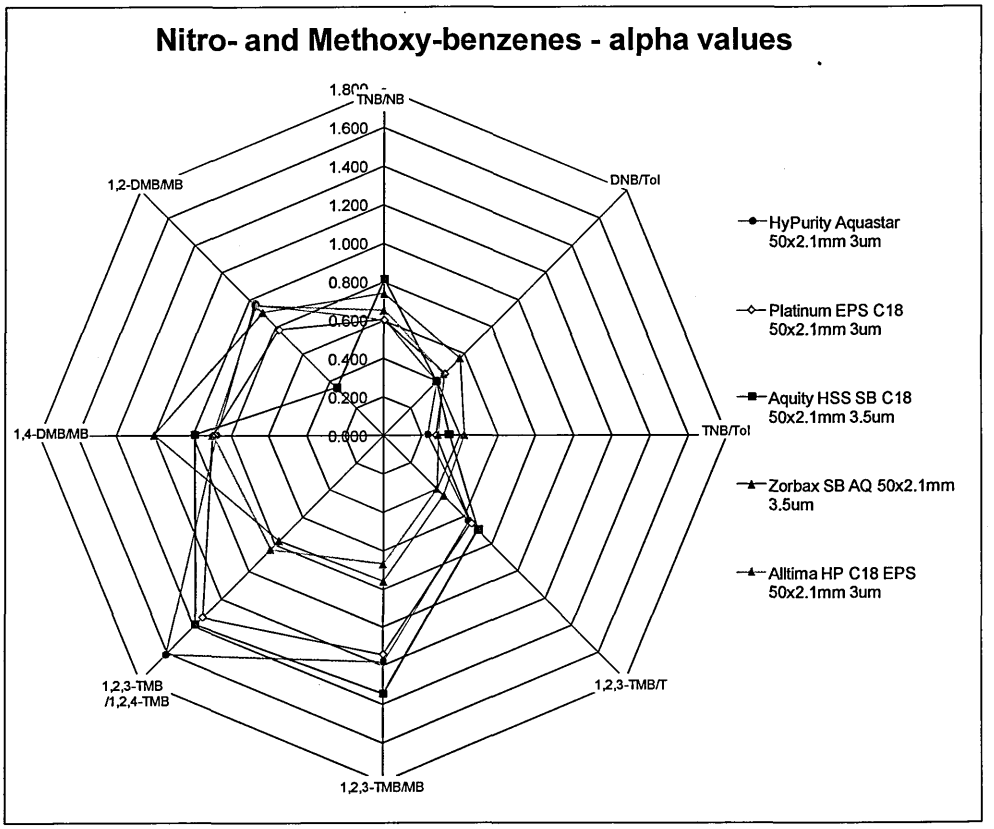

Appendix 3 **Retention factor (k) and alpha (α) values for Dinitro Benzene Characterisation for EPS phases**

	k' values			
	1,2-DNB	**1,3-DNB**	**1,4-DNB**	**Toluene**
HyPurity Aquastar 50x2.1mm 3um	1.476	1.456	1.165	4.636
Platinum EPS C18 50x2.1mm 3um	0.940	0.931	0.735	2.439
Aquity HSS SB C18 50x2.1mm 3.5um	2.721	2.843	2.227	8.088
Zorbax SB AQ 50x2.1mm 3.5um	2.319	2.222	2.004	4.486
Alltima HP C18 EPS 50x2.1mm 3um	0.471	0.591	0.601	1.582

	α values					
	1,2-DNB/T	**1,3-DNB/T**	**1,4-DNB/T**	**1,4-DNB/ 1,2-DNB**	**1,3-DNB/ 1,2-DNB**	**1,4-DNB/ 1,3-DNB**
HyPurity Aquastar 50x2.1mm 3um	0.318	0.314	0.251	0.790	0.987	0.800
Platinum EPS C18 50x2.1mm 3um	0.385	0.382	0.301	0.782	0.991	0.789
Aquity HSS SB C18 50x2.1mm 3.5um	0.336	0.351	0.275	0.818	1.045	0.783
Zorbax SB AQ 50x2.1mm 3.5um	0.517	0.495	0.447	0.864	0.958	0.902
Alltima HP C18 EPS 50x2.1mm 3um	0.298	0.374	0.380	1.277	1.255	1.017

Appendix 4 **Comparison of alpha values for Dinitro Benzene Characterisation for Competitor EPS phases**

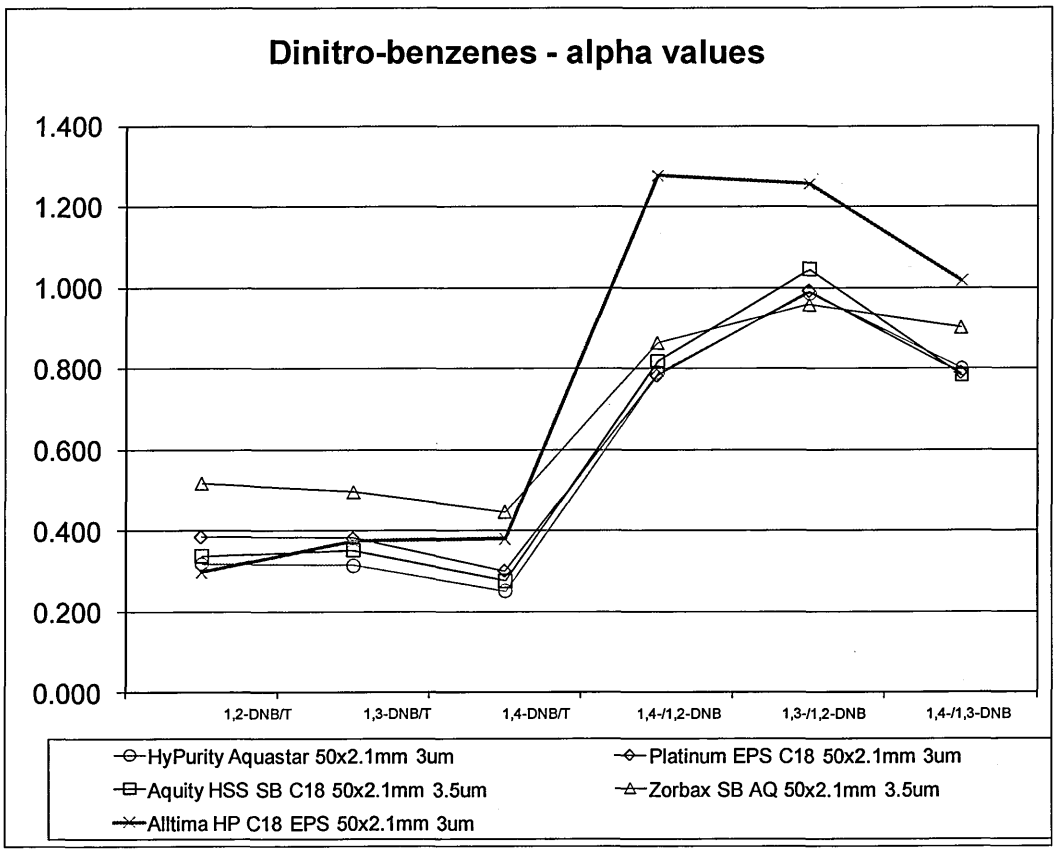

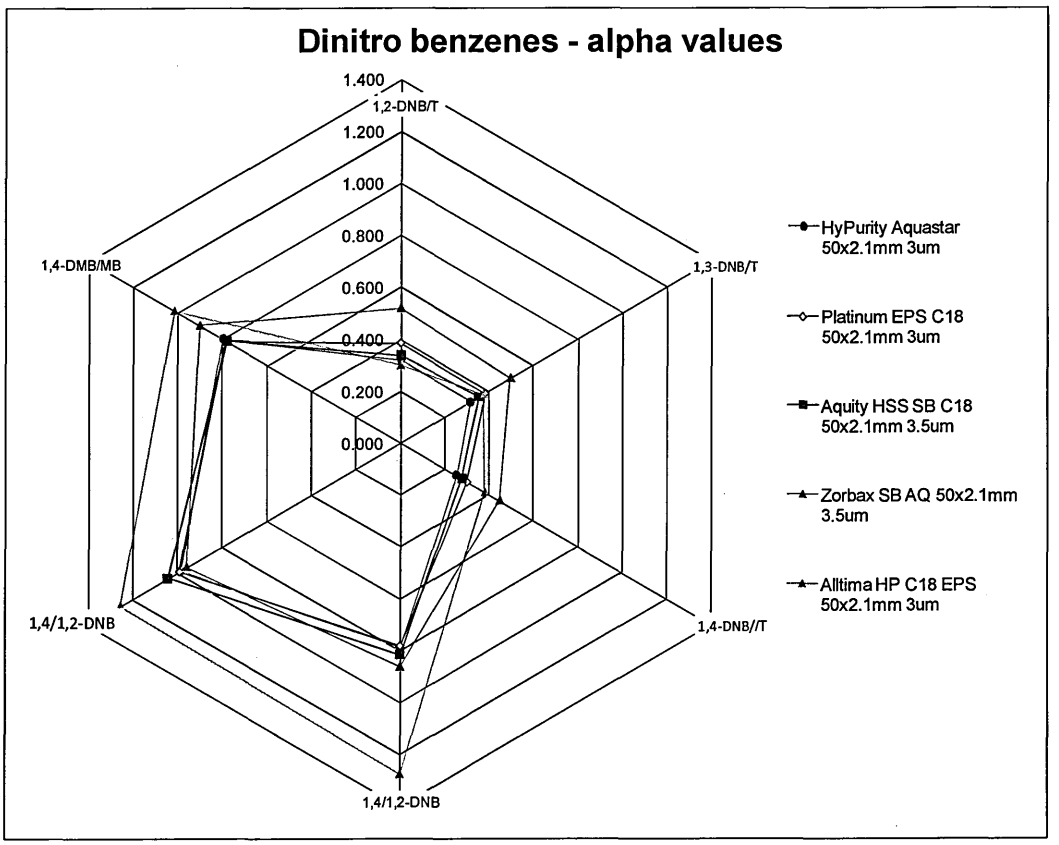

Appendix 5 Alpha Values of Acid Characterisation for Competitor EPS phases

Column characterization spreadsheet for acidic analytes - EPS Competitors
C:\Chem32\1\DATA\110509 (1200MD)

5 mM KH_2PO_4 pH 2.5 in water / MeOH (65:35 v/v)

Analytes	Apparent retention factors				
	HyPurity Aquastar 3um	Platinum C18 EPS 3um	Aquity HSS SB C18 3.5um	Zorbax SB-AQ 3.5um	Alltima HP C18 EPS 3um
4-Hydroxybenzoic acid (ρ)	0.52	0.38	0.80	1.00	0.27
3-Hydroxybenzoic acid (*m*)	0.61	0.45	0.95	1.10	0.32
Phenol (P)	0.87	0.53	1.31	1.19	0.36
Sorbic acid (S)	1.56	0.96	2.67	2.56	0.62
Benzoic acid (BN)	1.53	0.93	2.56	2.36	0.61
2-Hydroxybenzoic acid (σ)	1.23	0.72	2.04	1.97	0.50
3-Phenylpropionic acid (HC)	2.59	1.43	4.32	3.79	0.95
Dimethylphthalate (DMP)	2.59	1.70	5.07	5.43	1.02
Cinnamic acid (CA)	3.43	2.04	6.13	5.72	1.29
4-Hydroxybenzoic acid propyl ester (PP)	6.34	3.89	12.67	14.98	2.46

5 mM KH_2PO_4 pH 2.5 in water / MeOH (35:65 v/v)

Analytes	Apparent retention factors				
	HyPurity Aquastar 3um	Platinum C18 EPS 3um	Aquity HSS SB C18 3.5um	Zorbax SB-AQ 3.5um	Alltima HP C18 EPS 3um
Benzene sulphonic acid (BSA)	0.03	-0.05	0.05	0.08	0.01
Benzylalcohol (BA)	0.32	0.12	0.49	0.28	0.12
Phenol (P)	0.16	0.06	0.31	0.27	0.06
Toluene (Tl)	0.81	0.48	1.45	0.79	0.31

5 mM KH_2PO_4 pH 2.5 in water / MeOH (65:35 v/v)

	Selectivity factors						
	$\alpha_{P/DMP}$	$\alpha_{CA/HC}$	$\alpha_{\sigma/BN}$	$\alpha_{PP/P}$	$\alpha_{BN/S}$	$\alpha_{\sigma/\rho}$	$\alpha_{\sigma/m}$
HyPurity Aquastar 3um	0.34	1.33	0.81	7.27	0.98	2.38	2.00
Platinum C18 EPS 3um	0.31	1.43	0.77	7.41	0.97	1.90	1.58
Aquity HSS SB C18 3.5um	0.26	1.42	0.80	9.65	0.96	2.54	2.14
Zorbax SB-AQ 3.5um	0.22	1.51	0.83	12.64	0.92	1.96	1.79
Alltima HP C18 EPS 3um	0.35	1.35	0.81	6.87	0.99	1.86	1.58

5 mM KH_2PO_4 pH 2.5 in water / MeOH (35:65 v/v)

	Selectivity factors			
	$\alpha_{P/BA}$	$\alpha_{P/Tl}$	$\alpha_{BA/Tl}$	$\alpha_{BSA/Tl}$
HyPurity Aquastar 3um	0.49	0.19	0.39	0.03
Platinum C18 EPS 3um	0.49	0.12	0.25	-0.11
Aquity HSS SB C18 3.5um	0.64	0.22	0.34	0.04
Zorbax SB-AQ 3.5um	0.95	0.34	0.35	0.11
Alltima HP C18 EPS 3um	0.52	0.20	0.39	0.03

Appendix 6 Comparison Acid Characterisation for EPS phases

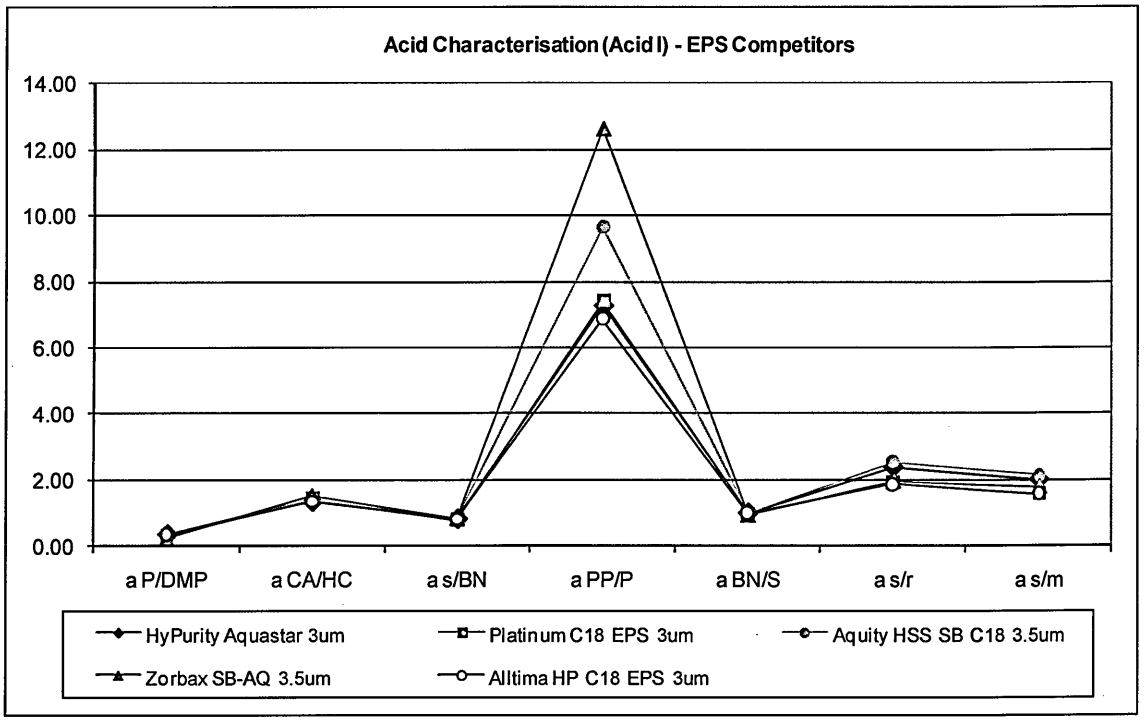

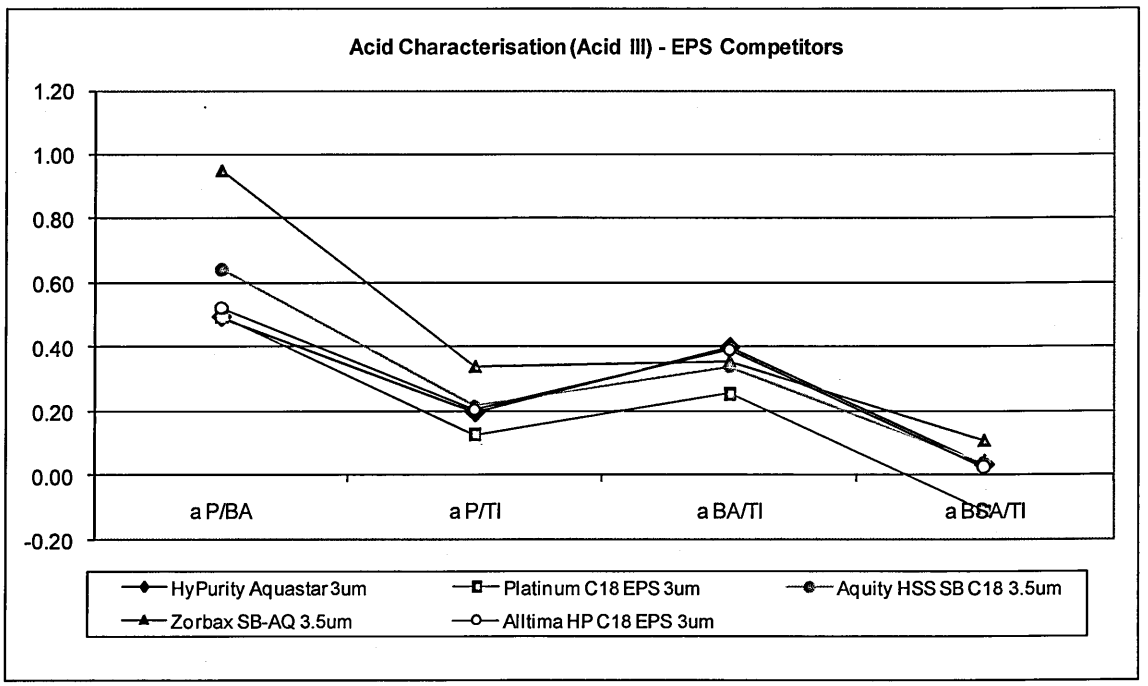

Appendix 7 Alpha Values of QC Test Characterisation for EPS phases

Phase: HyPurity Aquastar S/N 18968-39 # 6430

Analytes	t_R (min)	k
$t_{o\ (water)}$	0.74	
Benzene sulphonic acid (BSA)	0.79	0.07
Pindolol (Pin)	0.83	0.12
Caffeine (CA)	1.08	0.46
Phenol (P)	1.08	0.46
2-Hydroxybenzoic acid (HBA)	1.22	0.66
Piroxicam (Pir)	2.03	1.75
Carvedilol (Car)	2.80	2.80

Selectivity factors						
$a_{Pin/BSA}$	$a_{CA/BSA}$	$a_{P/CA}$	$a_{HBA/P}$	$a_{Car/Pir}$	$a_{Car/HBA}$	$a_{Car/BSA}/100$
1.67	6.22	1.00	1.42	1.60	4.25	0.38

C:\Chem32\1\DATA\110512-SB\QC000001-4 (1200MD)

Phase: Platinum EPS C18 S/N 18964-39 # 29-176

Analytes	t_R (min)	k
$t_{o\ (water)}$	0.72	
Benzene sulphonic acid (BSA)	0.67	-0.06
Pindolol (Pin)	0.96	0.35
Caffeine (CA)	1.08	0.51
Phenol (P)	0.92	0.29
2-Hydroxybenzoic acid (HBA)	1.08	0.51
Piroxicam (Pir)	1.98	1.77
Carvedilol (Car)	2.43	2.40

Selectivity factors						
$a_{Pin/BSA}$	$a_{CA/BSA}$	$a_{P/CA}$	$a_{HBA/P}$	$a_{Car/Pir}$	$a_{Car/HBA}$	$a_{Car/BSA}/100$
-5.51	-8.18	0.56	1.78	1.36	4.66	-0.38

C:\Chem32\1\DATA\110512-SB\QC000006-10 (1200MD)

Phase: Aquity HSS SB C18 S/N 18985-39

Analytes	t_R (min)	k
$t_{o\ (water)}$	0.69	
Benzene sulphonic acid (BSA)	0.76	0.10
Pindolol (Pin)	0.84	0.22
Caffeine (CA)	1.55	1.25
Phenol (P)	1.27	0.84
2-Hydroxybenzoic acid (HBA)	1.55	1.25
Piroxicam (Pir)	2.96	3.29
Carvedilol (Car)	4.67	5.76

Selectivity factors						
$a_{Pin/BSA}$	$a_{CA/BSA}$	$a_{P/CA}$	$a_{HBA/P}$	$a_{Car/Pir}$	$a_{Car/HBA}$	$a_{Car/BSA}/100$
2.14	12.15	0.67	1.49	1.75	4.61	0.56

C:\Chem32\1\DATA\110512-SB\QC000012-16 (1200MD)

Phase: Zorbax SB AQ S/N 18984-39 # B10313

Analytes	t_R (min)	k
$t_{o\ (water)}$	0.66	
Benzene sulphonic acid (BSA)	0.78	0.17
Pindolol (Pin)	0.78	0.17
Caffeine (CA)	1.64	1.48
Phenol (P)	1.12	0.68
2-Hydroxybenzoic acid (HBA)	1.38	1.08
Piroxicam (Pir)	2.20	2.31
Carvedilol (Car)	3.57	4.38

Selectivity factors						
$a_{Pin/BSA}$	$a_{CA/BSA}$	$a_{P/CA}$	$a_{HBA/P}$	$a_{Car/Pir}$	$a_{Car/HBA}$	$a_{Car/BSA}/100$
1.00	8.74	0.46	1.57	1.90	4.08	0.26

C:\Chem32\1\DATA\110512-SB\QC000018-22 (1200MD)

Phase: Alltima HP EPS C18 S/N 18962-39 # 36-132

Analytes	t_R (min)	k
$t_{o\ (water)}$	0.77	
Benzene sulphonic acid (BSA)	0.84	0.09
Pindolol (Pin)	0.84	0.09
Caffeine (CA)	0.98	0.28
Phenol (P)	0.91	0.19
2-Hydroxybenzoic acid (HBA)	0.98	0.28
Piroxicam (Pir)	1.38	0.80
Carvedilol (Car)	1.61	1.10

Selectivity factors						
$a_{Pin/BSA}$	$a_{CA/BSA}$	$a_{P/CA}$	$a_{HBA/P}$	$a_{Car/Pir}$	$a_{Car/HBA}$	$a_{Car/BSA}/100$
1.00	3.12	0.69	1.45	1.37	3.92	0.12

C:\Chem32\1\DATA\110512-SB\QC000024-28 (1200MD)

Appendix 8 Chromatograms of QC Tests for EPS phases

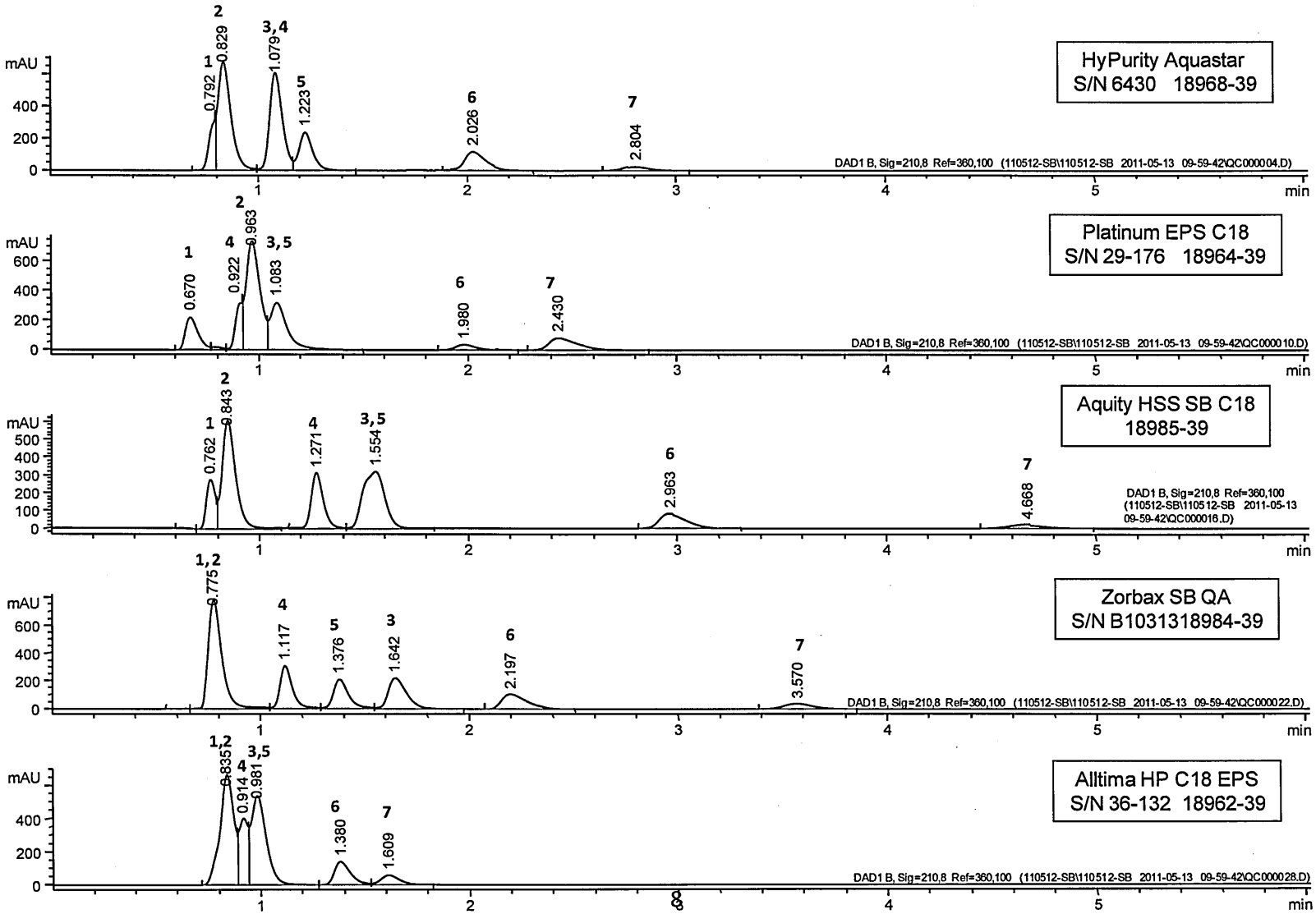

1. Benzenesulfonic acid, 2. Pindolol, 3. Caffeine , 4. Phenol, 5. 2-Hydroxybenzoic acid, 6. Piroxicam, 7. Carvedilol

Appendix 9 Comparison of alpha values of QC Tests for EPS phases

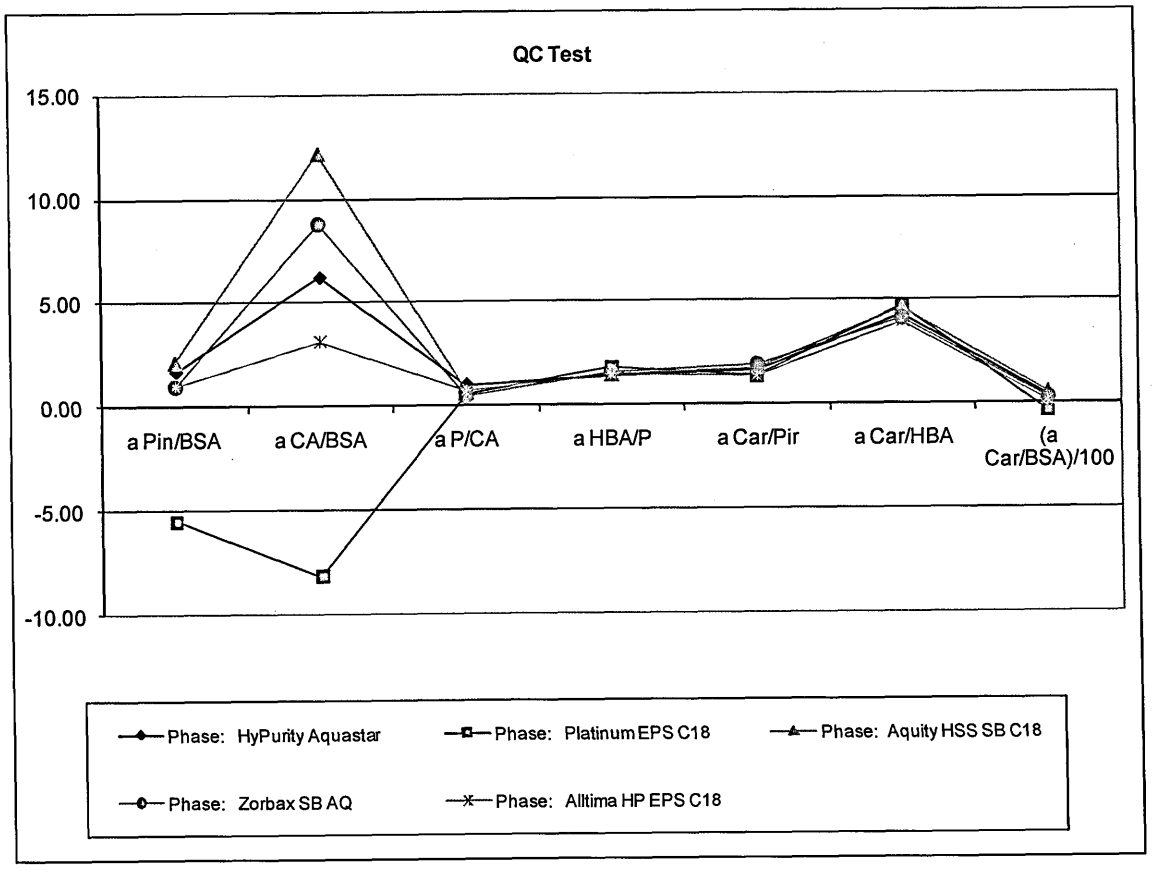

Appendix 10 QC toluene data for 100 Compounds in 0.03% FA in MeCN

Alltima HP EPS				
	R_t	Area	Peak width	Symmetry
Toluene 1	1.732	45.5	0.0298	0.929
Toluene 2	1.727	46.1	0.0309	0.93
Toluene 3	1.726	45.2	0.0321	0.908
Toluene 4	1.726	46.0	0.0298	0.943
Toluene 5	1.727	46.7	0.0308	0.935
Toluene 6	1.726	48.0	0.0299	0.947
Mean	**1.727**	**46.250**	**0.031**	**0.932**
SD	0.0023	1.0015	0.0009	0.0137
RSD (%)	**0.135**	**2.165**	**2.977**	**1.474**

ACE 3 C18				
	R_t	Area	Peak width	Symmetry
Toluene 1	3.083	42.2	0.0241	0.916
Toluene 2	3.081	41.9	0.0254	0.92
Toluene 3	3.078	41.5	0.0254	0.912
Toluene 4	3.079	41.5	0.0244	0.913
Toluene 5	3.083	42.6	0.0247	0.924
Toluene 6	3.079	43.5	0.0244	0.907
Mean	**3.081**	**42.2**	**0.025**	**0.915**
SD	0.0022	0.7642	0.0006	0.0061
RSD (%)	**0.070**	**1.811**	**2.224**	**0.662**

Platinum EPS C18				
	R_t	Area	Peak width	Symmetry
Toluene 1	1.915	50.6	0.028	0.851
Toluene 2	1.913	50.7	0.0282	0.85
Toluene 3	1.911	50.9	0.0283	0.845
Toluene 4	1.911	50.5	0.0282	0.858
Toluene 5	1.911	51.4	0.0282	0.843
Toluene 6	1.912	50.8	0.0283	0.857
Mean	**1.912**	**50.817**	**0.028**	**0.851**
SD	0.0016	0.3189	0.0001	0.0061
RSD (%)	**0.084**	**0.627**	**0.388**	**0.716**

Zorbax-SB AQ				
	R_t	Area	Peak width	Symmetry
Toluene 1	2.418	46.5	0.0271	0.954
Toluene 2	2.417	46.1	0.0258	1.001
Toluene 3	2.417	46.0	0.0258	1.000
Toluene 4	2.415	46.8	0.0271	0.942
Toluene 5	2.416	46.4	0.0259	0.977
Toluene 6	2.415	47.4	0.0269	0.978
Mean	**2.416**	**46.533**	**0.026**	**0.975**
SD	0.0012	0.5125	0.0007	0.0238
RSD (%)	**0.050**	**1.101**	**2.506**	**2.445**

X-Select HSS C18				
	R_t	Area	Peak width	Symmetry
Toluene 1	2.73	48.9	0.0244	0.911
Toluene 2	2.723	48.5	0.0242	0.911
Toluene 3	2.722	48.6	0.0253	0.923
Toluene 4	2.721	47.4	0.0244	0.932
Toluene 5	2.72	49.4	0.0248	0.867
Toluene 6	2.72	49.9	0.0246	0.917
Mean	**2.723**	**48.783**	**0.025**	**0.910**
SD	0.0038	0.8565	0.0004	0.0226
RSD (%)	**0.139**	**1.756**	**1.592**	**2.483**

HyPURITY Aquastar				
	R_t	Area	Peak width	Symmetry
Toluene 1	2.415	50.100	0.025	0.913
Toluene 2	2.398	51.500	0.027	0.893
Toluene 3	2.401	52.200	0.026	0.912
Toluene 4	2.399	51.500	0.026	0.916
Toluene 5	2.399	52.4	0.027	0.939
Tolene 6	2.397	50.900	0.026	0.965
Mean	**2.402**	**51.433**	**0.026**	**0.923**
SD	0.0067	0.8477	0.0008	0.0253
RSD (%)	**0.281**	**1.648**	**3.168**	**2.737**

Appendix 11 QC toluene data for 100 Compounds in 0.03% FA in MeOH

Alltima HP EPS				
	Rt	Area	Peak width	Symmetry
Toluene 1	1.928	36.6	0.041	0.807
Toluene 2	1.924	36.9	0.040	0.807
Toluene 3	1.925	37.6	0.040	0.815
Toluene 4	1.927	36.6	0.040	0.812
Toluene 5	1.928	37.2	0.040	0.814
Toluene 6	1.924	42.1	0.040	0.804
Mean	1.926	37.8	0.040	0.810
SD	0.002	2.125	0.000	0.004
RSD (%)	**0.099**	**5.616**	**0.730**	**0.549**

ACE 3 C18				
	Rt	Area	Peak width	Symmetry
Toluene 1	3.626	33.3	0.028	0.913
Toluene 2	3.629	33.2	0.028	0.925
Toluene 3	3.630	33.6	0.027	0.911
Toluene 4	3.630	33.1	0.028	0.934
Toluene 5	3.628	34.2	0.028	0.937
Toluene 6	3.627	38.0	0.027	0.922
Mean	3.628	34.2	0.027	0.924
SD	0.002	1.888	0.000	0.011
RSD (%)	**0.045**	**5.514**	**0.497**	**1.149**

Platinum EPS C18				
	Rt	Area	Peak width	Symmetry
Toluene 1	2.177	41.9	0.038	0.800
Toluene 2	2.180	40.9	0.038	0.804
Toluene 3	2.180	41.7	0.037	0.802
Toluene 4	2.178	41.2	0.037	0.801
Toluene 5	2.184	42.1	0.037	0.805
Toluene 6	2.181	44.3	0.037	0.795
Mean	2.180	42.0	0.038	0.801
SD	0.002	1.204	0.000	0.004
RSD (%)	**0.112**	**2.866**	**1.058**	**0.442**

Zorbax-SB AQ				
	Rt	Area	Peak width	Symmetry
Toluene 1	2.677	37.9	0.033	0.726
Toluene 2	2.673	37.0	0.036	0.735
Toluene 3	2.668	38.0	0.033	0.742
Toluene 4	2.667	36.5	0.033	0.744
Toluene 5	2.663	37.9	0.033	0.735
Toluene 6	2.663	41.9	0.033	0.734
Mean	2.669	38.2	0.033	0.736
SD	0.006	1.910	0.001	0.006
RSD (%)	**0.209**	**5.000**	**4.233**	**0.872**

X-Select HSS C18				
	Rt	Area	Peak width	Symmetry
Toluene 1	3.155	38.9	0.029	0.903
Toluene 2	3.148	38.1	0.029	0.908
Toluene 3	3.145	38.5	0.029	0.913
Toluene 4	3.142	38.2	0.029	0.911
Toluene 5	3.140	38.9	0.030	0.913
Toluene 6	3.141	41.9	0.029	0.916
Mean	3.145	39.1	0.029	0.911
SD	0.006	1.420	0.000	0.005
RSD (%)	**0.179**	**3.634**	**1.373**	**0.504**

HyPURITY Aquastar				
	Rt	Area	Peak width	Symmetry
Toluene 1	2.792	42.6	0.034	0.866
Toluene 2	2.792	42.6	0.034	0.866
Toluene 3	2.791	43.0	0.035	0.894
Toluene 4	2.789	41.8	0.036	0.920
Toluene 5	2.785	43.1	0.037	0.929
Tolene 6	2.784	45.9	0.038	0.939
Mean	2.789	43.2	0.036	0.902
SD	0.004	1.415	0.001	0.032
RSD (%)	**0.127**	**3.278**	**3.964**	**3.532**

Appendix 12 QC toluene data for 100 Compounds in 20mM KH_2PO_4 in MeOH

Alltima HP EPS				
	Rt	Area	Peak width	Symmetry
Toluene 1	2.082	7.0	0.051	0.825
Toluene 2	2.068	6.4	0.052	0.795
Toluene 3	2.066	8.0	0.049	0.762
Toluene 4	2.064	7.9	0.053	0.810
Toluene 5	2.058	12.4	0.051	0.787
Toluene 6	2.060	8.2	0.052	0.798
Mean	2.066	8.3	0.051	0.796
SD	0.009	2.115	0.001	0.021
RSD (%)	**0.413**	**25.432**	**2.521**	**2.681**

ACE 3 C18				
	Rt	Area	Peak width	Symmetry
Toluene 1	4.479	6.2	0.042	0.969
Toluene 2	4.471	9.4	0.051	1.001
Toluene 3	4.478	7.3	0.041	0.974
Toluene 4	4.478	6.9	0.042	0.955
Toluene 5	4.479	11.3	0.041	1.025
Toluene 6	4.483	7.2	0.042	1.012
Mean	4.478	8.1	0.043	0.989
SD	0.004	1.919	0.004	0.027
RSD (%)	**0.087**	**23.840**	**8.613**	**2.768**

Platinum EPS C18				
	Rt	Area	Peak width	Symmetry
Toluene 1	2.506	8.3	0.049	0.909
Toluene 2	2.496	7.8	0.046	0.866
Toluene 3	2.495	9.5	0.048	0.940
Toluene 4	2.491	8.8	0.050	0.972
Toluene 5	2.487	14.0	0.050	0.944
Toluene 6	2.490	9.6	0.053	0.998
Mean	2.494	9.7	0.049	0.938
SD	0.007	2.232	0.002	0.047
RSD (%)	**0.268**	**23.092**	**4.328**	**4.959**

Zorbax-SB AQ				
	Rt	Area	Peak width	Symmetry
Toluene 1	3.079	7.2	0.042	0.848
Toluene 2	3.054	6.8	0.043	0.881
Toluene 3	3.047	8.4	0.044	0.842
Toluene 4	3.043	8.0	0.042	0.865
Toluene 5	3.038	12.6	0.047	0.830
Toluene 6	3.039	8.4	0.045	0.861
Mean	3.050	8.6	0.044	0.855
SD	0.015	2.080	0.002	0.018
RSD (%)	**0.504**	**24.281**	**4.132**	**2.128**

X-Select HSS C18				
	Rt	Area	Peak width	Symmetry
Toluene 1	3.667	7.1	0.046	1.032
Toluene 2	3.658	6.7	0.046	0.993
Toluene 3	3.655	8.4	0.043	0.973
Toluene 4	3.654	8.0	0.043	0.981
Toluene 5	3.653	12.4	0.044	0.996
Toluene 6	3.652	8.3	0.043	0.998
Mean	3.657	8.5	0.044	0.996
SD	0.006	2.035	0.001	0.020
RSD (%)	**0.152**	**23.989**	**3.253**	**2.040**

HyPURITY Aquastar				
	Rt	Area	Peak width	Symmetry
Toluene 1	3.262	8.2	0.050	0.792
Toluene 2	3.260	7.6	0.049	0.810
Toluene 3	3.261	9.7	0.049	0.833
Toluene 4	3.262	8.8	0.051	0.844
Toluene 5	3.259	13.6	0.050	0.876
Tolene 6	3.256	9.0	0.051	0.843
Mean	3.260	9.5	0.050	0.833
SD	0.002	2.140	0.001	0.029
RSD (%)	**0.070**	**22.561**	**1.833**	**3.512**

Appendix 13 Zorbax-SB AQ 100 Compounds in 0.03% v/v FA in MeOH

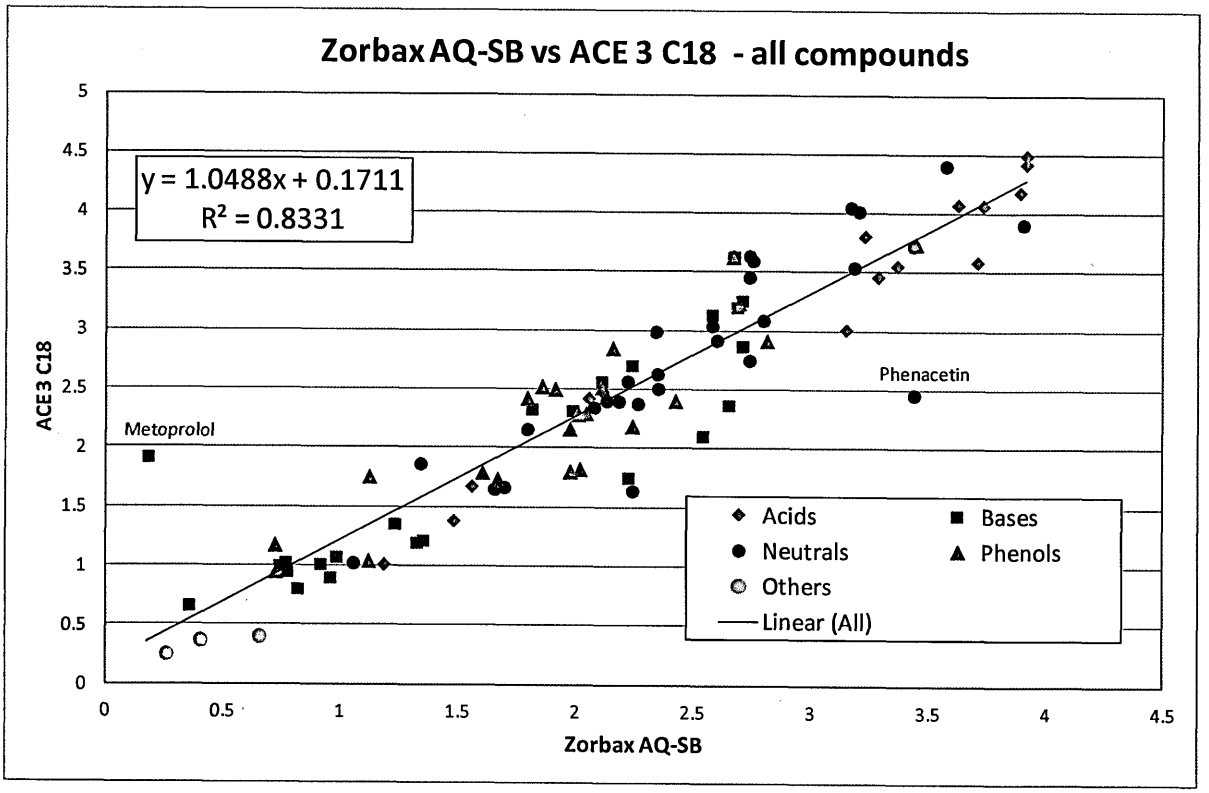

Appendix 14 XSelect HSS SB-C18 100 Compounds in 0.03% v/v FA in MeOH

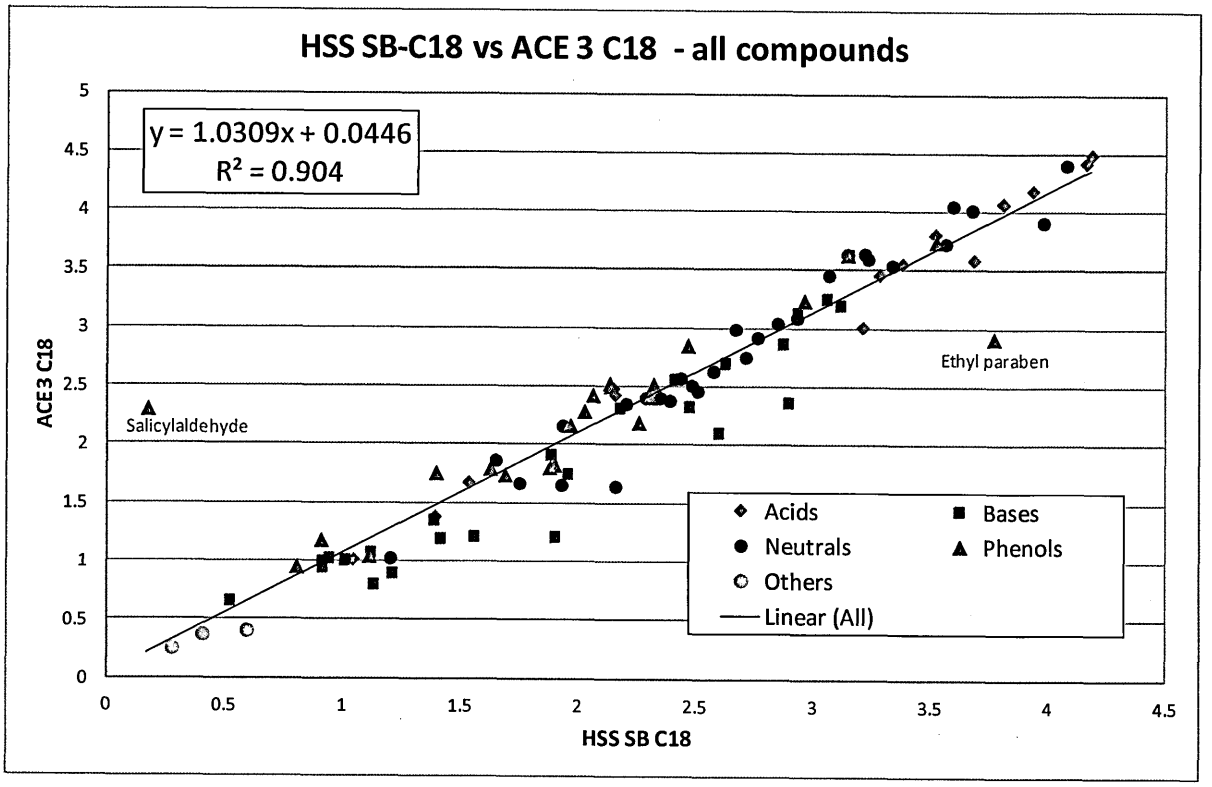

Appendix 15 Alltima HP C18 100 Compounds in 0.03% v/v FA in MeOH

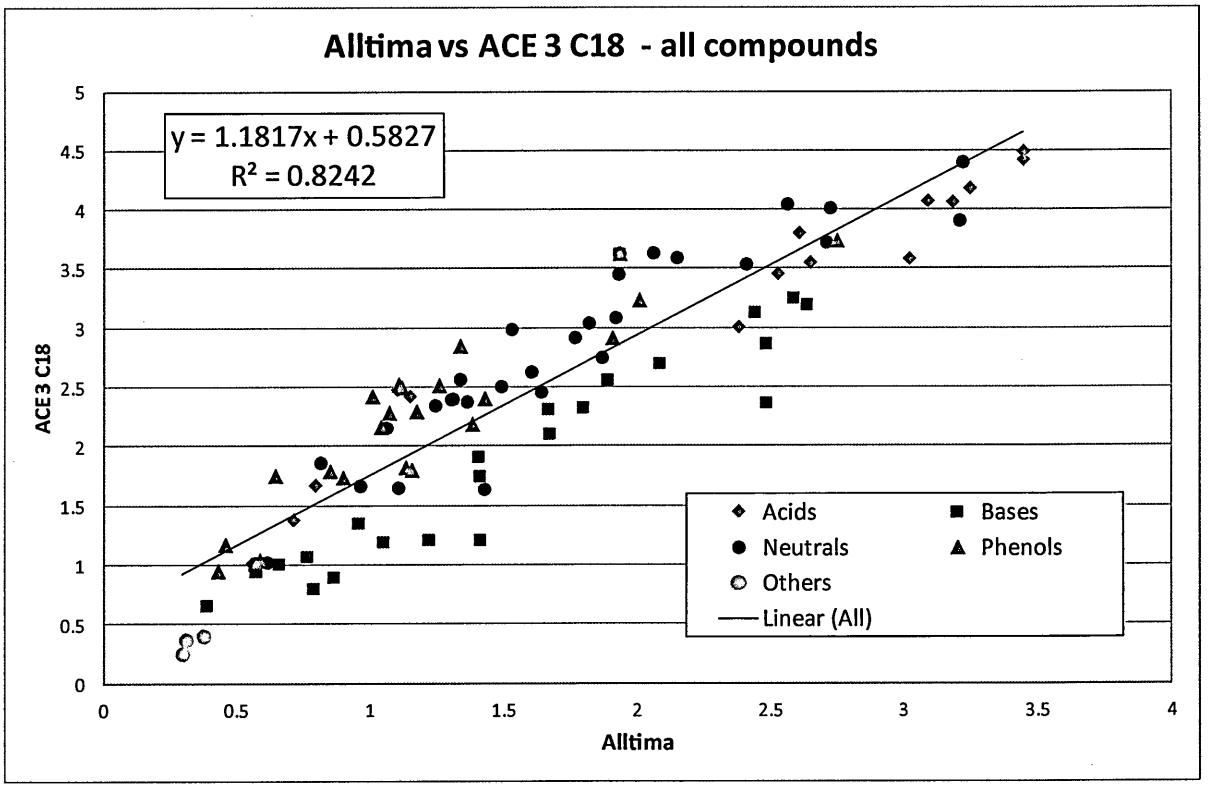

Appendix 16 Platinum EPS C18 100 Compounds in 0.03% v/v FA in MeOH

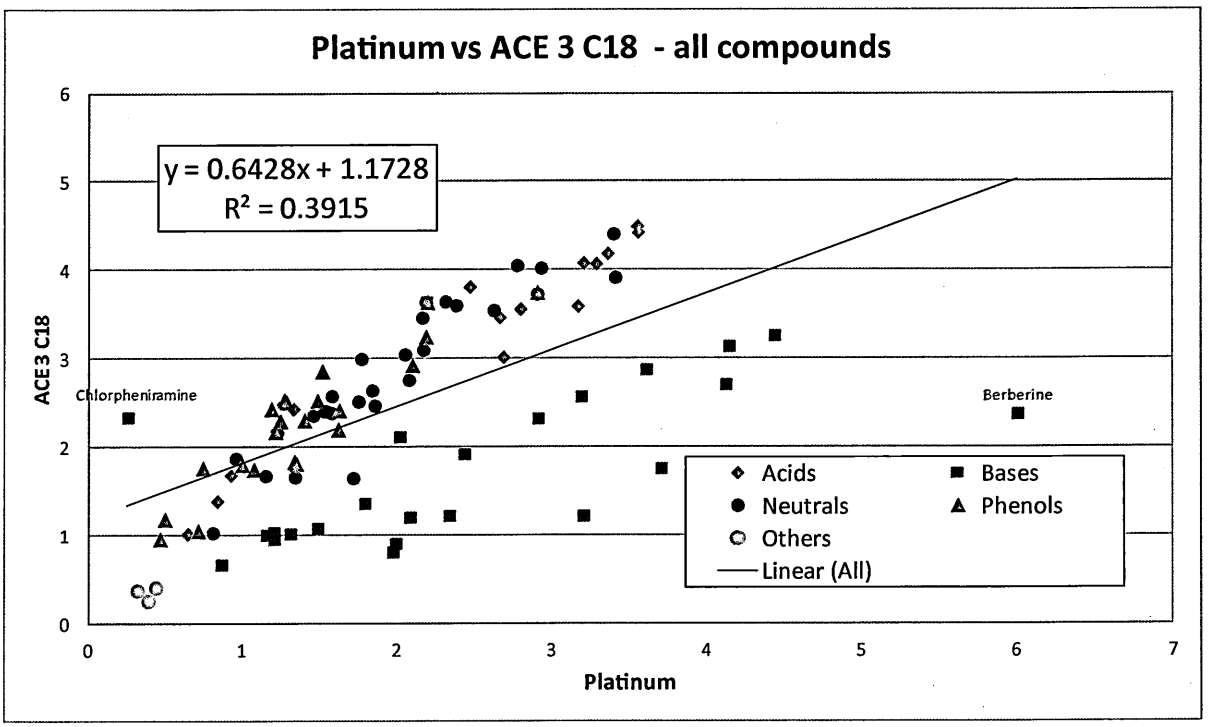

Appendix 17 HyPURITY Aquastar 100 Compounds in 0.03% v/v FA in MeOH

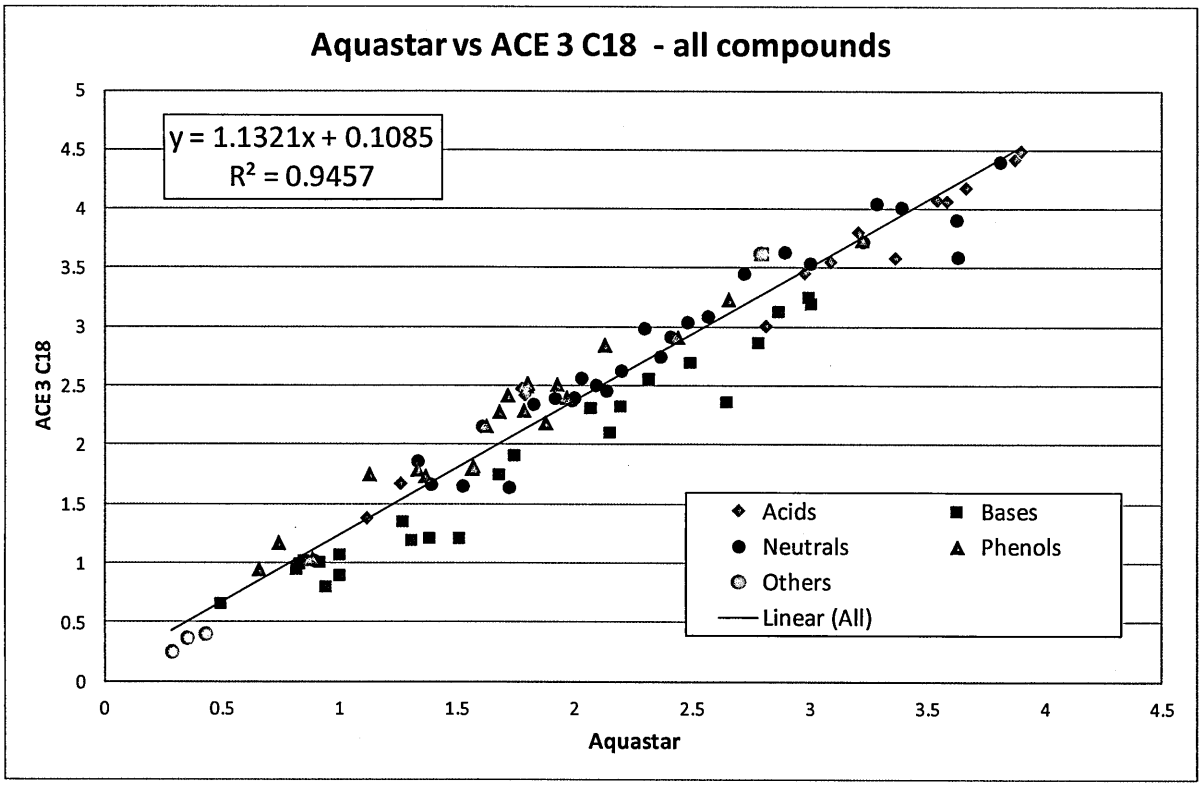

Appendix 18 Alltima HP C18 100 Compounds in 20mM KH_2PO_4 in MeOH

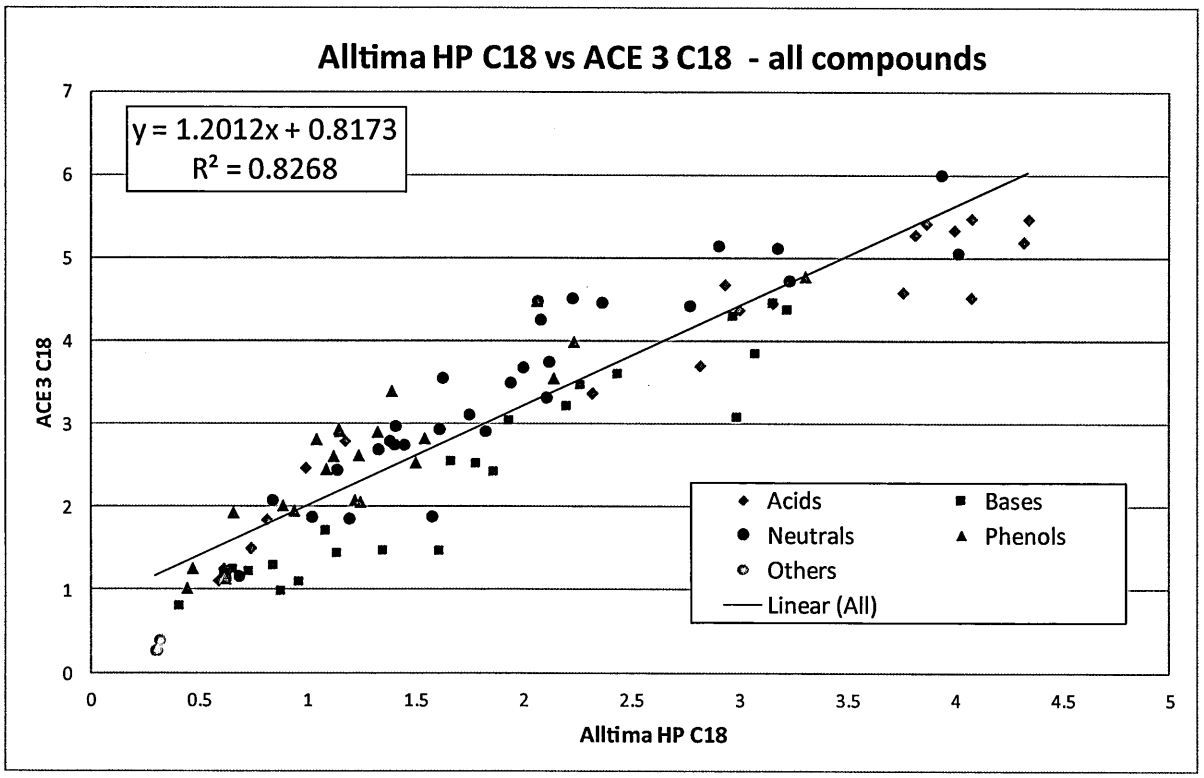

Appendix 19 Zorbax-SB AQ 100 Compounds in 20mM KH_2PO_4 in MeOH

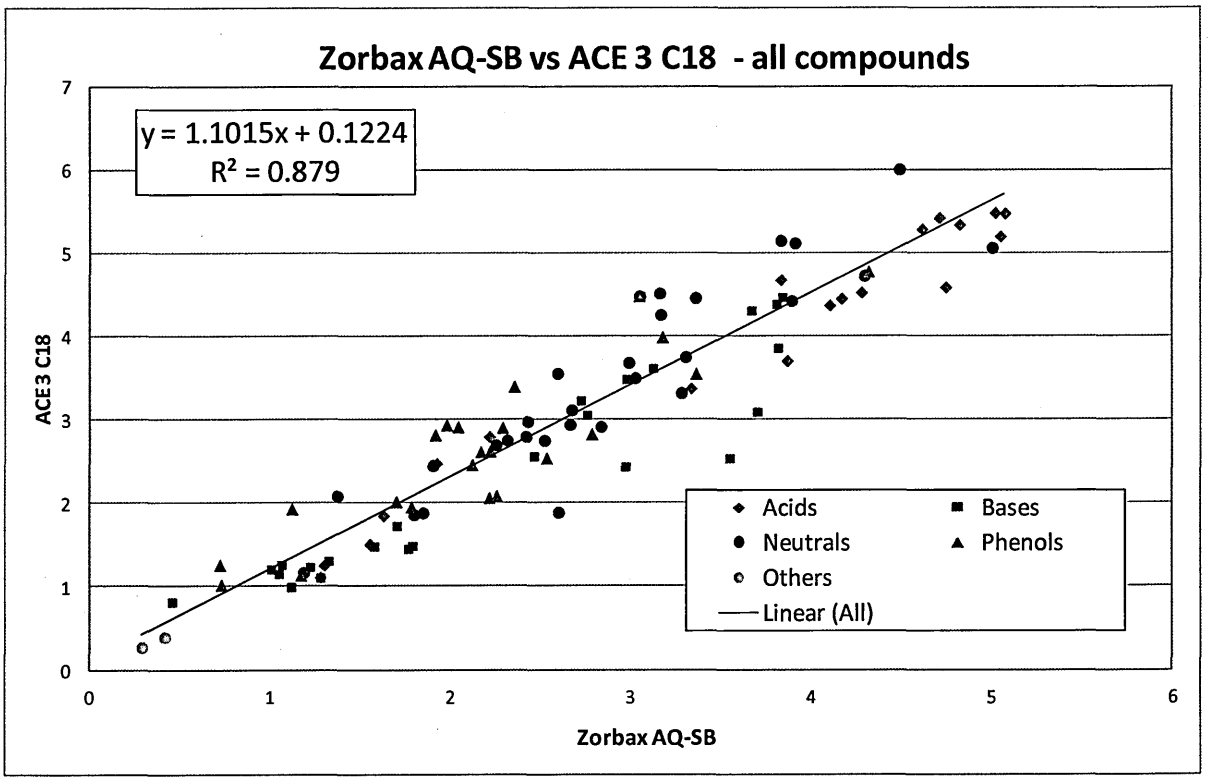

Appendix 20 XSelect HSS SB C18 100 Compounds in 20mM KH_2PO_4 in MeOH

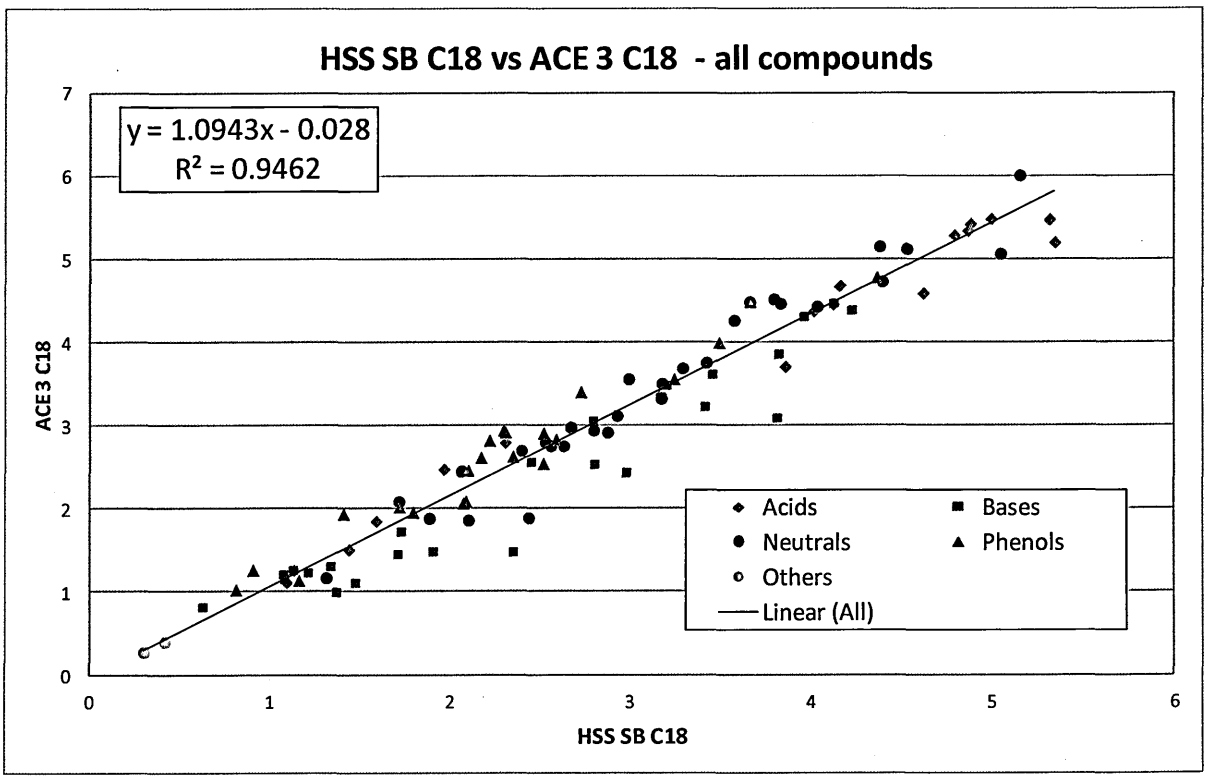

Appendix 21 Platinum EPS C18 100 Compounds in 20mM KH_2PO_4 in MeOH

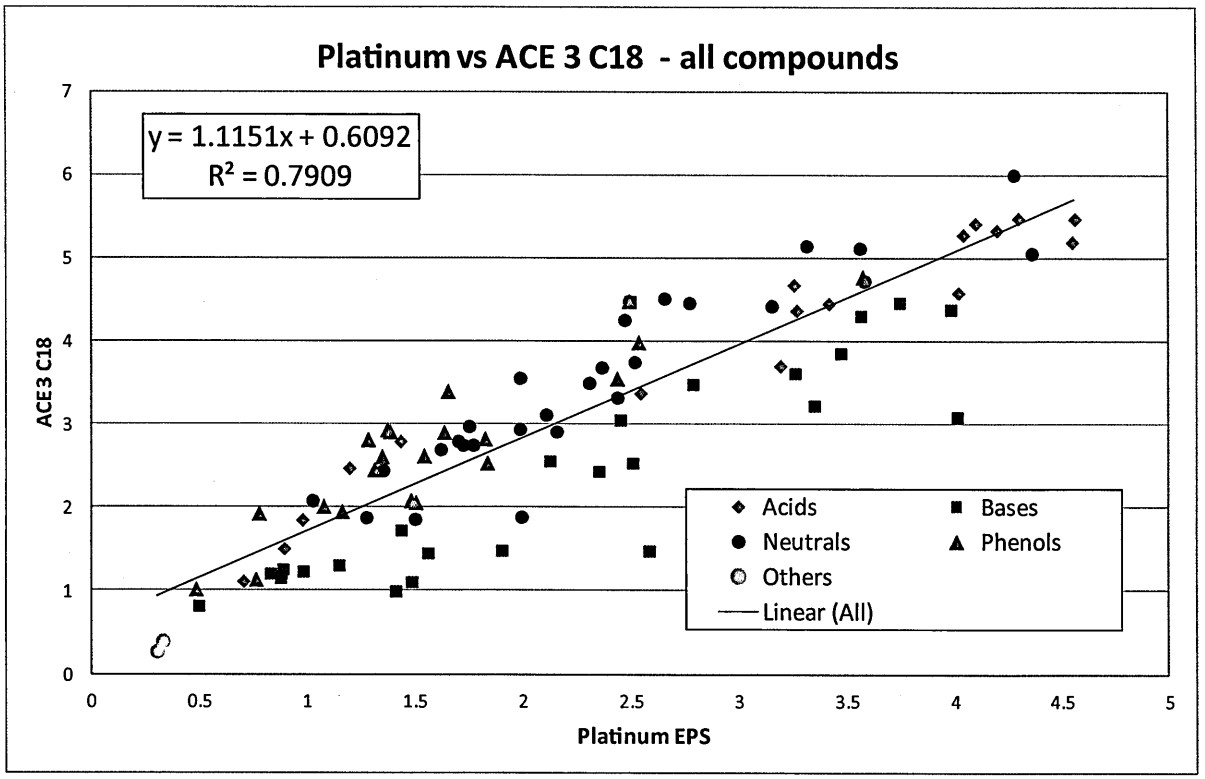

Appendix 22 HyPURITY Aquastar 100 Compounds in 20mM KH_2PO_4 in MeOH

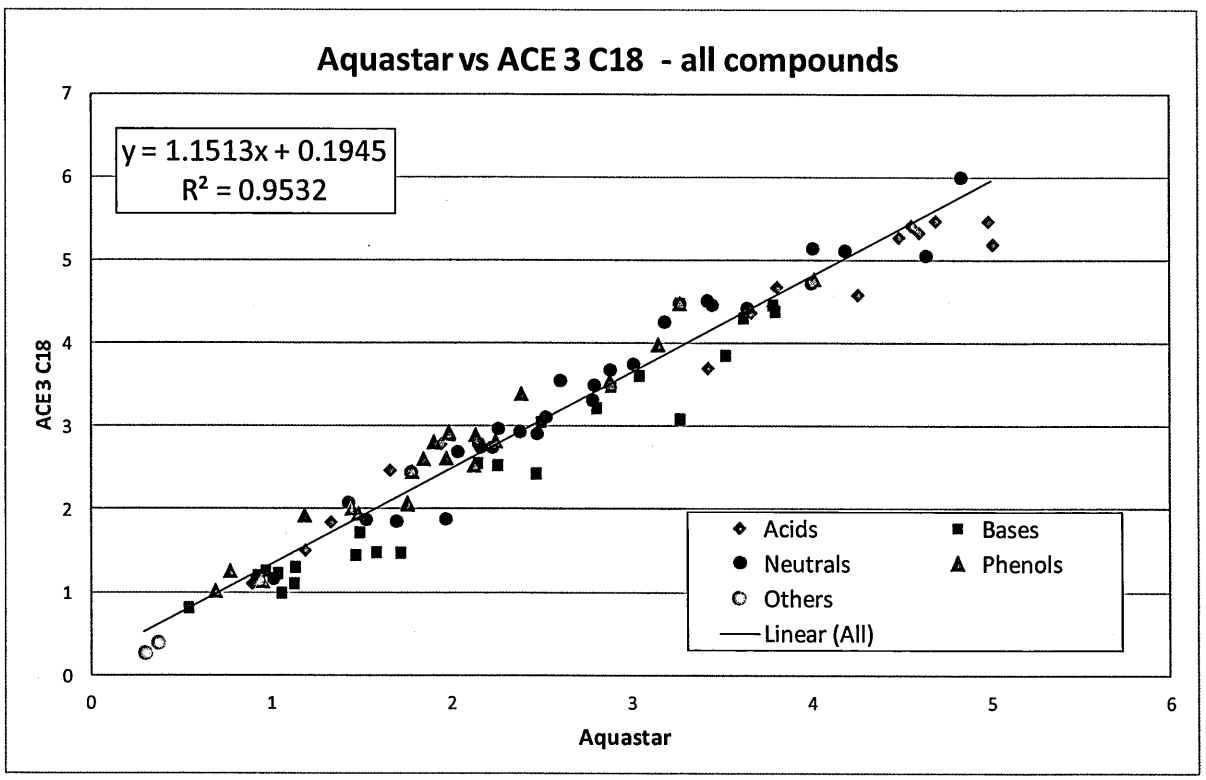

Appendix 23 Accelerated ACE 5 C18 stability results in 0.5% v/v TFA in 95:5 H_2O:MeOH

ACE 5 C18 Batch V10-2849 S/N: 18868-39 13/01/2011			ACE 5 C18 Batch V10-2849 S/N: 18869-39 24/01/2011			ACE 5 C18 Batch V10-2849 S/N: 18870-39 26/01/2011					
o-Cresol injections			**o-Cresol injections**			**o-Cresol injections**			**o-Cresol injections**		
Injection	RT/mins	% k'	Injection	RT/mins	% k'	Injection	RT/mins	% k'	Average	STD	RSD (%)
2	1.716	100.00	2	1.693	100.00	2	1.699	100.00	100.00	0.000	**0.000**
12	1.622	93.99	12	1.599	93.92	12	1.609	94.16	94.02	0.121	**0.128**
22	1.586	91.69	22	1.566	91.79	22	1.575	91.95	91.81	0.129	**0.141**
32	1.561	90.10	32	1.54	90.10	32	1.551	90.39	90.20	0.167	**0.186**
42	1.538	88.63	42	1.518	88.68	42	1.53	89.03	88.78	0.217	**0.244**
52	1.515	87.16	52	1.496	87.26	52	1.509	87.66	87.36	0.268	**0.306**
62	1.493	85.75	62	1.474	85.83	62	1.49	86.43	86.00	0.370	**0.430**
72	1.473	84.47	72	1.453	84.48	72	1.469	85.06	84.67	0.341	**0.403**
82	1.45	83.00	82	1.43	82.99	82	1.451	83.90	83.30	0.520	**0.624**
84	1.444	82.62	84	1.424	82.60	84	1.444	83.44	82.89	0.480	**0.579**

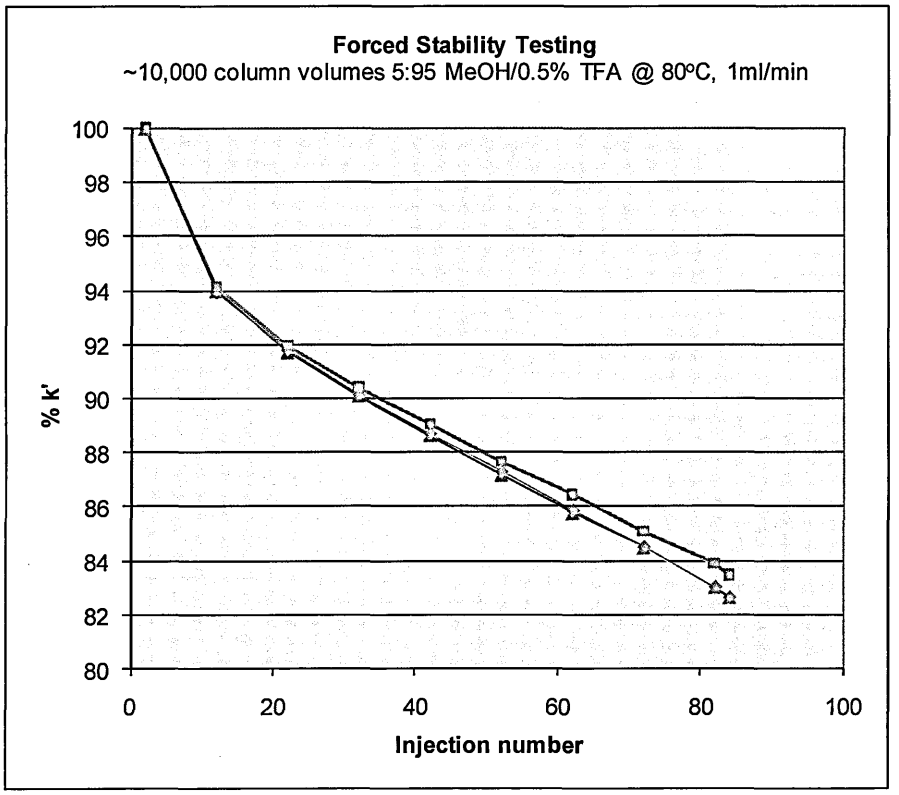

NB

Initial validation was carried out using methanol as the organic modifier, later this was changed to acetonitrile for the results published in the thesis. These results are given as an example of validation across three different columns, they are an accelerated stability testing and do not represent the stability of columns under normal analytical usage.

Appendix 24 Stability results for Alltima HP C18 phase in 10 mM KH_2PO_4 at pH 2.5 and 60°C

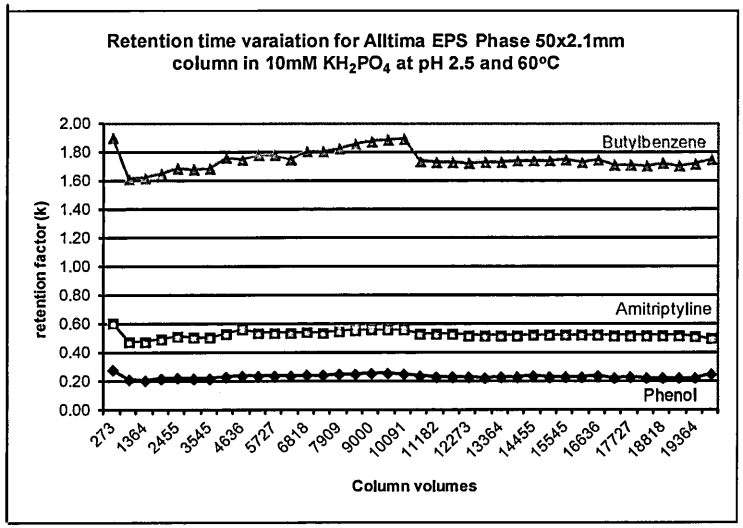

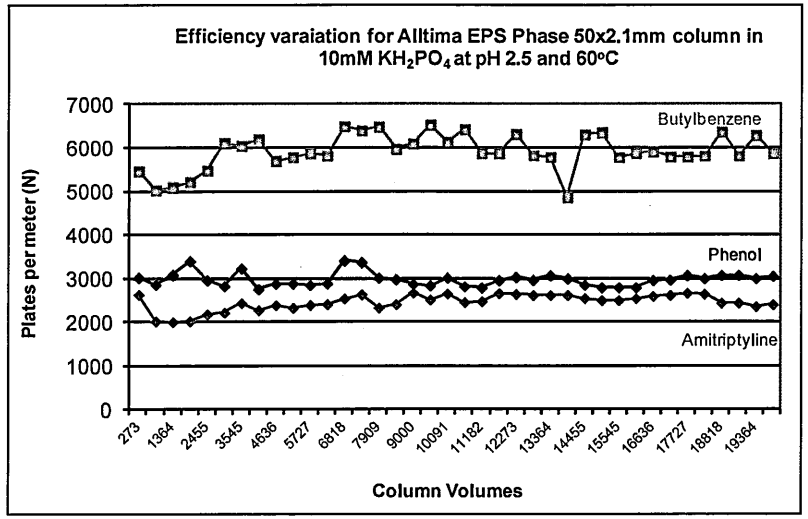

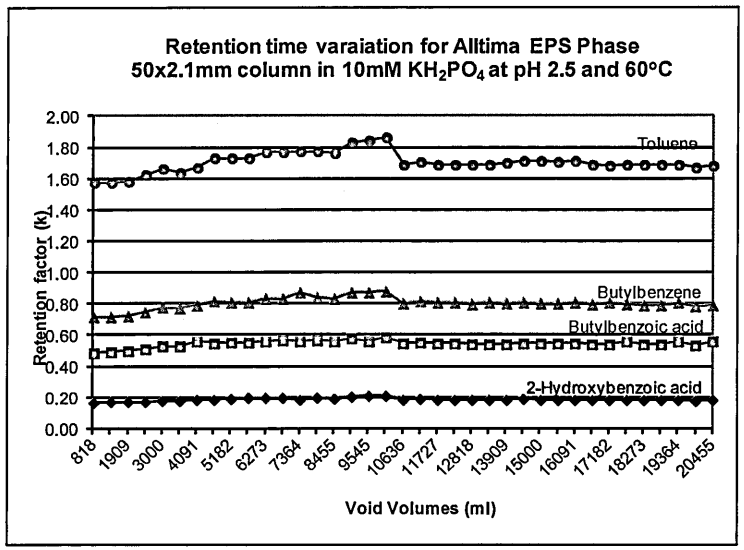

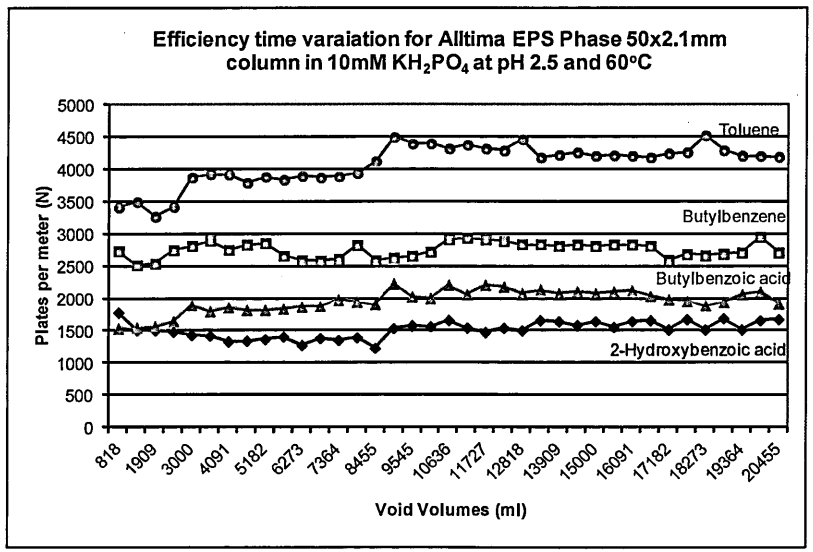

Appendix 25 Stability results for Alltima HP phase in 10 mM NH_3CH_3COOH at pH 6.8 and 60°C

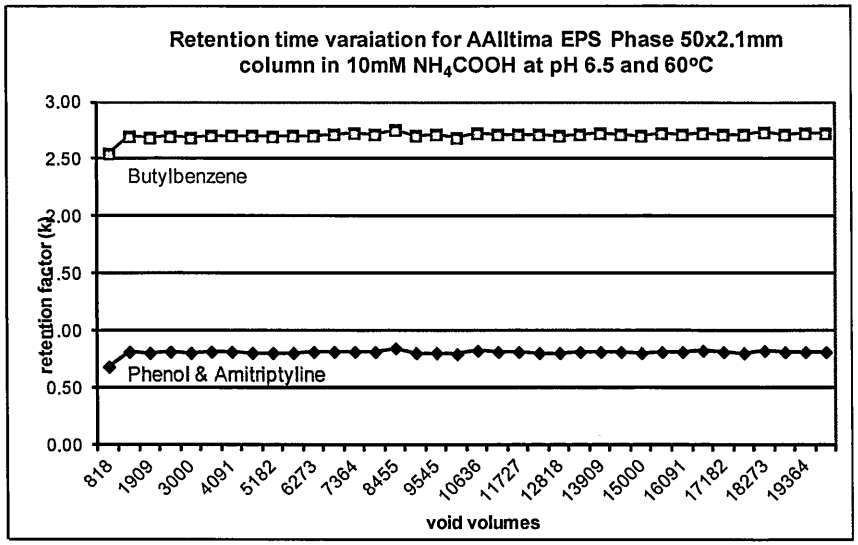

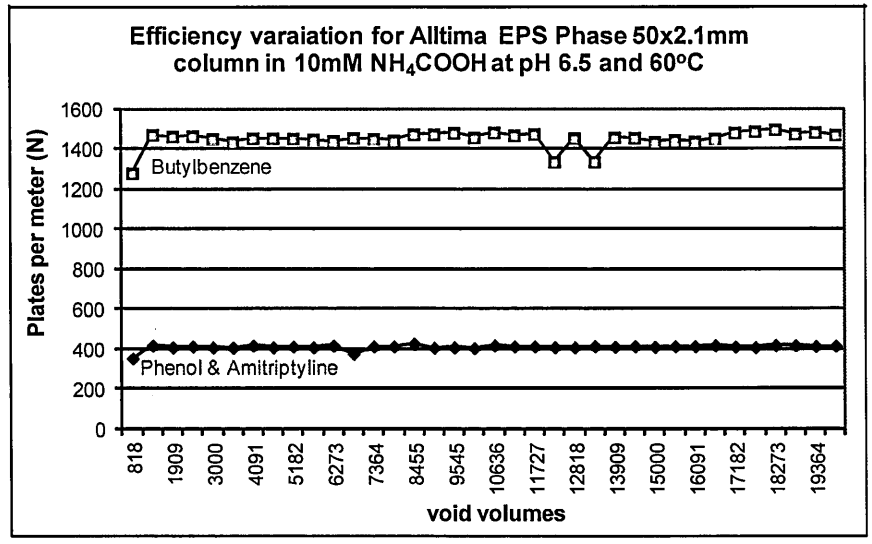

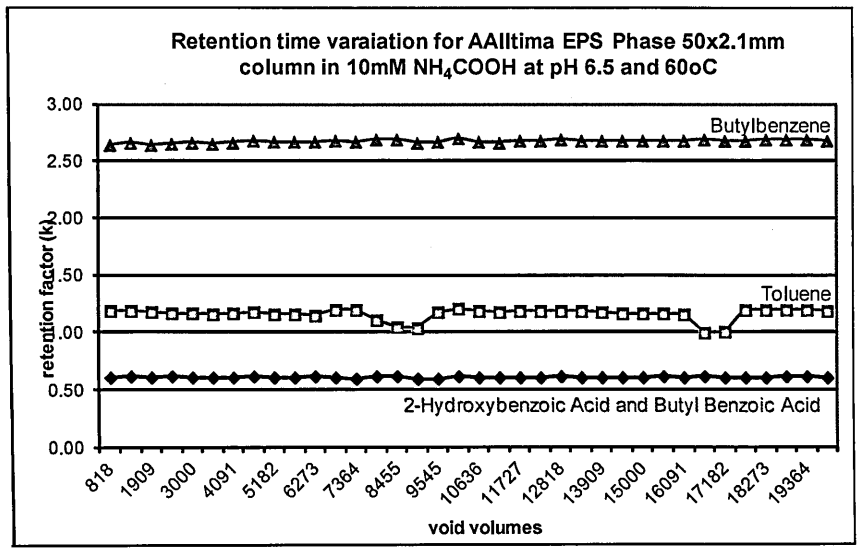

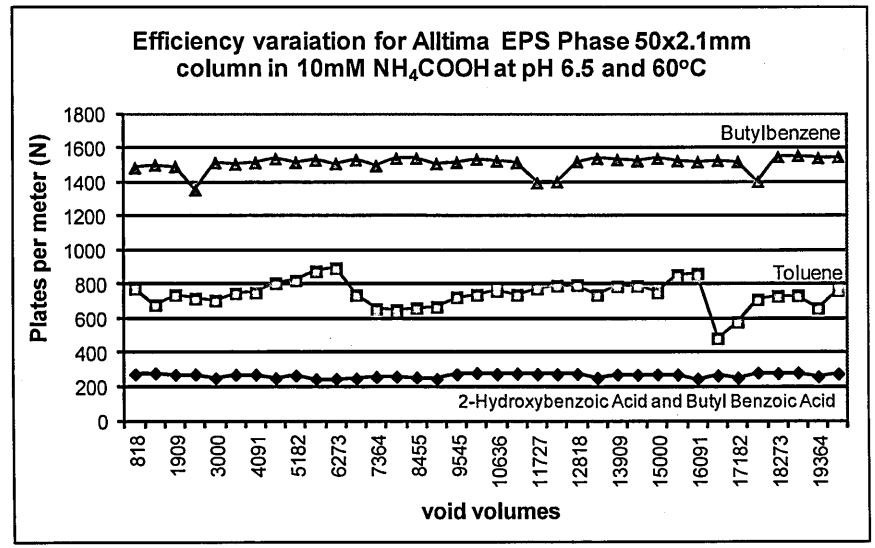

Appendix 26 Stability results for Alltima HP C18 phase in 10 mM KH_2PO_4 at pH 7.6 and 60°C

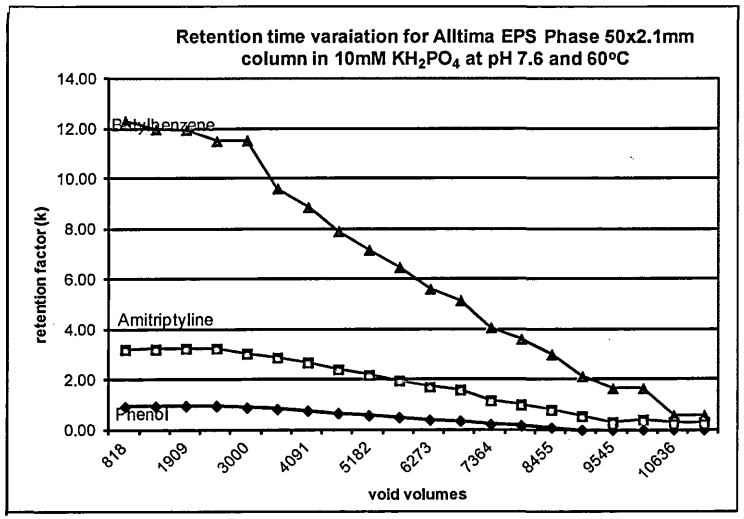

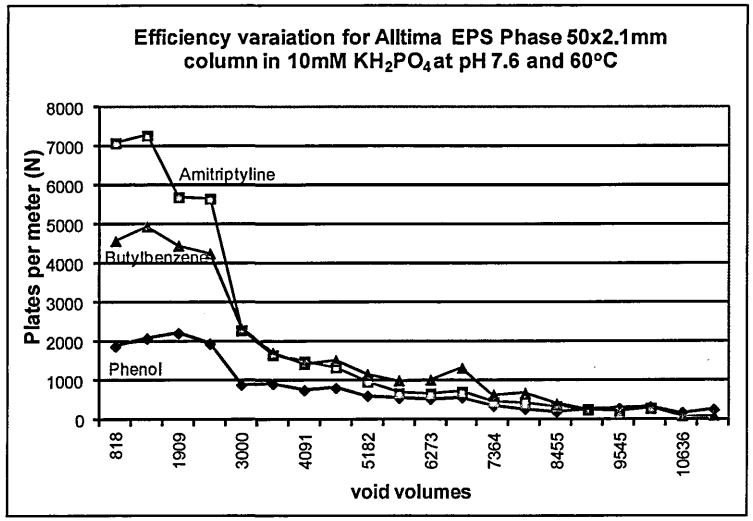

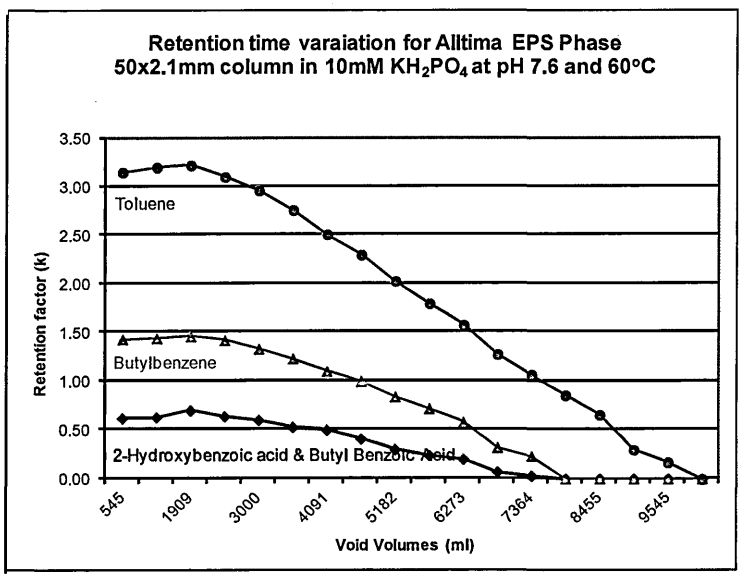

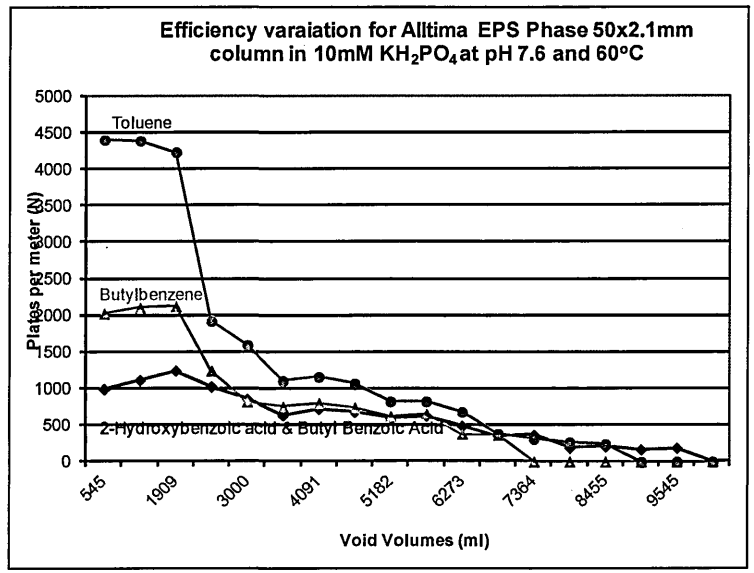

Appendix 27 Stability results for Platinum C18 phase in 10 mM KH_2PO_4 at pH 2.5 and 60°C

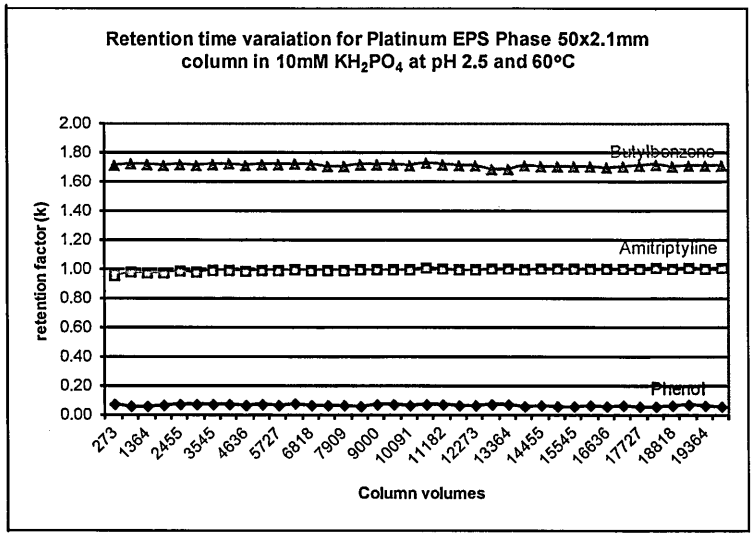

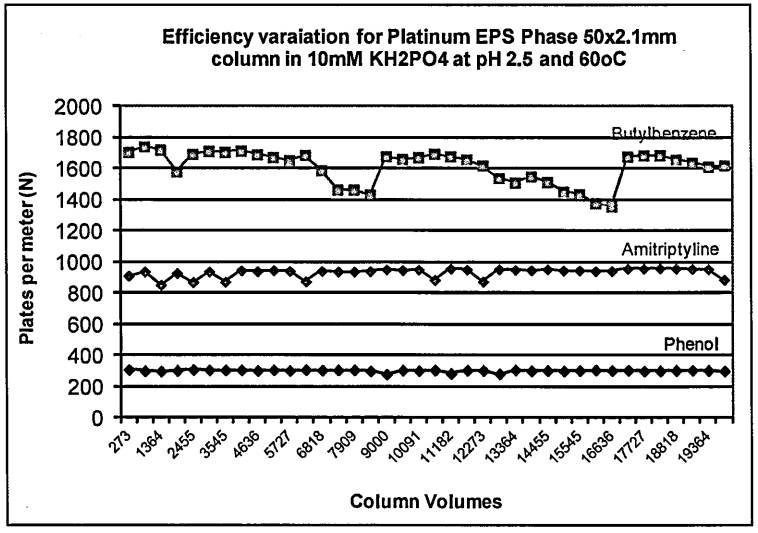

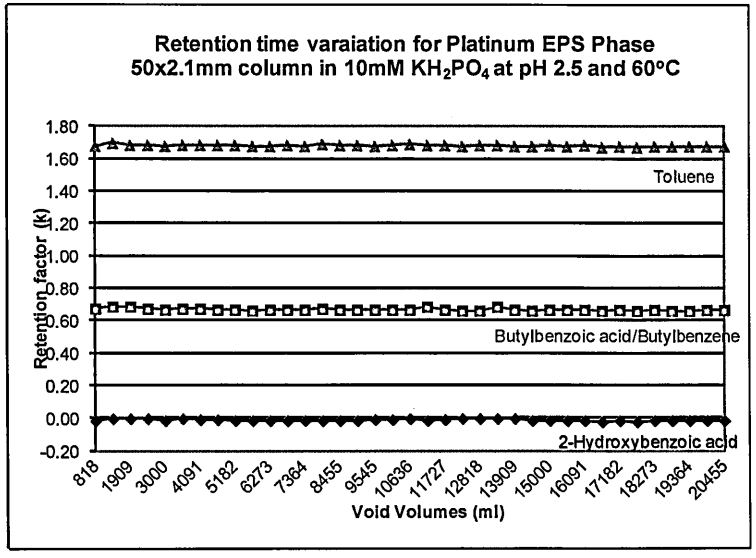

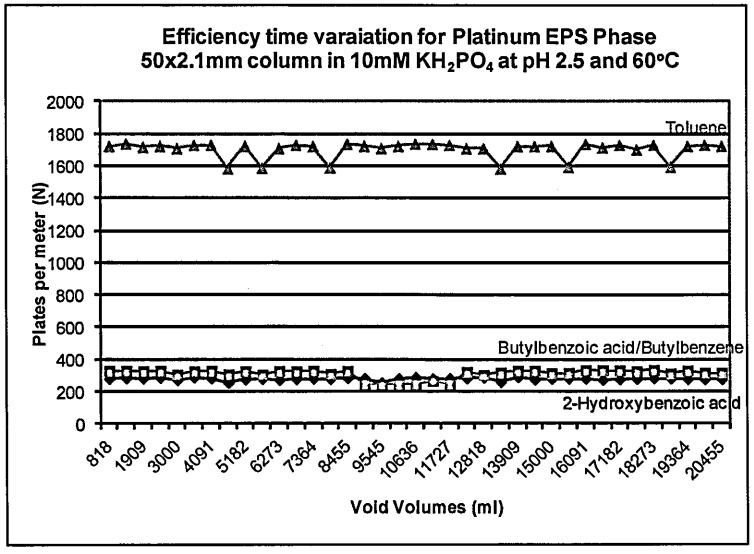

Appendix 28 Stability results for Platinum C18 phase in 10 mM NH_3CH_3COOHat pH 6.8 and 60°C

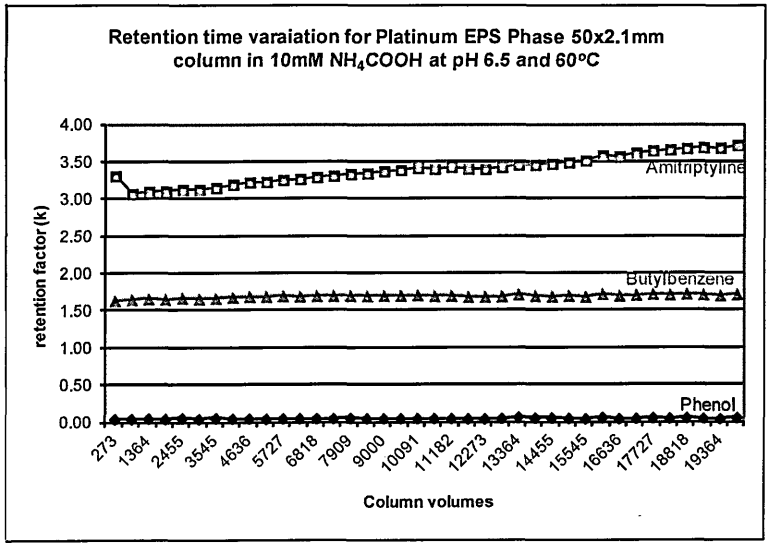

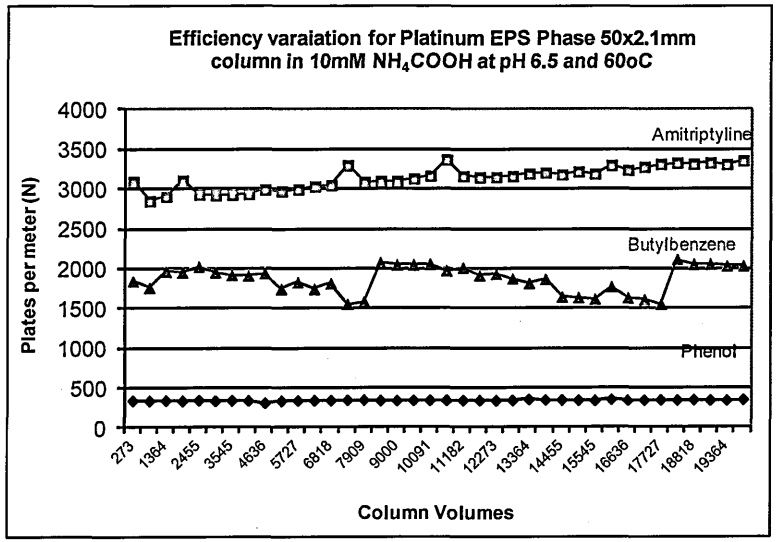

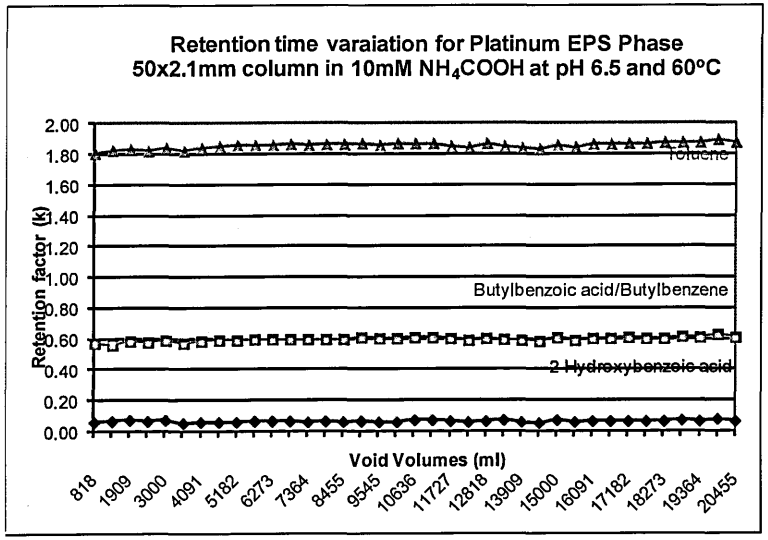

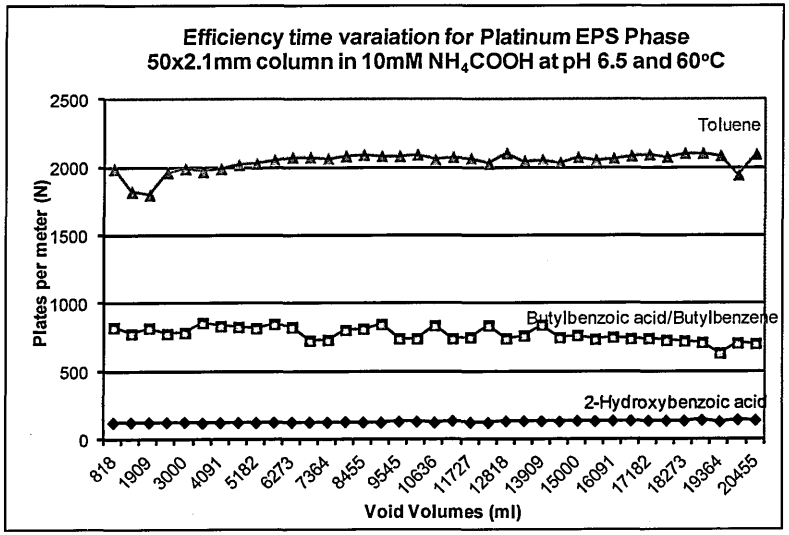

Appendix 29 Stability results for Platinum C18 phase in 10 mM KH_2PO_4 at pH 7.6 and 60°C

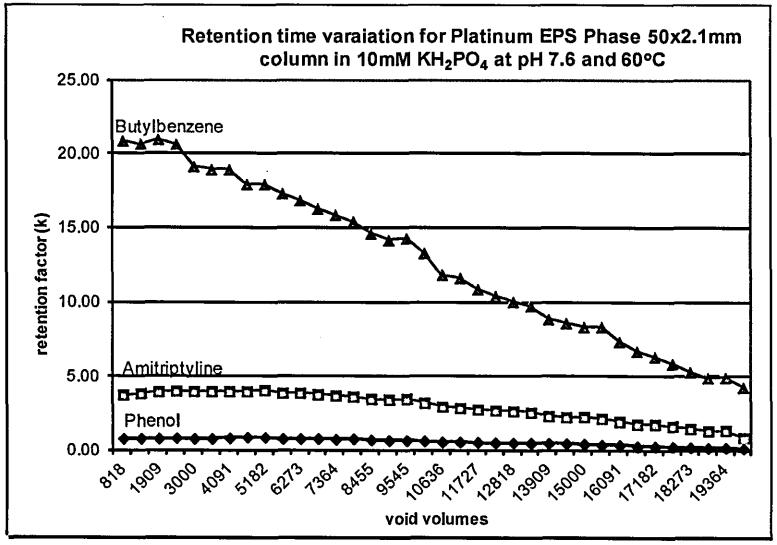

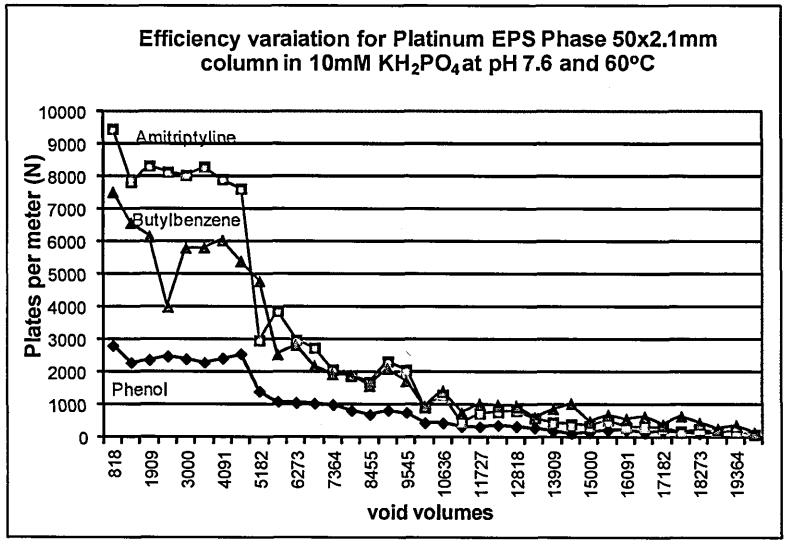

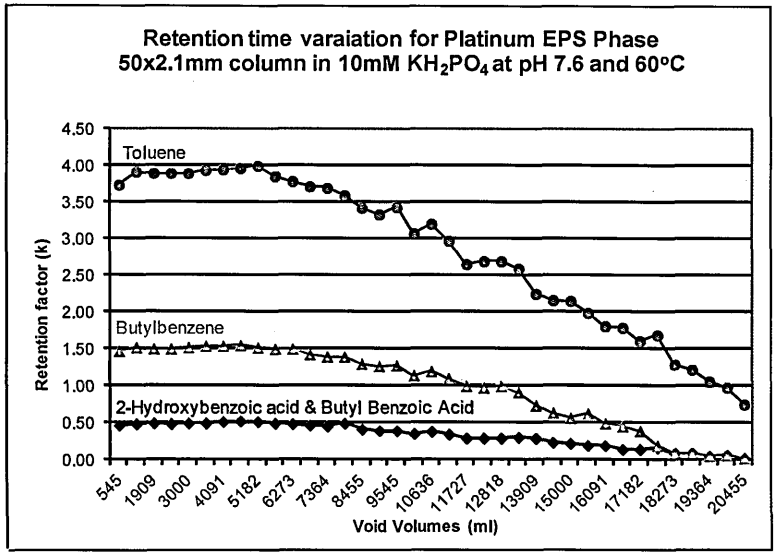

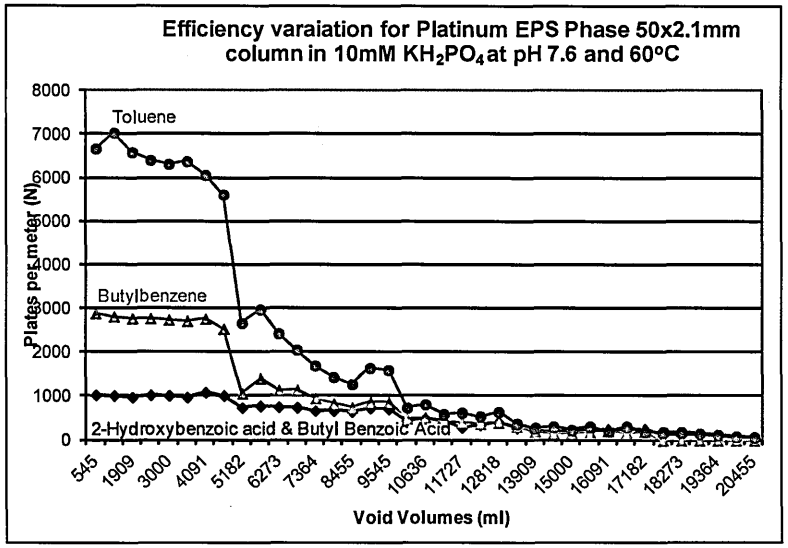

Appendix 30 Stability results for HyPURITY Aquastar phase in 10 mM KH_2PO_4 at pH 2.5 and 60°C

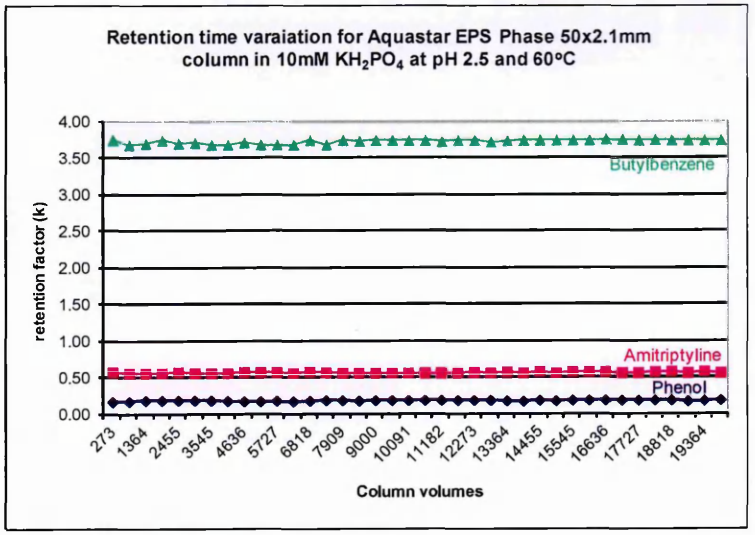

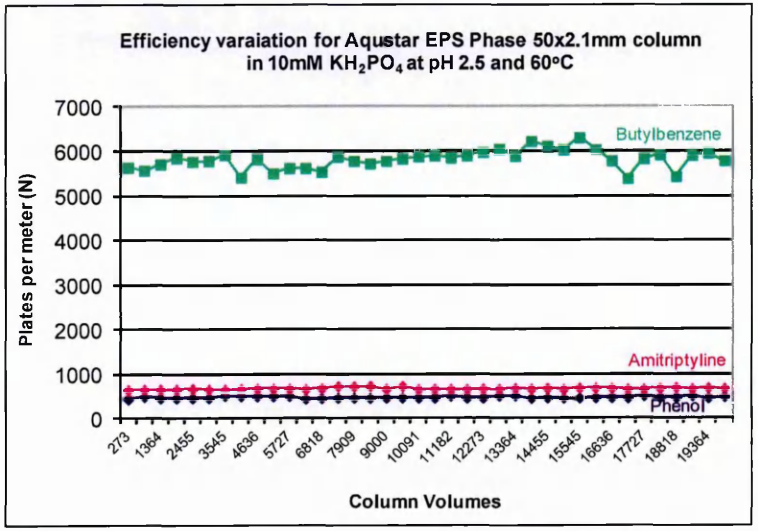

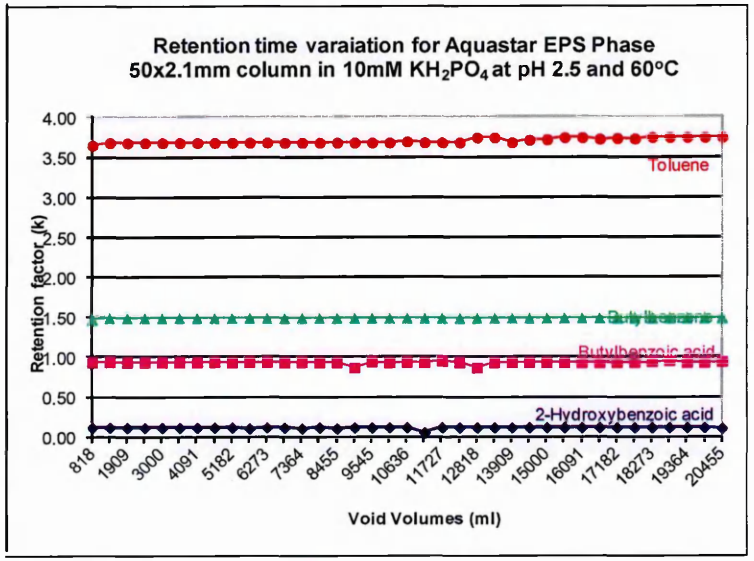

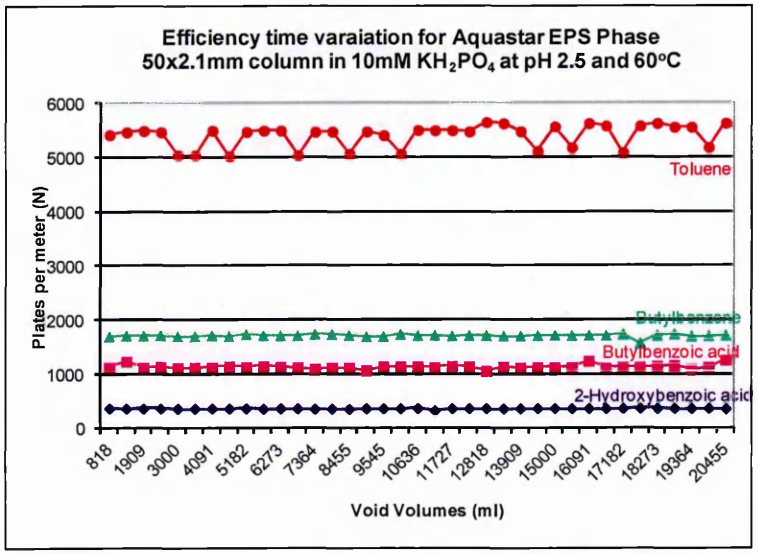

Appendix 31 Stability results for HyPURITY Aquastar in 10 mM NH_3CH_3COOHat pH 6.8 and 60°C

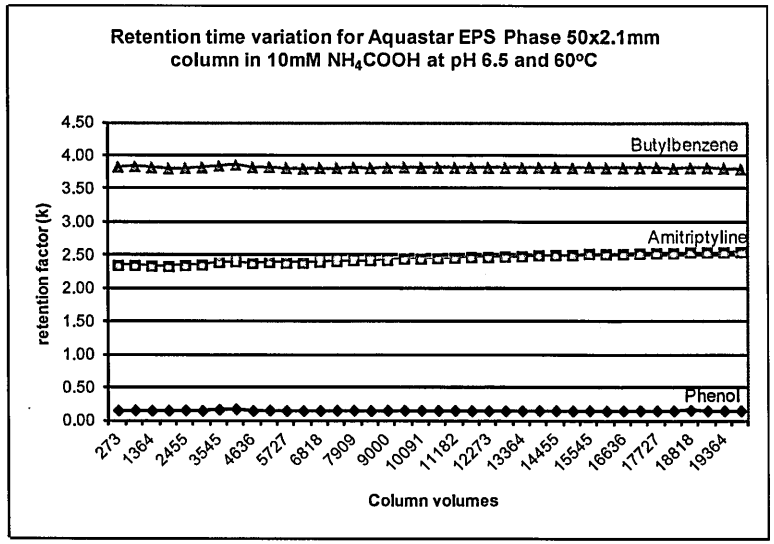

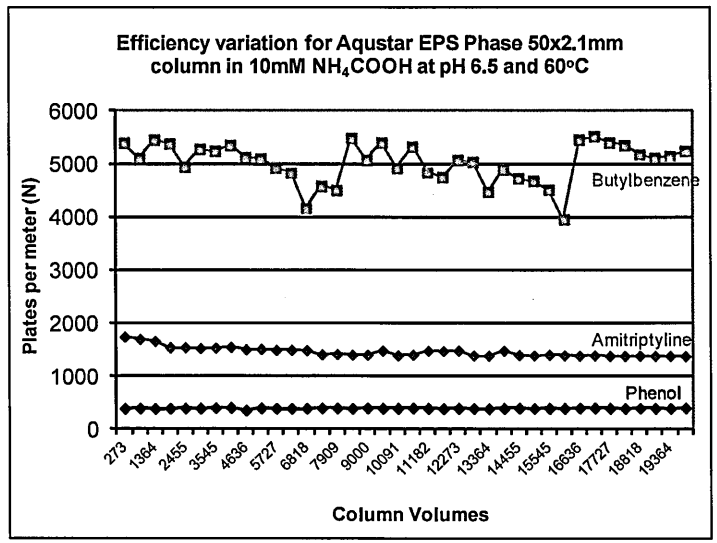

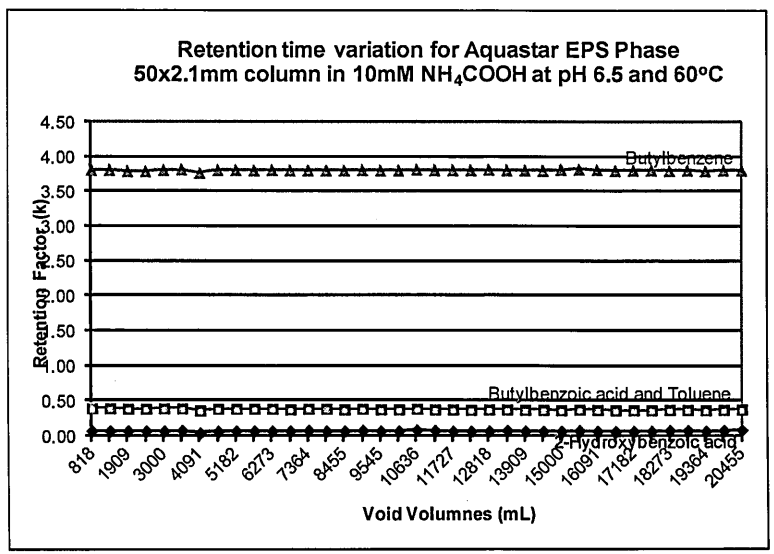

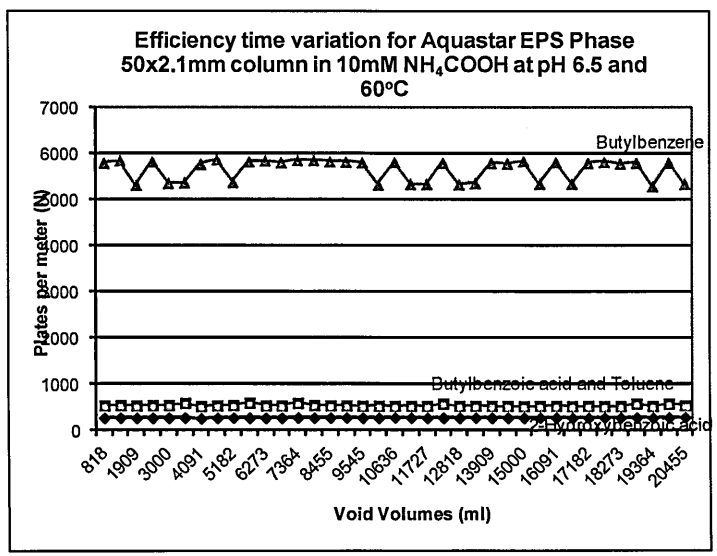

Appendix 32 Stability results for HyPURITY Aquastar phase in 10 mM KH_2PO_4 at pH 7.6 and 60°C

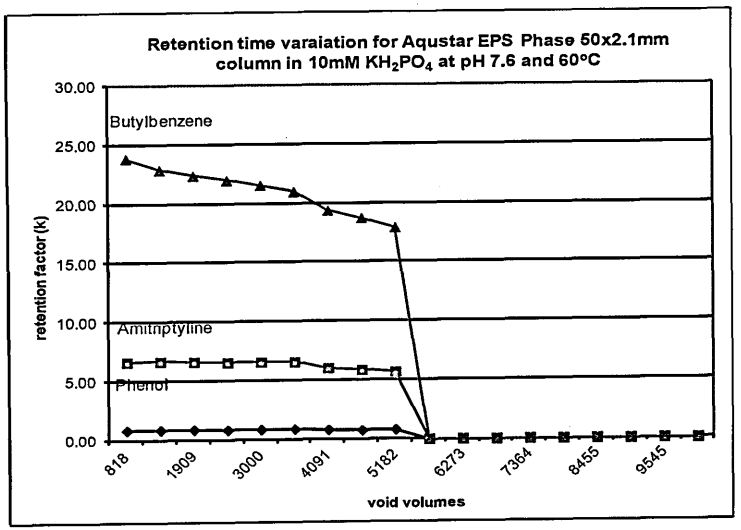

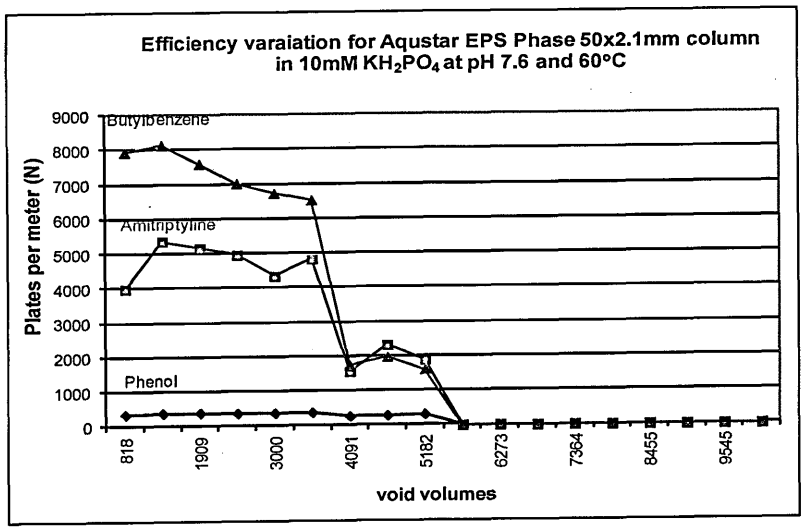

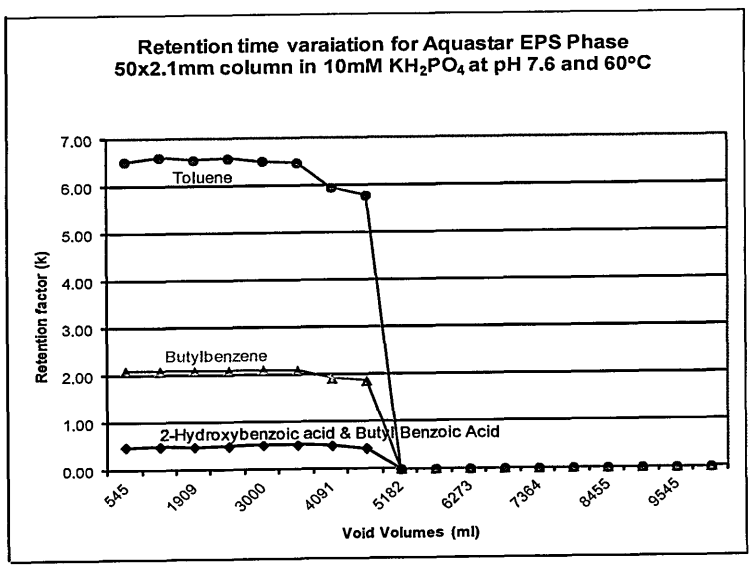

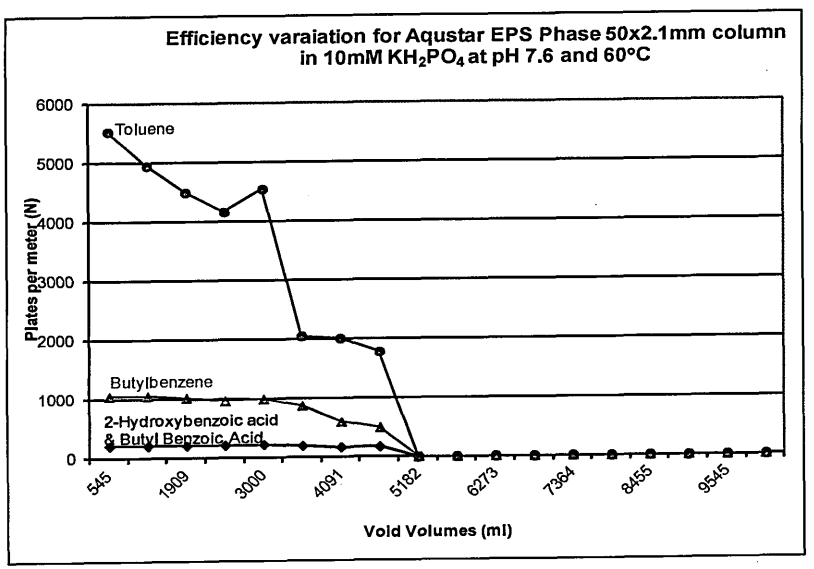

Appendix 33 Stability results for Zorbax-SB AQ phase in 10 mM KH_2PO_4 at pH 2.5 and 60°C

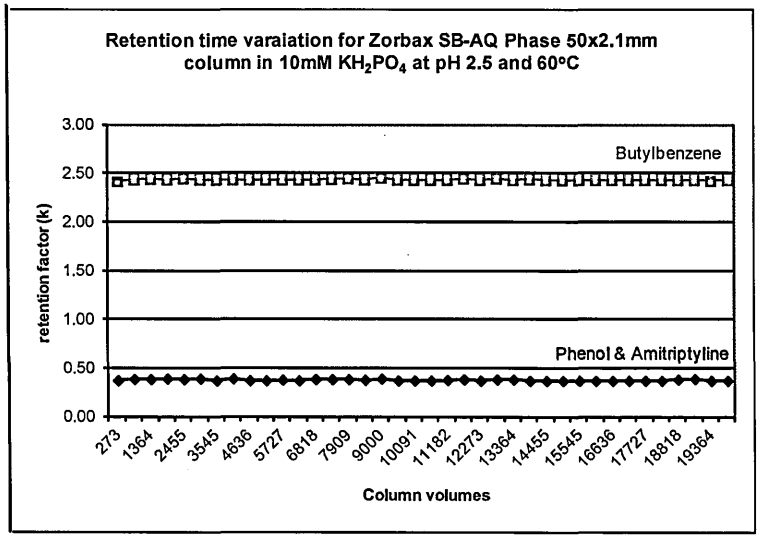

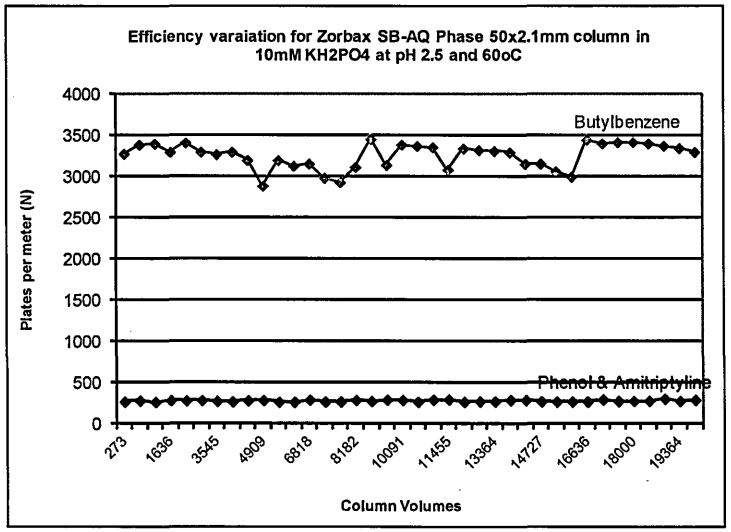

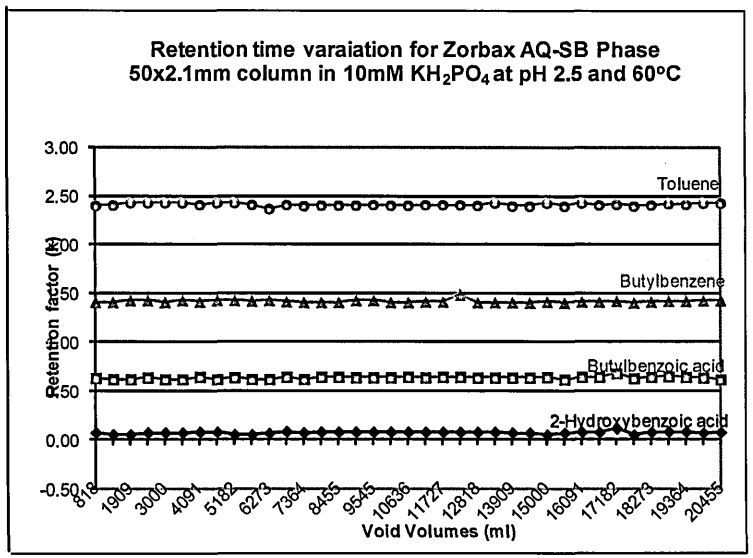

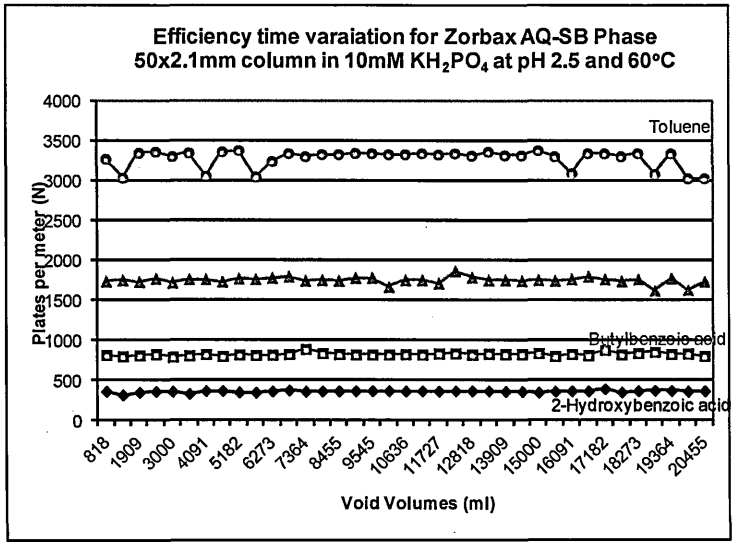

Appendix 34 Stability results for Zorbax-SB AQ phase in 10 mM NH_3CH_3COOHat pH 6.8 and 60°C

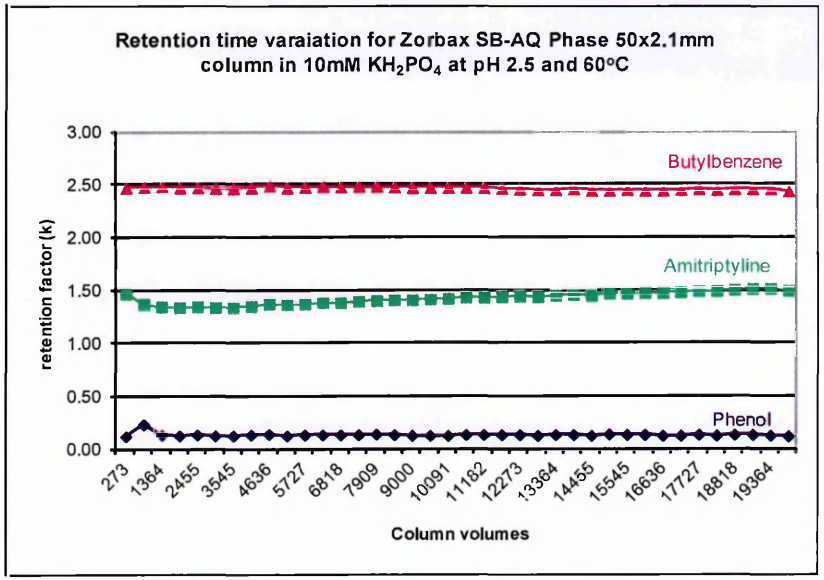

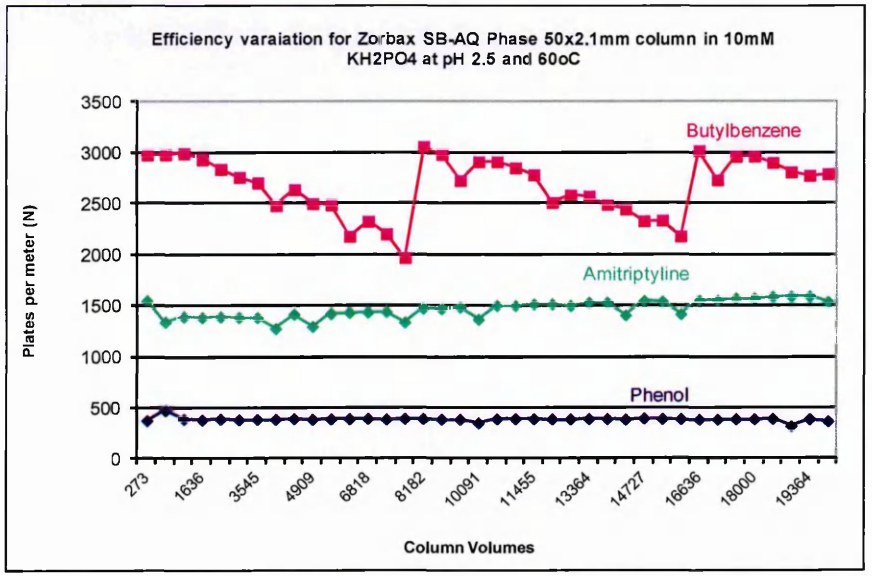

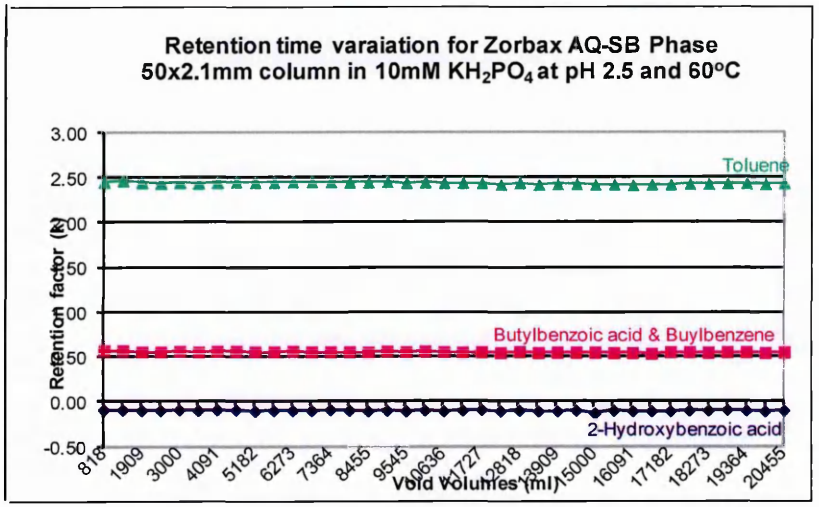

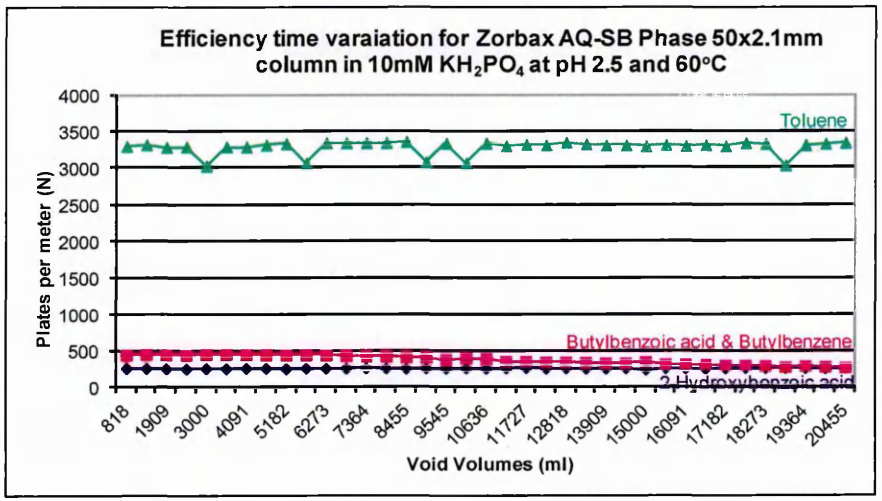

Appendix 35 Stability results for Zorbax-SB AQ phase in 10 mM KH_2PO_4 at pH 7.6 and 60°C

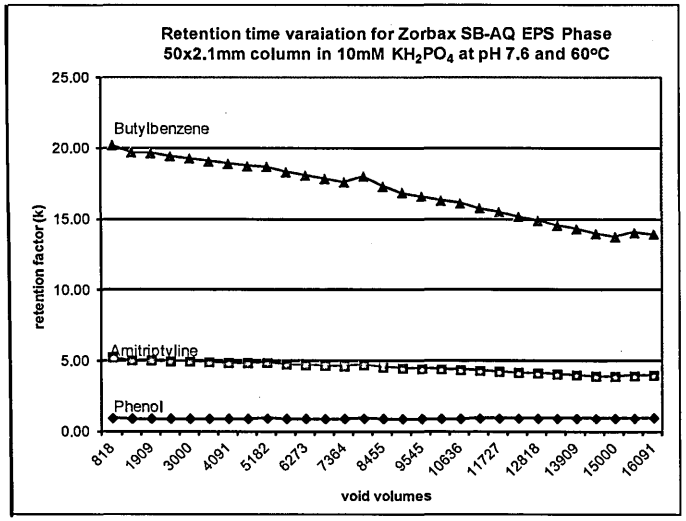

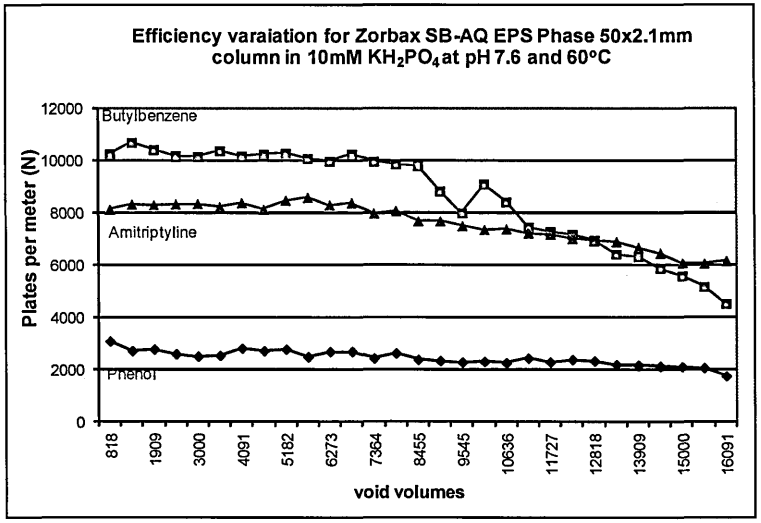

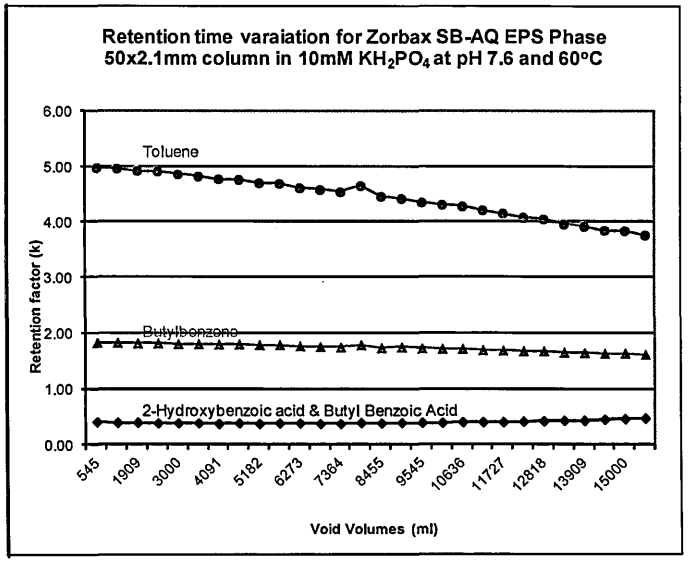

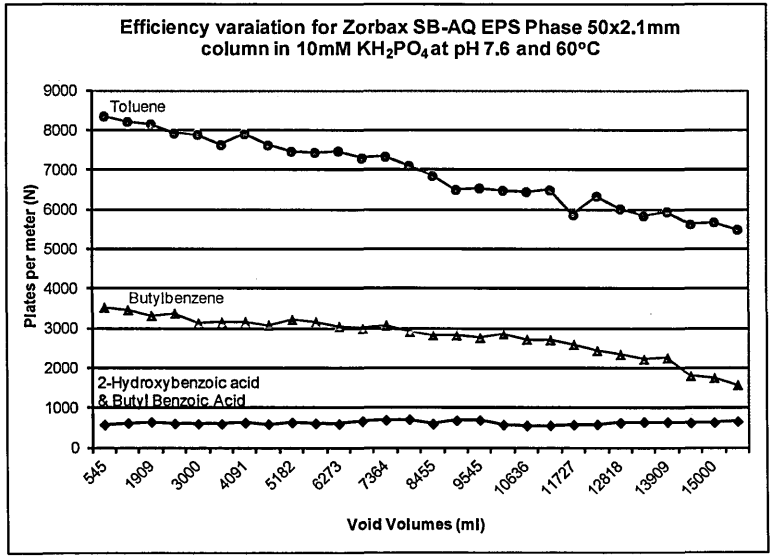

Appendix 36 Stability results for XSelect HSS SB C18 phase in 10 mM KH_2PO_4 at pH 2.5 and 60°C

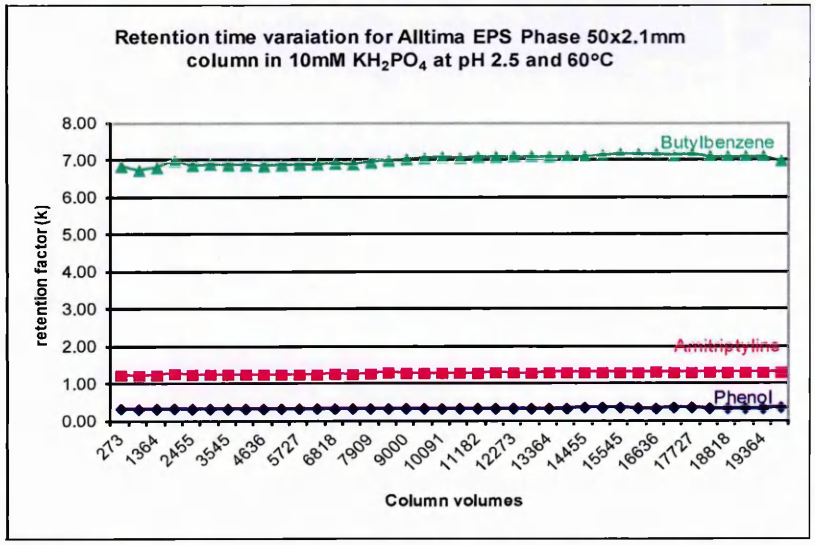

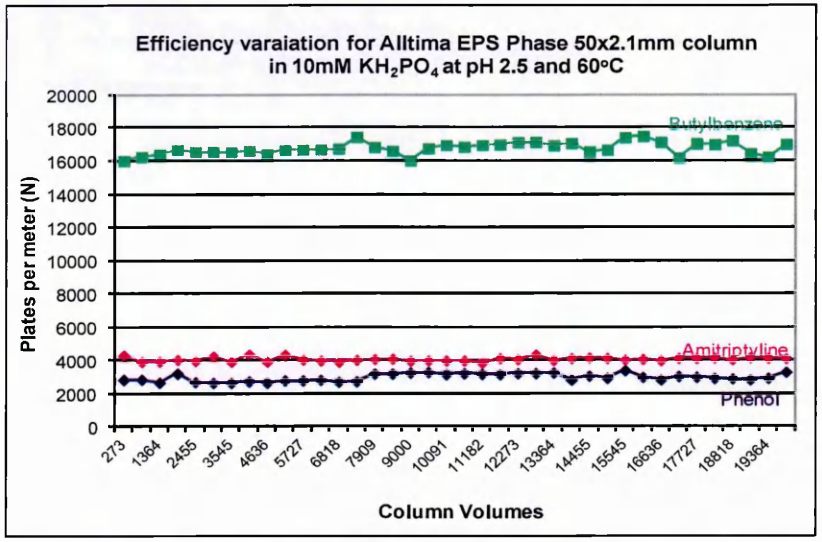

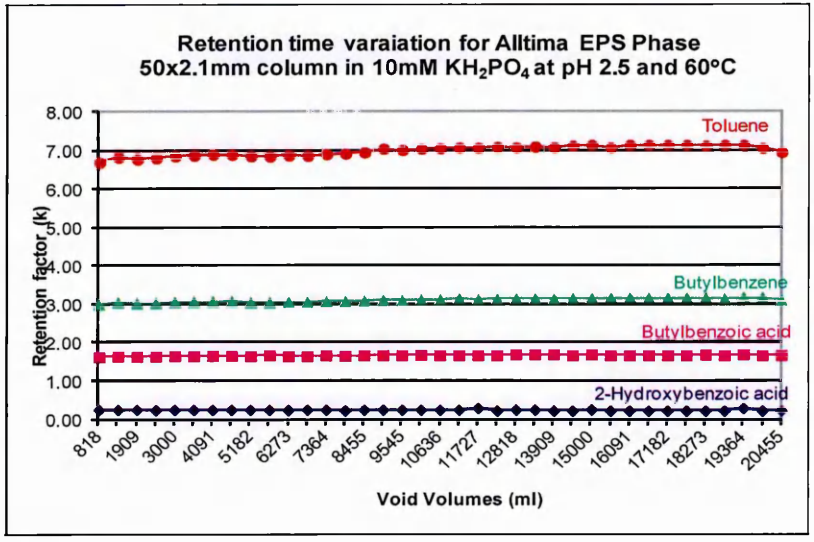

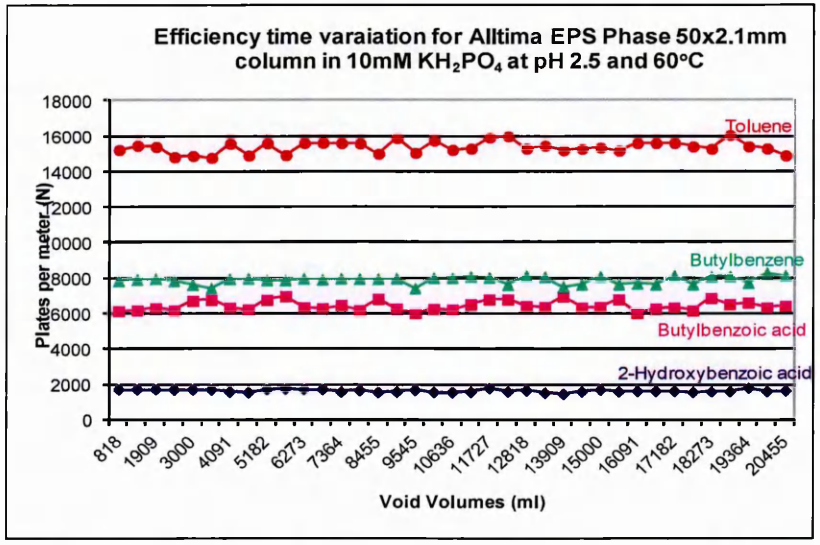

Appendix 37 Stability results for XSelect HSS SB C18 in 10 mM NH_3CH_3COOHat pH 6.8 and 60°C

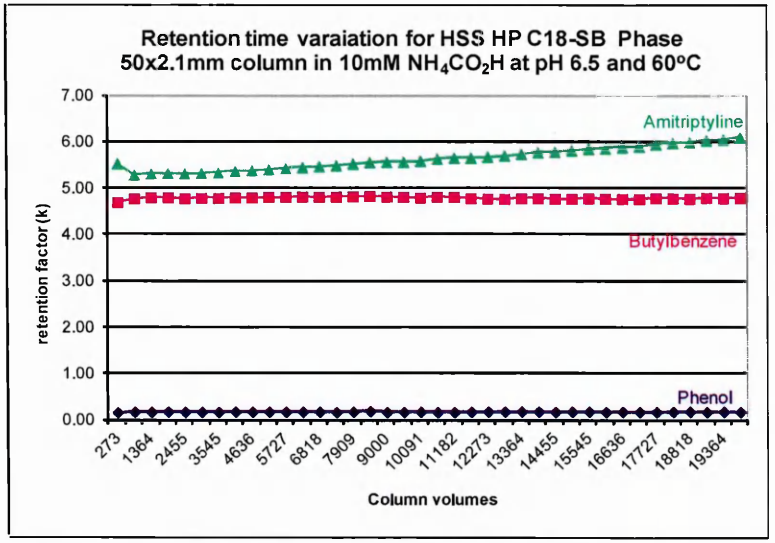

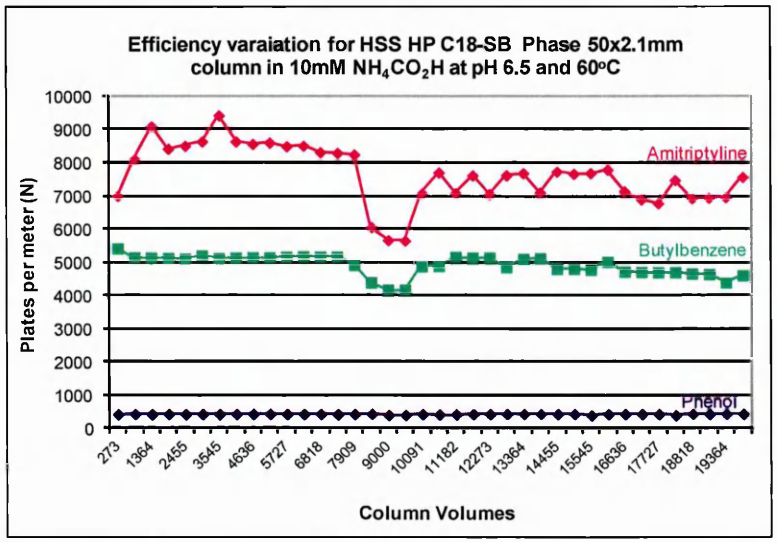

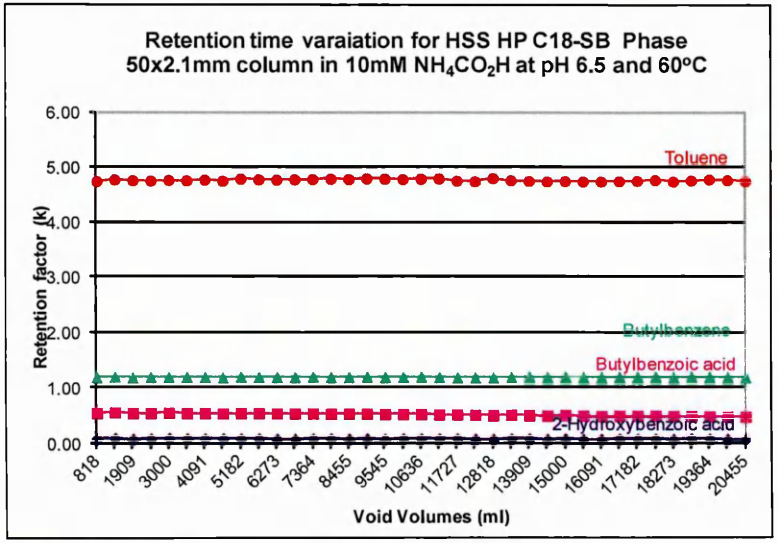

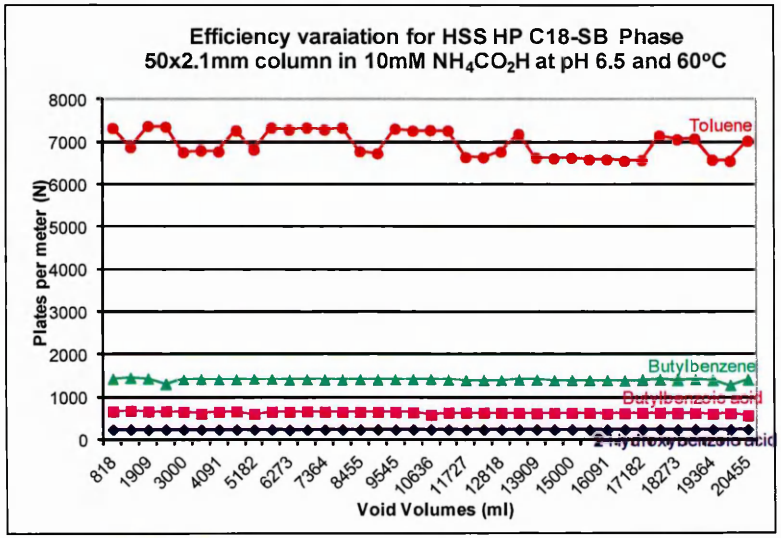

Appendix 38 Stability results for XSelect HSS SB C18 phase in 10 mM KH_2PO_4 at pH 7.6 and 60°C

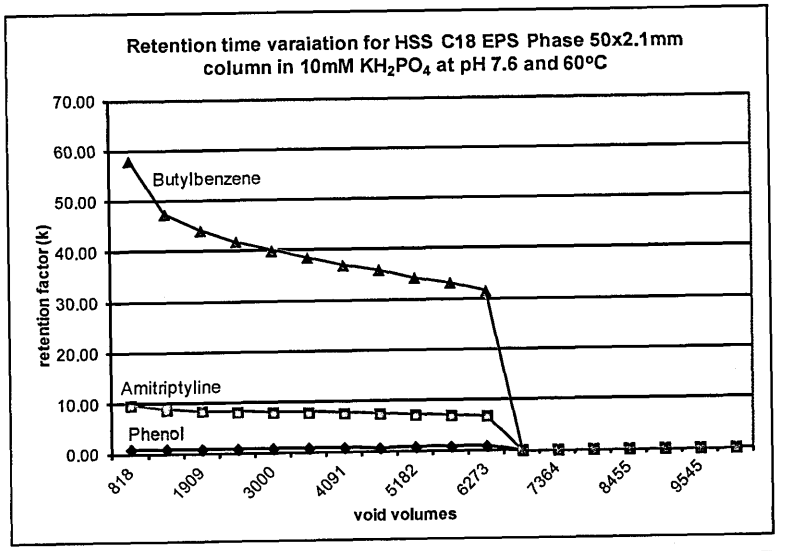

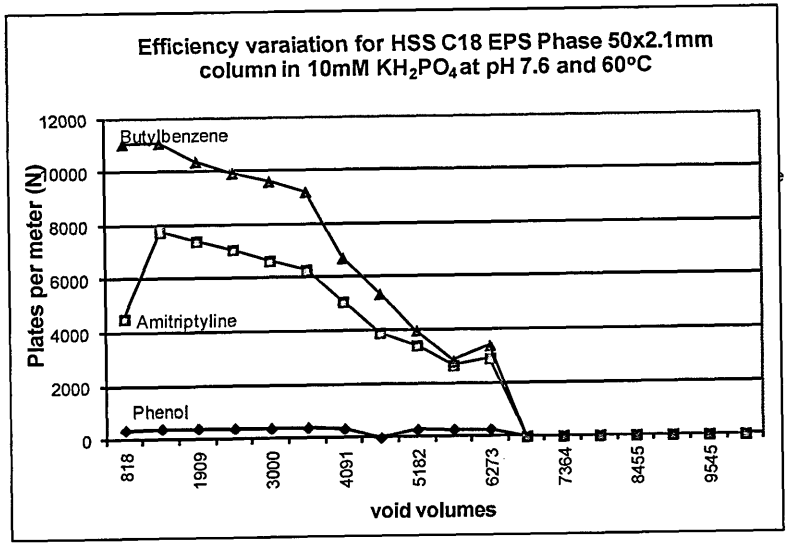

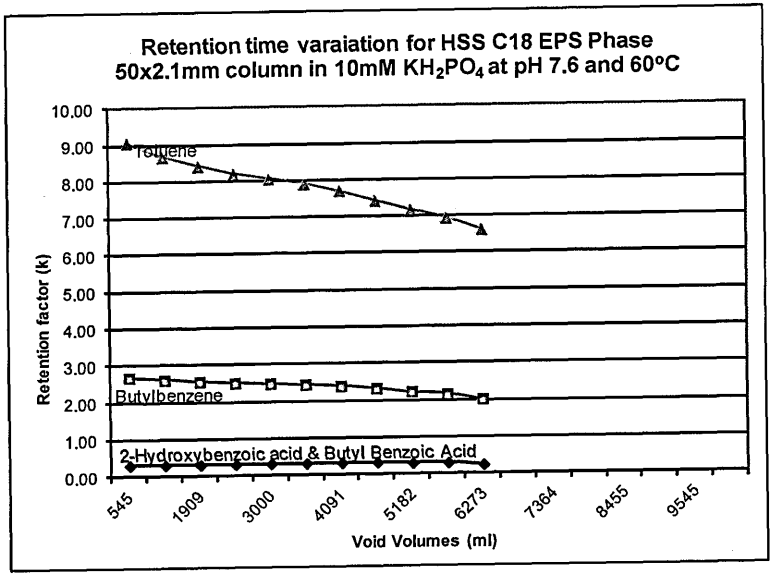

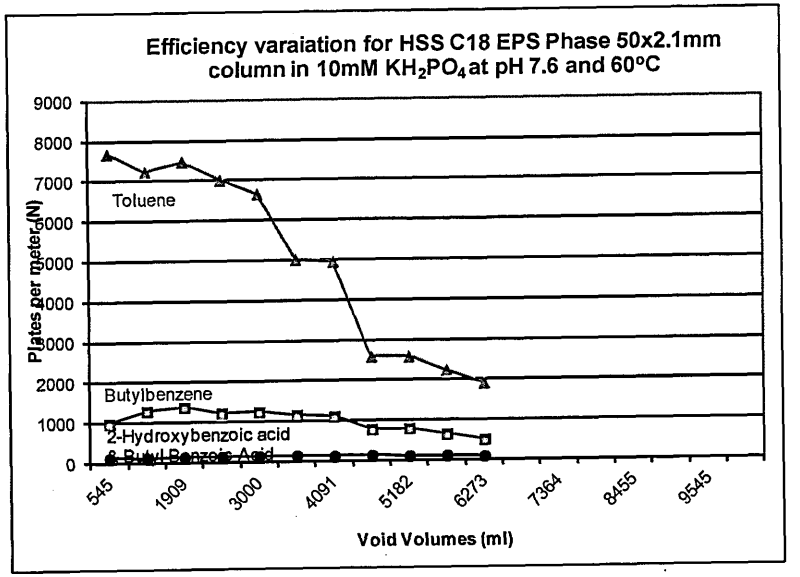

Appendix 39 GC-MS and ^{13}CNMR for HyPURITY Aquastar C18 phase

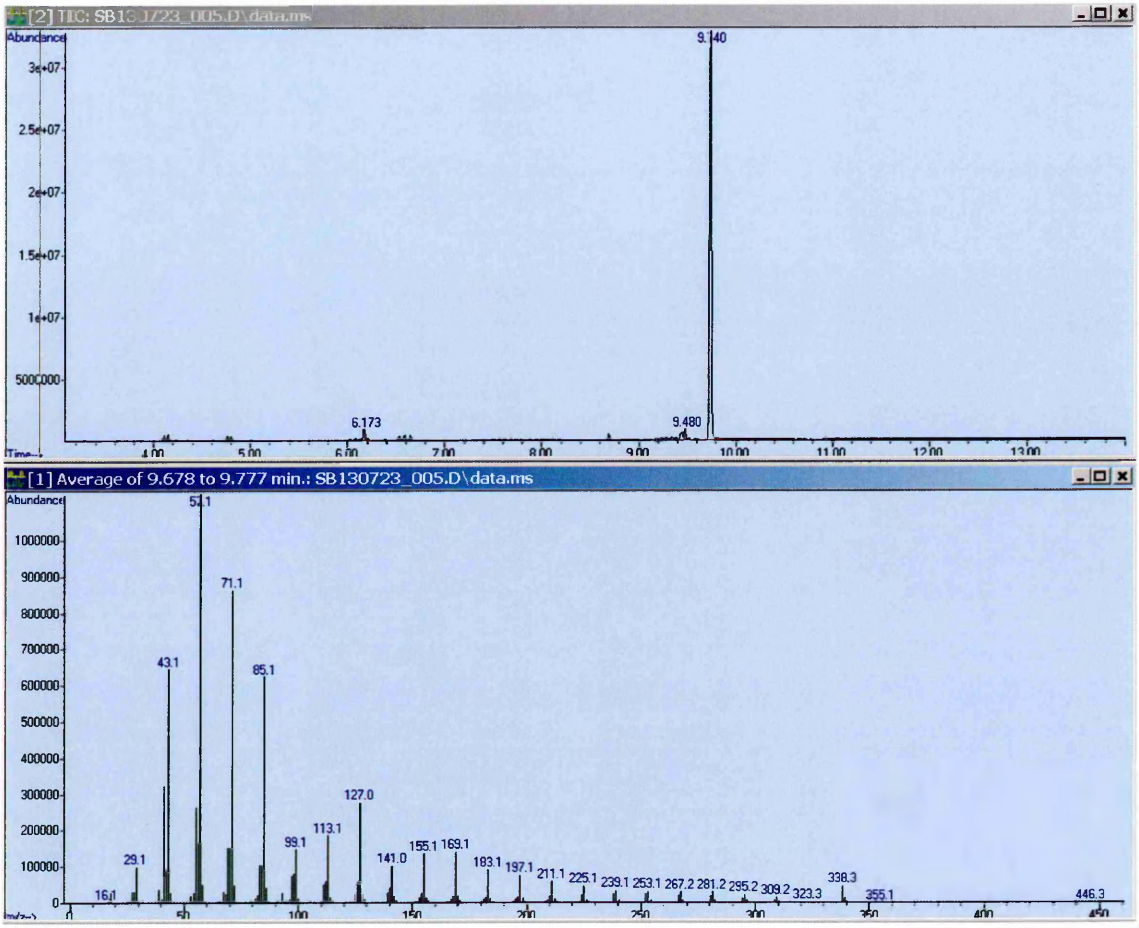

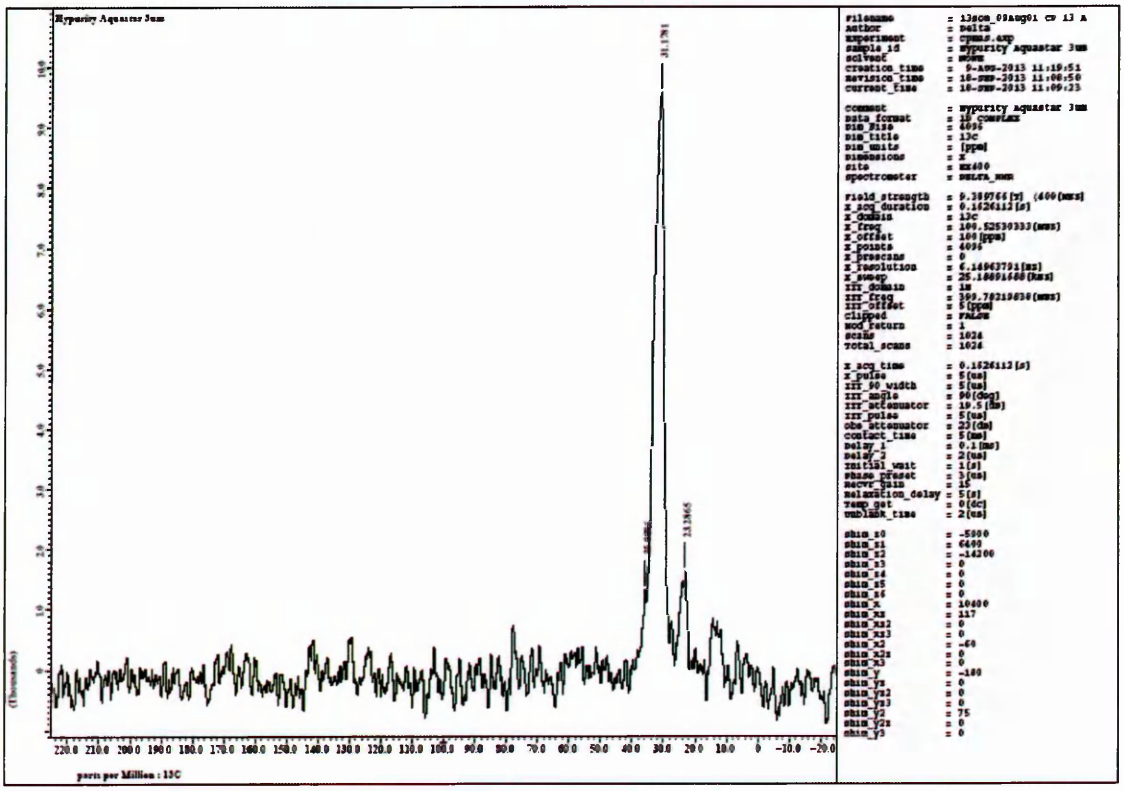

Appendix 40 GC-MS and ^{13}CNMR for Platinum EPS C18 phase

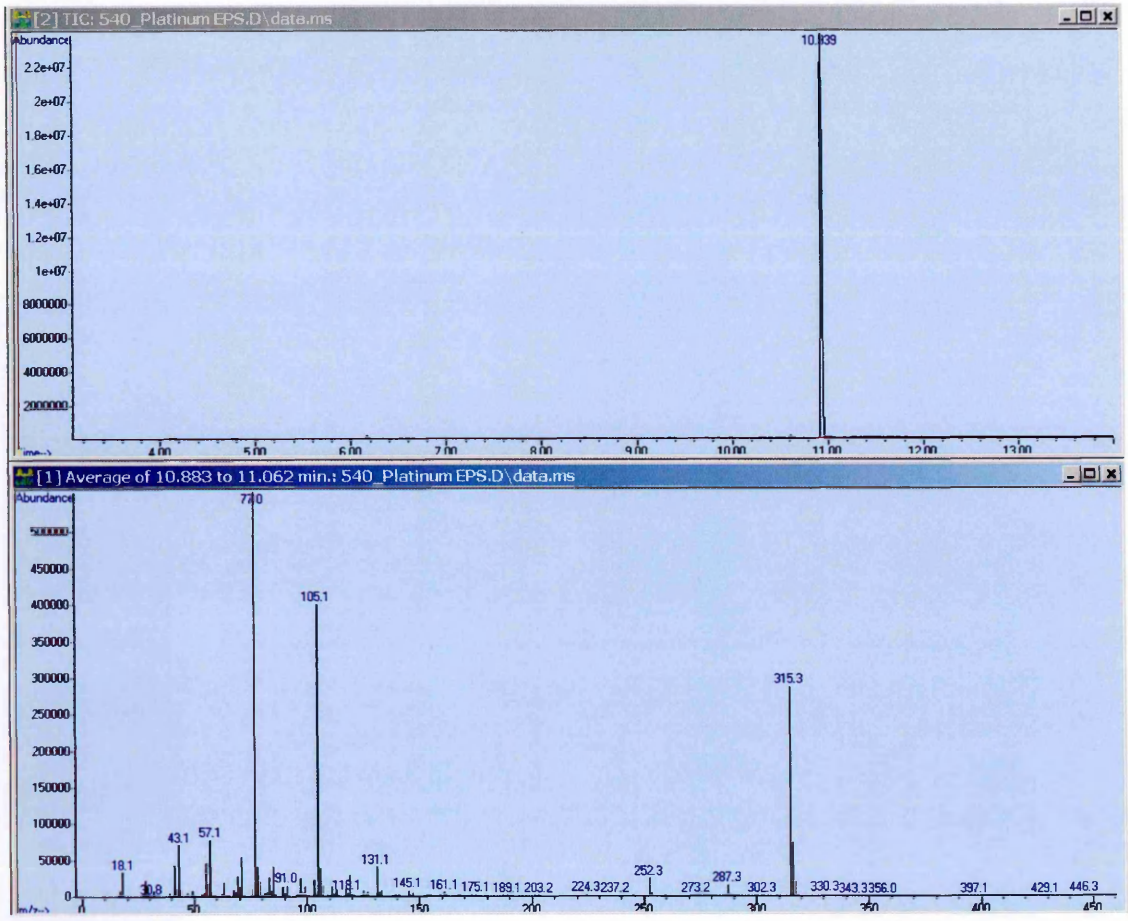

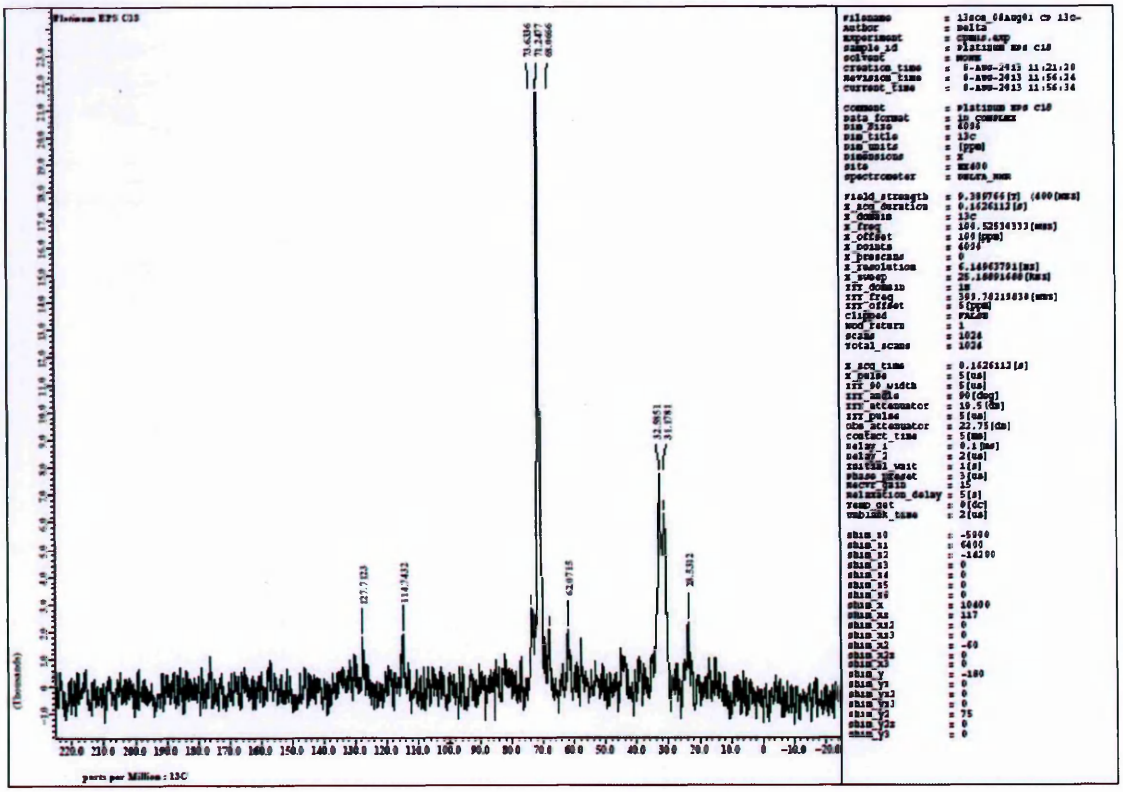

Appendix 41 GC-MS and ^{13}CNMR for Zorbax-SB AQ C18 phase

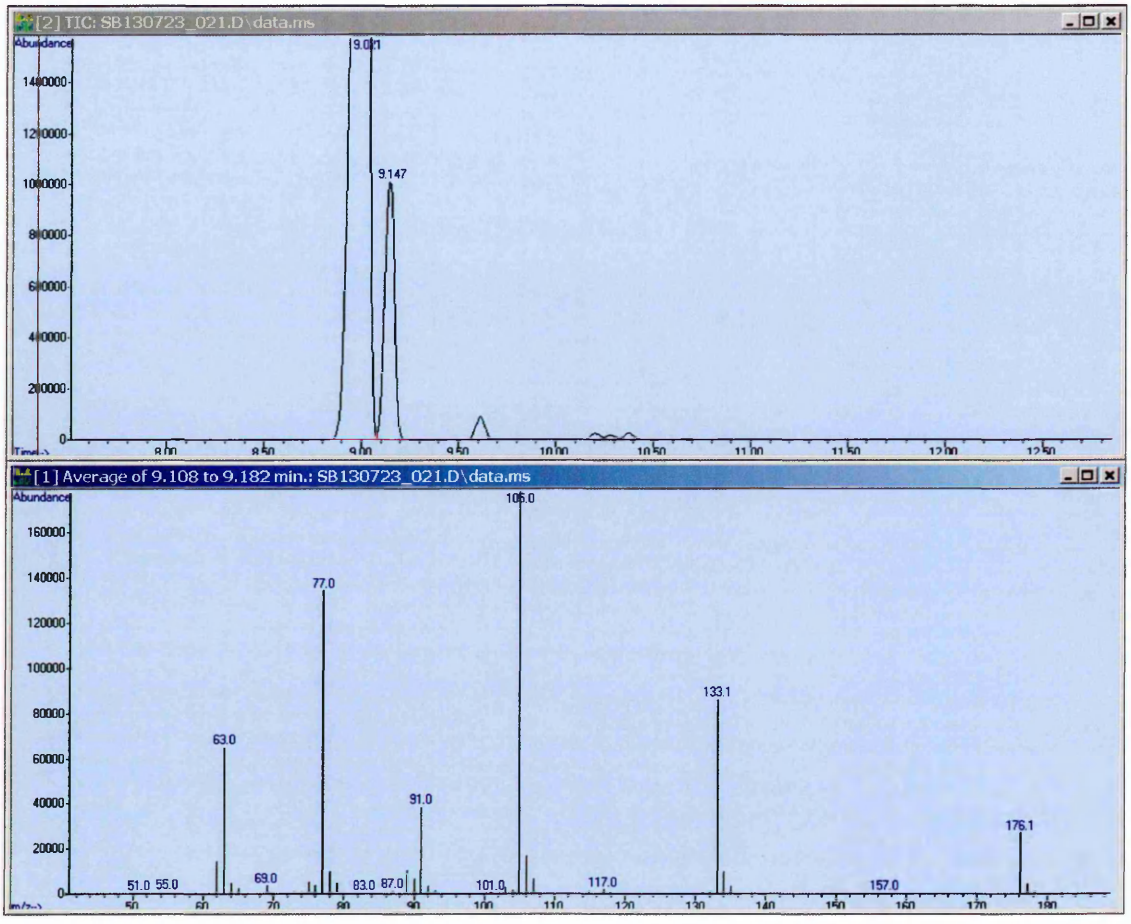

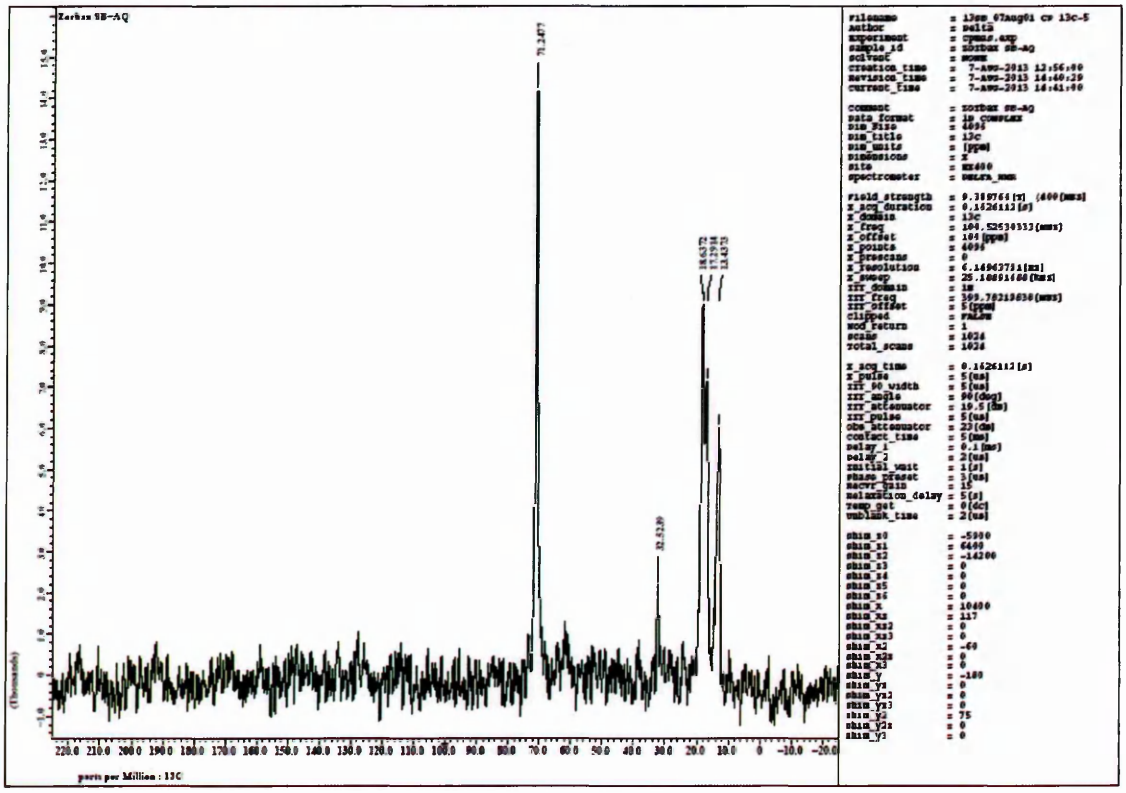

Appendix 42 GC-MS and ^{13}CNMR for XSelect HSS SB C18 phase

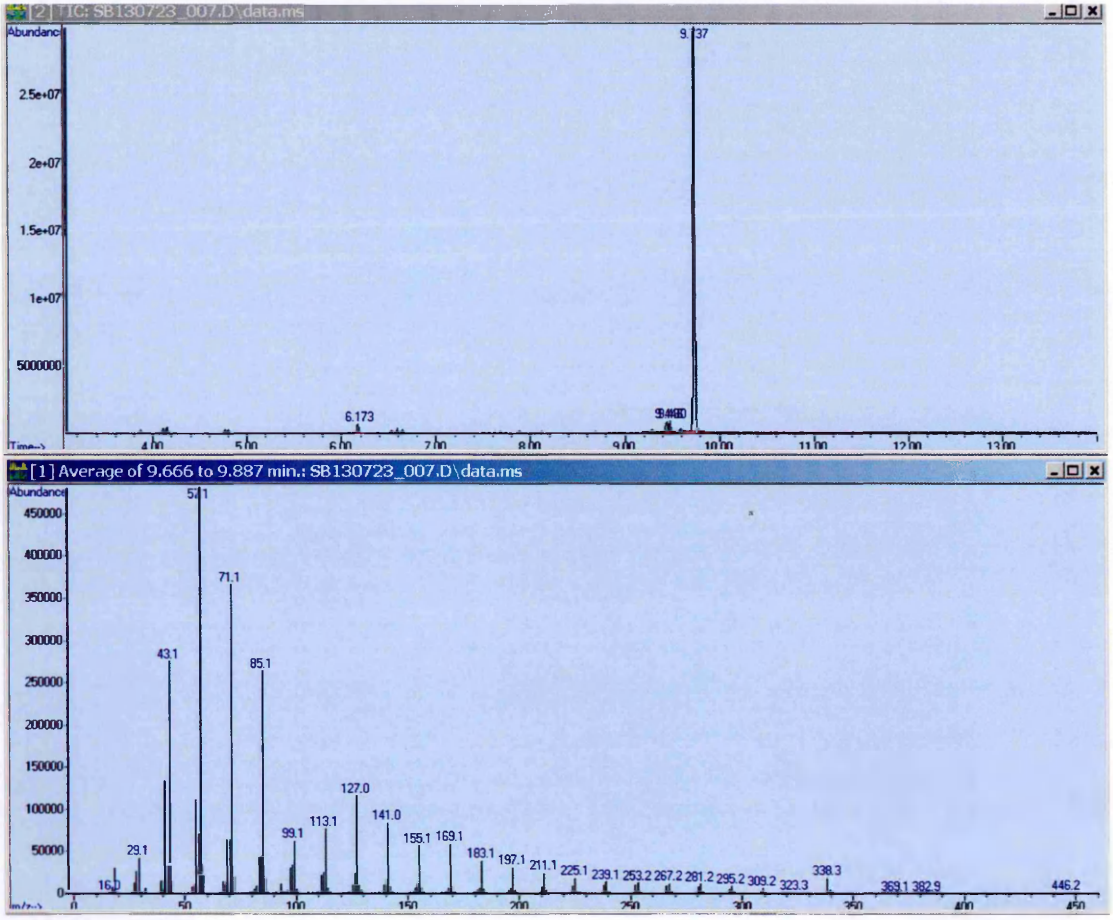

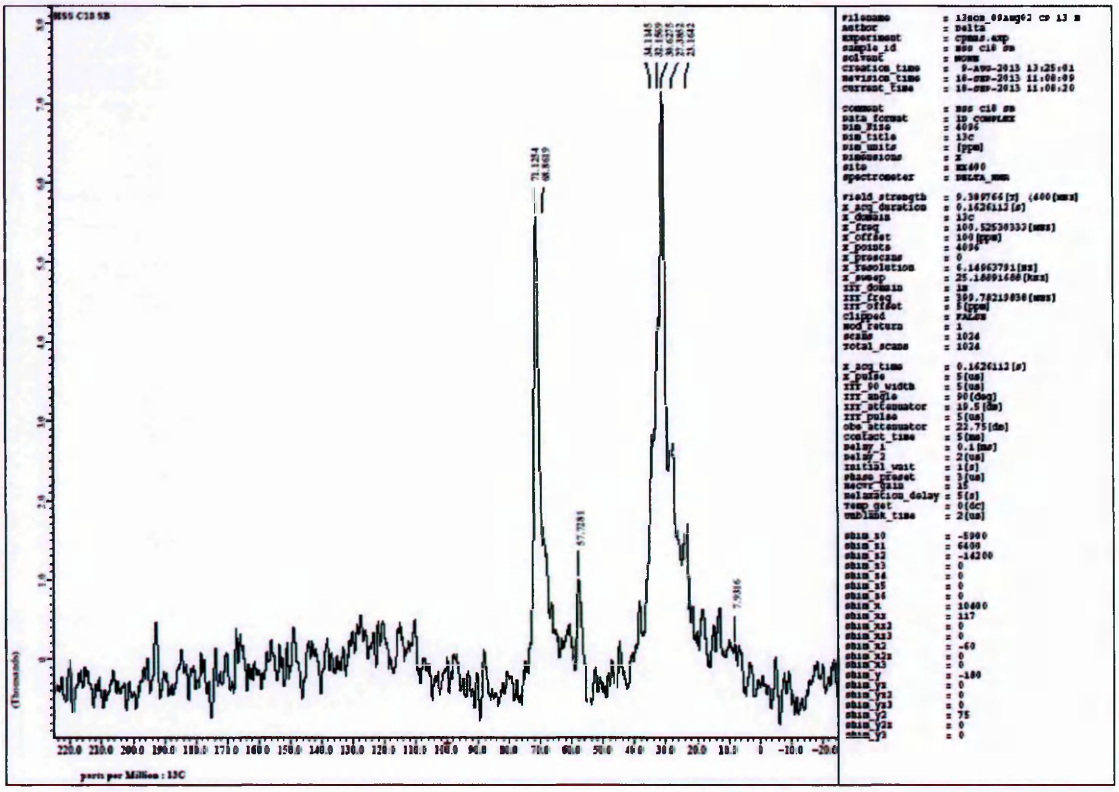

Appendix 43 GC-MS and ^{13}CNMR for Alltima HP C18 C18 phase

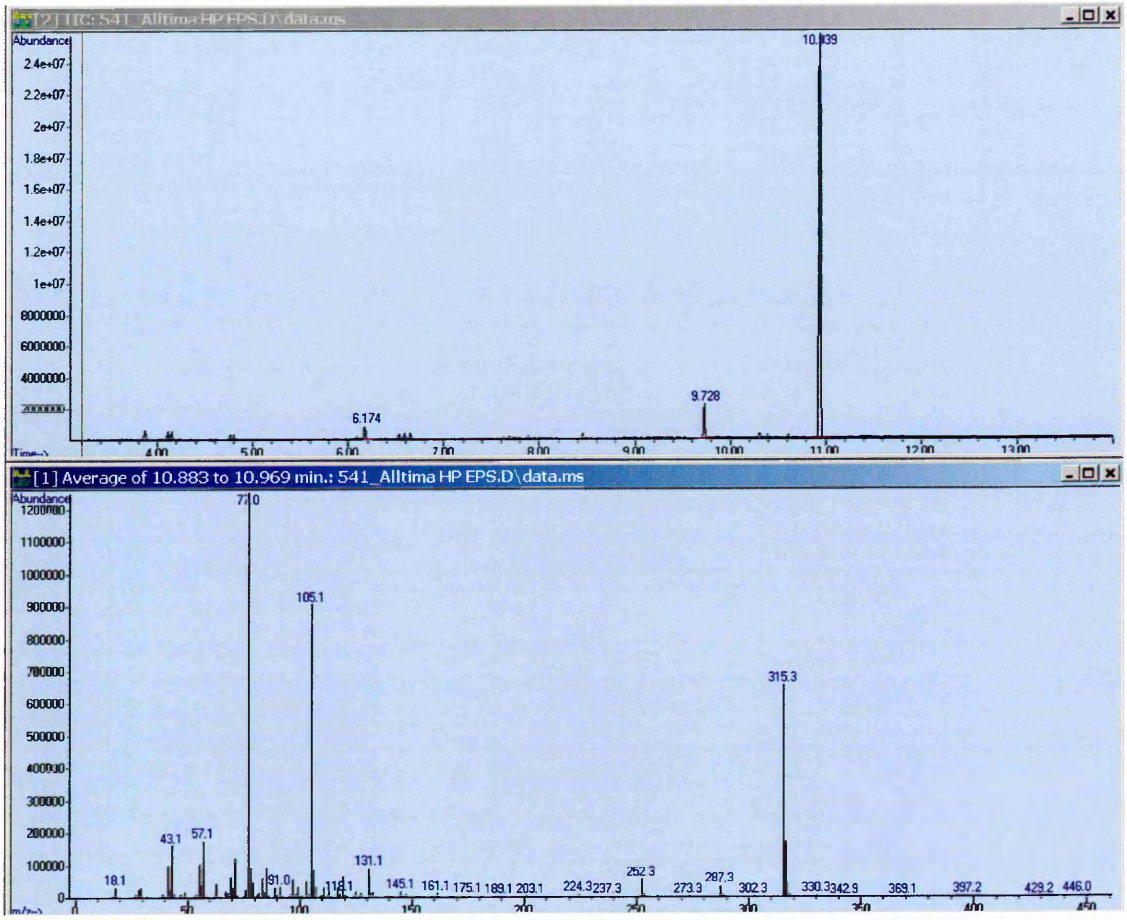

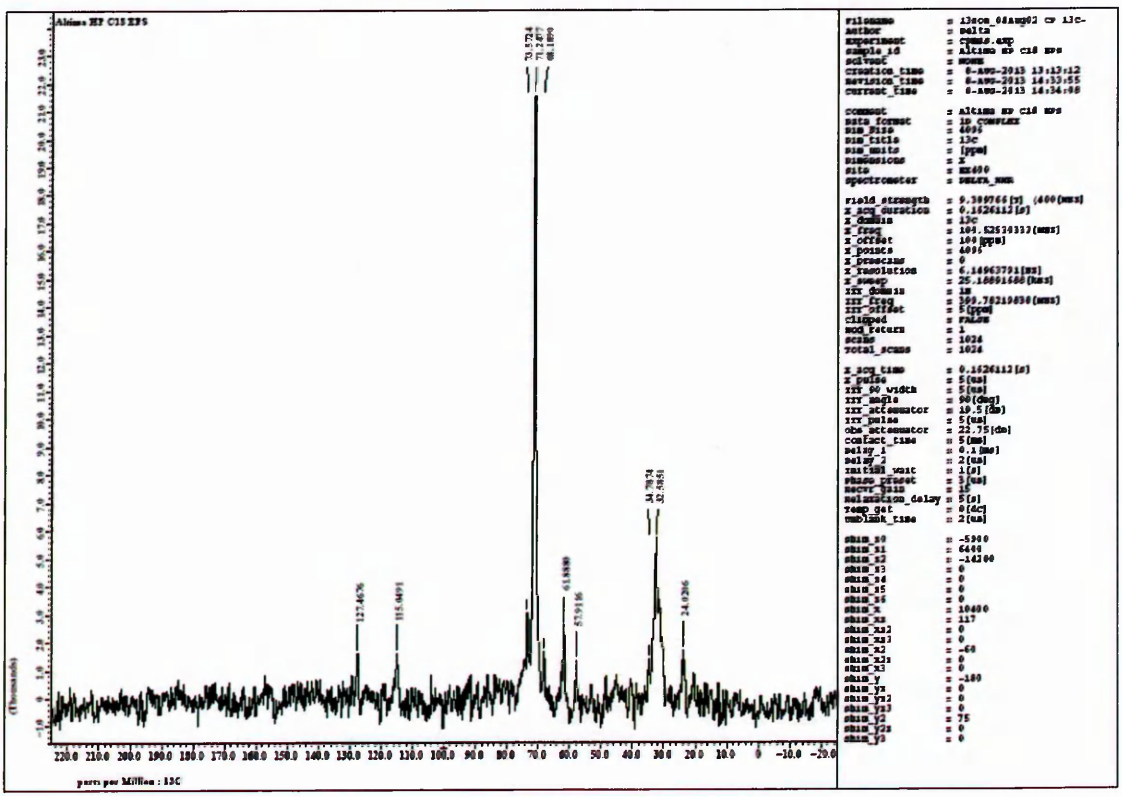

Appendix 44 Extended Tanaka data for TYPE-C™ Bidentate C18 phase

	Nitro- / Methoxy-aromatics characterisation k-values								
	k(NB)	k(DNB)	k(TNB)	k(T)	k(MB)	k(1,2-DMB)	k(1,4-DMB)	k(1,2,3-TMB)	k(1,2,4-TMB)
ACE 3 C18	1.93	1.60	1.23	7.69	3.24	1.58	2.58	0.82	1.58
Type C C18	4.26	3.20	1.89	12.43	5.79	3.06	4.80	1.45	2.79

	Nitro- / Methoxy-aromatics characterisation α-values							
	TNB/NB	DNB/T	TNB/T	1,2,3-TMB/T	1,2,3-TMB/MB	1,2,3-/1,2,4-TMB	1,4-DMB/MB	1,2-DMB/MB
ACE 3 C18	0.64	0.21	0.16	0.11	0.25	0.52	0.79	0.49
Type C C18	0.44	0.26	0.15	0.12	0.25	0.52	0.83	0.53

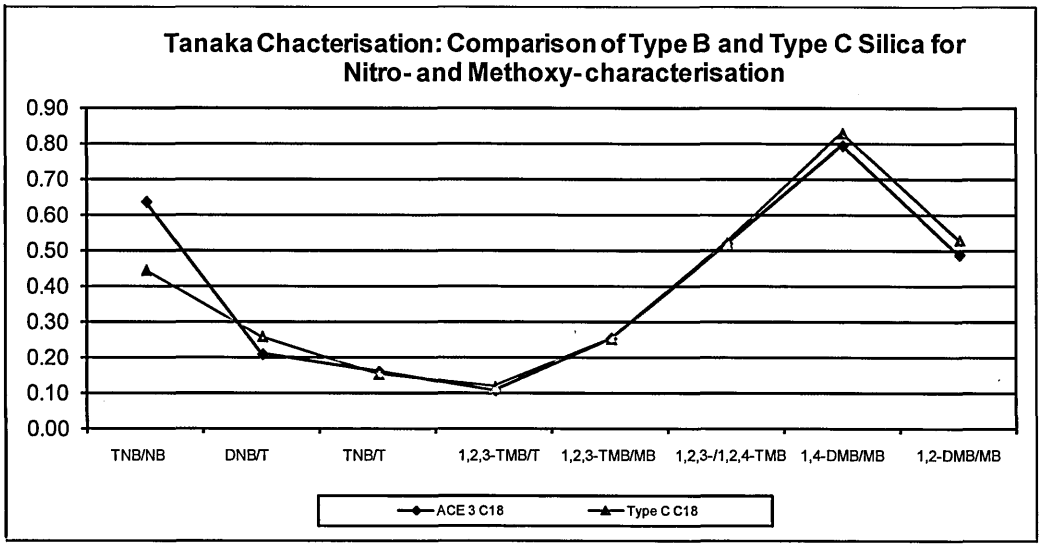

Dinitro-aromatics characterisation				
	k-values			
	k(1,2-DNB)	k(1,3-DNB)	k(1,4-DNB)	k(T)
ACE 3 C18	0.43	0.60	2.63	5.79
Type C C18	1.20	1.25	1.82	1.56

	α-values					
	1,2-DNB/T	1,3-DNB/T	1,4-DNB/T	1,4-/1,2-DNB	1,3-/1,2-DNB	1,4-/1,3-DNB
ACE 3 C18	0.08	0.10	0.45	6.05	1.37	4.40
Type C C18	0.77	0.80	1.16	1.52	1.04	1.46

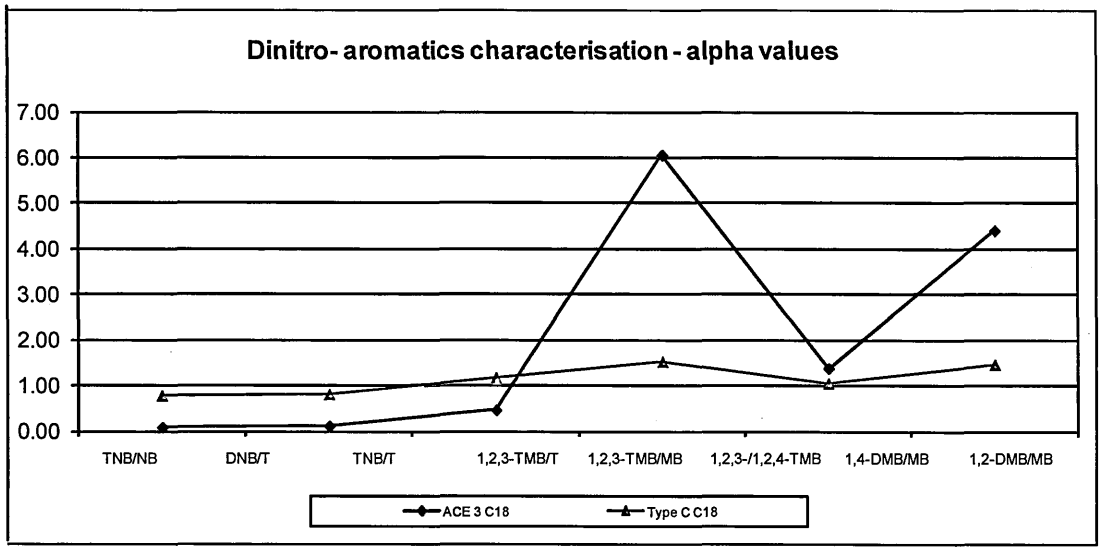

Appendix 45 Acid compounds data for TYPE-C™ Bidentate C18 phase

5 mM KH_2PO_4 pH 2.5 in water / MeOH (65:35 v/v)	Selectivity factors						
	$\alpha_{P/DMP}$	$\alpha_{CA/HC}$	$\alpha_{\sigma/BN}$	$\alpha_{PP/P}$	$\alpha_{BN/S}$	$\alpha_{\sigma/\rho}$	$\alpha_{\sigma/m}$
ACE 3 C18	0.33	1.23	0.74	10.83	1.00	3.67	2.50
TYPE-CTM Bidentate C18	0.25	1.35	0.71	10.73	1.00	3.53	2.61

5 mM KH_2PO_4 pH 2.5 in water / MeOH (35:65 v/v)	Selectivity factors			
	$\alpha_{P/BA}$	$\alpha_{P/TI}$	$\alpha_{BA/TI}$	$\alpha_{BSA/TI}$
ACE 3 C18	1.00	0.64	0.64	0.05
TYPE-CTM Bidentate C18	1.13	0.40	0.36	0.01

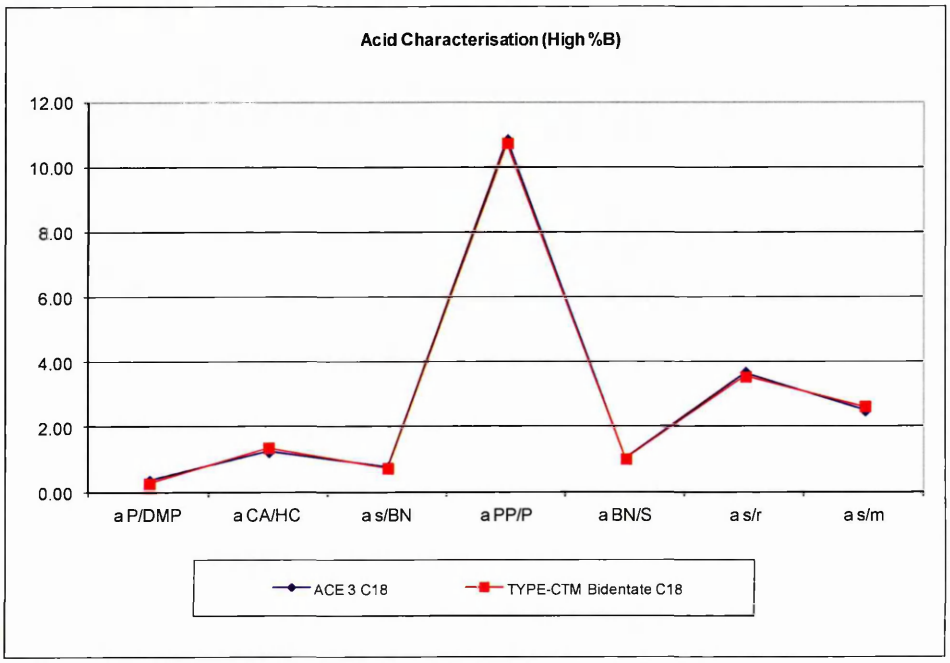

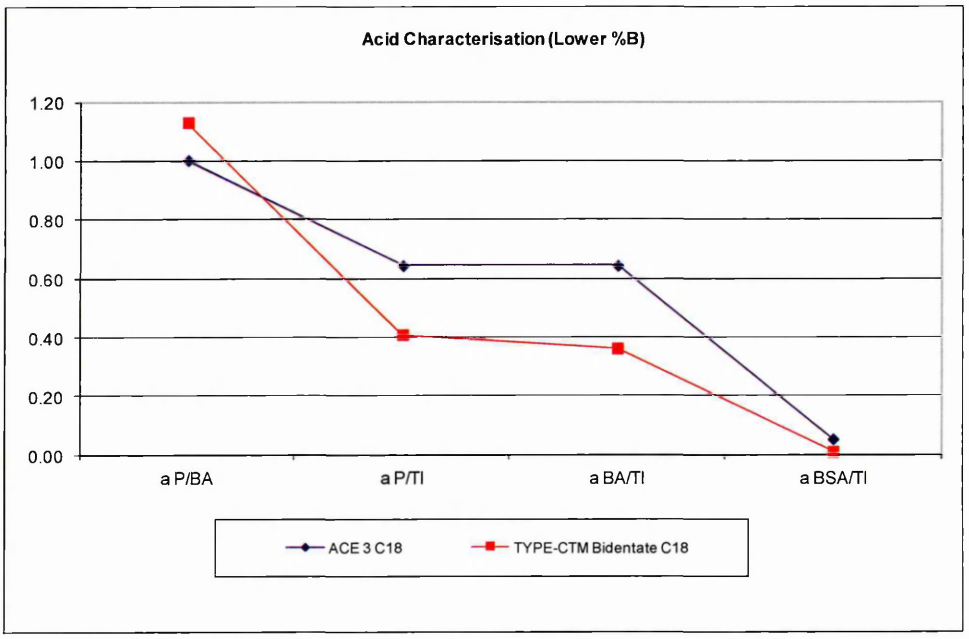

Appendix 46 QC toluene results for ACE 3 C18 and TYPE-C™ Bidentate C18 phase

ACE 3 C18: 0.03% v/v TFA in MeCN				
	Rt (min)	Area (mAU)	Peak Width	Symmetry
Toluene 1	3.778	15.0	0.0473	1.017
Toluene 2	3.778	15.0	0.0451	1.018
Toluene 3	3.778	15.0	0.0451	1.011
Average	**3.778**	**15.0**	**0.046**	**1.015**
	0.000	0.000	0.001	0.004
RSD(%)	**0.000**	**0.000**	**2.771**	**0.373**

TYPE-C™ Bidentate C18: 0.03% v/v TFA in MeCN				
	Rt (min)	Area (mAU)	Peak Width	Symmetry
Toluene 1	3.697	15.8	0.063	0.846
Toluene 2	3.693	15.6	0.070	0.832
Toluene 3	3.692	15.5	0.072	0.816
Average	**3.694**	**15.6**	**0.068**	**0.831**
	0.003	0.1528	0.005	0.015
RSD(%)	**0.072**	**0.977**	**6.819**	**1.806**

ACE 3 C18: 0.03%(v/v) $TFA_{(aq)}$ in Methanol				
	Rt (min)	Area (mAU)	Peak Width	Symmetry
Toluene 1	4.409	17.1	0.047	1.054
Toluene 2	4.407	17.2	0.047	1.047
Toluene 3	4.406	17.0	0.047	1.040
Average	**4.407**	**17.1**	**0.047**	**1.047**
	0.002	0.100	0.000	0.007
RSD(%)	**0.035**	**0.585**	**0.369**	**0.669**

TYPE-C™ Bidentate C18: 0.03%(v/v) $TFA_{(aq)}$ in Methanol				
	Rt (min)	Area (mAU)	Peak Width	Symmetry
Toluene 1	4.471	16.7	0.061	0.816
Toluene 2	4.469	16.9	0.066	0.832
Toluene 3	4.467	16.9	0.070	0.836
Average	**4.469**	**16.8**	**0.066**	**0.828**
	0.002	0.115	0.005	0.011
RSD(%)	**0.045**	**0.686**	**7.248**	**1.278**

ACE 3 C18: 20mM KH_2PO_4 in Methanol				
	Rt (min)	Area (mAU)	Peak Width	Symmetry
Toluene 1	5.598	16.3	0.05770	1.123
Toluene 2	5.597	16.5	0.05890	1.098
Toluene 3	5.596	16.5	0.05670	1.084
Average	**5.597**	**16.4**	**0.058**	**1.101667**
	0.001	0.115	0.001	0.020
RSD(%)	**0.018**	**0.703**	**1.907**	**1.793**

TYPE-C™ Bidentate C18: 20mM KH_2PO_4 in Methanol				
	Rt (min)	Area (mAU)	Peak Width	Symmetry
Toluene 1	5.819	15.9	0.10100	0.736
Toluene 2	5.808	15.7	0.10810	0.745
Toluene 3	5.807	15.9	0.10900	0.729
Average	**5.811**	**15.8**	**0.106**	**0.736667**
	0.007	0.115	0.004	0.008
RSD(%)	**0.115**	**0.729**	**4.133**	**1.089**

ACE 3 C18: 20mM KH_2PO_4 in Acetonitrile				
	Rt (min)	Area (mAU)	Peak Width	Symmetry
Toluene 1	4.8	15.8	0.05360	1.017
Toluene 2	4.799	15.5	0.05360	0.989
Toluene 3	4.8	15.1	0.05330	1.023
Average	**4.800**	**15.5**	**0.054**	**1.009667**
	0.001	0.351	0.000	0.018
RSD(%)	**0.012**	**2.271**	**0.324**	**1.797**

TYPE-C™ Bidentate C18: 20mM KH_2PO_4 in Acetonitrile				
	Rt (min)	Area (mAU)	Peak Width	Symmetry
Toluene 1	4.725	15.6	0.09090	0.72
Toluene 2	4.725	15.3	0.09180	0.739
Toluene 3	4.723	15.2	0.09340	0.738
Average	**4.724**	**15.4**	**0.092**	**0.732333**
	0.001	0.208	0.001	0.011
RSD(%)	**0.024**	**1.355**	**1.376**	**1.460**

Appendix 47 100 Compound on TYPE-C™ Bidentate C18 phase 0.03% v/v TFA in MeCN

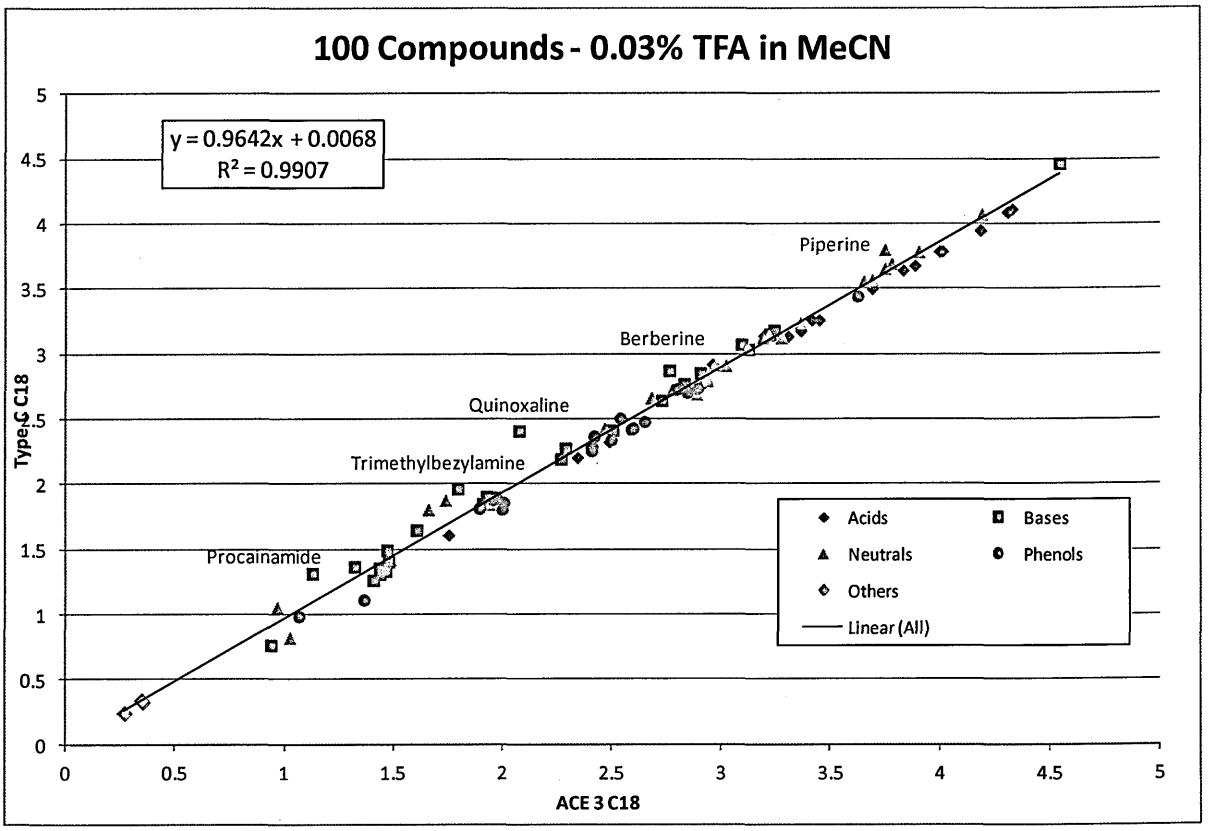

Appendix 48 100 Compound on TYPE-C™ Bidentate C18 phase 20mM KH_2PO_4 in MeOH

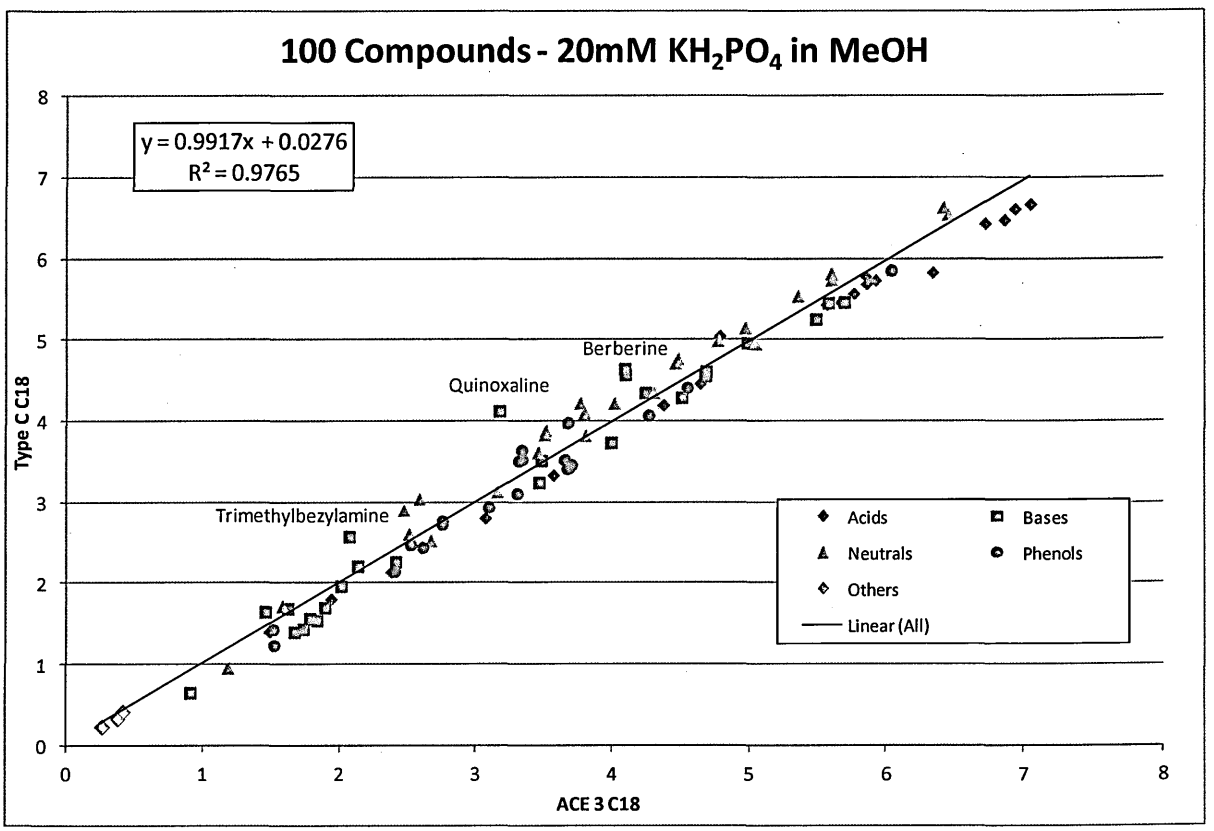

Appendix 49 100 Compound on TYPE-C™ Bidentate C18 phase 20mM KH_2PO_4 in MeCN

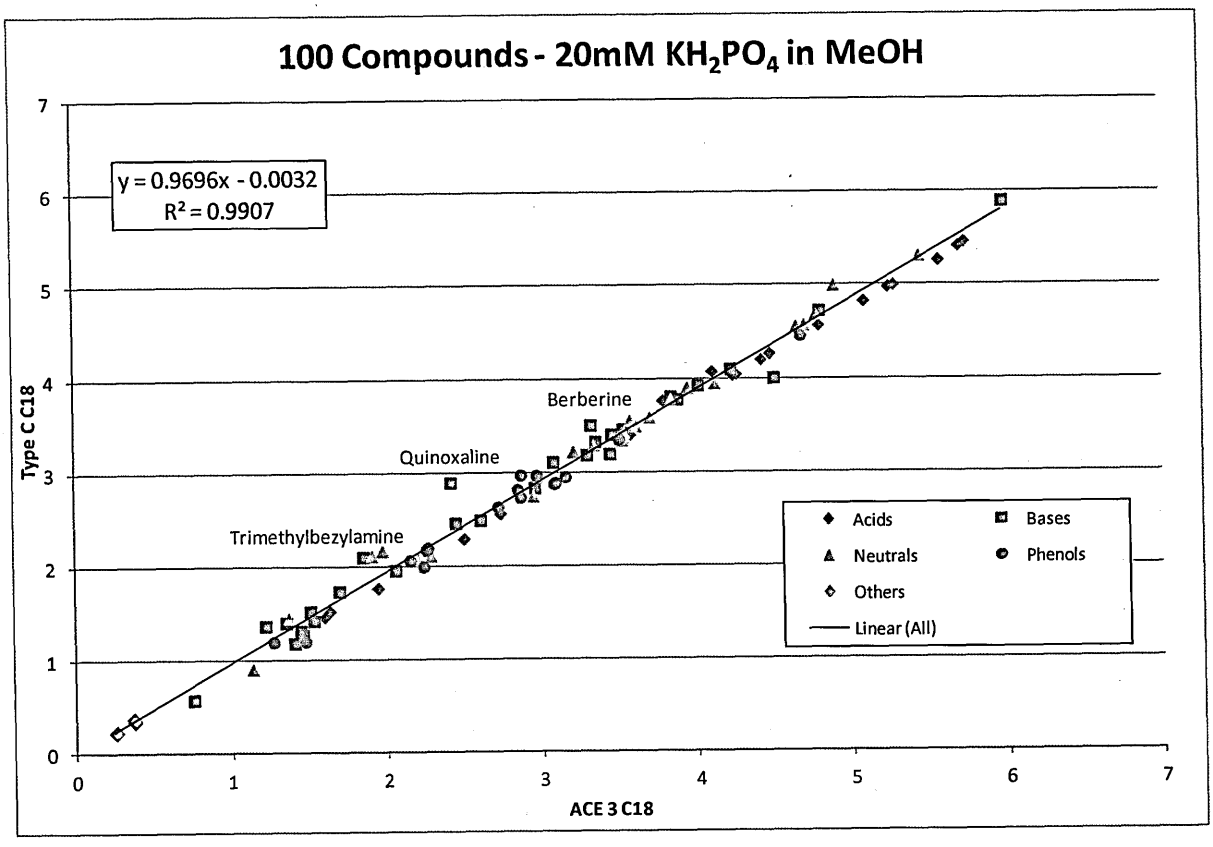

Appendix 50 QC Data on Zic-HILIC for Tanaka HILIC Characterisation

	Tanaka characterisation							
	α(pH)	α(CH2)	α(OH)	α(V/A)	α(2dG/3dG)	a(a/b)	α(AX)	α(CX)
ZIC-HILIC, 150 x 4.6 mm	1.22	1.65	1.99	1.47	1.10	1.14	0.14	3.05
ZIC-HILIC, 150 x 4.6 mm	1.16	1.63	1.97	1.47	1.10	1.14	0.14	3.04
ZIC-HILIC, 150 x 4.6 mm	1.15	1.66	2.00	1.35	1.11	1.15	0.13	3.01
Mean	1.177	1.647	1.985	1.430	1.104	1.144	0.137	3.032
SD	0.038	0.013	0.013	0.070	0.003	0.004	0.007	0.018
RSD (%)	3.269	0.765	0.667	4.861	0.246	0.308	5.331	0.589